PowerPoint File available:

http://bl831.als.lbl.gov/~jamesh/powerpoint/BioXFEL_SvN_2013.ppt

Acknowledgements

Chris Neilson Rick Kirian Nadia Zatsepin Ken Frankel

ALS 8.3.1 creator: Tom Alber

Integrated Diffraction Analysis Technologies (IDAT)
Center for Structure of Membrane Proteins (CSMP)
Membrane Protein Expression Center II (MPEC)
Center for HIV Accessory and Regulatory Complexes (HARC)

W. M. Keck Foundation
Plexxikon, Inc.
M D Anderson CRC
University of California Berkeley
University of California San Francisco
University of California Campus-Laboratory Collaboration Grant
Henry Wheeler

The Advanced Light Source is supported by the Director, Office of Science, Office of Basic Energy Sciences, Materials Sciences Division, of the US Department of Energy under contract No. DE-AC02-05CH11231 at Lawrence Berkeley National Laboratory.

“If you don’t have
good data,
then you have
no data at all.”

-Sung-Hou Kim

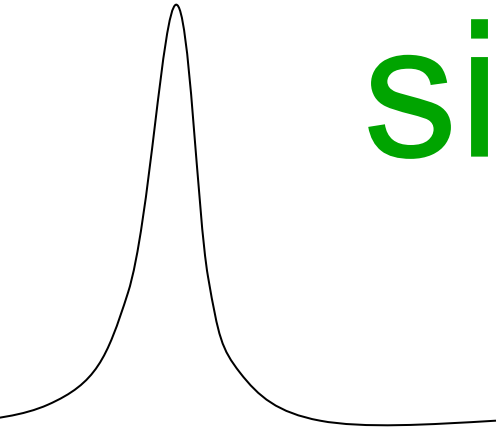

signal *vs* noise

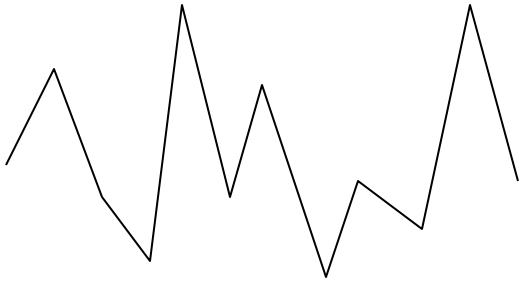

"If you don't have
good data,
then you have
no data at all."

-Sung-Hou Kim

Missing Overloads

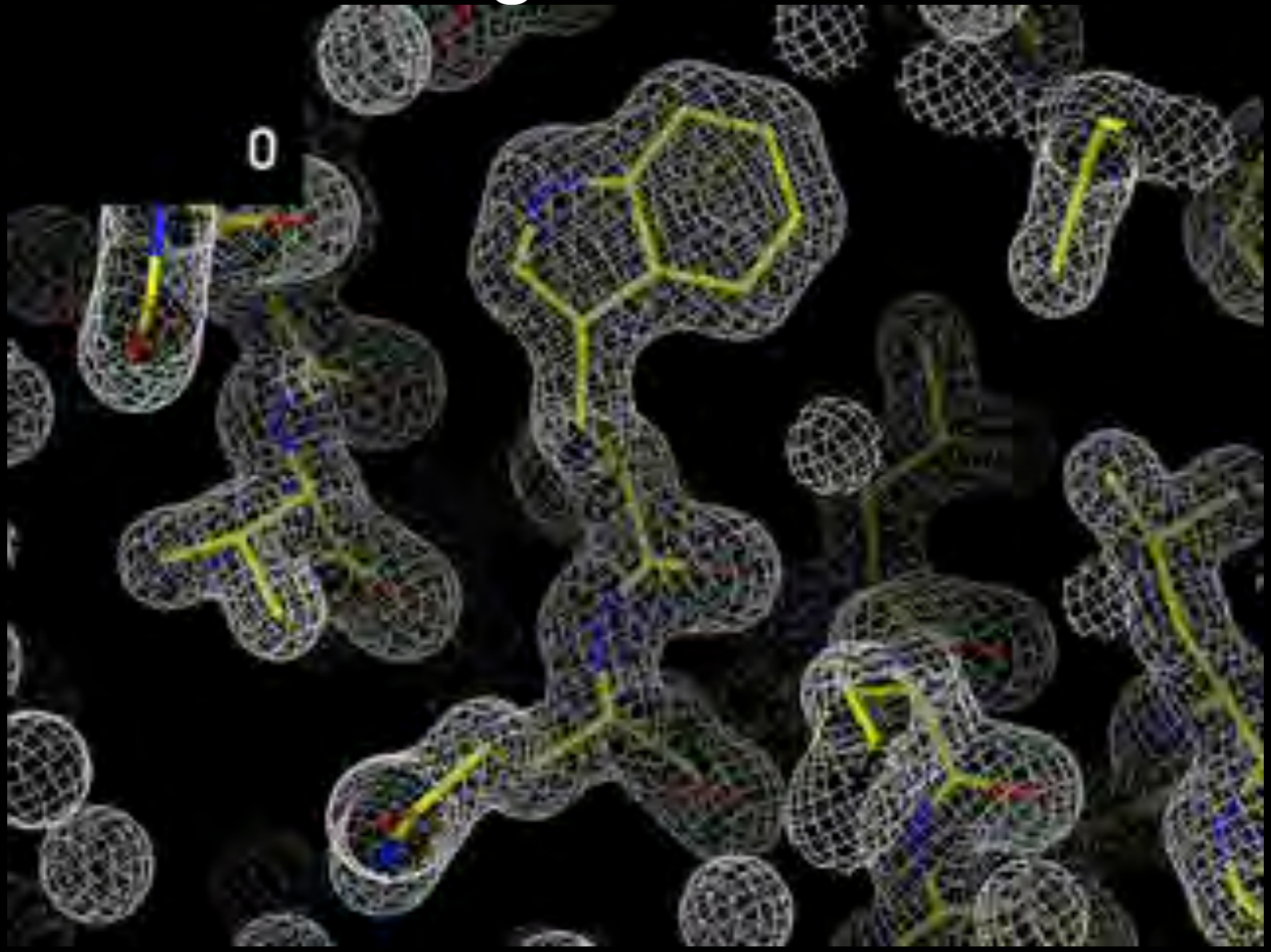

http://bl831.als.lbl.gov/~jamesh/movies/overloads.mpeg

Missing Overloads

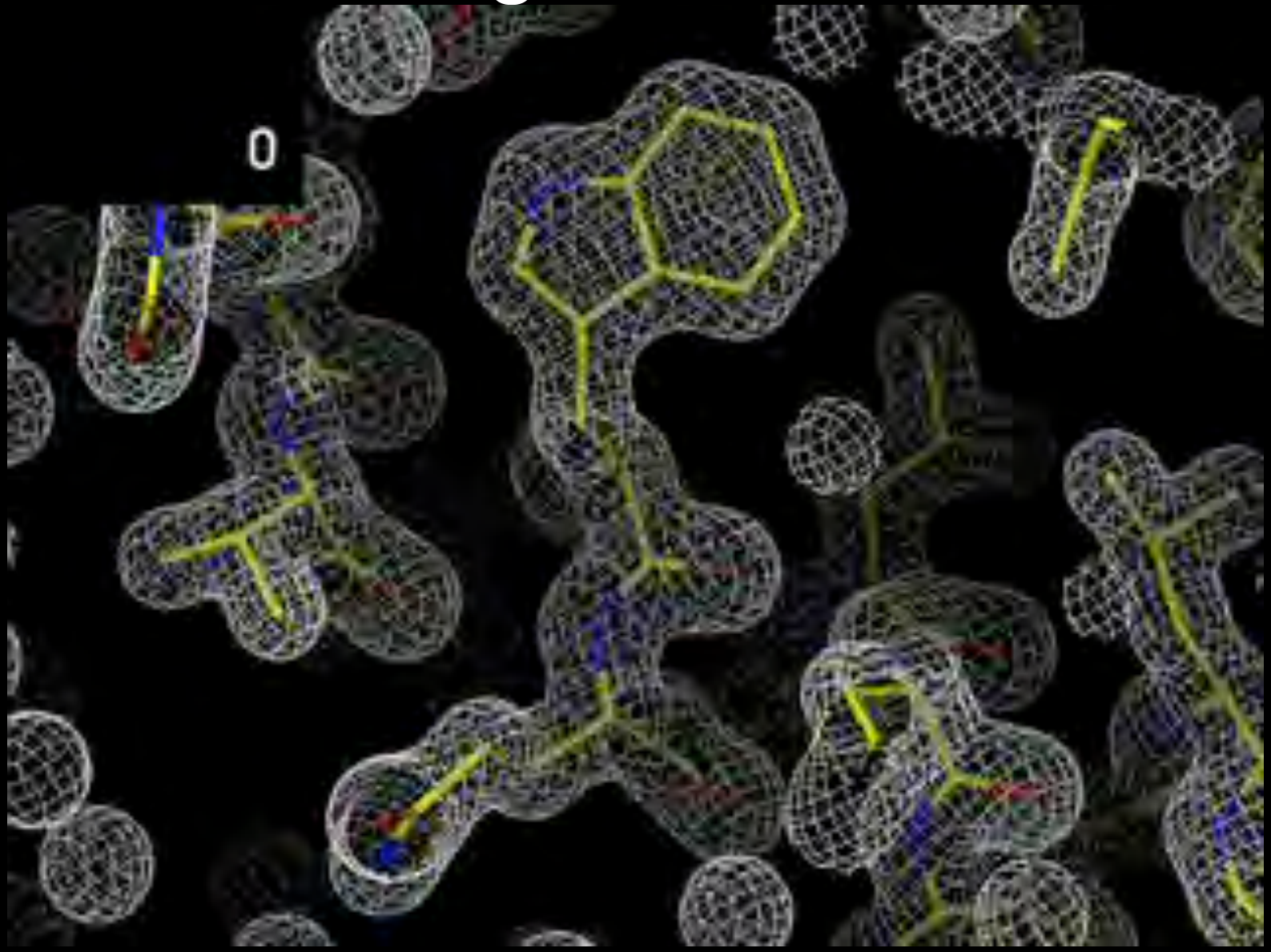

http://bl831.als.lbl.gov/~jamesh/movies/overloads.mpeg

Completeness: random deletion

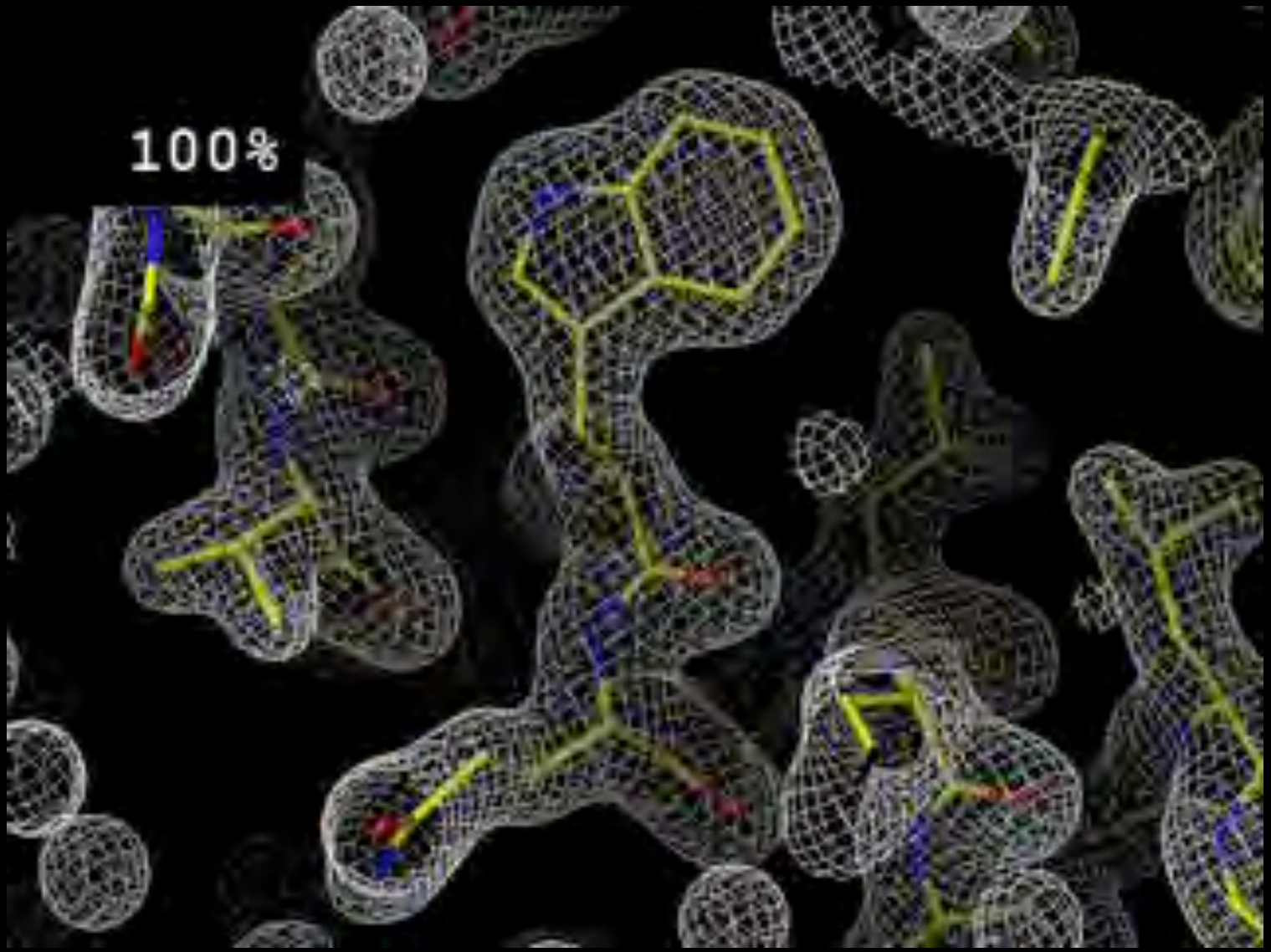

http://bl831.als.lbl.gov/~jamesh/movies/completeness.mpeg

Completeness: random deletion

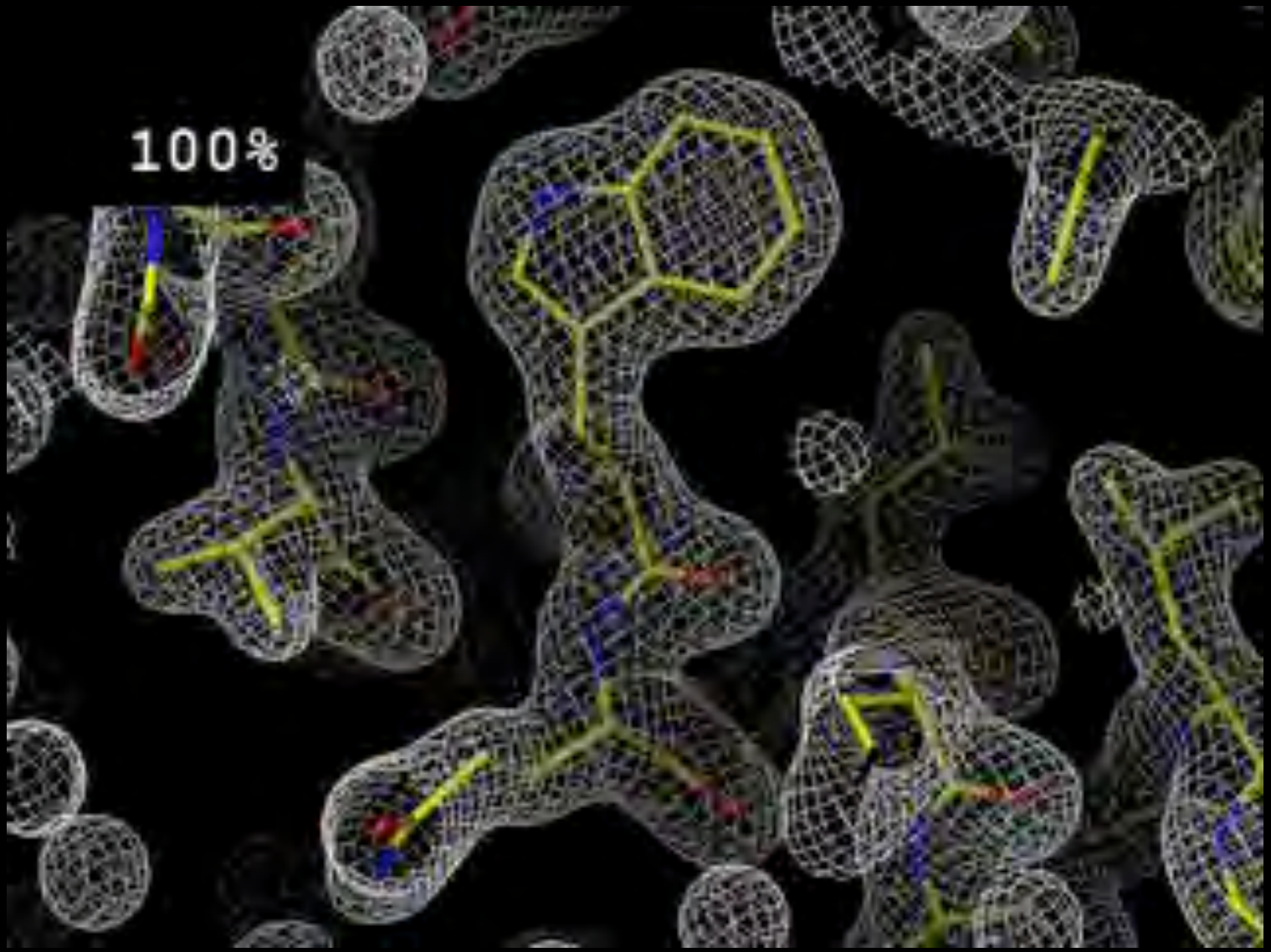

http://bl831.als.lbl.gov/~jamesh/movies/completeness.mpeg

R-factor

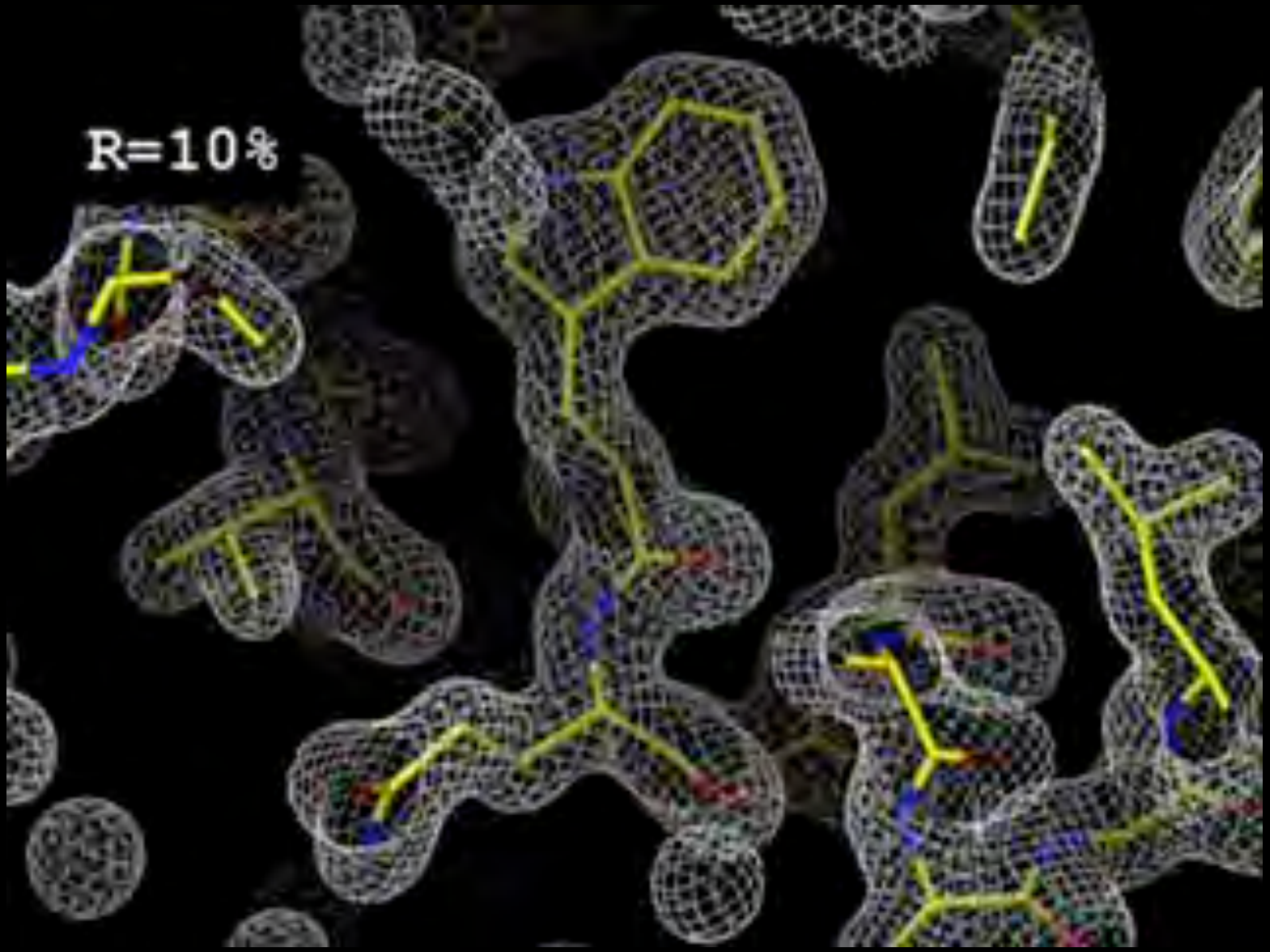

http://bl831.als.lbl.gov/~jamesh/movies/rfactor.mpeg

R-factor

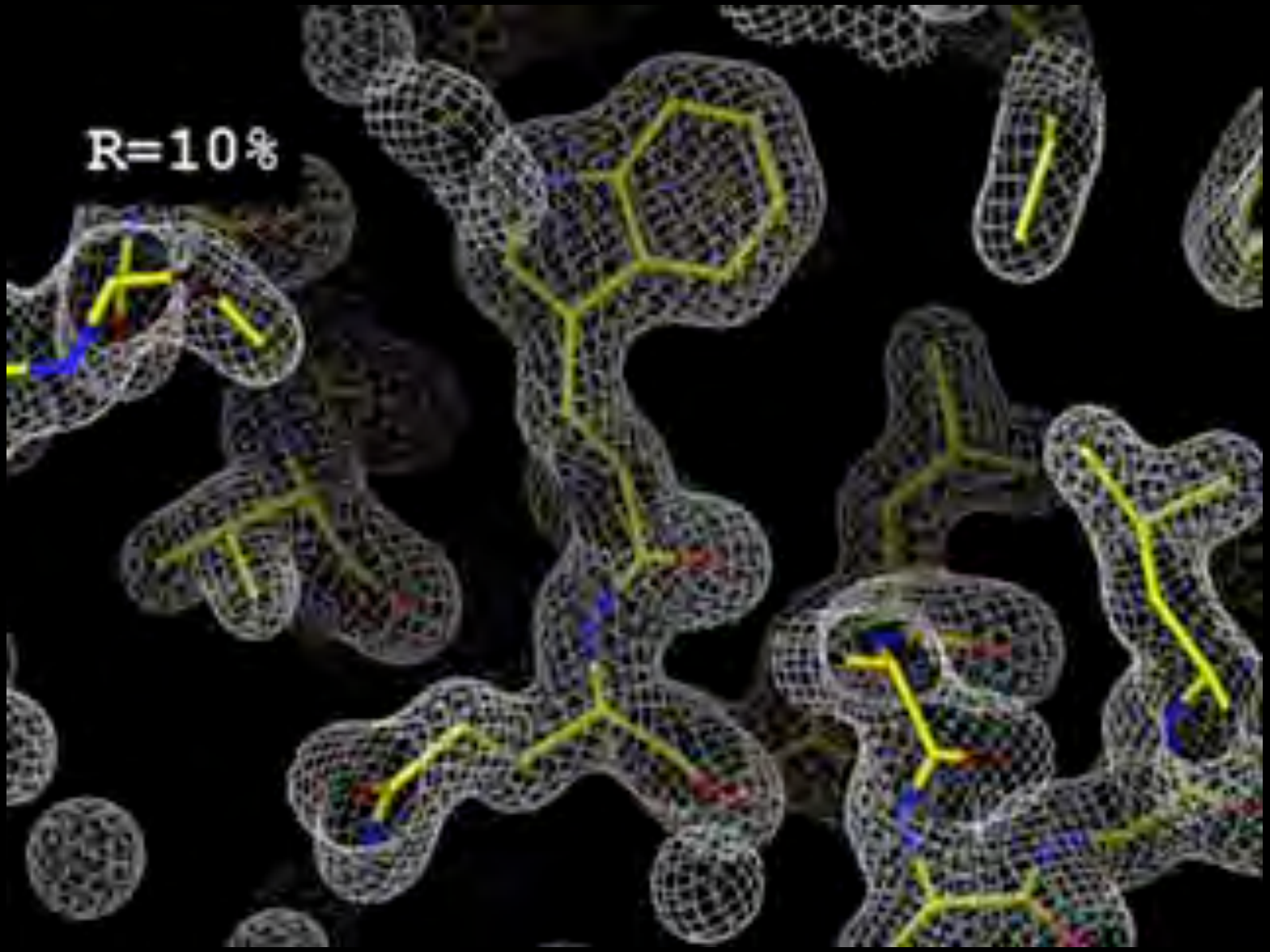

http://bl831.als.lbl.gov/~jamesh/movies/rfactor.mpeg

Figure of Merit

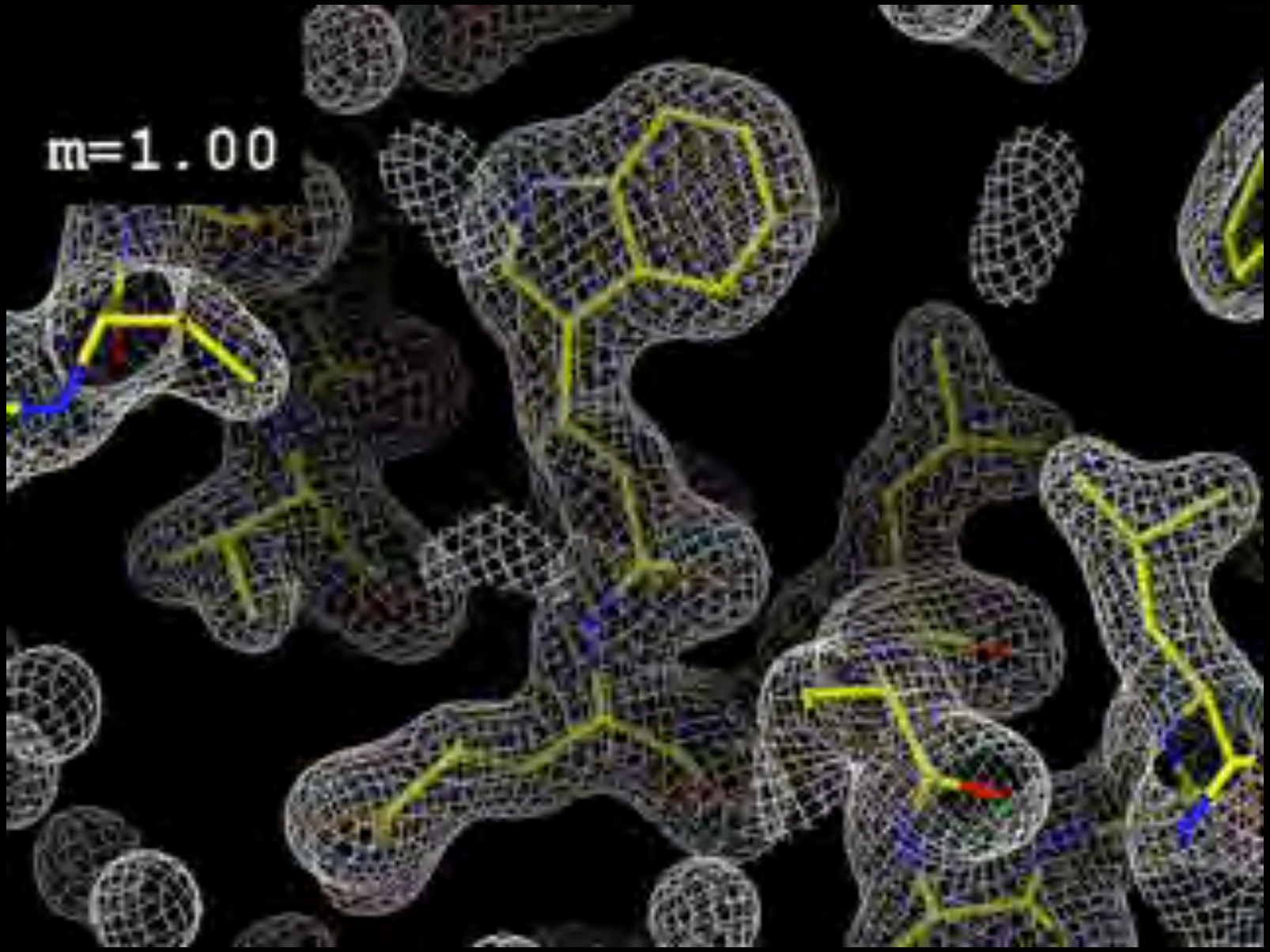

http://bl831.als.lbl.gov/~jamesh/movies/dephase.mpeg

Figure of Merit

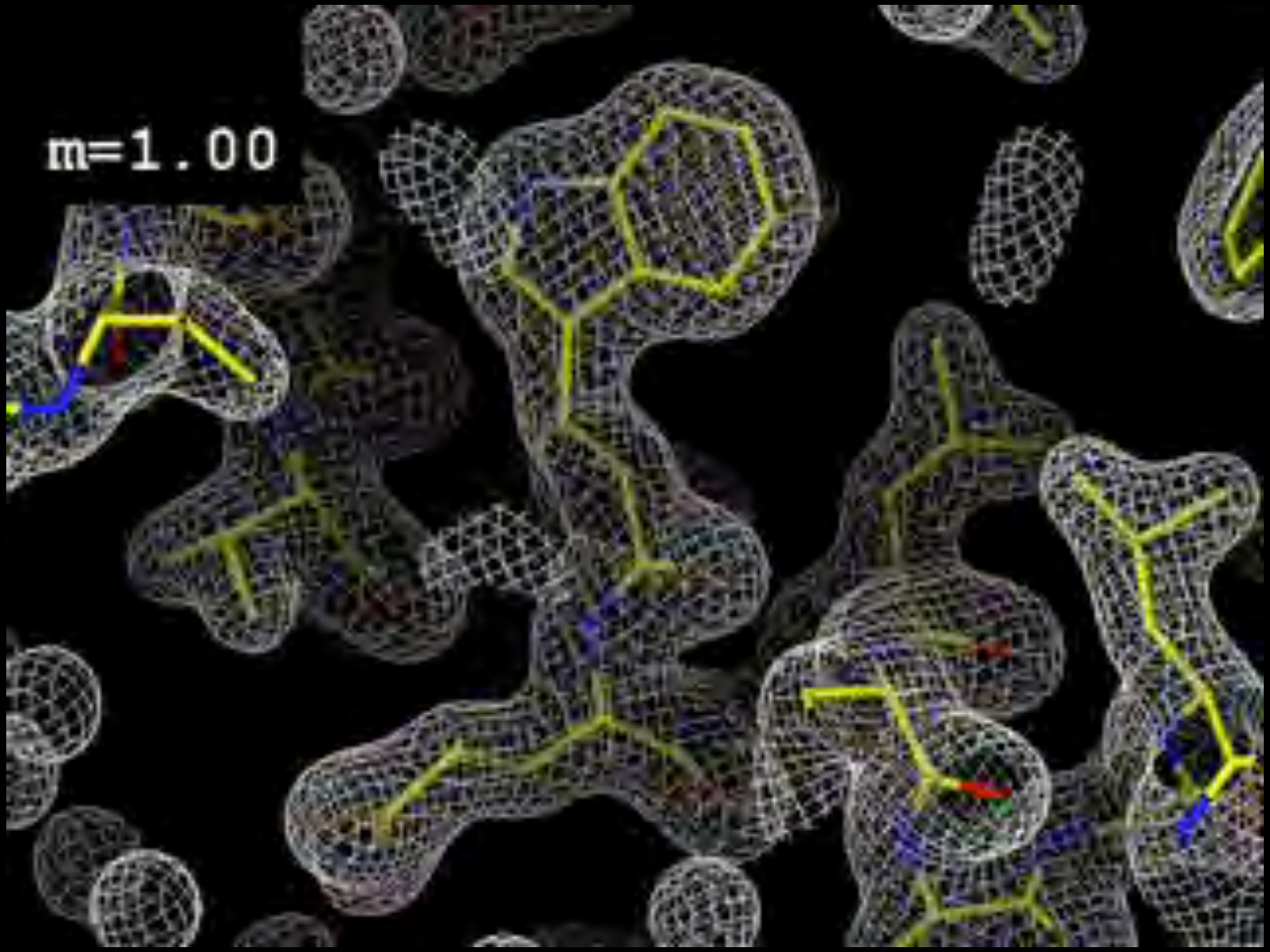

http://bl831.als.lbl.gov/~jamesh/movies/dephase.mpeg

Resolution

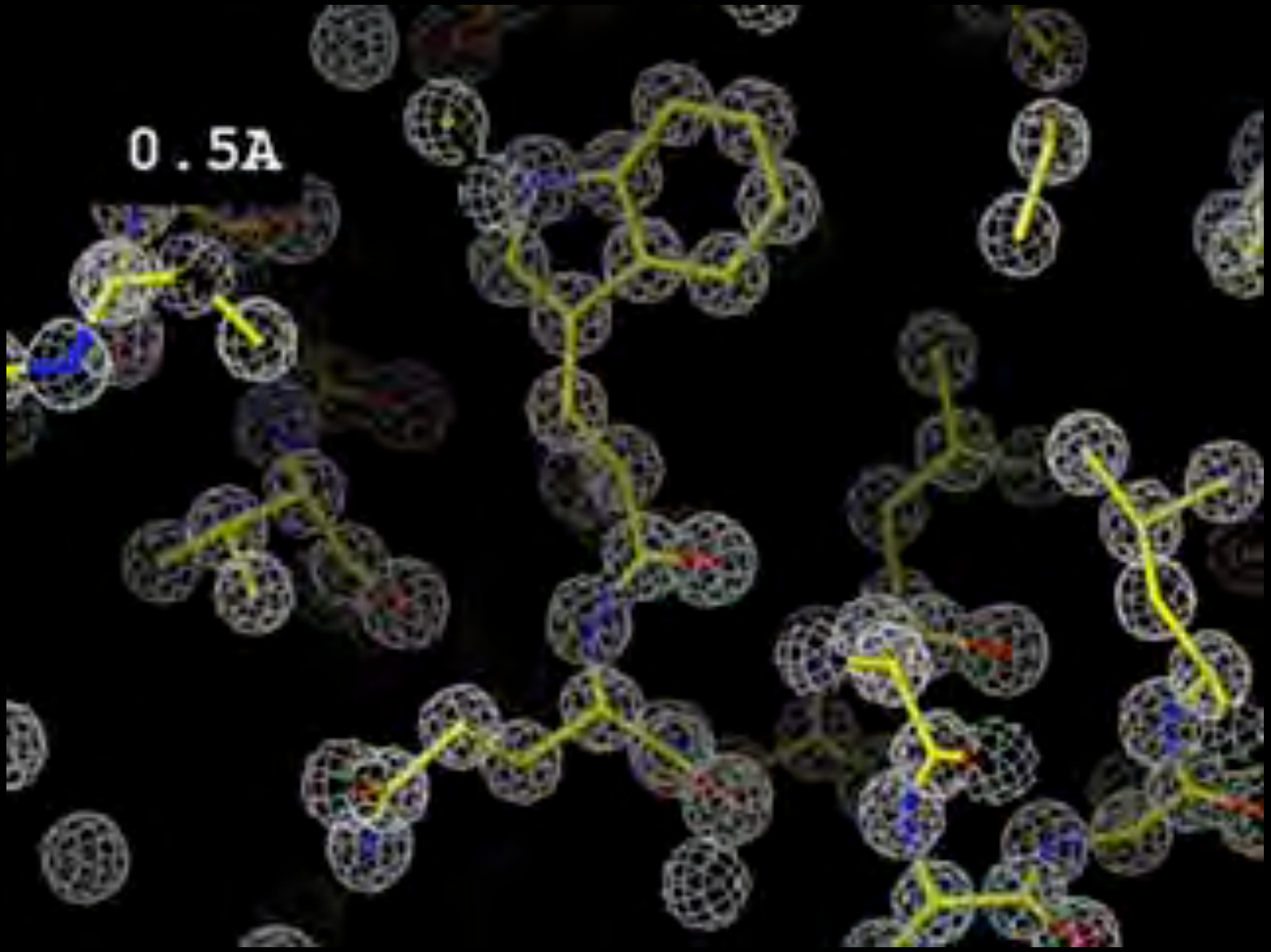

http://bl831.als.lbl.gov/~jamesh/movies/resolution.mpeg

Resolution

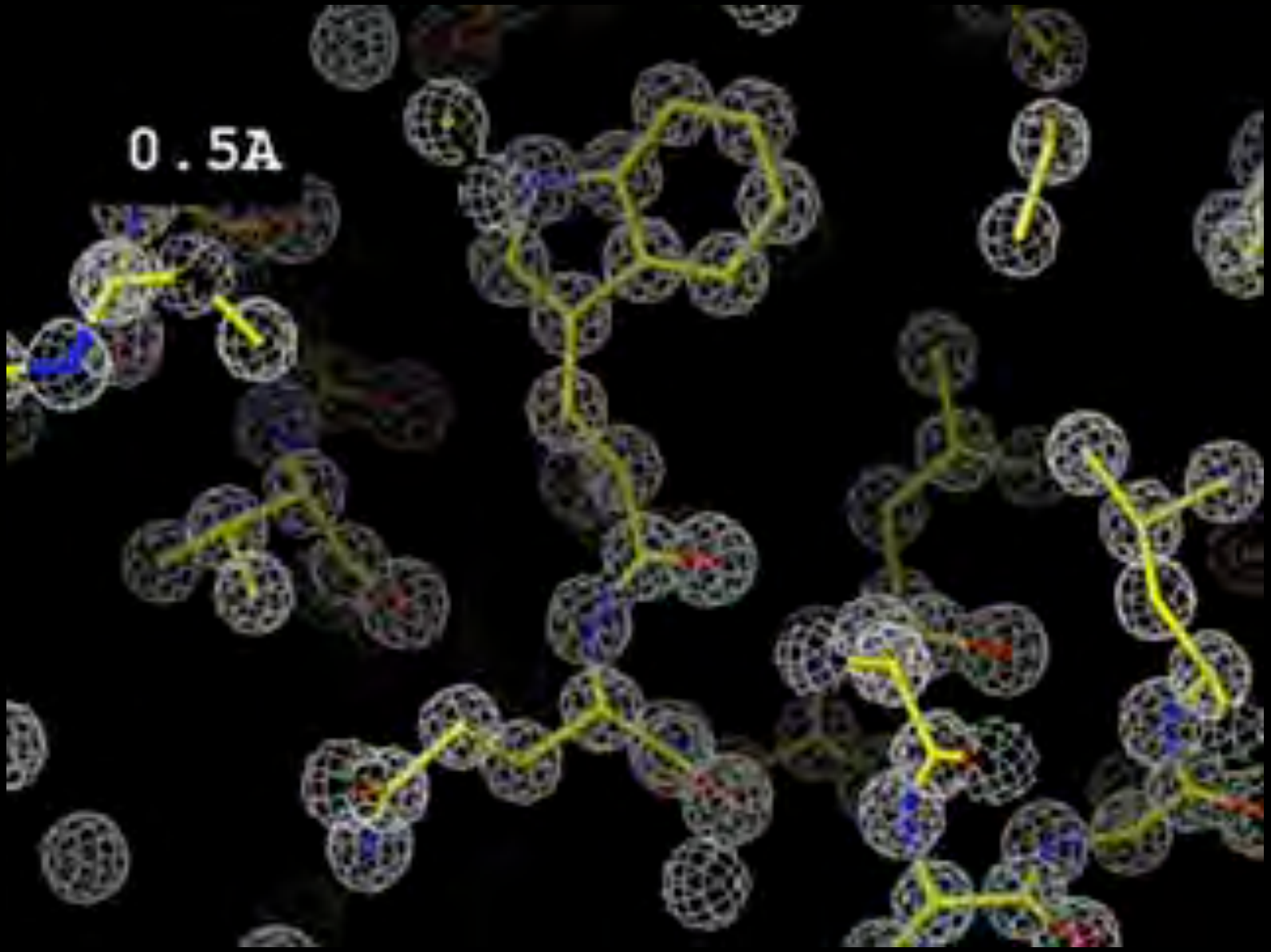

http://bl831.als.lbl.gov/~jamesh/movies/resolution.mpeg

signal *vs* noise

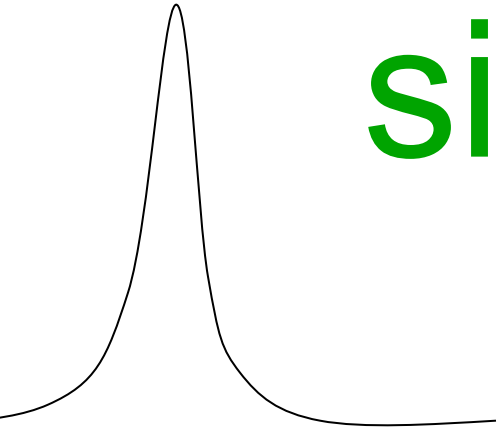

easy

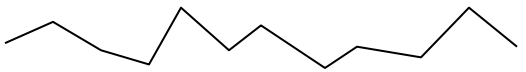

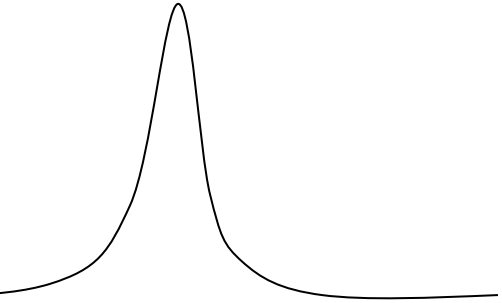

hard

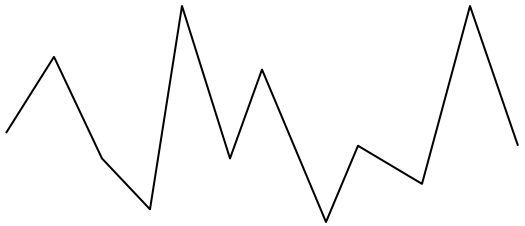

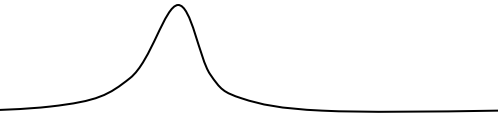

impossible

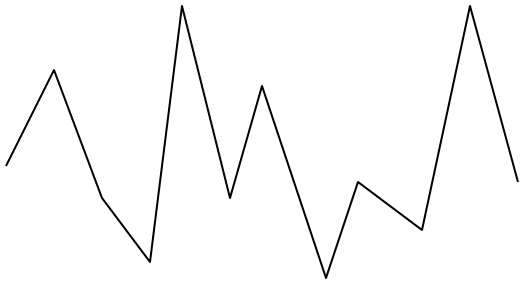

signal *vs* noise

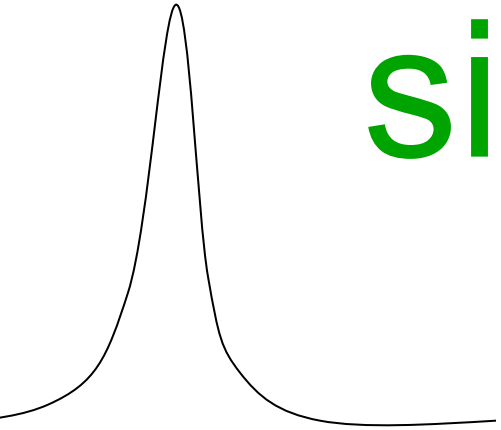

easy

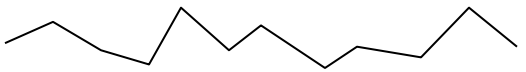

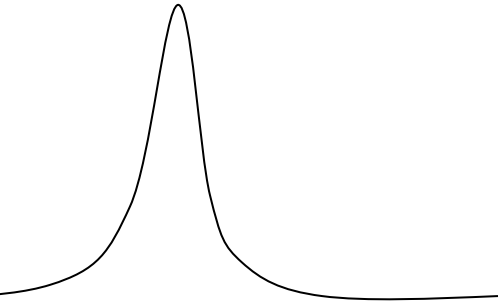

hard

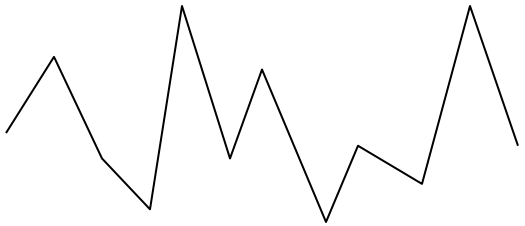

threshold of “solvability”

impossible

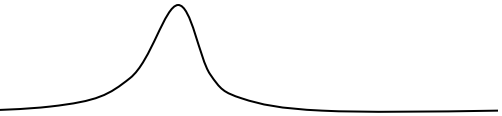

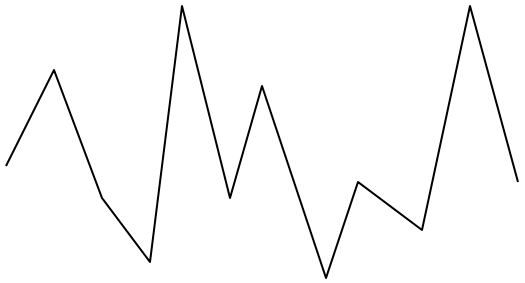

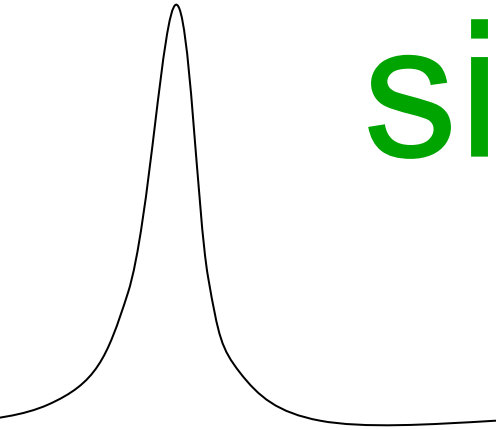

signal *vs* noise

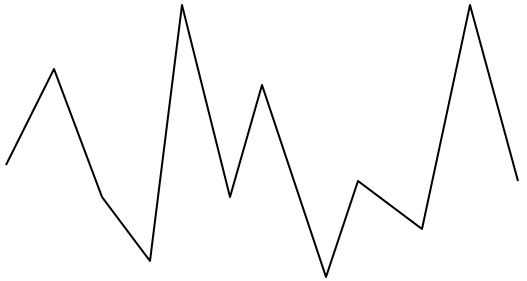

"If you don't have
good data,
then you must
learn statistics."

-James Holton

Adding noise

Adding noise

1 + 1 = 1.4

Adding noise

$$1 + 1 = 1.4$$

$$\sigma_{total}^2 = \sigma_1^2 + \sigma_2^2$$

Adding noise

$$1^2 + 1^2 = 1.4^2$$

$$\sigma_{total}^2 = \sigma_1^2 + \sigma_2^2$$

Adding noise

$$1^2 + 1^2 = 1.4^2$$

$$3^2 + 1^2 = 3.2^2$$

$$\sigma_{total}^2 = \sigma_1^2 + \sigma_2^2$$

Adding noise

$$1^2 + 1^2 = 1.4^2$$

$$3^2 + 1^2 = 3.2^2$$

$$10^2 + 1^2 = 10.05^2$$

Classes of error in MX

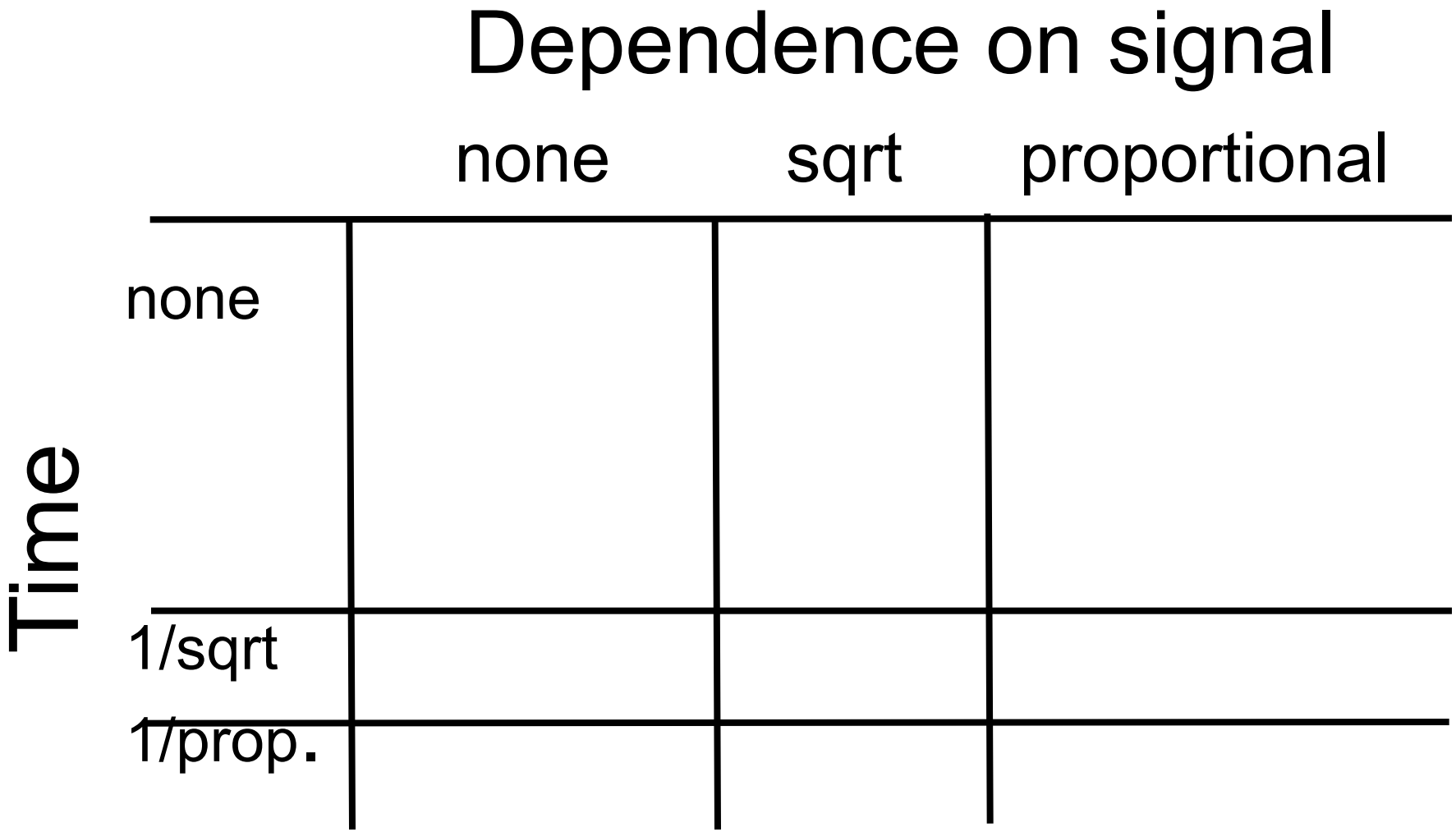

Classes of error in MX

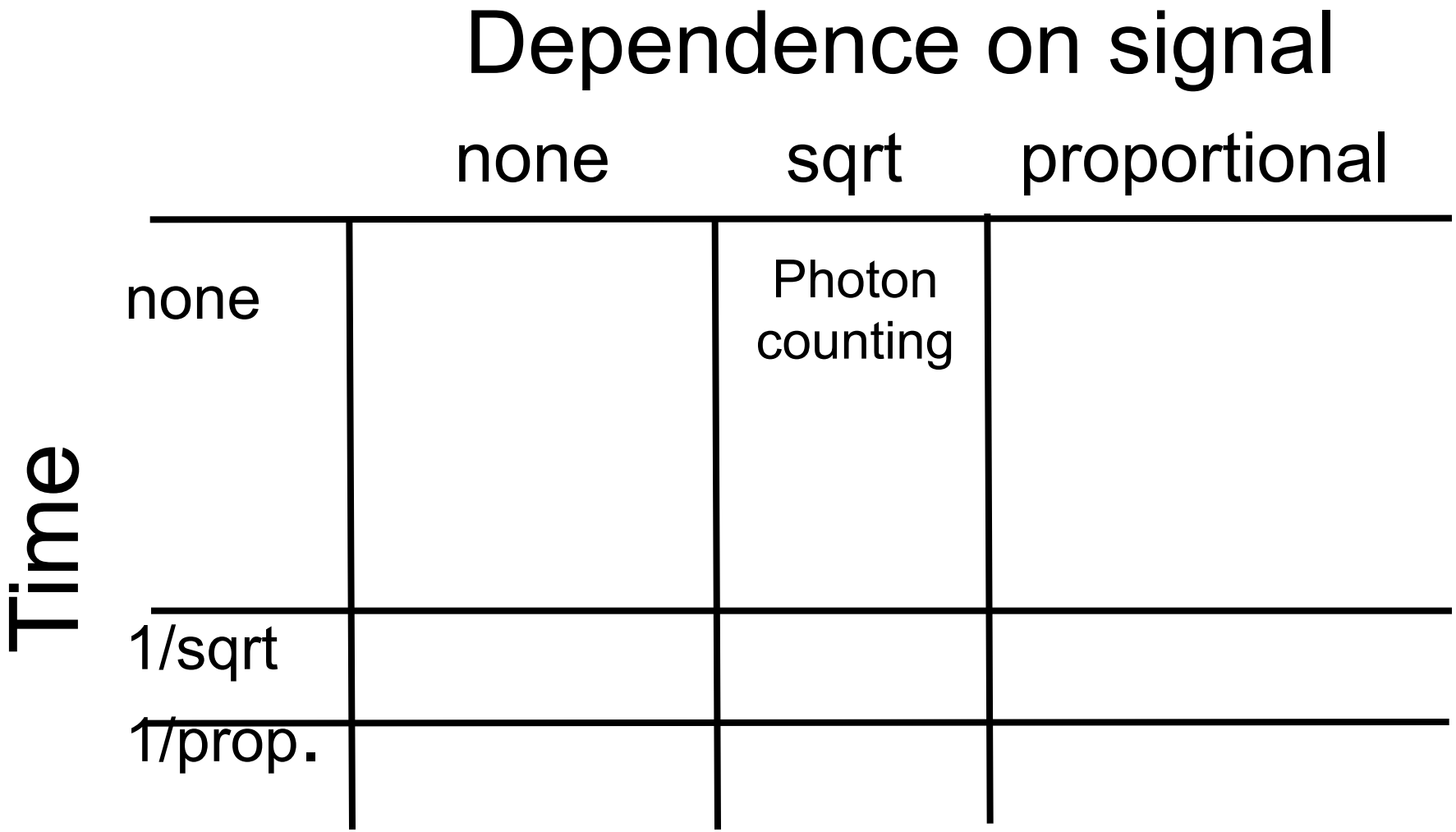

Classes of error in MX

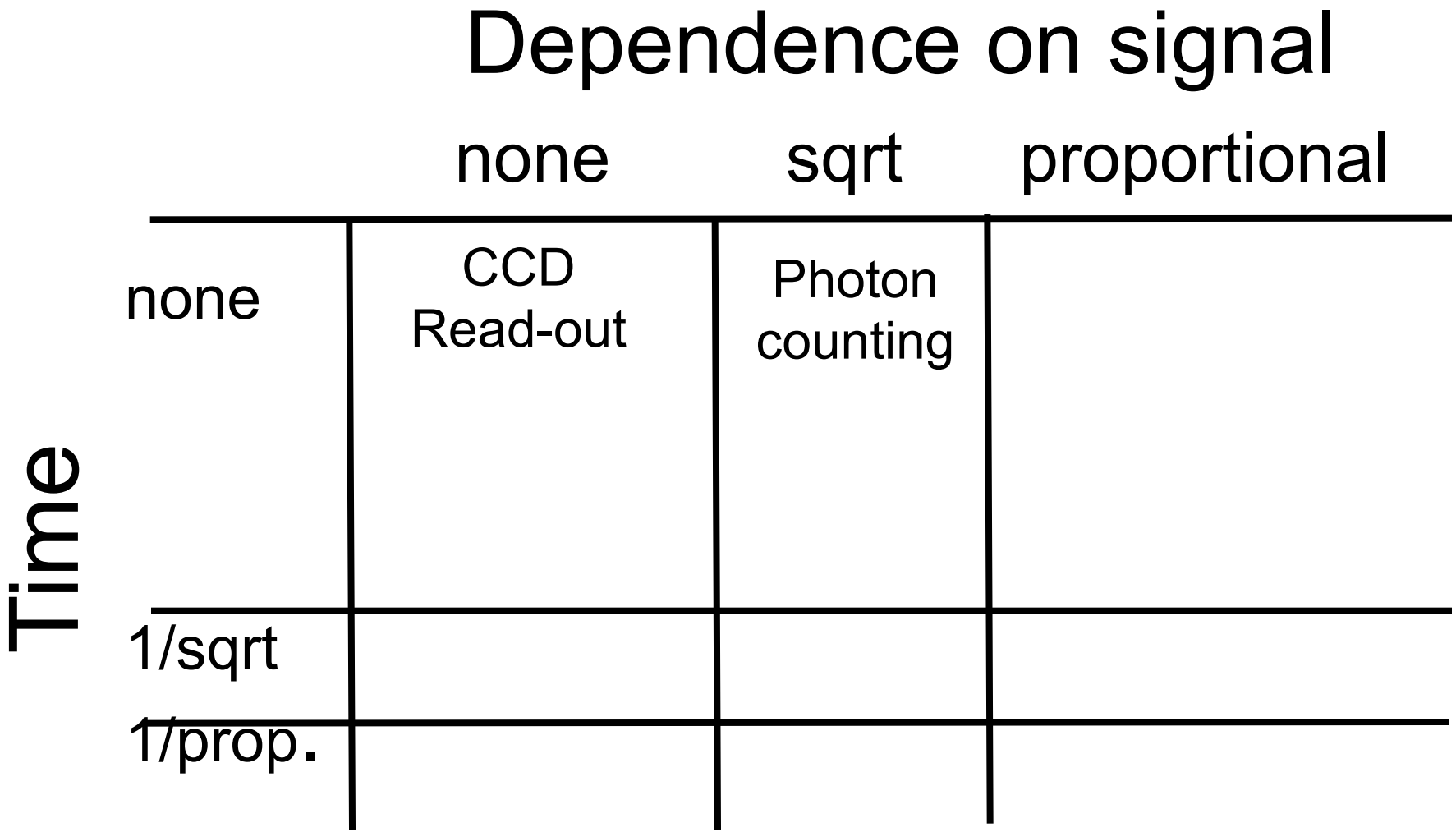

Classes of error in MX

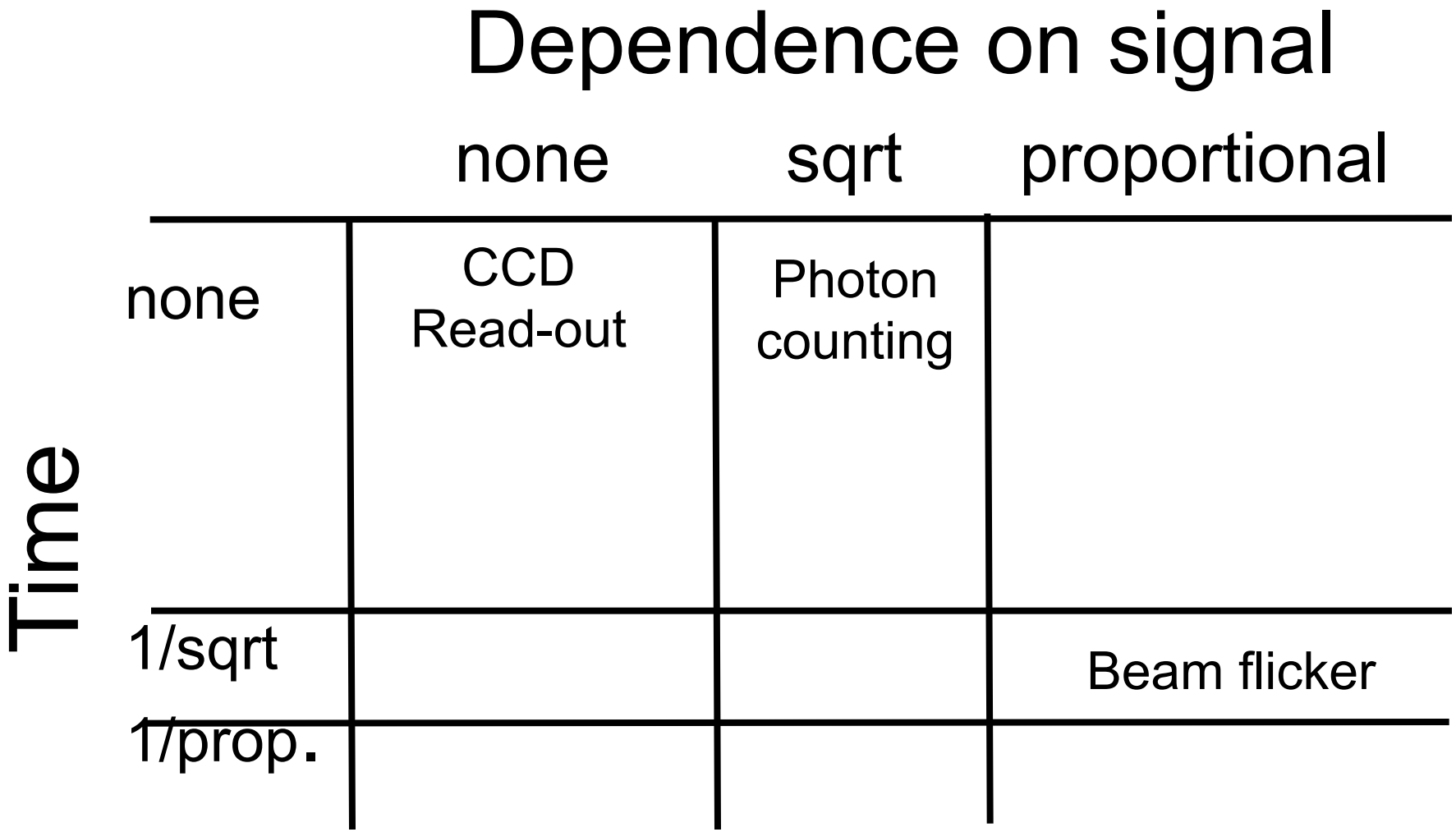

Classes of error in MX

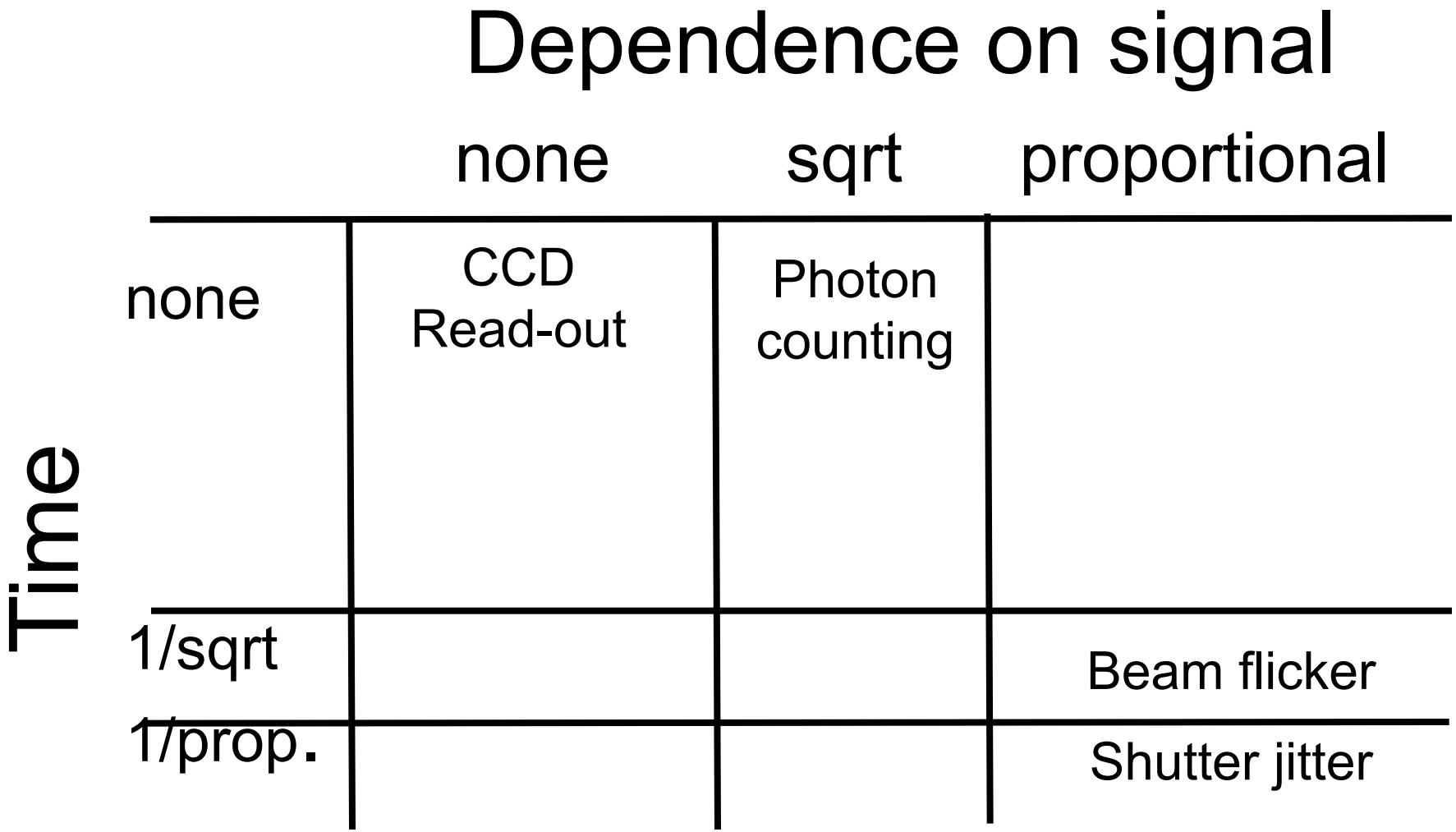

Classes of error in MX

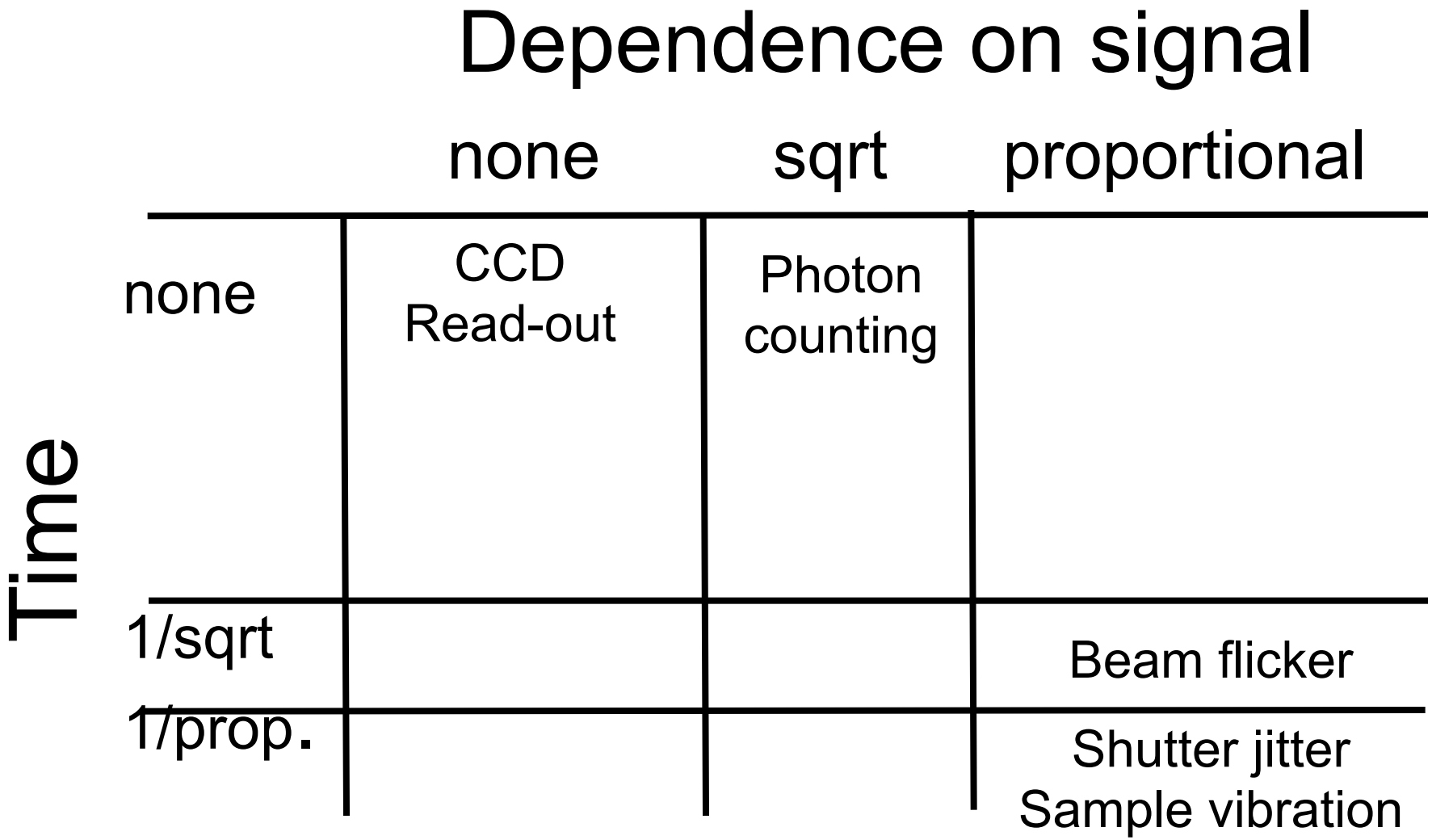

Classes of error in MX

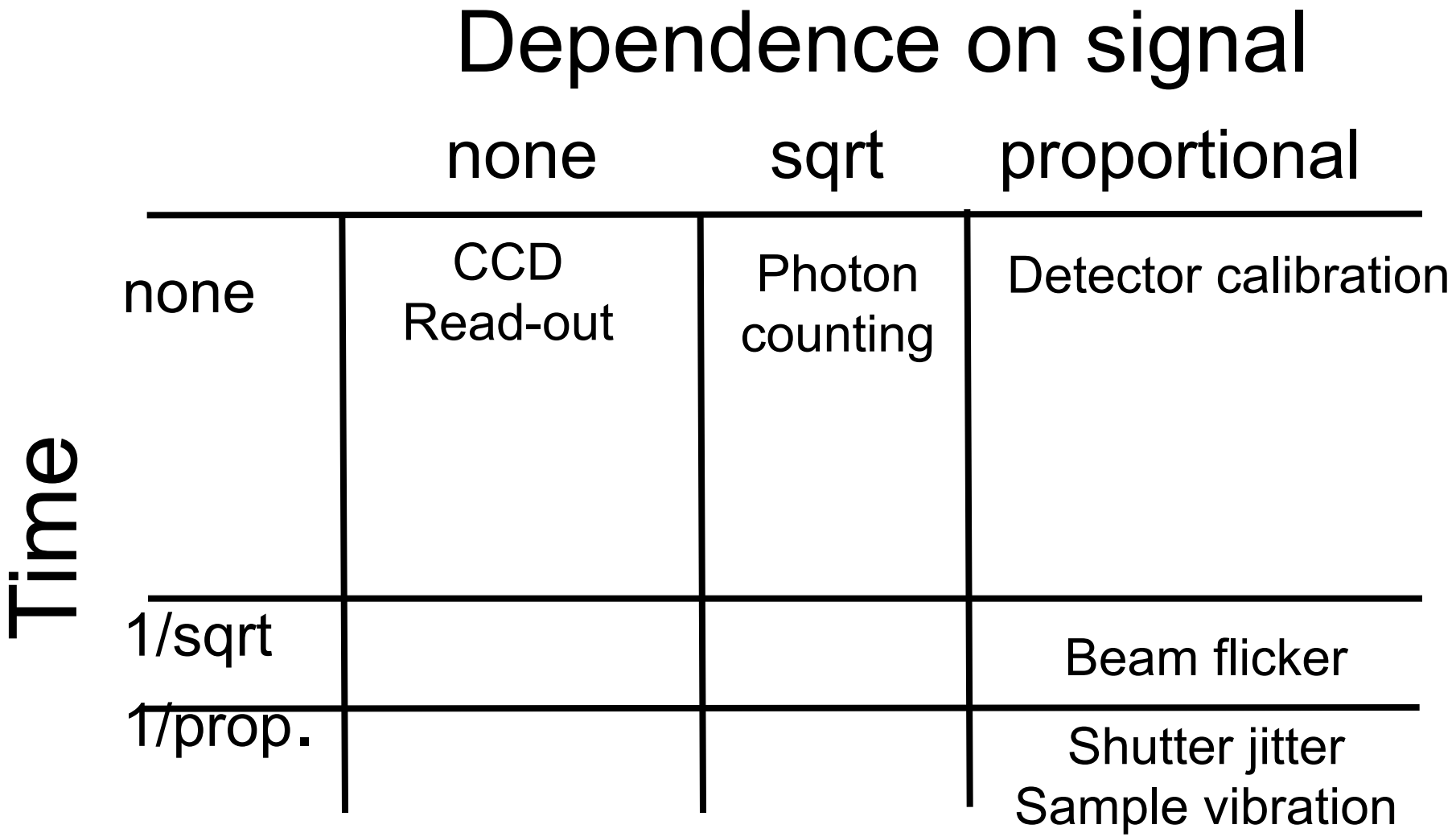

Classes of error in MX

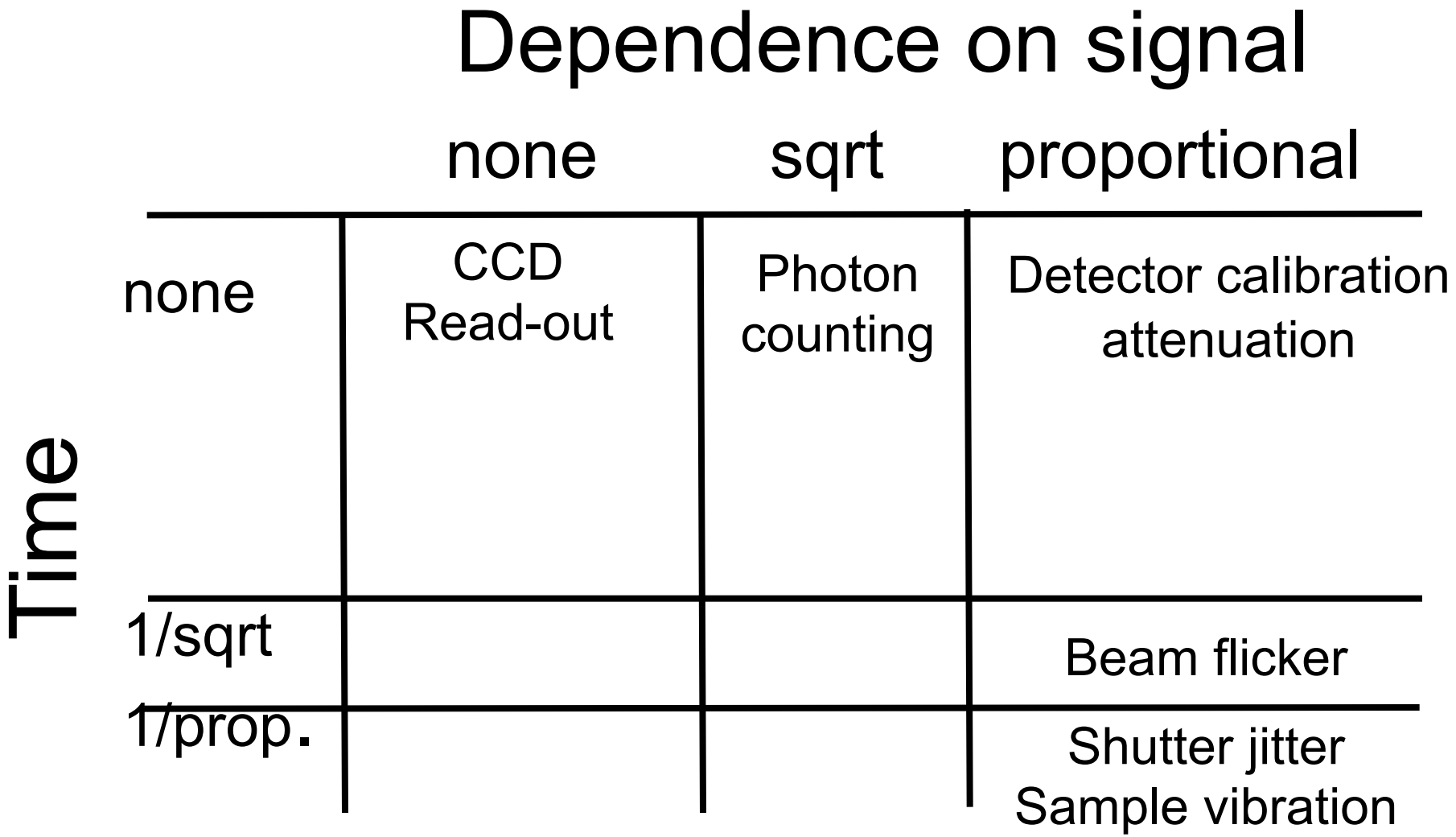

Classes of error in MX

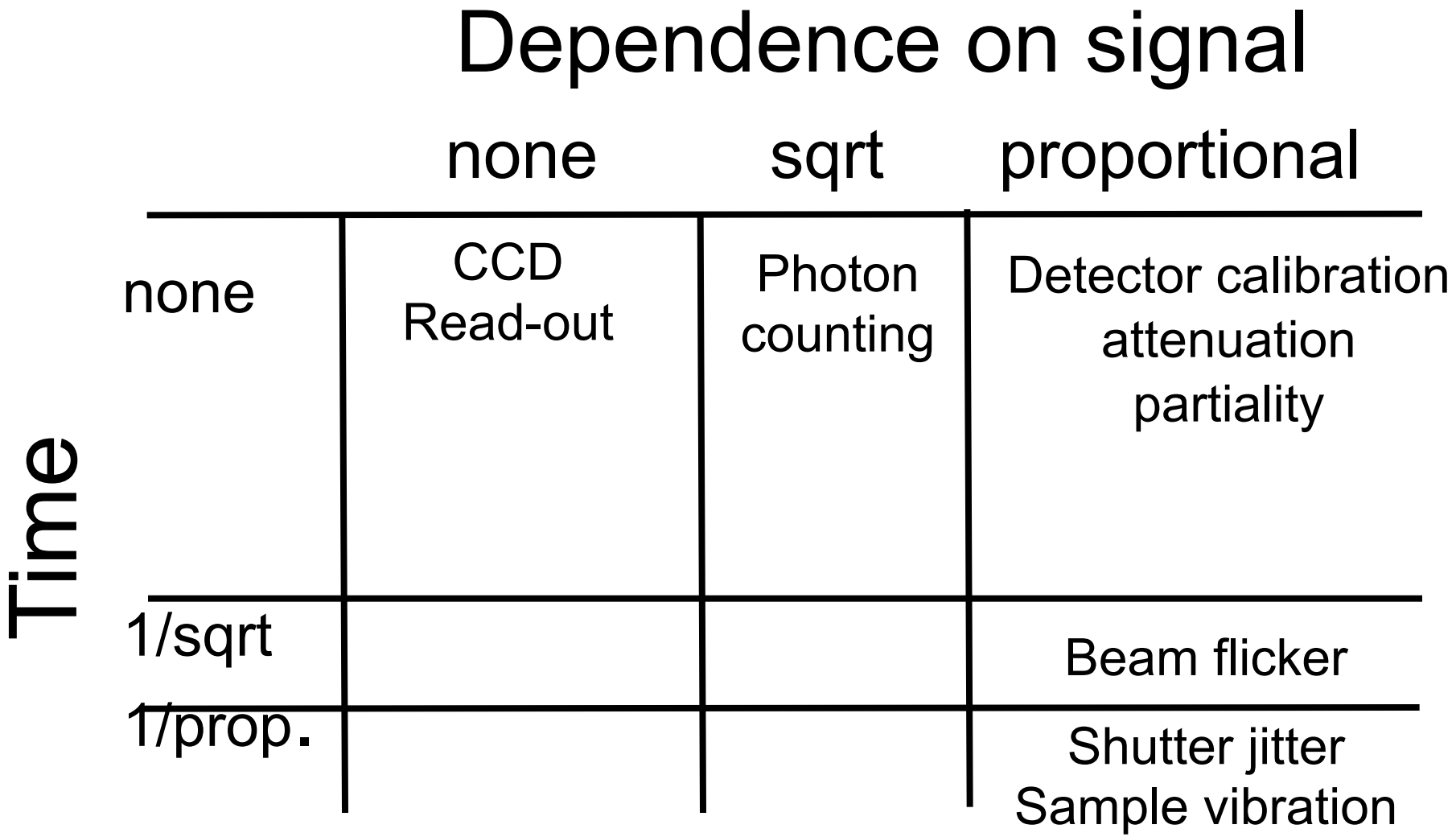

Classes of error in MX

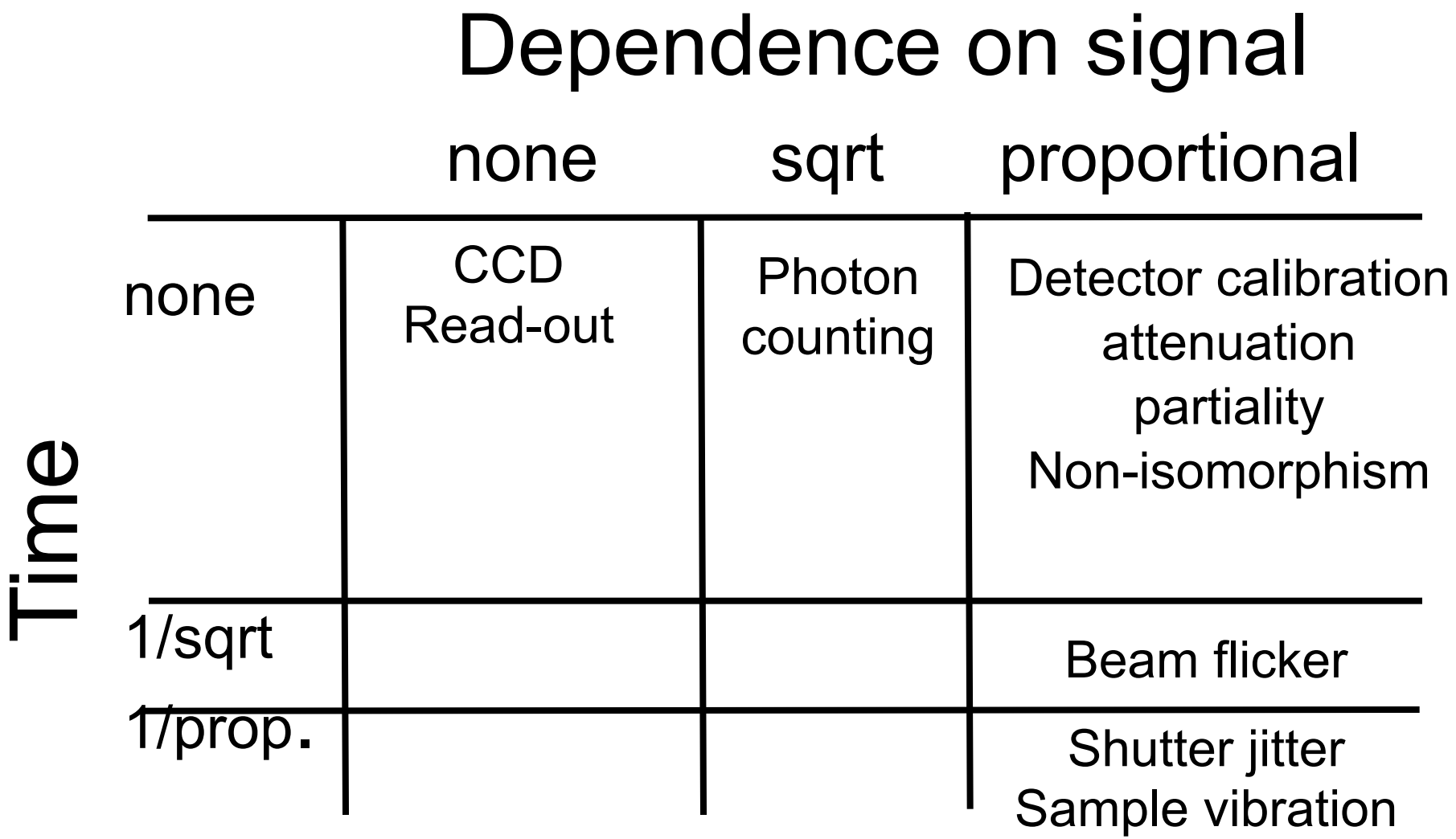

Classes of error in MX

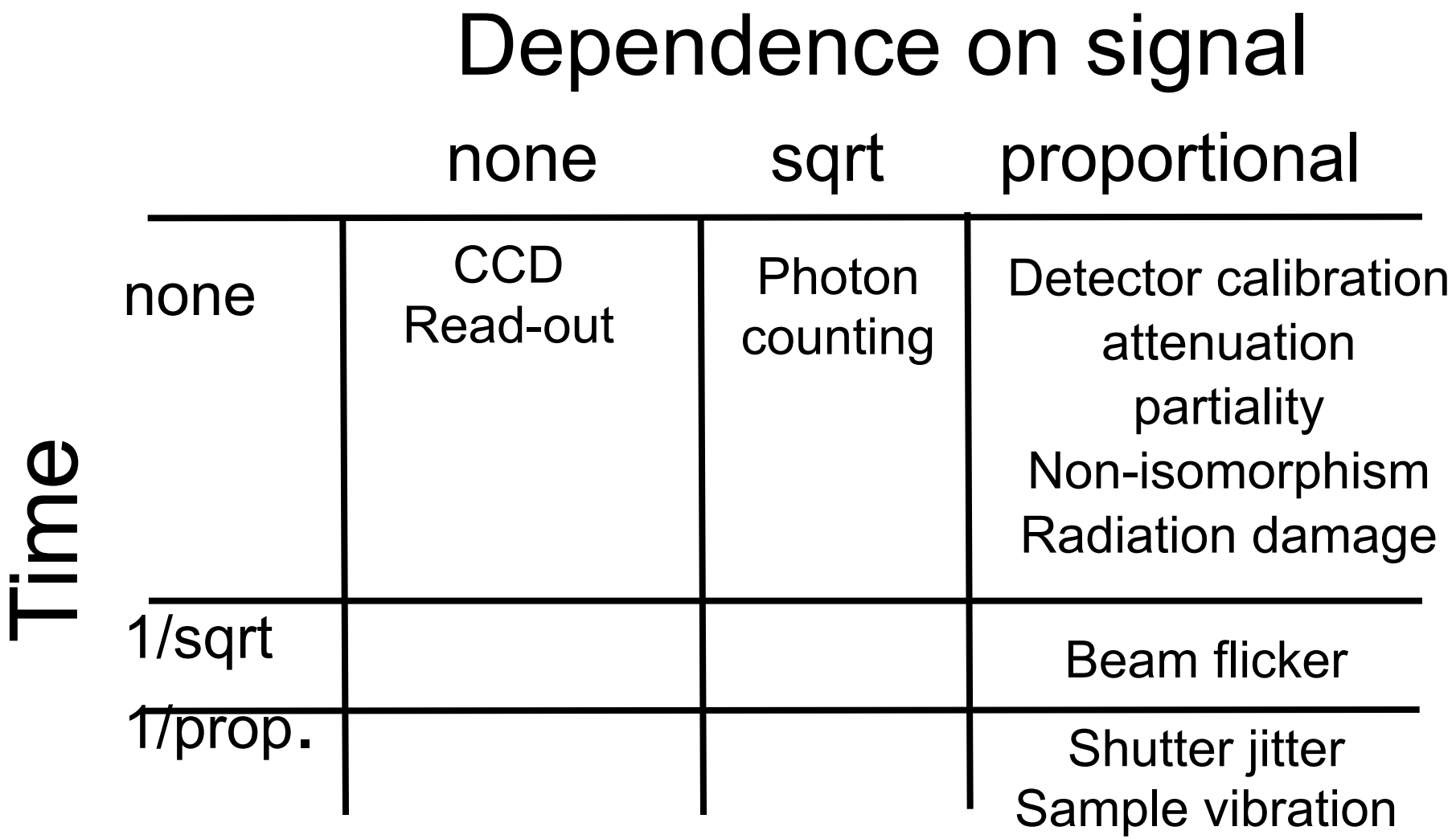

Classes of error in MX

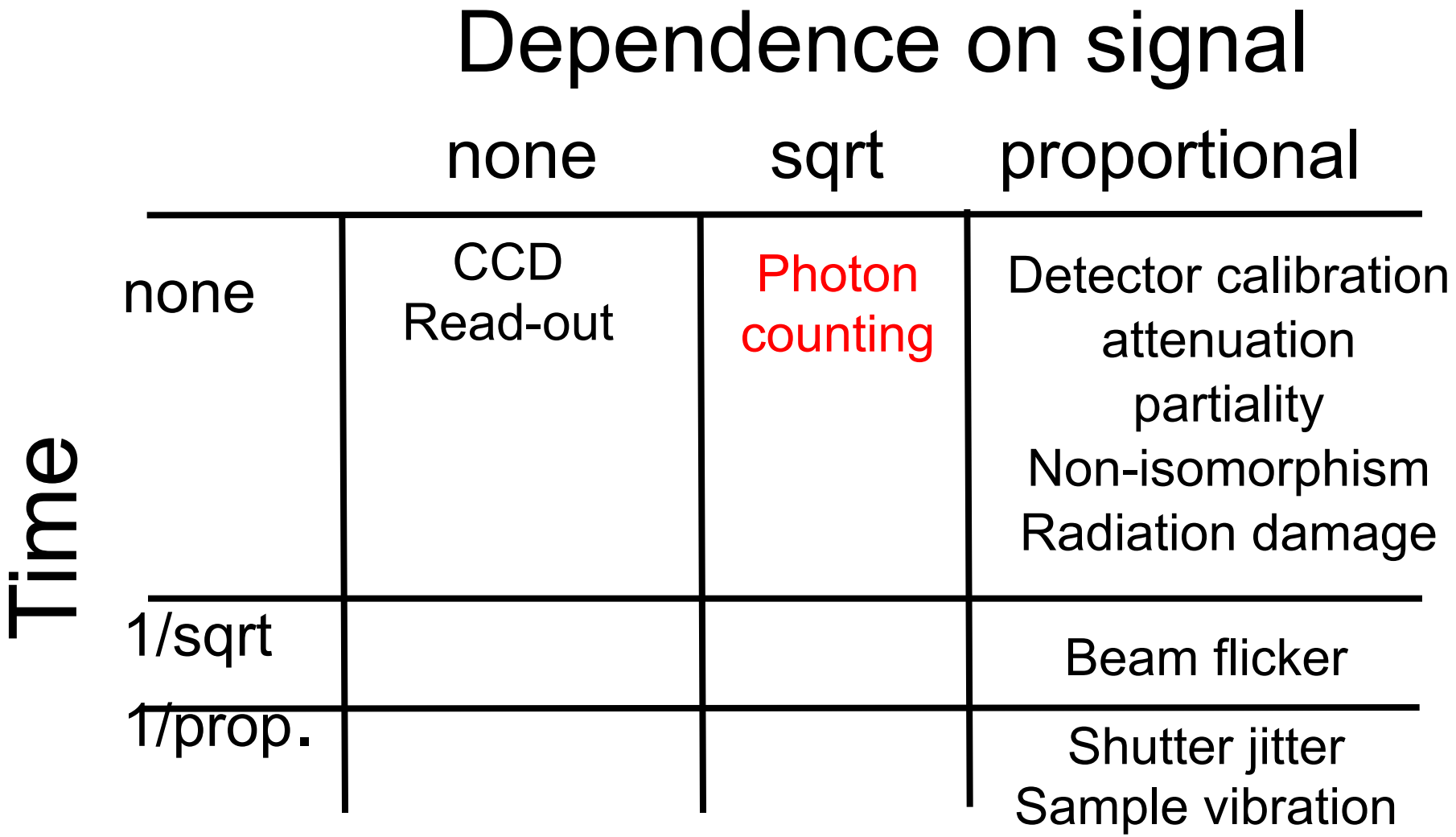

Classes of error in MX

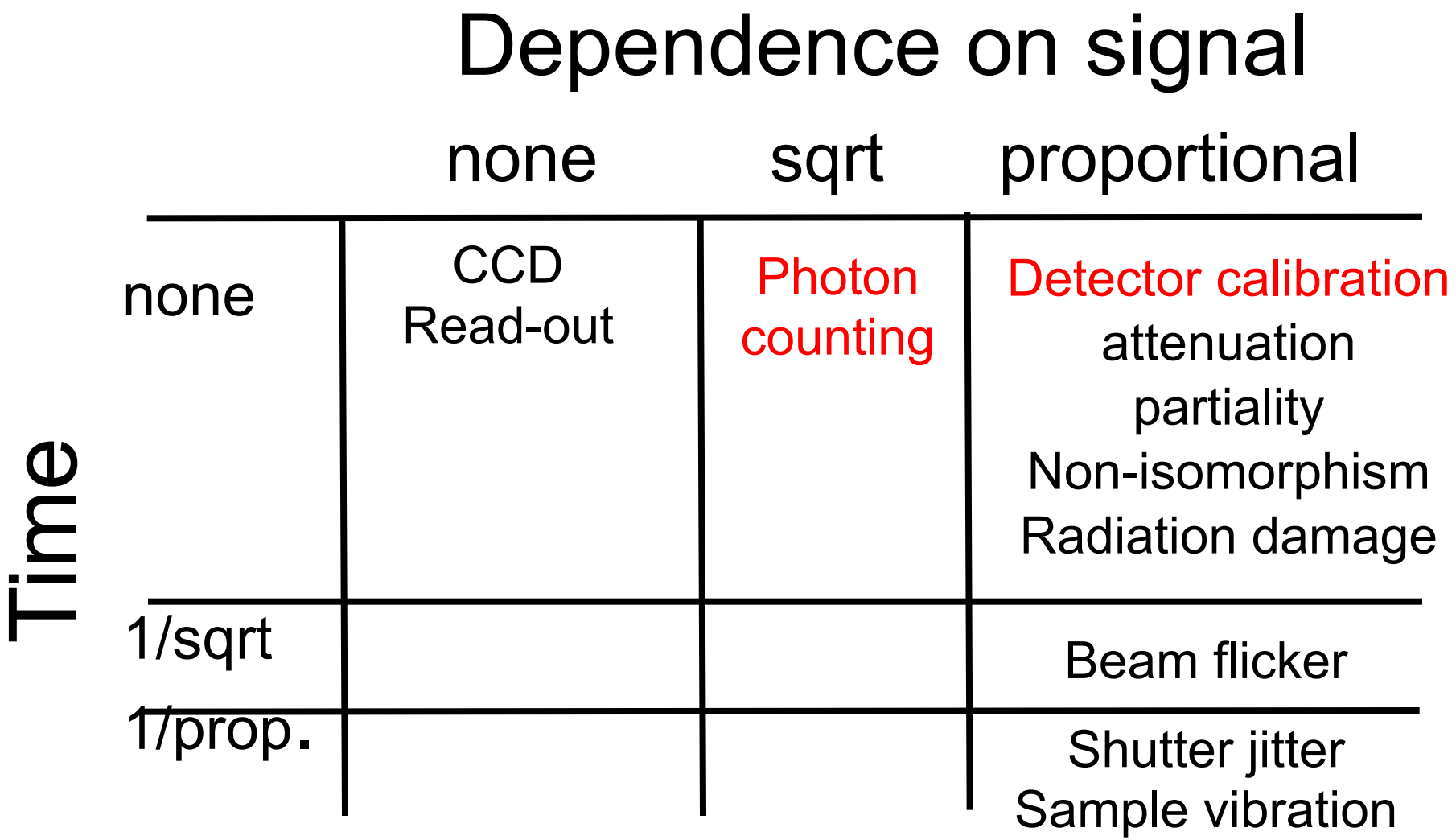

Fractional error

$$\text{mult} > \left(\frac{\sim 3\%}{\langle \Delta F/F \rangle} \right)^2$$

Fractional error at XFEL

$$\text{mult} > \left(\frac{\sim 100\%}{\langle \Delta F/F \rangle} \right)^2$$

Fractional error at XFEL

$$\text{mult} > \left(\frac{\sim 100\%}{\langle \Delta F/F \rangle} \right)^2$$

Gd lyso: $\Delta F/F = 8.7\% \rightarrow \text{mult} = 132$

The “partiality problem”

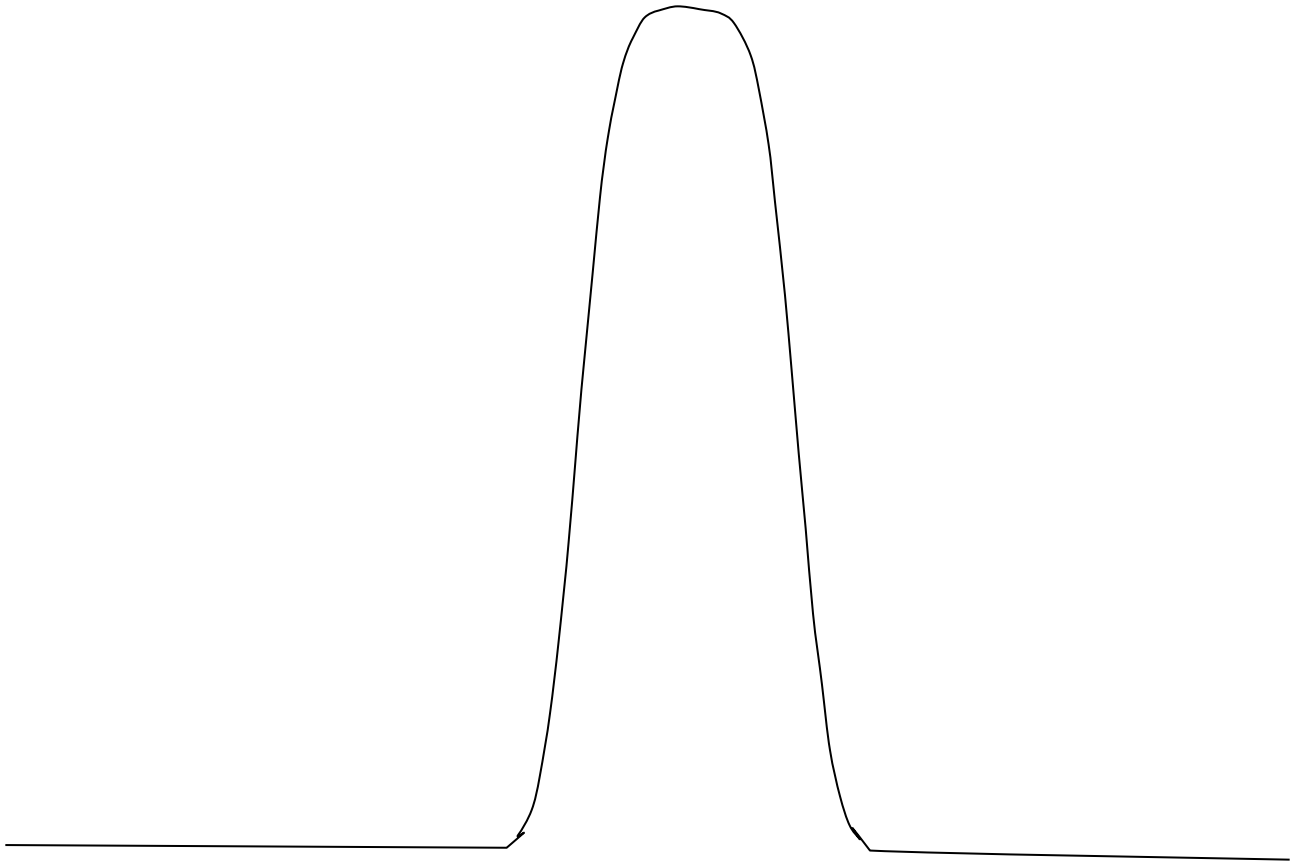

The “partiality problem”

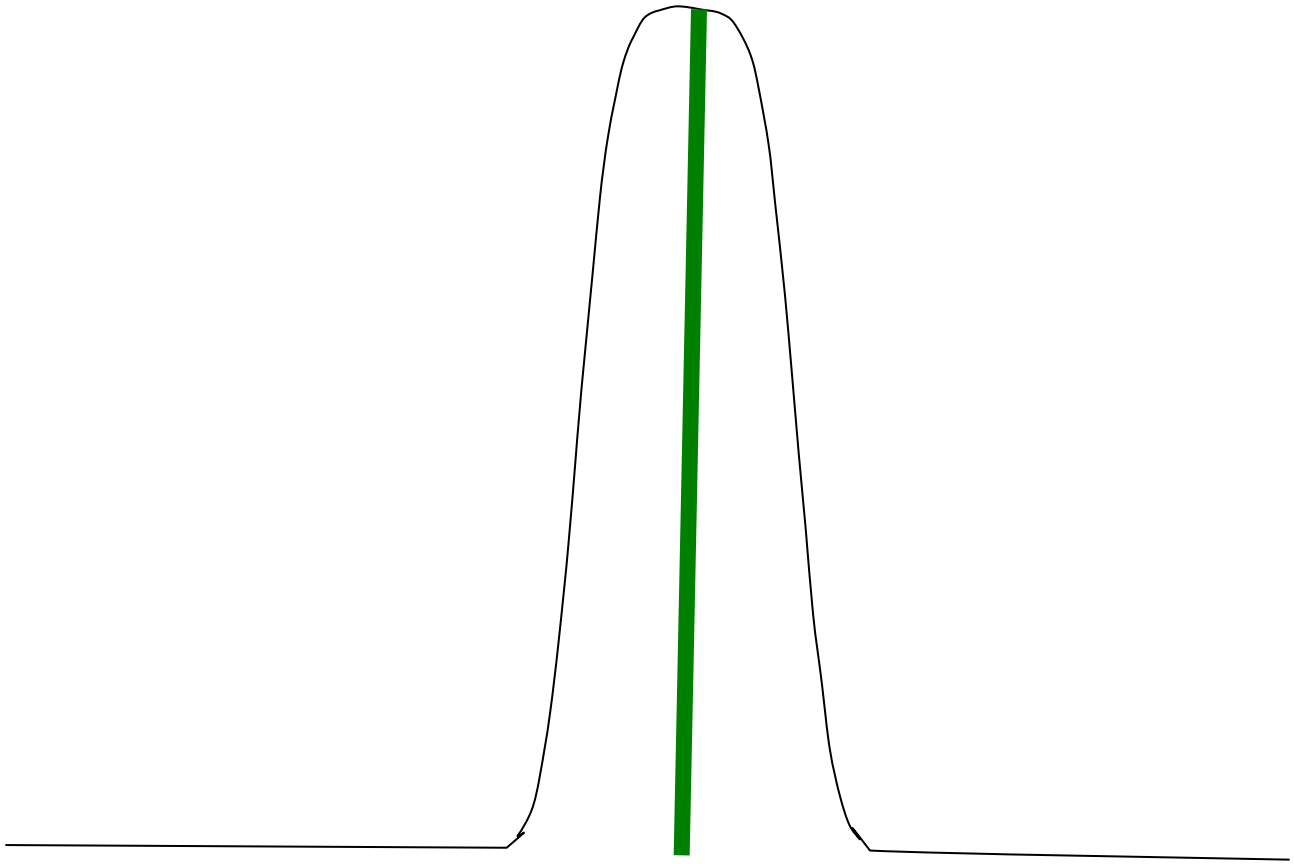

The “partiality problem”

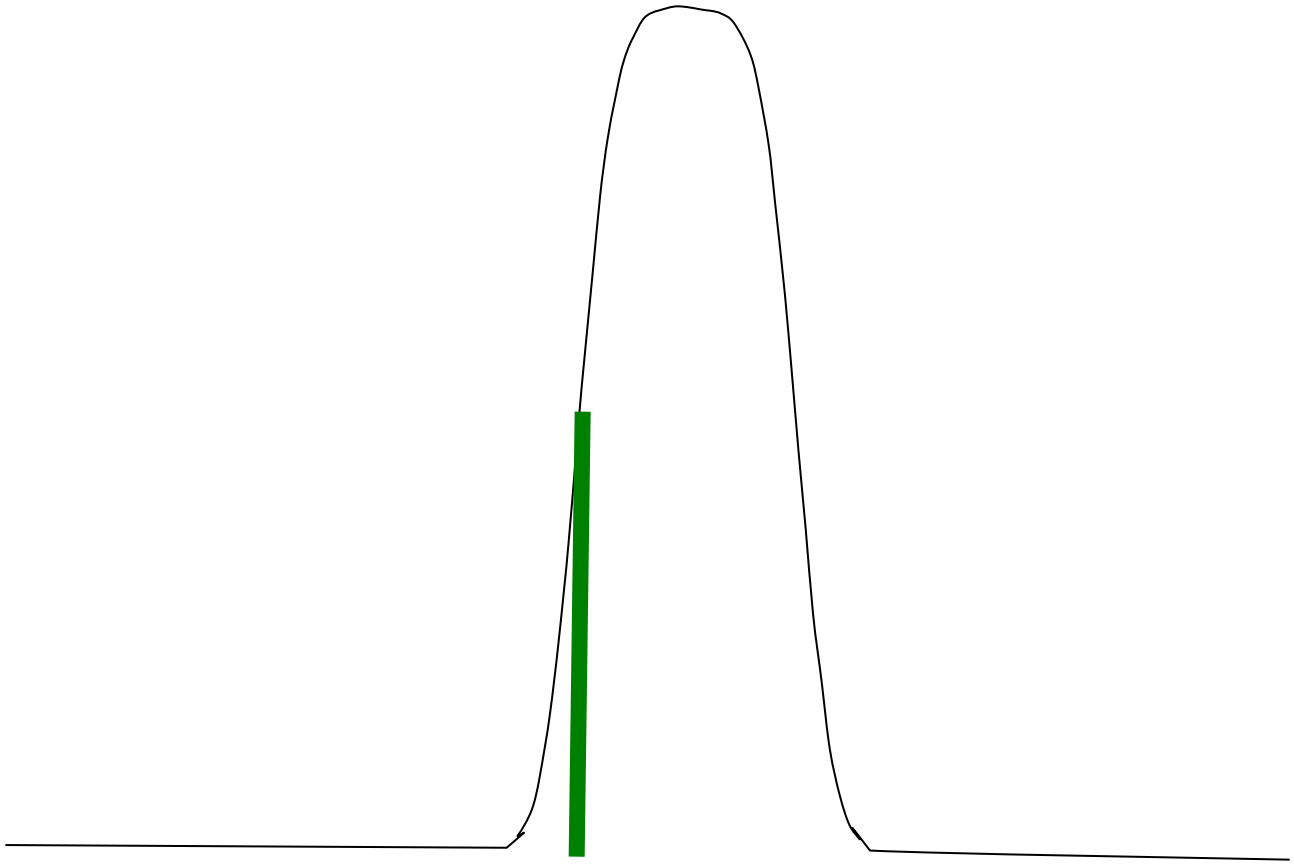

The “partiality problem”

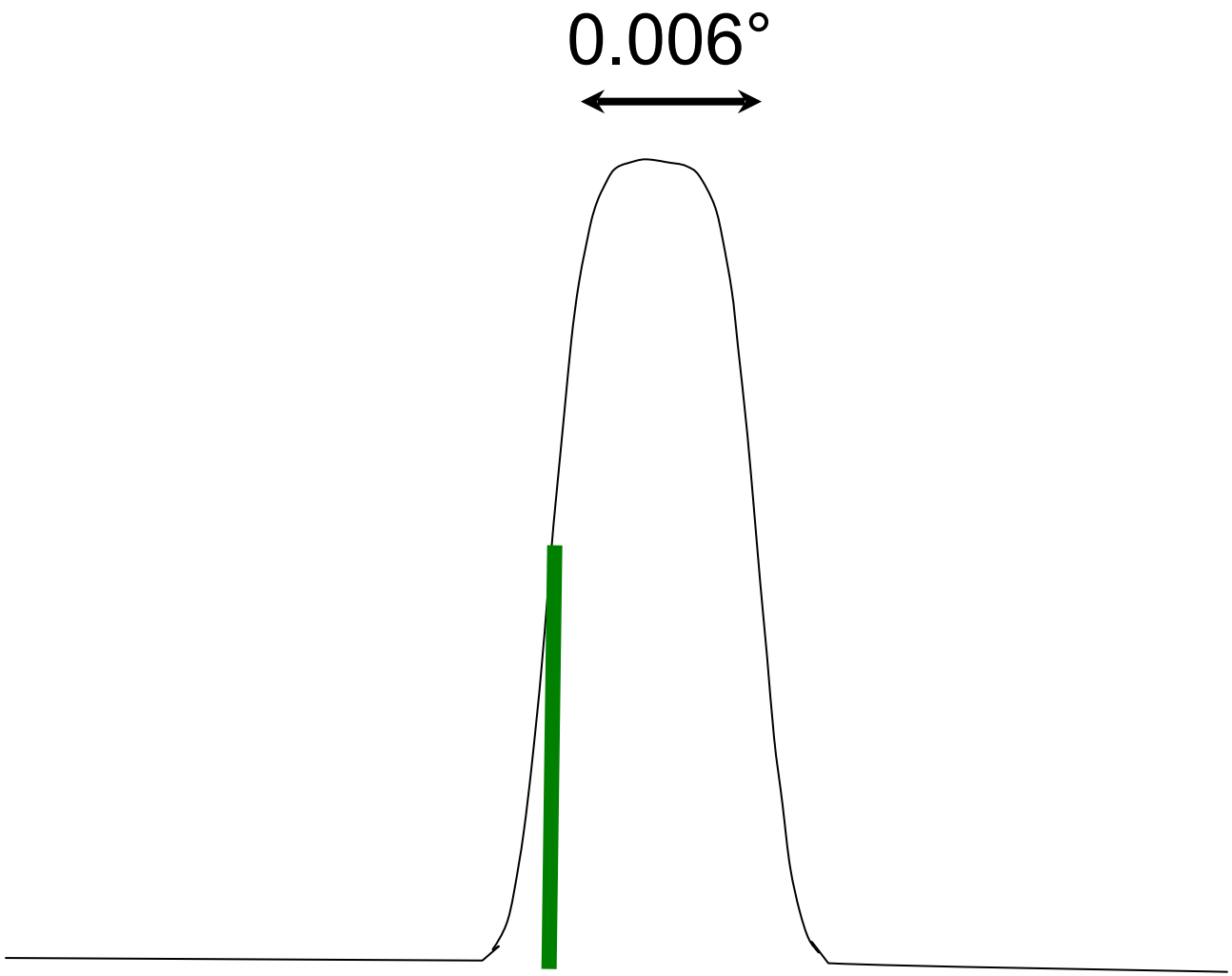

The “partiality problem”

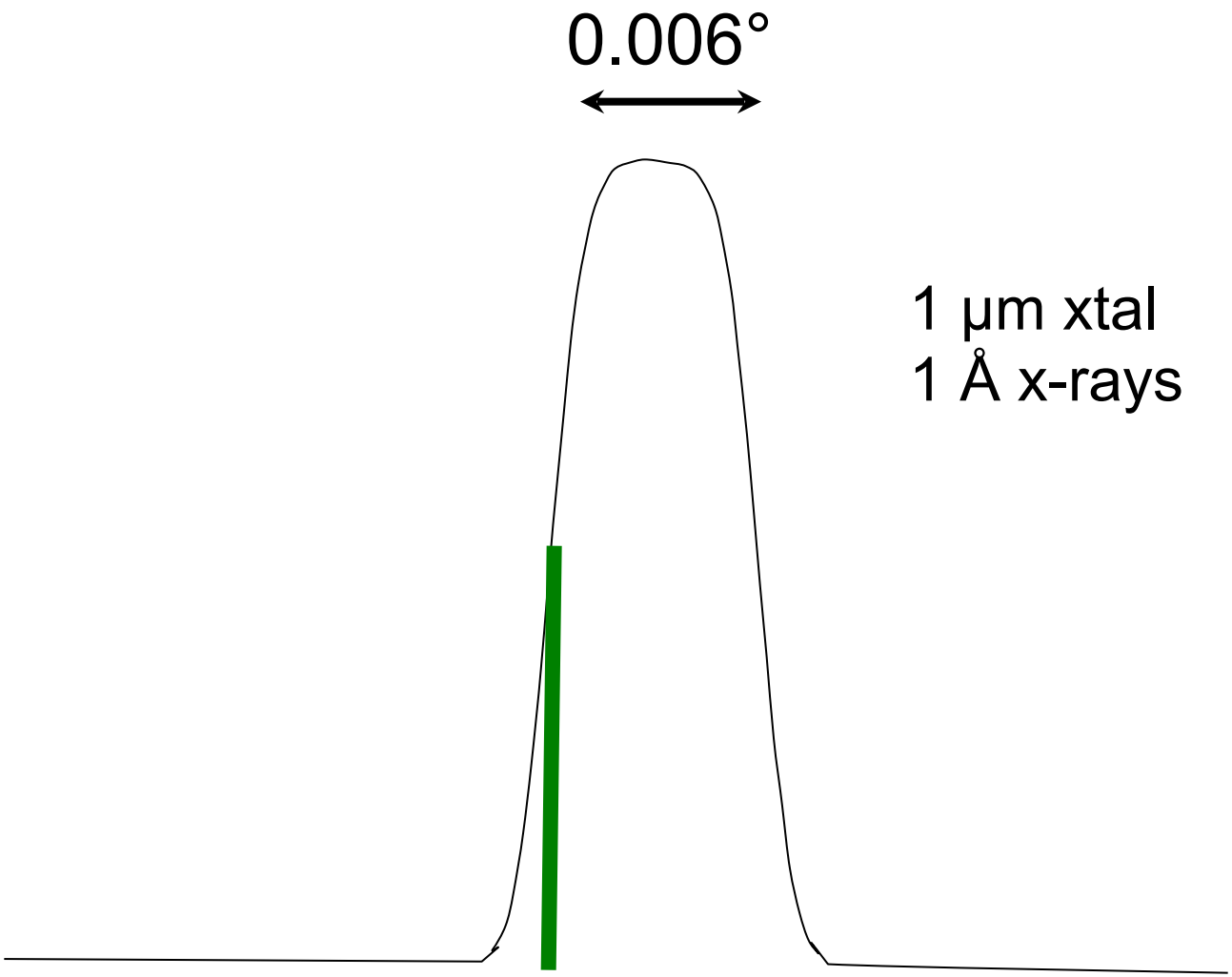

Classes of error in MX

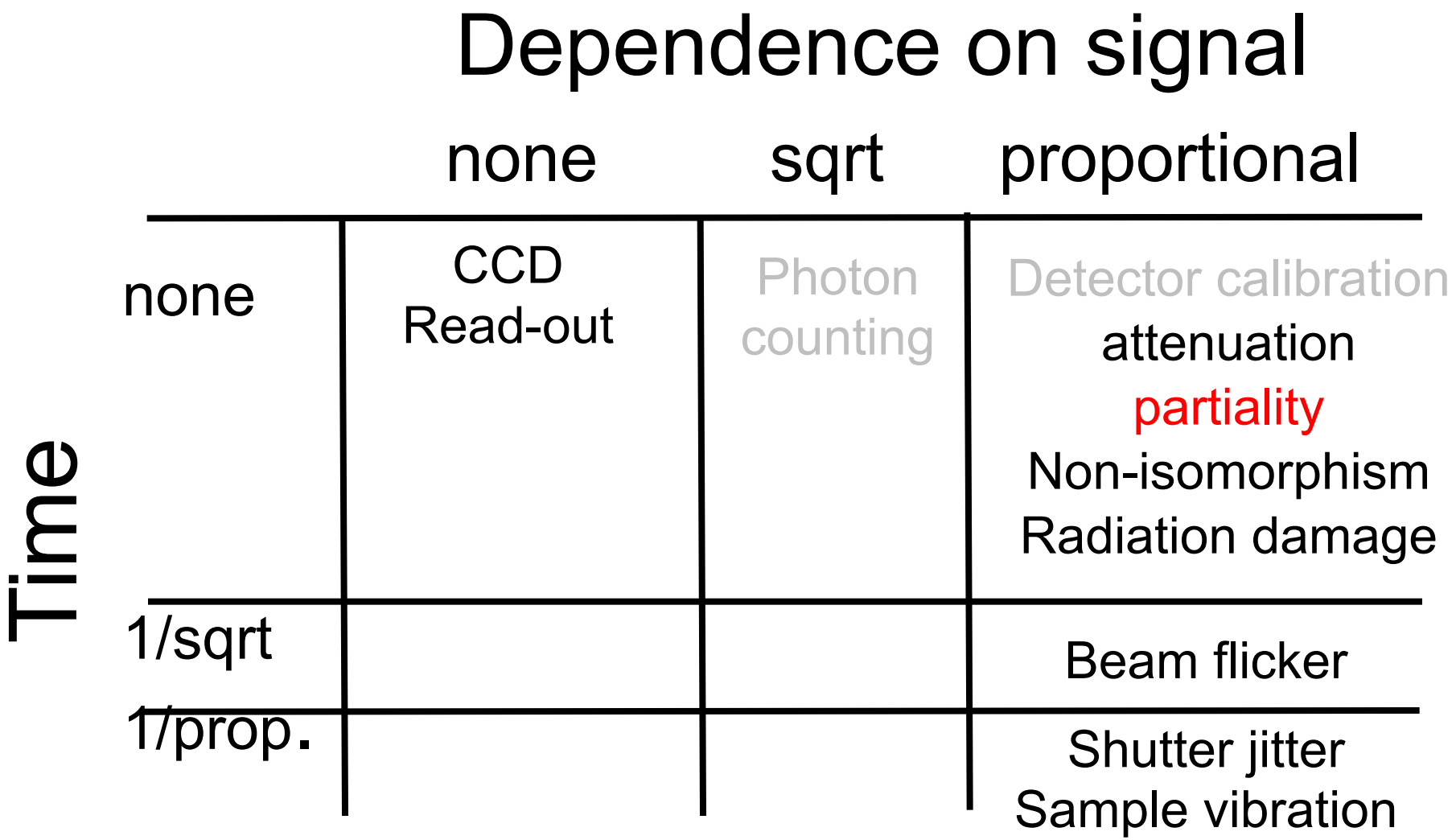

Intensity of a Bragg spot

$$I_{spot} = |F(hkl)|^2$$

Intensity of a Bragg spot

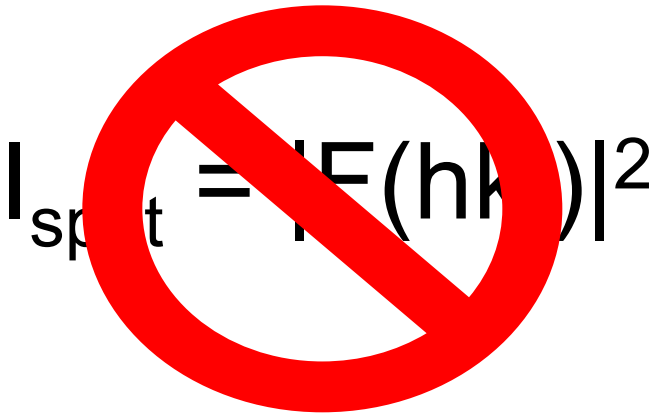

Intensity of a Bragg spot

$$I_{spot} = k * |F(hkl)|^2$$

Intensity of a Bragg spot

$$I_{spot} = k(d) * |F(hkl)|^2$$

Intensity of a Bragg spot

$$I_{spot} = k(d,\lambda) * |F(hkl)|^2$$

Intensity of a Bragg spot

$$I_{spot} = k(d,\lambda,P) * |F(hkl)|^2$$

Intensity of a Bragg spot

$$I_{spot} = k(d,\lambda,P,\omega) * |F(hkl)|^2$$

Intensity of a Bragg spot

$$I_{spot} = k(d,\lambda,P,\omega,X_{det},Y_{det}) * |F$$

Darwin's Formula

$$I(hkl) = I_{beam}\, r_e^2\, \frac{V_{xtal}}{V_{cell}}\, \frac{\lambda^3 L}{\omega V_{cell}}\, P\, A\, |\, F(hkl)\, |^2$$

I(hkl) - photons/spot (fully-recorded)

I_{beam} - incident (photons/s/m^2)

r_e - classical electron radius (2.818×10^{-15} m)

V_{xtal} - volume of crystal (in m^3)

V_{cell} - volume of unit cell (in m^3)

λ - x-ray wavelength (in meters!)

ω - rotation speed (radians/s)

L - Lorentz factor (speed/speed)

P - polarization factor

$(1+\cos^2(2\theta) - Pfac \cdot \cos(2\Phi)\sin^2(2\theta))/2$

A - attenuation factor

$\exp(-\mu_{xtal} \cdot l_{path})$

F(hkl) - structure amplitude (electrons)

C. G. Darwin (1914)

Darwin's Formula

$$I(hkl) = I_{beam}\, r_e^2\, \frac{V_{xtal}}{V_{cell}}\, \frac{\lambda^3 L}{\omega V_{cell}}\, P\, A\, |\, F(hkl)\, |^2$$

I(hkl) - photons/spot (fully-recorded)

I_{beam} - incident (photons/s/m^2)

r_e - classical electron radius (2.818×10^{-15} m)

V_{xtal} - volume of crystal (in m^3)

V_{cell} - volume of unit cell (in m^3)

λ - x-ray wavelength (in meters!)

ω - rotation speed (radians/s)

L - Lorentz factor (speed/speed)

P - polarization fa

$(1+\cos^2(2\theta)$ -Pfac·cc 2

A - attenuation fa

$\exp(-\mu_{xtal} \cdot l_{path})$

F(hkl) - structure amp s)

C. G. Darwin (1914)

Darwin's Formula

$$I(hkl) = I_{beam}\, r_e^2\, \frac{V_{xtal}}{V_{cell}}\, \frac{\lambda^3 L}{\omega V_{cell}}\, P\, A\, |F|$$

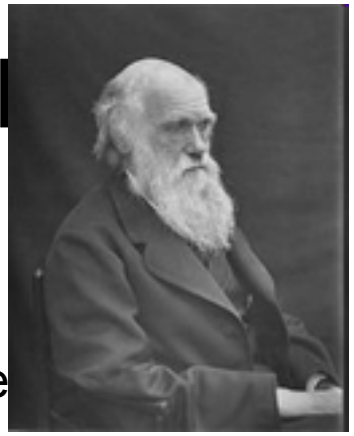

I(hkl) - photons/spot (fully-recorded)

I_{beam} - incident (photons/s/m^2)

r_e - classical electron radius (2.818×10^{-15} m)

V_{xtal} - volume of crystal (in m^3)

V_{cell} - volume of unit cell (in m^3)

λ - x-ray wavelength (in meters!)

ω - rotation spee

L - Lorentz factor (speed/speed)

P - polarization fa

$(1+\cos^2(2\theta)$ -Pfac·cc 2

A - attenuation fa

$\exp(-\mu_{xtal} \cdot l_{path})$

F(hkl) - structure amp s)

C. G. Darwin (1914)

Darwin's Formula

$$I(hkl) = I_{beam}\, r_e^2\, \frac{V_{xtal}}{V_{cell}}\, \frac{\lambda^3 L}{\omega V_{cell}}\, P\, A\, |F|$$

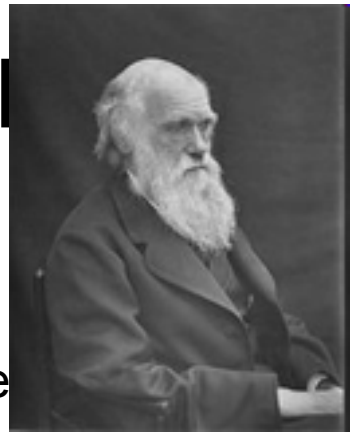

I(hkl) - photons/spot (fully-recorded)

I_{beam} - incident (photons/s/m^2)

r_e - classical electron radius (2.818×10^{-15} m)

V_{xtal} - volume of crystal (in m^3)

V_{cell} - volume of unit cell (in m^3)

λ - x-ray wavelength (in meters!)

ω - rotation spee

L - Lorentz factor (speed/speed)

P fa

(1+cc cc 2

A fa

th)

F(hkl) np s)

C. G. Darwin (1914)

Darwin's Formula

$$I(hkl) = I_{beam}\, r_e^2\, \frac{V_{xtal}}{V_{cell}}\, \frac{\lambda^3 L}{\omega V_{cell}}\, P\, A\, |\, F(hkl)\, |^2$$

I(hkl) - photons/spot (fully-recorded)

I_{beam} - incident (photons/s/m^2)

r_e - classical electron radius (2.818×10^{-15} m)

V_{xtal} - volume of crystal (in m^3)

V_{cell} - volume of unit cell (in m^3)

λ - x-ray wavelength (in meters!)

ω - rotation speed (radians/s)

L - Lorentz factor (speed/speed)

P - polarization factor

$(1+\cos^2(2\theta) - Pfac \cdot \cos(2\Phi)\sin^2(2\theta))/2$

A - attenuation factor

$\exp(-\mu_{xtal} \cdot l_{path})$

F(hkl) - structure amplitude (electrons)

C. G. Darwin (1914)

Darwin's Formula

$$I(hkl) = I_{beam}\, r_e^2\, \frac{V_{xtal}}{V_{cell}}\, \frac{\lambda^3 L}{\omega V_{cell}}\, P\, A\, |\, F(hkl)\, |^2$$

I(hkl) - photons/spot (fully-recorded)

I_{beam} - incident (photons/s/m^2)

r_e - classical electron radius (2.818×10^{-15} m)

V_{xtal} - volume of crystal (in m^3)

V_{cell} - volume of unit cell (in m^3)

λ - x-ray wavelength (in meters!)

ω - rotation speed (radians/s)

L - Lorentz factor (speed/speed)

P - polarization factor

$(1+\cos^2(2\theta) - Pfac \cdot \cos(2\Phi)\sin^2(2\theta))/2$

A - attenuation factor

$\exp(-\mu_{xtal} \cdot l_{path})$

F(hkl) - structure amplitude (electrons)

C. G. Darwin (1914)

Take home lesson:

Darwin's Formula does not work at XFELs!

Take home lesson:

Darwin's Formula does not work at XFELs!

Mosflm, XDS, Denzo will not work

Can’t we just rotate the crystal?

Can’t we just rotate the crystal?

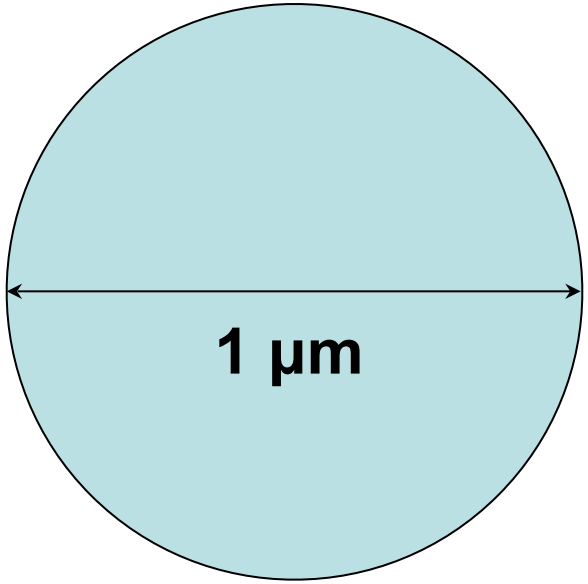

Can’t we just rotate the crystal?

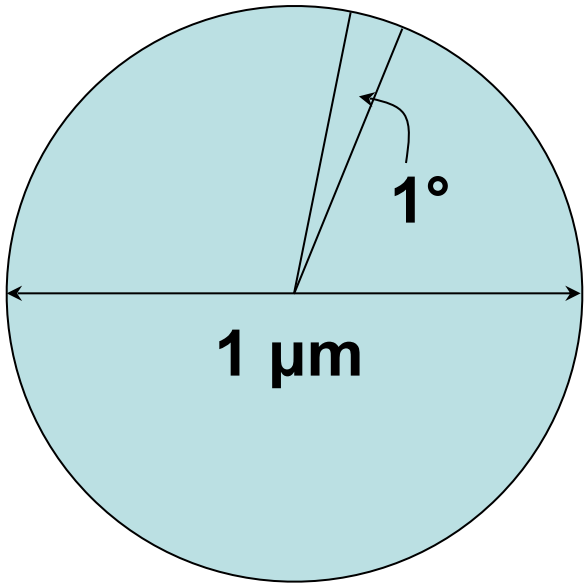

Can’t we just rotate the crystal?

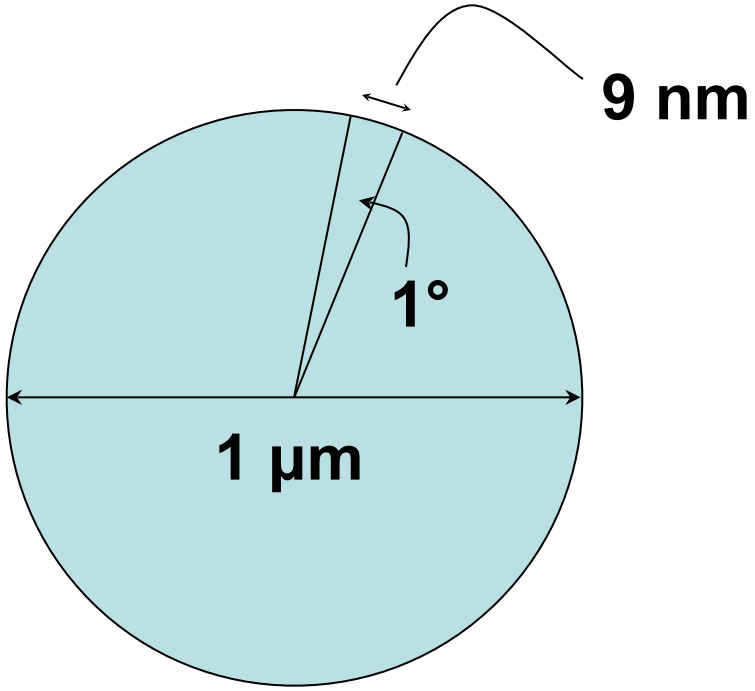

Can’t we just rotate the crystal?

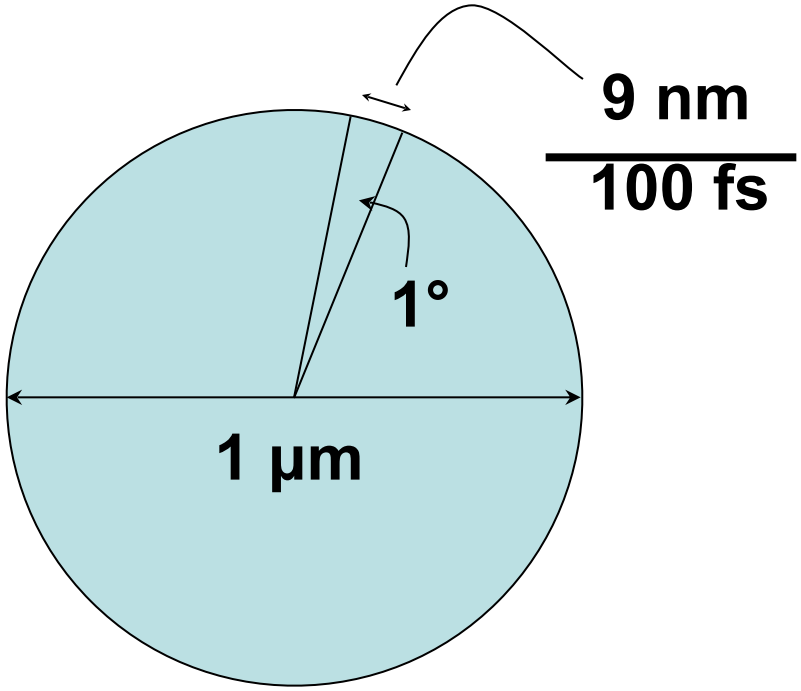

Can’t we just rotate the crystal?

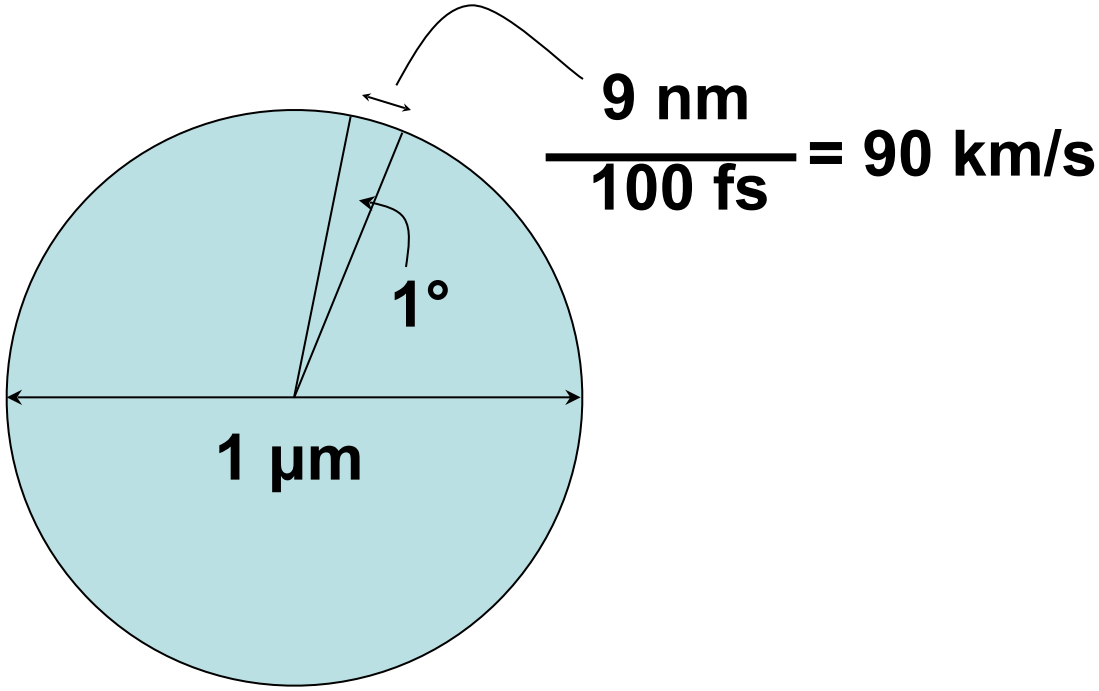

Can’t we just rotate the crystal?

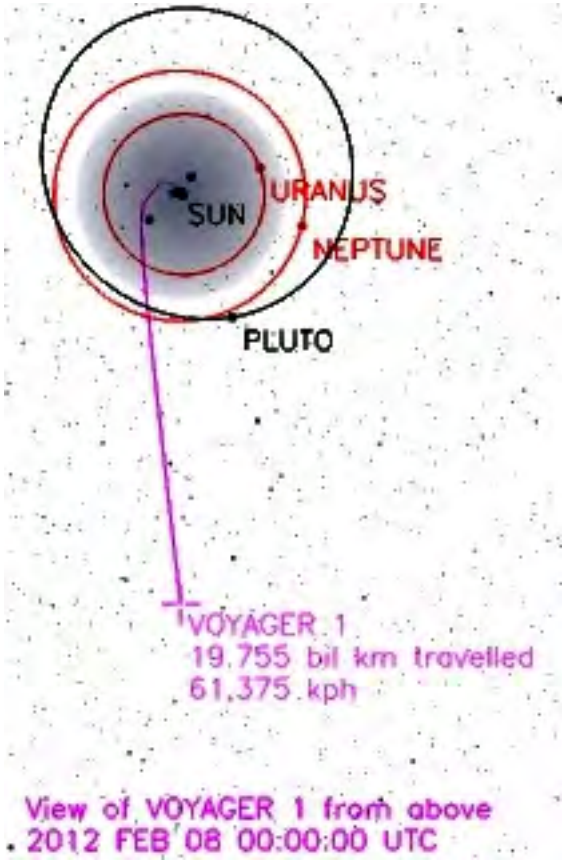

17.26 km/s

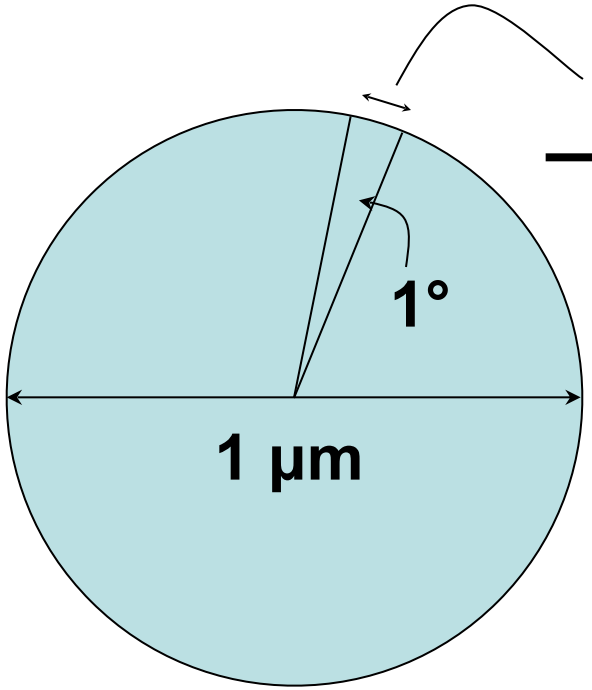

$$\frac{9\ \text{nm}}{100\ \text{fs}} = 90\ \text{km/s}$$

Can’t we just rotate the crystal?

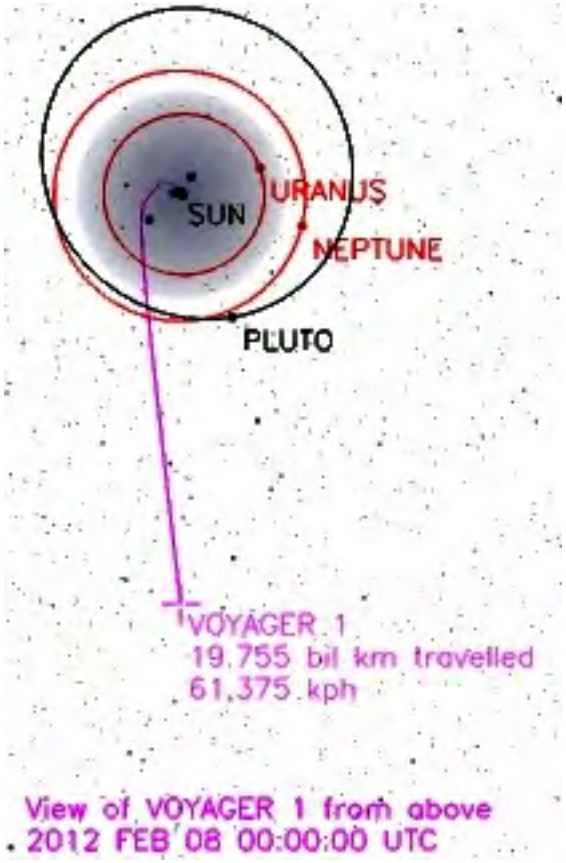

17.26 km/s

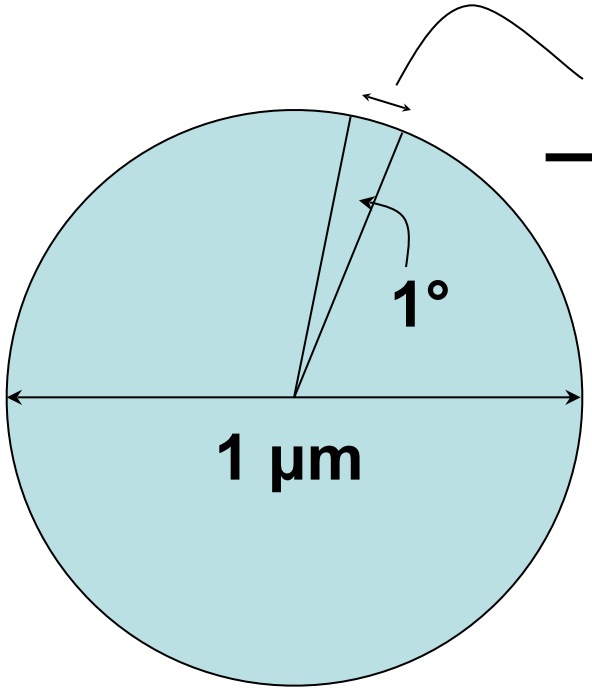

$$\frac{9\ \text{nm}}{100\ \text{fs}} = 90\ \text{km/s}$$

$$\frac{(90\ \text{km/s})^2}{0.5\ \mu\text{m}}$$

Can’t we just rotate the crystal?

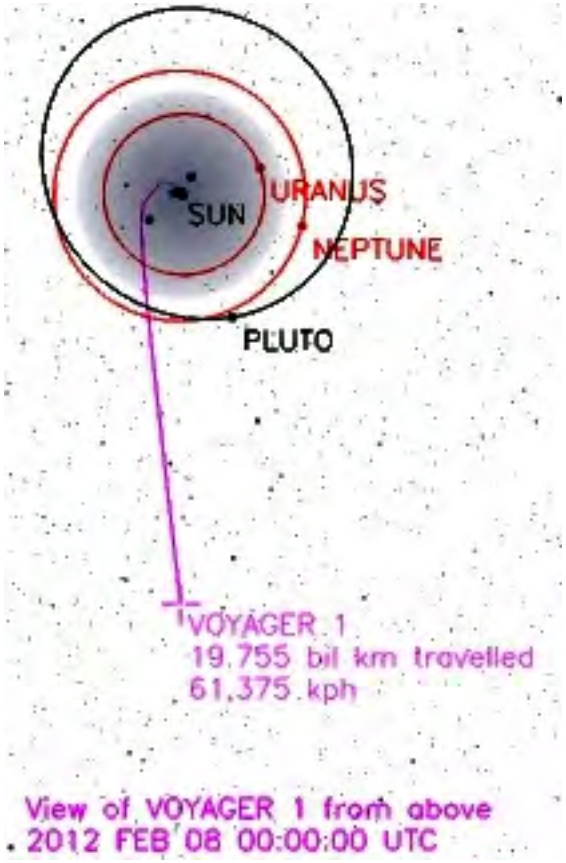

17.26 km/s

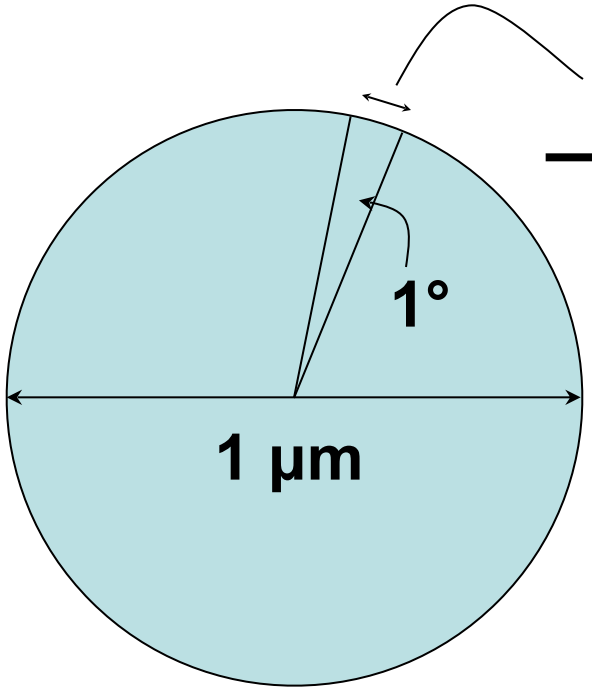

$$\frac{9\ \text{nm}}{100\ \text{fs}} = 90\ \text{km/s}$$

$$\frac{(90\ \text{km/s})^2}{0.5\ \mu\text{m}} = 1.5 \times 10^{15}\ \text{G}$$

Can’t we just rotate the crystal?

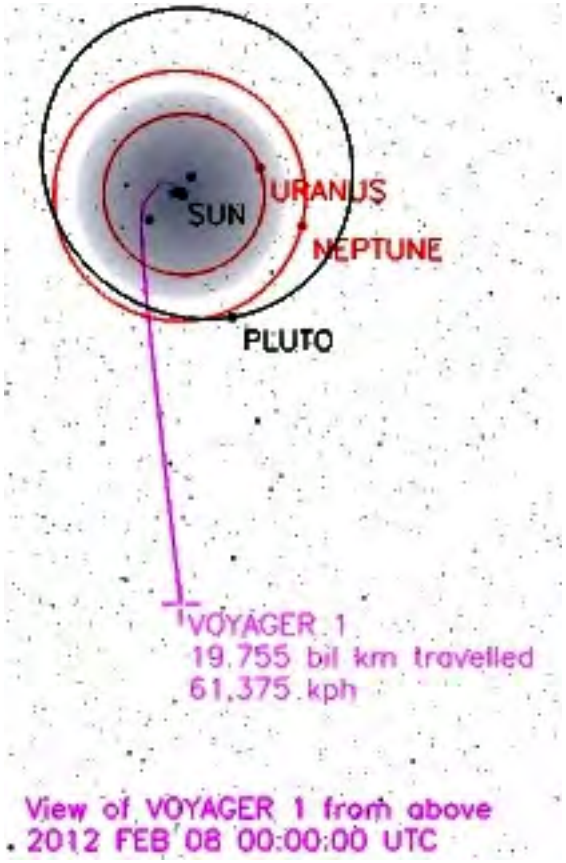

17.26 km/s

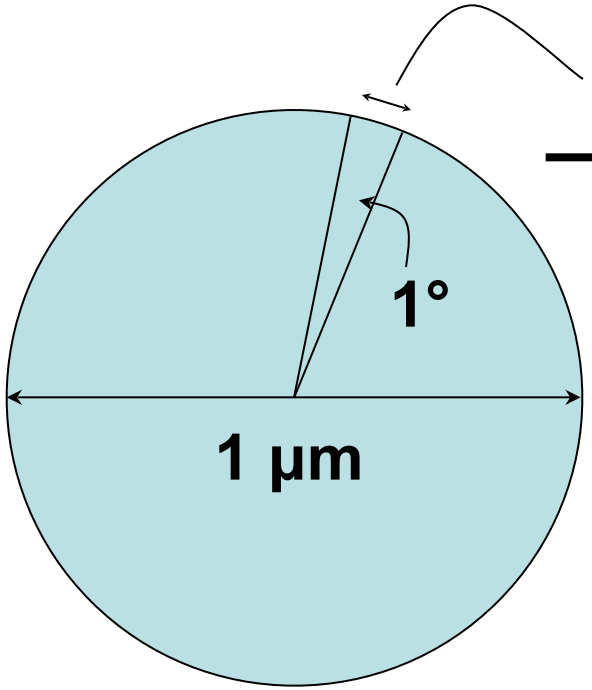

$$\frac{9\ \text{nm}}{100\ \text{fs}} = 90\ \text{km/s}$$

$$\frac{(90\ \text{km/s})^2}{0.5\ \mu\text{m}} = 1.5 \times 10^{15}\ \text{G} = 0.5\ \text{nN}$$

Can’t we just rotate the crystal?

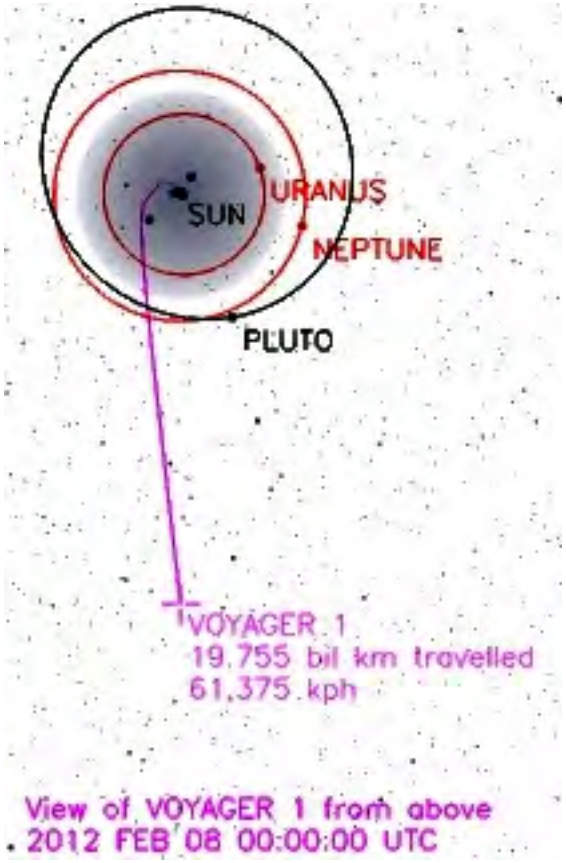

17.26 km/s

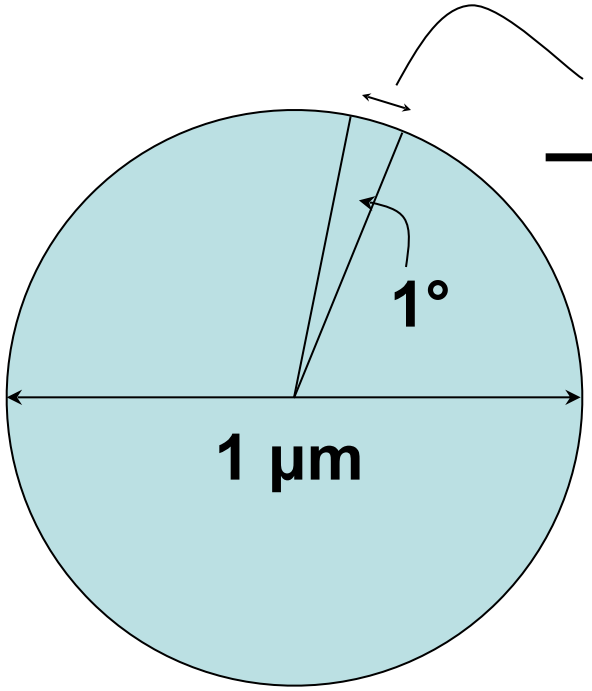

$$\frac{9\ \text{nm}}{100\ \text{fs}} = 90\ \text{km/s}$$

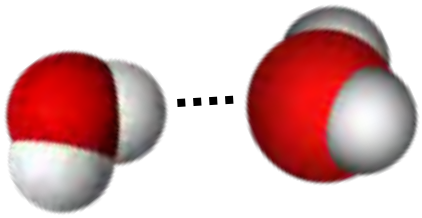

$$\frac{(90\ \text{km/s})^2}{0.5\ \mu\text{m}} = 1.5 \times 10^{15}\ \text{G} = 0.5\ \text{nN}$$

Can’t we just rotate the crystal?

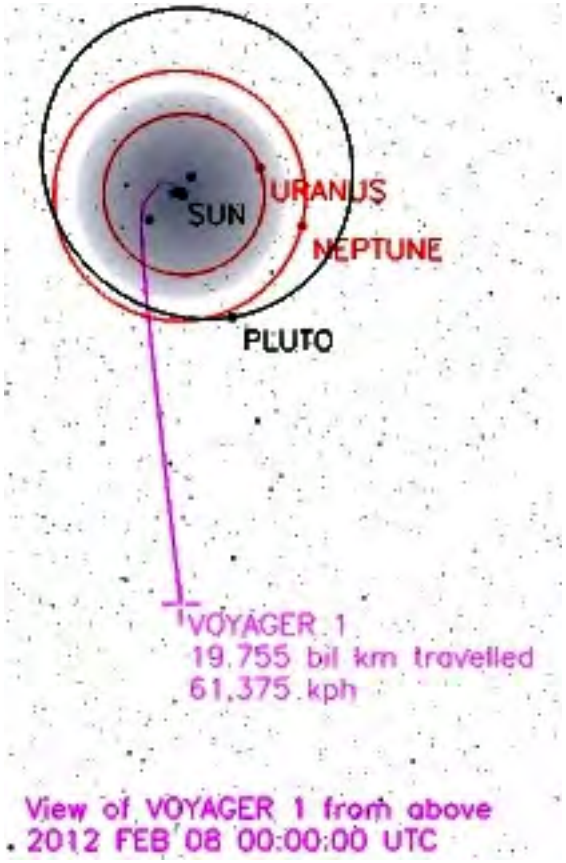

17.26 km/s

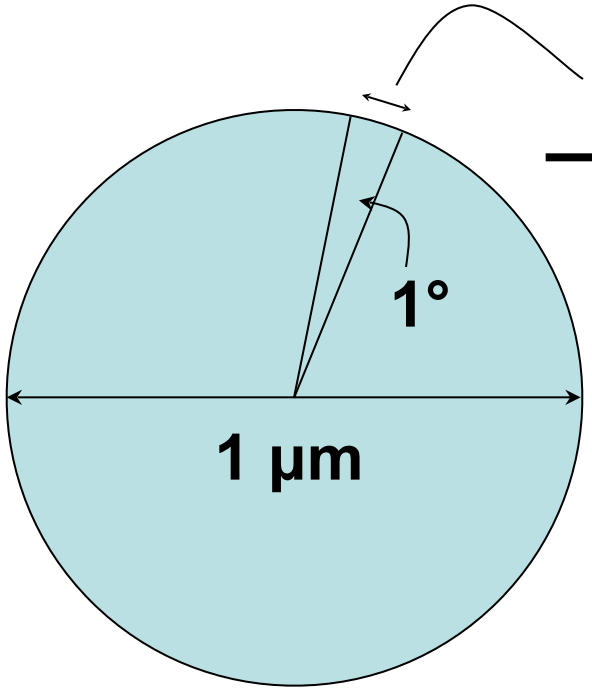

$$\frac{9\ \text{nm}}{100\ \text{fs}} = 90\ \text{km/s}$$

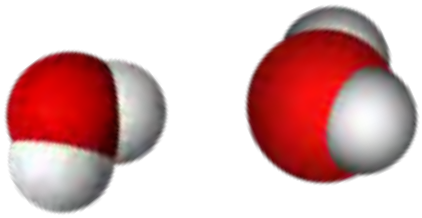

$$\frac{(90\ \text{km/s})^2}{0.5\ \mu\text{m}} = 1.5 \times 10^{15}\ \text{G} = 0.5\ \text{nN}$$

Can’t we just rotate the crystal?

NO

Can’t we just rotate the crystal?

NO

Why do we want to rotate the crystal?

The “nanocrystal advantage”

$$I_{spot} = k\, N_{cells}$$

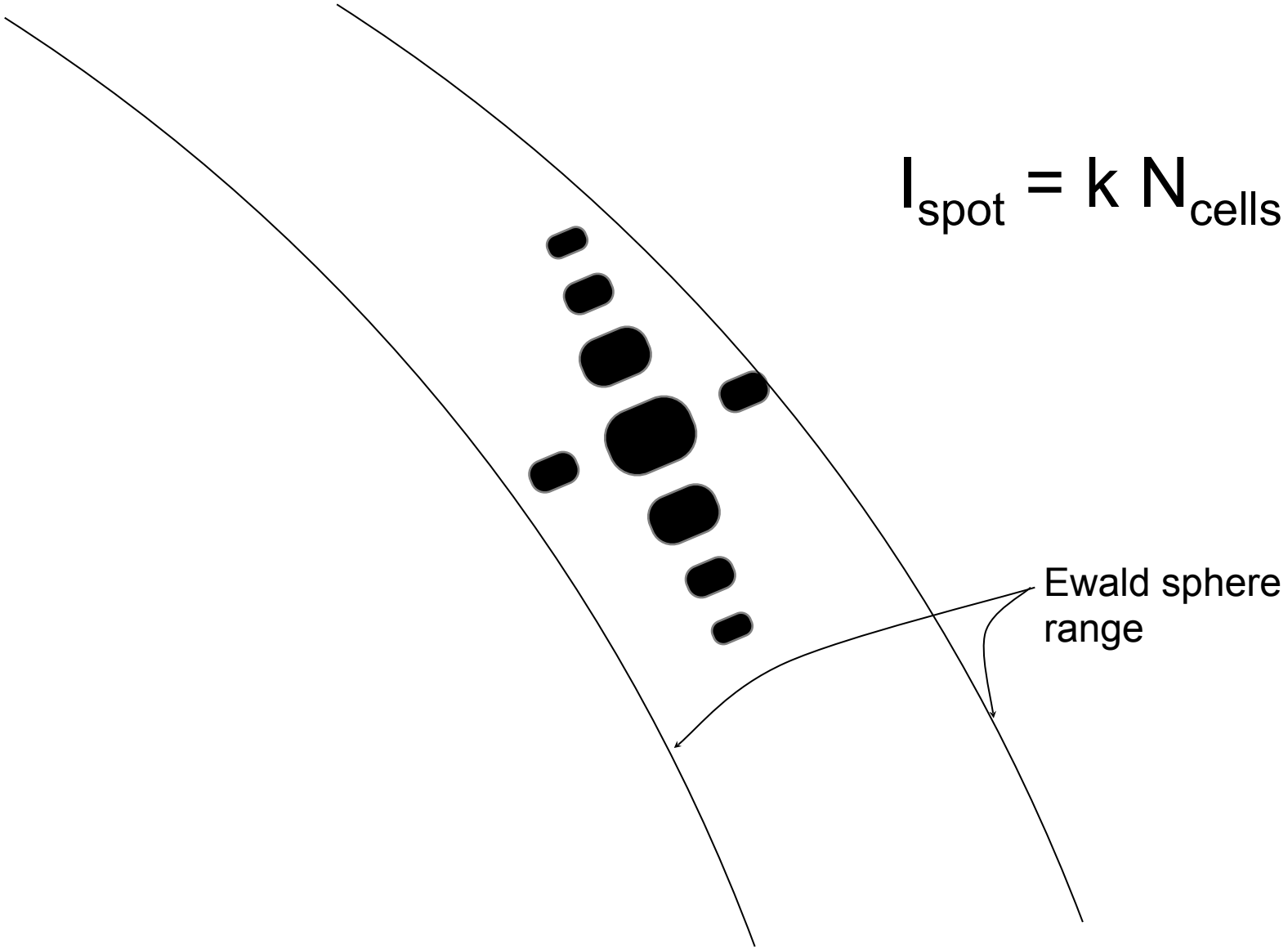

The “nanocrystal advantage”

$$I_{spot} = k\, N_{cells}^{2}$$

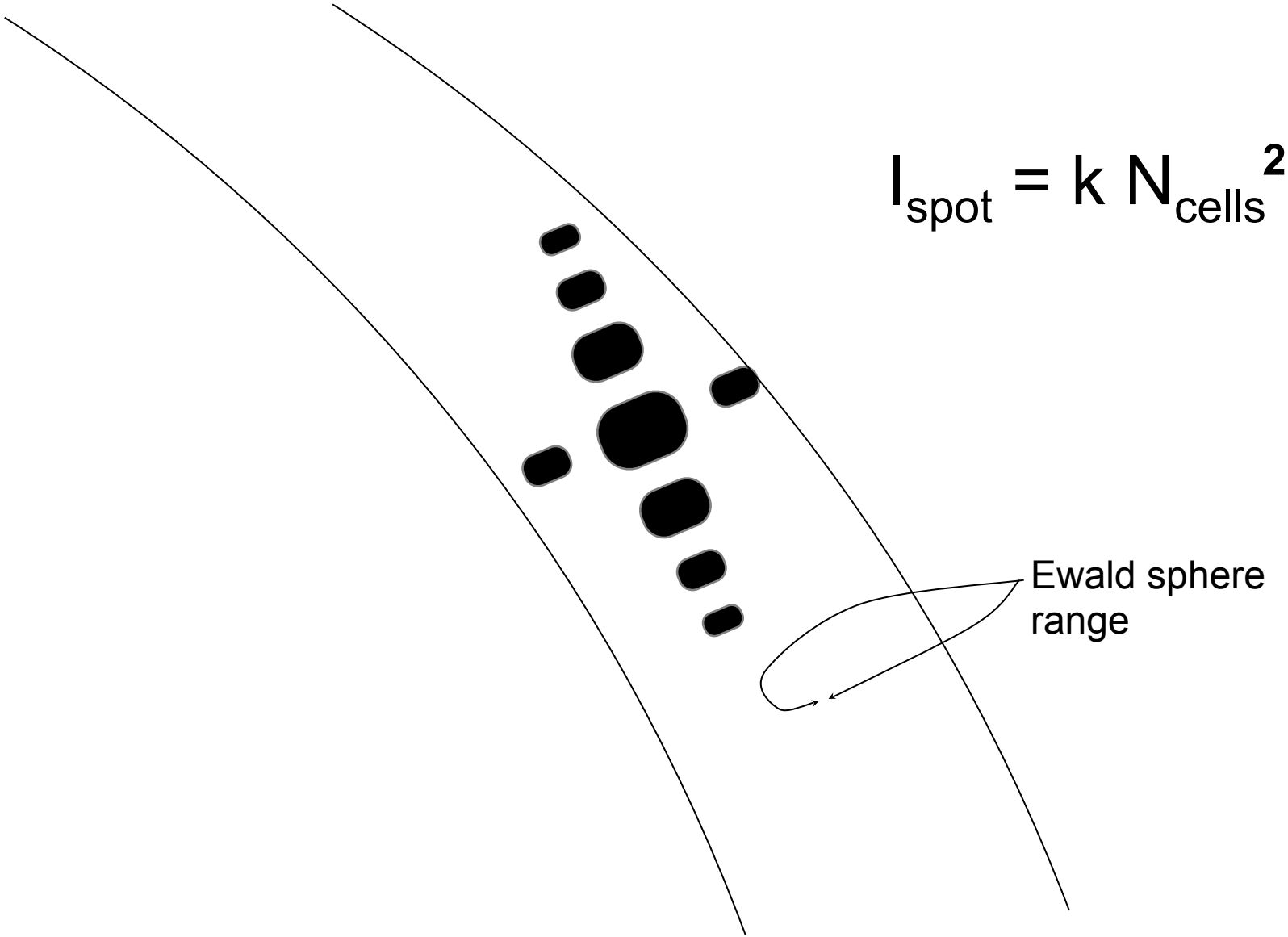

Fraunhofer's Formula

$$I_{pixel} = I_{beam}\, r_e^2\, \Omega \left(\frac{\sin(\pi N \cdot hkl)}{\sin(\pi \cdot hkl)} \right)^2 P\, A\, |\, F(hkl)\, |^2$$

I_{pixel} - photons/pixel/s

I_{beam} - incident (photons/s/m^2)

r_e - classical electron radius (2.818×10^{-15} m)

hkl - index of pixel (**$a \cdot (u_p + u_s)/\lambda$**)

a - orientation (recip. cell vectors)

u_p,u_s - unit vector pointing at pixel,source

λ - x-ray wavelength (in meters!)

N - number of cells (each direction)

Ω - solid angle of pixel (steradian)

P - polarization factor

$(1+\cos^2(2\theta) - Pfac \cdot \cos(2\Phi)\sin^2(2\theta))/2$

A - attenuation factor

$\exp(-\mu_{xtal} \cdot l_{path})$

F(hkl) - structure amplitude (electrons)

see: Kirian et al. (2010)

fastBragg

http://bl831.als.lbl.gov/~jamesh/fastBragg/

$$I_{pixel} = I_{beam}\, r_e^2\, \Omega \left\langle \frac{\sin(\pi N \cdot hkl)}{\sin(\pi \cdot hkl)} \right\rangle P\, A\, |\, F(hkl)\, |^2$$

A series of readings plotted in this way is shown in fig. 1. The readings are at first approximately constant, being due to the general radiation. As the position at which the chamber is set approaches that at which homogeneous rays

Fig. 1.

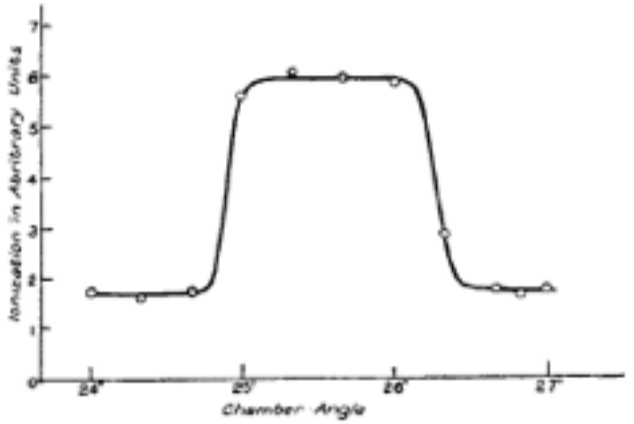

are received, the ionization rises rapidly, remains constant again as long as the whole pencil of homogeneous rays enters the chamber, and then falls to a value approximately equal to its former steady value when the homogeneous rays are no longer received.

6. When comparing two crystal faces, this survey is made in each case. One of the faces is then mounted in the spectrometer, the chamber set so that it receives the homogeneous beam, and a series of readings taken by sweeping the crystal backwards and forwards. The crystal faces are interchanged, the chamber reset, and a series of readings taken for the other face. This process is repeated several times, and the means of the intensities for the faces are compared. The preliminary survey indicates what fraction of the total intensity observed must be subtracted, for each face, in order to allow for the general radiation; and when this has been done, the ratio of the corrected readings gives the ratio of the intensity of reflexion by the two faces. A series of readings obtained in this way is given below. It is a comparison of the reflexion by the (311) face of NaCl, mounted so as to face left on the spectrometer, of the same face turned through 180° so that it faces right, and of the third-order reflexion from the face (100) mounted so as to face right. The difference between the values for (311) L and (311) R is due to inaccurate grinding of the crystal

surface, the effect of which will be discussed later. It can be shown that, although they differ greatly, their mean represents accurately the strength of reflexion if the face were cut true. In taking the readings, the crystal was turned 5 minutes of arc for every beat of a metronome, beating 100 to the minute.

Comparison of (311) L, (311) R, and (300) R.

Face.	Sweep of crystal.	Chamber angle.	Potentiometer scale.	Readings.	Mean of readings.
	° °	°			
(311) L	8 50–11 20	20 50	2	(71, 73, 73, 72)	72·2
(311) R	10 05–12 35	21 00	2	(57, 55, 58, 57, 56, 56)	56·5
(311) L	8 50–11 20	20 50	2	(73, 74, 74, 75)	74·0
(300) R	17 30–20 00	38 25	3	(77, 78, 78, 78)	77·8
(311) L	8 50–11 20	20 50	2	(72, 71, 70, 72, 71, 70)	71·0
(300) R	17 30–20 00	38 25	3	(78, 78, 79, 80, 80)	79·0

A survey of the three reflexions showed that the homogeneous radiation was responsible for 76·9 per cent. of the total effect in the case of the (300) R reflexion, 33·0 per cent. for the (311) R, and 32·2 per cent. for the (311) L reflexion. Since the intensity is very much greater for the (300) face than for the (311) face, different scales on the potentiometer were used. A reading of 72·2 on the second scale represents 72·2 per cent. of a total voltage of 15·72, the corresponding voltage for the third scale being 22·79.

Taking this into account and allowing for the general radiation, one gets a ratio

$$\frac{\text{Mean intensity, face (311)}}{\text{Intensity, face (300) R}} = \frac{3{\cdot}22}{13{\cdot}45} = 0{\cdot}2395.$$

In another experiment, (300) R and (300) L were compared, and in this way the relative mean intensities of (311) and (300) measured.

In order to have a uniform system of indicating both the order of reflexion and the face at which it is taking place, the convention of multiplying the indices of the face by the order has been adopted. Thus, by the reflexion from (622) is meant the second order of reflexion from the face (311).

The crystal is not turned continuously during each reading; its setting is altered five minutes of arc at each beat of a metronome by means of a series of spokes on the tangent screw. It would be preferable to turn the crystal with a uniform angular velocity, but it is unlikely that any appreciable error was caused by the method used. In order

A series of readings plotted in this way is shown in fig. 1. The readings are at first approximately constant, being due to the general radiation. As the position at which the chamber is set approaches that at which homogeneous rays

Fig. 1.

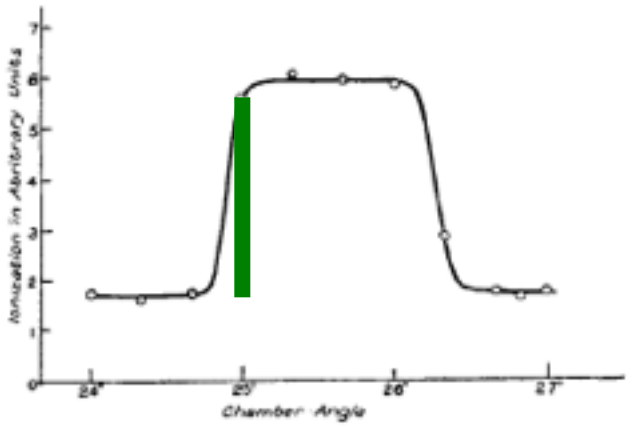

are received, the ionization rises rapidly, remains constant again as long as the whole pencil of homogeneous rays enters the chamber, and then falls to a value approximately equal to its former steady value when the homogeneous rays are no longer received.

6. When comparing two crystal faces, this survey is made in each case. One of the faces is then mounted in the spectrometer, the chamber set so that it receives the homogeneous beam, and a series of readings taken by sweeping the crystal backwards and forwards. The crystal faces are interchanged, the chamber reset, and a series of readings taken for the other face. This process is repeated several times, and the means of the intensities for the faces are compared. The preliminary survey indicates what fraction of the total intensity observed must be subtracted, for each face, in order to allow for the general radiation; and when this has been done, the ratio of the corrected readings gives the ratio of the intensity of reflexion by the two faces. A series of readings obtained in this way is given below. It is a comparison of the reflexion by the (311) face of NaCl, mounted so as to face left on the spectrometer, of the same face turned through 180° so that it faces right, and of the third-order reflexion from the face (100) mounted so as to face right. The difference between the values for (311) L and (311) R is due to inaccurate grinding of the crystal

surface, the effect of which will be discussed later. It can be shown that, although they differ greatly, their mean represents accurately the strength of reflexion if the face were cut true. In taking the readings, the crystal was turned 5 minutes of arc for every beat of a metronome, beating 100 to the minute.

Comparison of (311) L, (311) R, and (300) R.

Face.	Sweep of crystal.	Chamber angle.	Potentiometer scale.	Readings.	Mean of readings.
	° °	°			
(311) L	8 50–11 20	20 50	2	(71, 73, 73, 72)	72·2
(311) R	10 05–12 35	21 00	2	(57, 55, 58, 57, 56, 56)	56·5
(311) L	8 50–11 20	20 50	2	(73, 74, 74, 75)	74·0
(300) R	17 30–20 00	38 25	3	(77, 78, 78, 78)	77·8
(311) L	8 50–11 20	20 50	2	(72, 71, 70, 72, 71, 70)	71·0
(300) R	17 30–20 00	38 25	3	(78, 78, 79, 80, 80)	79·0

A survey of the three reflexions showed that the homogeneous radiation was responsible for 76·9 per cent. of the total effect in the case of the (300) R reflexion, 33·0 per cent. for the (311) R, and 32·2 per cent. for the (311) L reflexion. Since the intensity is very much greater for the (300) face than for the (311) face, different scales on the potentiometer were used. A reading of 72·2 on the second scale represents 72·2 per cent. of a total voltage of 15·72, the corresponding voltage for the third scale being 22·79.

Taking this into account and allowing for the general radiation, one gets a ratio

$$\frac{\text{Mean intensity, face (311)}}{\text{Intensity, face (300) R}} = \frac{3{\cdot}22}{13{\cdot}45} = 0{\cdot}2395.$$

In another experiment, (300) R and (300) L were compared, and in this way the relative mean intensities of (311) and (300) measured.

In order to have a uniform system of indicating both the order of reflexion and the face at which it is taking place, the convention of multiplying the indices of the face by the order has been adopted. Thus, by the reflexion from (622) is meant the second order of reflexion from the face (311).

The crystal is not turned continuously during each reading; its setting is altered five minutes of arc at each beat of a metronome by means of a series of spokes on the tangent screw. It would be preferable to turn the crystal with a uniform angular velocity, but it is unlikely that any appreciable error was caused by the method used. In order

A series of readings plotted in this way is shown in fig. 1. The readings are at first approximately constant, being due to the general radiation. As the position at which the chamber is set approaches that at which homogeneous rays

Fig. 1.

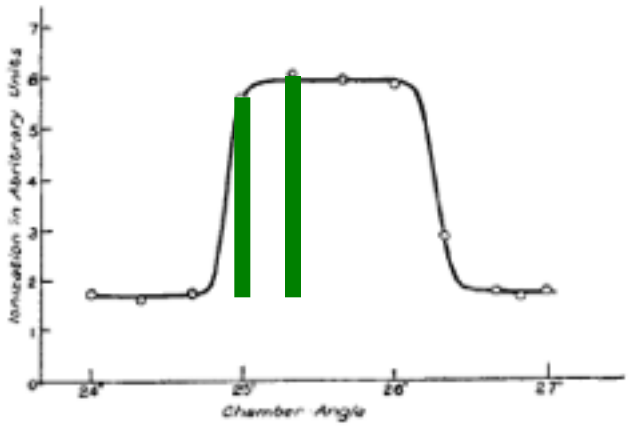

are received, the ionization rises rapidly, remains constant again as long as the whole pencil of homogeneous rays enters the chamber, and then falls to a value approximately equal to its former steady value when the homogeneous rays are no longer received.

6. When comparing two crystal faces, this survey is made in each case. One of the faces is then mounted in the spectrometer, the chamber set so that it receives the homogeneous beam, and a series of readings taken by sweeping the crystal backwards and forwards. The crystal faces are interchanged, the chamber reset, and a series of readings taken for the other face. This process is repeated several times, and the means of the intensities for the faces are compared. The preliminary survey indicates what fraction of the total intensity observed must be subtracted, for each face, in order to allow for the general radiation; and when this has been done, the ratio of the corrected readings gives the ratio of the intensity of reflexion by the two faces. A series of readings obtained in this way is given below. It is a comparison of the reflexion by the (311) face of NaCl, mounted so as to face left on the spectrometer, of the same face turned through 180° so that it faces right, and of the third-order reflexion from the face (100) mounted so as to face right. The difference between the values for (311) L and (311) R is due to inaccurate grinding of the crystal

surface, the effect of which will be discussed later. It can be shown that, although they differ greatly, their mean represents accurately the strength of reflexion if the face were cut true. In taking the readings, the crystal was turned 5 minutes of arc for every beat of a metronome, beating 100 to the minute.

Comparison of (311) L, (311) R, and (300) R.

Face.	Sweep of crystal.	Chamber angle.	Potentiometer scale.	Readings.	Mean of readings.
	° °	°			
(311) L	8 50–11 20	20 50	2	(71, 73, 73, 72)	72·2
(311) R	10 05–12 35	21 00	2	(57, 55, 58, 57, 56, 56)	56·5
(311) L	8 50–11 20	20 50	2	(73, 74, 74, 75)	74·0
(300) R	17 30–20 00	38 25	3	(77, 78, 78, 78)	77·8
(311) L	8 50–11 20	20 50	2	(72, 71, 70, 72, 71, 70)	71·0
(300) R	17 30–20 00	38 25	3	(78, 78, 79, 80, 80)	79·0

A survey of the three reflexions showed that the homogeneous radiation was responsible for 76·9 per cent. of the total effect in the case of the (300) R reflexion, 33·0 per cent. for the (311) R, and 32·2 per cent. for the (311) L reflexion. Since the intensity is very much greater for the (300) face than for the (311) face, different scales on the potentiometer were used. A reading of 72·2 on the second scale represents 72·2 per cent. of a total voltage of 15·72, the corresponding voltage for the third scale being 22·79.

Taking this into account and allowing for the general radiation, one gets a ratio

$$\frac{\text{Mean intensity, face (311)}}{\text{Intensity, face (300) R}} = \frac{3{\cdot}22}{13{\cdot}45} = 0{\cdot}2395.$$

In another experiment, (300) R and (300) L were compared, and in this way the relative mean intensities of (311) and (300) measured.

In order to have a uniform system of indicating both the order of reflexion and the face at which it is taking place, the convention of multiplying the indices of the face by the order has been adopted. Thus, by the reflexion from (622) is meant the second order of reflexion from the face (311).

The crystal is not turned continuously during each reading; its setting is altered five minutes of arc at each beat of a metronome by means of a series of spokes on the tangent screw. It would be preferable to turn the crystal with a uniform angular velocity, but it is unlikely that any appreciable error was caused by the method used. In order

A series of readings plotted in this way is shown in fig. 1. The readings are at first approximately constant, being due to the general radiation. As the position at which the chamber is set approaches that at which homogeneous rays

Fig. 1.

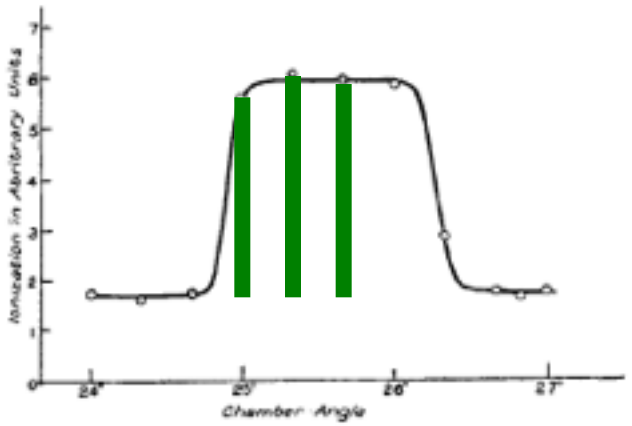

are received, the ionization rises rapidly, remains constant again as long as the whole pencil of homogeneous rays enters the chamber, and then falls to a value approximately equal to its former steady value when the homogeneous rays are no longer received.

6. When comparing two crystal faces, this survey is made in each case. One of the faces is then mounted in the spectrometer, the chamber set so that it receives the homogeneous beam, and a series of readings taken by sweeping the crystal backwards and forwards. The crystal faces are interchanged, the chamber reset, and a series of readings taken for the other face. This process is repeated several times, and the means of the intensities for the faces are compared. The preliminary survey indicates what fraction of the total intensity observed must be subtracted, for each face, in order to allow for the general radiation; and when this has been done, the ratio of the corrected readings gives the ratio of the intensity of reflexion by the two faces. A series of readings obtained in this way is given below. It is a comparison of the reflexion by the (311) face of NaCl, mounted so as to face left on the spectrometer, of the same face turned through 180° so that it faces right, and of the third-order reflexion from the face (100) mounted so as to face right. The difference between the values for (311) L and (311) R is due to inaccurate grinding of the crystal

surface, the effect of which will be discussed later. It can be shown that, although they differ greatly, their mean represents accurately the strength of reflexion if the face were cut true. In taking the readings, the crystal was turned 5 minutes of arc for every beat of a metronome, beating 100 to the minute.

Comparison of (311) L, (311) R, and (300) R.

Face.	Sweep of crystal.	Chamber angle.	Potentiometer scale.	Readings.	Mean of readings.
	° °	°			
(311) L	8 50–11 20	20 50	2	(71, 73, 73, 72)	72·2
(311) R	10 05–12 35	21 00	2	(57, 55, 58, 57, 56, 56)	56·5
(311) L	8 50–11 20	20 50	2	(73, 74, 74, 75)	74·0
(300) R	17 30–20 00	38 25	3	(77, 78, 78, 78)	77·8
(311) L	8 50–11 20	20 50	2	(72, 71, 70, 72, 71, 70)	71·0
(300) R	17 30–20 00	38 25	3	(78, 78, 79, 80, 80)	79·0

A survey of the three reflexions showed that the homogeneous radiation was responsible for 76·9 per cent. of the total effect in the case of the (300) R reflexion, 33·0 per cent. for the (311) R, and 32·2 per cent. for the (311) L reflexion. Since the intensity is very much greater for the (300) face than for the (311) face, different scales on the potentiometer were used. A reading of 72·2 on the second scale represents 72·2 per cent. of a total voltage of 15·72, the corresponding voltage for the third scale being 22·79.

Taking this into account and allowing for the general radiation, one gets a ratio

$$\frac{\text{Mean intensity, face (311)}}{\text{Intensity, face (300) R}} = \frac{3{\cdot}22}{13{\cdot}45} = 0{\cdot}2395.$$

In another experiment, (300) R and (300) L were compared, and in this way the relative mean intensities of (311) and (300) measured.

In order to have a uniform system of indicating both the order of reflexion and the face at which it is taking place, the convention of multiplying the indices of the face by the order has been adopted. Thus, by the reflexion from (622) is meant the second order of reflexion from the face (311).

The crystal is not turned continuously during each reading; its setting is altered five minutes of arc at each beat of a metronome by means of a series of spokes on the tangent screw. It would be preferable to turn the crystal with a uniform angular velocity, but it is unlikely that any appreciable error was caused by the method used. In order

A series of readings plotted in this way is shown in fig. 1. The readings are at first approximately constant, being due to the general radiation. As the position at which the chamber is set approaches that at which homogeneous rays

Fig. 1.

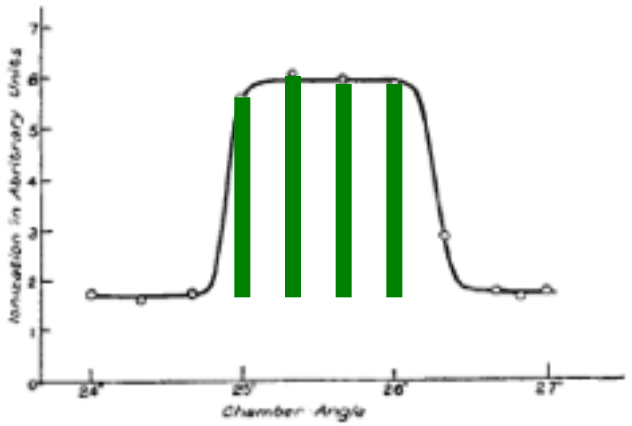

are received, the ionization rises rapidly, remains constant again as long as the whole pencil of homogeneous rays enters the chamber, and then falls to a value approximately equal to its former steady value when the homogeneous rays are no longer received.

6. When comparing two crystal faces, this survey is made in each case. One of the faces is then mounted in the spectrometer, the chamber set so that it receives the homogeneous beam, and a series of readings taken by sweeping the crystal backwards and forwards. The crystal faces are interchanged, the chamber reset, and a series of readings taken for the other face. This process is repeated several times, and the means of the intensities for the faces are compared. The preliminary survey indicates what fraction of the total intensity observed must be subtracted, for each face, in order to allow for the general radiation; and when this has been done, the ratio of the corrected readings gives the ratio of the intensity of reflexion by the two faces. A series of readings obtained in this way is given below. It is a comparison of the reflexion by the (311) face of NaCl, mounted so as to face left on the spectrometer, of the same face turned through 180° so that it faces right, and of the third-order reflexion from the face (100) mounted so as to face right. The difference between the values for (311) L and (311) R is due to inaccurate grinding of the crystal

surface, the effect of which will be discussed later. It can be shown that, although they differ greatly, their mean represents accurately the strength of reflexion if the face were cut true. In taking the readings, the crystal was turned 5 minutes of arc for every beat of a metronome, beating 100 to the minute.

Comparison of (311) L, (311) R, and (300) R.

Face.	Sweep of crystal.	Chamber angle.	Potentiometer scale.	Readings.	Mean of readings.
	° °	°			
(311) L	8 50–11 20	20 50	2	(71, 73, 73, 72)	72·2
(311) R	10 05–12 35	21 00	2	(57, 55, 58, 57, 56, 56)	56·5
(311) L	8 50–11 20	20 50	2	(73, 74, 74, 75)	74·0
(300) R	17 30–20 00	38 25	3	(77, 78, 78, 78)	77·8
(311) L	8 50–11 20	20 50	2	(72, 71, 70, 72, 71, 70)	71·0
(300) R	17 30–20 00	38 25	3	(78, 78, 79, 80, 80)	79·0

A survey of the three reflexions showed that the homogeneous radiation was responsible for 76·9 per cent. of the total effect in the case of the (300) R reflexion, 33·0 per cent. for the (311) R, and 32·2 per cent. for the (311) L reflexion. Since the intensity is very much greater for the (300) face than for the (311) face, different scales on the potentiometer were used. A reading of 72·2 on the second scale represents 72·2 per cent. of a total voltage of 15·72, the corresponding voltage for the third scale being 22·79.

Taking this into account and allowing for the general radiation, one gets a ratio

$$\frac{\text{Mean intensity, face (311)}}{\text{Intensity, face (300) R}} = \frac{3{\cdot}22}{13{\cdot}45} = 0{\cdot}2395.$$

In another experiment, (300) R and (300) L were compared, and in this way the relative mean intensities of (311) and (300) measured.

In order to have a uniform system of indicating both the order of reflexion and the face at which it is taking place, the convention of multiplying the indices of the face by the order has been adopted. Thus, by the reflexion from (622) is meant the second order of reflexion from the face (311).

The crystal is not turned continuously during each reading; its setting is altered five minutes of arc at each beat of a metronome by means of a series of spokes on the tangent screw. It would be preferable to turn the crystal with a uniform angular velocity, but it is unlikely that any appreciable error was caused by the method used. In order

A series of readings plotted in this way is shown in fig. 1. The readings are at first approximately constant, being due to the general radiation. As the position at which the chamber is set approaches that at which homogeneous rays

Fig. 1.

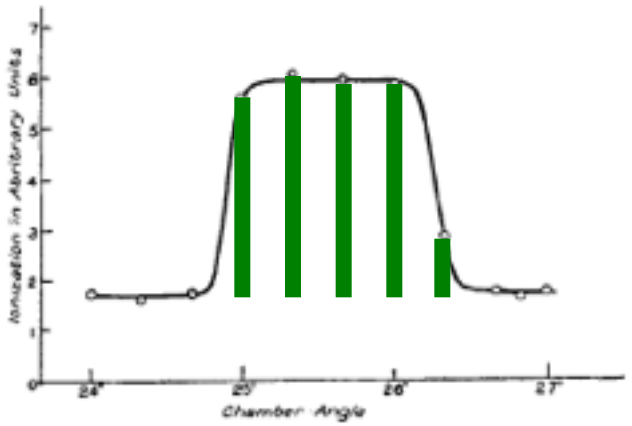

are received, the ionization rises rapidly, remains constant again as long as the whole pencil of homogeneous rays enters the chamber, and then falls to a value approximately equal to its former steady value when the homogeneous rays are no longer received.

6. When comparing two crystal faces, this survey is made in each case. One of the faces is then mounted in the spectrometer, the chamber set so that it receives the homogeneous beam, and a series of readings taken by sweeping the crystal backwards and forwards. The crystal faces are interchanged, the chamber reset, and a series of readings taken for the other face. This process is repeated several times, and the means of the intensities for the faces are compared. The preliminary survey indicates what fraction of the total intensity observed must be subtracted, for each face, in order to allow for the general radiation; and when this has been done, the ratio of the corrected readings gives the ratio of the intensity of reflexion by the two faces. A series of readings obtained in this way is given below. It is a comparison of the reflexion by the (311) face of NaCl, mounted so as to face left on the spectrometer, of the same face turned through 180° so that it faces right, and of the third-order reflexion from the face (100) mounted so as to face right. The difference between the values for (311) L and (311) R is due to inaccurate grinding of the crystal

surface, the effect of which will be discussed later. It can be shown that, although they differ greatly, their mean represents accurately the strength of reflexion if the face were cut true. In taking the readings, the crystal was turned 5 minutes of arc for every beat of a metronome, beating 100 to the minute.

Comparison of (311) L, (311) R, and (300) R.

Face.	Sweep of crystal.	Chamber angle.	Potentiometer scale.	Readings.	Mean of readings.
	° °	°			
(311) L	8 50–11 20	20 50	2	(71, 73, 73, 72)	72·2
(311) R	10 05–12 35	21 00	2	(57, 55, 58, 57, 56, 56)	56·5
(311) L	8 50–11 20	20 50	2	(73, 74, 74, 75)	74·0
(300) R	17 30–20 00	38 25	3	(77, 78, 78, 78)	77·8
(311) L	8 50–11 20	20 50	2	(72, 71, 70, 72, 71, 70)	71·0
(300) R	17 30–20 00	38 25	3	(78, 78, 79, 80, 80)	79·0

A survey of the three reflexions showed that the homogeneous radiation was responsible for 76·9 per cent. of the total effect in the case of the (300) R reflexion, 33·0 per cent. for the (311) R, and 32·2 per cent. for the (311) L reflexion. Since the intensity is very much greater for the (300) face than for the (311) face, different scales on the potentiometer were used. A reading of 72·2 on the second scale represents 72·2 per cent. of a total voltage of 15·72, the corresponding voltage for the third scale being 22·79.

Taking this into account and allowing for the general radiation, one gets a ratio

$$\frac{\text{Mean intensity, face (311)}}{\text{Intensity, face (300) R}} = \frac{3{\cdot}22}{13{\cdot}45} = 0{\cdot}2395.$$

In another experiment, (300) R and (300) L were compared, and in this way the relative mean intensities of (311) and (300) measured.

In order to have a uniform system of indicating both the order of reflexion and the face at which it is taking place, the convention of multiplying the indices of the face by the order has been adopted. Thus, by the reflexion from (622) is meant the second order of reflexion from the face (311).

The crystal is not turned continuously during each reading; its setting is altered five minutes of arc at each beat of a metronome by means of a series of spokes on the tangent screw. It would be preferable to turn the crystal with a uniform angular velocity, but it is unlikely that any appreciable error was caused by the method used. In order

A series of readings plotted in this way is shown in fig. 1. The readings are at first approximately constant, being due to the general radiation. As the position at which the chamber is set approaches that at which homogeneous rays

Fig. 1.

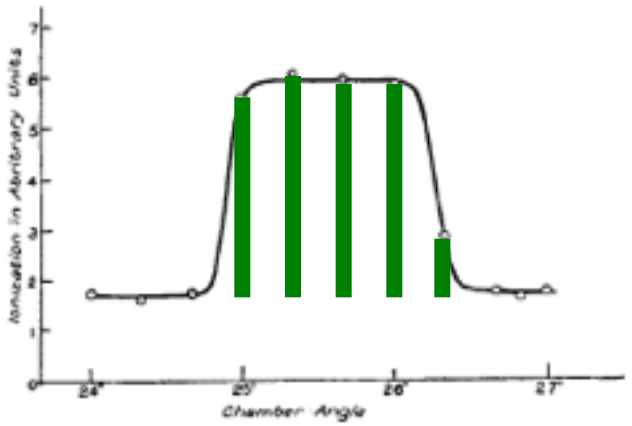

are received, the ionization rises rapidly, remains constant again as long as the whole pencil of homogeneous rays enters the chamber, and then falls to a value approximately equal to its former steady value when the homogeneous rays are no longer received.

6. When comparing two crystal faces, this survey is made in each case. One of the faces is then mounted in the spectrometer, the chamber set so that it receives the homogeneous beam, and a series of readings taken by sweeping the crystal backwards and forwards. The crystal faces are interchanged, the chamber reset, and a series of readings taken for the other face. This process is repeated several times, and the means of the intensities for the faces are compared. The preliminary survey indicates what fraction of the total intensity observed must be subtracted, for each face, in order to allow for the general radiation; and when this has been done, the ratio of the corrected readings gives the ratio of the intensity of reflexion by the two faces. A series of readings obtained in this way is given below. It is a comparison of the reflexion by the (311) face of NaCl, mounted so as to face left on the spectrometer, of the same face turned through 180° so that it faces right, and of the third-order reflexion from the face (100) mounted so as to face right. The difference between the values for (311) L and (311) R is due to inaccurate grinding of the crystal

surface, the effect of which will be discussed later. It can be shown that, although they differ greatly, their mean represents accurately the strength of reflexion if the face were cut true. In taking the readings, the crystal was turned 5 minutes of arc for every beat of a metronome, beating 100 to the minute.

Comparison of (311) L, (311) R, and (300) R.

Face.	Sweep of crystal.	Chamber angle.	Potentiometer scale.	Readings.	Mean of readings.
	° °	°			
(311) L	8 50–11 20	20 50	2	(71, 73, 73, 72)	72·2
(311) R	10 05–12 35	21 00	2	(57, 55, 58, 57, 56, 56)	56·5
(311) L	8 50–11 20	20 50	2	(73, 74, 74, 75)	74·0
(300) R	17 30–20 00	38 25	3	(77, 78, 78, 78)	77·8
(311) L	8 50–11 20	20 50	2	(72, 71, 70, 72, 71, 70)	71·0
(300) R	17 30–20 00	38 25	3	(78, 78, 79, 80, 80)	79·0

A survey of the three reflexions showed that the homogeneous radiation was responsible for 76·9 per cent. of the total effect in the case of the (300) R reflexion, 33·0 per cent. for the (311) R, and 32·2 per cent. for the (311) L reflexion. Since the intensity is very much greater for the (300) face than for the (311) face, different scales on the potentiometer were used. A reading of 72·2 on the second scale represents 72·2 per cent. of a total voltage of 15·72, the corresponding voltage for the third scale being 22·79.

Taking this into account and allowing for the general radiation, one gets a ratio

$$\frac{\text{Mean intensity, face (311)}}{\text{Intensity, face (300) R}} = \frac{3{\cdot}22}{13{\cdot}45} = 0{\cdot}2395.$$

In another experiment, (300) R and (300) L were compared, and in this way the relative mean intensities of (311) and (300) measured.

In order to have a uniform system of indicating both the order of reflexion and the face at which it is taking place, the convention of multiplying the indices of the face by the order has been adopted. Thus, by the reflexion from (622) is meant the second order of reflexion from the face (311).

The crystal is not turned continuously during each reading; its setting is altered five minutes of arc at each beat of a metronome by means of a series of spokes on the tangent screw. It would be preferable to turn the crystal with a uniform angular velocity, but it is unlikely that any appreciable error was caused by the method used. In order

A series of readings plotted in this way is shown in fig. 1. The readings are at first approximately constant, being due to the general radiation. As the position at which the chamber is set approaches that at which homogeneous rays

Fig. 1.

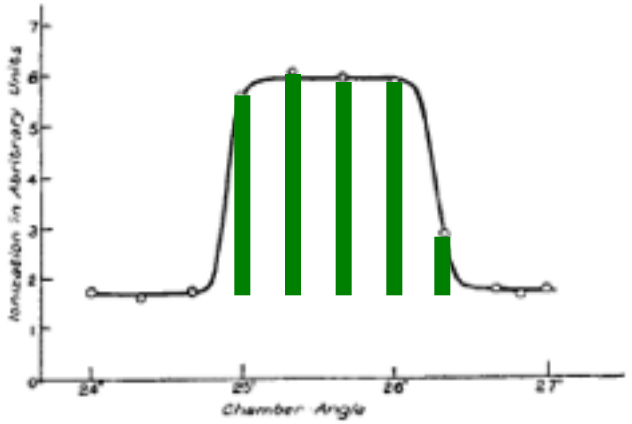

are received, the ionization rises rapidly, remains constant again as long as the whole pencil of homogeneous rays enters the chamber, and then falls to a value approximately equal to its former steady value when the homogeneous rays are no longer received.

6. When comparing two crystal faces, this survey is made in each case. One of the faces is then mounted in the spectrometer, the chamber set so that it receives the homogeneous beam, and a series of readings taken by sweeping the crystal backwards and forwards. The crystal faces are interchanged, the chamber reset, and a series of readings taken for the other face. This process is repeated several times, and the means of the intensities for the faces are compared. The preliminary survey indicates what fraction of the total intensity observed must be subtracted, for each face, in order to allow for the general radiation; and when this has been done, the ratio of the corrected readings gives the ratio of the intensity of reflexion by the two faces. A series of readings obtained in this way is given below. It is a comparison of the reflexion by the (311) face of NaCl, mounted so as to face left on the spectrometer, of the same face turned through 180° so that it faces right, and of the third-order reflexion from the face (100) mounted so as to face right. The difference between the values for (311) L and (311) R is due to inaccurate grinding of the crystal

surface, the effect of which will be discussed later. It can be shown that, although they differ greatly, their mean represents accurately the strength of reflexion if the face were cut true. In taking the readings, the crystal was turned 5 minutes of arc for every beat of a metronome, beating 100 to the minute.

Comparison of (311) L, (311) R, and (300) R.

Face.	Sweep of crystal.	Chamber angle.	Potentiometer scale.	Readings.	Mean of readings.
	° ′ ° ′	° ′			
(311) L	8 50–11 20	20 50	2	(71, 73, 73, 72)	72·2
(311) R	10 05–12 35	21 00	2	(57, 55, 58, 57, 56, 56)	56·5
(311) L	8 50–11 20	20 50	2	(73, 74, 74, 75)	74·0
(300) R	17 30–20 00	38 25	3	(77, 78, 78, 78)	77·8
(311) L	8 50–11 20	20 50	2	(72, 71, 70, 72, 71, 70)	71·0
(300) R	17 30–20 00	38 25	3	(78, 78, 79, 80, 80)	79·0

A survey of the three reflexions showed that the homogeneous radiation was responsible for 76·9 per cent. of the total effect in the case of the (300) R reflexion, 33·0 per cent. for the (311) R, and 32·2 per cent. for the (311) L reflexion. Since the intensity is very much greater for the (300) face than for the (311) face, different scales on the potentiometer were used. A reading of 72·2 on the second scale represents 72·2 per cent. of a total voltage of 15·72, the corresponding voltage for the third scale being 22·79.

Taking this into account and allowing for the general radiation, one gets a ratio

$$\frac{\text{Mean intensity, face (311)}}{\text{Intensity, face (300) R}} = \frac{3{\cdot}22}{13{\cdot}45} = 0{\cdot}2395.$$

In another experiment, (300) R and (300) L were compared, and in this way the relative mean intensities of (311) and (300) measured.

In order to have a uniform system of indicating both the order of reflexion and the face at which it is taking place, the convention of multiplying the indices of the face by the order has been adopted. Thus, by the reflexion from (622) is meant the second order of reflexion from the face (311).

The crystal is not turned continuously during each reading; its setting is altered five minutes of arc at each beat of a metronome by means of a series of spokes on the tangent screw. It would be preferable to turn the crystal with a uniform angular velocity, but it is unlikely that any appreciable error was caused by the method used. In order

What is “partiality”?

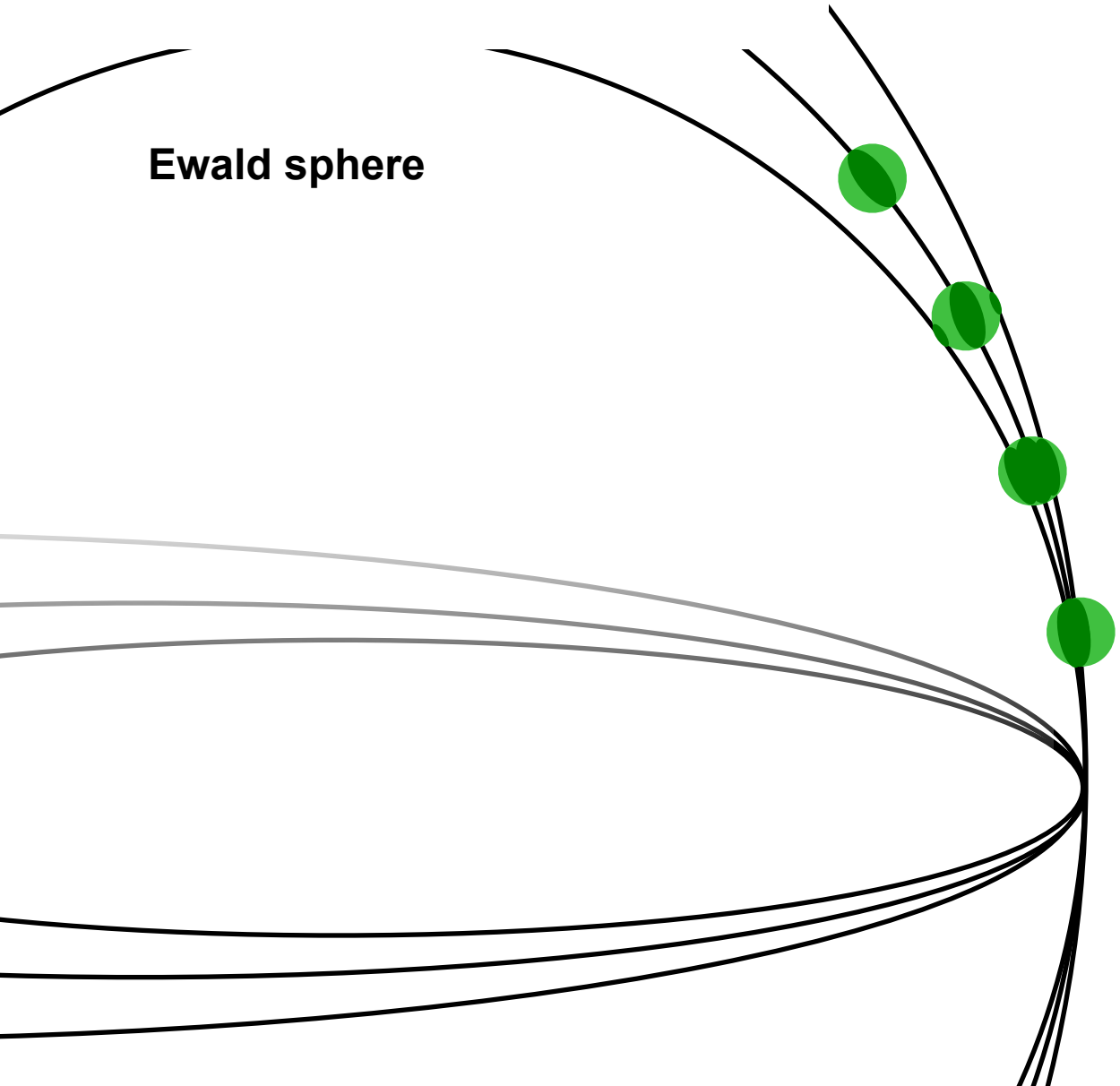

What is “partiality”?

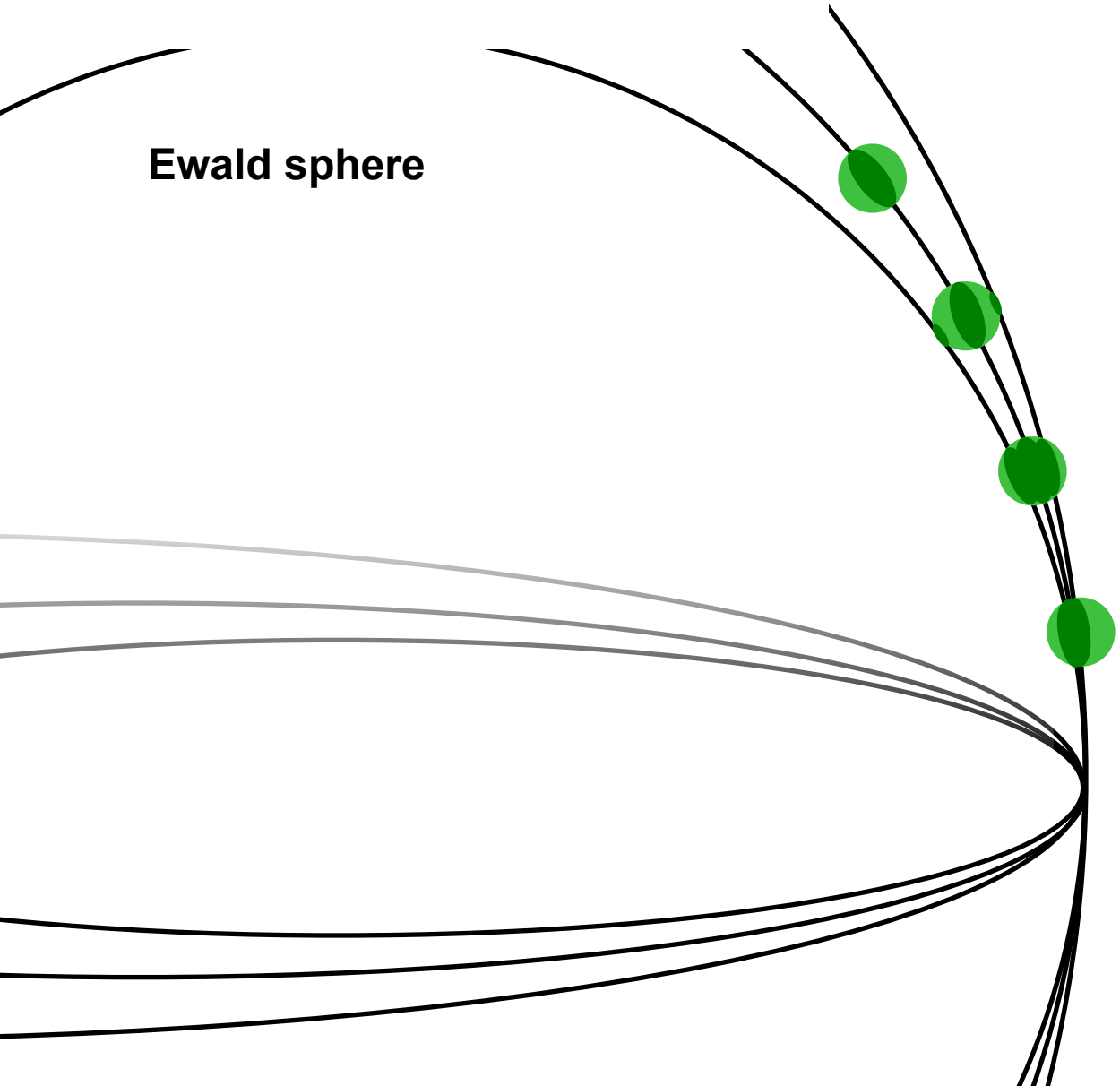

How can I know I’m doing it right?

How can I know I’m doing it right?

Cheat!

How can I know I'm doing it right?

Cheat!

http://bl831a.als.lbl.gov/example_data_sets/Illuin/LCLS/

How can I know I'm doing it right?

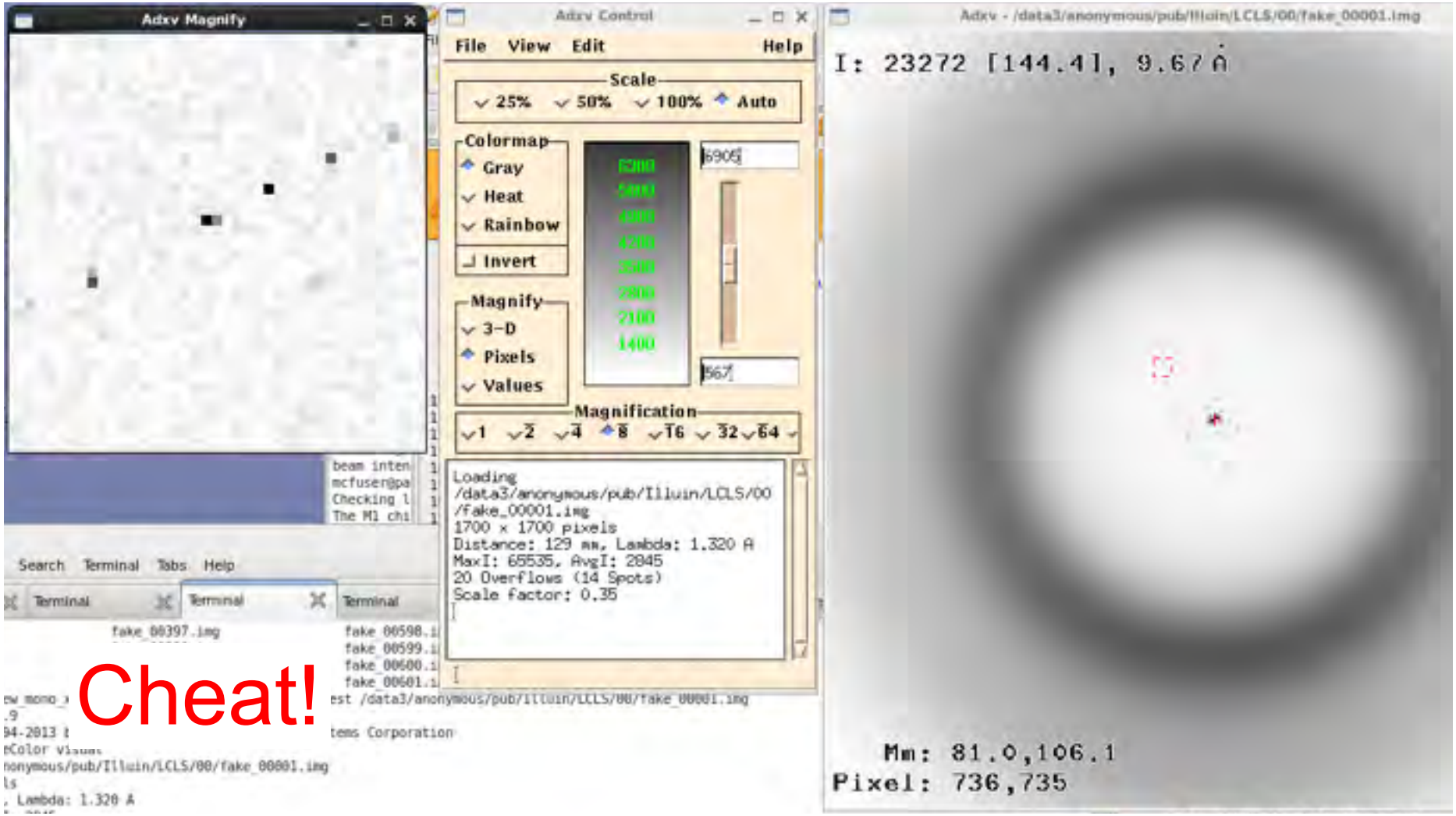

http://bl831a.als.lbl.gov/example_data_sets/Illuin/LCLS/

Check the Wilson plot!

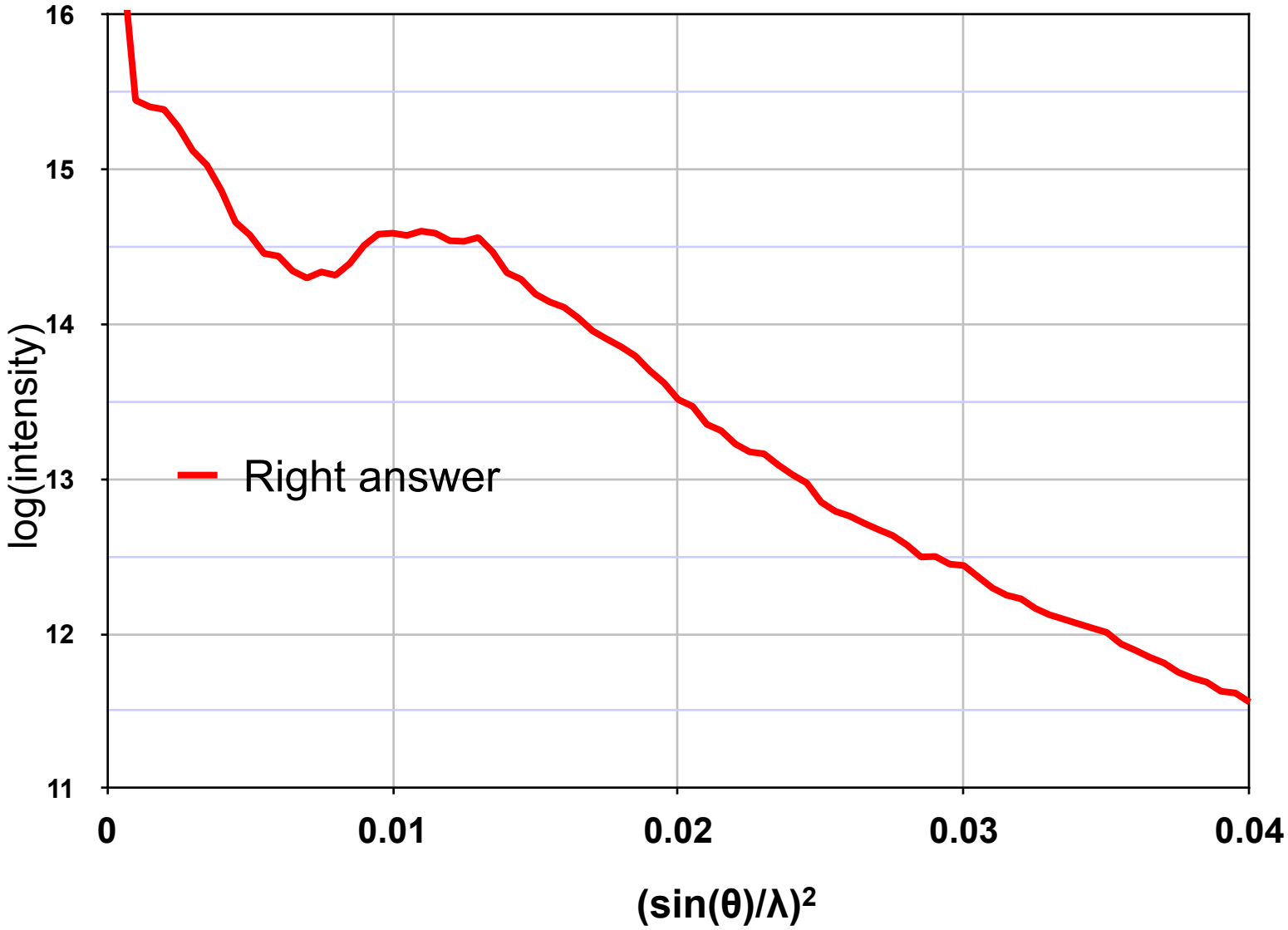

Check the Wilson plot!

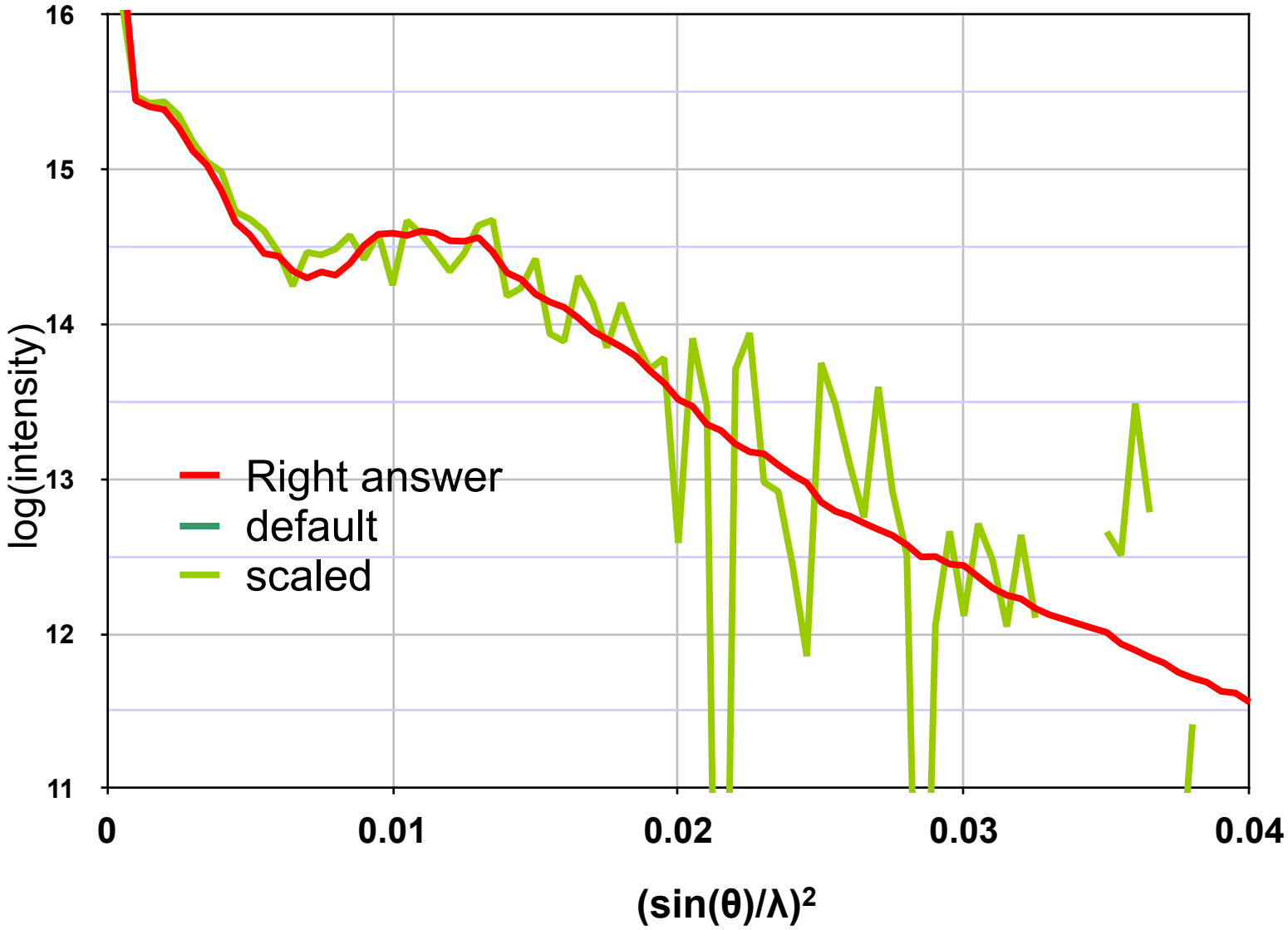

Check the Wilson plot!

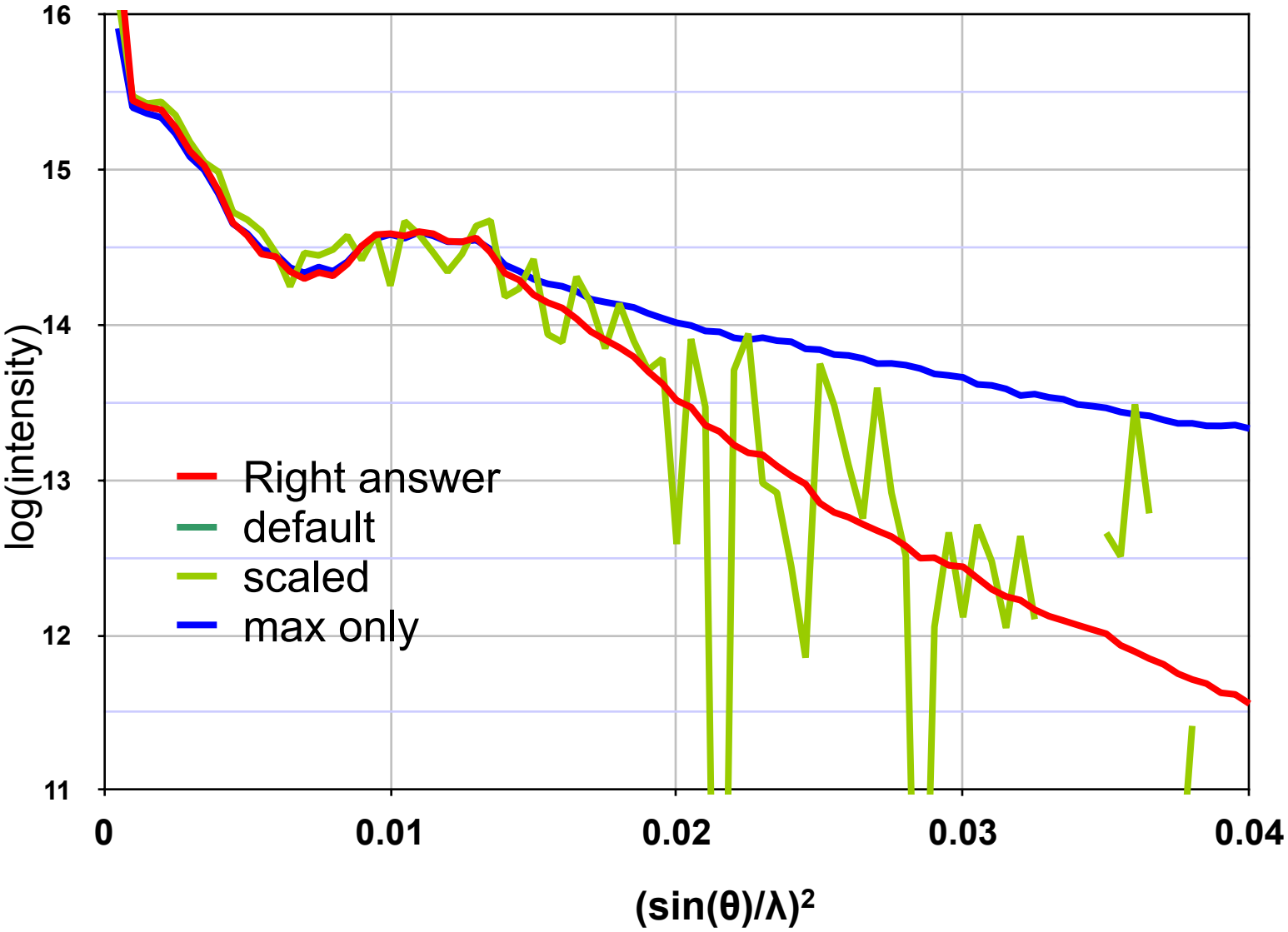

Check the Wilson plot!

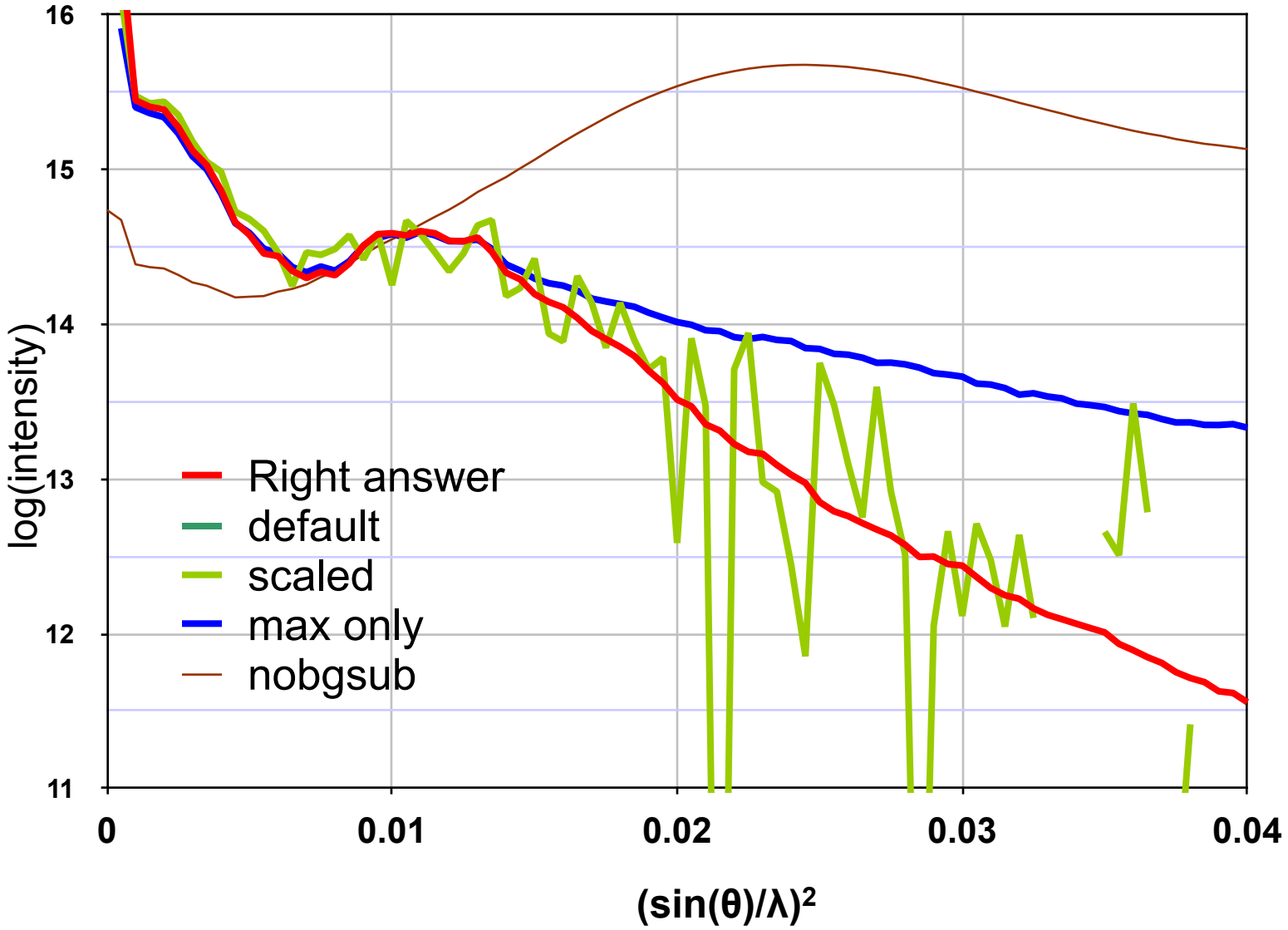

Check the Wilson plot!

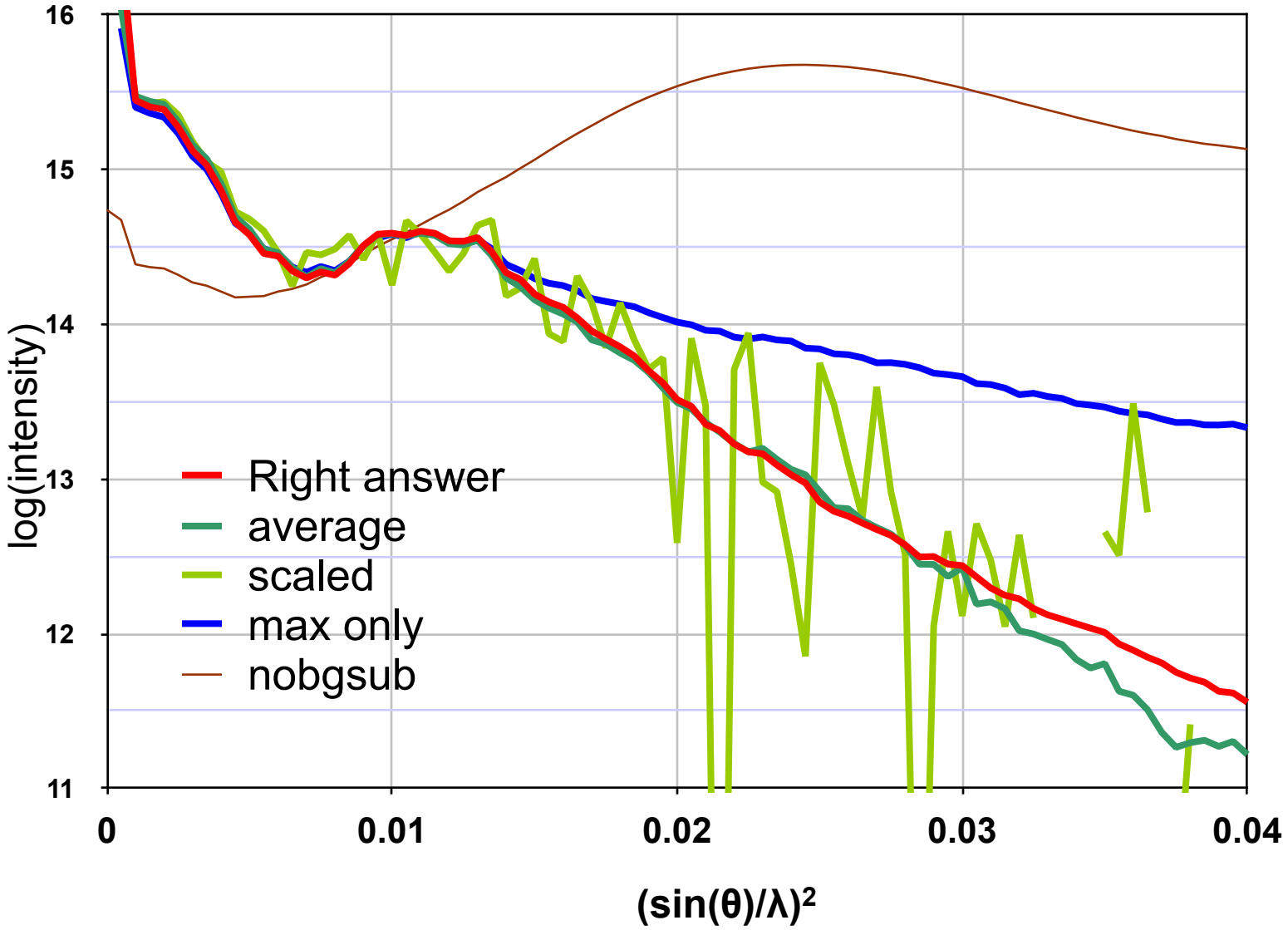

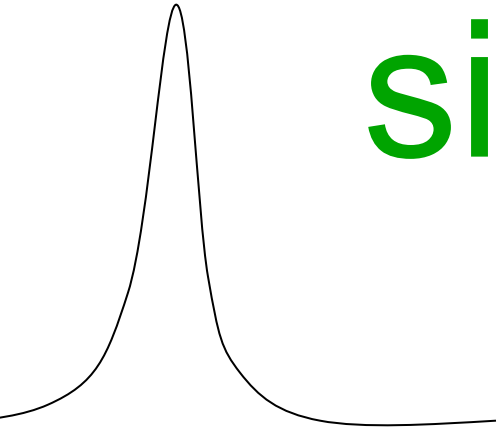

signal *vs* noise

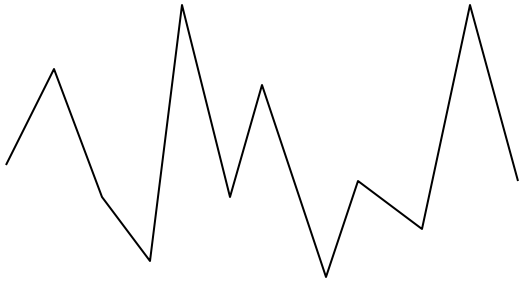

"Control! Control!
you must learn
CONTROL!!!"

-Yoda

nearBragg program

http://bl831.als.lbl.gov/~jamesh/nearBragg/

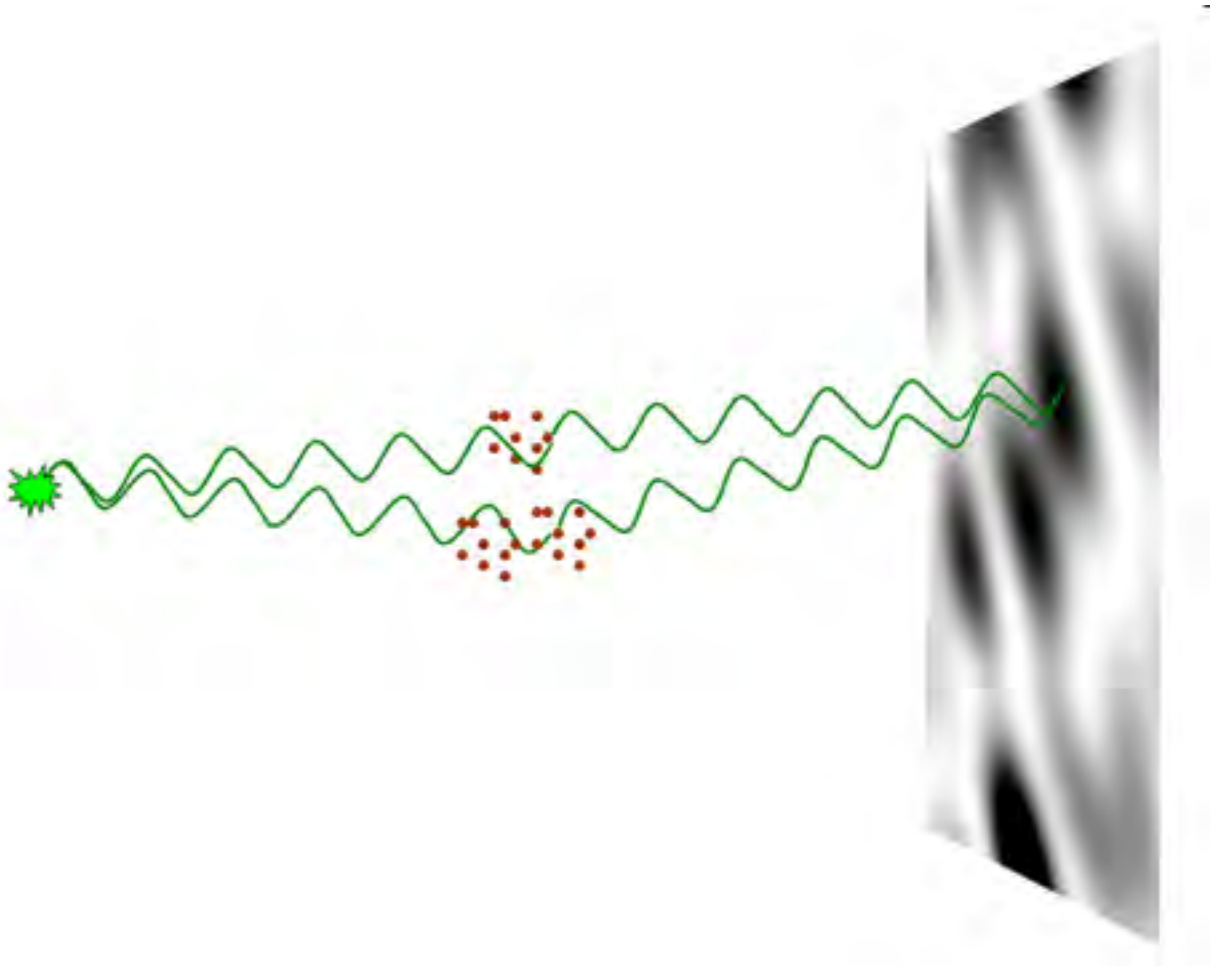

nearBragg program

http://bl831.als.lbl.gov/~jamesh/nearBragg/

- "assumption-free" total scattering

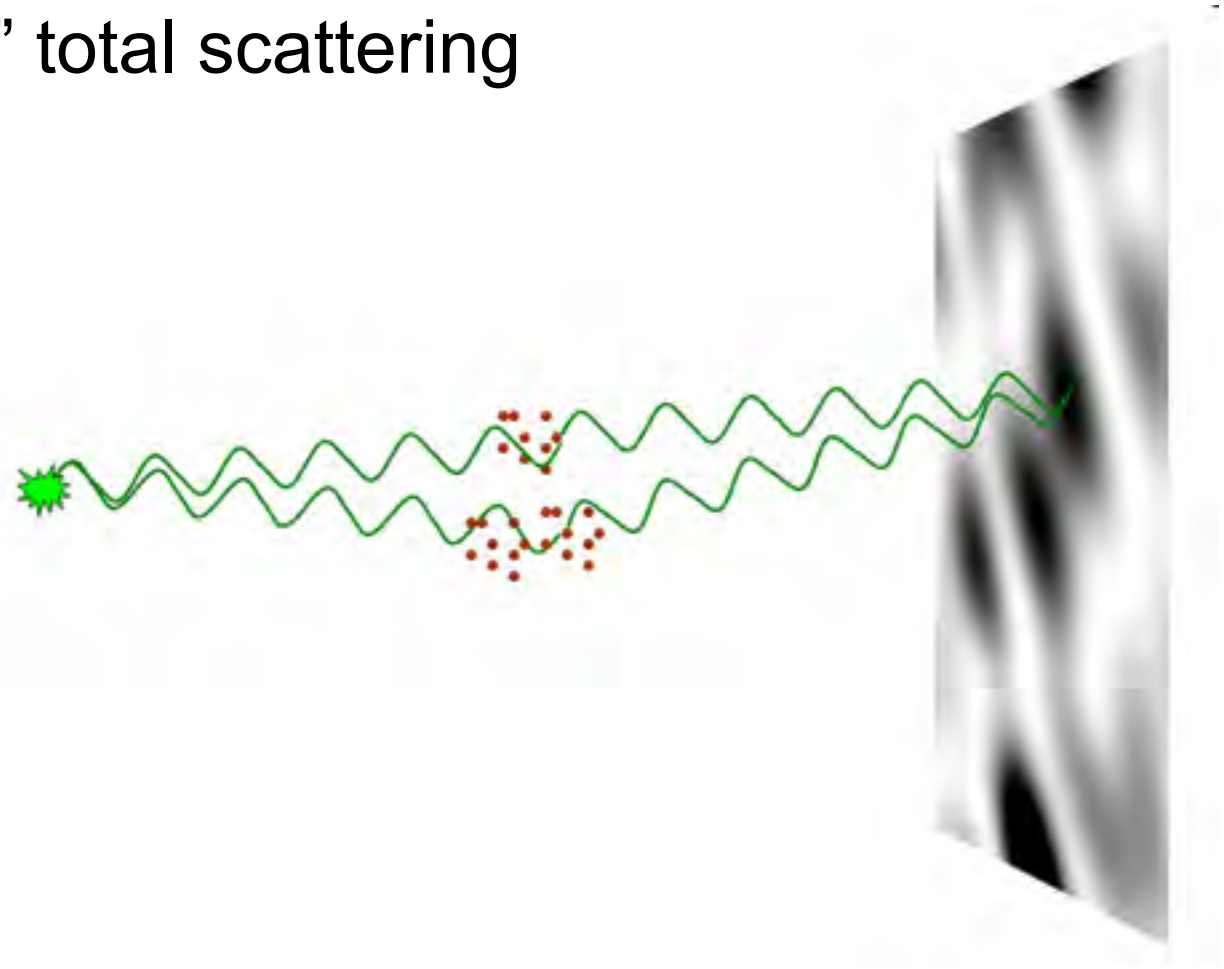

nearBragg program

http://bl831.als.lbl.gov/~jamesh/nearBragg/

- "assumption-free" total scattering
- no Fourier Transform

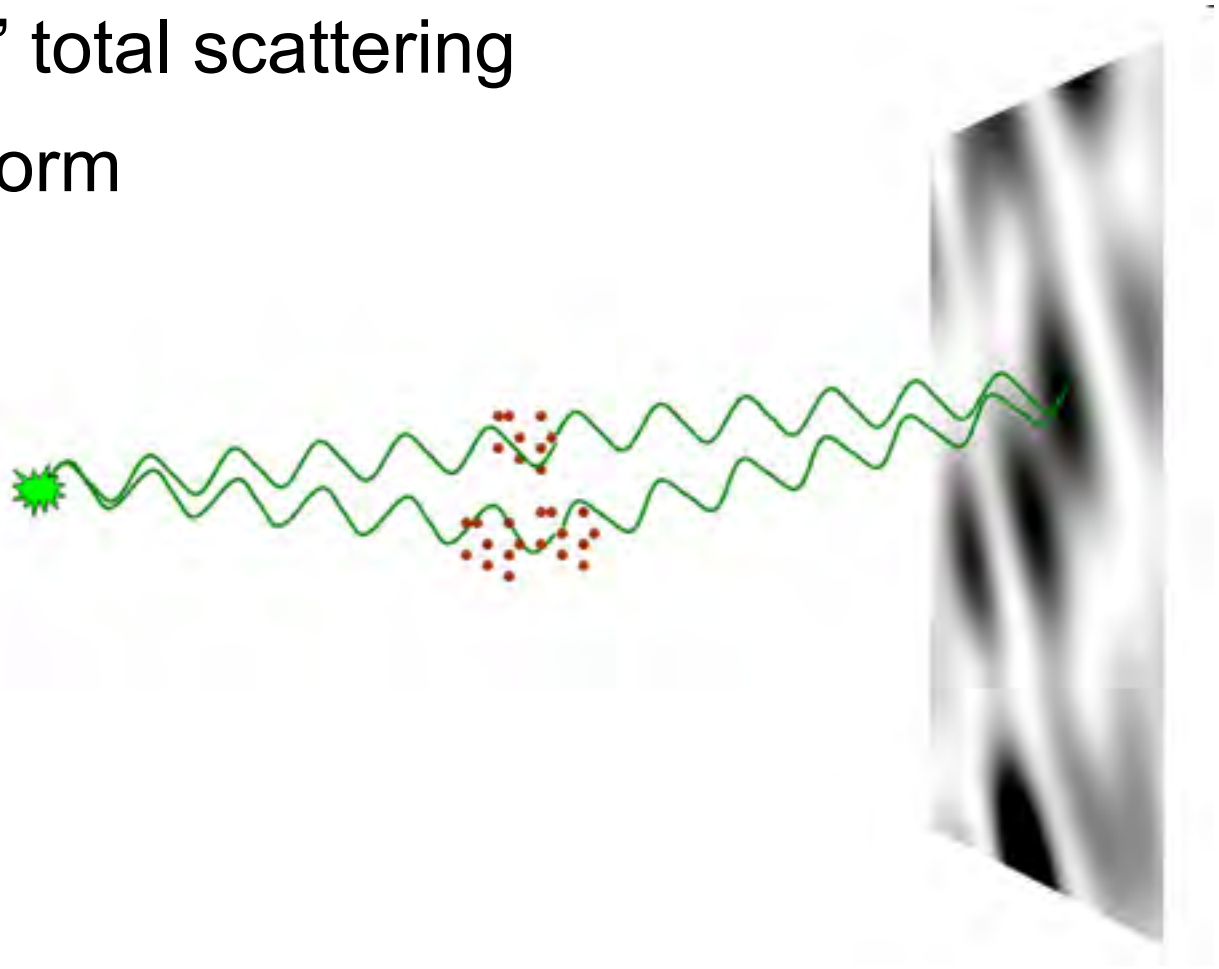

nearBragg program

http://bl831.als.lbl.gov/~jamesh/nearBragg/

- "assumption-free" total scattering
- no Fourier Transform
- no unit cells

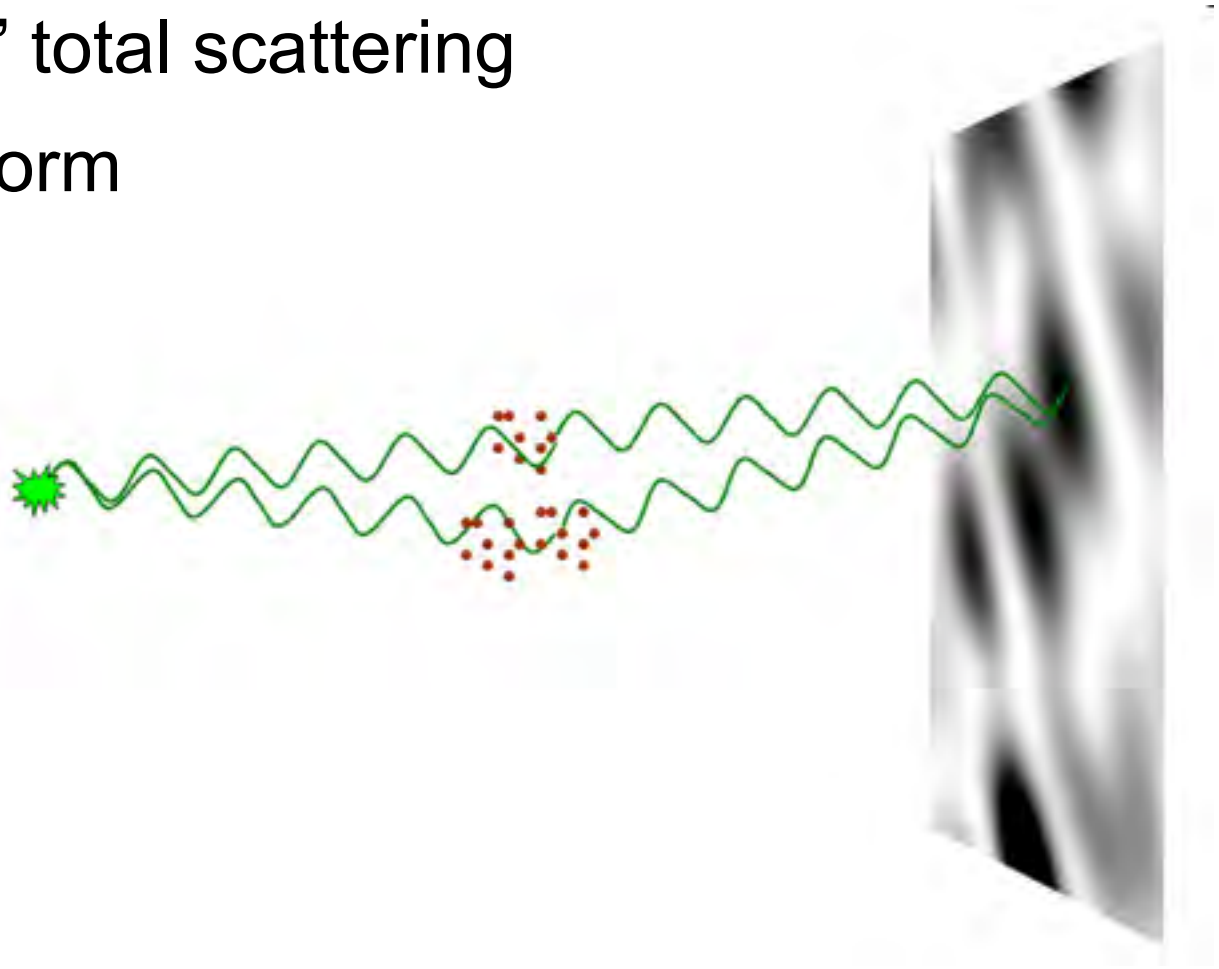

nearBragg program

http://bl831.als.lbl.gov/~jamesh/nearBragg/

- "assumption-free" total scattering
- no Fourier Transform
- no unit cells
- no "mosaicity"

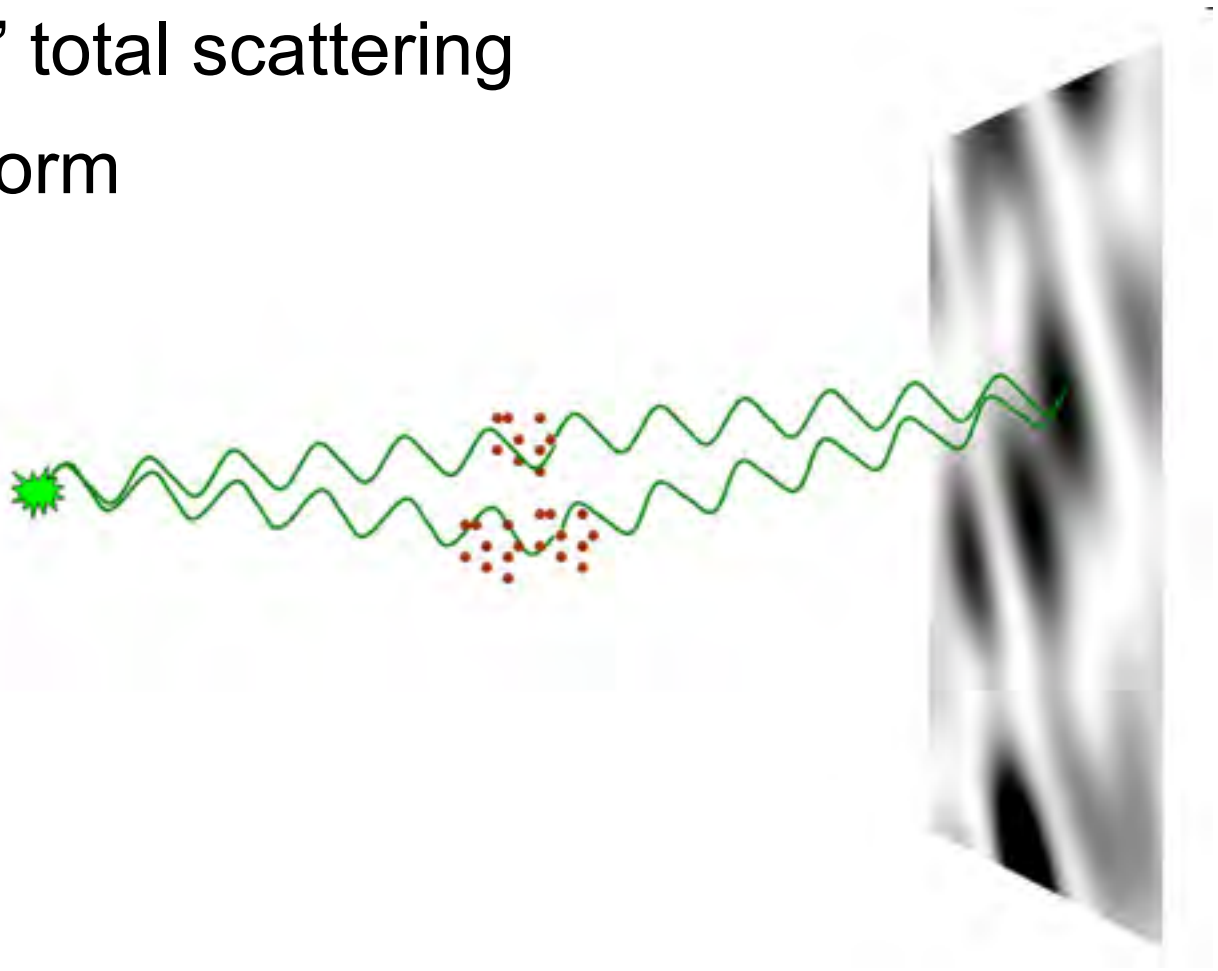

nearBragg program

http://bl831.als.lbl.gov/~jamesh/nearBragg/

- "assumption-free" total scattering
- no Fourier Transform
- no unit cells
- no "mosaicity"
- arbitrary "atoms"

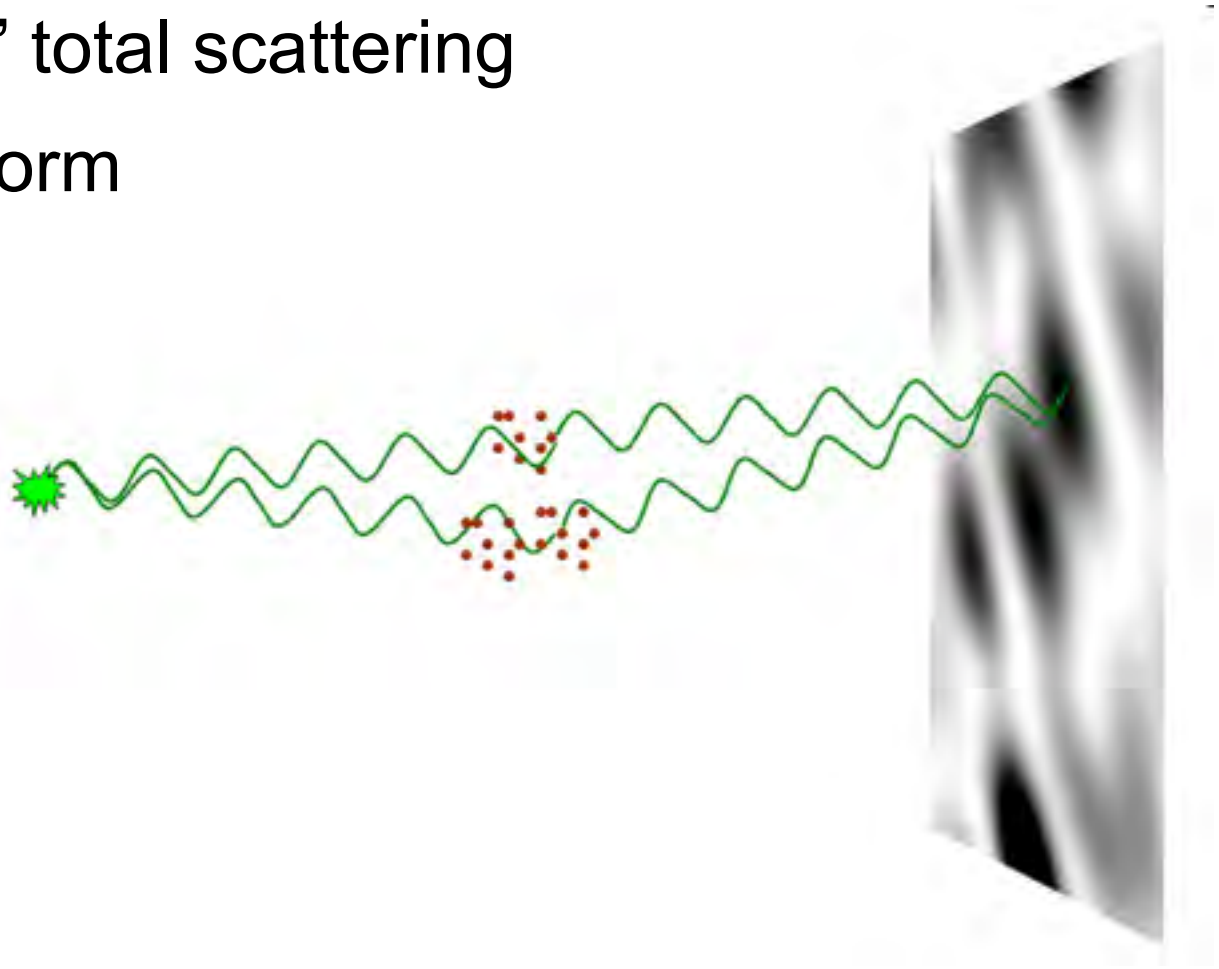

nearBragg program

http://bl831.als.lbl.gov/~jamesh/nearBragg/

- "assumption-free" total scattering
- no Fourier Transform
- no unit cells
- no "mosaicity"
- arbitrary "atoms"
- arbitrary "source"

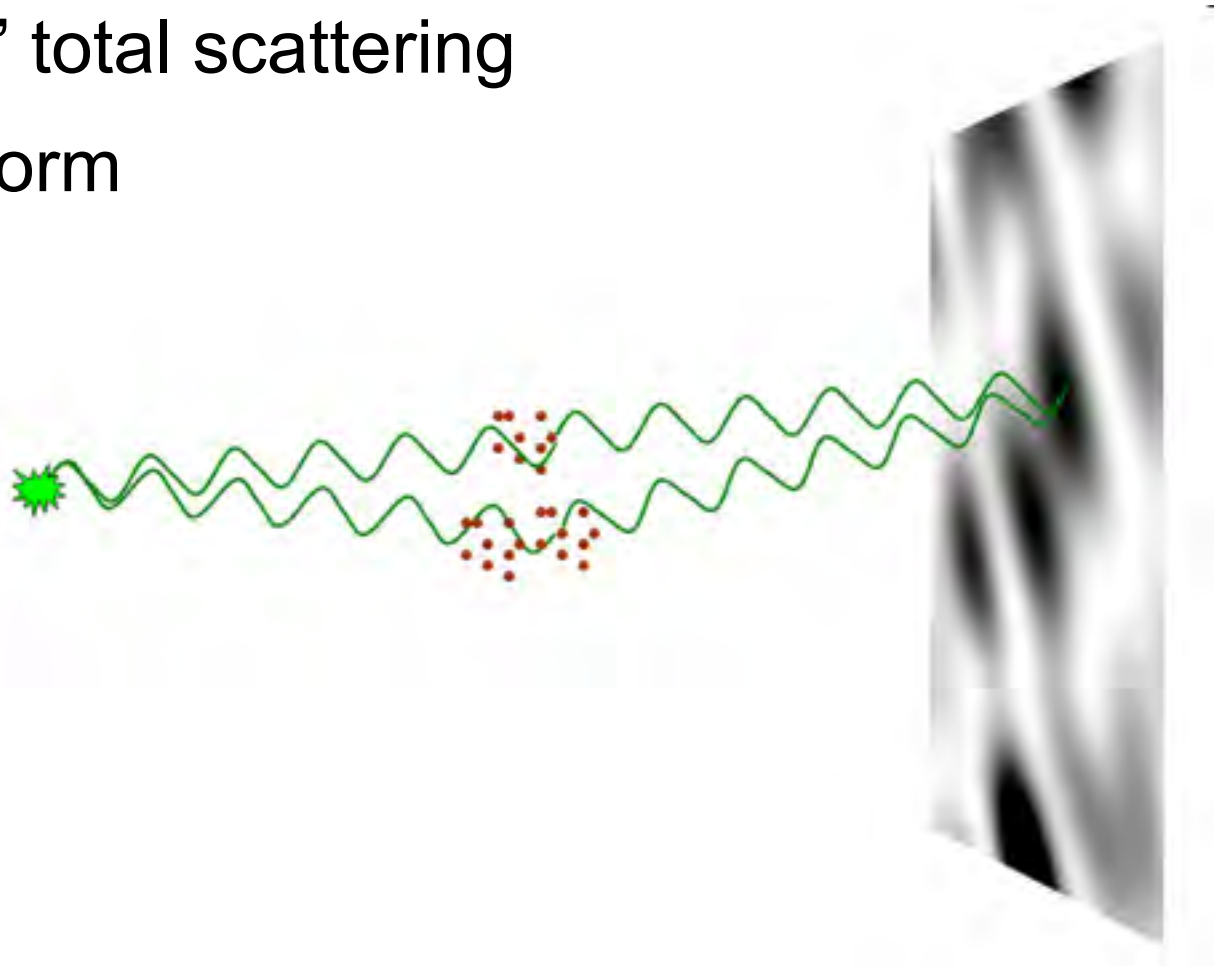

nearBragg program

http://bl831.als.lbl.gov/~jamesh/nearBragg/

- "assumption-free" total scattering
- no Fourier Transform
- no unit cells
- no "mosaicity"
- arbitrary "atoms"
- arbitrary "source"
- coherent or not

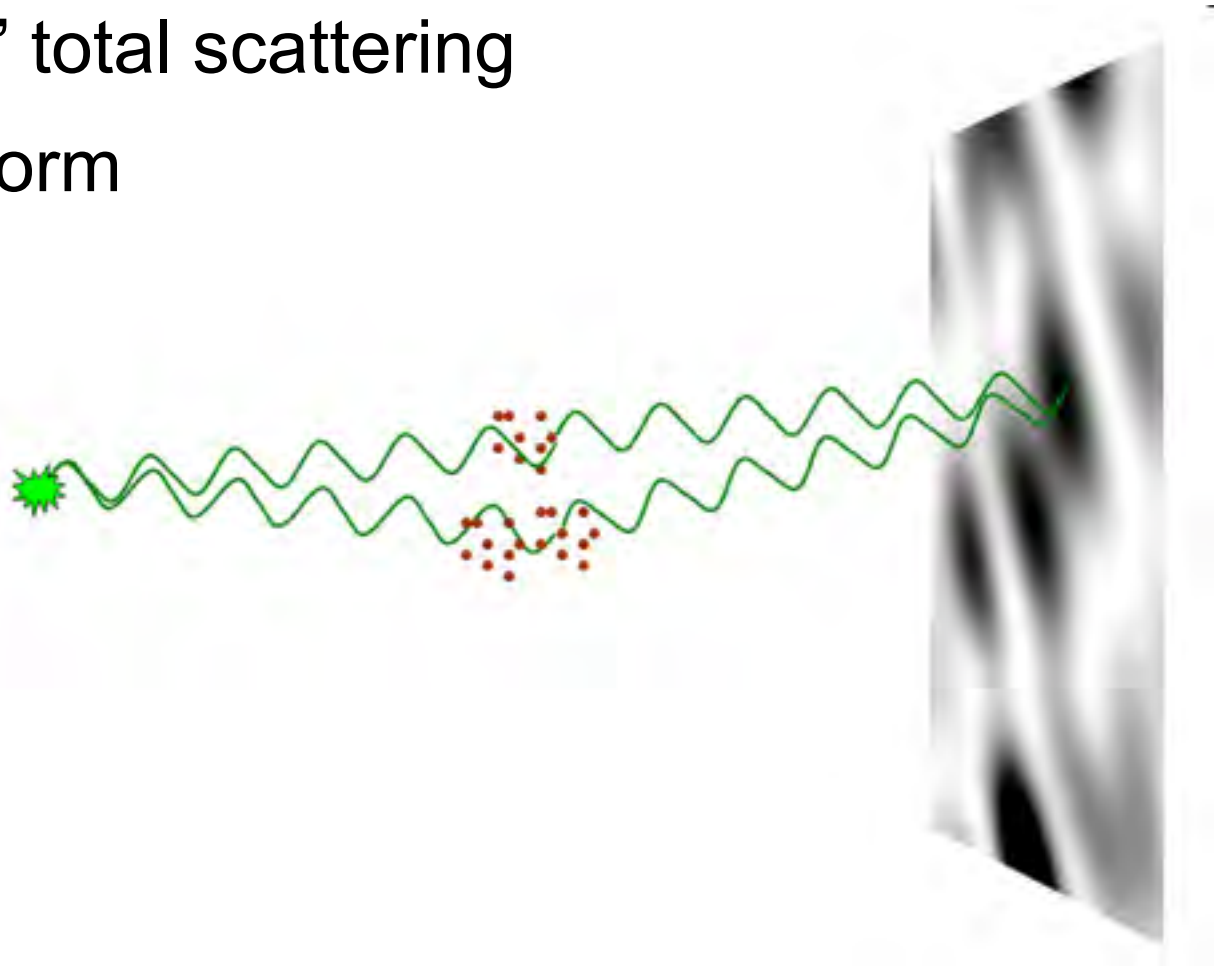

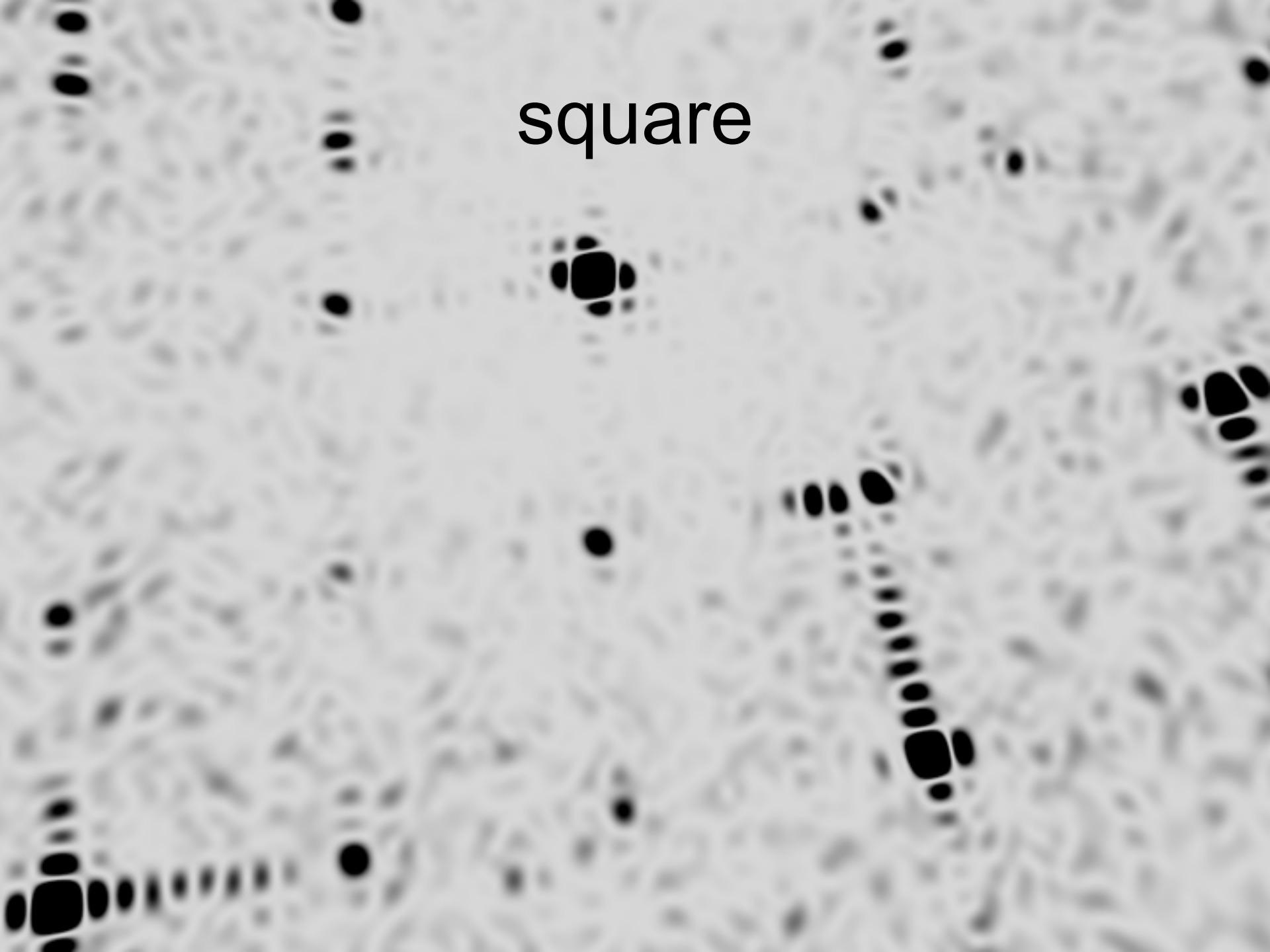
square

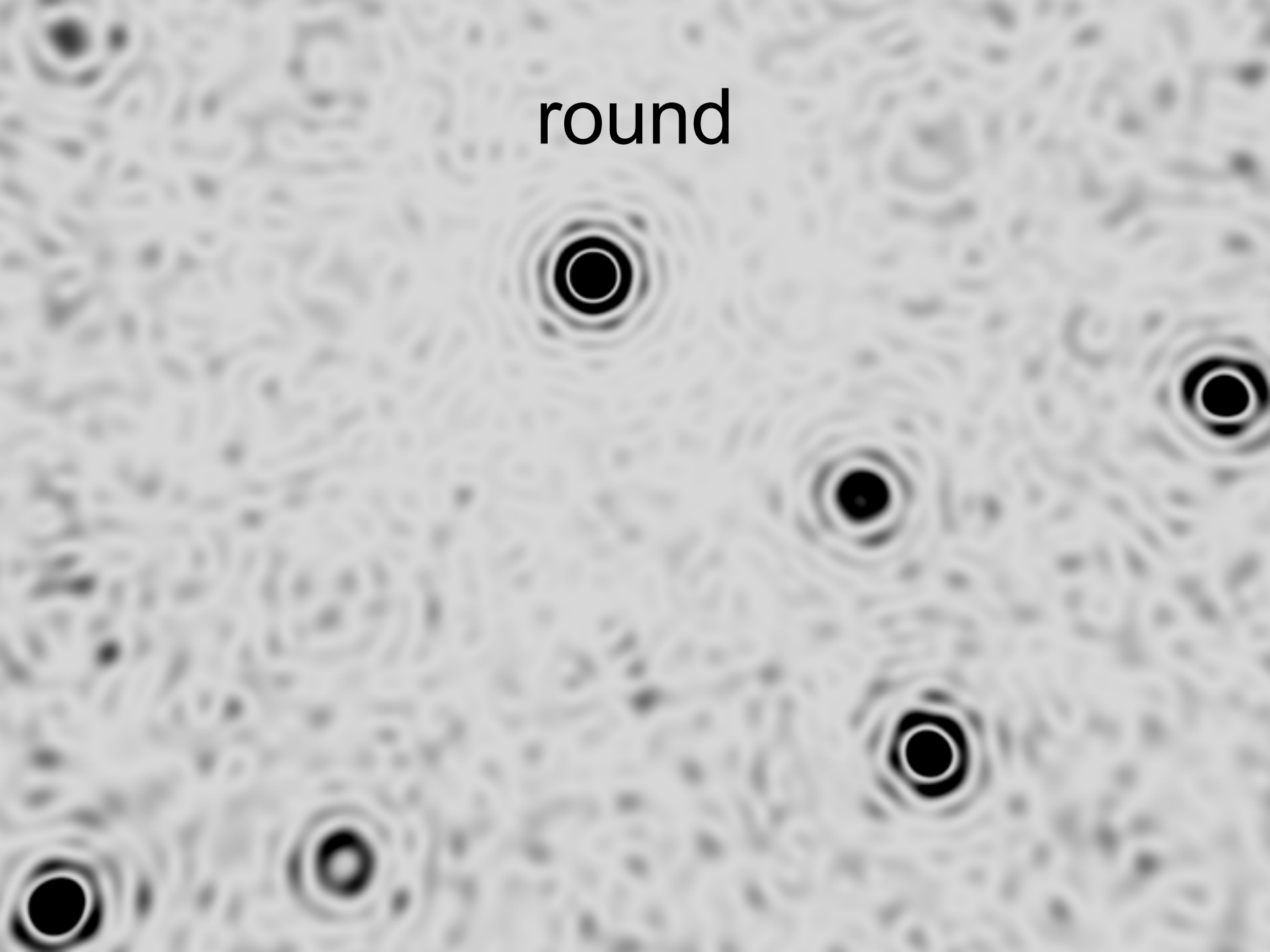
round

scattering from a crystal structure

False color intensity

sample

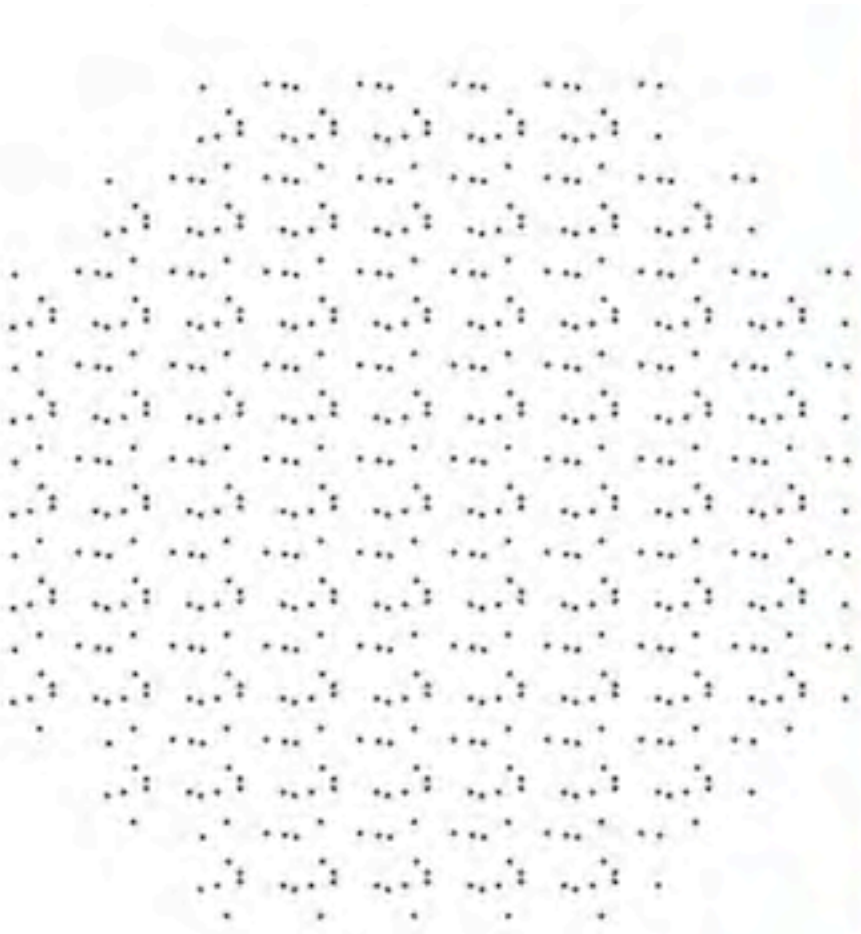

detector

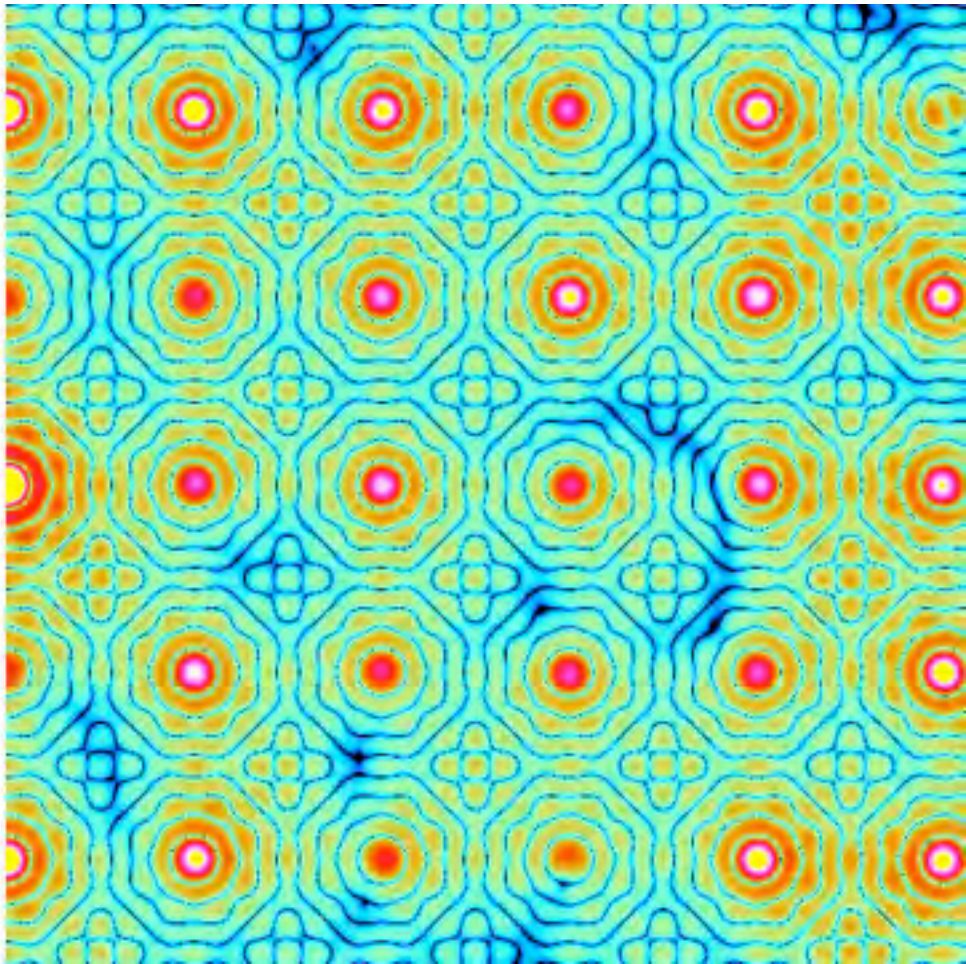

scattering from a crystal structure

False color intensity

sample

detector

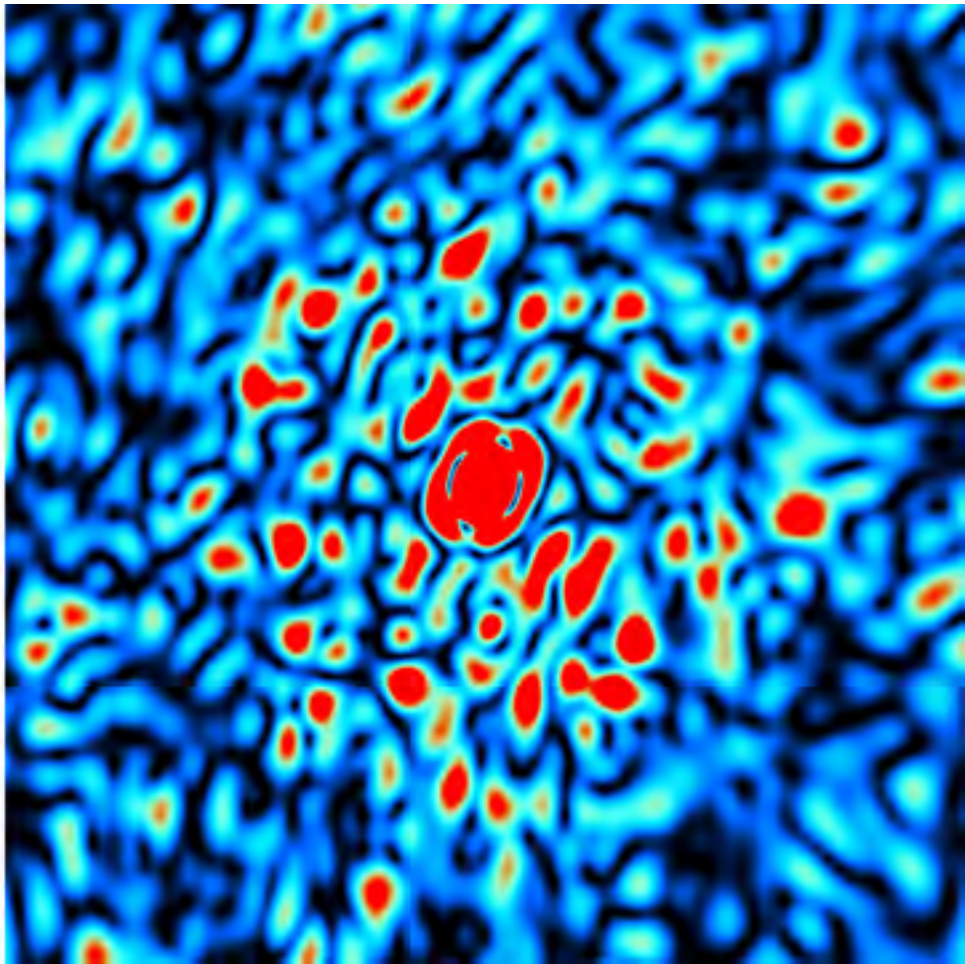

scattering from a crystal structure

False color intensity

sample

detector

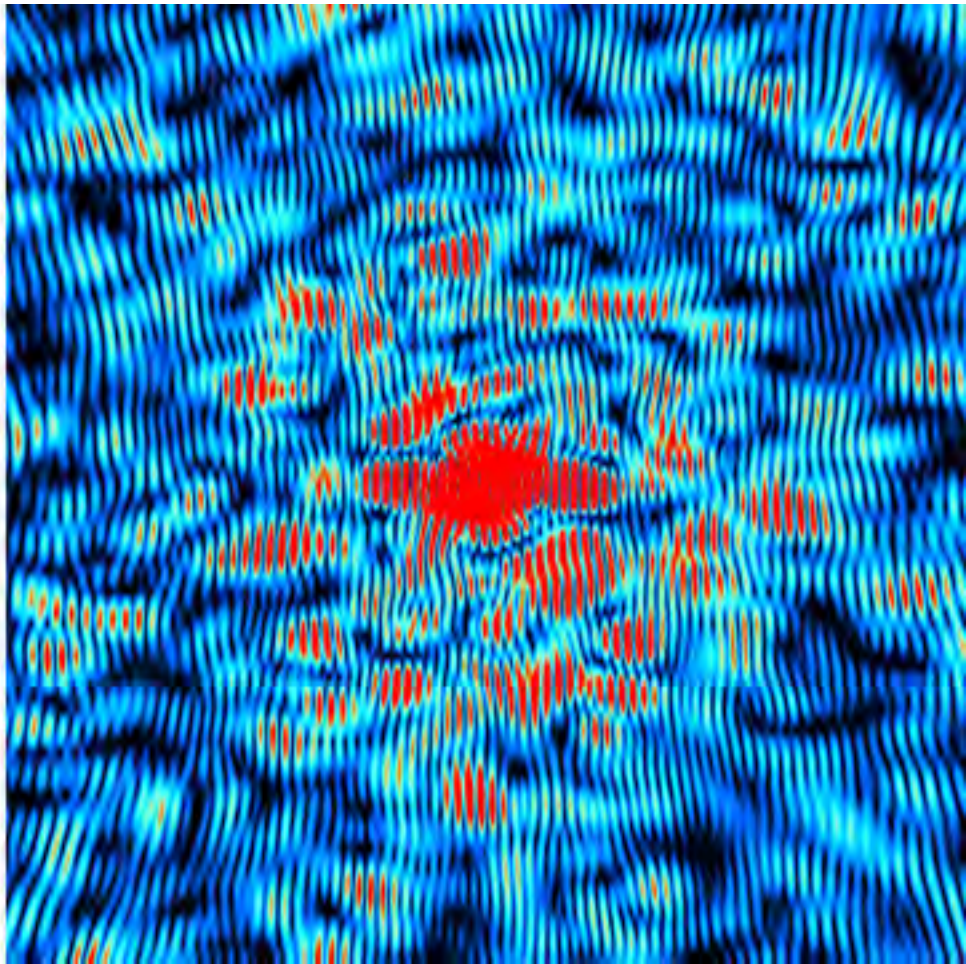

Classes of error in MX

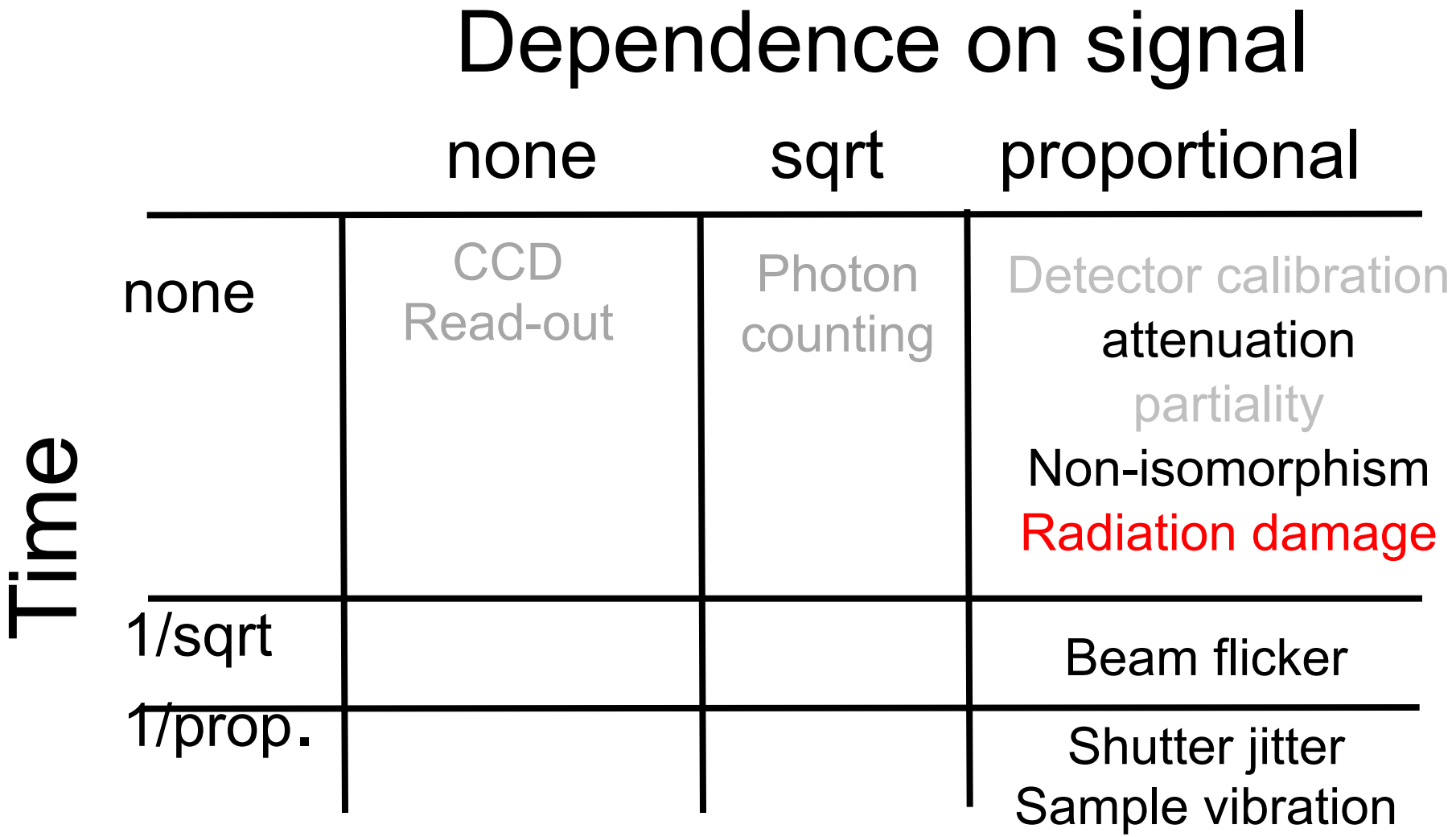

100 fs damage “threshold”

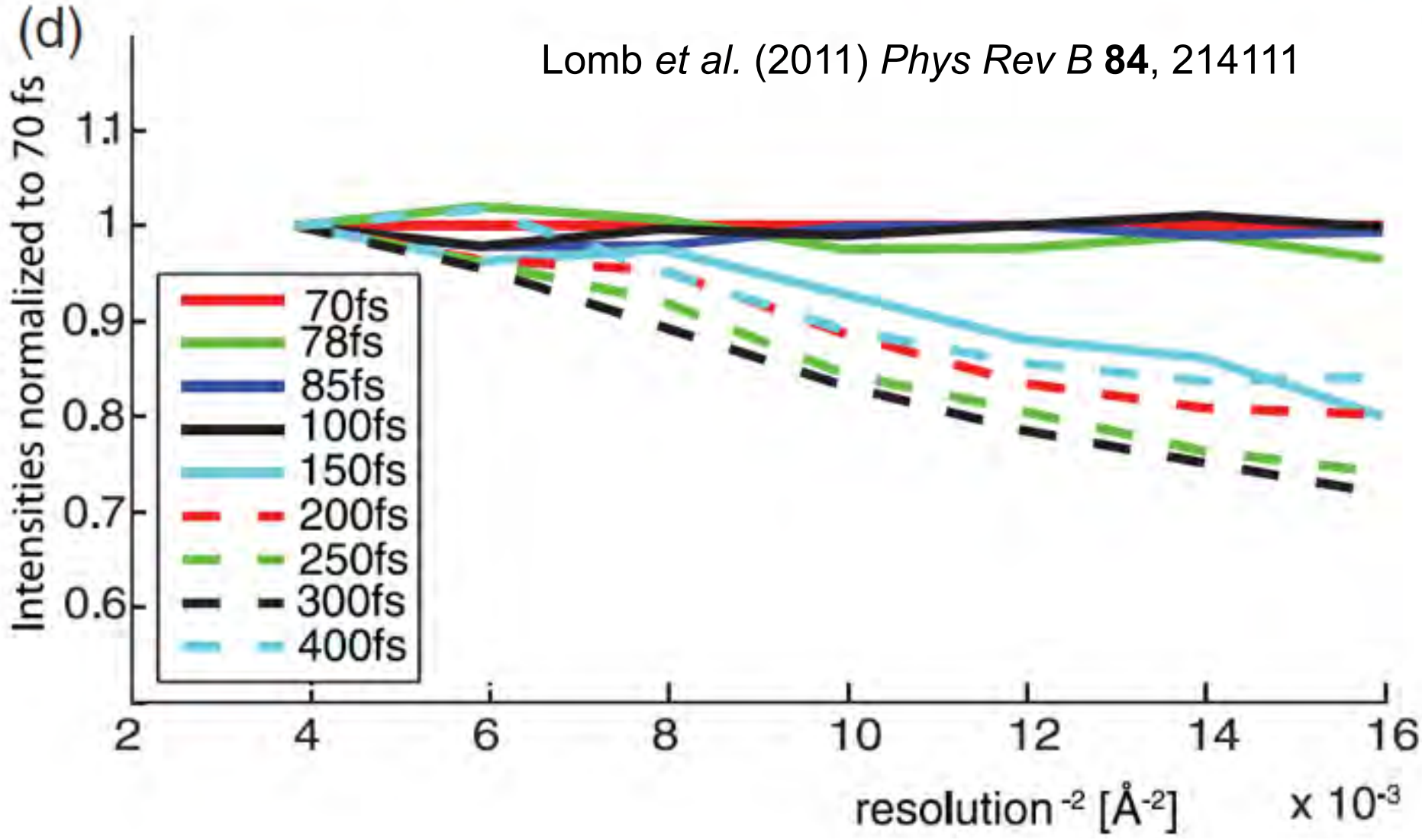

Lomb *et al.* (2011) *Phys Rev B* **84**, 214111

Rough values of energy quanta

Rough values of energy quanta

1 MeV	100 GJ/mol	Medical radiation therapy
100 keV	10 GJ/mol	Medical imaging
10 keV	1 GJ/mol	X-ray crystallography
1 keV	100 MJ/mol	S and P K-edges
100 eV	10 MJ/mol	“water window”
10 eV	1 MJ/mol	C≡C bond
1 eV	100 kJ/mol	C-C bond, visible light
100 meV	10 kJ/mol	hydrogen bond
10 meV	1 kJ/mol	heat (~300 K)

Dose-rate dependence of damage

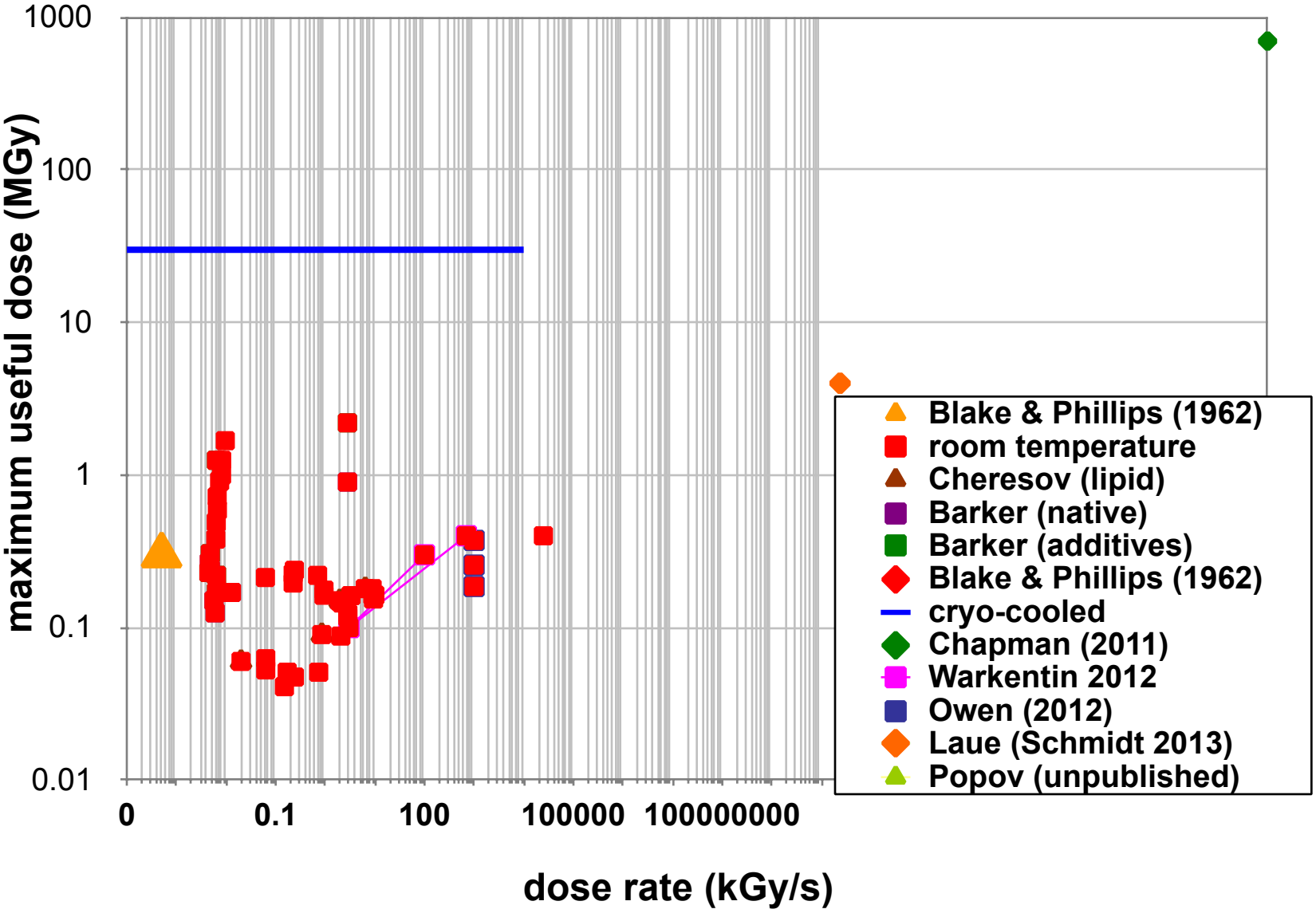

Nonisomorphism from damage

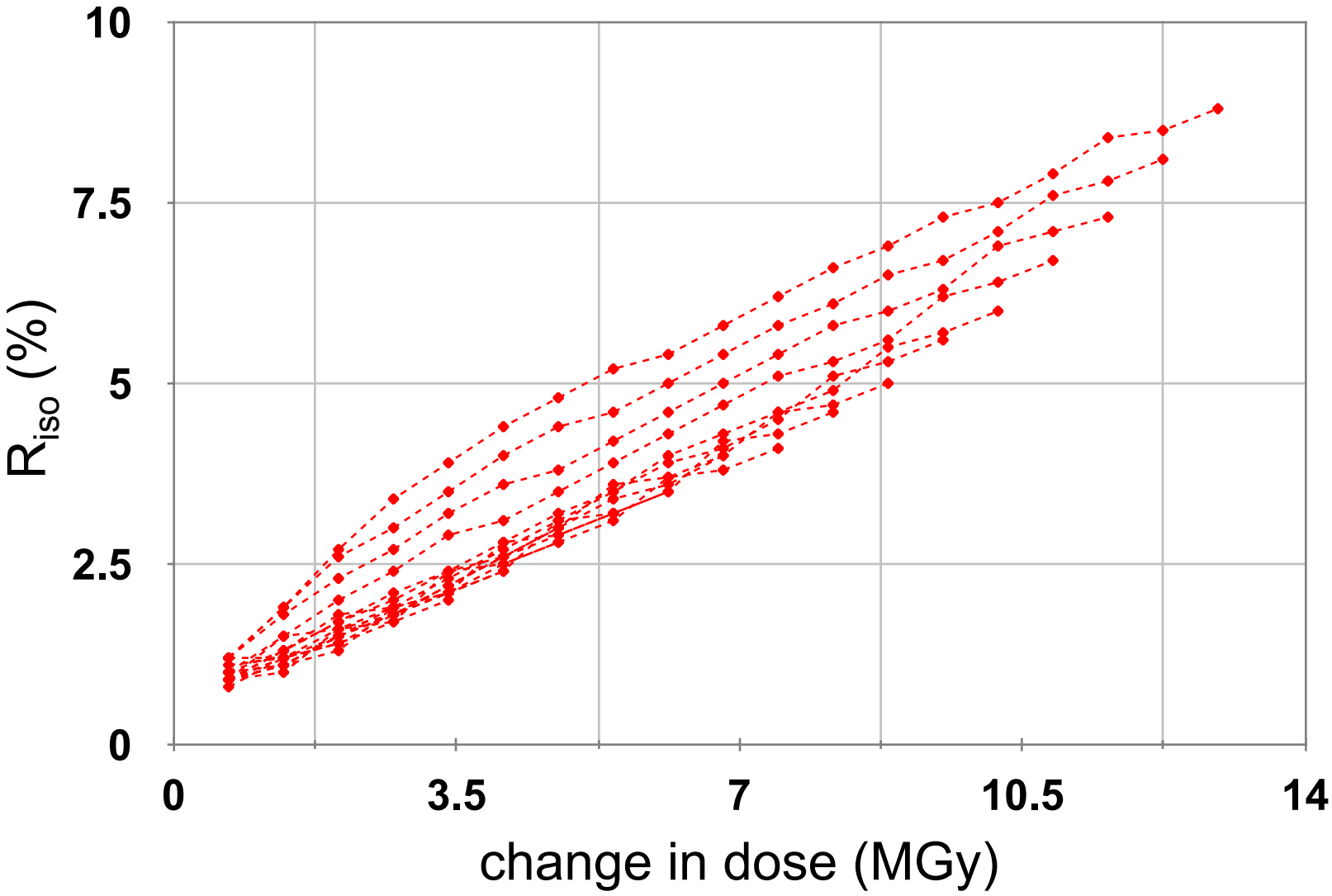

data taken from Banumathi, *et al.* (2004) *Acta Cryst. D* **60**, 1085-1093.

Nonisomorphism from damage

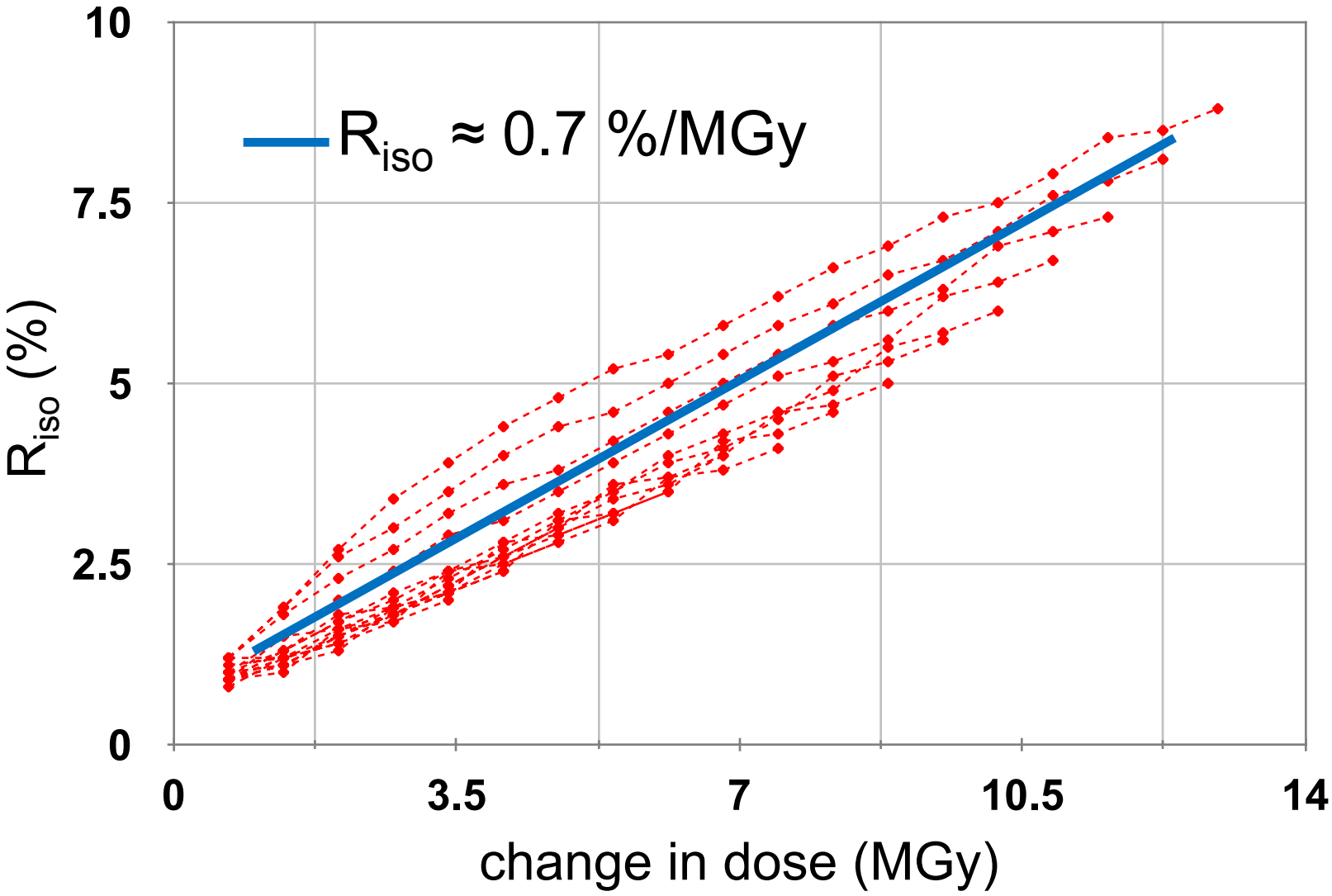

data taken from Banumathi, *et al.* (2004) *Acta Cryst. D* **60**, 1085-1093.

Classes of error in MX

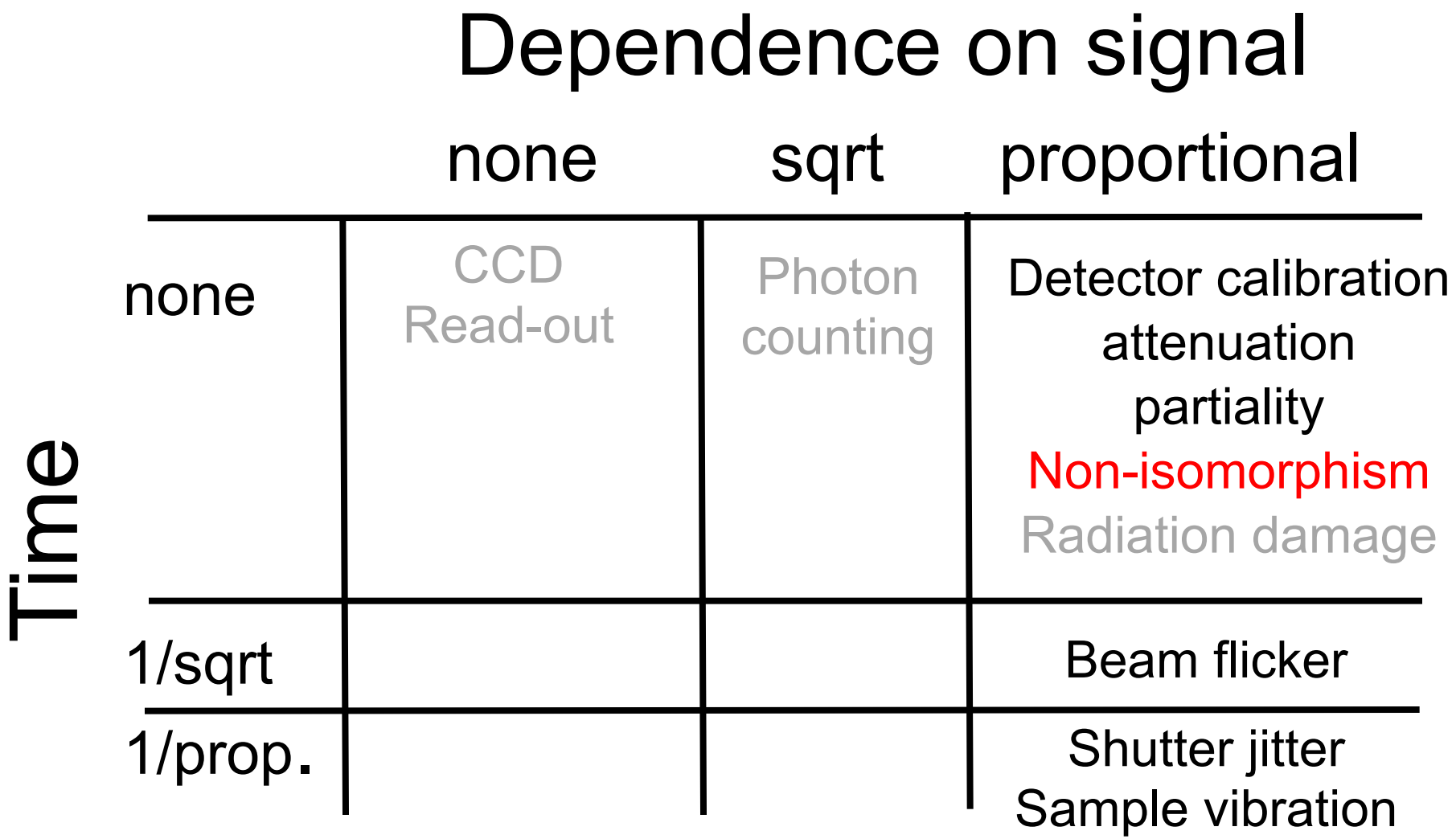

Multi-crystal strategies

The data for each derivative were recorded on twenty-two precession photographs ; a separate crystal had to be used for each photograph to keep radiation damage within acceptable limits. The results from the different photographs were scaled together on the computer, the best set of scaling factors being determined by solving an appropriate 22×22 matrix[5]. The degree of isomorphism of each derivative was tested, and found adequate, by means of a computer programme which used the $h0l$ reflexions to refine the preliminary values of the heavy-atom parameters, temperature factor, etc., and then compared the values of $\delta F_{\text{obs.}}$ and $\delta F_{\text{calc.}}$ as a function of $\sin\theta$. The co-ordinates of the heavy atoms were further refined using correlation functions[6] computed by means of programmes devised by Dr. M. G. Rossmann, and finally refined again during the process of phase determination itself. The phases were determined by essentially the same method as before, but owing to the very large

Multi-crystal strategies

The data for each derivative were recorded on twenty-two precession photographs ; a separate crystal had to be used for each photograph to keep radiation damage within acceptable limits. The results from the different photographs were scaled together on the computer, the best set of scaling factors being determined by solving an appropriate 22×22 matrix[5]. The degree of isomorphism of each derivative was tested, and found adequate, by means of a computer programme which used the $h0l$ reflexions to refine the preliminary values of the heavy-atom parameters, temperature factor, etc., and then compared the values of $\delta F_{\text{obs.}}$ and $\delta F_{\text{calc.}}$ as a function of $\sin\theta$. The co-ordinates of the heavy atoms were further refined using correlation functions[6] computed by means of programmes devised by Dr. M. G. Rossmann, and finally refined again during the process of phase determination itself. The phases were determined by essentially the same method as before, but owing to the very large

Multi-crystal strategies

The data for each derivative were recorded on twenty-two precession photographs ; a separate crystal had to be used for each photograph to keep radiation damage within acceptable limits. The results from the different photographs were scaled together on the computer, the best set of scaling factors being determined by solving an appropriate 22×22 matrix[5]. The degree of isomorphism of each derivative was tested, and found adequate, by means of a computer programme which used the $h0l$ reflexions to refine the preliminary values of the heavy-atom parameters, temperature factor, etc., and then compared the values of $\delta F_{\text{obs.}}$ and $\delta F_{\text{calc.}}$ as a function of $\sin\theta$. The co-ordinates of the heavy atoms were further refined using correlation functions[6] computed by means of programmes devised by Dr. M. G. Rossmann, and finally refined again during the process of phase determination itself. The phases were determined by essentially the same method as before, but owing to the very large

Multi-crystal strategies

The data for each derivative were recorded on twenty-two precession photographs ; a separate crystal had to be used for each photograph to keep radiation damage within acceptable limits. The results from the different photographs were scaled together on the computer, the best set of scaling factors being determined by solving an appropriate 22×22 matrix[5]. The degree of isomorphism of each derivative was tested, and found adequate, by means of a computer programme which used the $h0l$ reflexions to refine the preliminary values of the heavy-atom parameters, temperature factor, etc., and then compared the values of $\delta F_{\text{obs.}}$ and $\delta F_{\text{calc.}}$ as a function of $\sin\theta$. The co-ordinates of the heavy atoms were further refined using correlation functions[6] computed by means of programmes devised by Dr. M. G. Rossmann, and finally refined again during the process of phase determination itself. The phases were determined by essentially the same method as before, but owing to the very large

Multi-crystal strategies

The data for each derivative were recorded on twenty-two precession photographs ; a separate crystal had to be used for each photograph to keep radiation damage within acceptable limits. The results from the different photographs were scaled together on the computer, the best set of scaling factors being determined by solving an appropriate 22×22 matrix[5]. The degree of isomorphism of each derivative was tested, and found adequate, by means of a computer programme which used the $h0l$ reflexions to refine the preliminary values of the heavy-atom parameters, temperature factor, etc., and then compared the values of $\delta F_{\text{obs.}}$ and $\delta F_{\text{calc.}}$ as a function of $\sin\theta$. The co-ordinates of the heavy atoms were further refined using correlation functions[6] computed by means of programmes devised by Dr. M. G. Rossmann, and finally refined again during the process of phase determination itself. The phases were determined by essentially the same method as before, but owing to the very large

Multi-crystal strategies

The data for each derivative were recorded on twenty-two precession photographs ; a separate crystal had to be used for each photograph to keep radiation damage within acceptable limits. The results from the different photographs were scaled together on the computer, the best set of scaling factors being determined by solving an appropriate 22×22 matrix[5]. The degree of isomorphism of each derivative was tested, and found adequate, by means of a computer programme which used the $h0l$ reflexions to refine the preliminary values of the heavy-atom parameters, temperature factor, etc., and then compared the values of $\delta F_{\text{obs.}}$ and $\delta F_{\text{calc.}}$ as a function of $\sin\theta$. The co-ordinates of the heavy atoms were further refined using correlation functions[6] computed by means of programmes devised by Dr. M. G. Rossmann, and finally refined again during the process of phase determination itself. The phases were determined by essentially the same method as before, but owing to the very large

Kendrew *et al.* (1960) "Structure of Myoglobin" *Nature* **185**, 422-427.

Multi-crystal strategies

The data for each derivative were recorded on twenty-two precession photographs ; a separate crystal had to be used for each photograph to keep radiation damage within acceptable limits. The results from the different photographs were scaled together on the computer, the best set of scaling factors being determined by solving an appropriate 22×22 matrix[5]. The degree of isomorphism of each derivative was tested, and found adequate, by means of a computer programme which used the $h0l$ reflexions to refine the preliminary values of the heavy-atom parameters, temperature factor, etc., and then compared the values of $\delta F_{\text{obs.}}$ and $\delta F_{\text{calc.}}$ as a function of $\sin\theta$. The co-ordinates of the heavy atoms were further refined using correlation functions[6] computed by means of programmes devised by Dr. M. G. Rossmann, and finally refined again during the process of phase determination itself. The phases were determined by essentially the same method as before, but owing to the very large

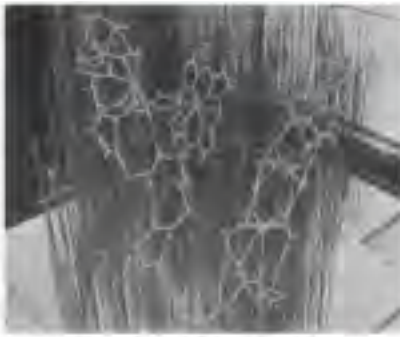

Kendrew *et al.* (1960) "Structure of Myoglobin" *Nature* **185**, 422-427.

Multi-crystal strategies

The data for each derivative were recorded on twenty-two precession photographs; a separate crystal had to be used for each photograph to keep radiation damage within acceptable limits. The results from the different photographs were scaled together on the computer, the best set of scaling factors being determined by solving an appropriate 22×22 matrix[5]. The degree of isomorphism of each derivative was tested, and found adequate, by means of a computer programme which used the $h0l$ reflexions to refine the preliminary values of the heavy-atom parameters, temperature factor, etc., and then compared the values of $\delta F_{obs.}$ and $\delta F_{calc.}$ as a function of $\sin\theta$. The co-ordinates of the heavy atoms were further refined using correlation functions[6] computed by means of programmes devised by Dr. M. G. Rossmann, and finally refined again during the process of phase determination itself. The phases were determined by essentially the same method as before, but owing to the very large

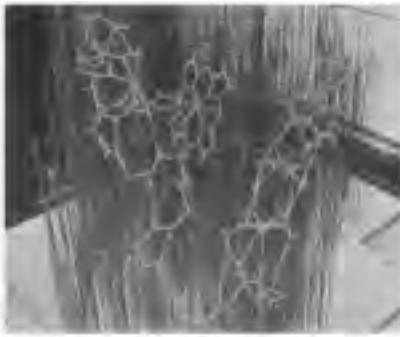

Kendrew *et al.* (1960) "Structure of Myoglobin" *Nature* **185**, 422-427.

Multi-crystal strategies

The data for each derivative were recorded on twenty-two precession photographs; a separate crystal had to be used for each photograph to keep radiation damage within acceptable limits. The results from the different photographs were scaled together on the computer, the best set of scaling factors being determined by solving an appropriate 22×22 matrix[5]. The degree of isomorphism of each derivative was tested, and found adequate, by means of a computer programme which used the $h0l$ reflexions to refine the preliminary values of the heavy-atom parameters, temperature factor, etc., and then compared the values of $\delta F_{obs.}$ and $\delta F_{calc.}$ as a function of $\sin\theta$. The co-ordinates of the heavy atoms were further refined using correlation functions[6] computed by means of programmes devised by Dr. M. G. Rossmann, and finally refined again during the process of phase determination itself. The phases were determined by essentially the same method as before, but owing to the very large

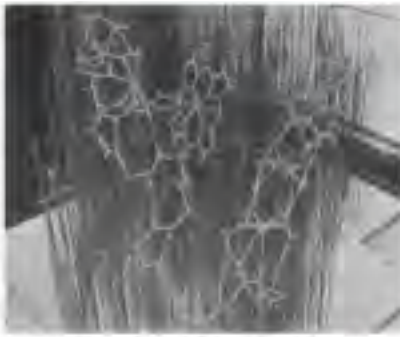

Kendrew *et al.* (1960) "Structure of Myoglobin" *Nature* **185**, 422-427.

The sources of inaccuracy in isomorphous replacement may be classed as follows:

(1) Errors due to technical limitations, e.g. variation of X-ray intensity of the source, absorption errors, setting errors, errors in measuring intensities, and so forth.
(2) Changes due to lack of strict isomorphism, apparently due to variation in the composition of the solvent and to the added molecules.
(3) Errors due to slight changes in the vapor pressure surrounding the crystal. This produces the new shrinkage phenomenon already mentioned.

We can summarize our results by saying that the errors due to (3) can under certain circumstances be considerable, but can be eliminated; that errors due to (1) are usually very small; but those due to (2) appear difficult to avoid in the case of ribonuclease II, and will probably be the limiting factor in a structure determination by isomorphous replacement.

Magdoff & Crick (1955) “Ribonuclease II. Accuracy of measurement and shrinkage”, *Acta Cryst.* **8**, 461-8.

The sources of inaccuracy in isomorphous replacement may be classed as follows:

(1) Errors due to technical limitations, e.g. variation of X-ray intensity of the source, absorption errors, setting errors, errors in measuring intensities, and so forth.

(2) Changes due to lack of strict isomorphism, apparently due to variation in the composition of the solvent and to the added molecules.

(3) Errors due to slight changes in the vapor pressure surrounding the crystal. This produces the new shrinkage phenomenon already mentioned.

We can summarize our results by saying that the errors due to (3) can under certain circumstances be considerable, but can be eliminated; that errors due to (1) are usually very small; but those due to (2) appear difficult to avoid in the case of ribonuclease II, and will probably be the limiting factor in a structure determination by isomorphous replacement.

Magdoff & Crick (1955) “Ribonuclease II. Accuracy of measurement and shrinkage”, *Acta Cryst.* **8**, 461-8.

The sources of inaccuracy in isomorphous replacement may be classed as follows:

(1) Errors due to technical limitations, e.g. variation of X-ray intensity of the source, absorption errors, setting errors, errors in measuring intensities, and so forth.

(2) Changes due to lack of strict isomorphism, apparently due to variation in the composition of the solvent and to the added molecules.

(3) Errors due to slight changes in the vapor pressure surrounding the crystal. This produces the new shrinkage phenomenon already mentioned.

We can summarize our results by saying that the errors due to (3) can under certain circumstances be considerable, but can be eliminated; that errors due to (1) are usually very small; but those due to (2) appear difficult to avoid in the case of ribonuclease II, and will probably be the limiting factor in a structure determination by isomorphous replacement.

Magdoff & Crick (1955) “Ribonuclease II. Accuracy of measurement and shrinkage”, *Acta Cryst.* **8**, 461-8.

The sources of inaccuracy in isomorphous replacement may be classed as follows:

(1) Errors due to technical limitations, e.g. variation of X-ray intensity of the source, absorption errors, setting errors, errors in measuring intensities, and so forth.

(2) Changes due to lack of strict isomorphism, apparently due to variation in the composition of the solvent and to the added molecules.

(3) Errors due to slight changes in the vapor pressure surrounding the crystal. This produces the new shrinkage phenomenon already mentioned.

We can summarize our results by saying that the errors due to (3) can under certain circumstances be considerable, but can be eliminated; that errors due to (1) are usually very small; but those due to (2) appear difficult to avoid in the case of ribonuclease II, and will probably be the limiting factor in a structure determination by isomorphous replacement.

Magdoff & Crick (1955) “Ribonuclease II. Accuracy of measurement and shrinkage”, *Acta Cryst.* **8**, 461-8.

The sources of inaccuracy in isomorphous replacement may be classed as follows:

(1) Errors due to technical limitations, e.g. variation of X-ray intensity of the source, absorption errors, setting errors, errors in measuring intensities, and so forth.

(2) Changes due to lack of strict isomorphism, apparently due to variation in the composition of the solvent and to the added molecules.

(3) Errors due to slight changes in the vapor pressure surrounding the crystal. This produces the new shrinkage phenomenon already mentioned.

We can summarize our results by saying that the errors due to (3) can under certain circumstances be considerable, but can be eliminated; that errors due to (1) are usually very small; but those due to (2) appear difficult to avoid in the case of ribonuclease II, and will probably be the limiting factor in a structure determination by isomorphous replacement.

Magdoff & Crick (1955) “Ribonuclease II. Accuracy of measurement and shrinkage”, *Acta Cryst.* **8**, 461-8.

Crick & Magdoff (1956) “The theory of the method of isomorphous replacement for protein crystals”, *Acta Cryst.* **9**, 901-8.

Non-isomorphism in lysozyme

RH 84.2% vs 71.9%

Non-isomorphism in lysozyme

RH 84.2% vs 71.9% RMSD = 0.18 Å

Non-isomorphism in lysozyme

RH 84.2% vs 71.9% RMSD = 0.18 Å R_{iso} = 44.5%

Non-isomorphism in lysozyme

Dear James

The story of the two forms of lysozyme crystals goes back to about 1964 when it was found that the diffraction patterns from different crystals could be placed in one of two classes depending on their intensities. This discovery was a big set back at the time and I can remember a lecture title being changed from the 'The structure of lysozyme' to 'The structure of lysozyme two steps forward and one step back'. Thereafter the crystals were screened based on intensities of the (11,11,l) rows to distinguish them (e.g. 11,11,4 > 11,11,5 in one form and vice versa in another). Data were collected only for those that fulfilled the Type II criteria. (These reflections were easy to measure on the linear diffractometer because crystals were mounted to rotate about the diagonal axis). As I recall both Type I and Type II could be found in the same crystallisation batch . Although sometimes the external morphology allowed recognition this was not infallible.

The structure was based on Type II crystals. Later a graduate student Helen Handoll examined Type I. The work, which was in the early days and before refinement programmes, seemed to suggest that the differences lay in the arrangement of water or chloride molecules (Lysozyme was crystallised from NaCl). But the work was never written up. Keith Wilson at one stage was following this up as lysozyme was being used to test data collection strategies but I do not know the outcome.

An account of this is given in International Table Volume F (Rossmann and Arnold edited 2001) p760.

Tony North was much involved in sorting this out and if you wanted more info he would be the person to contact. I hope this is helpful. Do let me know if you need more.

Best wishes

Louise

Non-isomorphism in lysozyme

Dear James

The story of the two forms of lysozyme crystals goes back to about 1964 when it was found that the diffraction patterns from different crystals could be placed in one of two classes depending on their intensities. This discovery was a big set back at the time and I can remember a lecture title being changed from the 'The structure of lysozyme' to 'The structure of lysozyme two steps forward and one step back'. Thereafter the crystals were screened based on intensities of the (11,11,l) rows to distinguish them (e.g. 11,11,4 > 11,11,5 in one form and vice versa in another). Data were collected only for those that fulfilled the Type II criteria. (These reflections were easy to measure on the linear diffractometer because crystals were mounted to rotate about the diagonal axis). As I recall both Type I and Type II could be found in the same crystallisation batch . Although sometimes the external morphology allowed recognition this was not infallible.

The structure was based on Type II crystals. Later a graduate student Helen Handoll examined Type I. The work, which was in the early days and before refinement programmes, seemed to suggest that the differences lay in the arrangement of water or chloride molecules (Lysozyme was crystallised from NaCl). But the work was never written up. Keith Wilson at one stage was following this up as lysozyme was being used to test data collection strategies but I do not know the outcome.

An account of this is given in International Table Volume F (Rossmann and Arnold edited 2001) p760.

Tony North was much involved in sorting this out and if you wanted more info he would be the person to contact. I hope this is helpful. Do let me know if you need more.

Best wishes

Louise

“same drop” ?

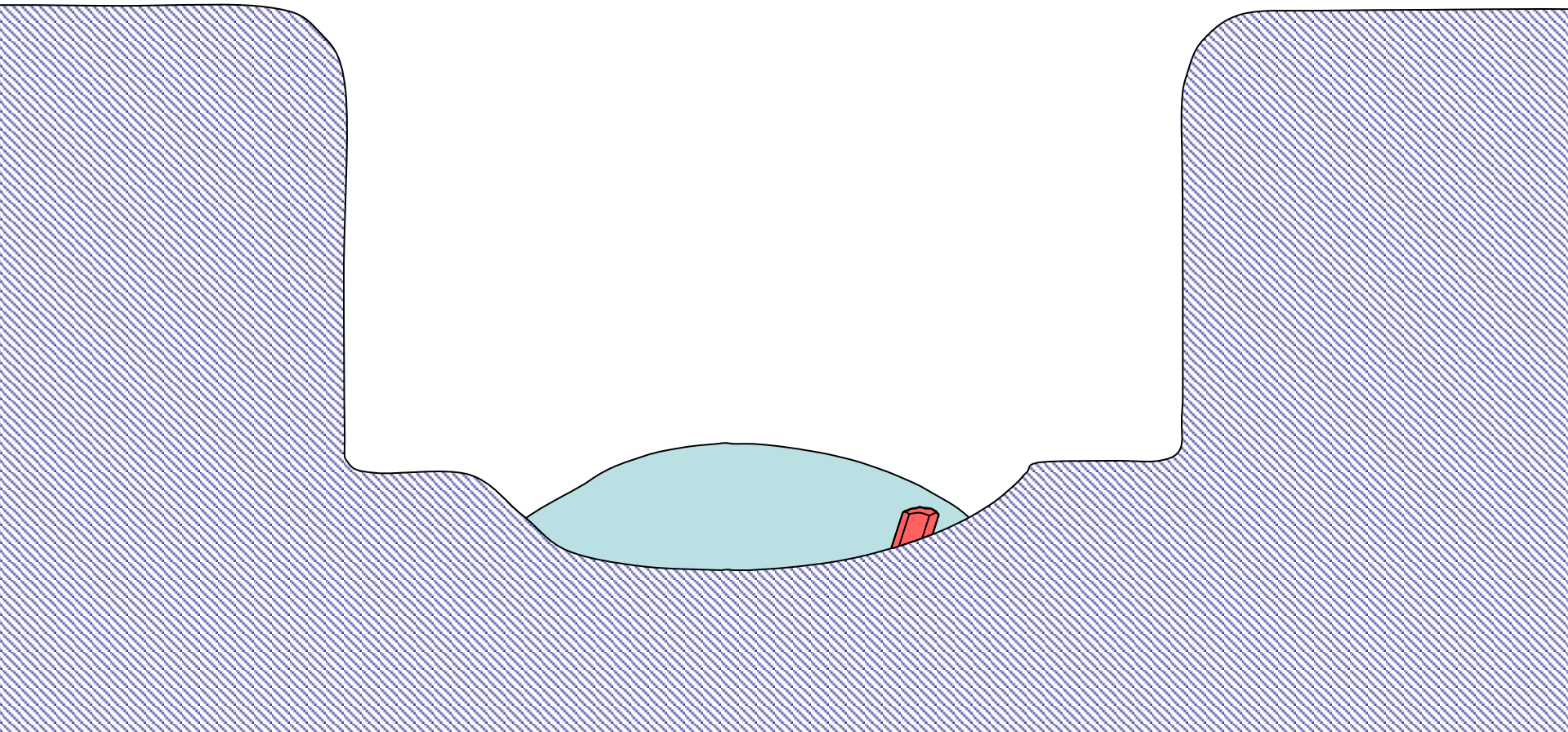

“same drop” ?

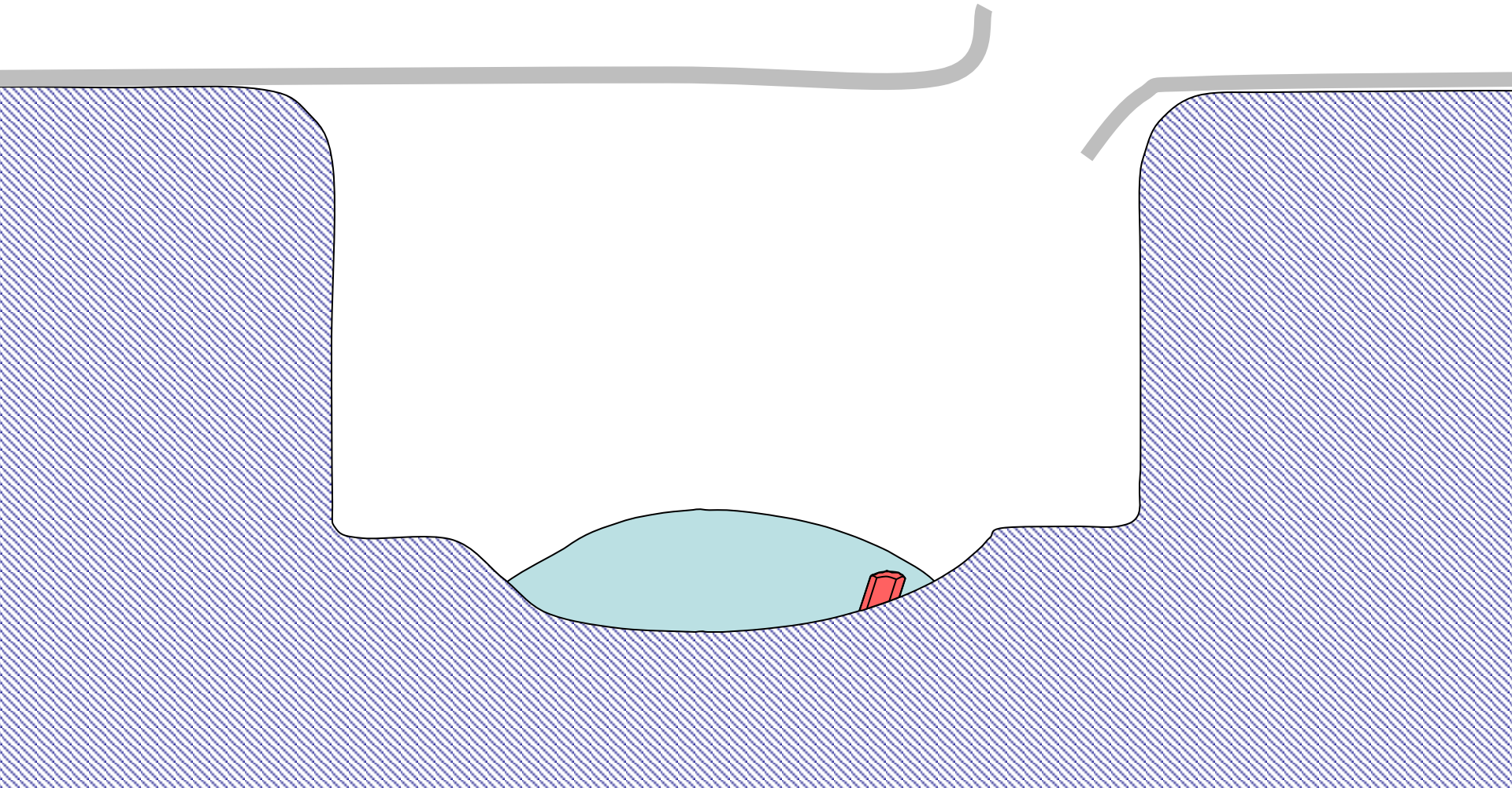

“same drop” ?

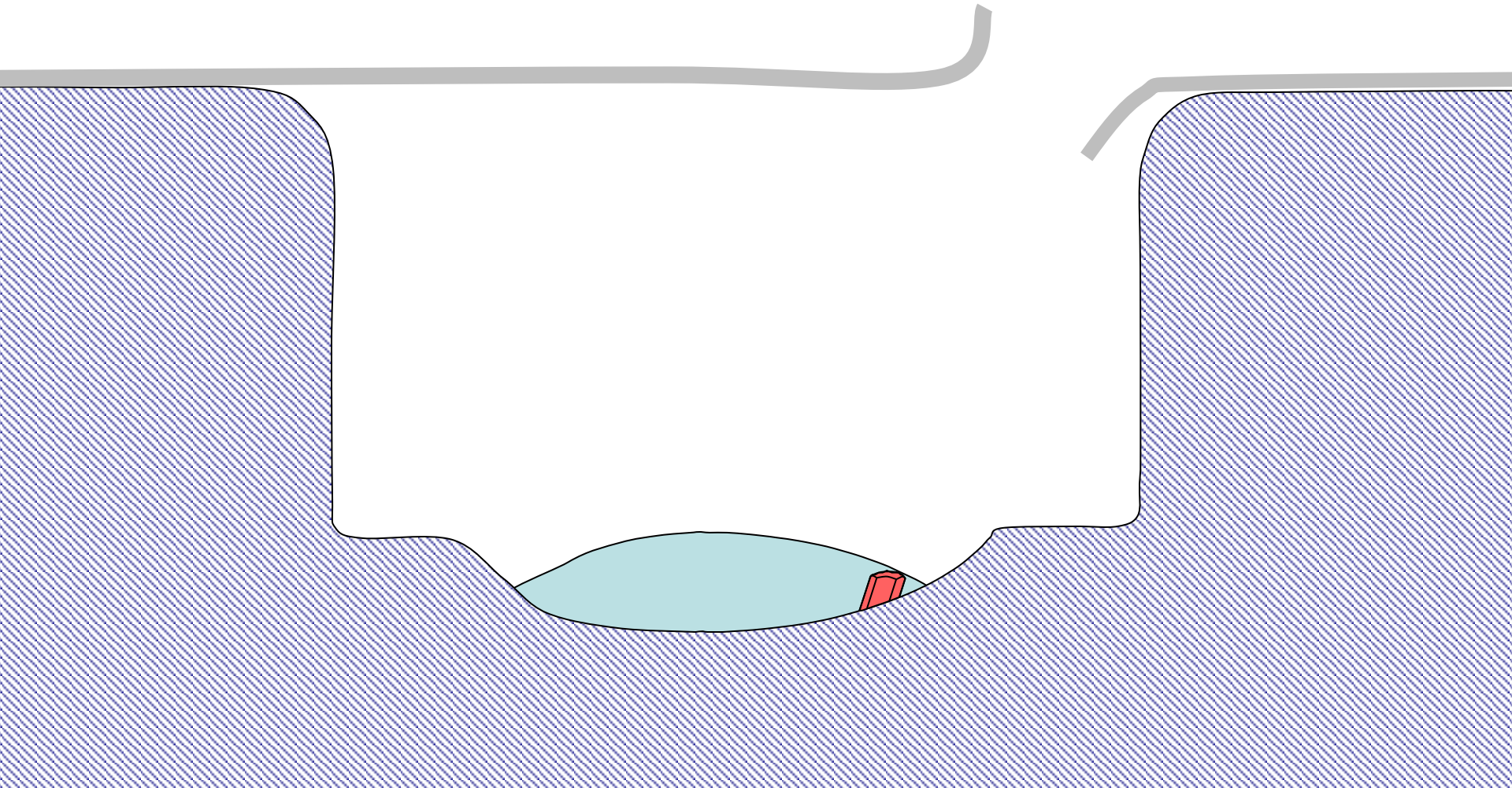

Elastic deformation
= non-isomorphism

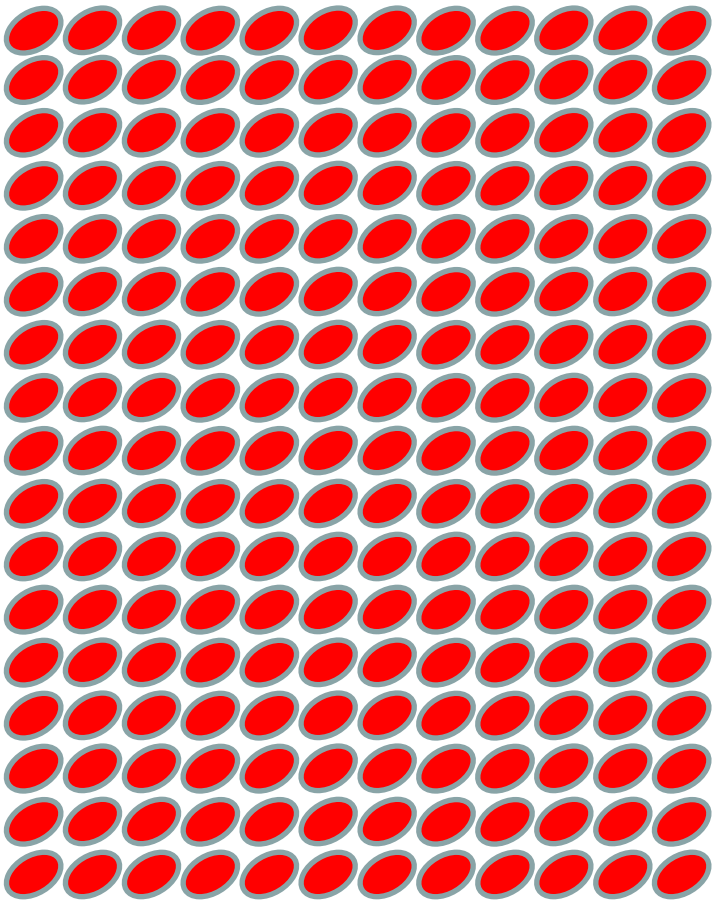

Elastic deformation
= non-isomorphism

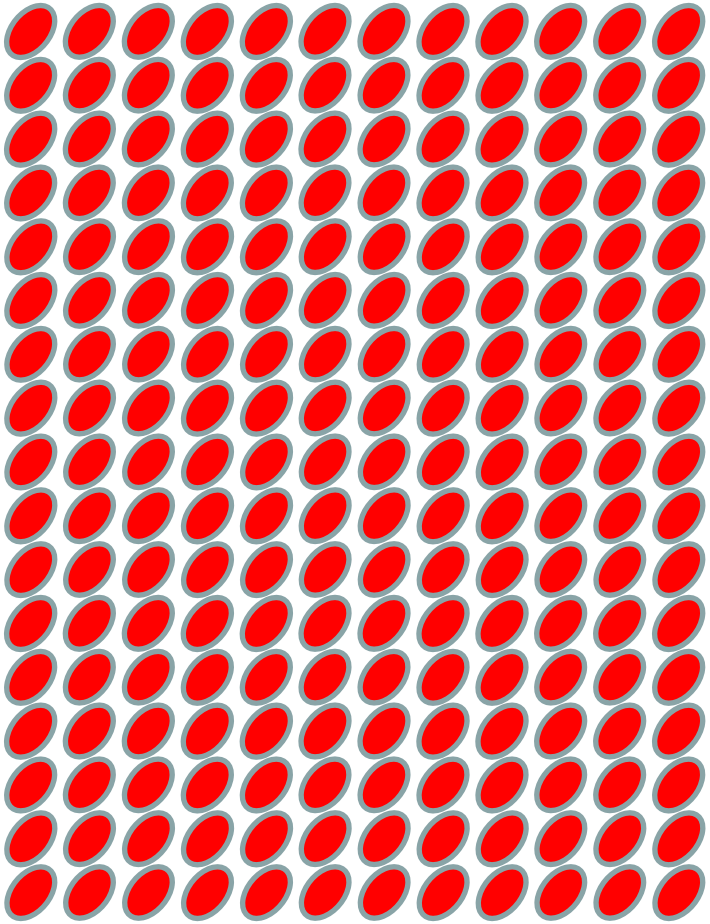

Plastic deformation = poor diffraction

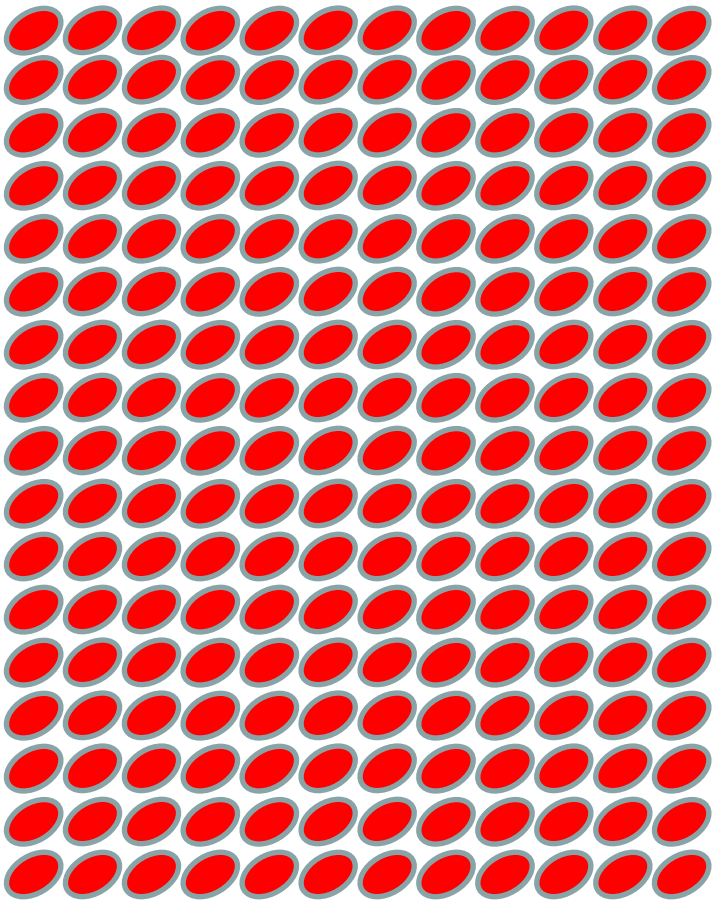

Plastic deformation = poor diffraction

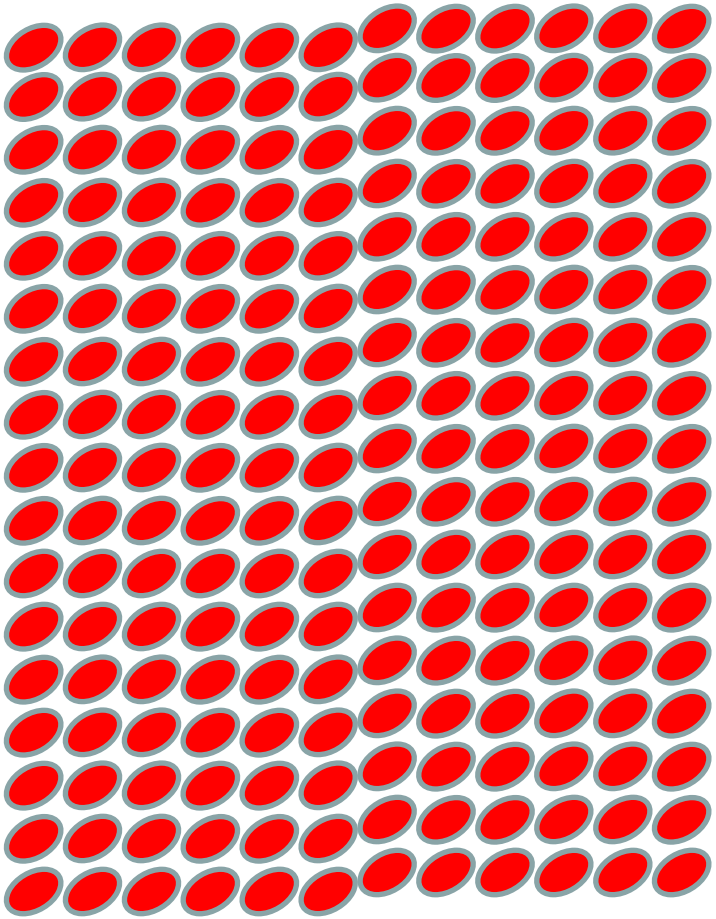

Vicker's hardness

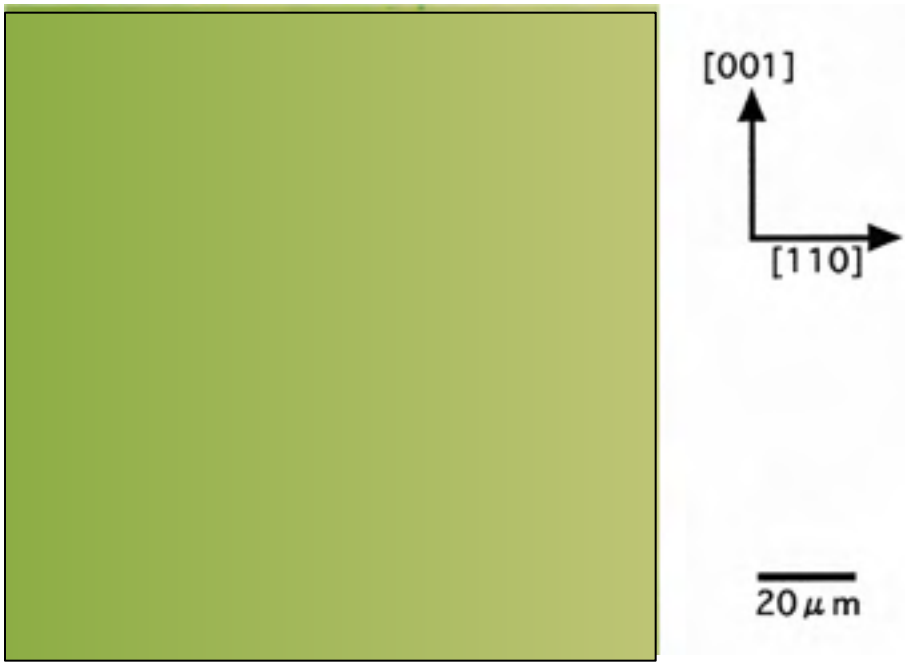

Tachibana *et al.* (1999) *J. Cryst. Growth* **198**, 661-664.
Koizumi *et al.* (2009) *Physical Review E* **79**, 61917.

Vicker's hardness

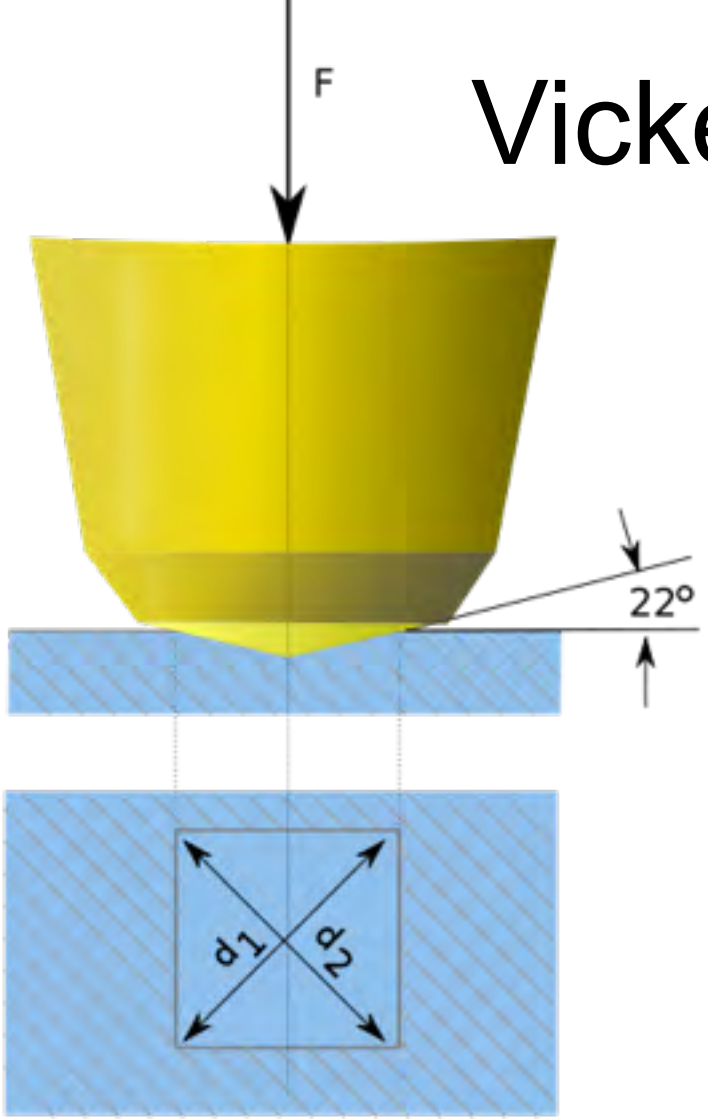

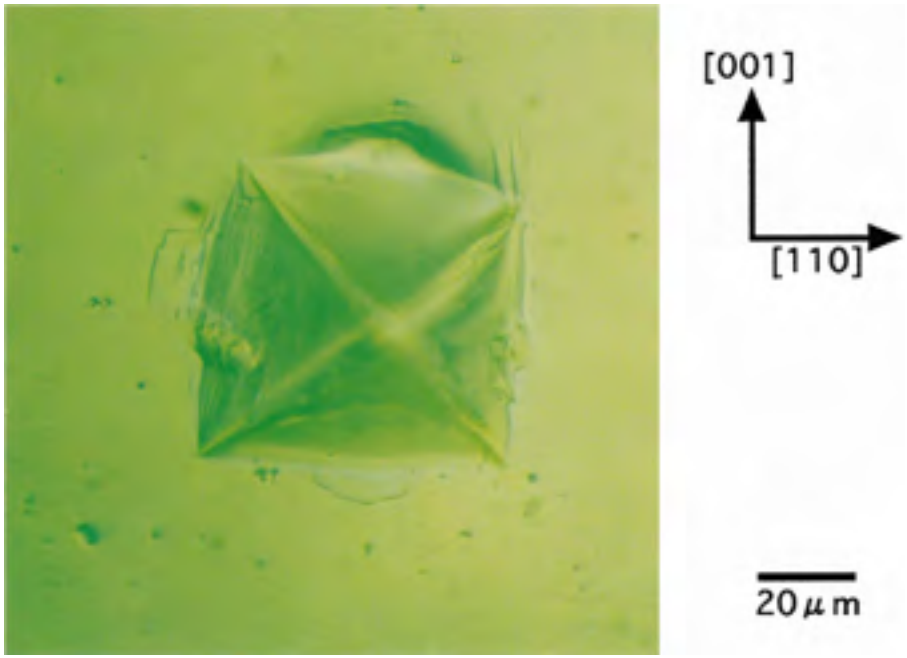

Tachibana *et al.* (1999) *J. Cryst. Growth* **198**, 661-664.
Koizumi *et al.* (2009) *Physical Review E* **79**, 61917.

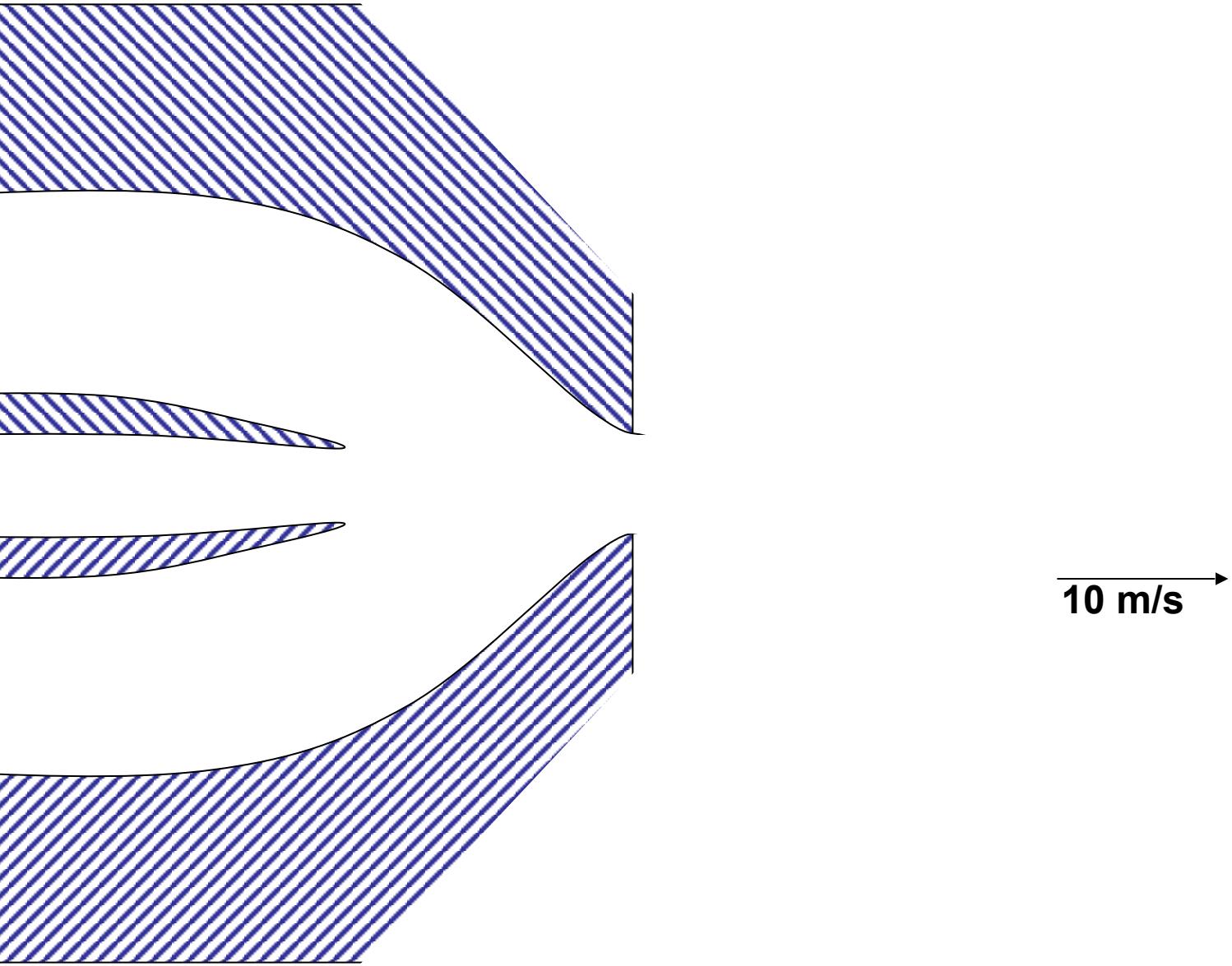
10 m/s

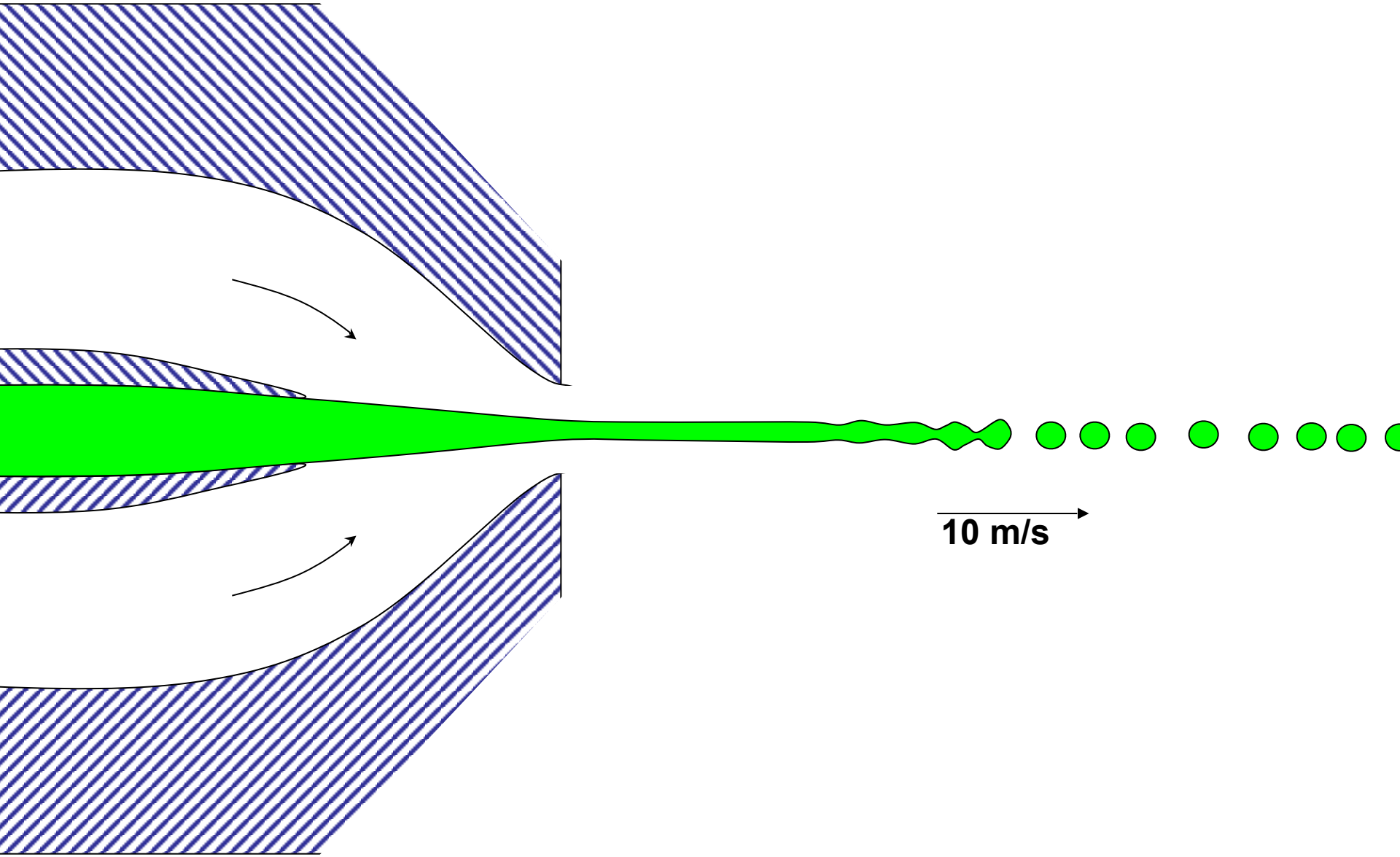
10 m/s

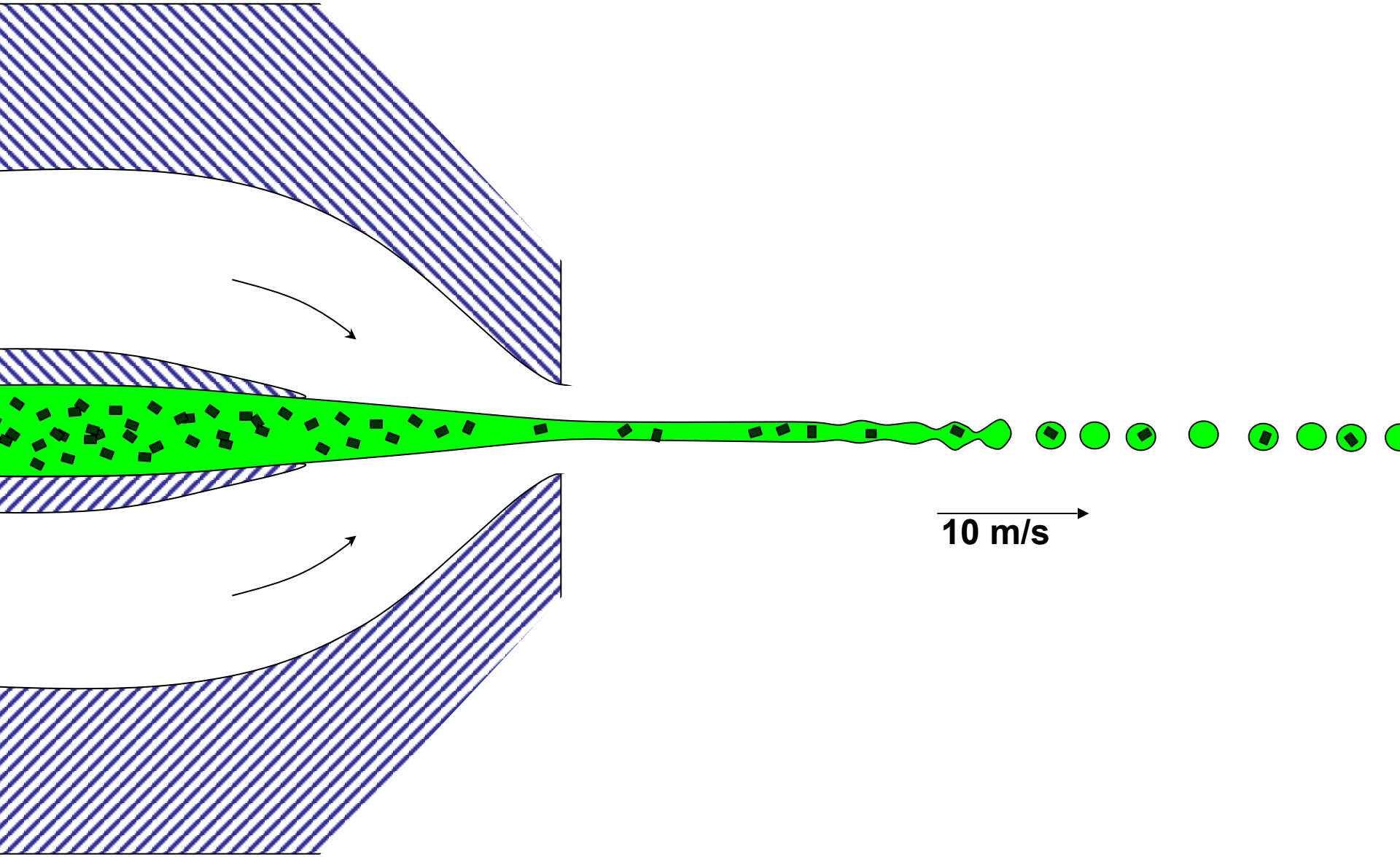
10 m/s

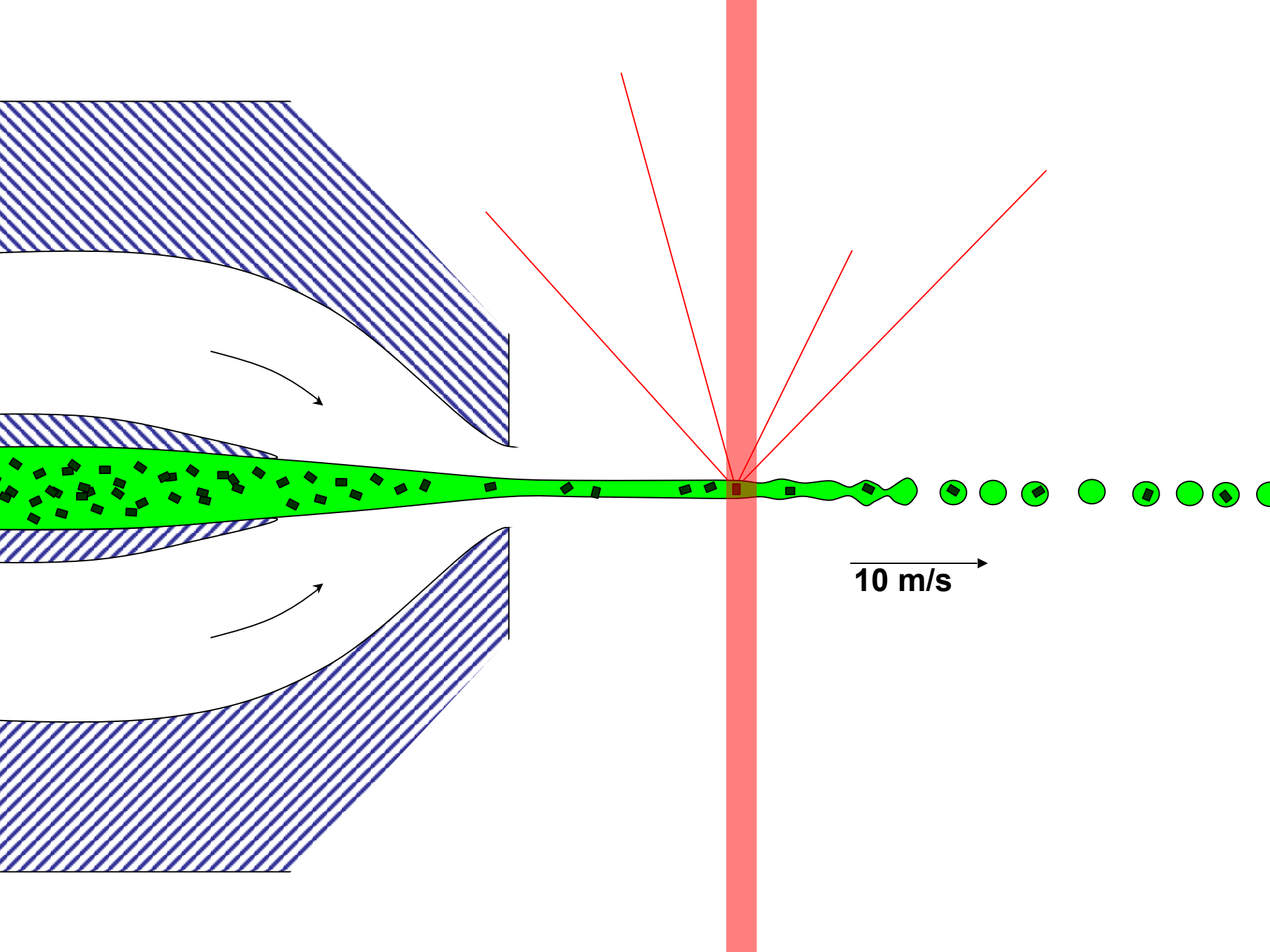
10 m/s

Dehydration: 1934

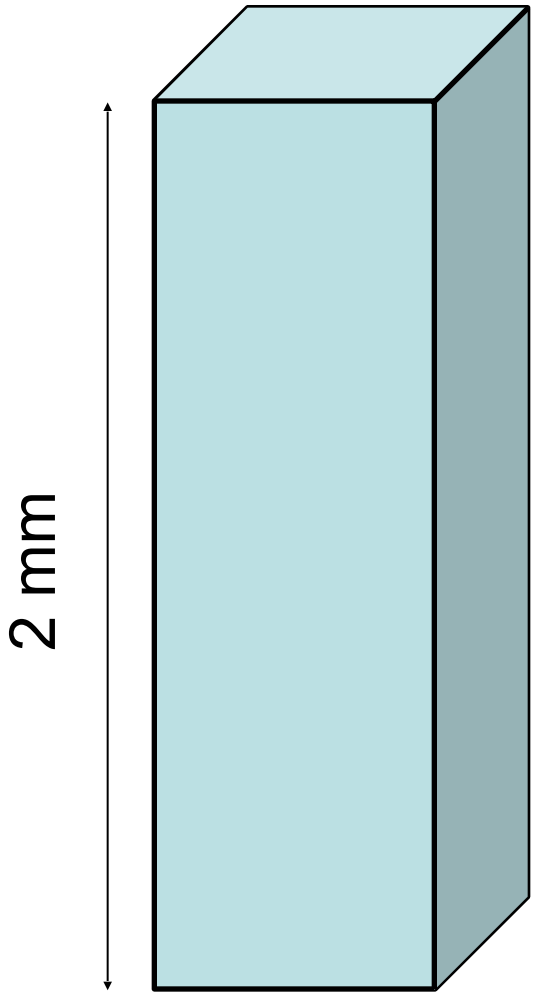

Dehydration: 1934

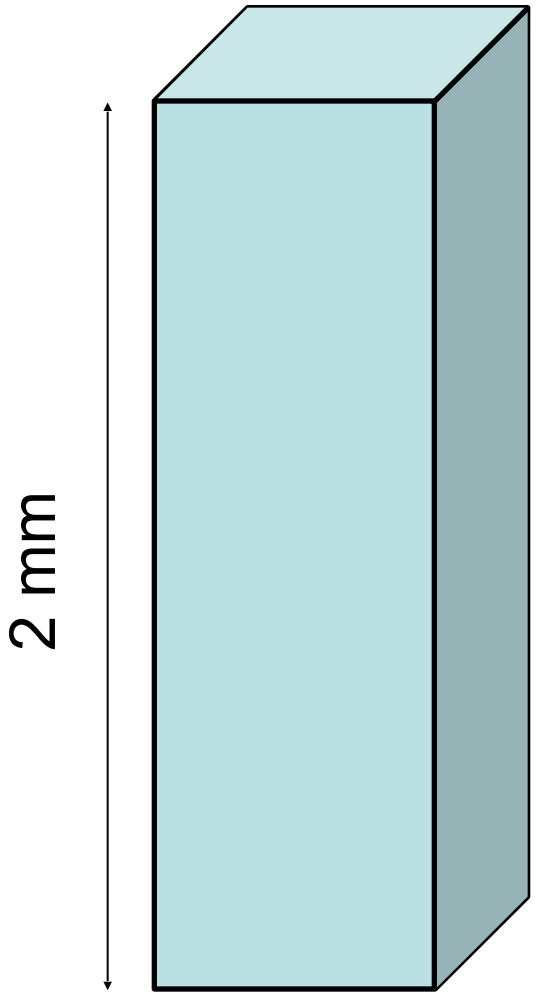

= 1.5 µL

Dehydration: 1934 and 2014?

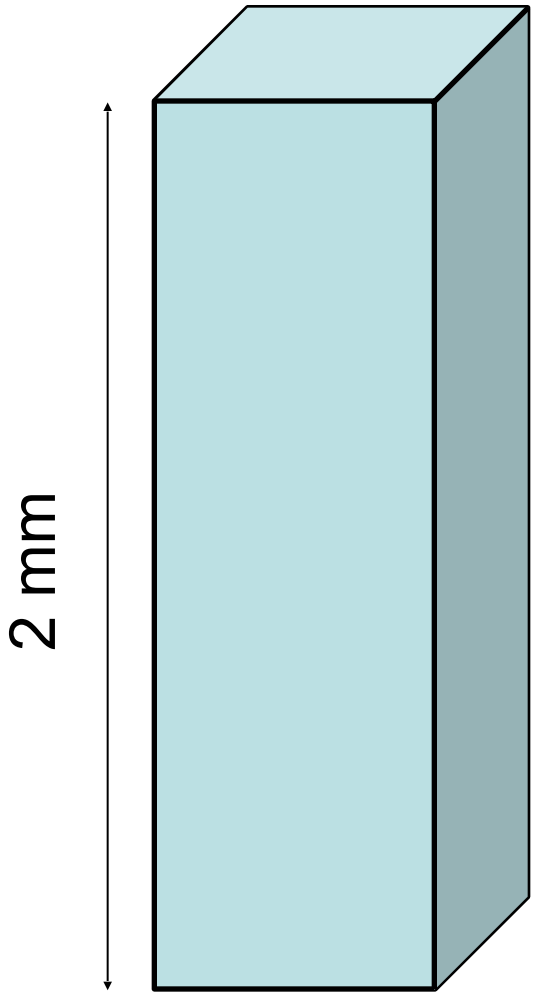

= 1.5 µL

Dehydration: 1934 and 2014?

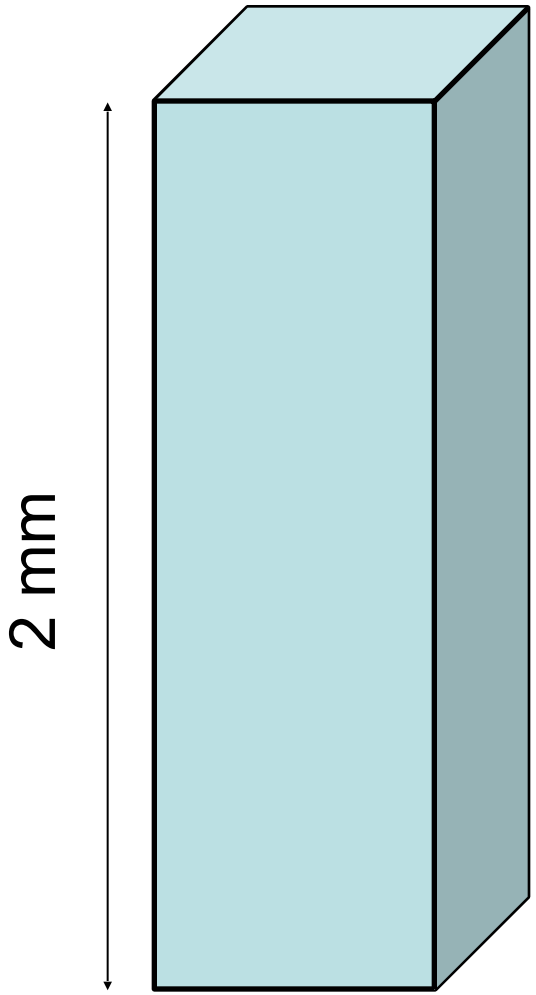

= 1.5 µL

100 µm 

Dehydration: 1934 and 2014?

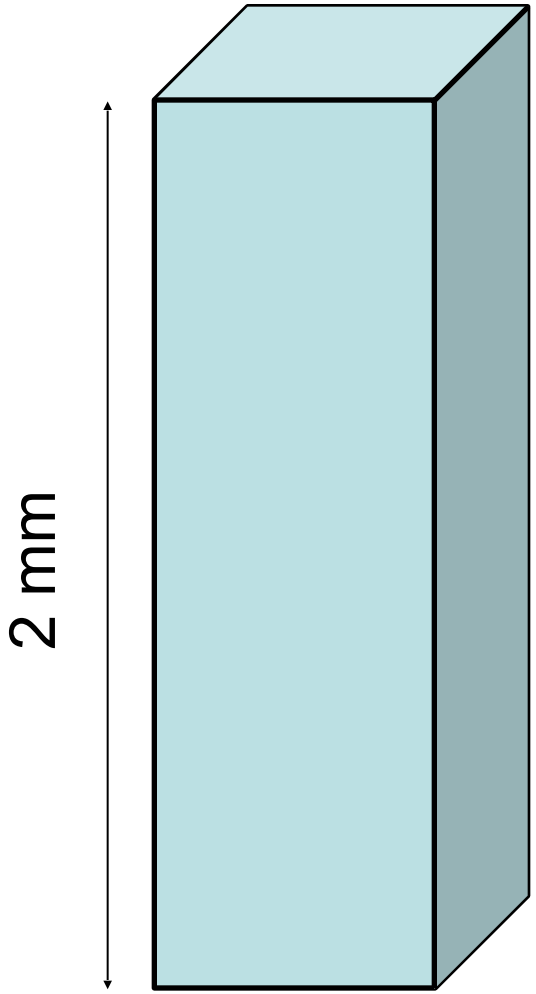

= 1.5 µL

100 µm  = 1.0 nL

Dehydration: 1934 and 2014?

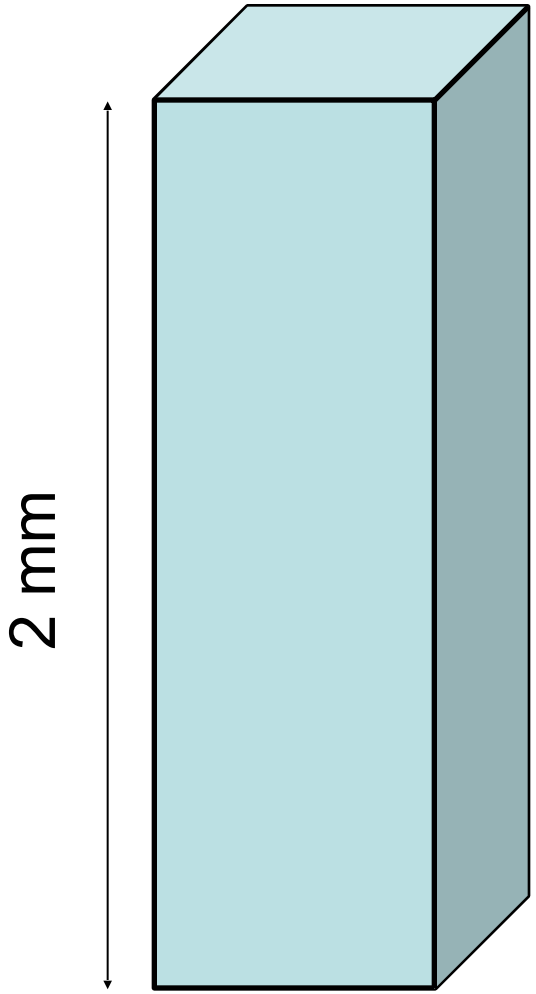

= 1.5 µL

100 µm = 1.0 nL

10 µm = 1.0 pL

Dehydration: 1934 and 2014?

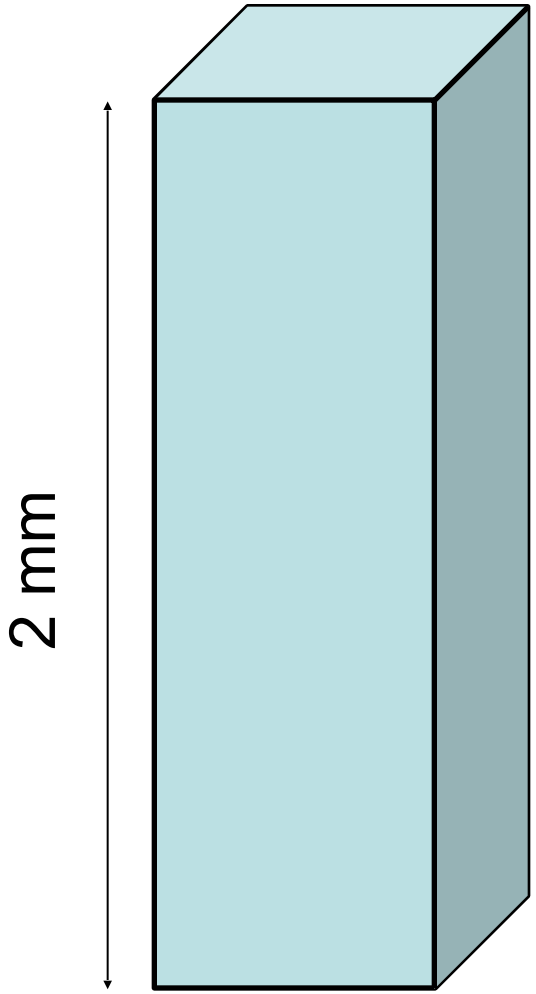

= 1.5 µL

100 µm = 1.0 nL

10 µm = 1.0 pL

1 µm = 1.0 fL

Tris buffer vs temperature

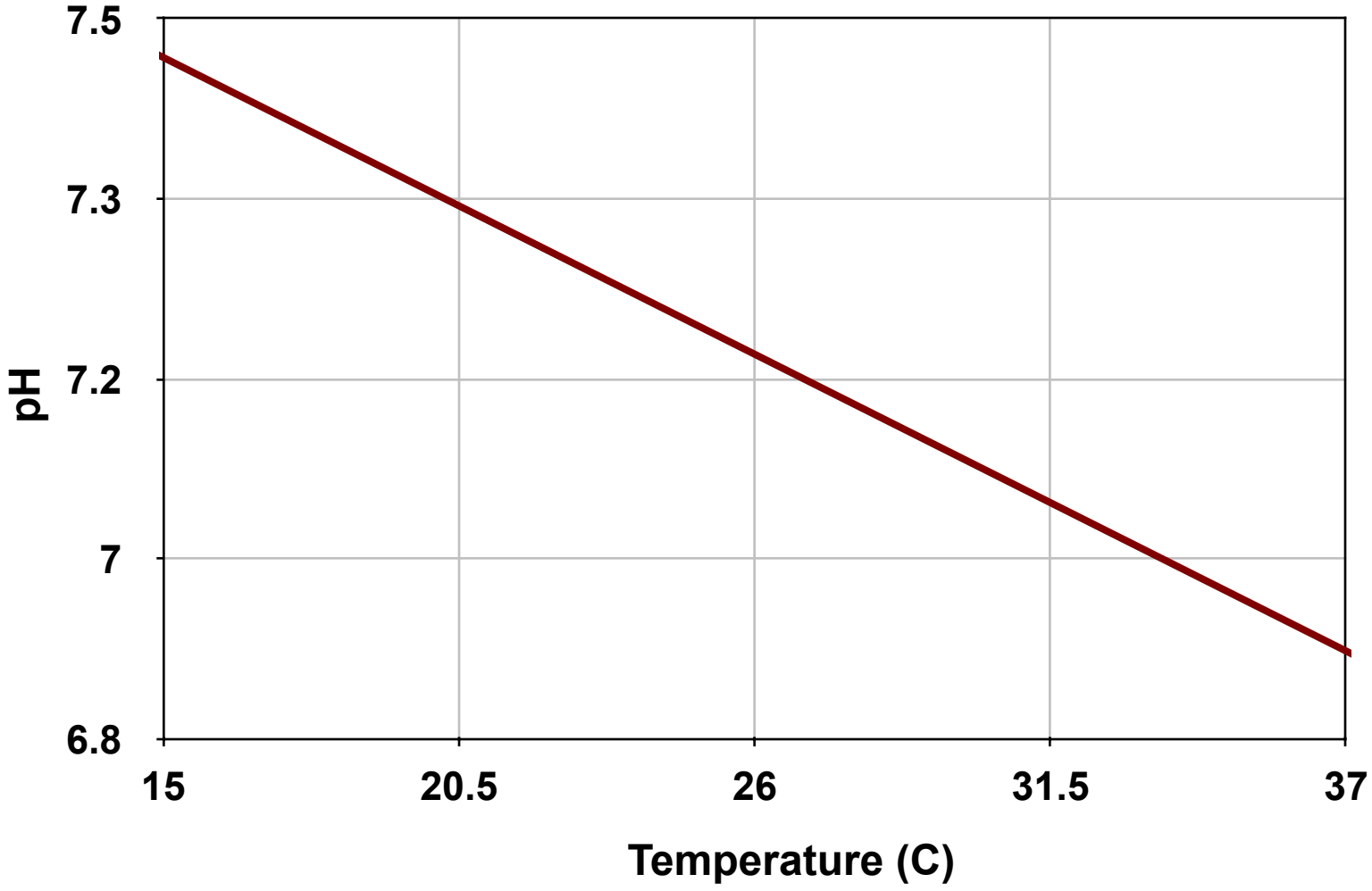

Tris buffer under cryo

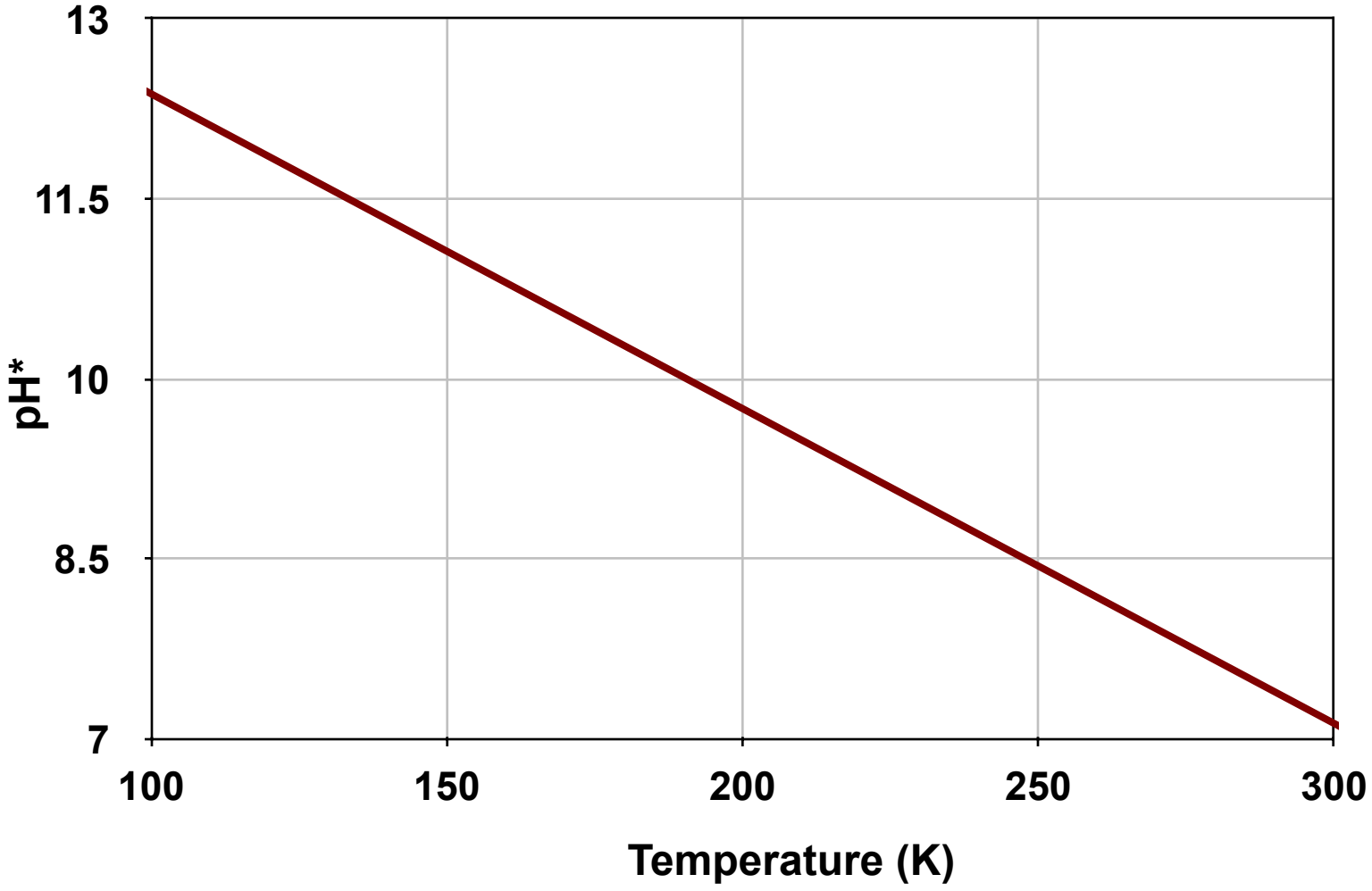

Douzou (1977) *Cryobiochemistry*. Academic Press.

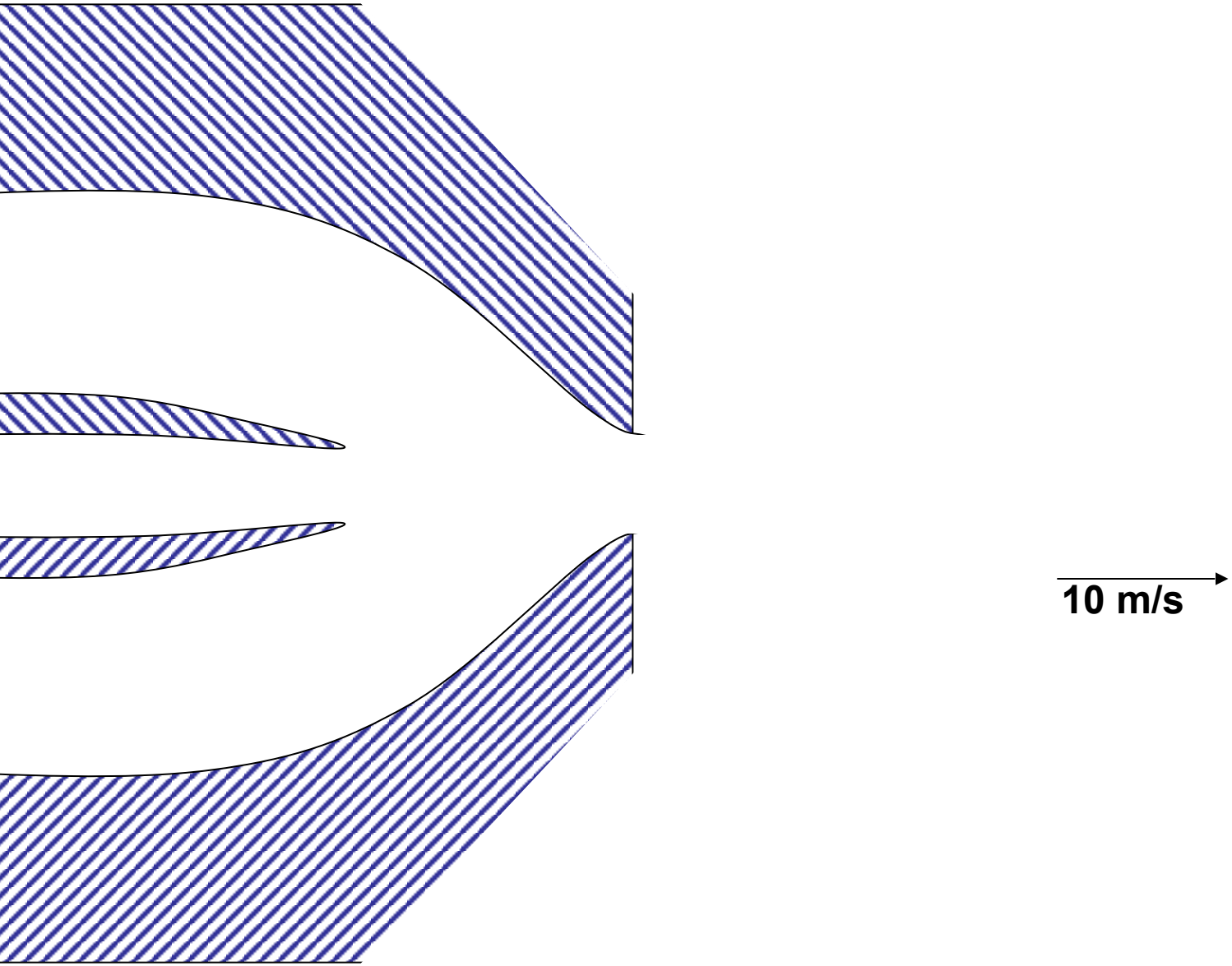
10 m/s

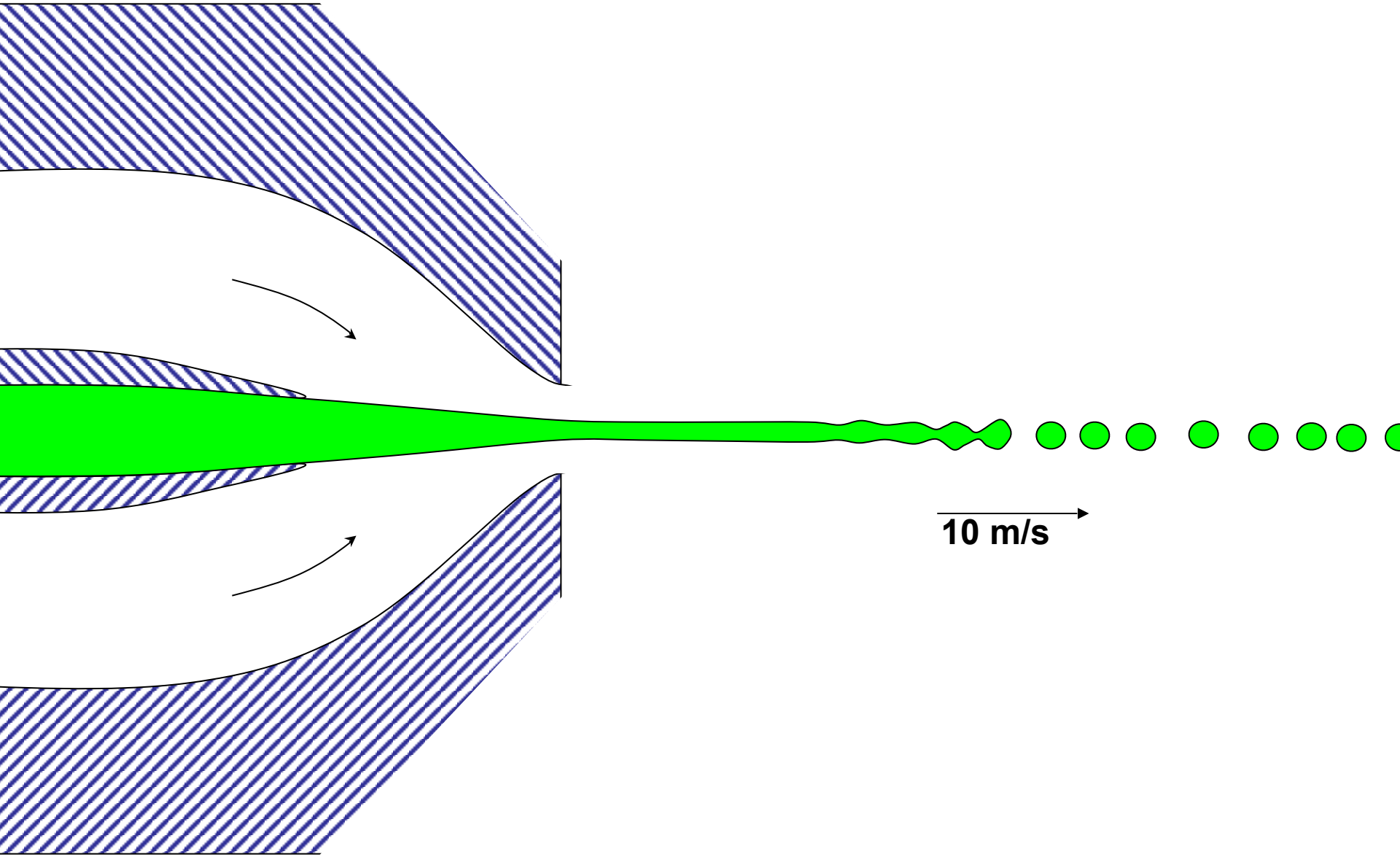
10 m/s

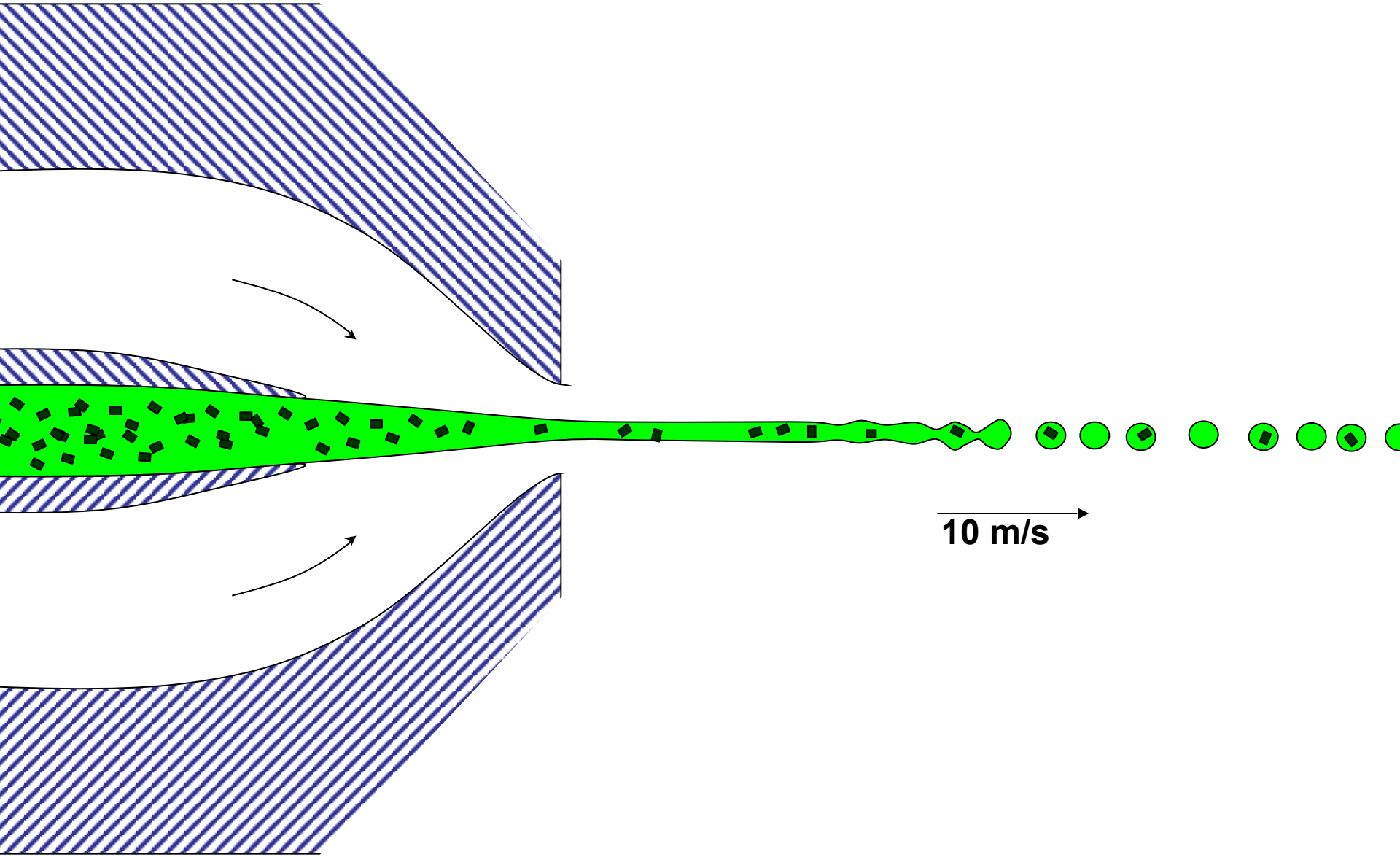
10 m/s

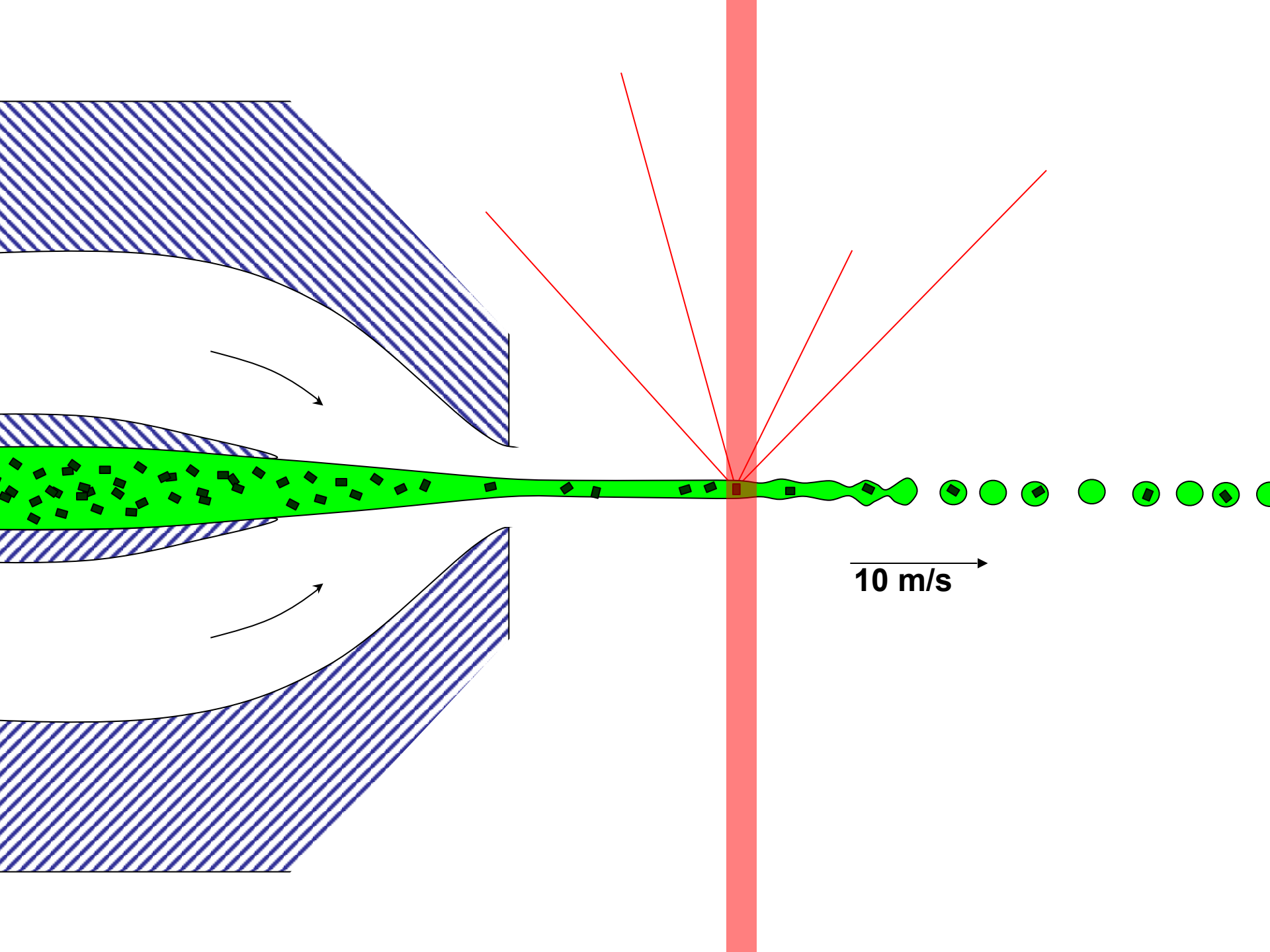
10 m/s

Classes of error in MX

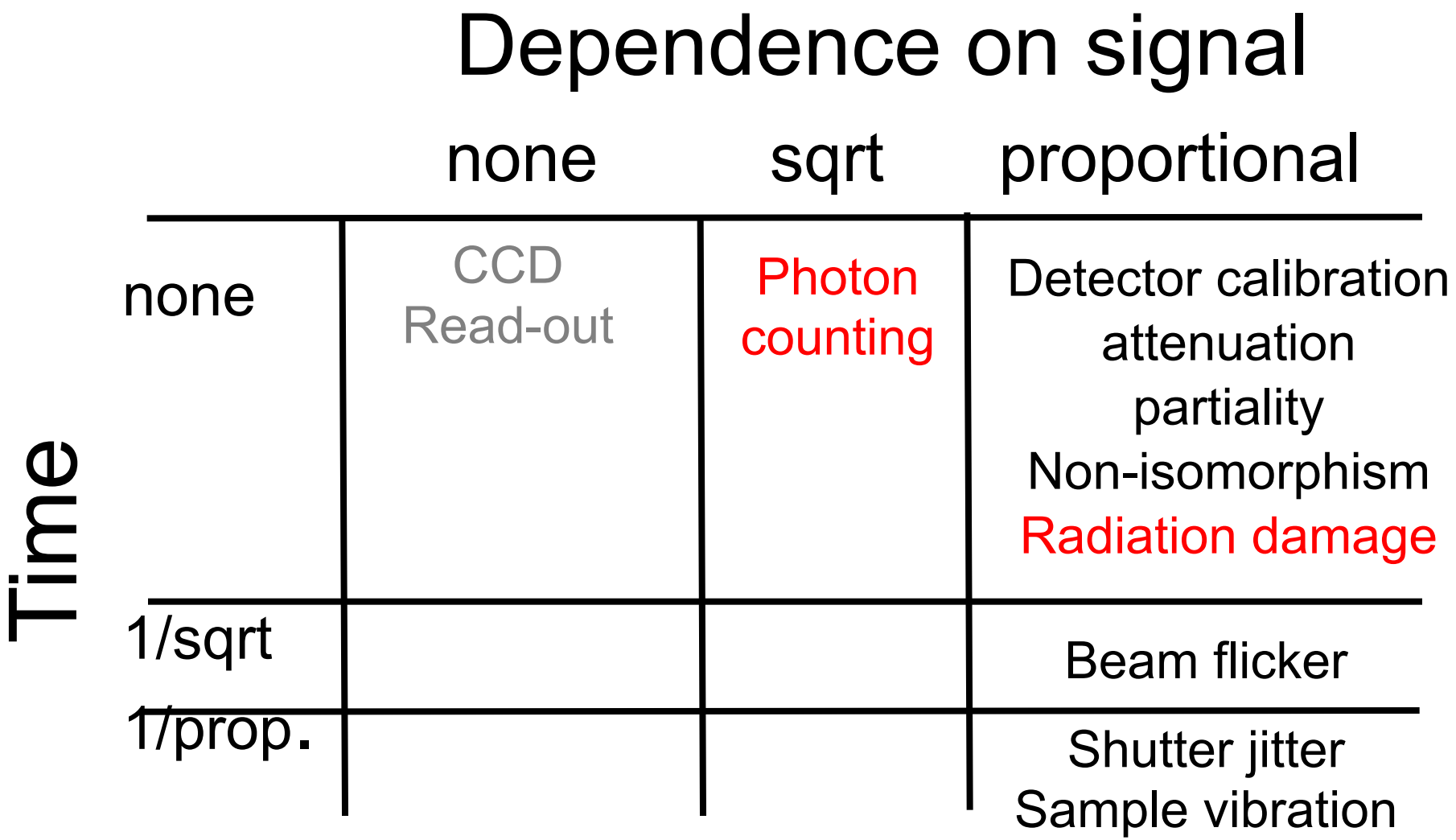

Self-calibrated damage limit

$$\langle I \rangle_{DL} = \frac{2\pi}{9} \frac{10^5 r_e^{\,2}}{hc} \frac{\mathrm{f}_{decayed} \rho R^4 \lambda^4}{\mathrm{f}_{NH} n_{ASU} M_r V_M^{\,2}} \frac{0.5 \lambda H}{\ln(2) \sin\theta} \frac{\mathrm{T}_{\mathrm{sphere}}(2\theta, \mu, R)}{\left(1 - T_{sphere}(0, \mu_{en}, R)\right)} \frac{(3 + \cos 4\theta)}{\sin\theta} \frac{\langle f_a^{\,2} \rangle}{\langle M_a \rangle} \exp\left(-2B\left(\frac{\sin\theta}{\lambda}\right)^2\right)$$

Where:

$\langle I \rangle_{DL}$	- average damage-limited intensity (photons/hkl) at a given resolution
10^5	- converting R from μm to m, r_e from m to Å, ρ from g/cm^3 to kg/m^3 and MGy to Gy
r_e	- classical electron radius (2.818 x 10^{-15} m/electron)
h	- Planck's constant (6.626 x 10^{-34} J·s)
c	- speed of light (299792458 m/s)
$\mathrm{f}_{decayed}$	- fractional progress toward completely faded spots at end of data set
ρ	- density of crystal (~1.2 g/cm^3)
R	- radius of the spherical crystal (μm)
λ	- X-ray wavelength (Å)
f_{NH}	- the Nave & Hill (2005) dose capture fraction (1 for large crystals)
n_{ASU}	- number of proteins in the asymmetric unit
M_r	- molecular weight of the protein (Daltons or g/mol)
V_M	- Matthews's coefficient (~2.4 Å^3/Dalton)
H	- Howells's criterion (10 MGy/Å)
θ	- Bragg angle
$\langle f_a^{\,2} \rangle$	- number-averaged squared structure factor per protein atom (electron^2)
$\langle M_a \rangle$	- number-averaged atomic weight of a protein atom (~7.1 Daltons)
B	- average (Wilson) temperature factor (Å^2)
μ	- attenuation coefficient of sphere material (m^{-1})
μ_{en}	- mass energy-absorption coefficient of sphere material (m^{-1})

Holton & Frankel (2010) *Acta D* **66** 393-408.

Self-calibrated damage limit

$$\langle I \rangle_{DL} = \frac{2\pi}{9} \frac{10^5 r_e^{\,2}}{hc} \frac{f_{decayed}\,\rho R^4 \lambda^4}{f_{NH}\, n_{ASU}\, M_r V_M^{\,2}} \frac{0.5\lambda H}{\ln(2)\sin\theta} \frac{T_{sphere}(2\theta,\mu,R)}{\left(1 - T_{sphere}(0,\mu_{en},R)\right)} \frac{(3+\cos 4\theta)}{\sin\theta} \frac{\langle f_a^{\,2} \rangle}{\langle M_a \rangle} \exp\left(-2B\left(\frac{\sin\theta}{\lambda}\right)^2\right)$$

Where:

$\langle I \rangle_{DL}$	- average damage-limited intensity (photons/hkl) at a given resolution
10^5	- converting R from μm to m, r_e from m to Å, ρ from g/cm^3 to kg/m^3 and MGy to Gy
r_e	- classical electron radius (2.818 x 10^{-15} m/electron)
h	- Planck's constant (6.626 x 10^{-34} J·s)
c	- speed of light (299792458 m/s)
$f_{decayed}$	- fractional progress toward completely faded spots at end of data set
ρ	- density of crystal (~1.2 g/cm^3)
R	- radius of the spherical crystal (μm)
λ	- X-ray wavelength (Å)
f_{NH}	- the Nave & Hill (2005) dose capture fraction (1 for large crystals)
n_{ASU}	- number of proteins in the asymmetric unit
M_r	- molecular weight of the protein (Daltons or g/mol)
V_M	- Matthews's coefficient (~2.4 Å^3/Dalton)
H	- Howells's criterion (10 MGy/Å)
θ	- Bragg angle
$\langle f_a^{\,2} \rangle$	- number-averaged squared structure factor per protein atom (electron^2)
$\langle M_a \rangle$	- number-averaged atomic weight of a protein atom (~7.1 Daltons)
B	- average (Wilson) temperature factor (Å^2)
μ	- attenuation coefficient of sphere material (m^{-1})
μ_{en}	- mass energy-absorption coefficient of sphere material (m^{-1})

Holton & Frankel (2010) *Acta D* **66** 393-408.

Self-calibrated damage limit

$$\langle I \rangle_{DL} = \frac{2\pi}{9}\frac{10^5 r_e^{\,2}}{hc}\frac{f_{decayed}\rho R^4 \lambda^4}{f_{NH} n_{ASU} M_r V_M^{\,2}}\frac{0.5\lambda H}{\ln(2)\sin\theta}\frac{T_{sphere}(2\theta,\mu,R)}{(1-T_{sphere}(0,\mu_{en},R))}\frac{(3+\cos 4\theta)}{\sin\theta}\frac{\langle f_a^{\,2}\rangle}{\langle M_a\rangle}\exp\left(-2B\left(\frac{\sin\theta}{\lambda}\right)^2\right)$$

Where:

$\langle I \rangle_{DL}$	- average damage-limited intensity (photons/hkl) at a given resolution
10^5	- converting R from μm to m, r_e from m to Å, ρ from g/cm^3 to kg/m^3 and MGy to Gy
r_e	- classical electron radius (2.818 x 10^{-15} m/electron)
h	- Planck's constant (6.626 x 10^{-34} J·s)
c	- speed of light (299792458 m/s)
$f_{decayed}$	- fractional progress toward completely faded spots at end of data set
ρ	- density of crystal (~1.2 g/cm^3)
R	- radius of the spherical crystal (μm)
λ	- X-ray wavelength (Å)
f_{NH}	- the Nave & Hill (2005) dose capture fraction (1 for large crystals)
n_{ASU}	- number of proteins in the asymmetric unit
M_r	- molecular weight of the protein (Daltons or g/mol)
V_M	- Matthews's coefficient (~2.4 Å^3/Dalton)
H	- Howells's criterion (10 MGy/Å)
θ	- Bragg angle
$\langle f_a^{\,2} \rangle$	- number-averaged squared structure factor per protein atom (electron^2)
$\langle M_a \rangle$	- number-averaged atomic weight of a protein atom (~7.1 Daltons)
B	- average (Wilson) temperature factor (Å^2)
μ	- attenuation coefficient of sphere material (m^{-1})
μ_{en}	- mass energy-absorption coefficient of sphere material (m^{-1})

Holton & Frankel (2010) *Acta D* **66** 393-408.

Self-calibrated damage limit

$$\langle I \rangle_{DL} = \frac{2\pi}{9} \frac{10^5 r_e^{\,2}}{hc} \frac{\mathrm{f}_{decayed} \rho R^4 \lambda^4}{\mathrm{f}_{NH} n_{ASU} M_r V_M^{\,2}} \frac{0.5 \lambda H}{\ln(2) \sin\theta} \frac{\mathrm{T}_{\mathrm{sphere}}(2\theta, \mu, R)}{\left(1 - T_{sphere}(0, \mu_{en}, R)\right)} \frac{(3 + \cos 4\theta)}{\sin\theta} \frac{\langle f_a^{\,2} \rangle}{\langle M_a \rangle} \exp\left(-2B\left(\frac{\sin\theta}{\lambda}\right)^2\right)$$

Where:

$\langle I \rangle_{DL}$	- average damage-limited intensity (photons/hkl) at a given resolution
10^5	- converting R from μm to m, r_e from m to Å, ρ from g/cm^3 to kg/m^3 and MGy to Gy
r_e	- classical electron radius (2.818 x 10^{-15} m/electron)
h	- Planck's constant (6.626 x 10^{-34} J·s)
c	- speed of light (299792458 m/s)
$\mathrm{f}_{decayed}$	- fractional progress toward completely faded spots at end of data set
ρ	- density of crystal (~1.2 g/cm^3)
R	- radius of the spherical crystal (μm)
λ	- X-ray wavelength (Å)
f_{NH}	- the Nave & Hill (2005) dose capture fraction (1 for large crystals)
n_{ASU}	- number of proteins in the asymmetric unit
M_r	- molecular weight of the protein (Daltons or g/mol)
V_M	- Matthews's coefficient (~2.4 Å^3/Dalton)
H	- Howells's criterion (10 MGy/Å)
θ	- Bragg angle
$\langle f_a^{\,2} \rangle$	- number-averaged squared structure factor per protein atom (electron^2)
$\langle M_a \rangle$	- number-averaged atomic weight of a protein atom (~7.1 Daltons)
B	- average (Wilson) temperature factor (Å^2)
μ	- attenuation coefficient of sphere material (m^{-1})
μ_{en}	- mass energy-absorption coefficient of sphere material (m^{-1})

Holton & Frankel (2010) *Acta D* **66** 393-408.

Self-calibrated damage limit

$$\langle I \rangle_{DL} = \frac{2\pi}{9} \frac{10^5 r_e^{\,2}}{hc} \frac{\mathrm{f}_{decayed}\, \rho R^4 \lambda^4}{\mathrm{f}_{NH}\, n_{ASU} M_r V_M^{\,2}} \frac{0.5\lambda H}{\ln(2)\sin\theta} \frac{\mathrm{T}_{\mathrm{sphere}}(2\theta, \mu, R)}{\left(1 - T_{sphere}(0, \mu_{en}, R)\right)} \frac{(3+\cos 4\theta)}{\sin\theta} \frac{\langle f_a^{\,2} \rangle}{\langle M_a \rangle} \exp\left(-2B\left(\frac{\sin\theta}{\lambda}\right)^2\right)$$

Where:

$\langle I \rangle_{DL}$	- average damage-limited intensity (photons/hkl) at a given resolution
10^5	- converting R from μm to m, r_e from m to Å, ρ from g/cm^3 to kg/m^3 and MGy to Gy
r_e	- classical electron radius (2.818 x 10^{-15} m/electron)
h	- Planck's constant (6.626 x 10^{-34} J·s)
c	- speed of light (299792458 m/s)
$\mathrm{f}_{decayed}$	- fractional progress toward completely faded spots at end of data set
ρ	- density of crystal (~1.2 g/cm^3)
R	- radius of the spherical crystal (μm)
λ	- X-ray wavelength (Å)
f_{NH}	- the Nave & Hill (2005) dose capture fraction (1 for large crystals)
n_{ASU}	- number of proteins in the asymmetric unit
M_r	- molecular weight of the protein (Daltons or g/mol)
V_M	- Matthews's coefficient (~2.4 Å^3/Dalton)
H	- Howells's criterion (10 MGy/Å)
θ	- Bragg angle
$\langle f_a^{\,2} \rangle$	- number-averaged squared structure factor per protein atom (electron^2)
$\langle M_a \rangle$	- number-averaged atomic weight of a protein atom (~7.1 Daltons)
B	- average (Wilson) temperature factor (Å^2)
μ	- attenuation coefficient of sphere material (m^{-1})
μ_{en}	- mass energy-absorption coefficient of sphere material (m^{-1})

Holton & Frankel (2010) *Acta D* **66** 393-408.

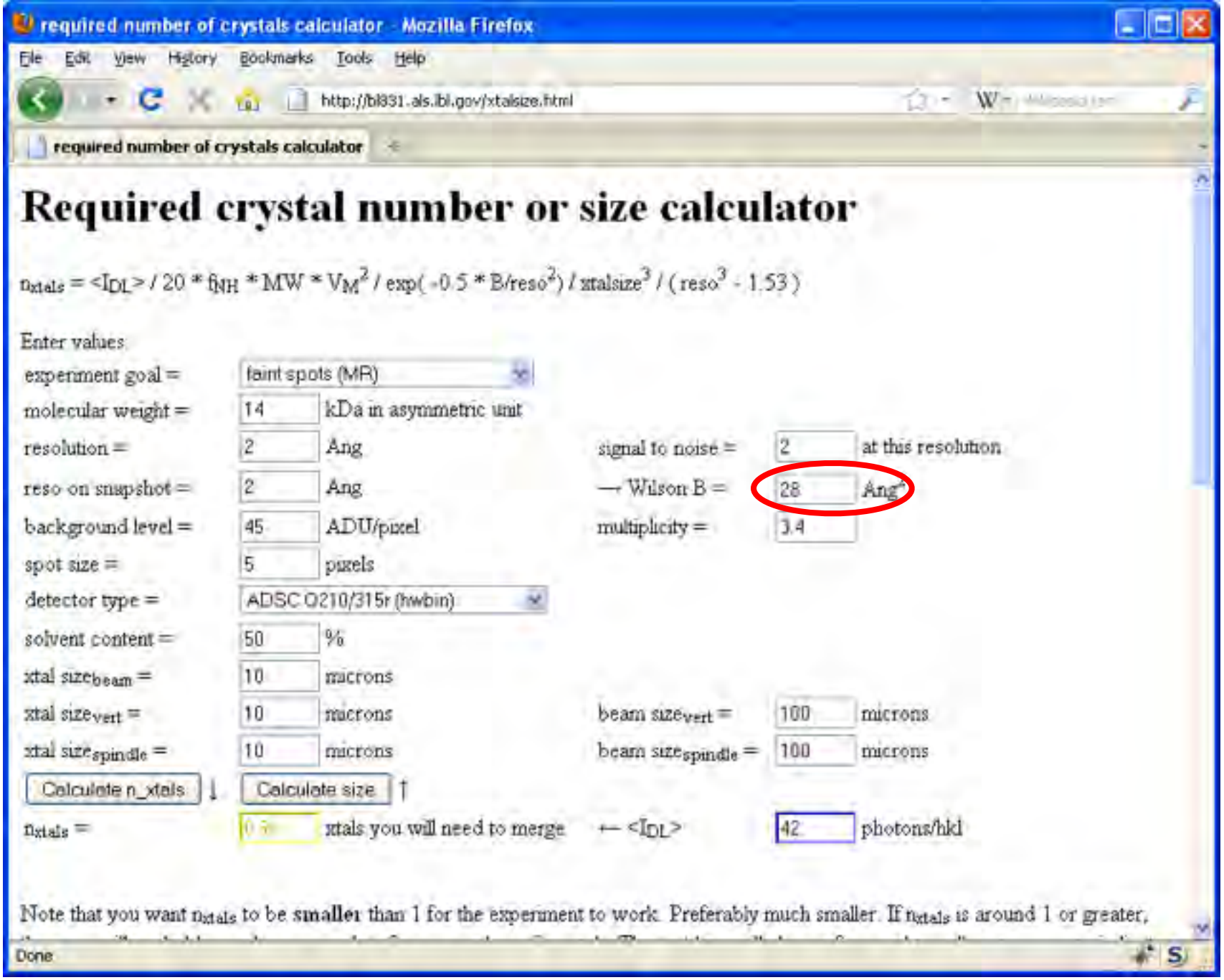

Holton & Frankel (2010) *Acta D* **66** 393-408.

Classes of error in MX

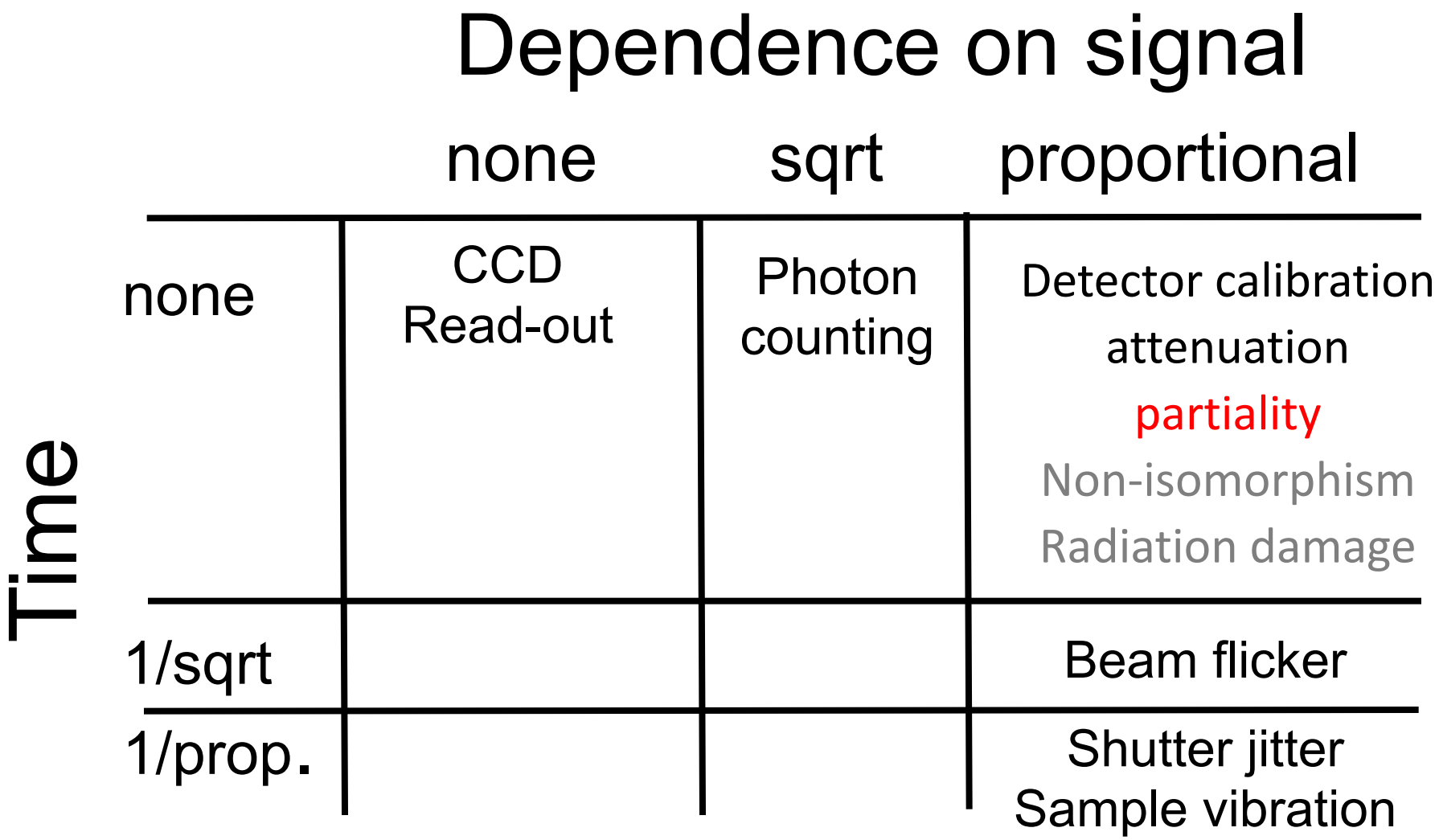

Summary

http://bl831a.als.lbl.gov/
~jamesh/powerpoint/BioXFEL_SvN_2014.pptx
http://bl831a.als.lbl.gov/
example_data_sets/Illuin/LCLS/

Summary

http://bl831a.als.lbl.gov/
~jamesh/powerpoint/BioXFEL_SvN_2014.pptx
http://bl831a.als.lbl.gov/
example_data_sets/Illuin/LCLS/

Partiality is backwards with stills

Summary

http://bl831a.als.lbl.gov/
~jamesh/powerpoint/BioXFEL_SvN_2014.pptx
http://bl831a.als.lbl.gov/
example_data_sets/Illuin/LCLS/

Partiality is backwards with stills

Check your Wilson plot

Summary

http://bl831a.als.lbl.gov/
~jamesh/powerpoint/BioXFEL_SvN_2014.pptx
http://bl831a.als.lbl.gov/
example_data_sets/Illuin/LCLS/

Partiality is backwards with stills

Check your Wilson plot

Control: try fake data

Summary

http://bl831a.als.lbl.gov/
~jamesh/powerpoint/BioXFEL_SvN_2014.pptx
http://bl831a.als.lbl.gov/
example_data_sets/Illuin/LCLS/

Partiality is backwards with stills

Check your Wilson plot

Control: try fake data

The B factor is everything

My questions:

http://bl831a.als.lbl.gov/
example_data_sets/Illuin/LCLS/

My questions:

How do I convert SMV to XTC?

`http://bl831a.als.lbl.gov/example_data_sets/Illuin/LCLS/`

My questions:

How do I convert SMV to XTC?

How do I convert XTC to SMV?

`http://bl831a.als.lbl.gov/example_data_sets/Illuin/LCLS/`

My questions:

How do I convert SMV to XTC?

How do I convert XTC to SMV?

Can you get Fs from my fastBragg data?

`http://bl831a.als.lbl.gov/example_data_sets/Illuin/LCLS/`

Classes of error in MX

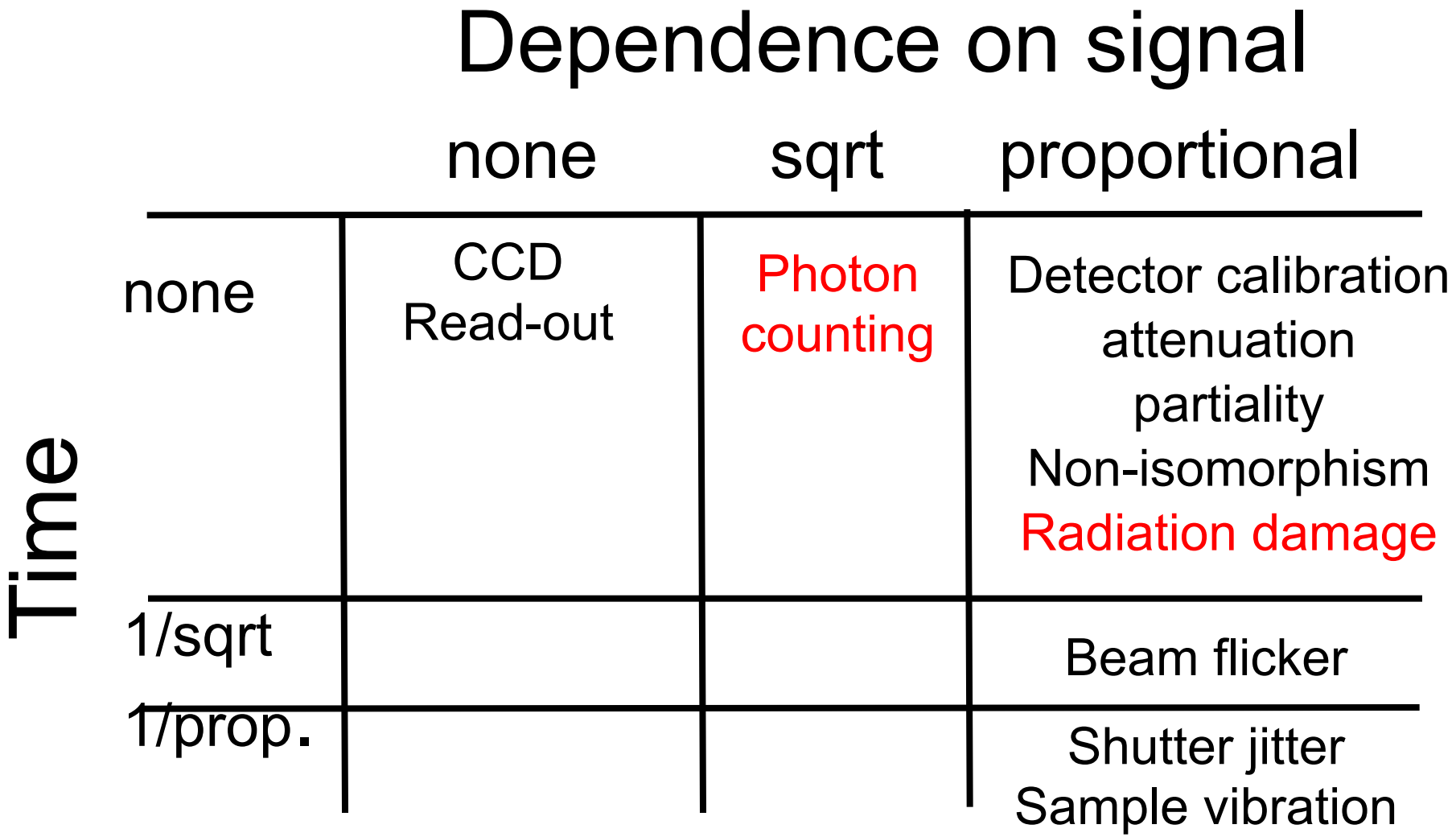

Classes of error in MX

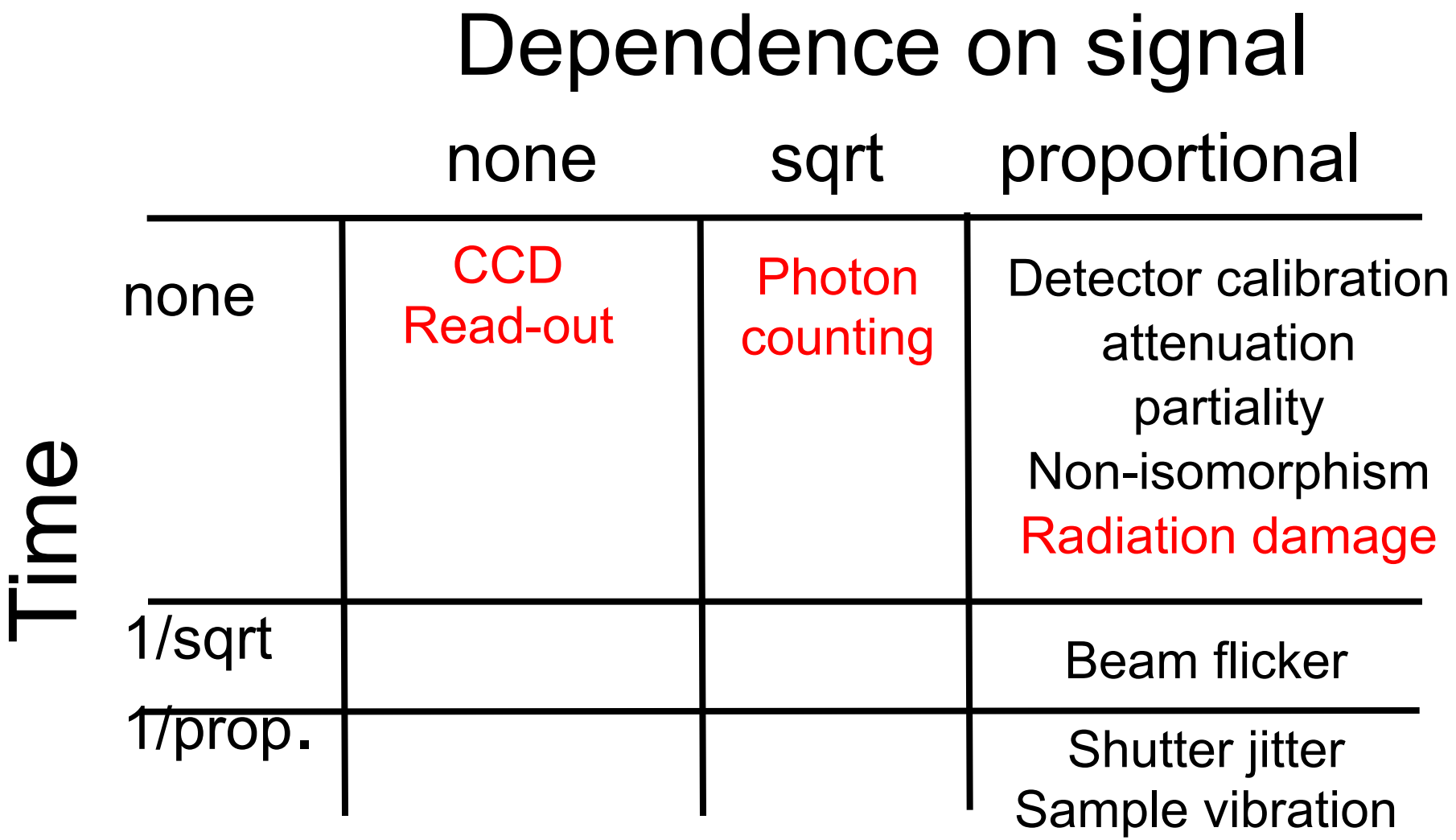

Optimal exposure time

(faint spots)

$$t_{hr} = t_{ref} \frac{10 \cdot m \cdot \sigma_0^{\,2}}{gain \cdot \left(bg_{ref} - bg_0 \right)}$$

t_{hr}	Optimal exposure time for data set (s)
t_{ref}	exposure time of reference image (s)
bg_{ref}	background level near weak spots on reference image (ADU)
bg_0	ADC offset of detector (ADU)
bg_{hr}	optimal background level (via t_{hr})
σ_0	rms read-out noise (ADU)
gain	ADU/photon
m	multiplicity of data set (including partials)

Optimal exposure time

(faint spots)

$$t_{hr} = t_{ref} \frac{10 \cdot m \cdot \sigma_0^{\,2}}{gain \cdot \left(bg_{ref} - bg_0 \right)}$$

t_{hr}	Optimal exposure time for data set (s)
t_{ref}	exposure time of reference image (s)
bg_{ref}	background level near weak spots on reference image (ADU)
bg_0	ADC offset of detector (ADU)
bg_{hr}	optimal background level (via t_{hr})
σ_0	rms read-out noise (ADU)
gain	ADU/photon
m	multiplicity of data set (including partials)

Optimal exposure time

(faint spots)

$$t_{hr} = t_{ref} \frac{10 \cdot m \cdot \sigma_0^{\,2}}{gain \cdot (bg_{ref} - bg_0)}$$

t_{hr}	Optimal exposure time for data set (s)
t_{ref}	exposure time of reference image (s)
bg_{ref}	background level near weak spots on reference image (ADU)
bg_0	ADC offset of detector (ADU)
bg_{hr}	optimal background level (via t_{hr})
σ_0	rms read-out noise (ADU)
$gain$	ADU/photon
m	multiplicity of data set (including partials)

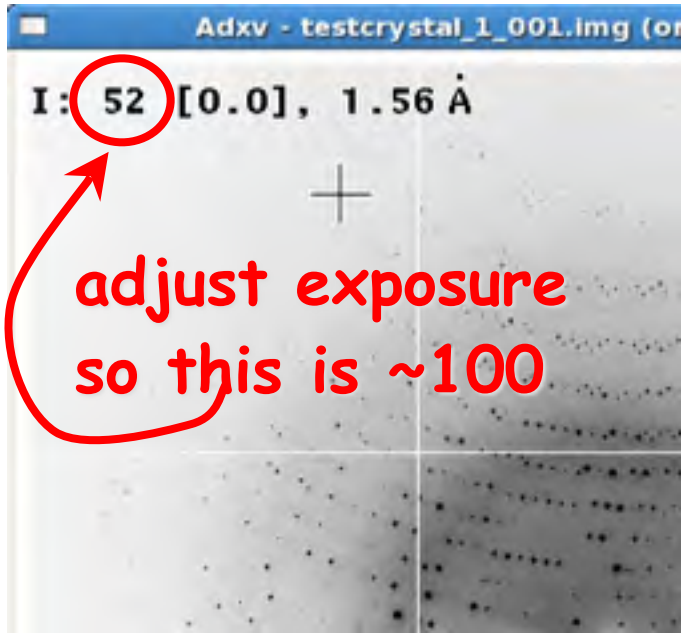

Classes of error in MX

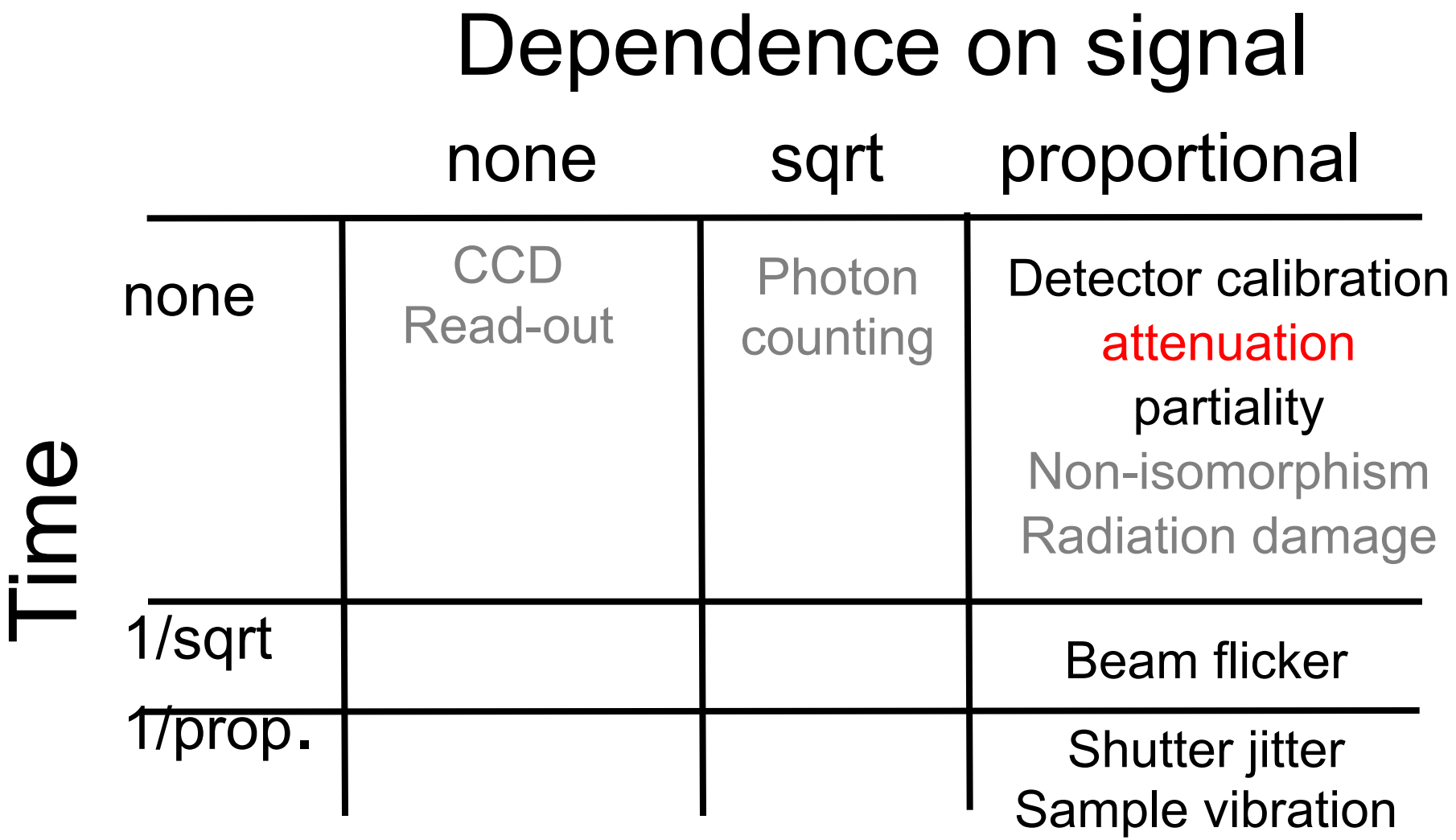

attenuation factor

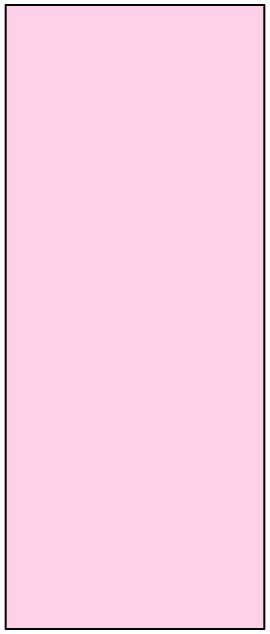

attenuation factor

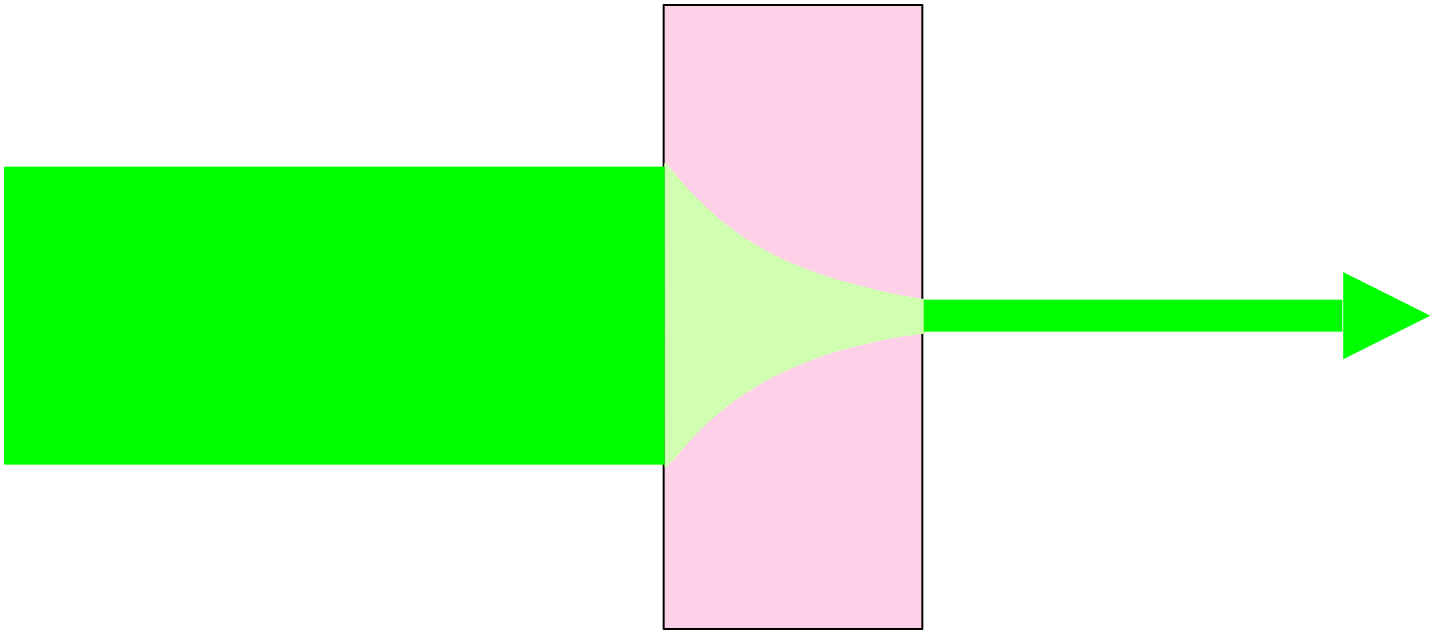

attenuation factor

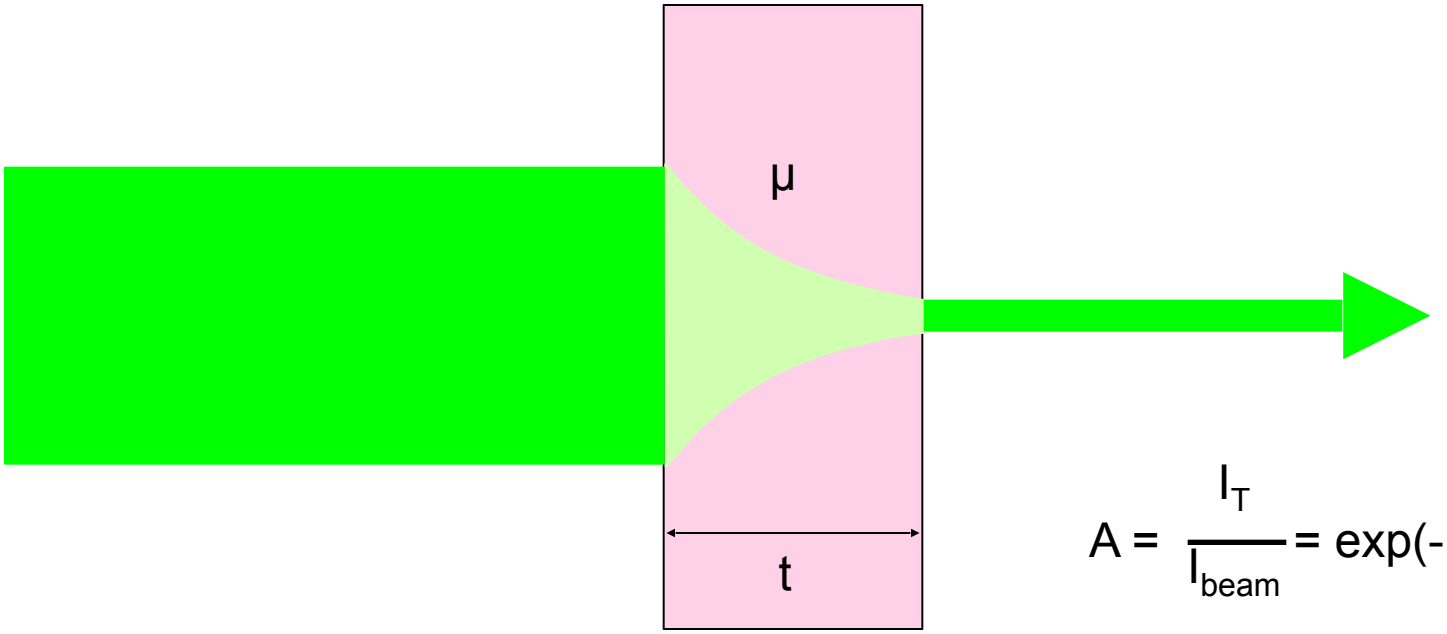

$$A = \frac{I_T}{I_{beam}} = \exp(-\mu t)$$

attenuation factor

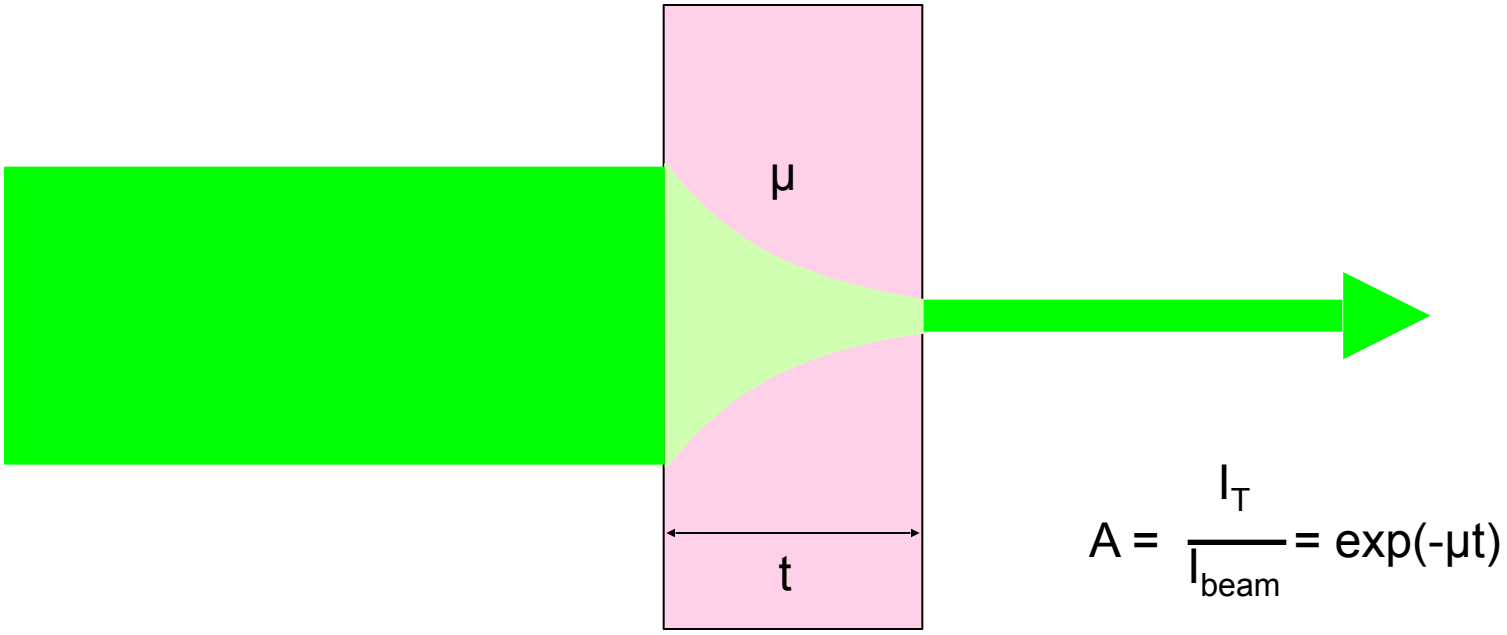

Bouguer, P. (1729). *Essai d'optique sur la gradation de la lumière*.
Lambert, J. H. (1760). *Photometria: sive De mensura et gradibus luminis, colorum et umbrae*. E. Klett.
Beer, A. (1852)."Bestimmung der Absorption des rothen Lichts in farbigen Flüssigkeiten", *Ann. Phys. Chem* **86**, 78-90.

attenuation factor

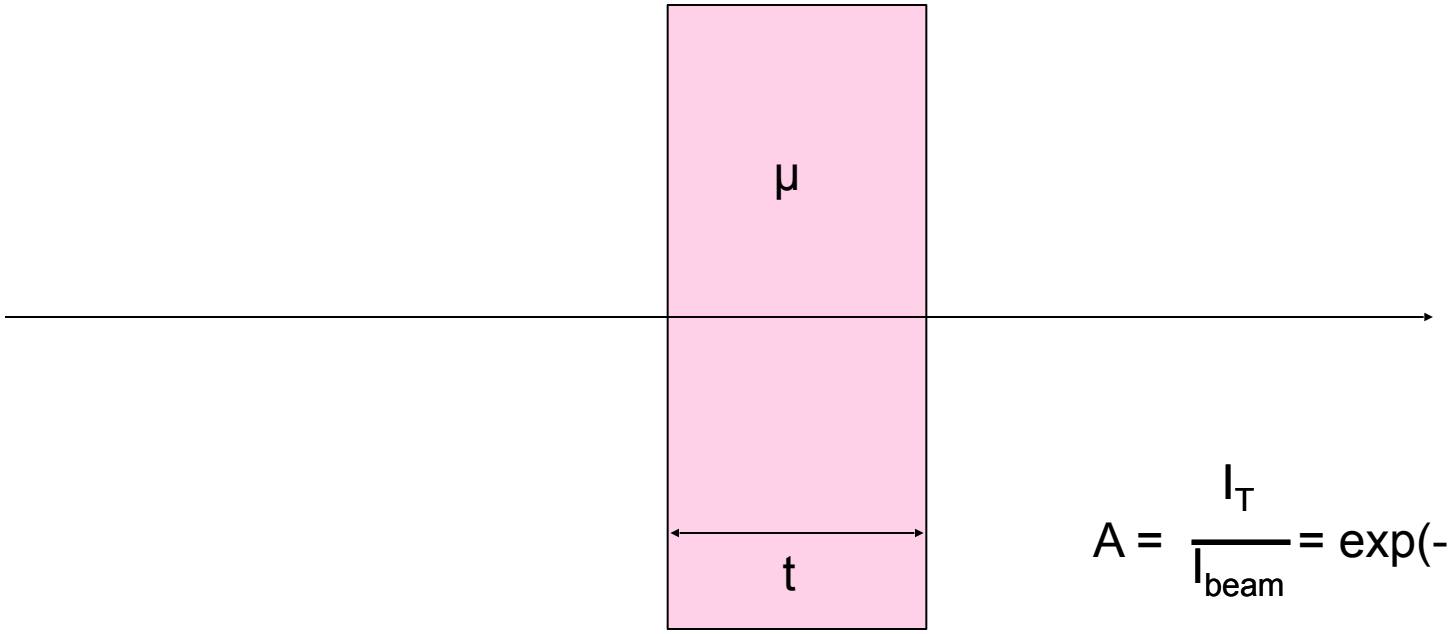

$$A = \frac{I_T}{I_{beam}} = \exp(-\mu t)$$

Bouguer, P. (1729). *Essai d'optique sur la gradation de la lumière*.
Lambert, J. H. (1760). *Photometria: sive De mensura et gradibus luminis, colorum et umbrae*. E. Klett.
Beer, A. (1852)."Bestimmung der Absorption des rothen Lichts in farbigen Flüssigkeiten", *Ann. Phys. Chem* **86**, 78-90.

attenuation factor

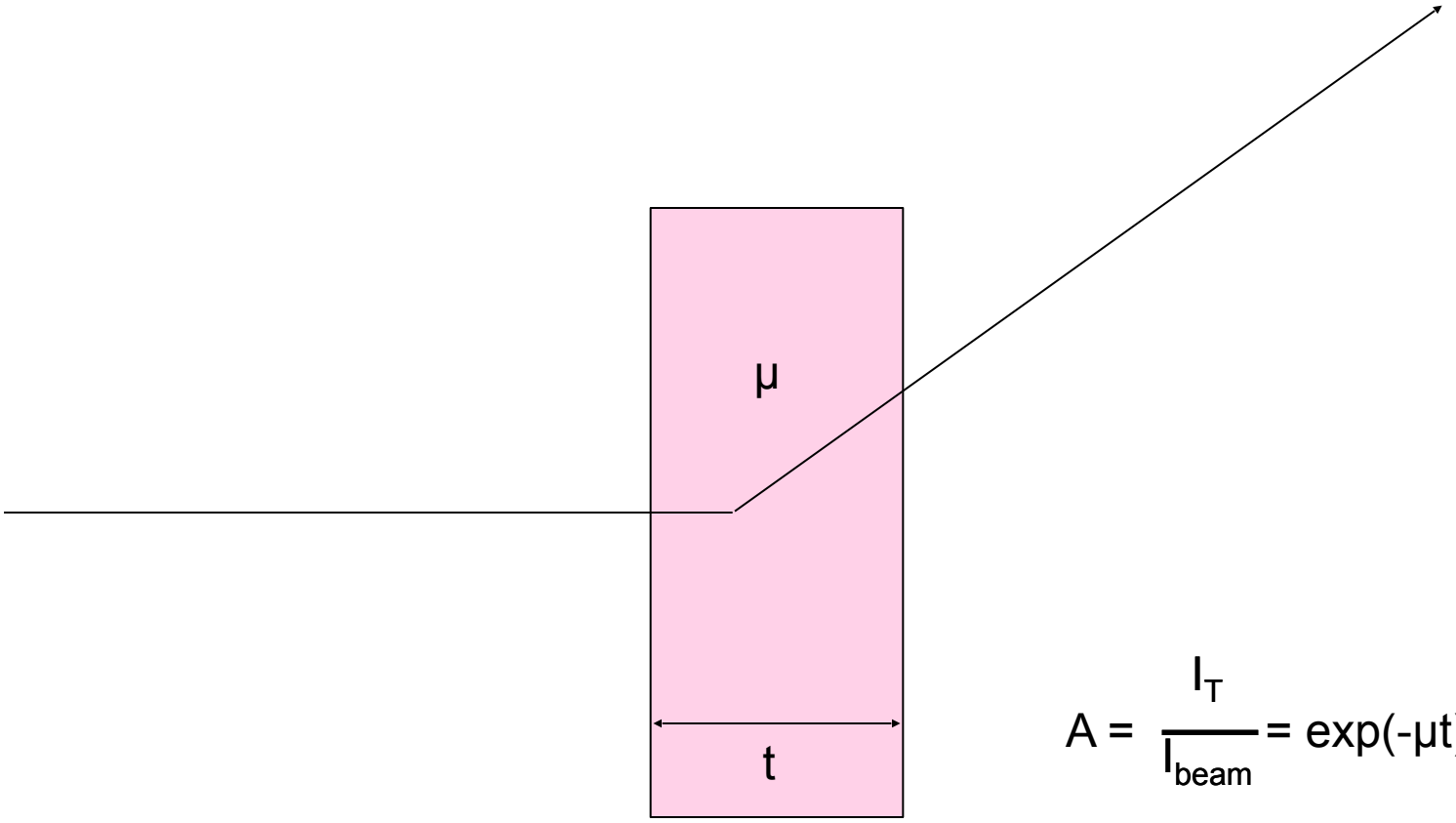

$$A = \frac{I_T}{I_{beam}} = \exp(-\mu t)$$

Bouguer, P. (1729). *Essai d'optique sur la gradation de la lumière*.
Lambert, J. H. (1760). *Photometria: sive De mensura et gradibus luminis, colorum et umbrae*. E. Klett.
Beer, A. (1852)."Bestimmung der Absorption des rothen Lichts in farbigen Flüssigkeiten", *Ann. Phys. Chem* **86**, 78-90.

attenuation factor

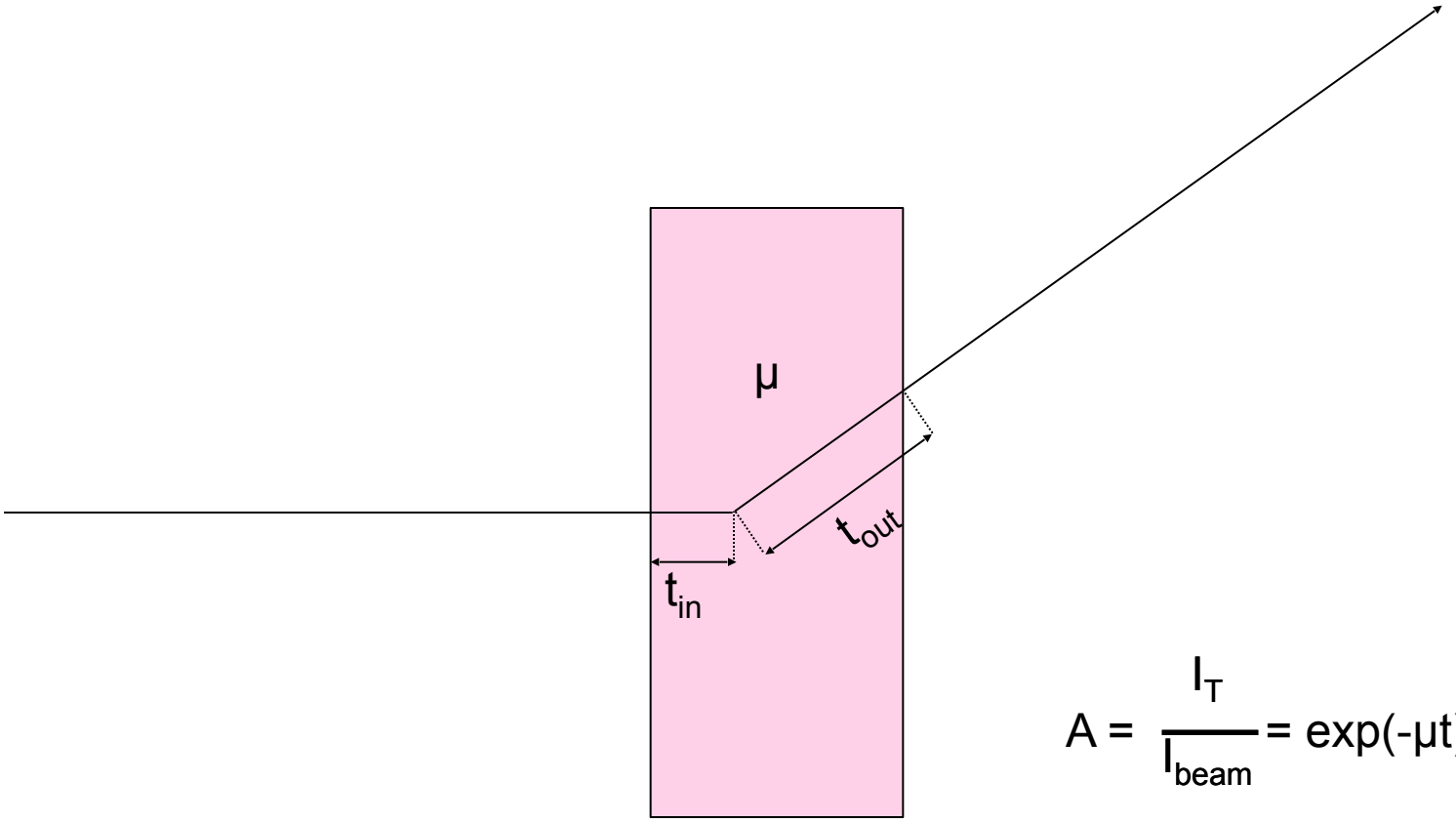

$$A = \frac{I_T}{I_{beam}} = \exp(-\mu t)$$

Bouguer, P. (1729). *Essai d'optique sur la gradation de la lumière*.

Lambert, J. H. (1760). *Photometria: sive De mensura et gradibus luminis, colorum et umbrae*. E. Klett.

Beer, A. (1852)."Bestimmung der Absorption des rothen Lichts in farbigen Flüssigkeiten", *Ann. Phys. Chem* **86**, 78-90.

attenuation factor

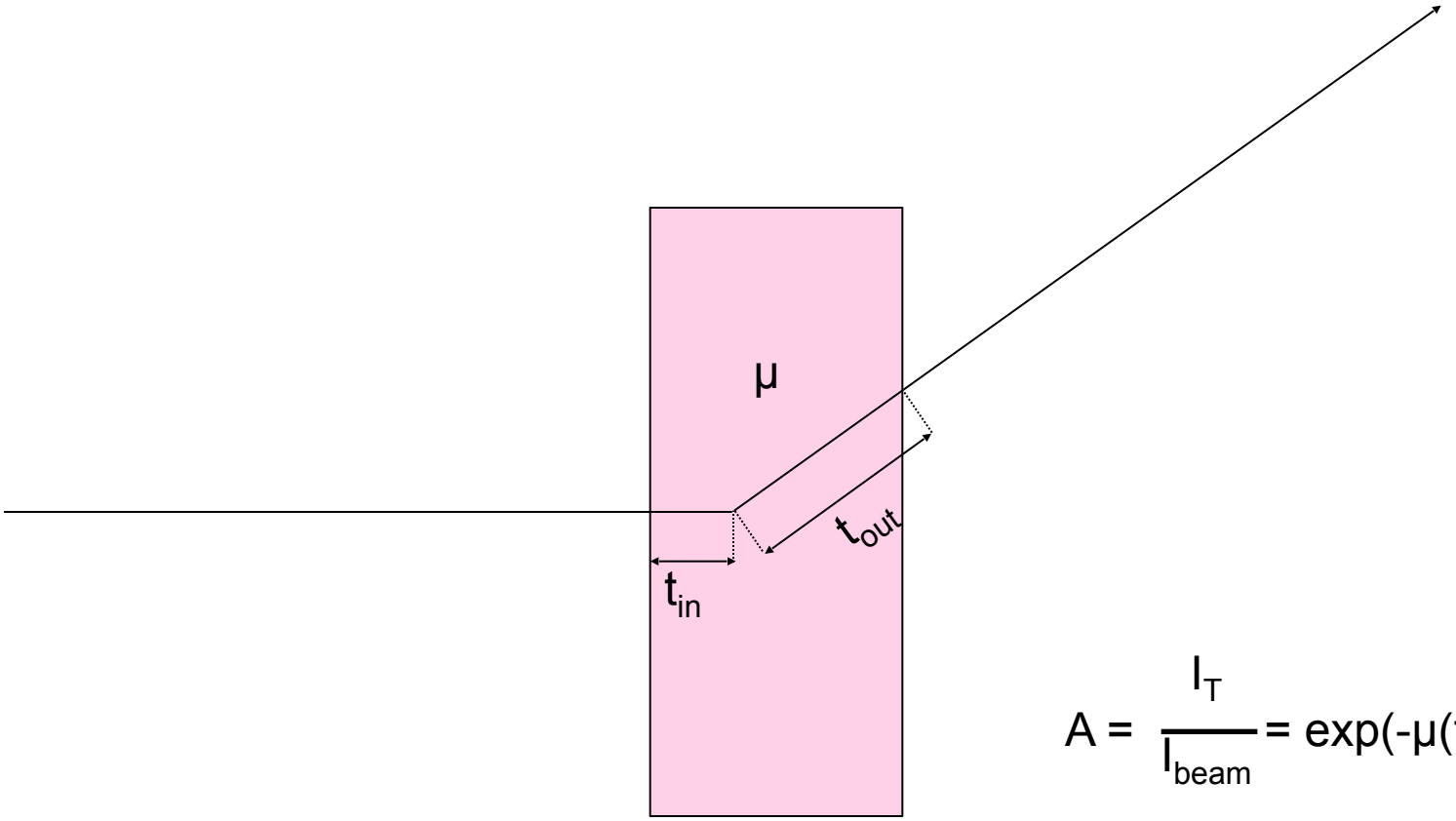

$$A = \frac{I_T}{I_{beam}} = \exp(-\mu(t_{in} + t_{out}))$$

Bouguer, P. (1729). *Essai d'optique sur la gradation de la lumière*.

Lambert, J. H. (1760). *Photometria: sive De mensura et gradibus luminis, colorum et umbrae*. E. Klett.

Beer, A. (1852)."Bestimmung der Absorption des rothen Lichts in farbigen Flüssigkeiten", *Ann. Phys. Chem* **86**, 78-90.

attenuation factor

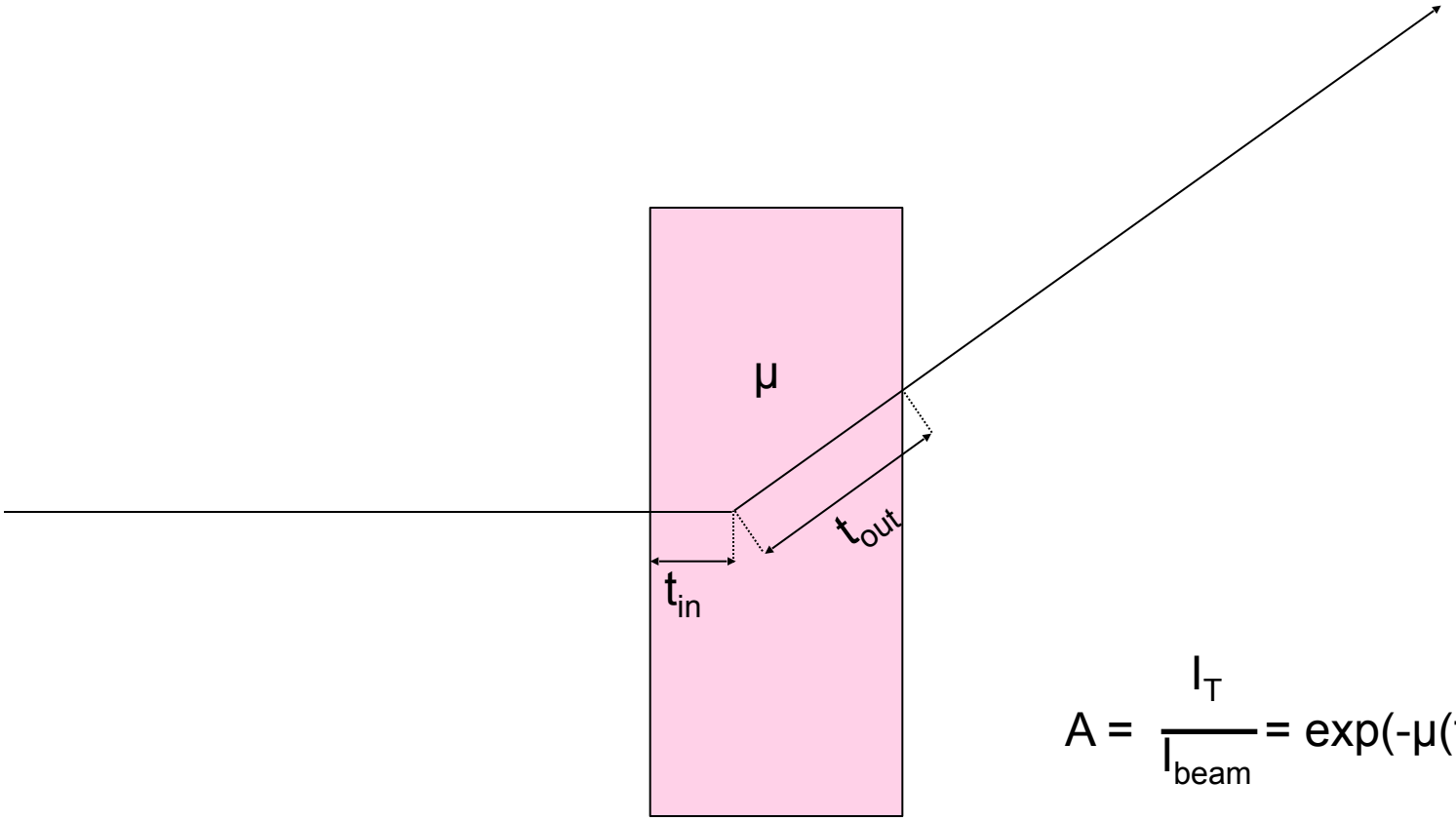

$$A = \frac{I_T}{I_{beam}} = \exp(-\mu(t_{in} + t_{out}))$$

Bouguer, P. (1729). *Essai d'optique sur la gradation de la lumière*.

Lambert, J. H. (1760). *Photometria: sive De mensura et gradibus luminis, colorum et umbrae*. E. Klett.

Beer, A. (1852)."Bestimmung der Absorption des rothen Lichts in farbigen Flüssigkeiten", *Ann. Phys. Chem* **86**, 78-90.

attenuation factor

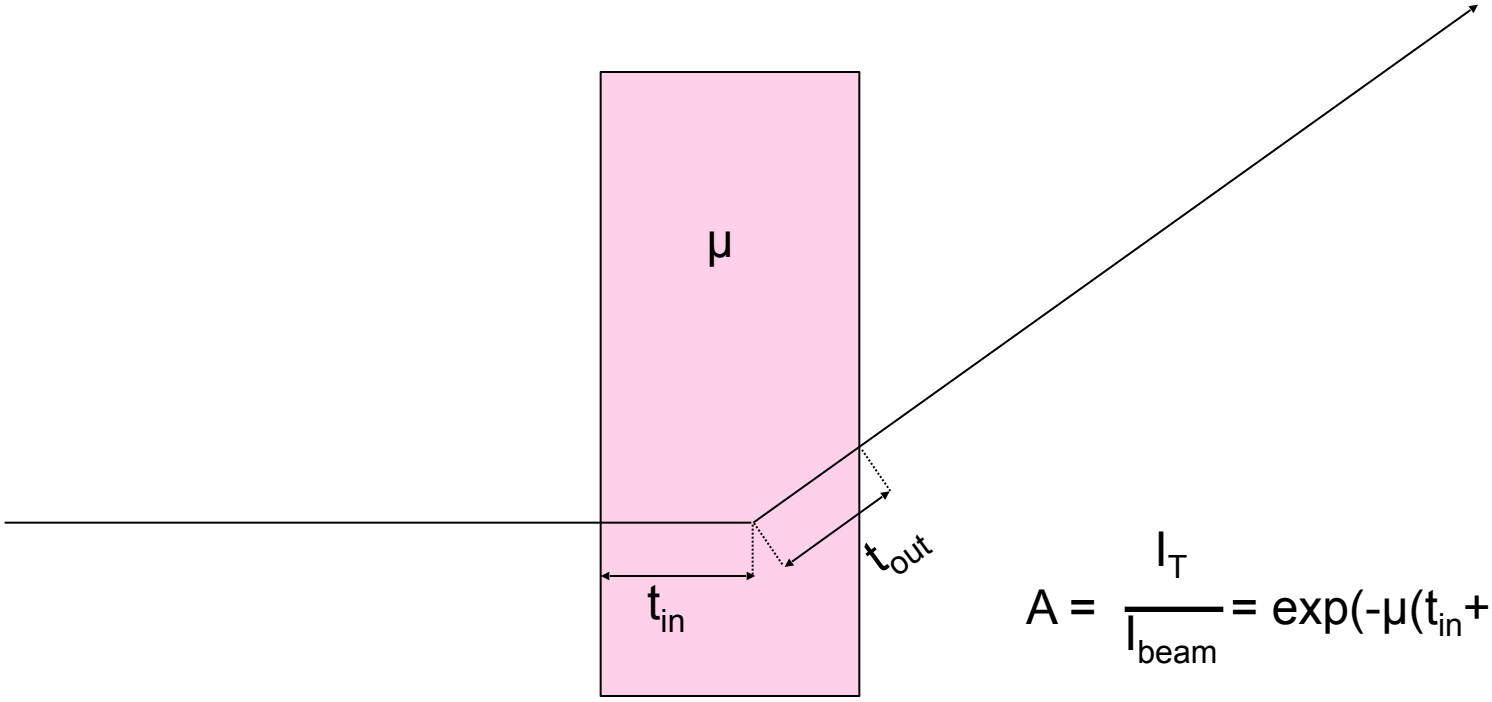

Bouguer, P. (1729). *Essai d'optique sur la gradation de la lumière*.

Lambert, J. H. (1760). *Photometria: sive De mensura et gradibus luminis, colorum et umbrae*. E. Klett.

Beer, A. (1852)."Bestimmung der Absorption des rothen Lichts in farbigen Flüssigkeiten", *Ann. Phys. Chem* **86**, 78-90.

attenuation factor

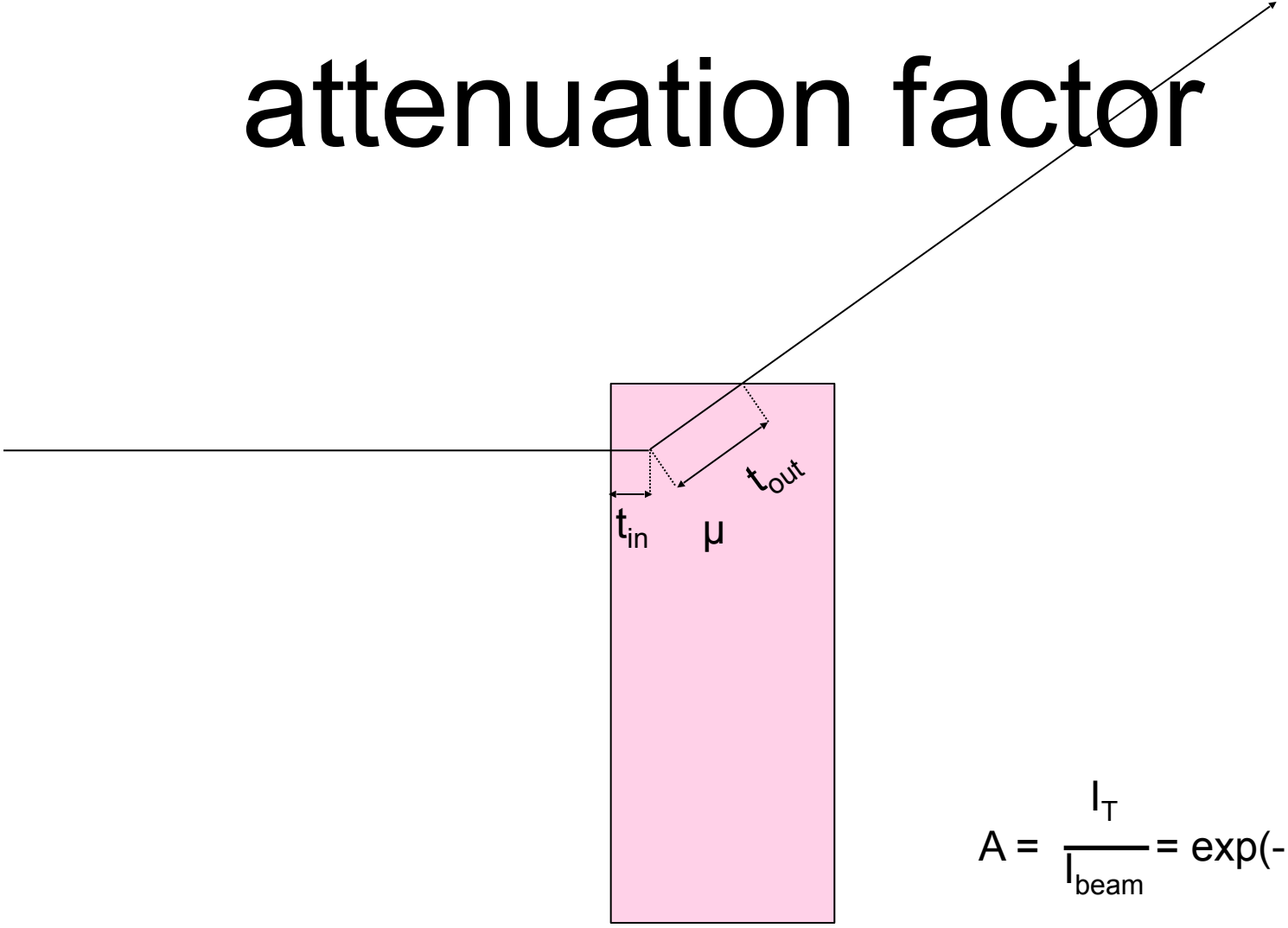

$$A = \frac{I_T}{I_{beam}} = \exp(-\mu(t_{in} + t_{out}))$$

Bouguer, P. (1729). *Essai d'optique sur la gradation de la lumière*.

Lambert, J. H. (1760). *Photometria: sive De mensura et gradibus luminis, colorum et umbrae*. E. Klett.

Beer, A. (1852)."Bestimmung der Absorption des rothen Lichts in farbigen Flüssigkeiten", *Ann. Phys. Chem* **86**, 78-90.

attenuation factor

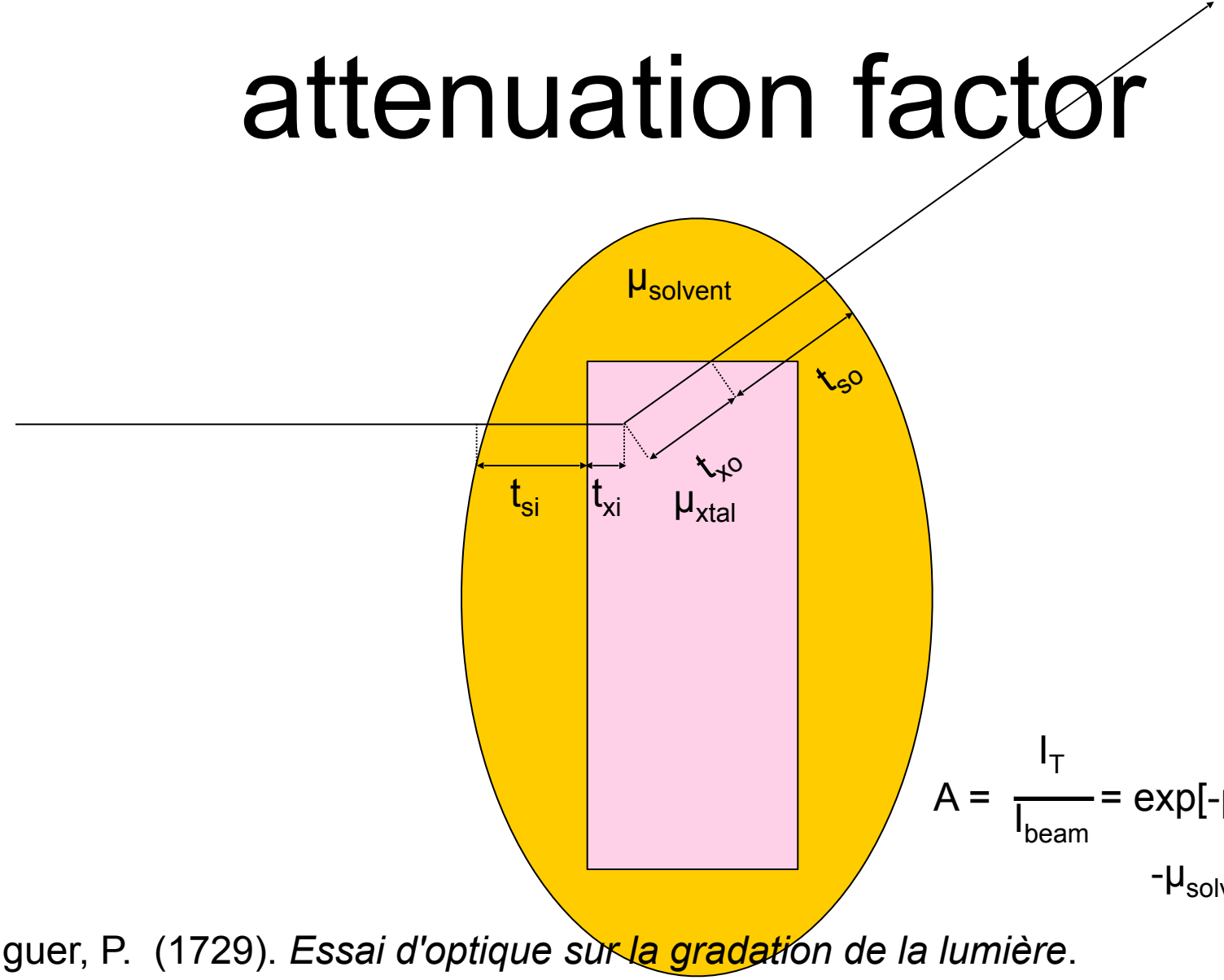

$$A = \frac{I_T}{I_{beam}} = \exp[-\mu_{xtal}(t_{xi} + t_{xo}) - \mu_{solvent}(t_{si} + t_{so})]$$

Bouguer, P. (1729). *Essai d'optique sur la gradation de la lumière*.

Lambert, J. H. (1760). *Photometria: sive De mensura et gradibus luminis, colorum et umbrae*. E. Klett.

Beer, A. (1852)."Bestimmung der Absorption des rothen Lichts in farbigen Flüssigkeiten", *Ann. Phys. Chem* **86**, 78-90.

attenuation factor

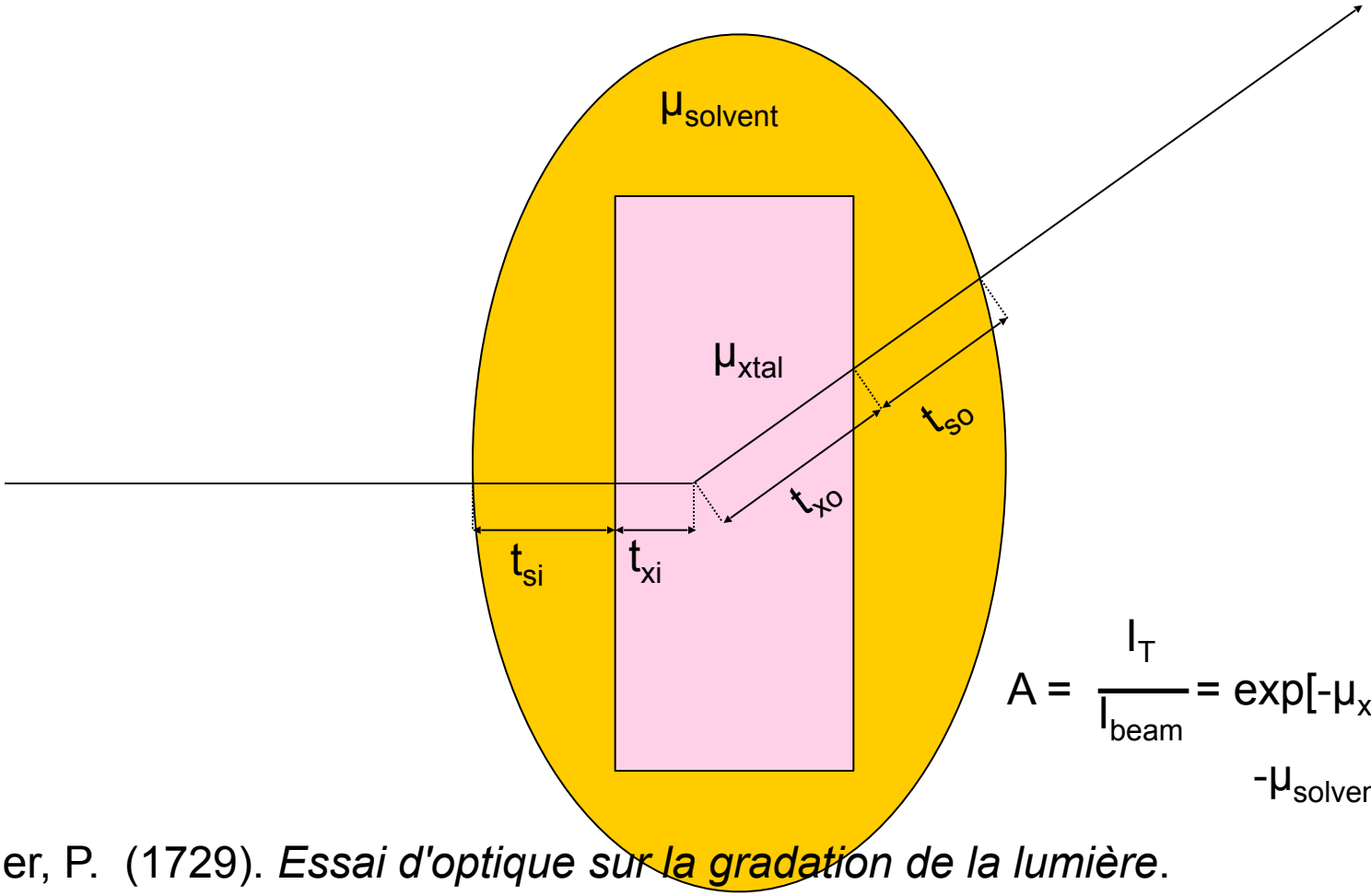

$$A = \frac{I_T}{I_{beam}} = \exp[-\mu_{xtal}(t_{xi} + t_{xo}) - \mu_{solvent}(t_{si} + t_{so})]$$

Bouguer, P. (1729). *Essai d'optique sur la gradation de la lumière*.

Lambert, J. H. (1760). *Photometria: sive De mensura et gradibus luminis, colorum et umbrae*. E. Klett.

Beer, A. (1852)."Bestimmung der Absorption des rothen Lichts in farbigen Flüssigkeiten", *Ann. Phys. Chem* **86**, 78-90.

attenuation factor

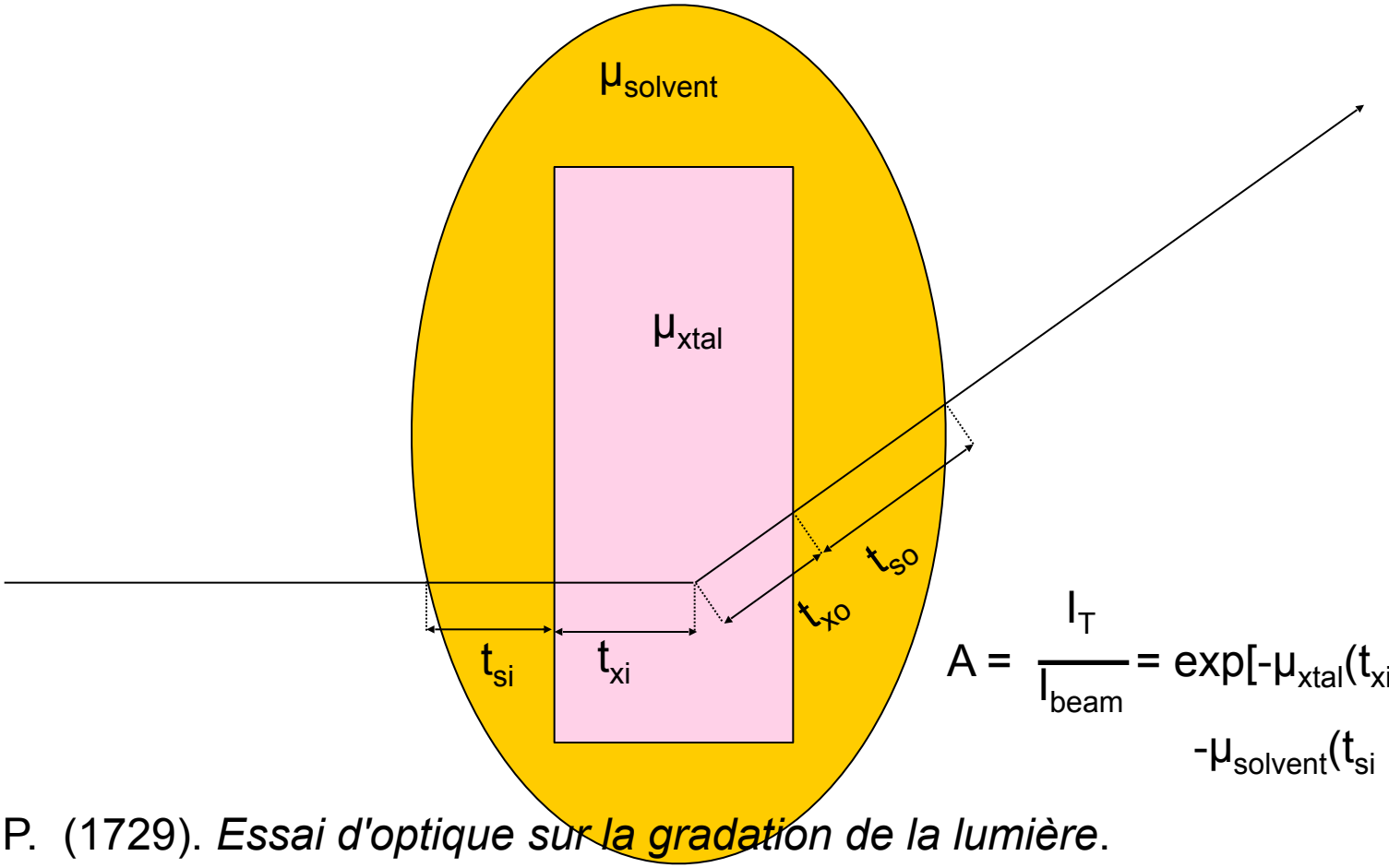

$$A = \frac{I_T}{I_{beam}} = \exp[-\mu_{xtal}(t_{xi} + t_{xo}) - \mu_{solvent}(t_{si} + t_{so})]$$

Bouguer, P. (1729). *Essai d'optique sur la gradation de la lumière*.

Lambert, J. H. (1760). *Photometria: sive De mensura et gradibus luminis, colorum et umbrae*. E. Klett.

Beer, A. (1852)."Bestimmung der Absorption des rothen Lichts in farbigen Flüssigkeiten", *Ann. Phys. Chem* **86**, 78-90.

Where do photons go?

Protein
1A x-rays

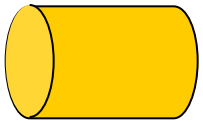

beamstop

Where do photons go?

Protein
1A x-rays

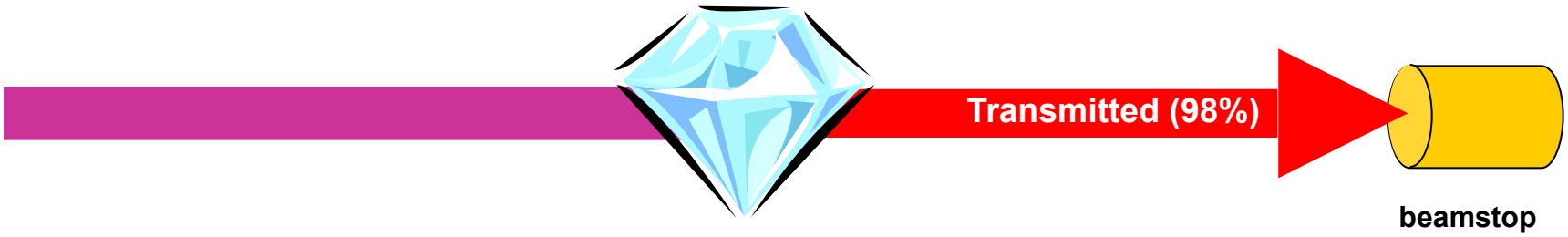

Where do photons go?

Protein
1A x-rays

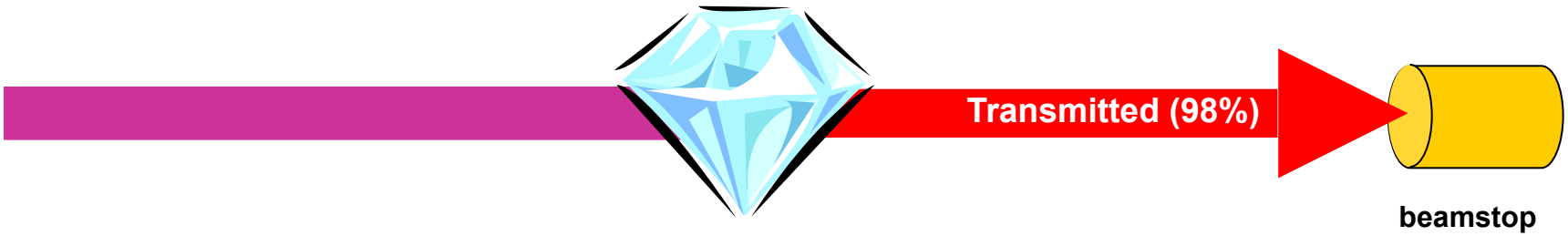

attenuation correction cannot be > ~2%
for 100 μm xtal at 1 Å

Classes of error in MX

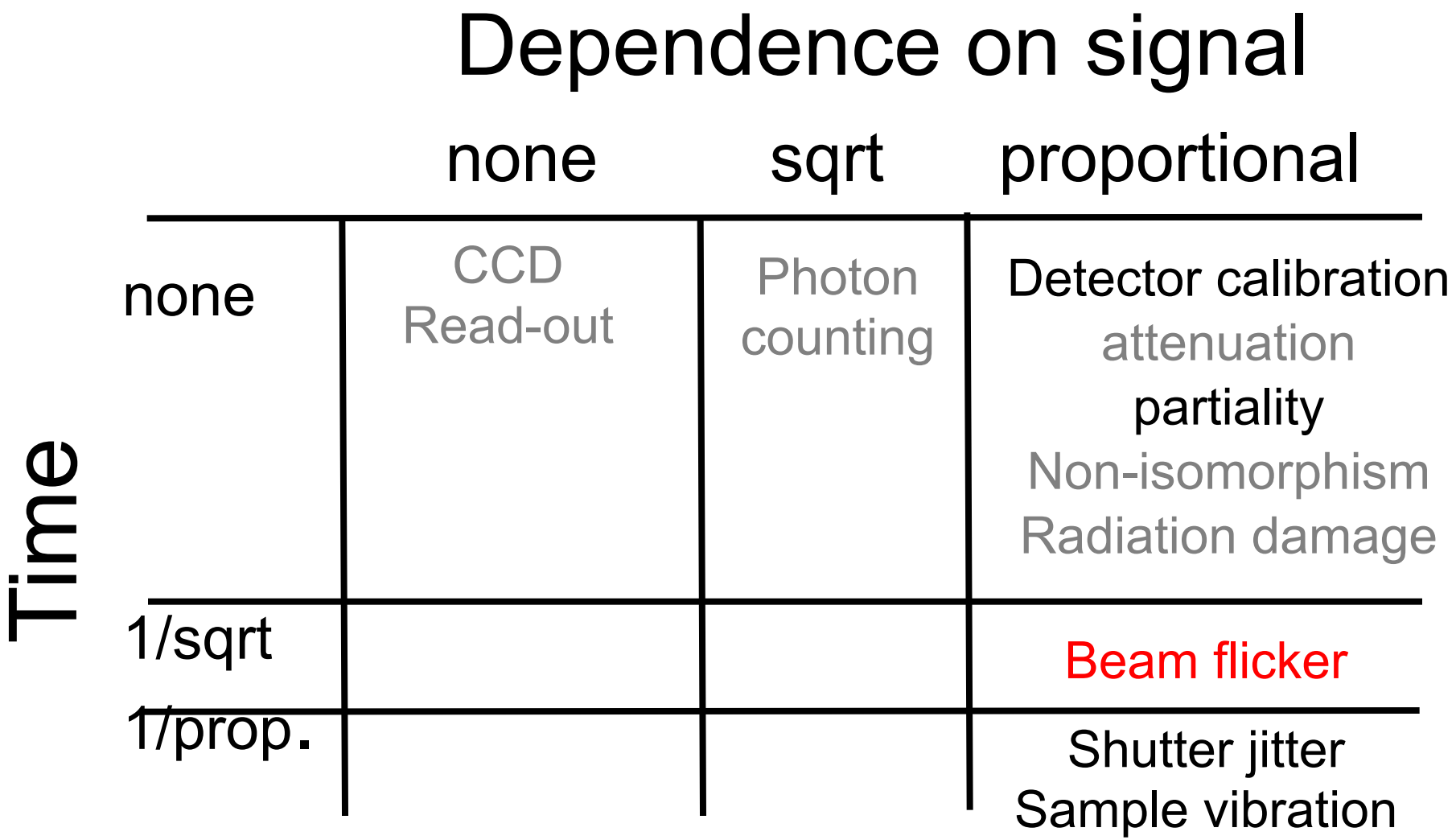

Beam Flicker

1/f noise or “flicker noise”

comes from everything

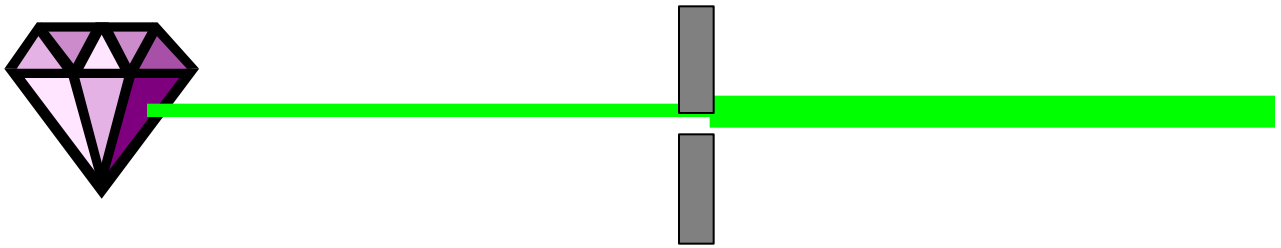

Beam Flicker

1/f noise or “flicker noise”

comes from everything

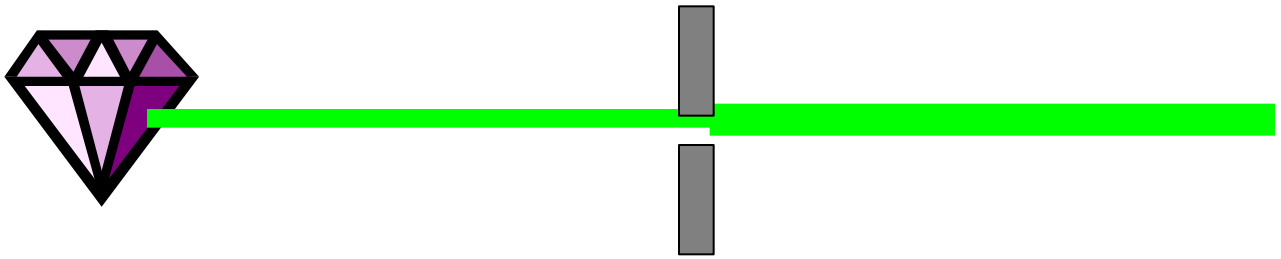

Beam Flicker

1/f noise or “flicker noise”

comes from everything

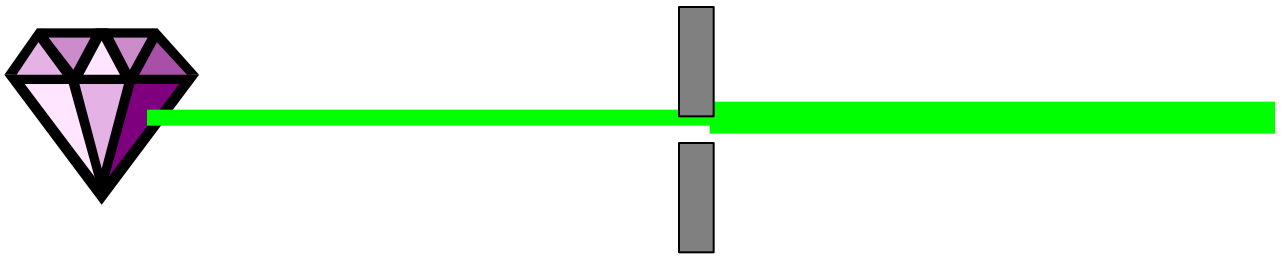

Beam Flicker

1/f noise or “flicker noise”

comes from everything

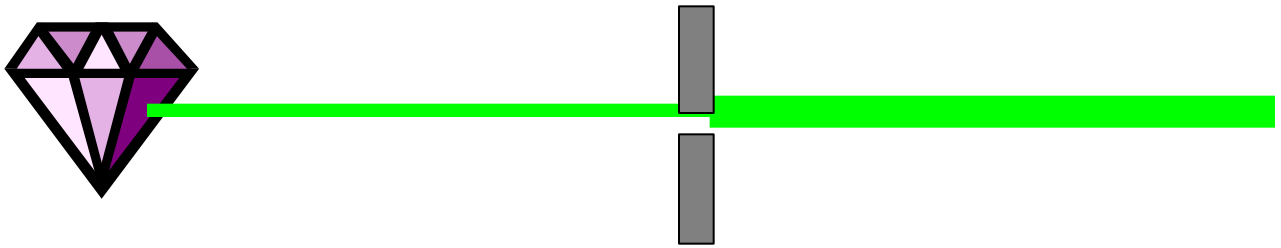

Beam Flicker

1/f noise or “flicker noise”

comes from everything

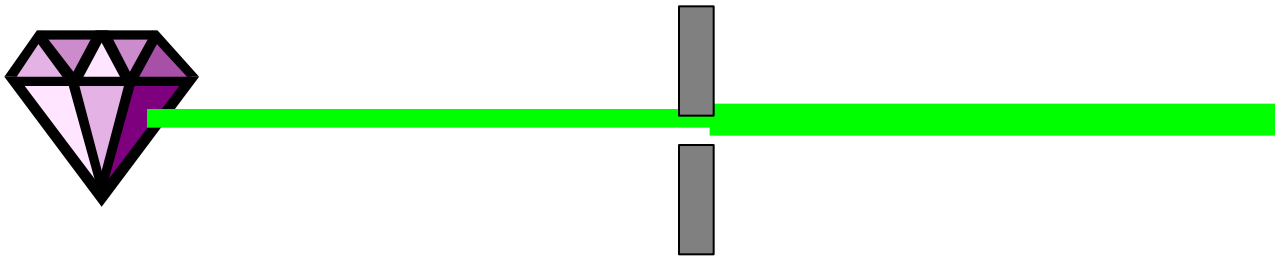

Beam Flicker

1/f noise or “flicker noise”

comes from everything

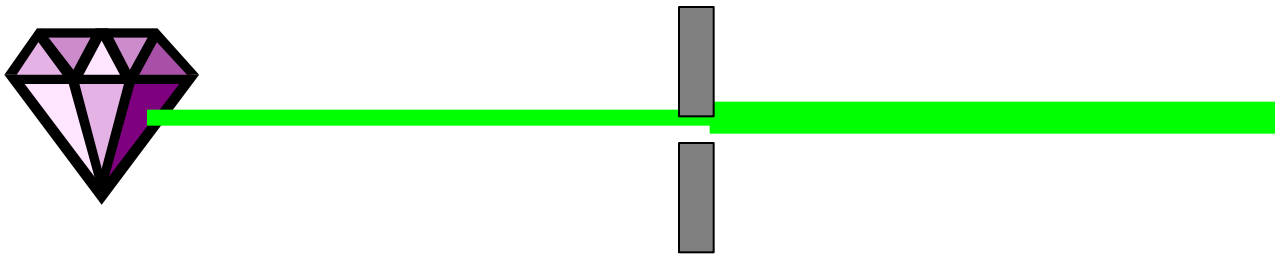

Beam Flicker

1/f noise or “flicker noise”

comes from everything

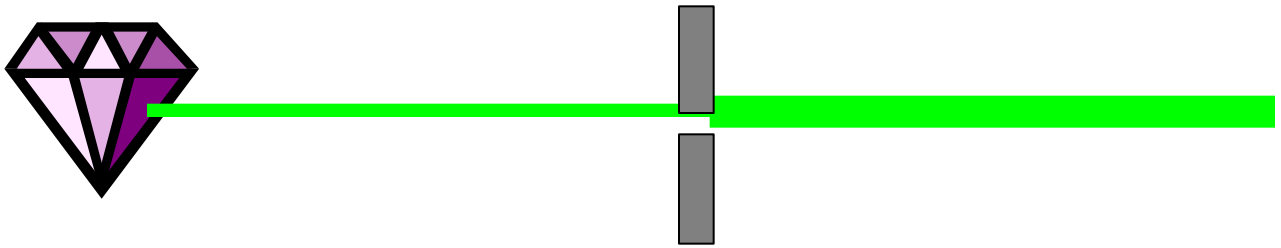

Beam Flicker

1/f noise or “flicker noise”

comes from everything

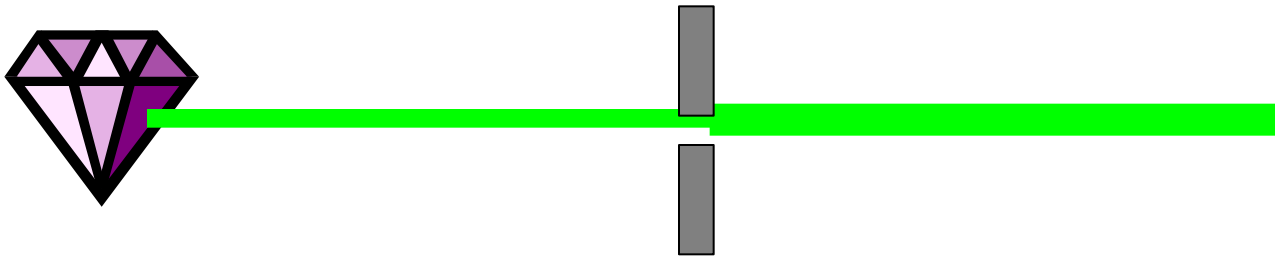

Beam Flicker

1/f noise or “flicker noise”

comes from everything

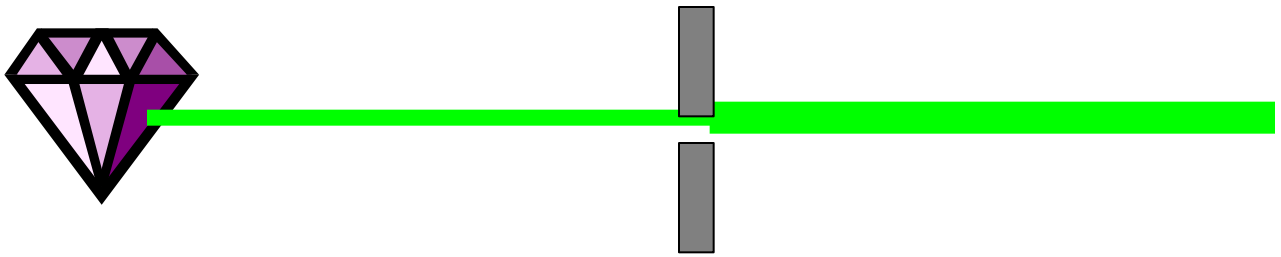

Beam Flicker

1/f noise or “flicker noise”

comes from everything

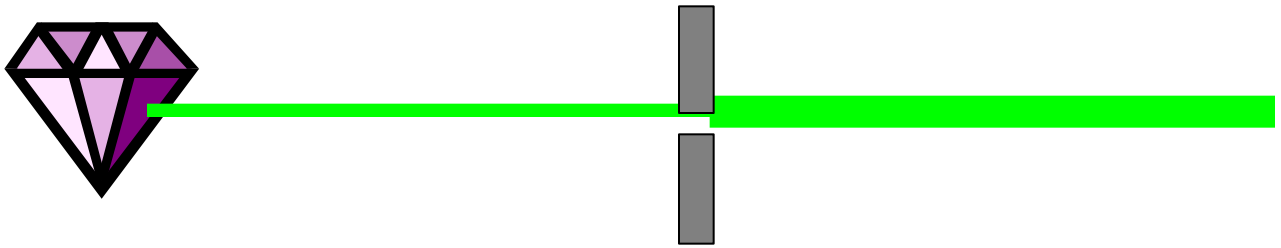

Beam Flicker

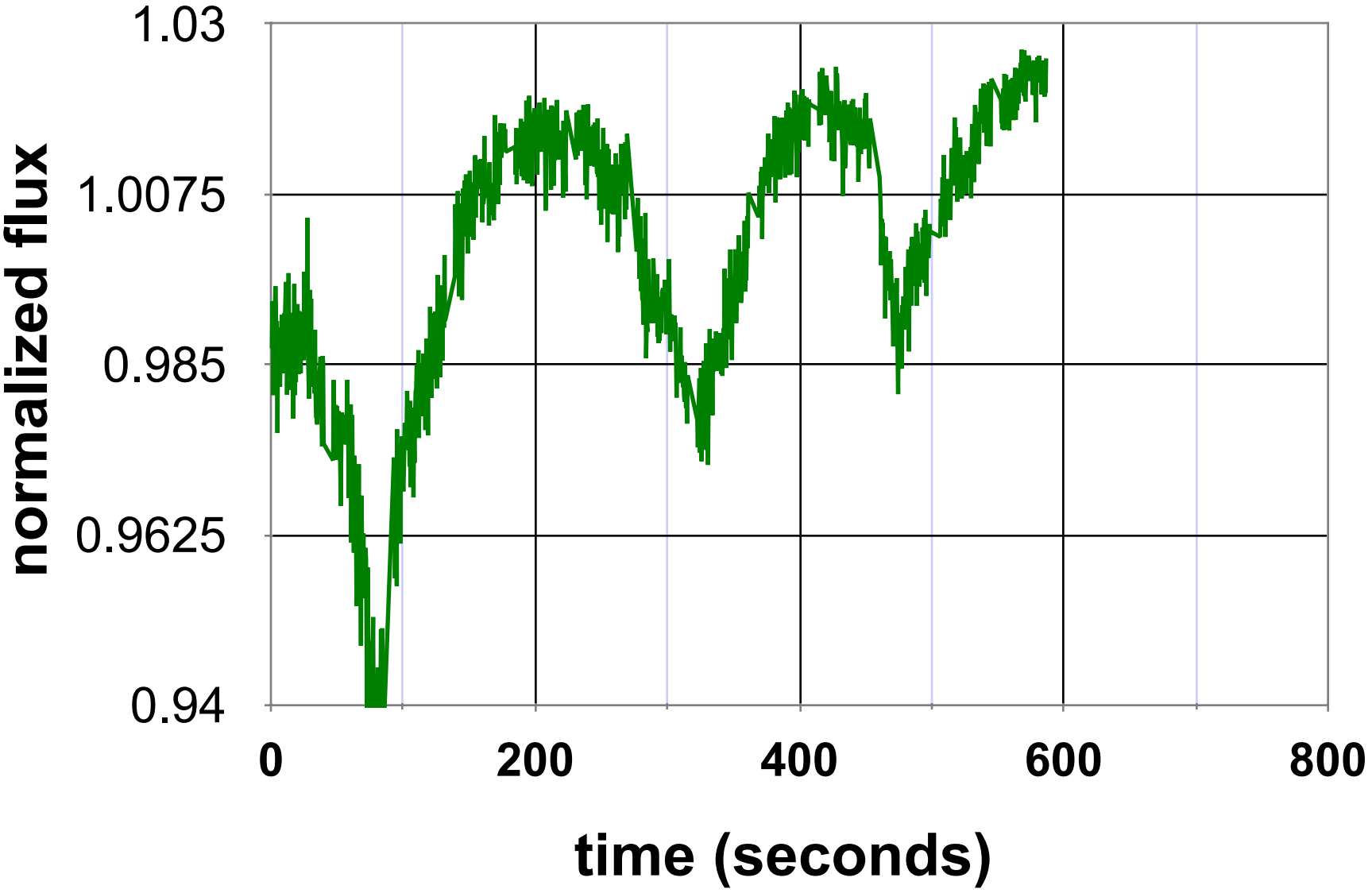

Beam Flicker

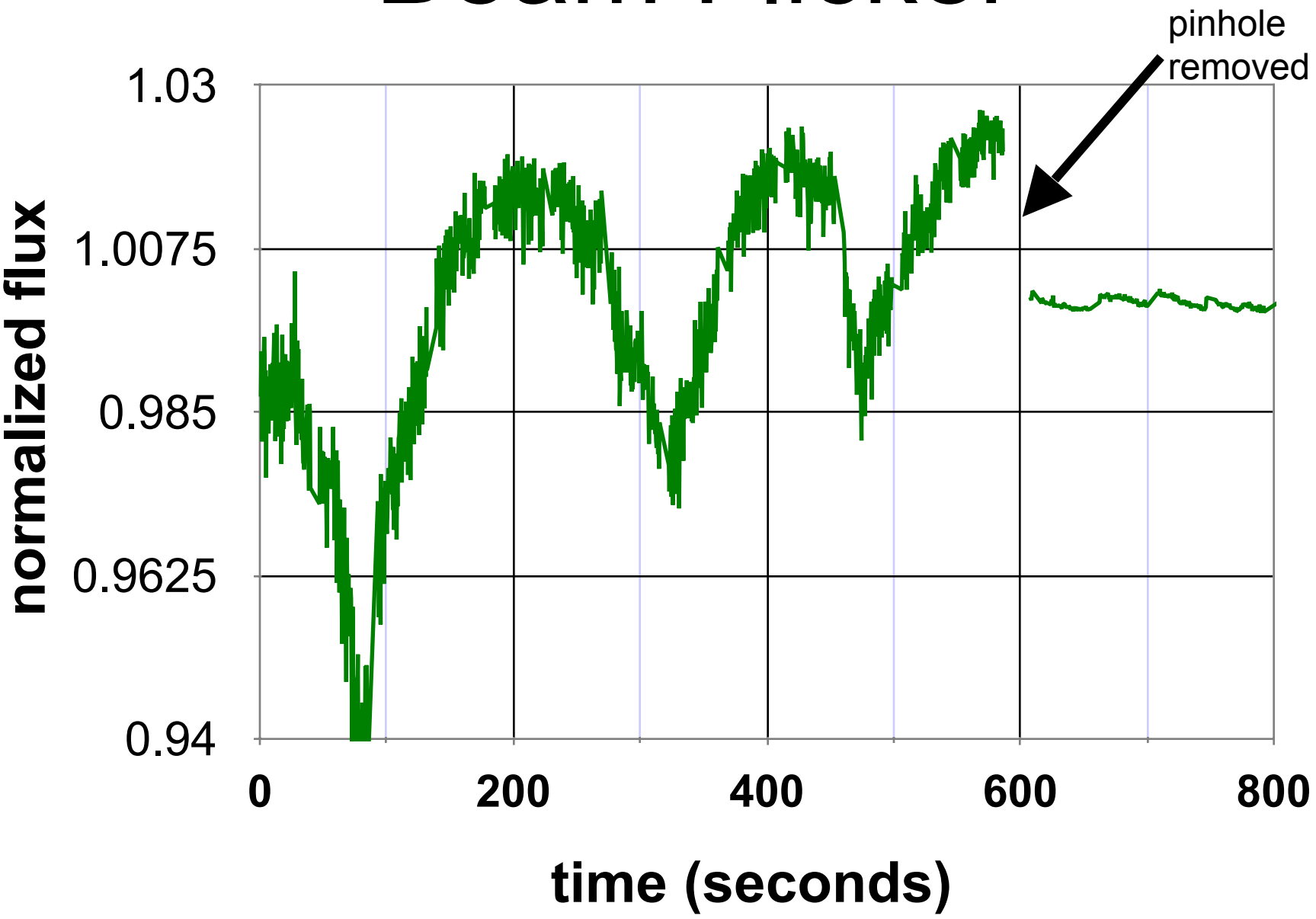

Beam Flicker

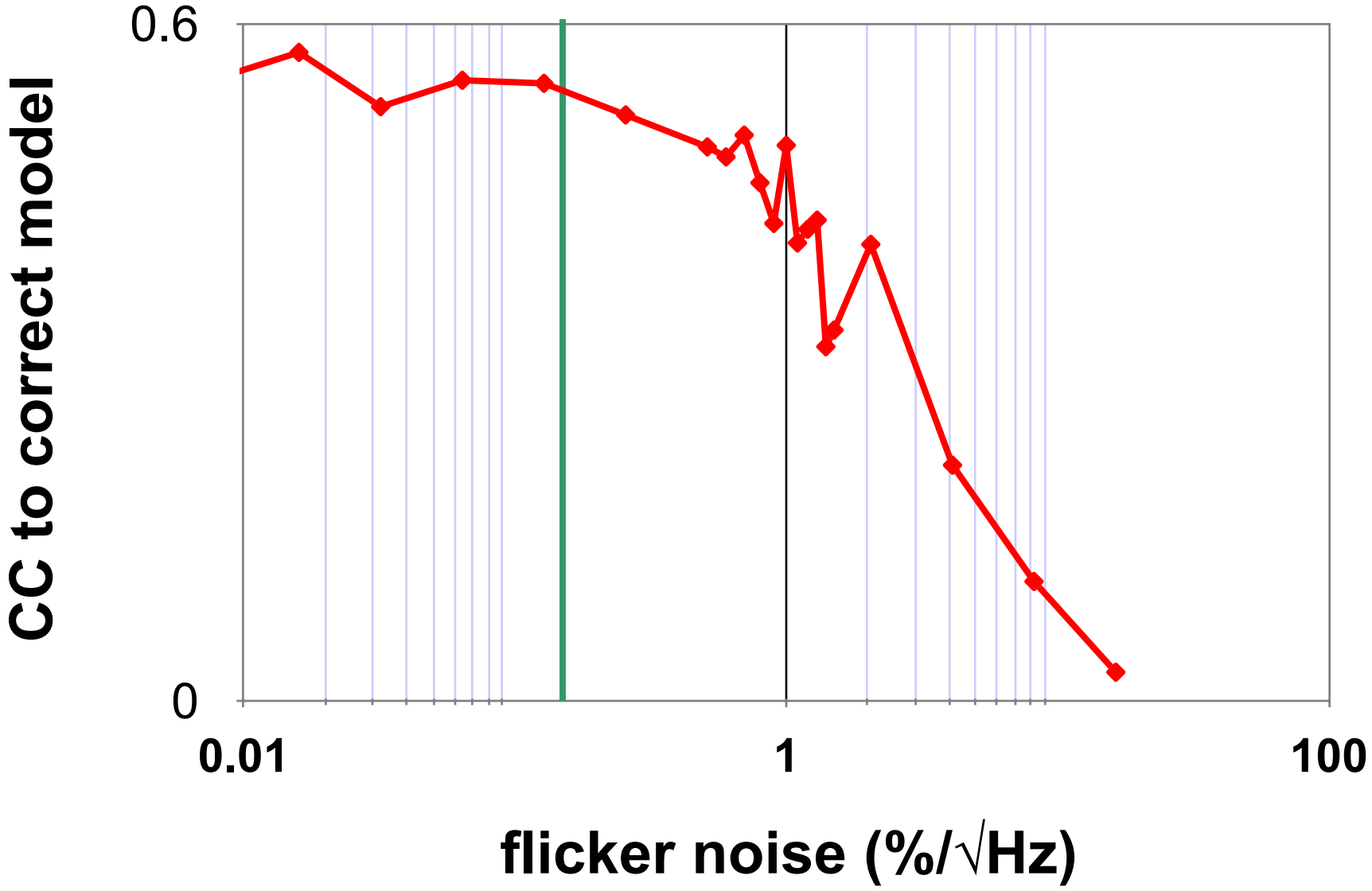

Classes of error in MX

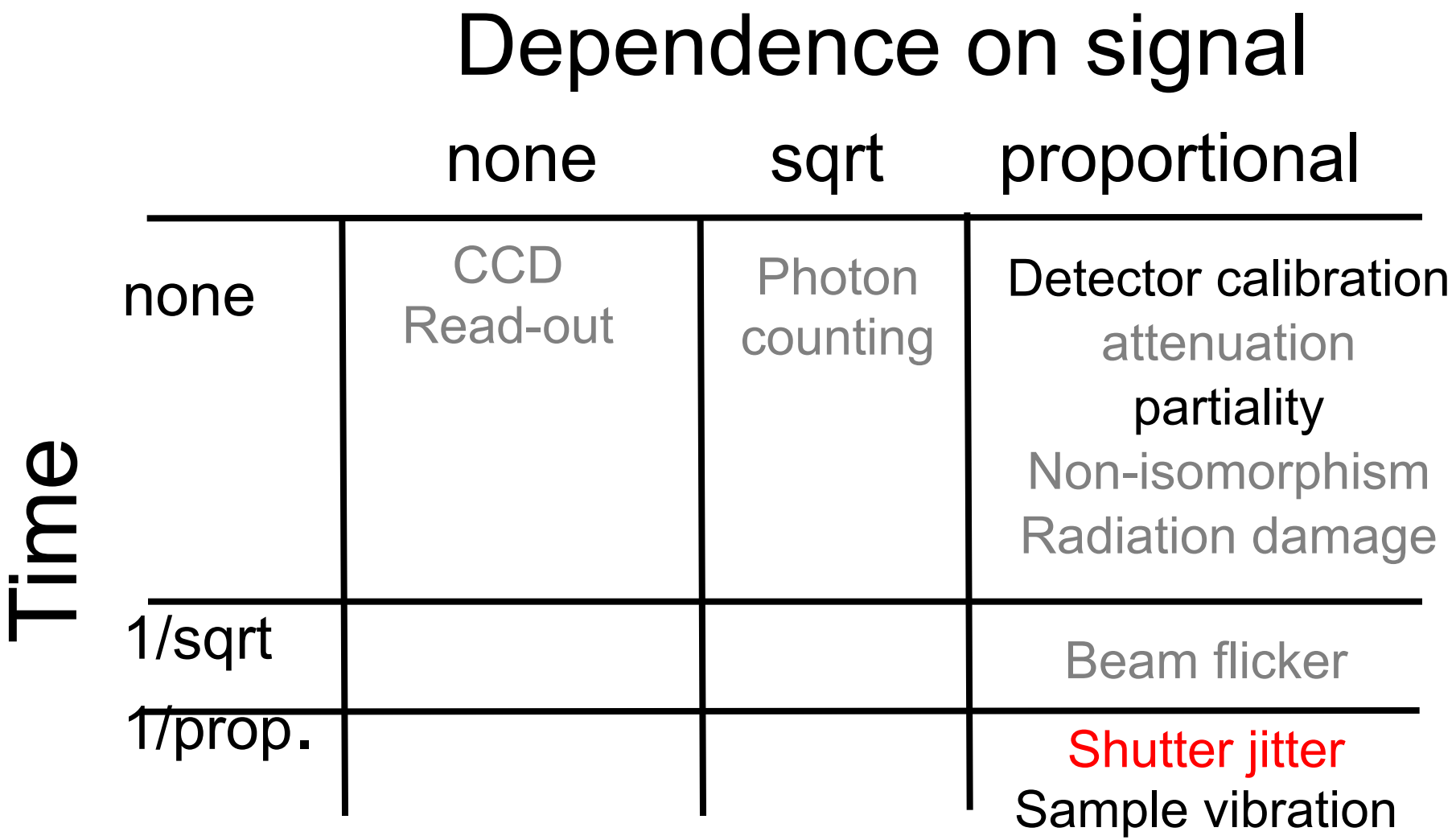

Shutter Jitter

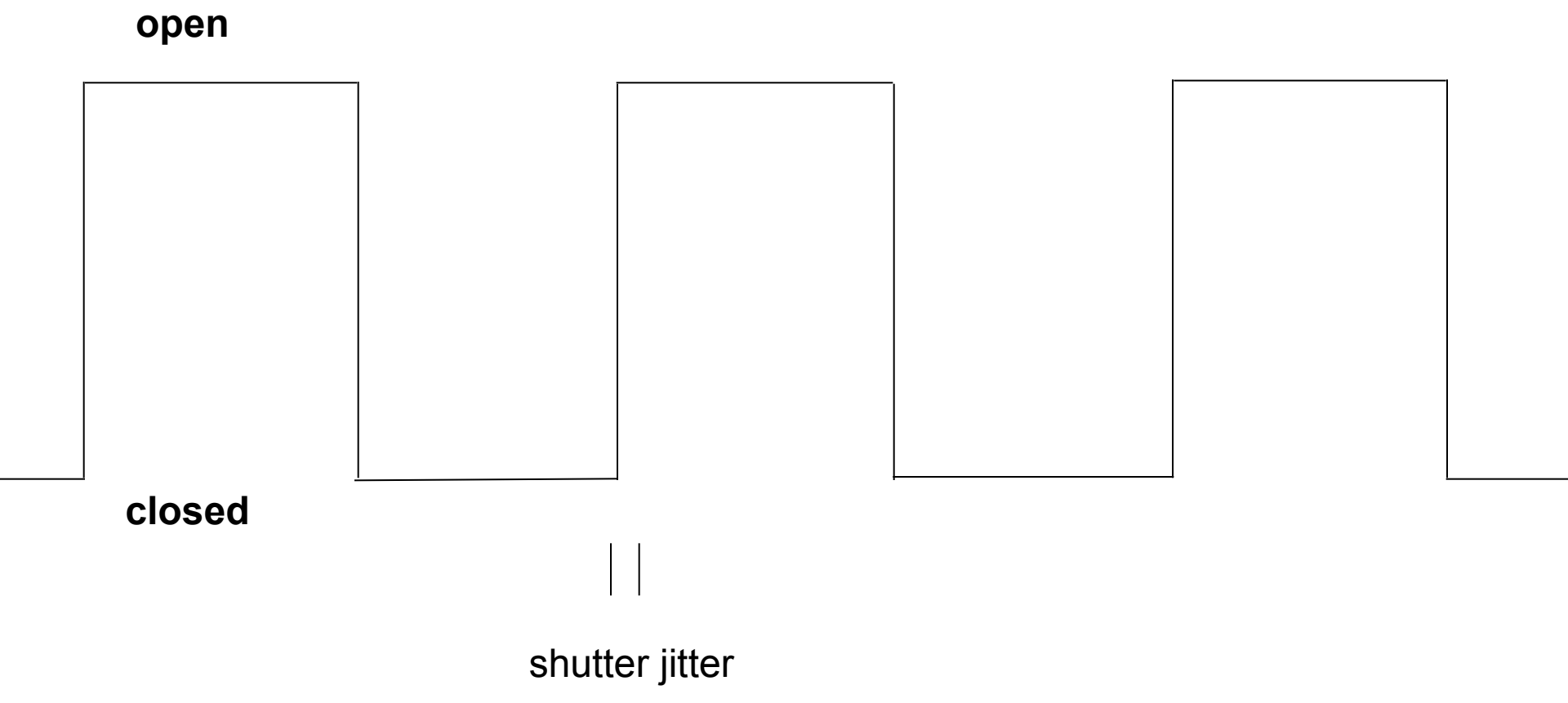

Shutter Jitter

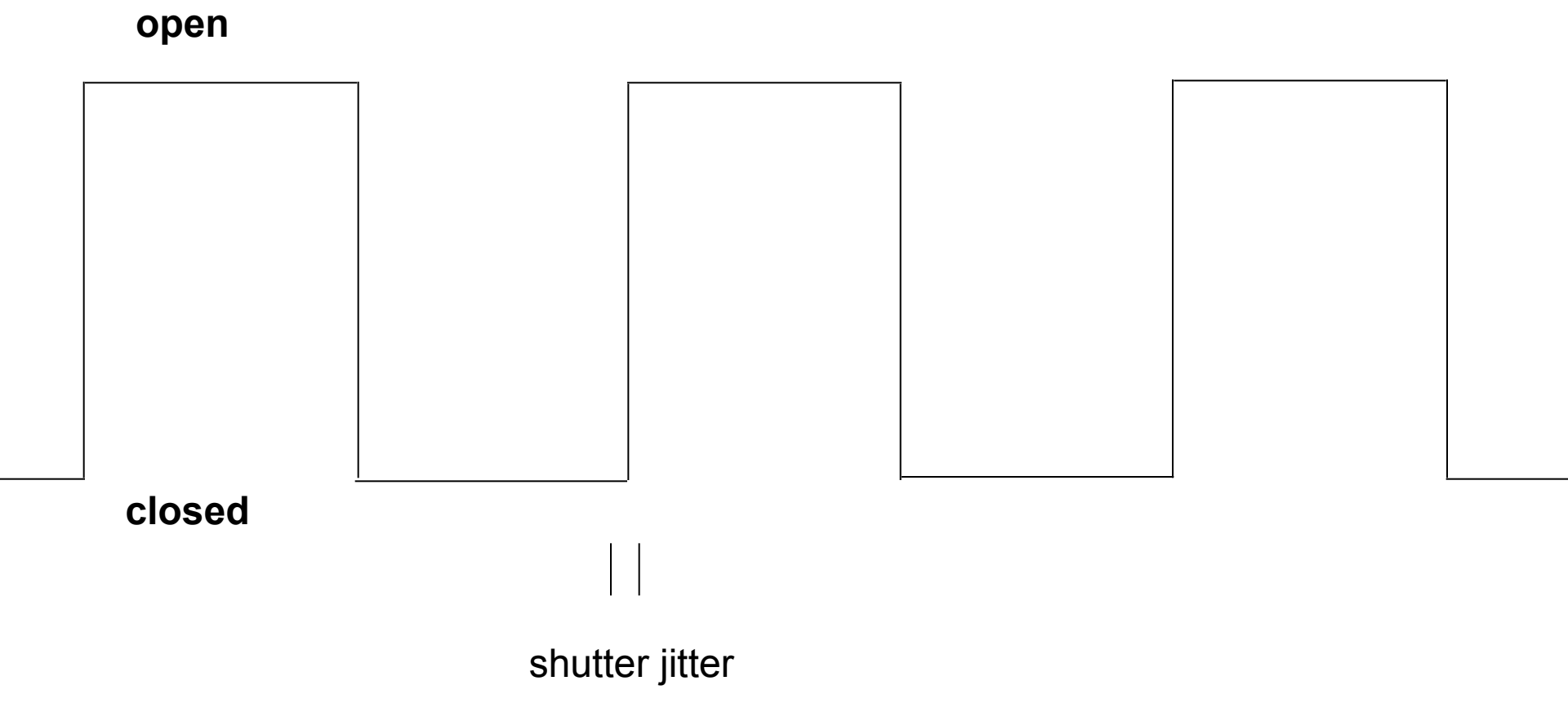

Shutter Jitter

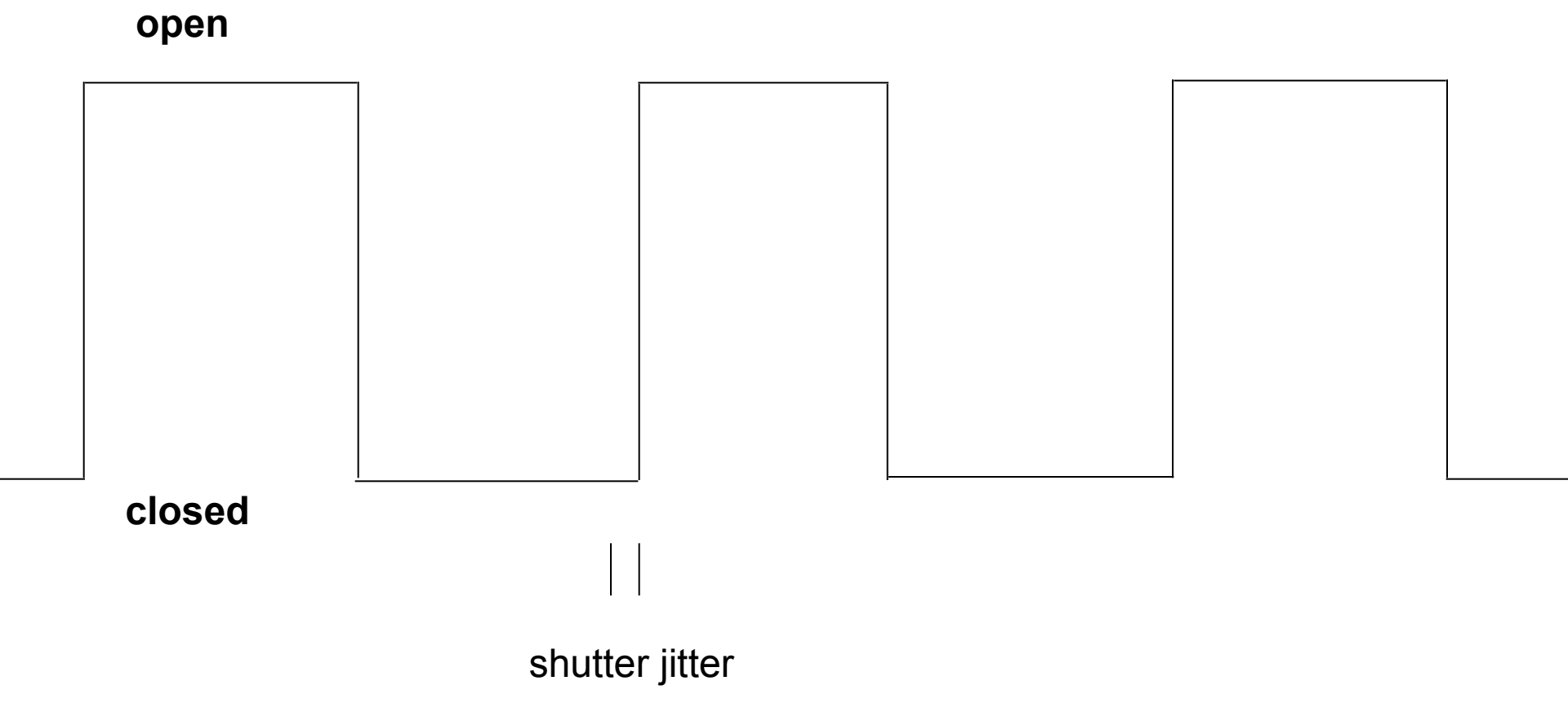

Shutter Jitter

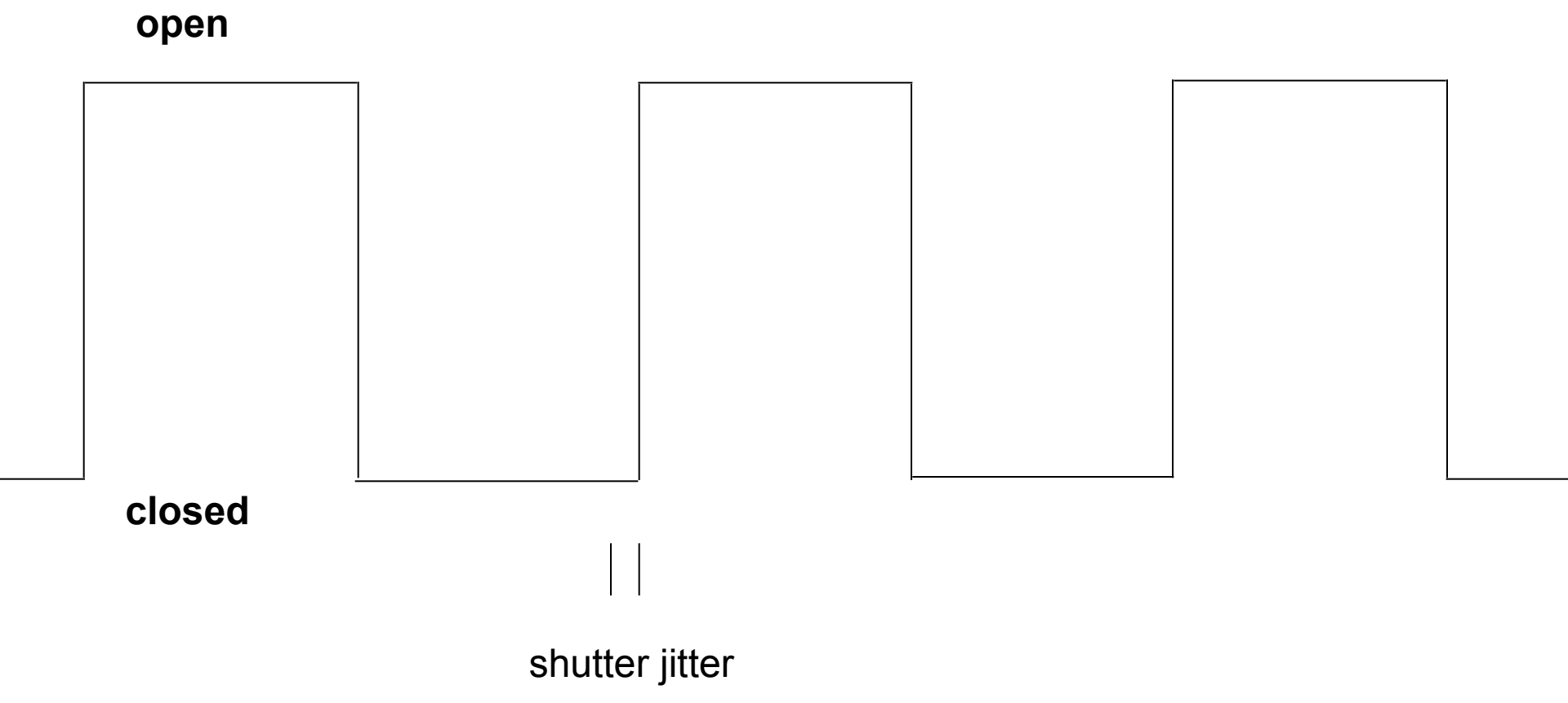

Shutter Jitter

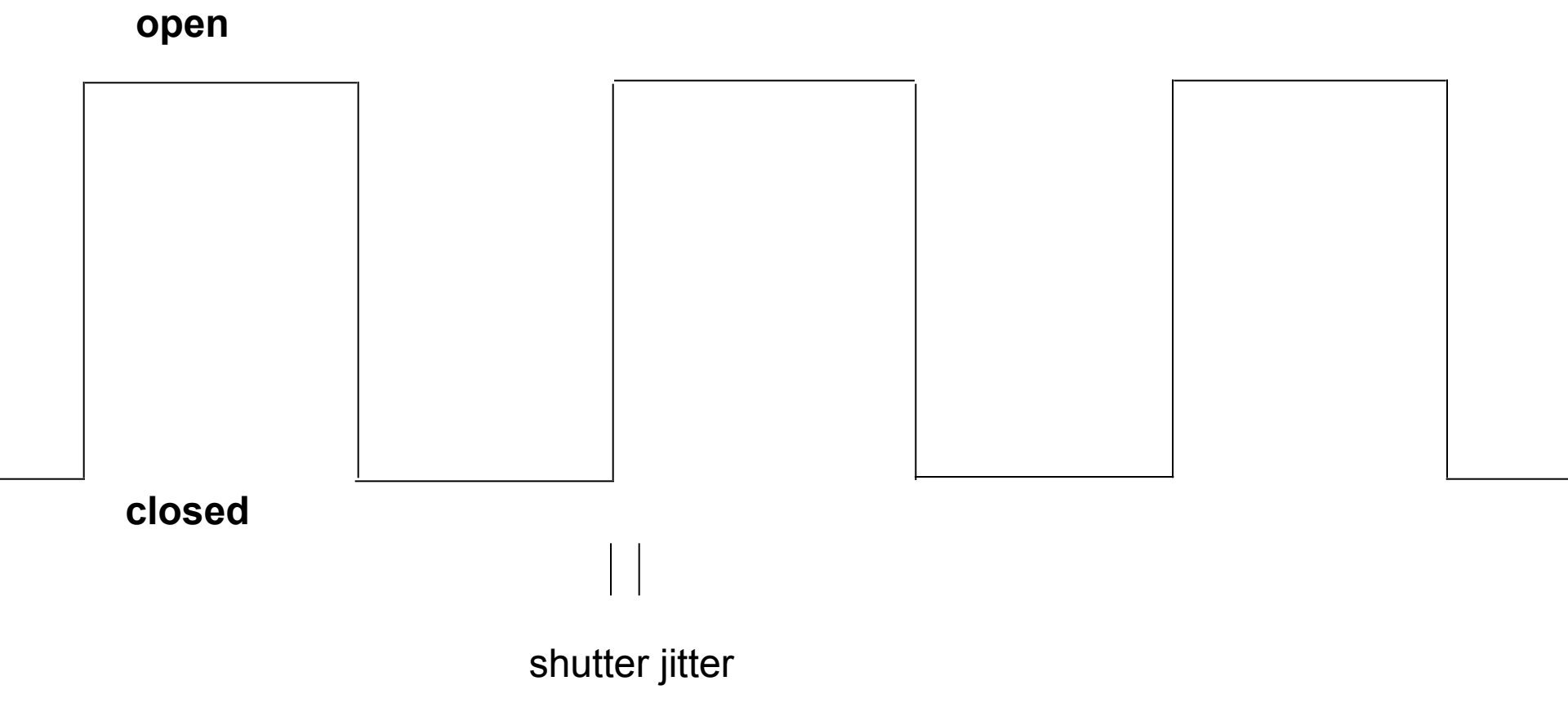

Shutter Jitter

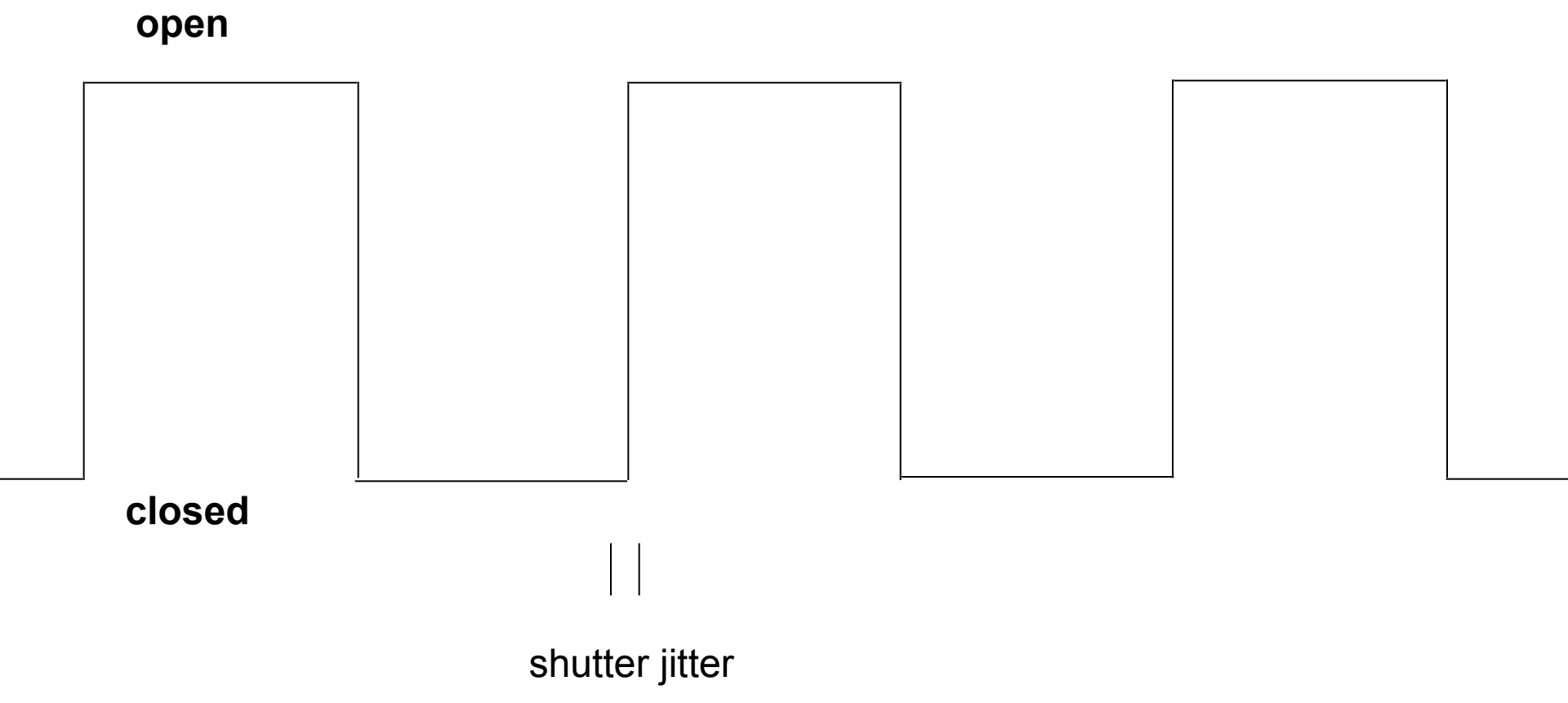

Shutter Jitter

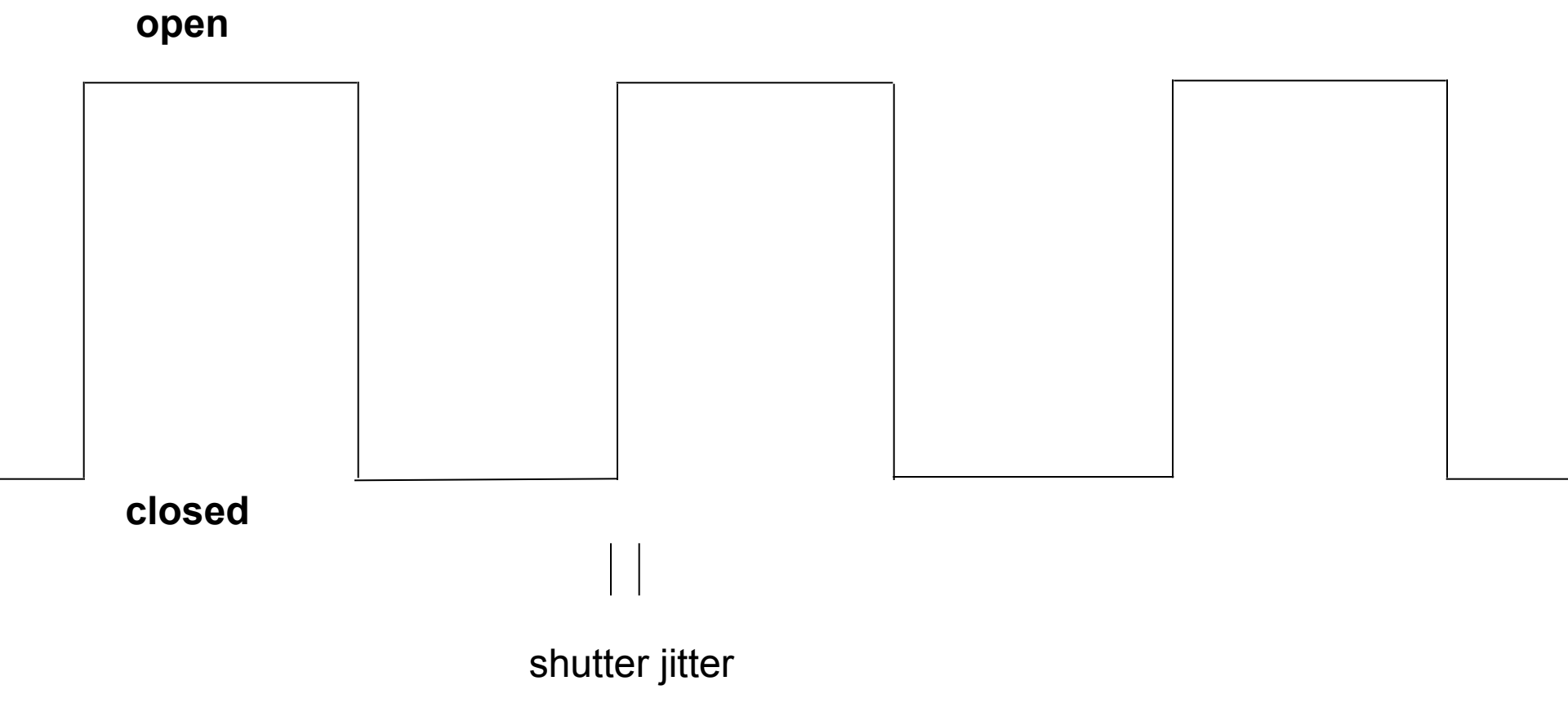

Shutter Jitter

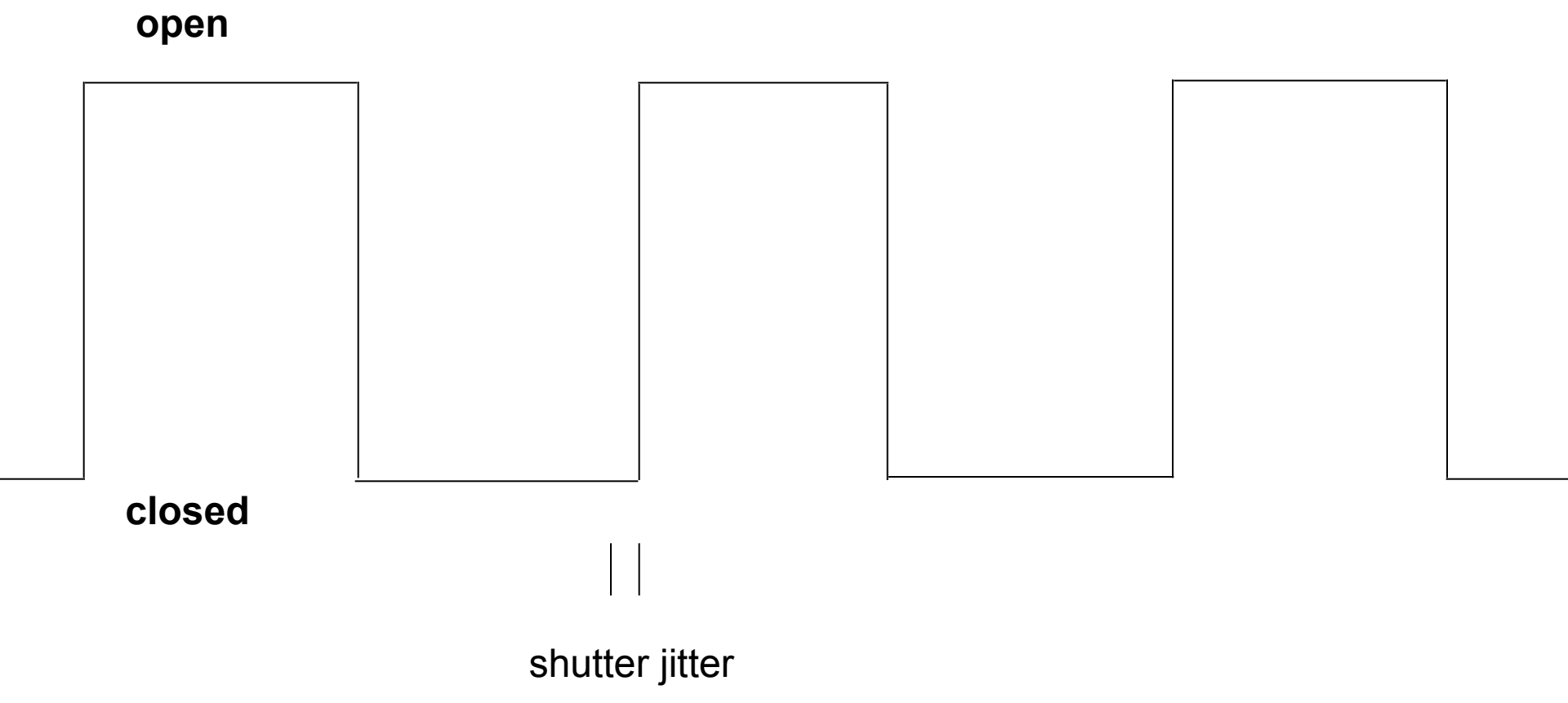

Shutter Jitter

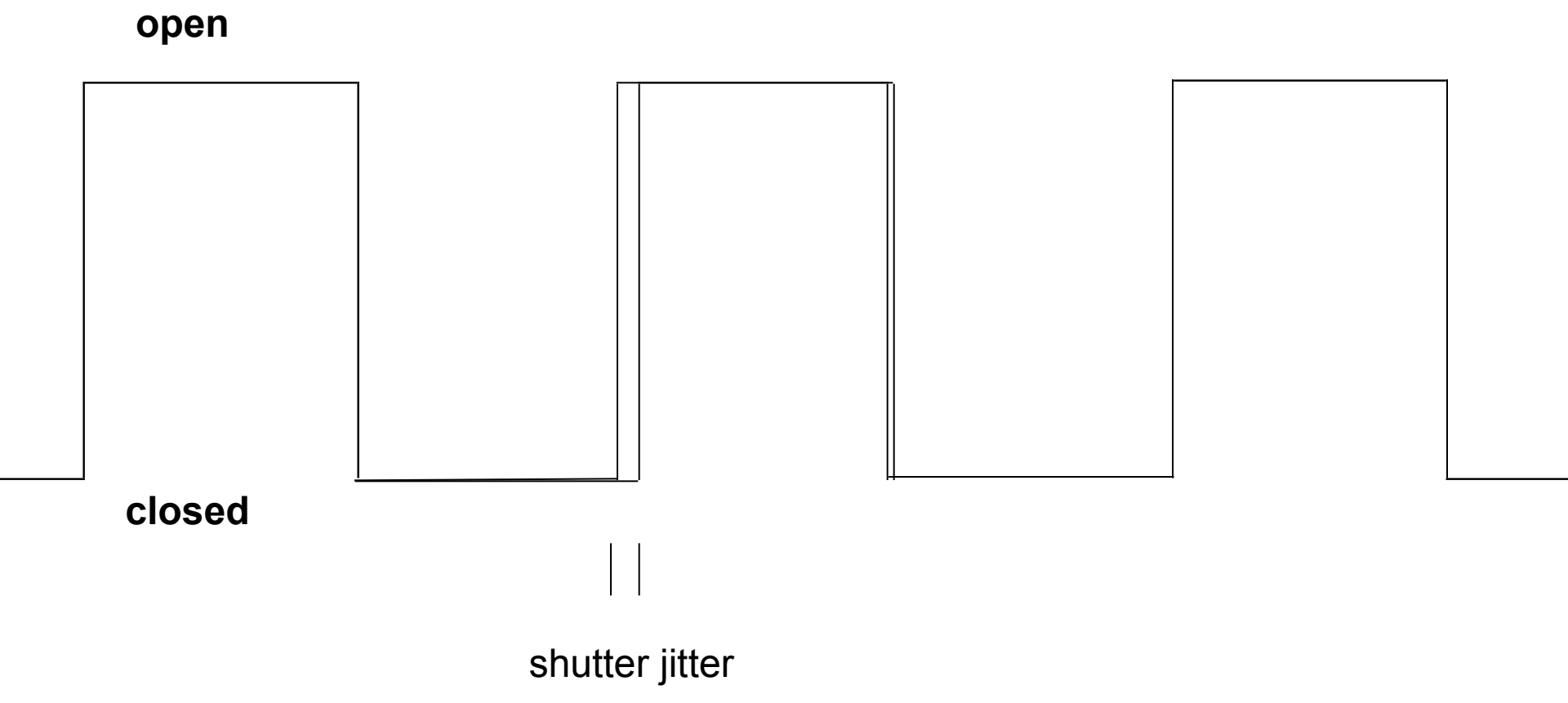

Shutter Jitter

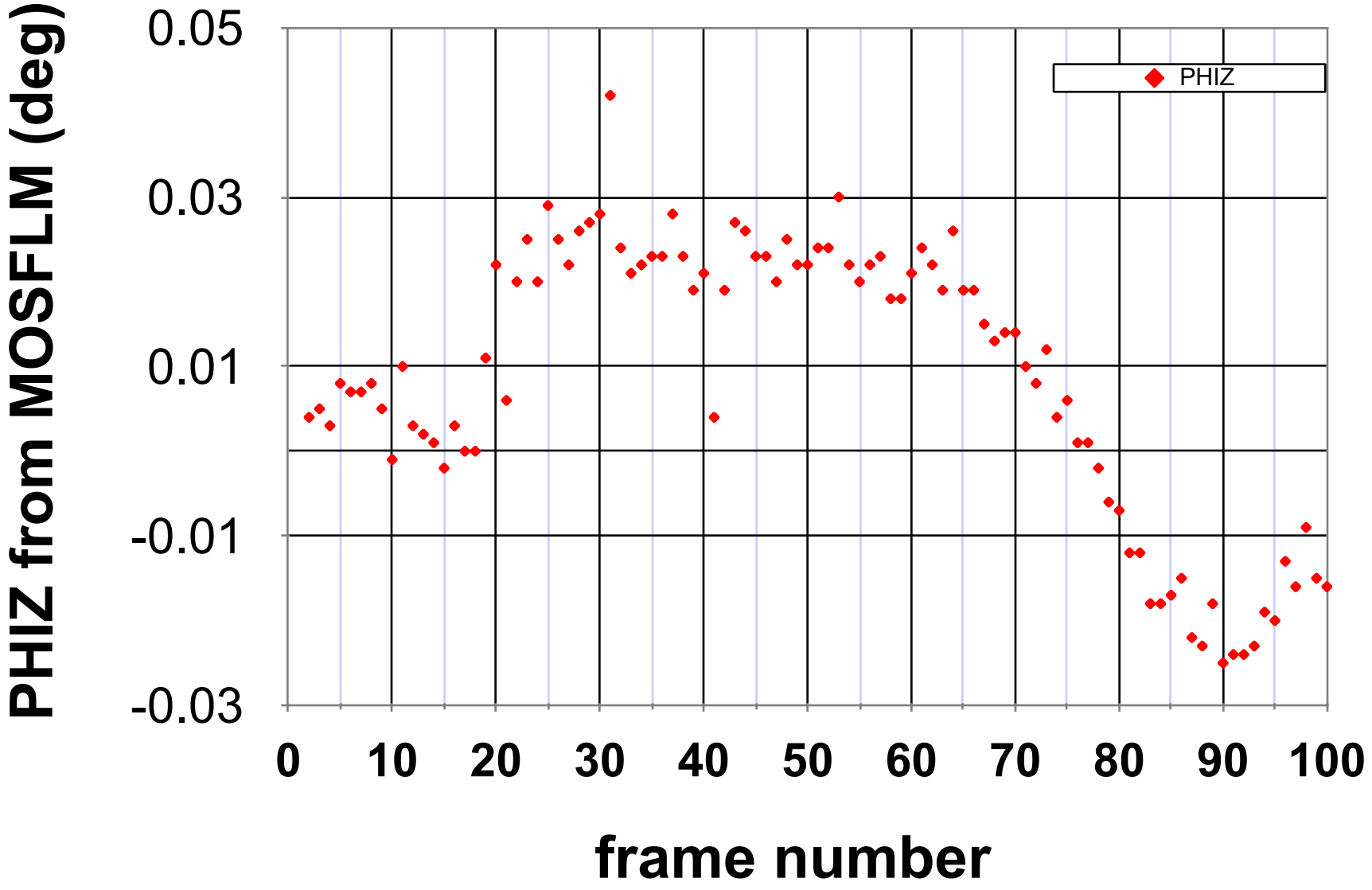

Shutter Jitter

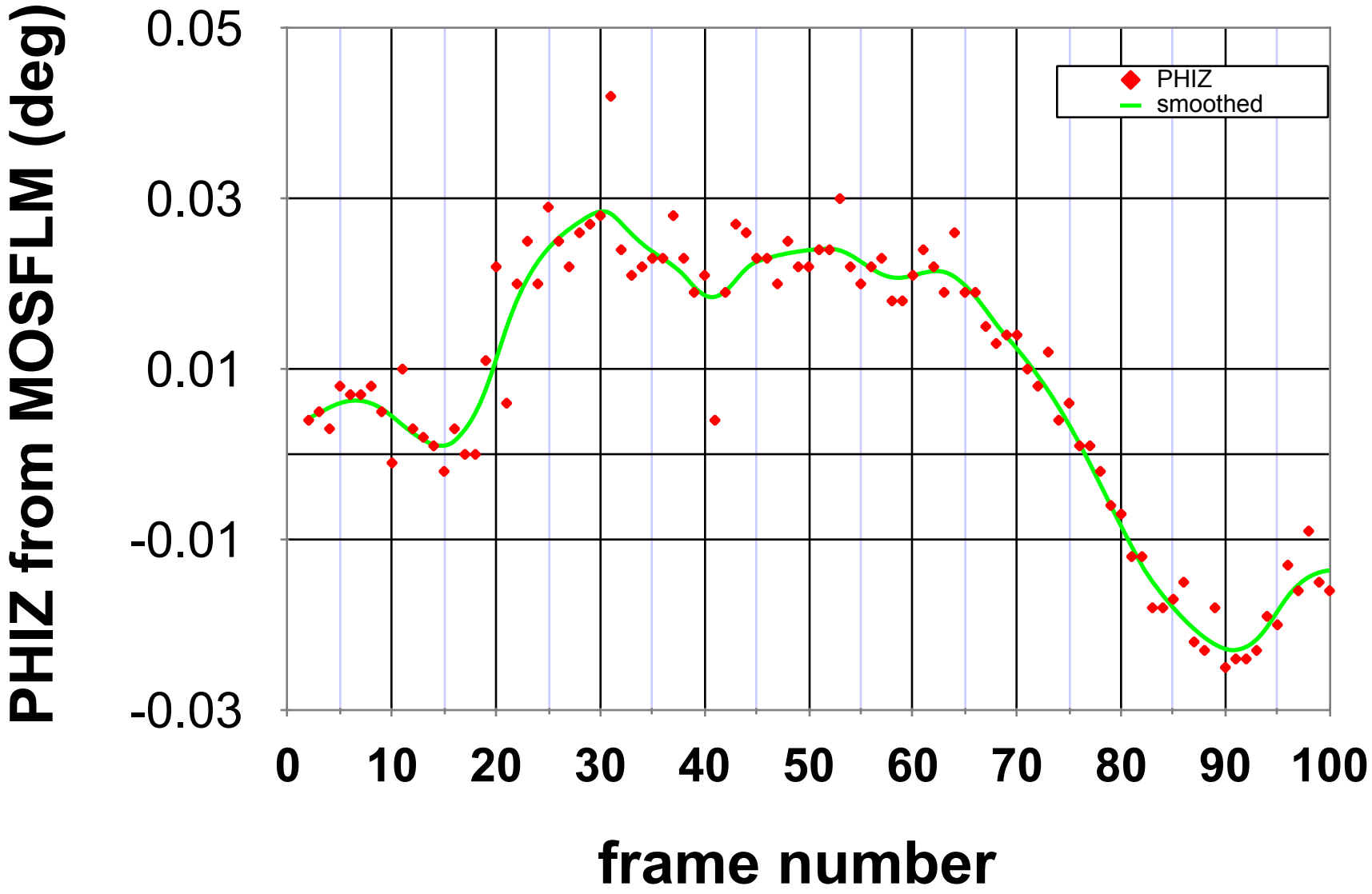

Shutter Jitter

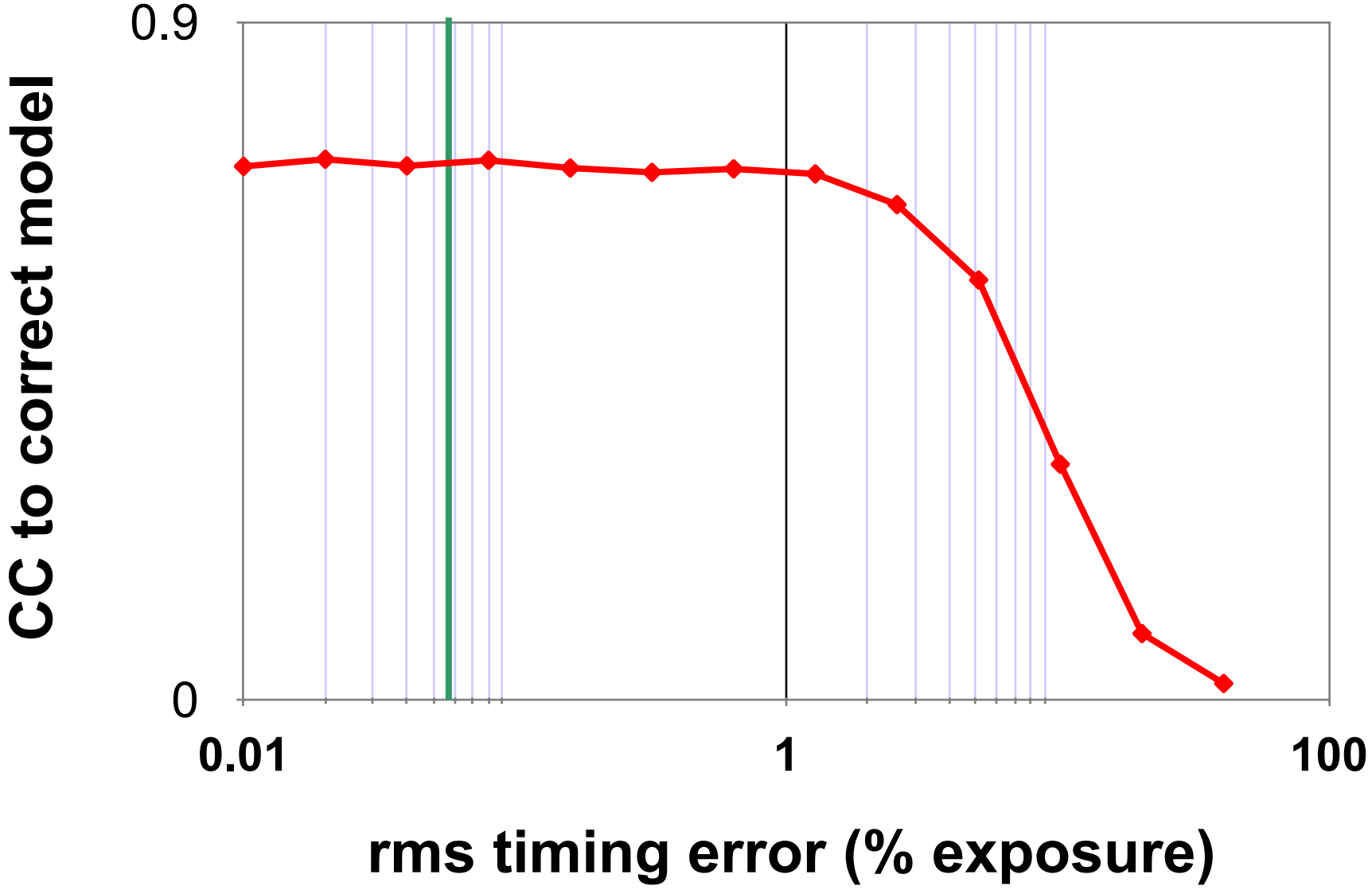

Classes of error in MX

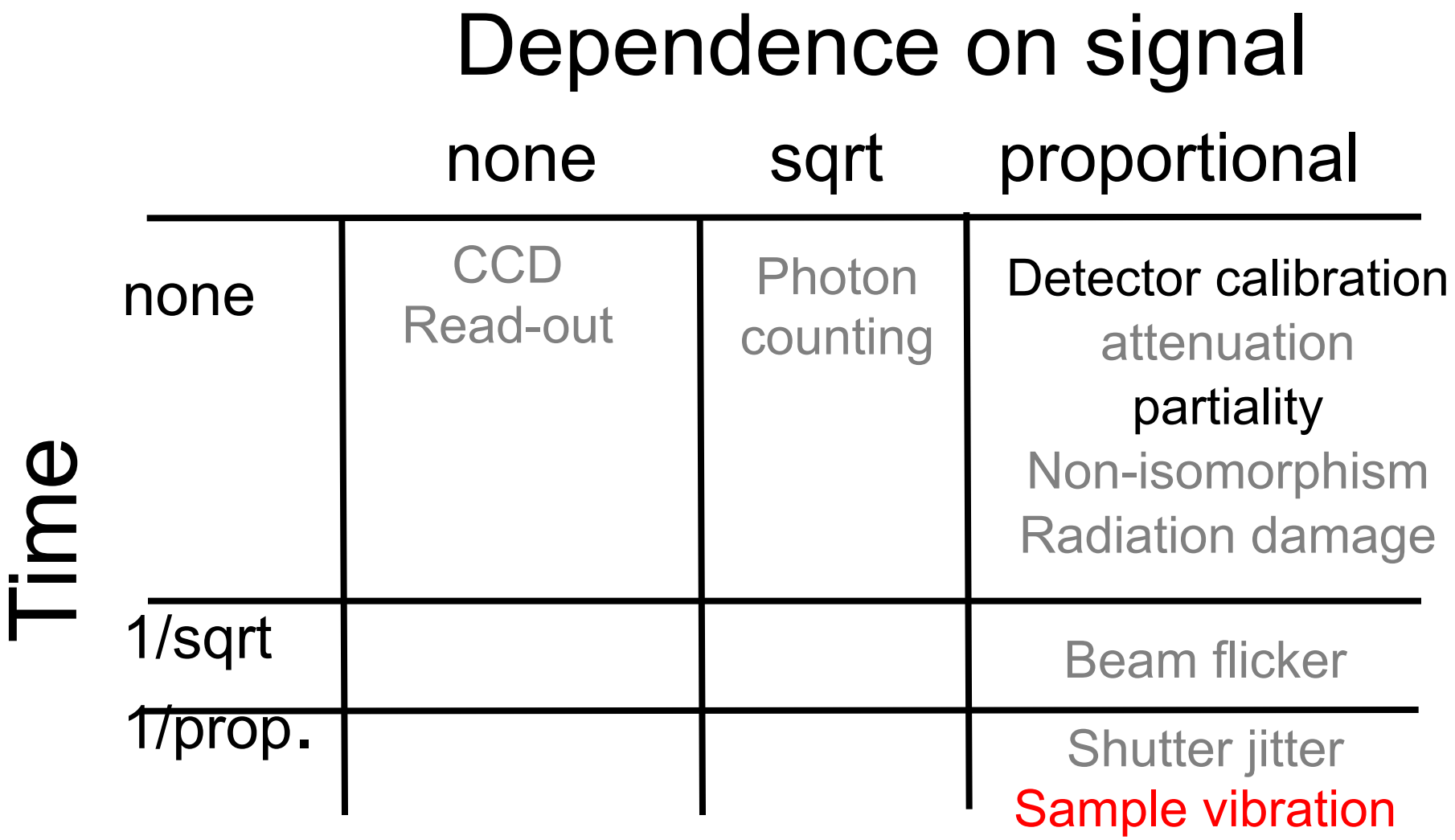

xtal vibration noise

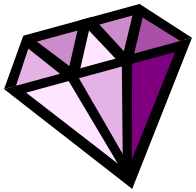

see: Alkire *et al.* (2008)."Is your cold-stream working for you or against you? An in-depth look at temperature and sample motion", *J. Appl. Cryst.* **41**, 1122-1133.

xtal vibration noise

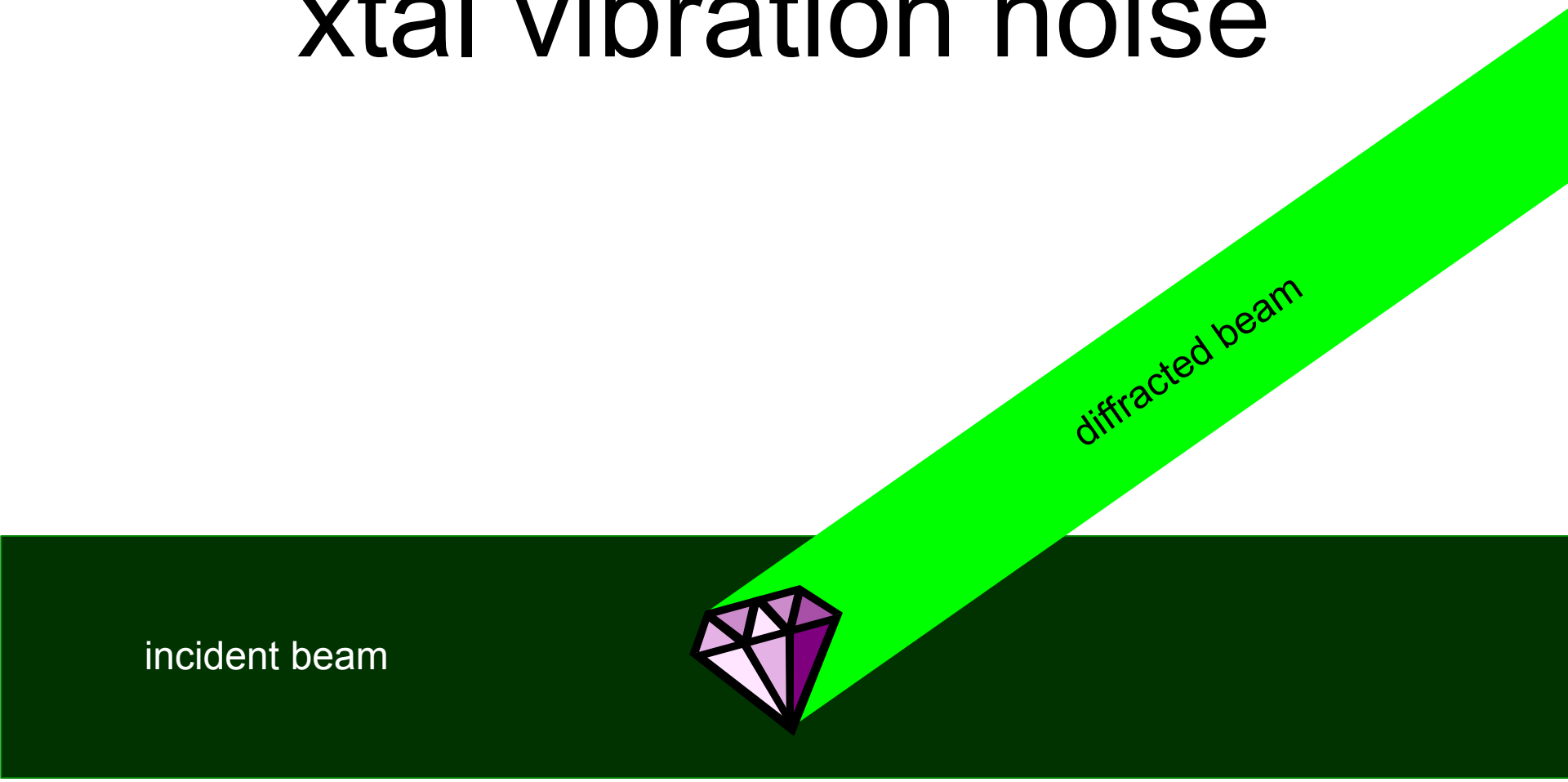

see: Alkire *et al.* (2008)."Is your cold-stream working for you or against you? An in-depth look at temperature and sample motion", *J. Appl. Cryst.* **41**, 1122-1133.

xtal vibration noise

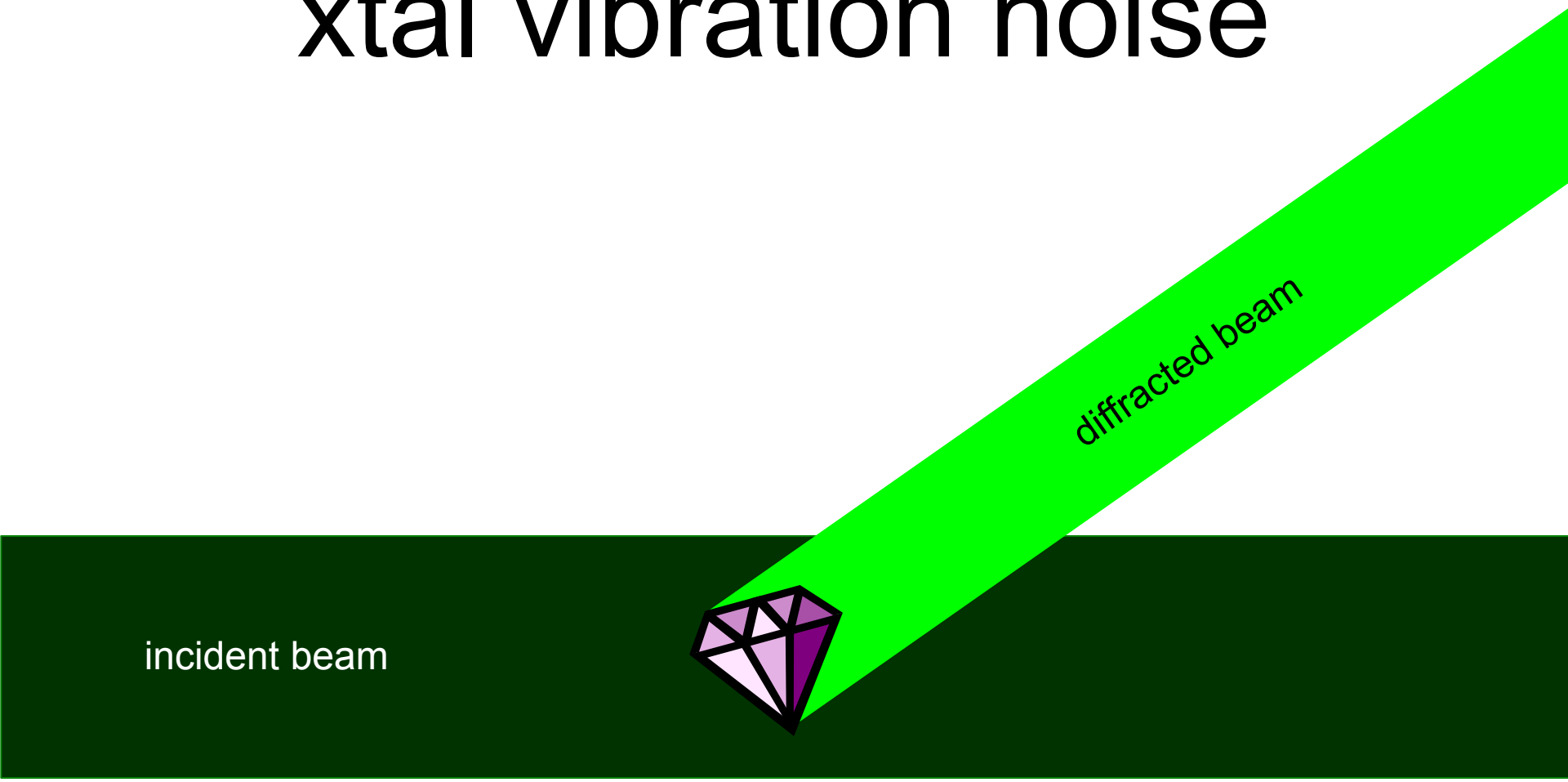

see: Alkire *et al.* (2008)."Is your cold-stream working for you or against you? An in-depth look at temperature and sample motion", *J. Appl. Cryst.* **41**, 1122-1133.

xtal vibration noise

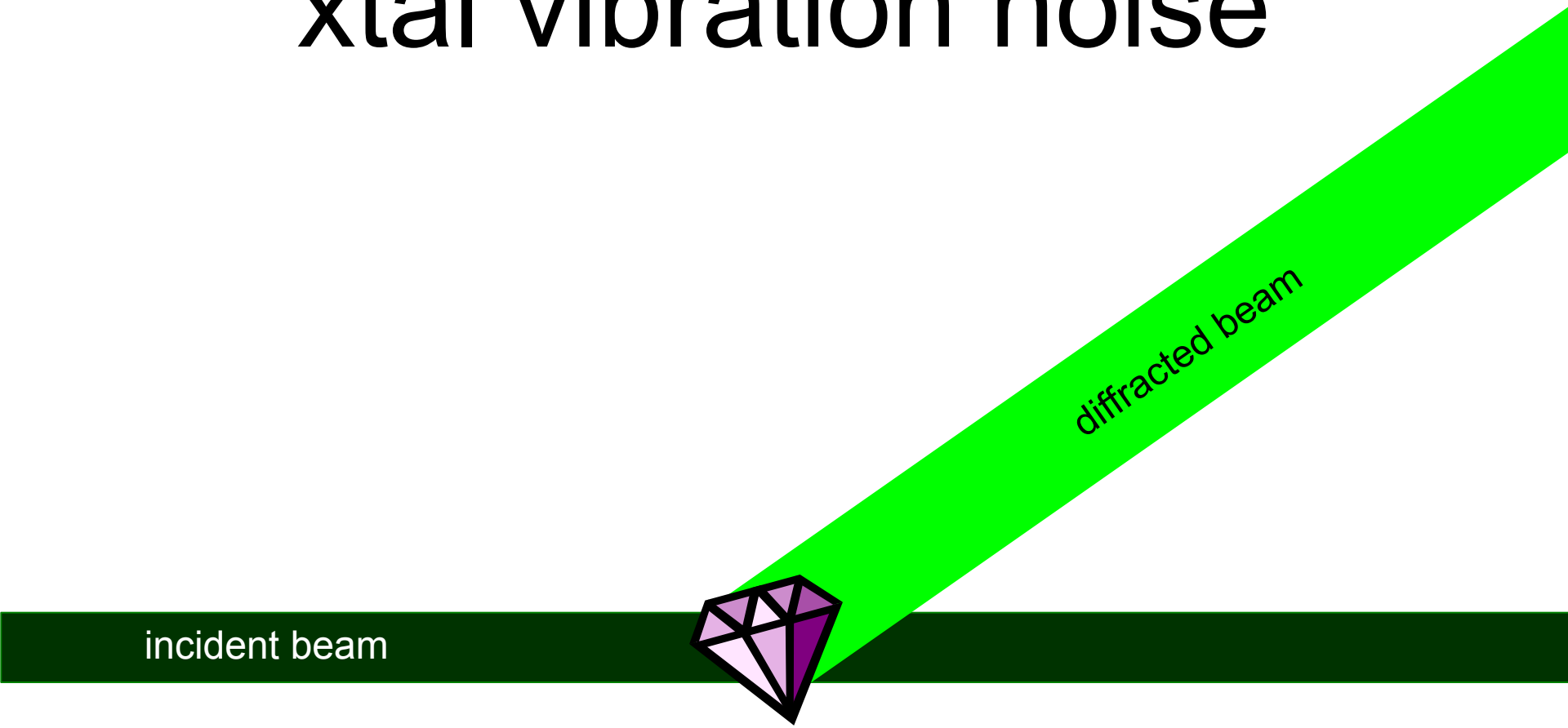

see: Alkire *et al.* (2008)."Is your cold-stream working for you or against you? An in-depth look at temperature and sample motion", *J. Appl. Cryst.* **41**, 1122-1133.

xtal vibration noise

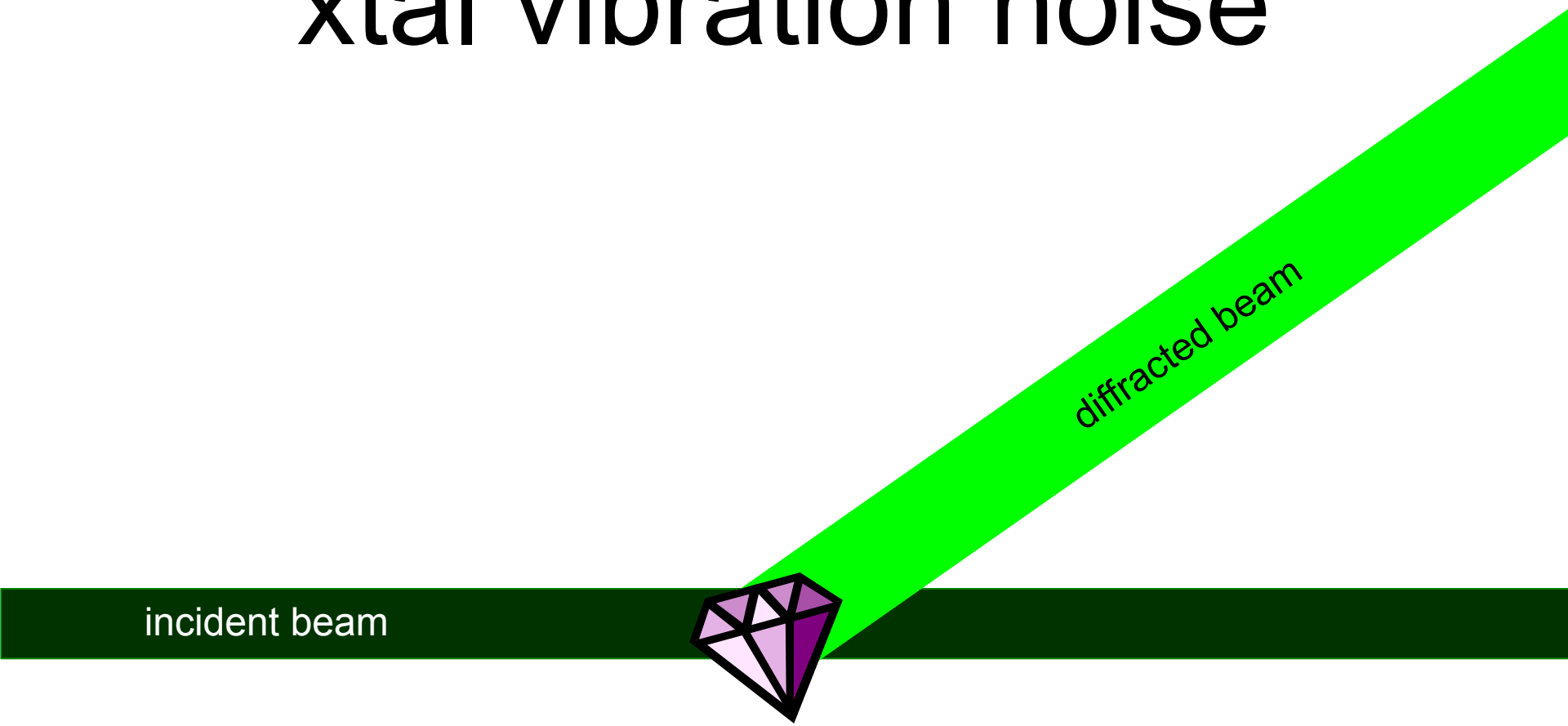

see: Alkire *et al.* (2008)."Is your cold-stream working for you or against you? An in-depth look at temperature and sample motion", *J. Appl. Cryst.* **41**, 1122-1133.

xtal vibration noise

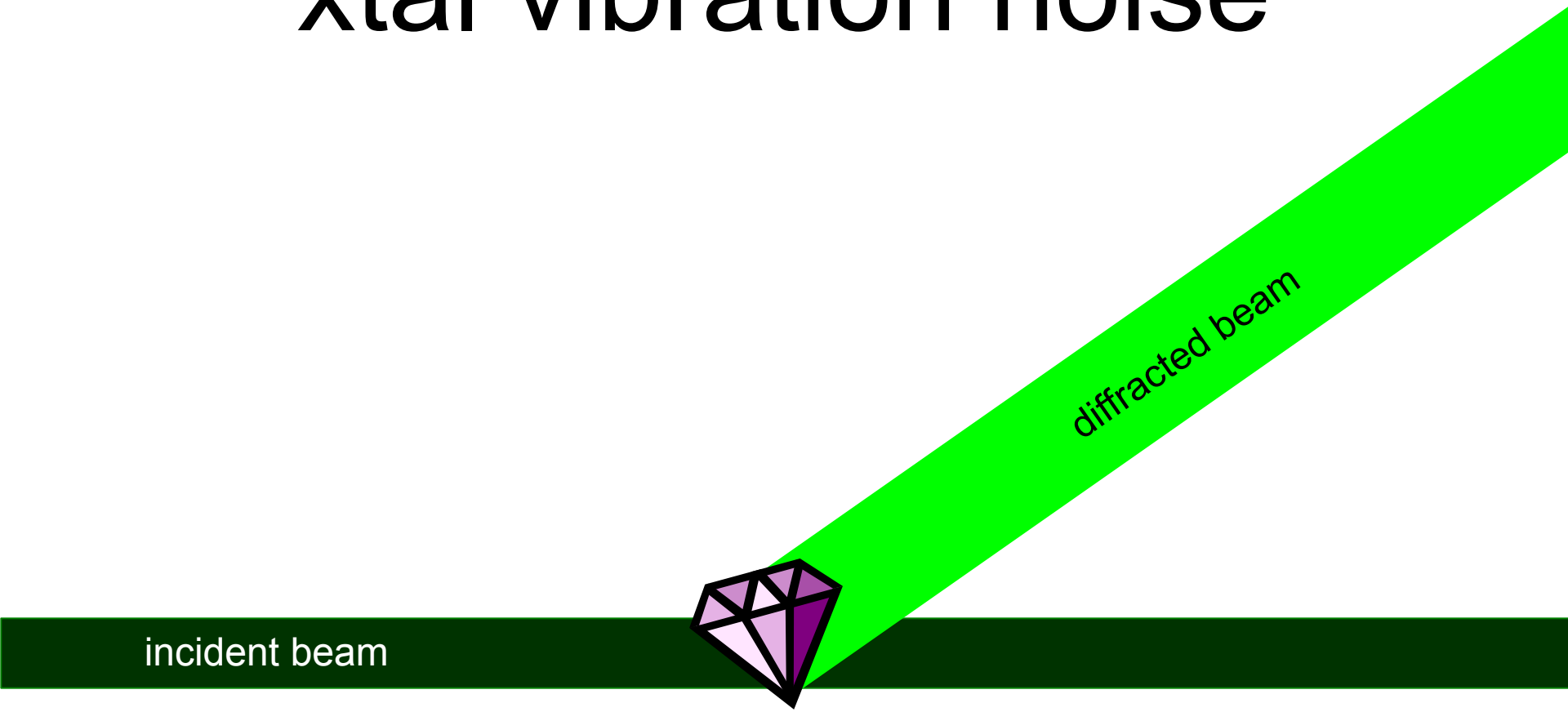

see: Alkire *et al.* (2008)."Is your cold-stream working for you or against you? An in-depth look at temperature and sample motion", *J. Appl. Cryst.* **41**, 1122-1133.

xtal vibration noise

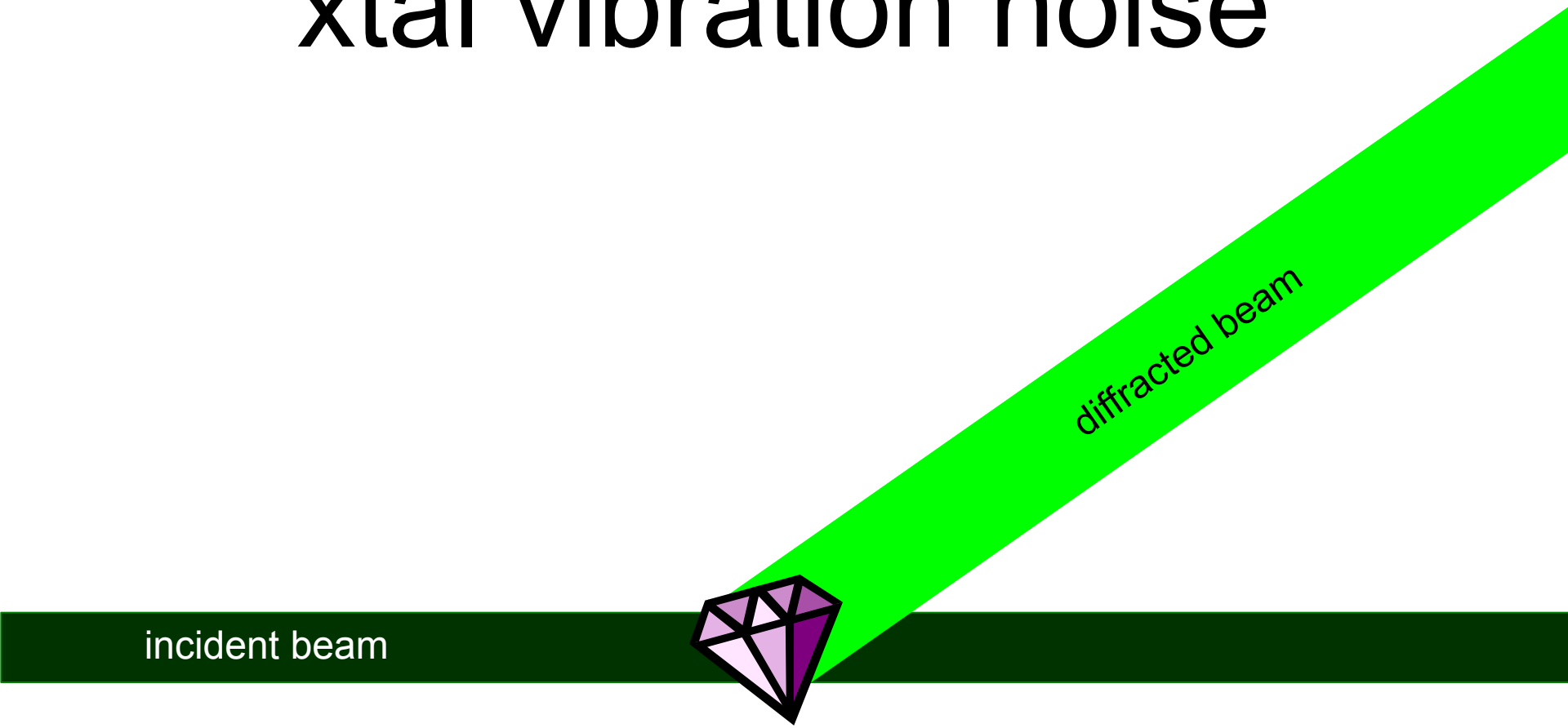

see: Alkire *et al.* (2008)."Is your cold-stream working for you or against you? An in-depth look at temperature and sample motion", *J. Appl. Cryst.* **41**, 1122-1133.

xtal vibration noise

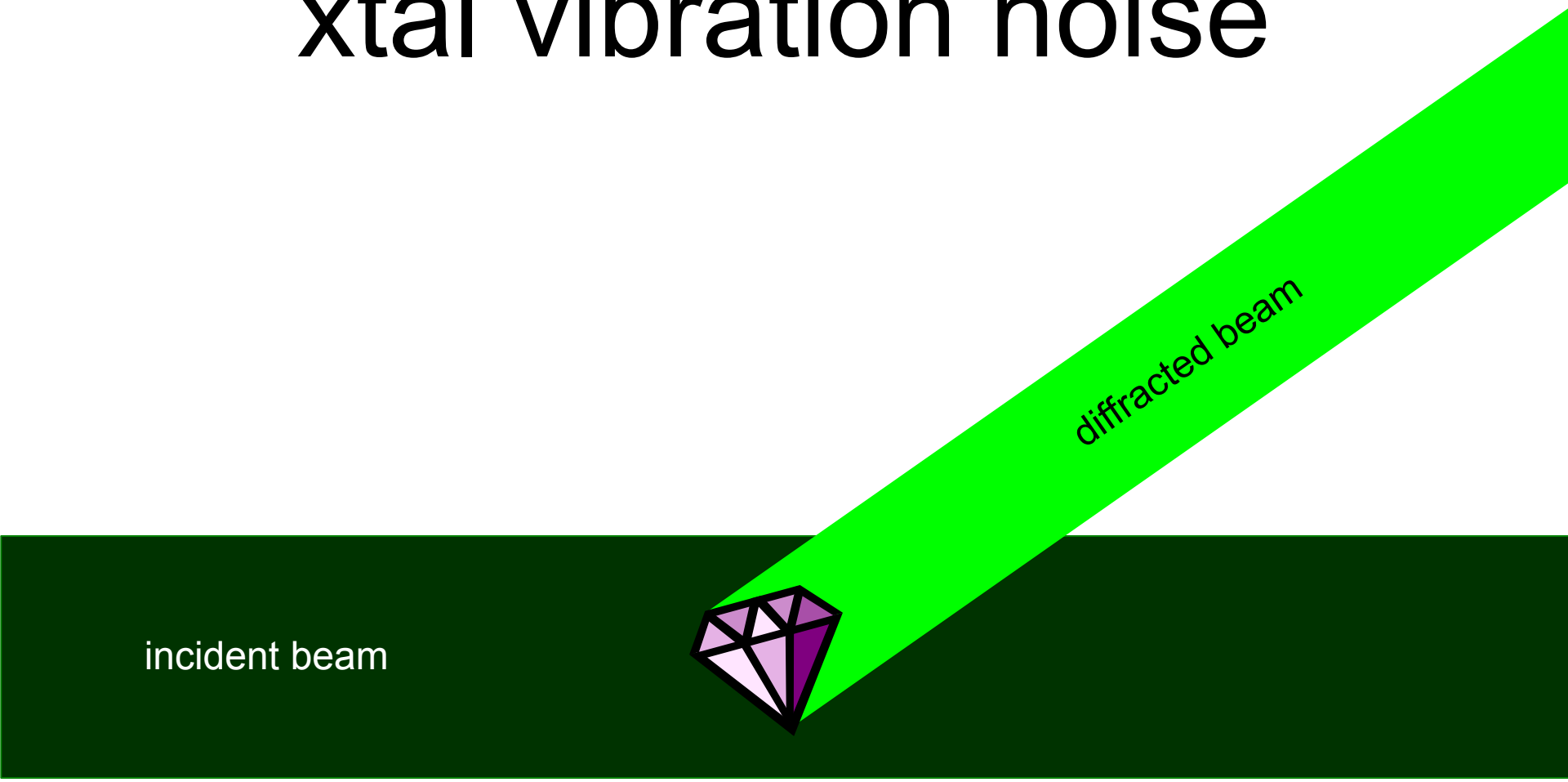

see: Alkire *et al.* (2008)."Is your cold-stream working for you or against you? An in-depth look at temperature and sample motion", *J. Appl. Cryst.* **41**, 1122-1133.

xtal vibration noise

incident beam

see: Alkire *et al.* (2008)."Is your cold-stream working for you or against you? An in-depth look at temperature and sample motion", *J. Appl. Cryst.* **41**, 1122-1133.

xtal vibration noise

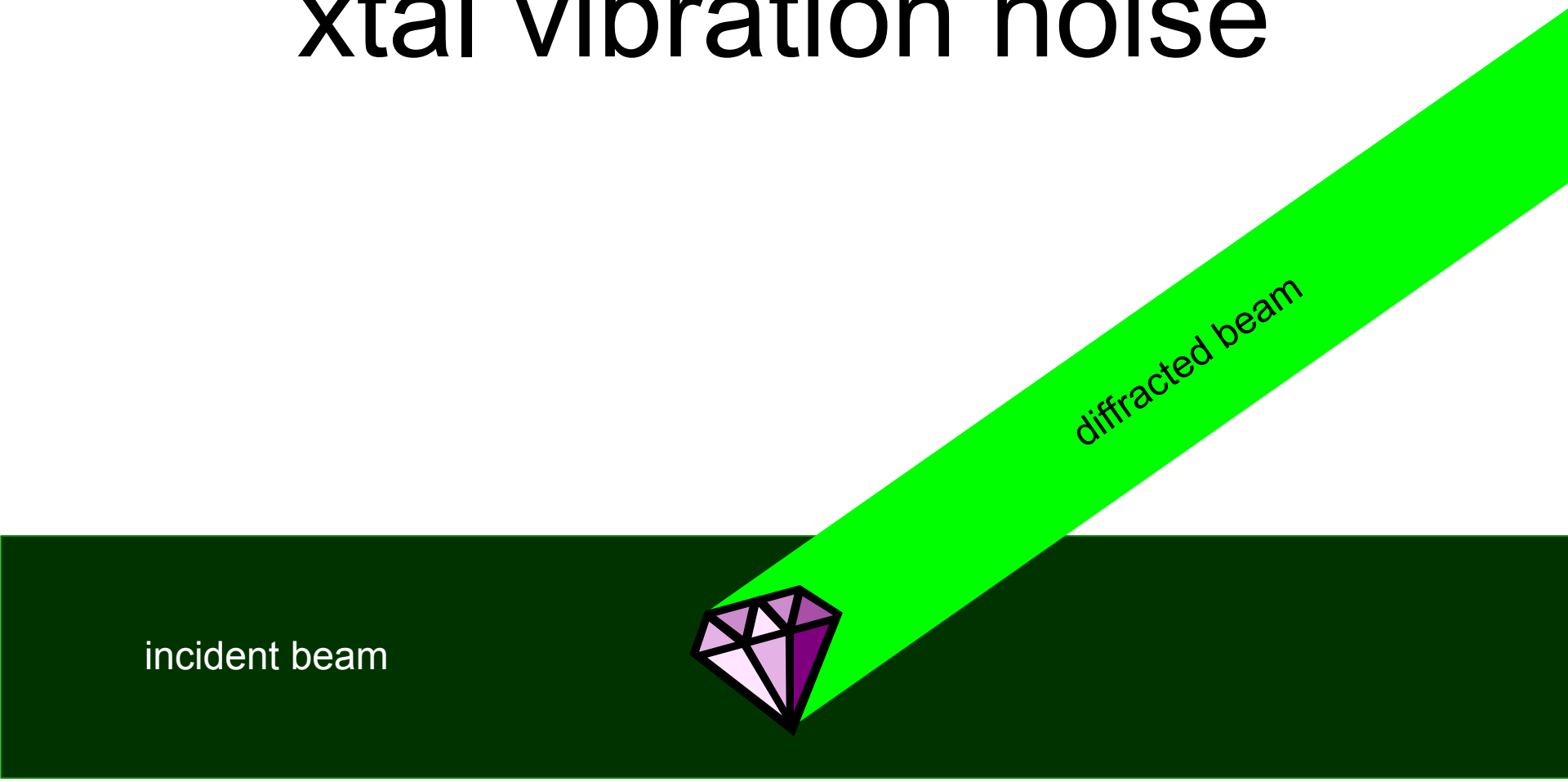

see: Alkire *et al.* (2008)."Is your cold-stream working for you or against you? An in-depth look at temperature and sample motion", *J. Appl. Cryst.* **41**, 1122-1133.

xtal vibration noise

incident beam

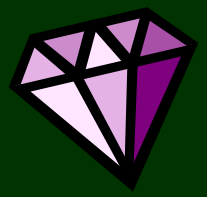

see: Alkire *et al.* (2008)."Is your cold-stream working for you or against you? An in-depth look at temperature and sample motion", *J. Appl. Cryst.* **41**, 1122-1133.

Classes of error in MX

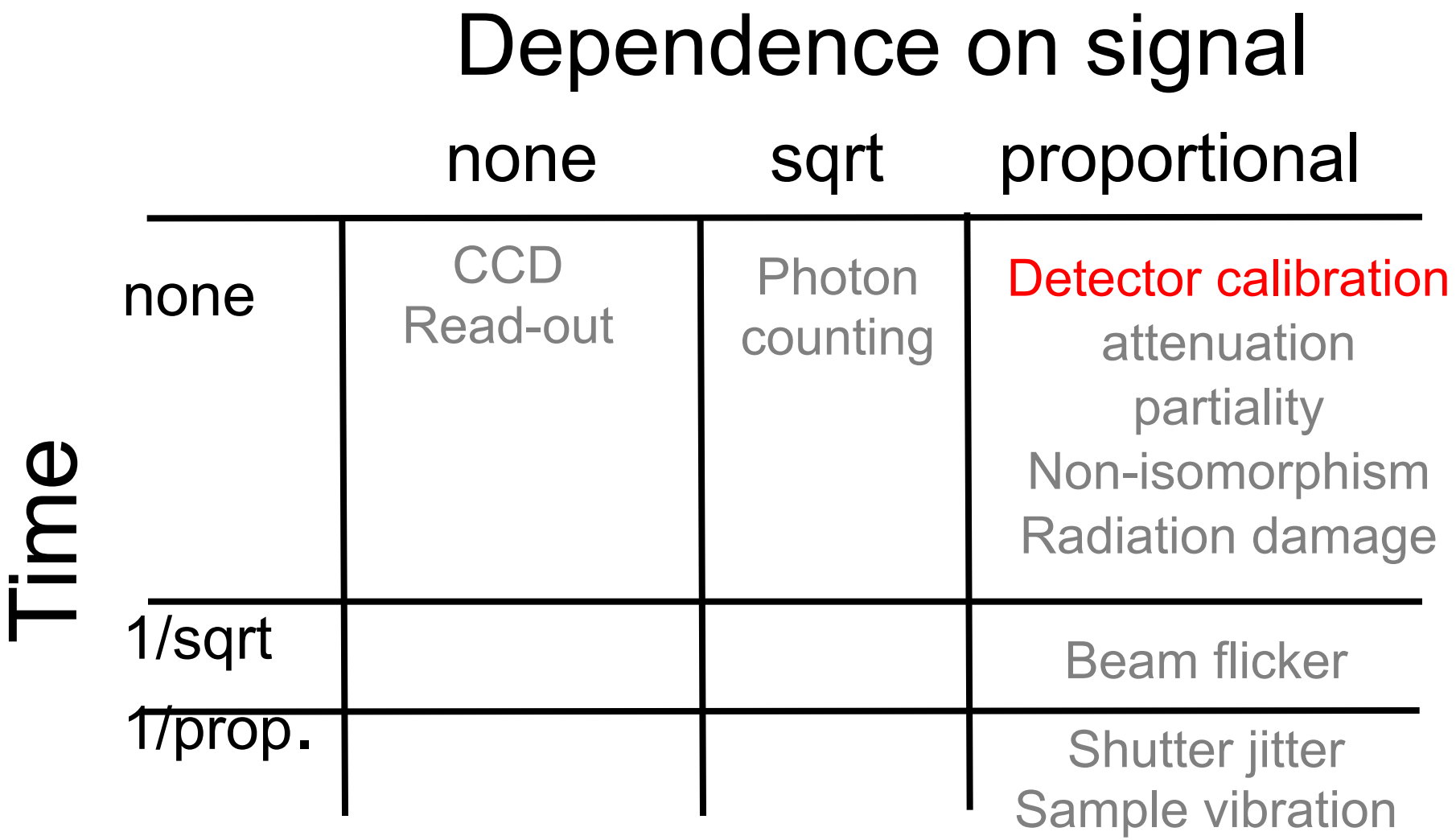

Detector calibration

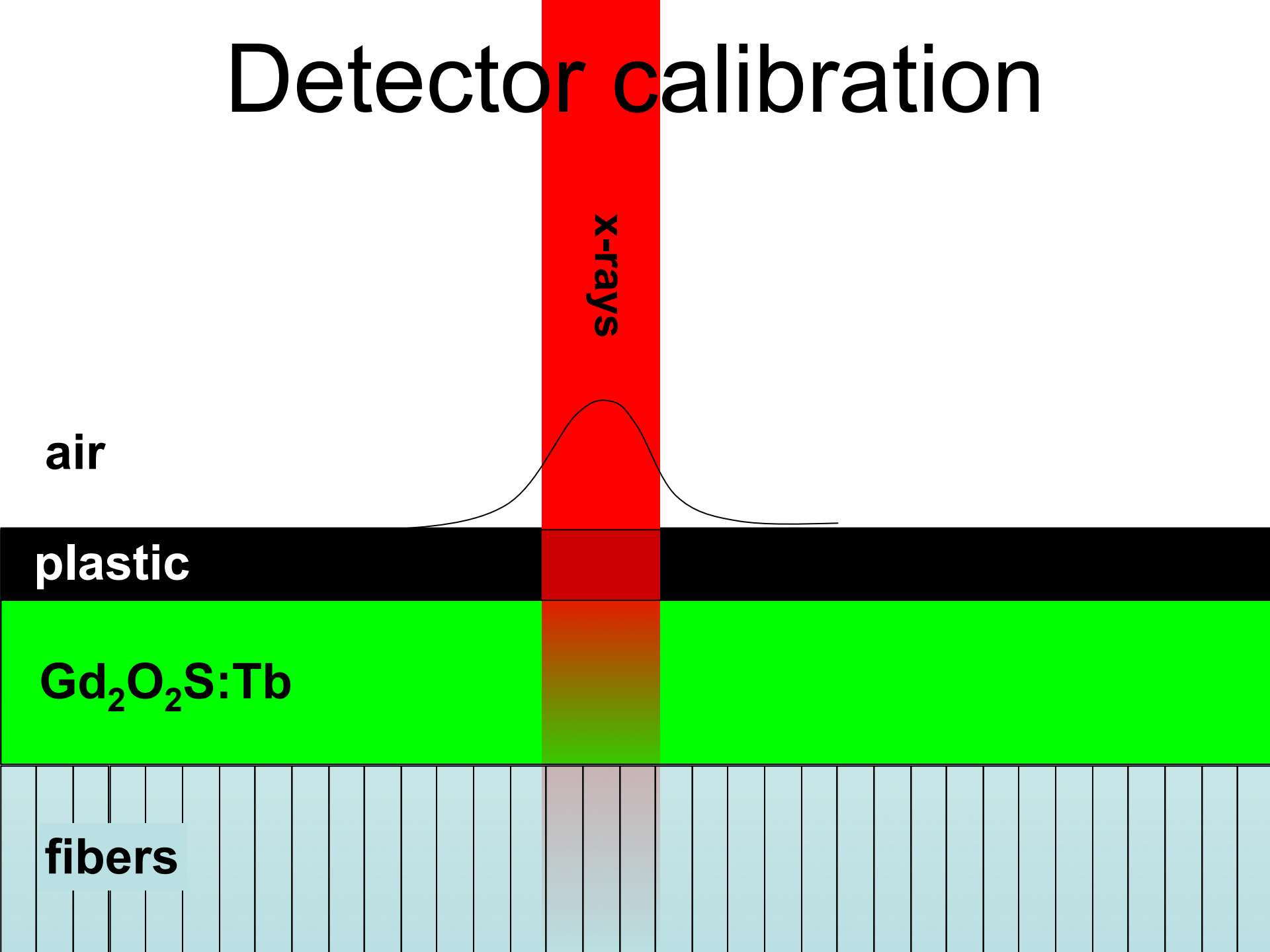

Detector calibration

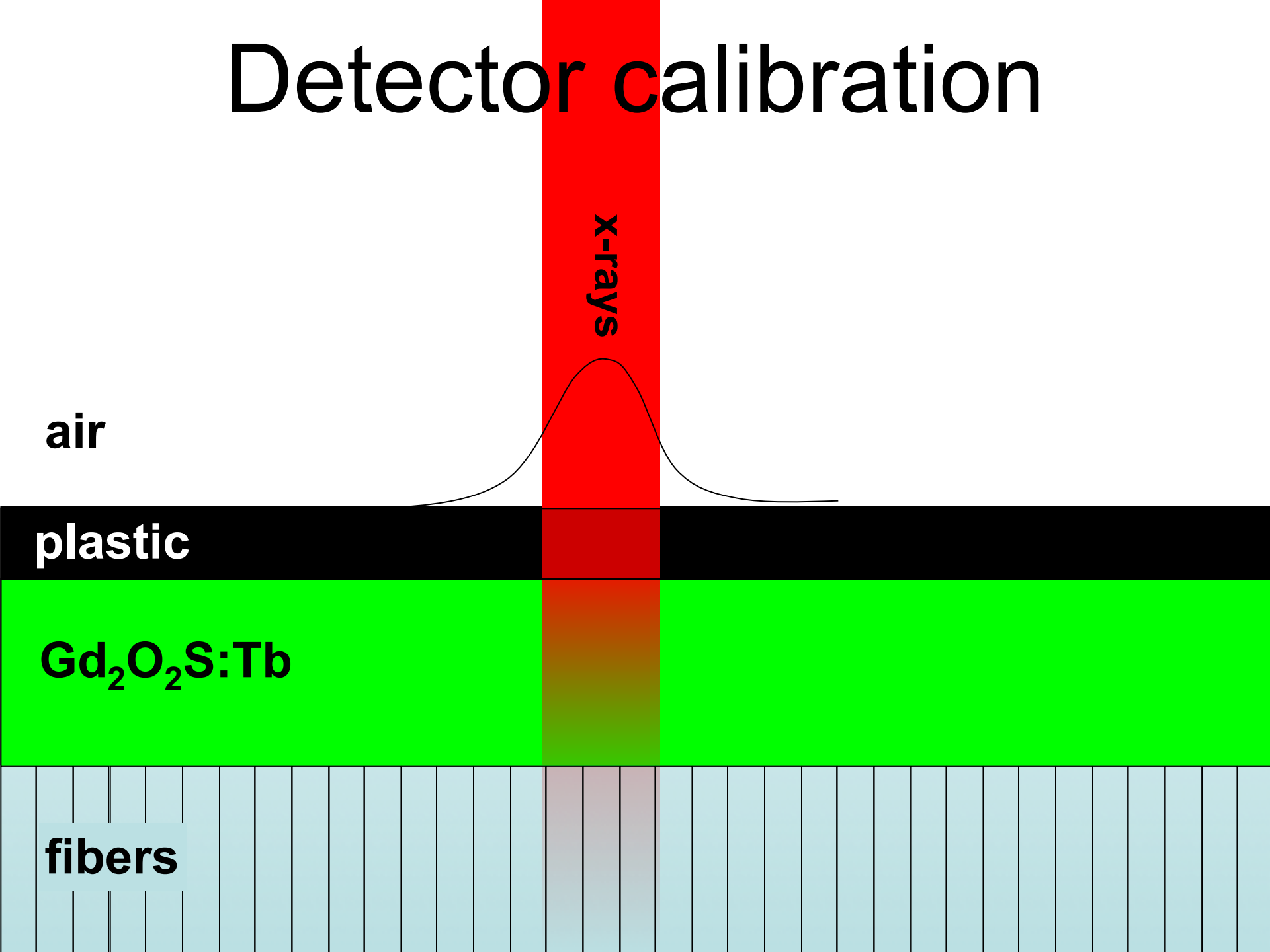

Detector calibration: 7247 eV

target:
oil

distance:
900 mm

2θ: 12°

Detector calibration: 7235 eV

target:
oil

distance:
900 mm

2θ: 12°

Detector calibration: ALS 8.3.1

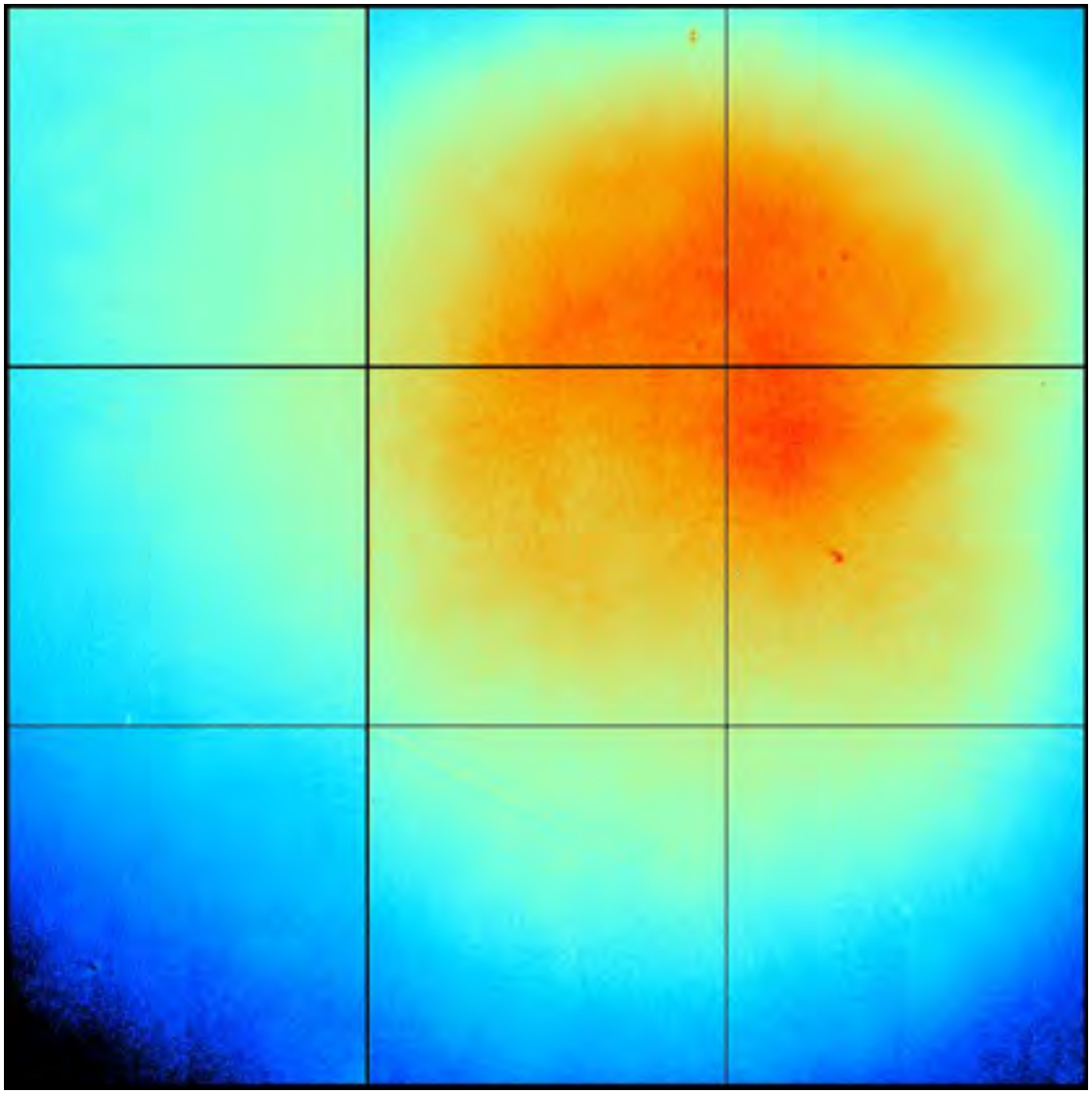

Detector calibration errors: detector 2

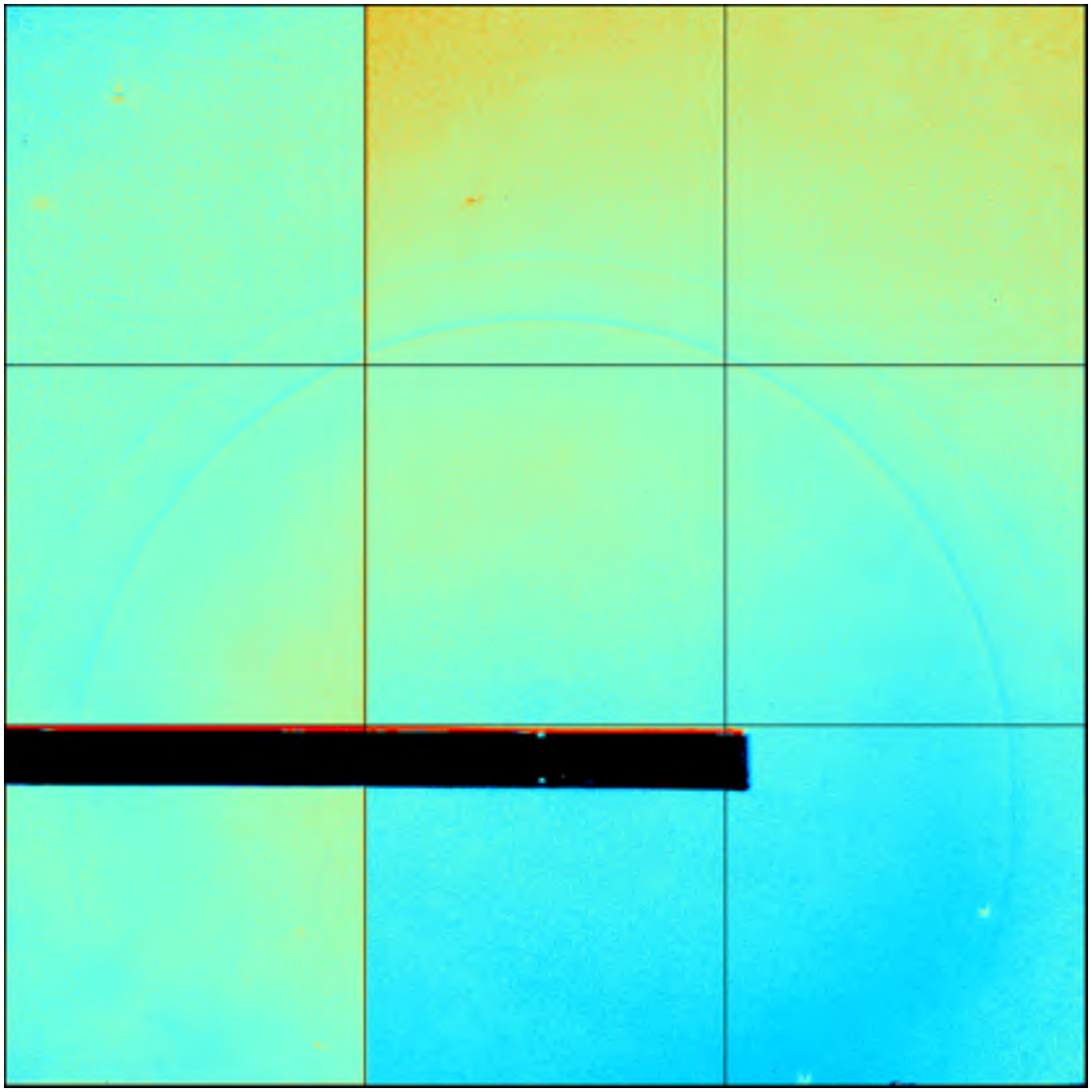

Detector calibration errors: detector 3

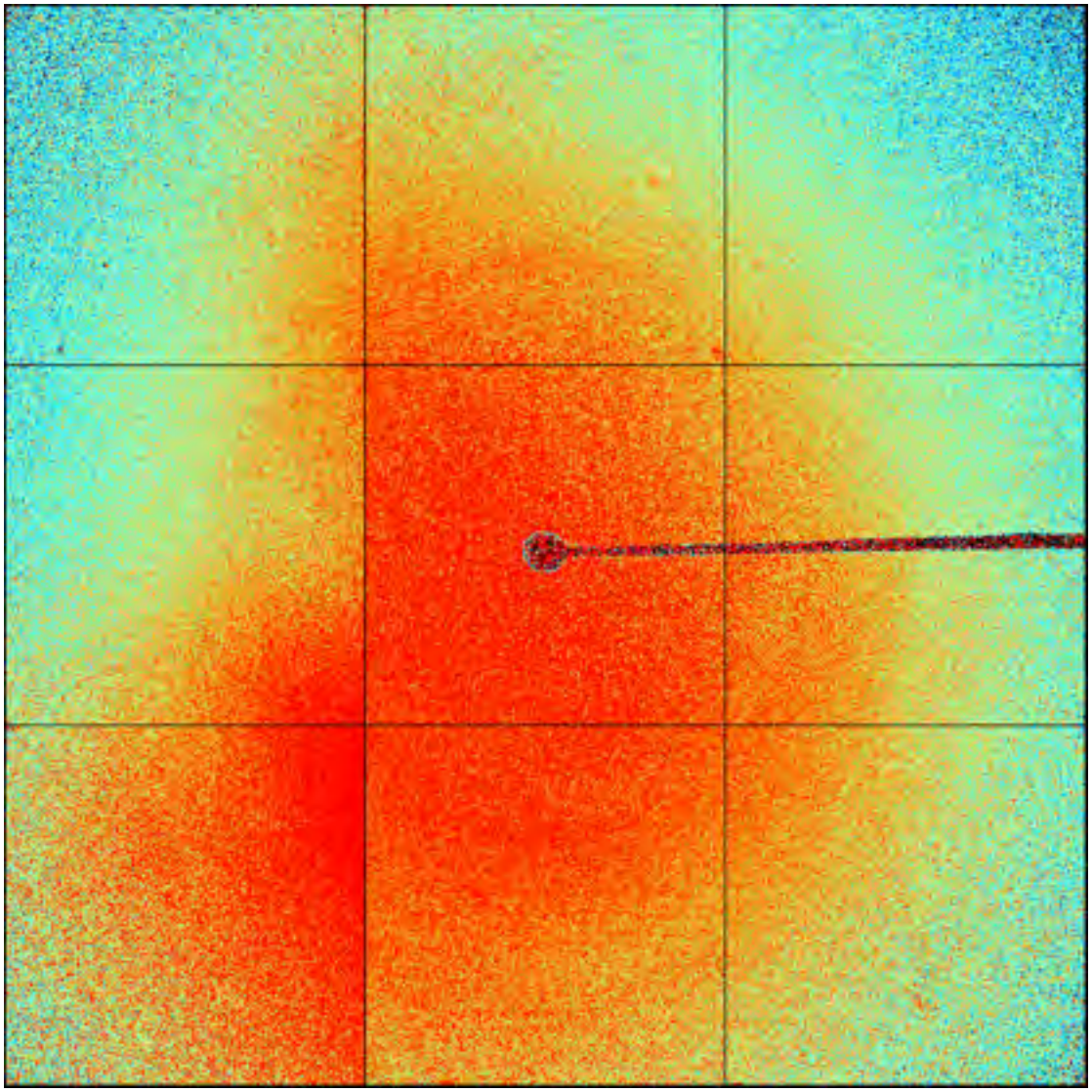

Detector calibration

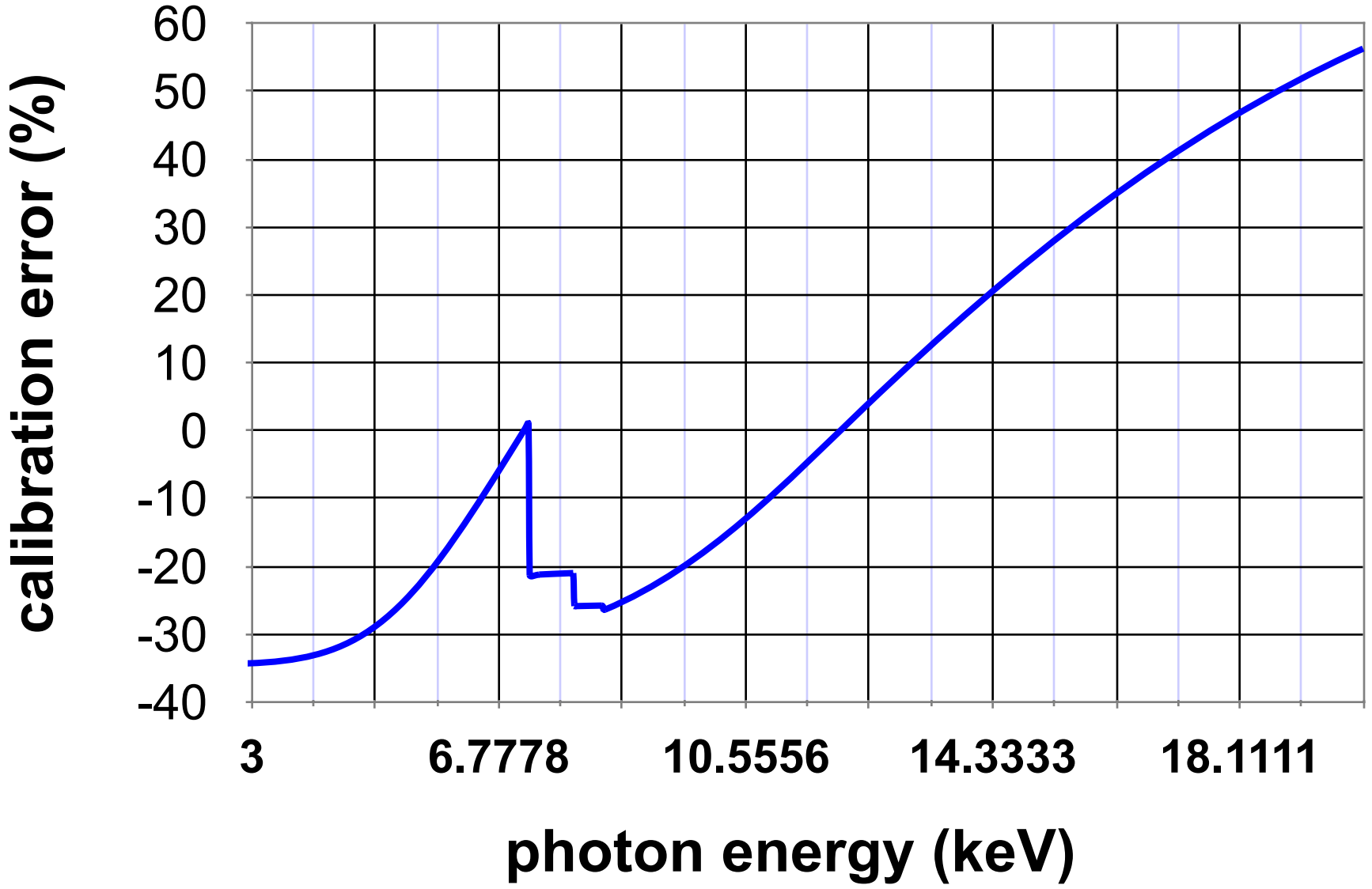

Detector calibration

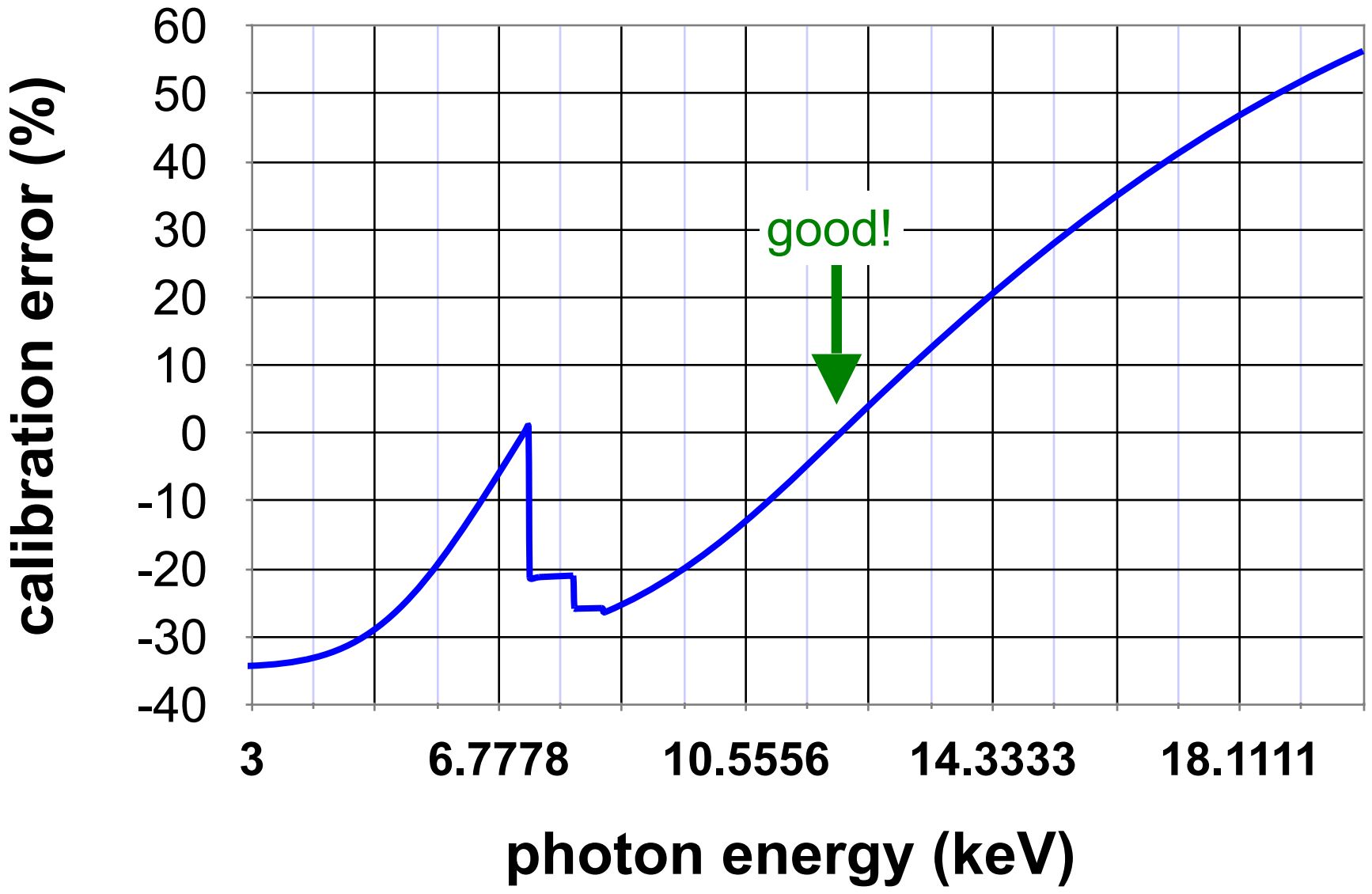

Detector calibration

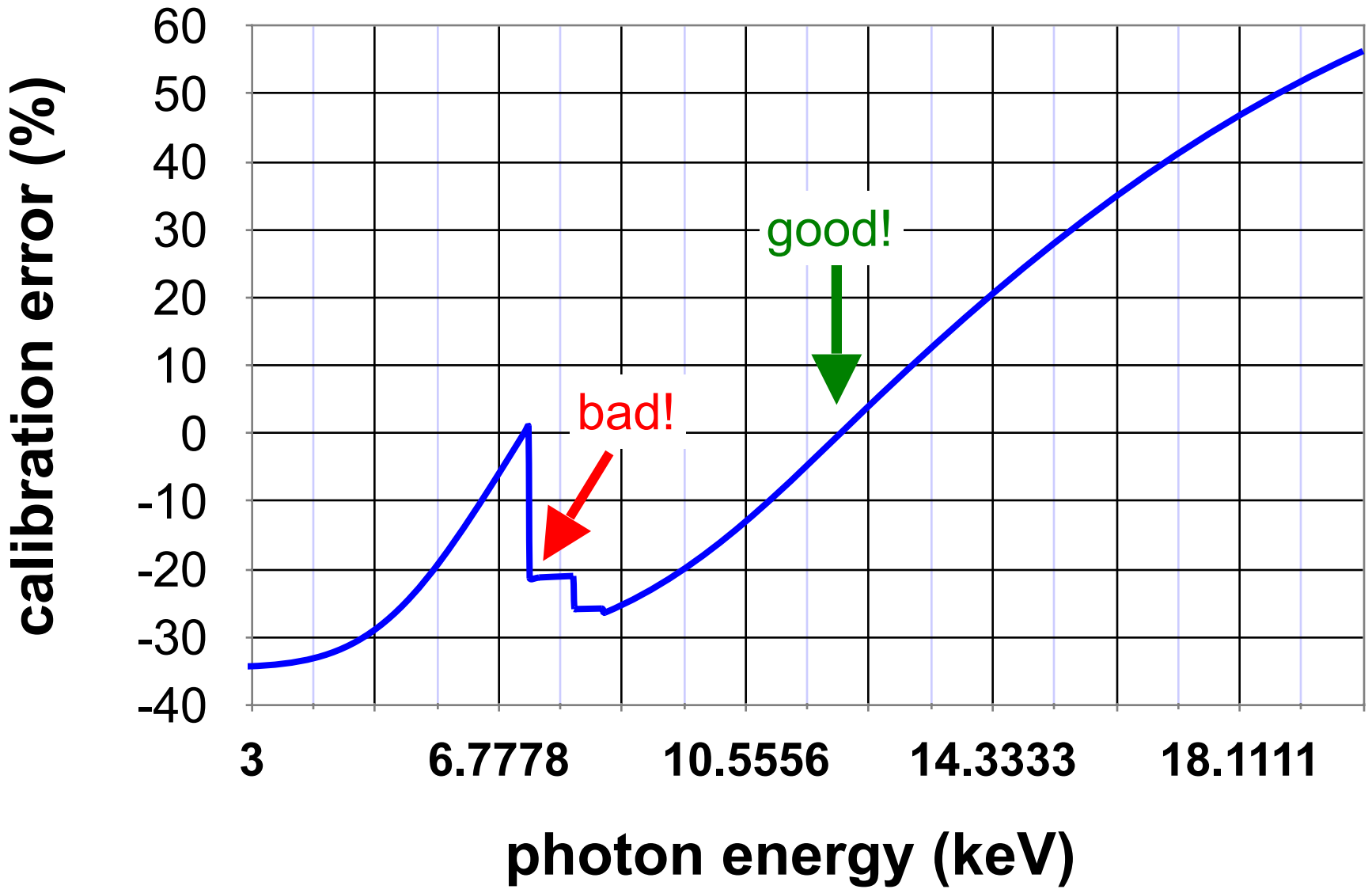

Detector calibration

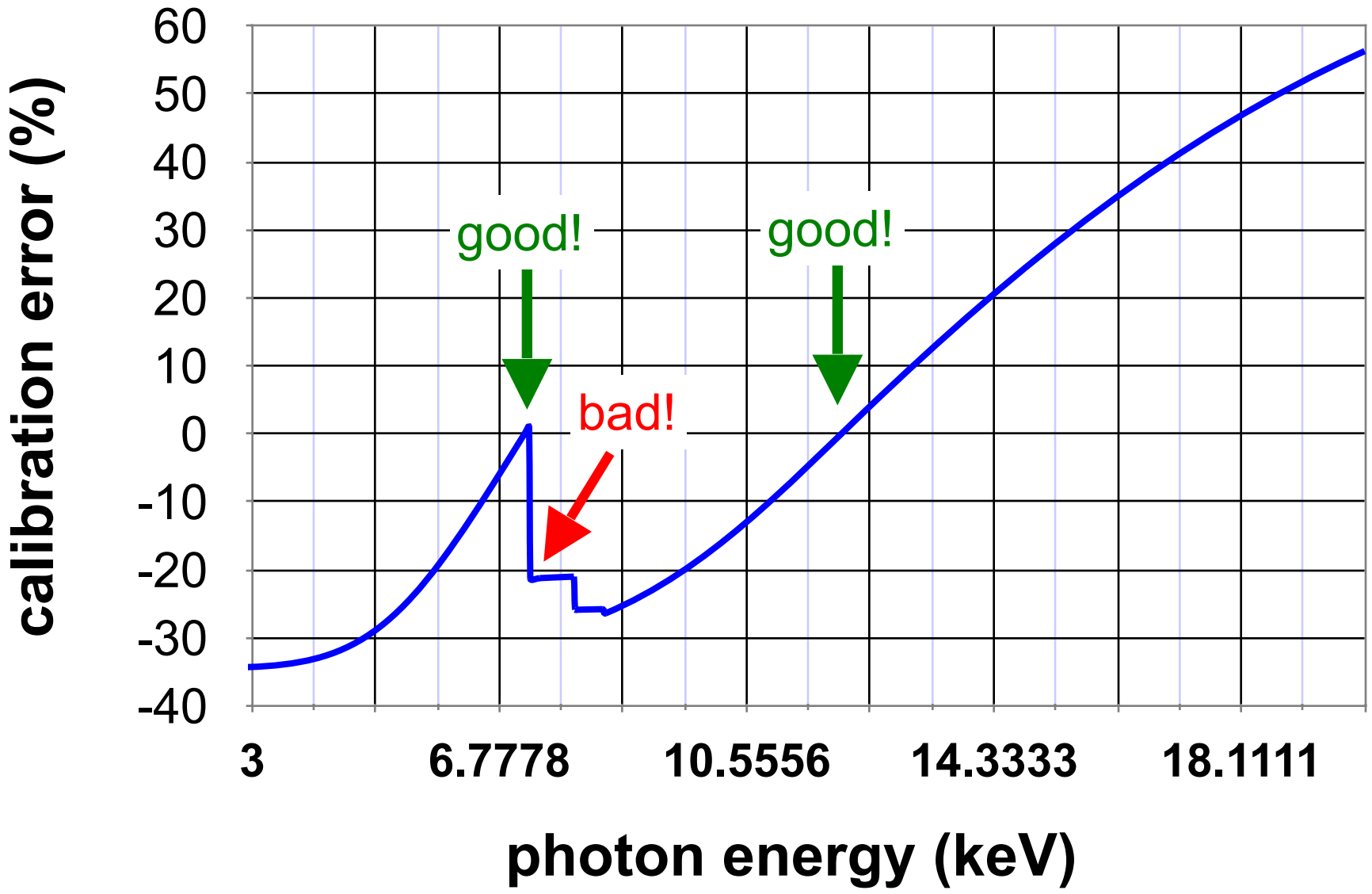

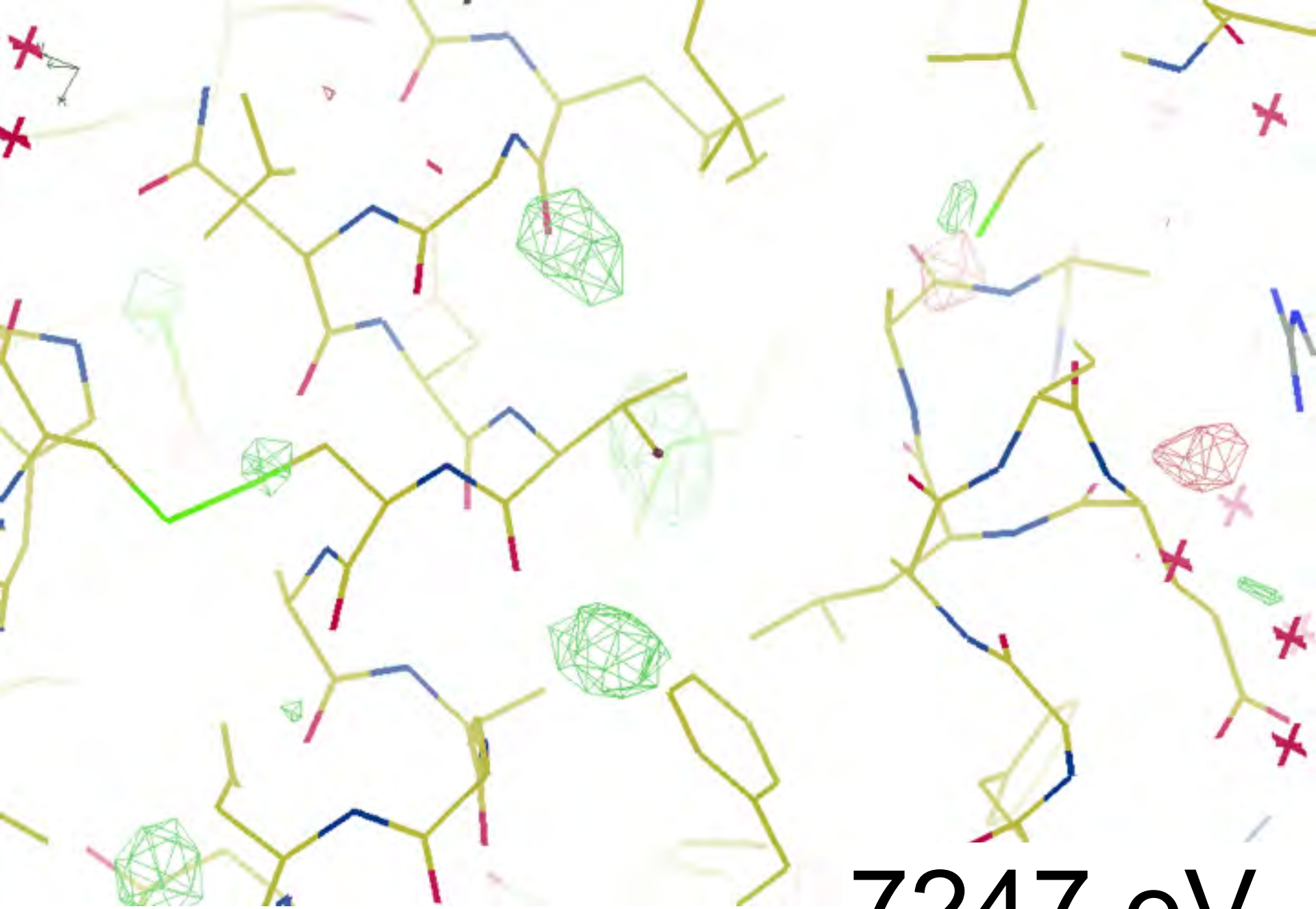
7247 eV

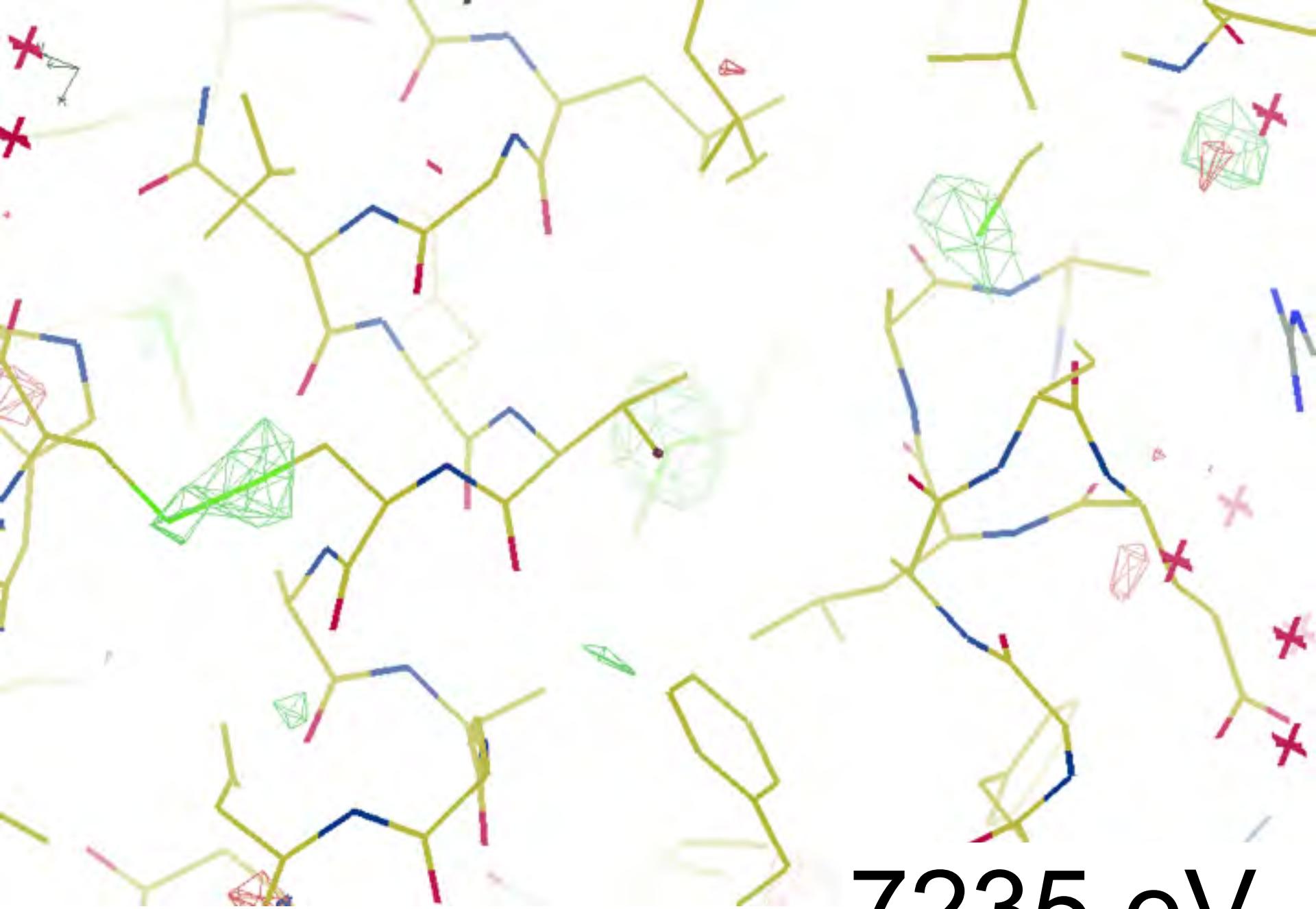
7235 eV

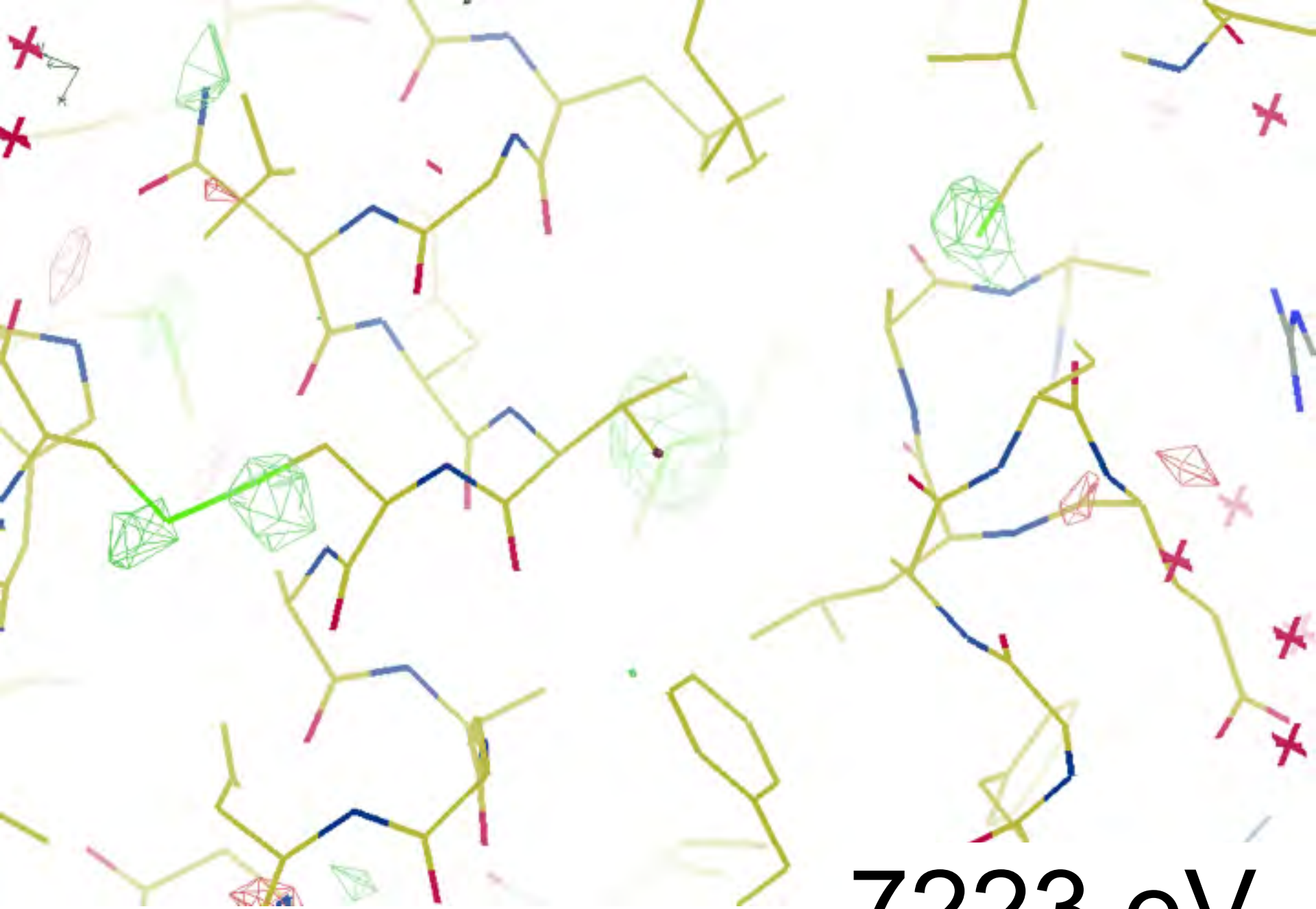
7223 eV

Calibration Error

Calibration Error

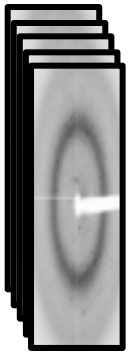

Calibration Error

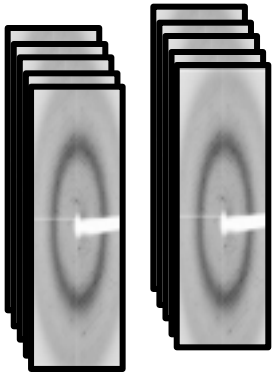

Calibration Error

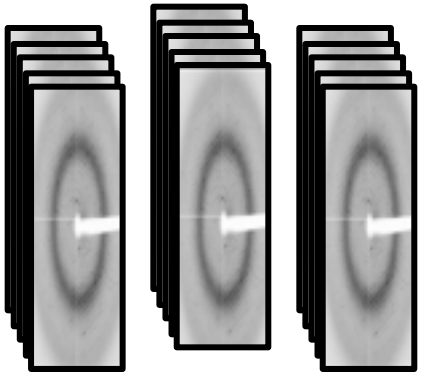

Calibration Error

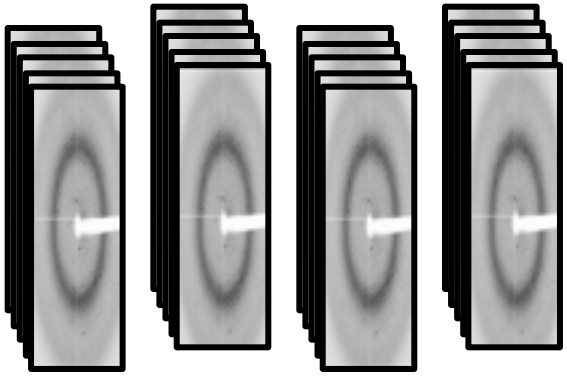

Calibration Error

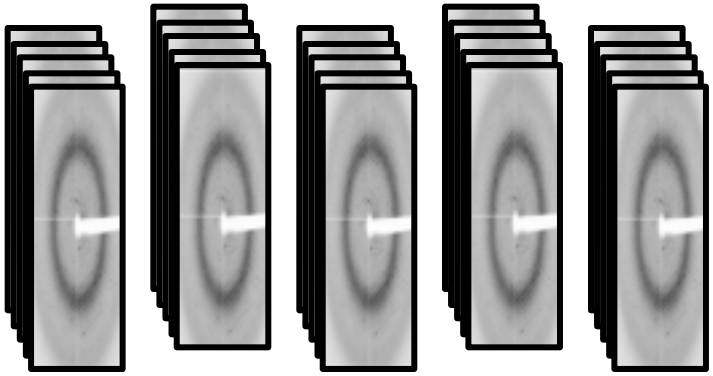

Calibration Error

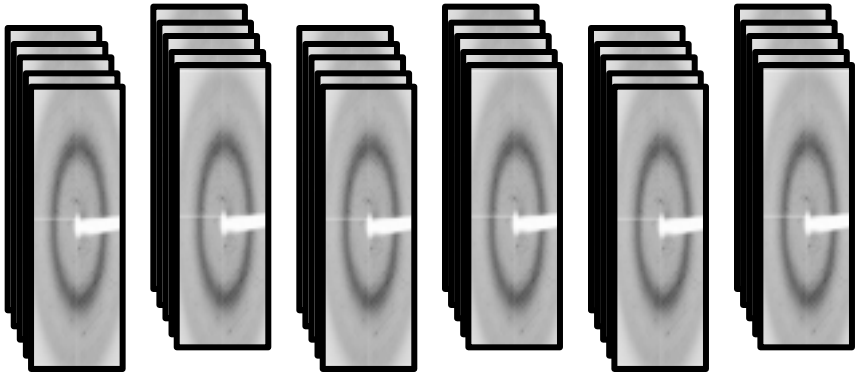

Calibration Error

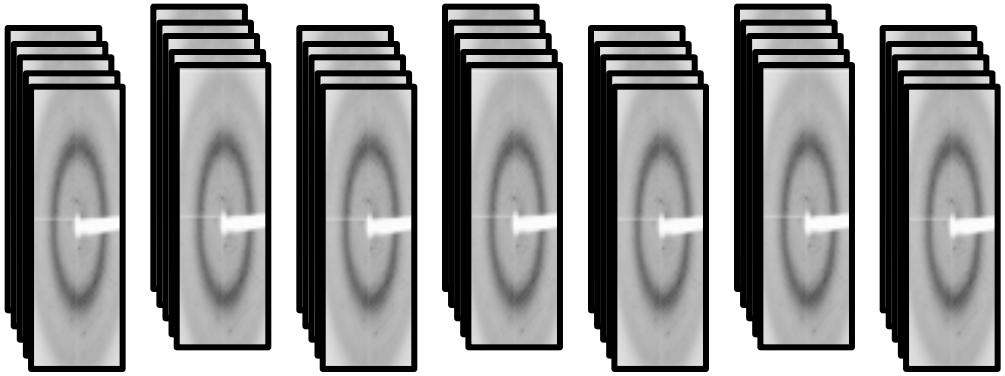

Calibration Error

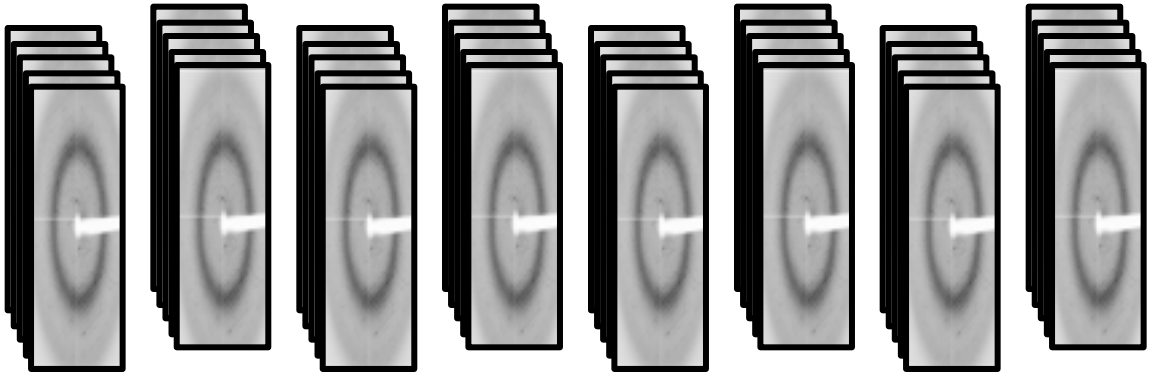

Calibration Error

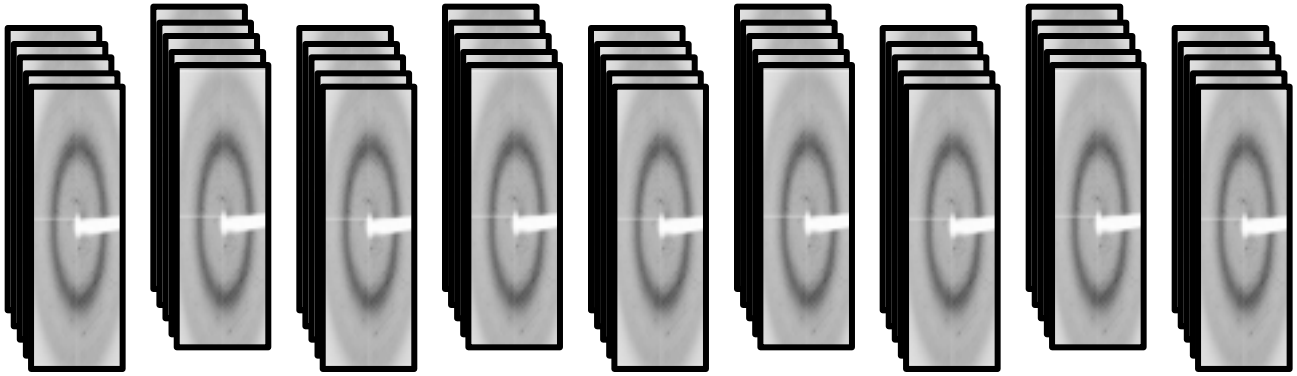

Calibration Error

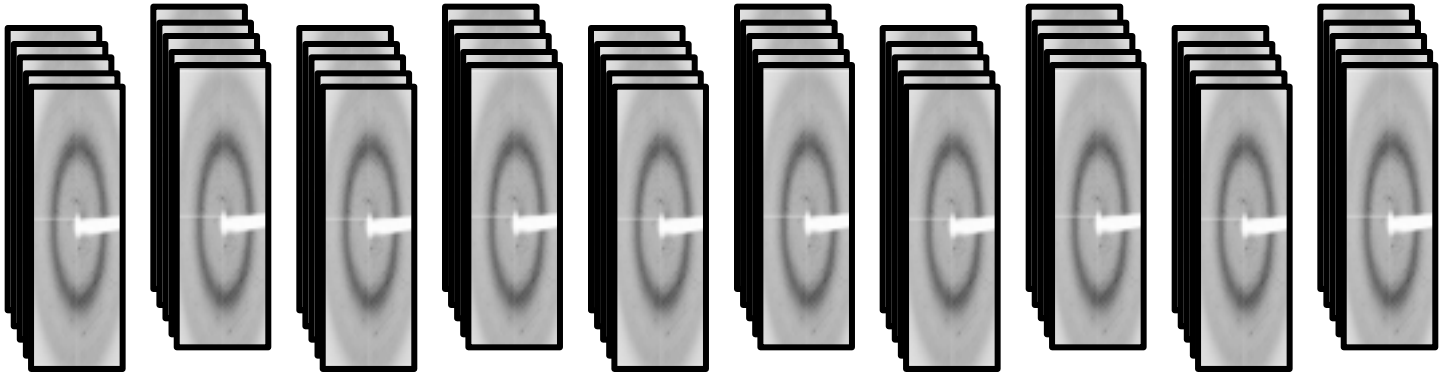

Calibration Error

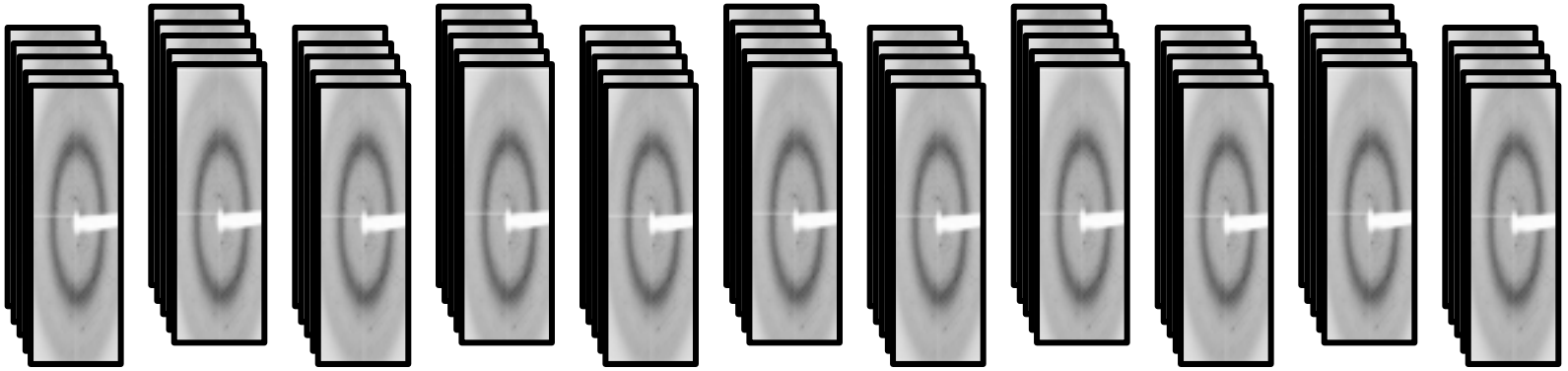

Calibration Error

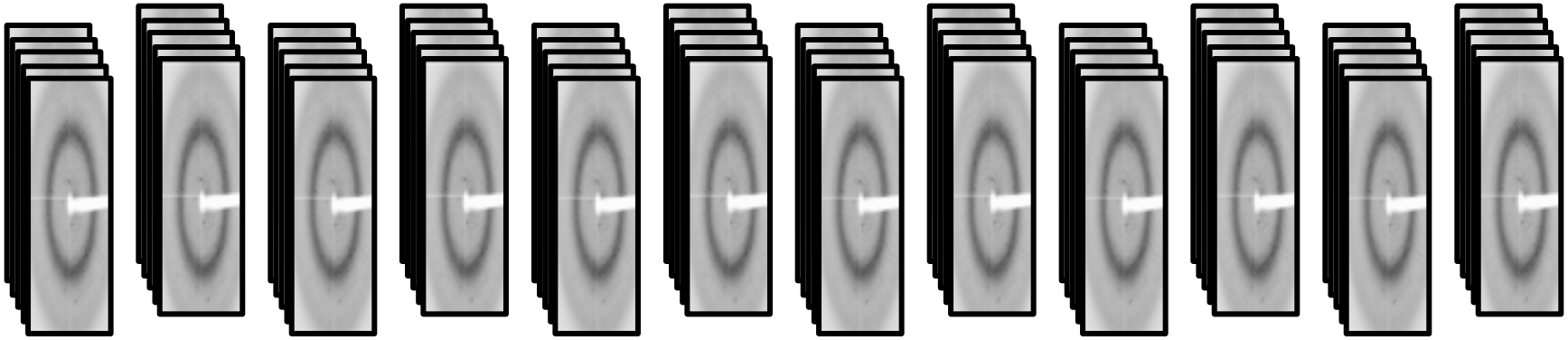

Calibration Error

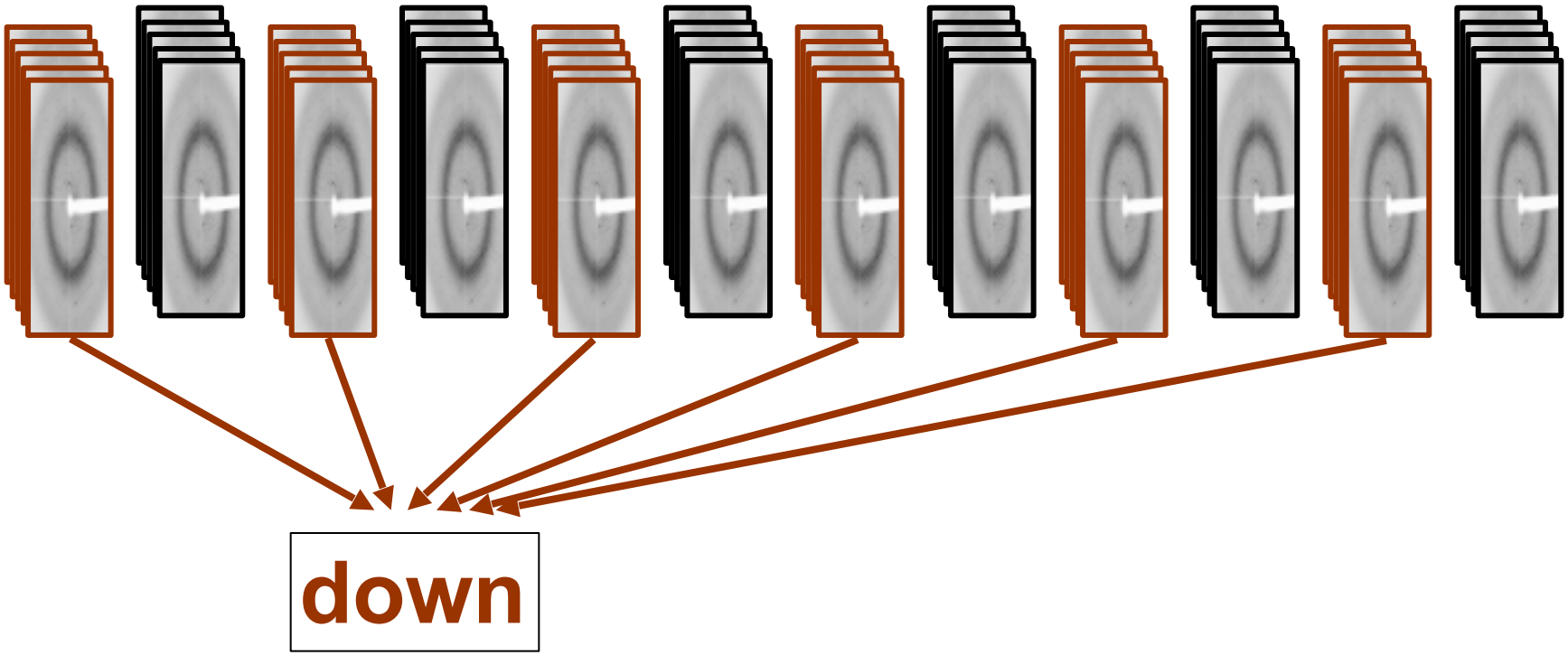

Calibration Error

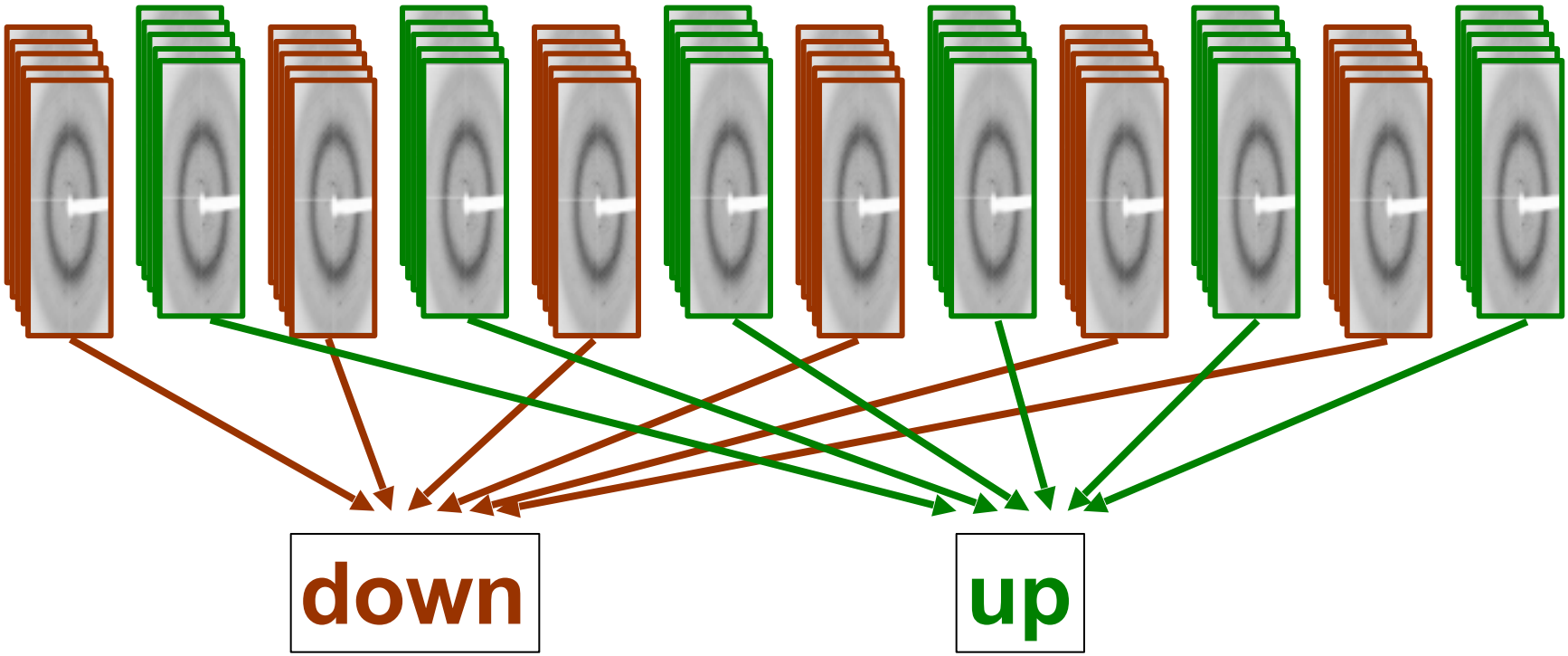

Calibration Error

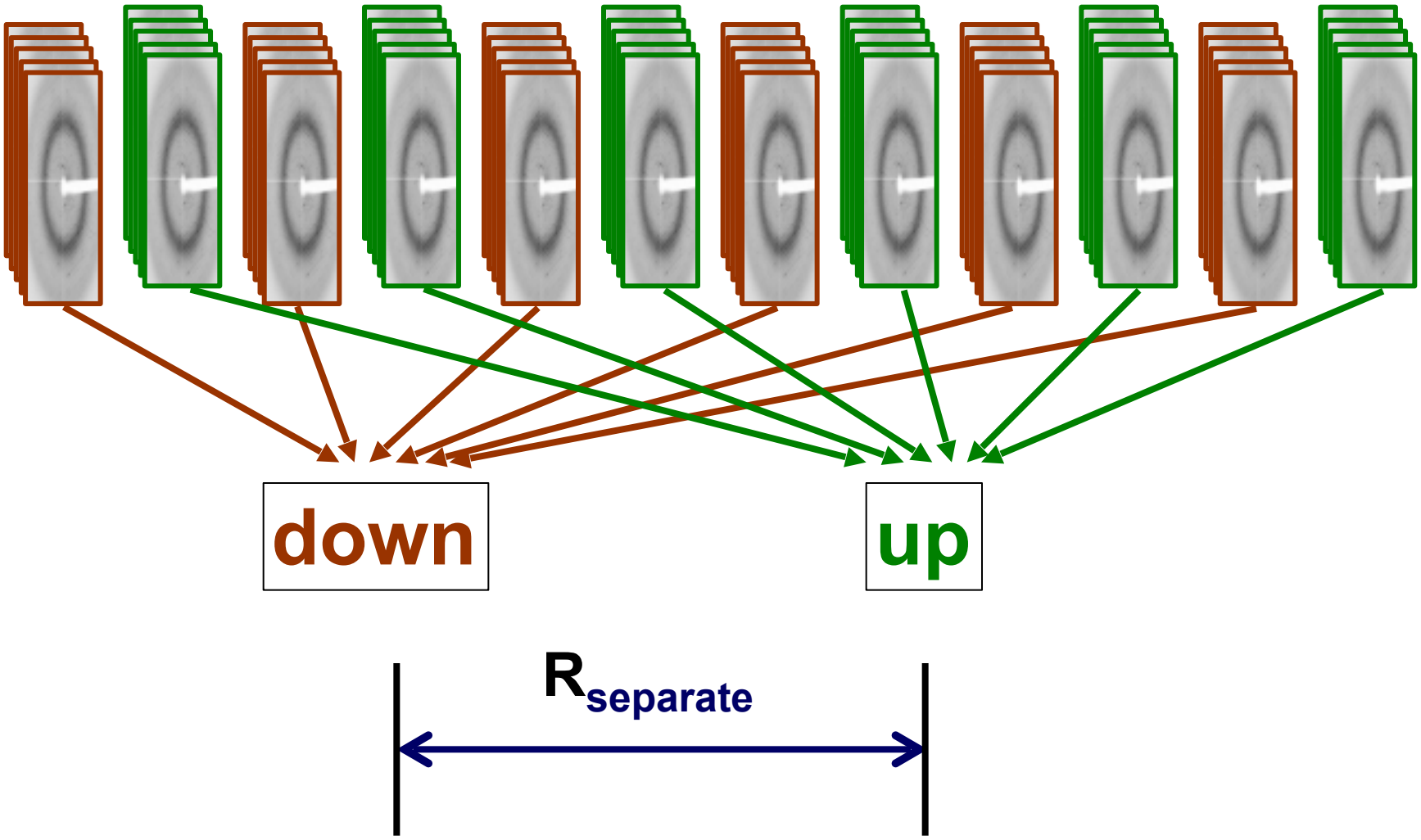

Calibration Error

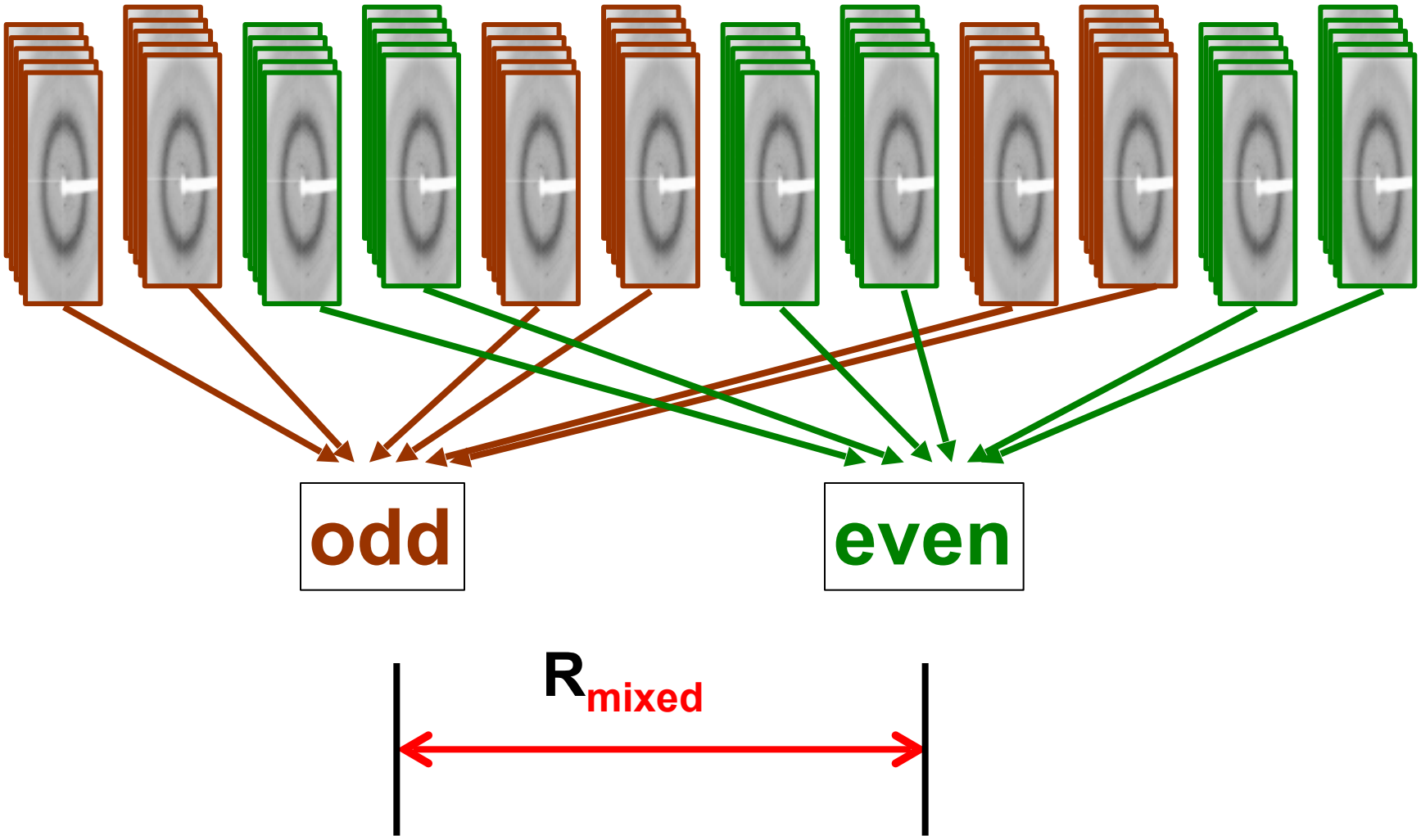

Calibration Error

separate: 2.5%

Calibration Error

separate: 2.5%

mixed: 0.9%

Calibration Error

separate: 2.5%

mixed: 0.9%

$2.5\%^2 - 0.9\%^2 = 2.3\%^2$

Detector calibration: 7235 eV

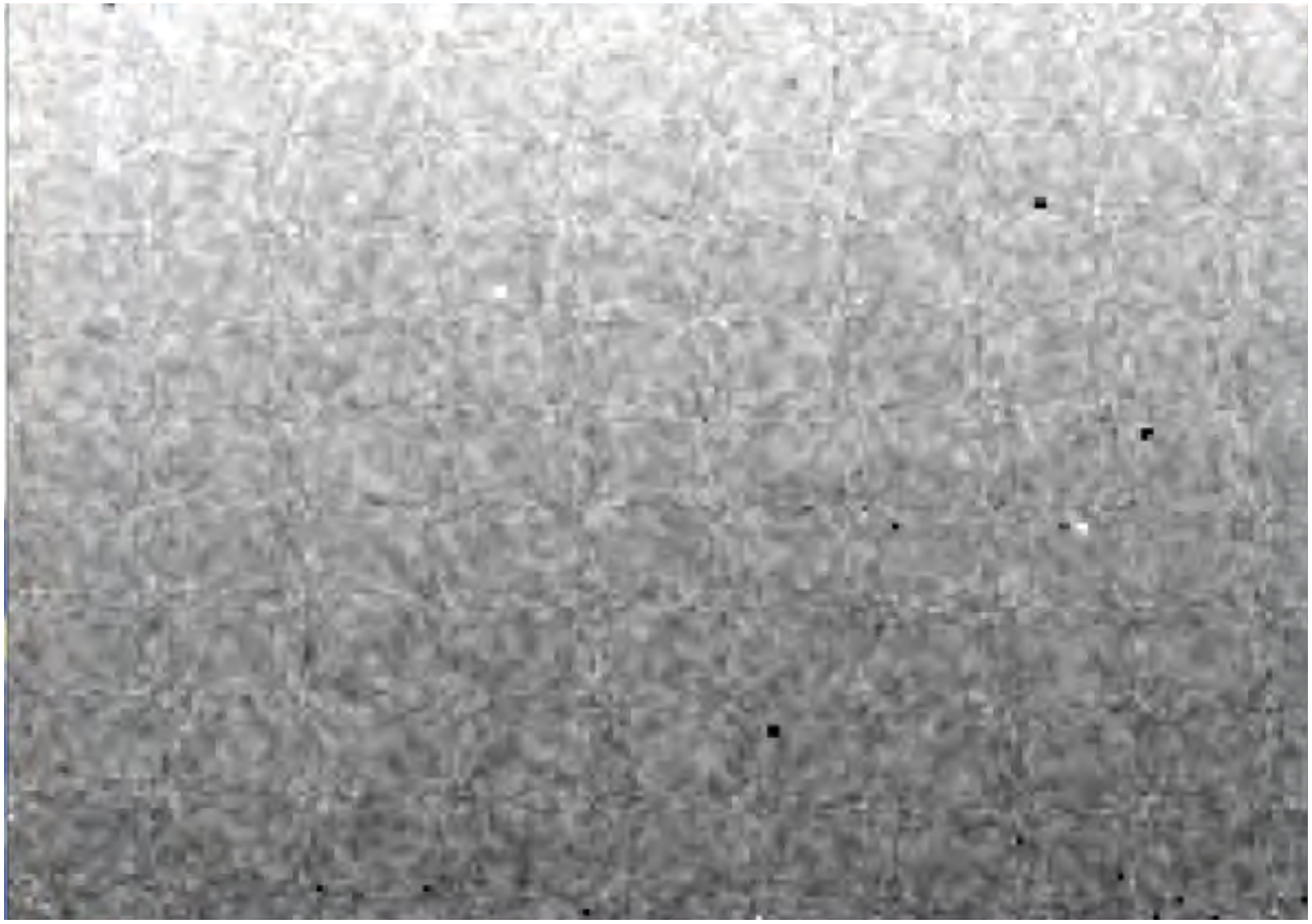

Detector calibration: 7247 eV

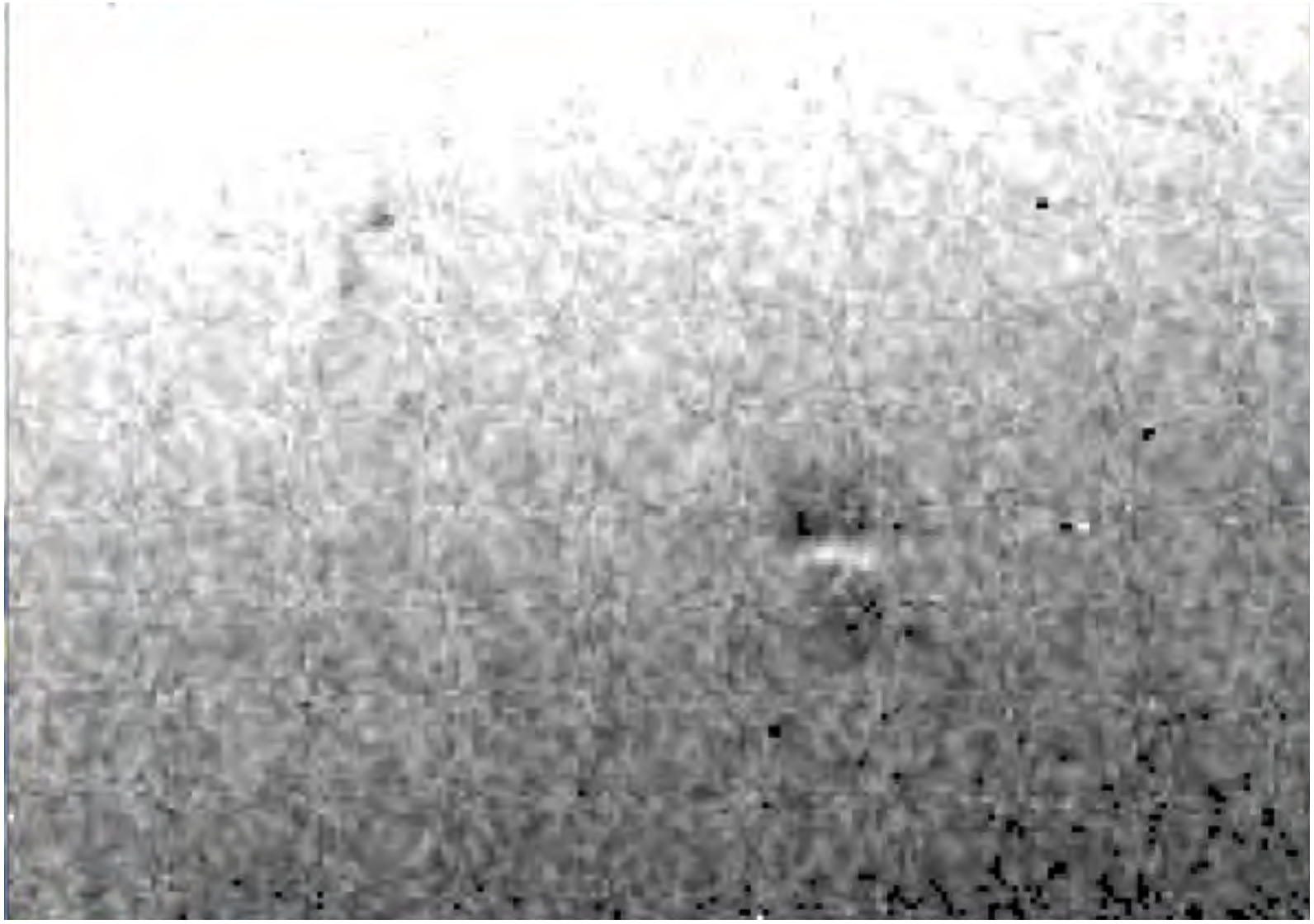

Gadox calibration vs energy

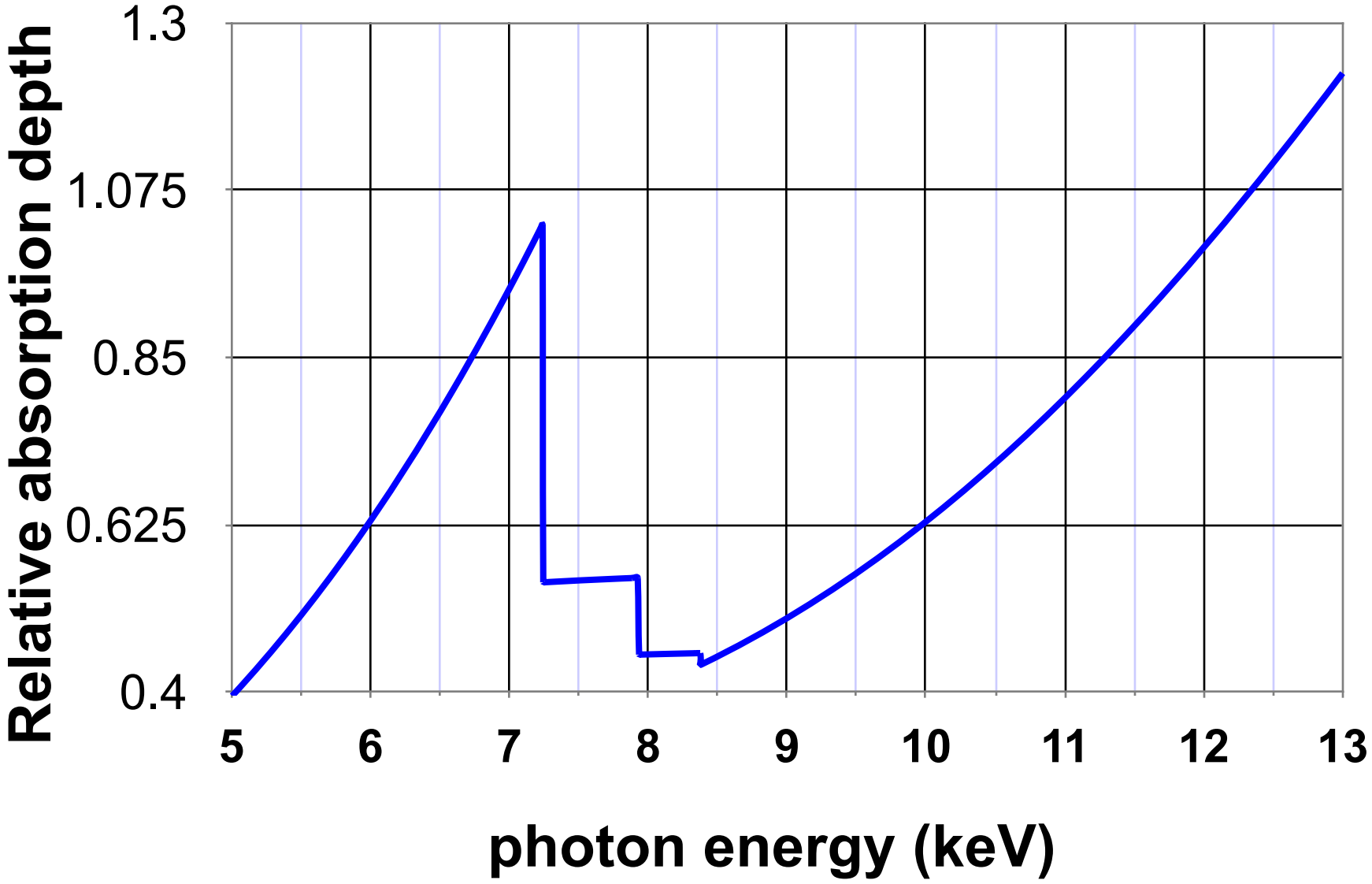

Gadox calibration vs energy

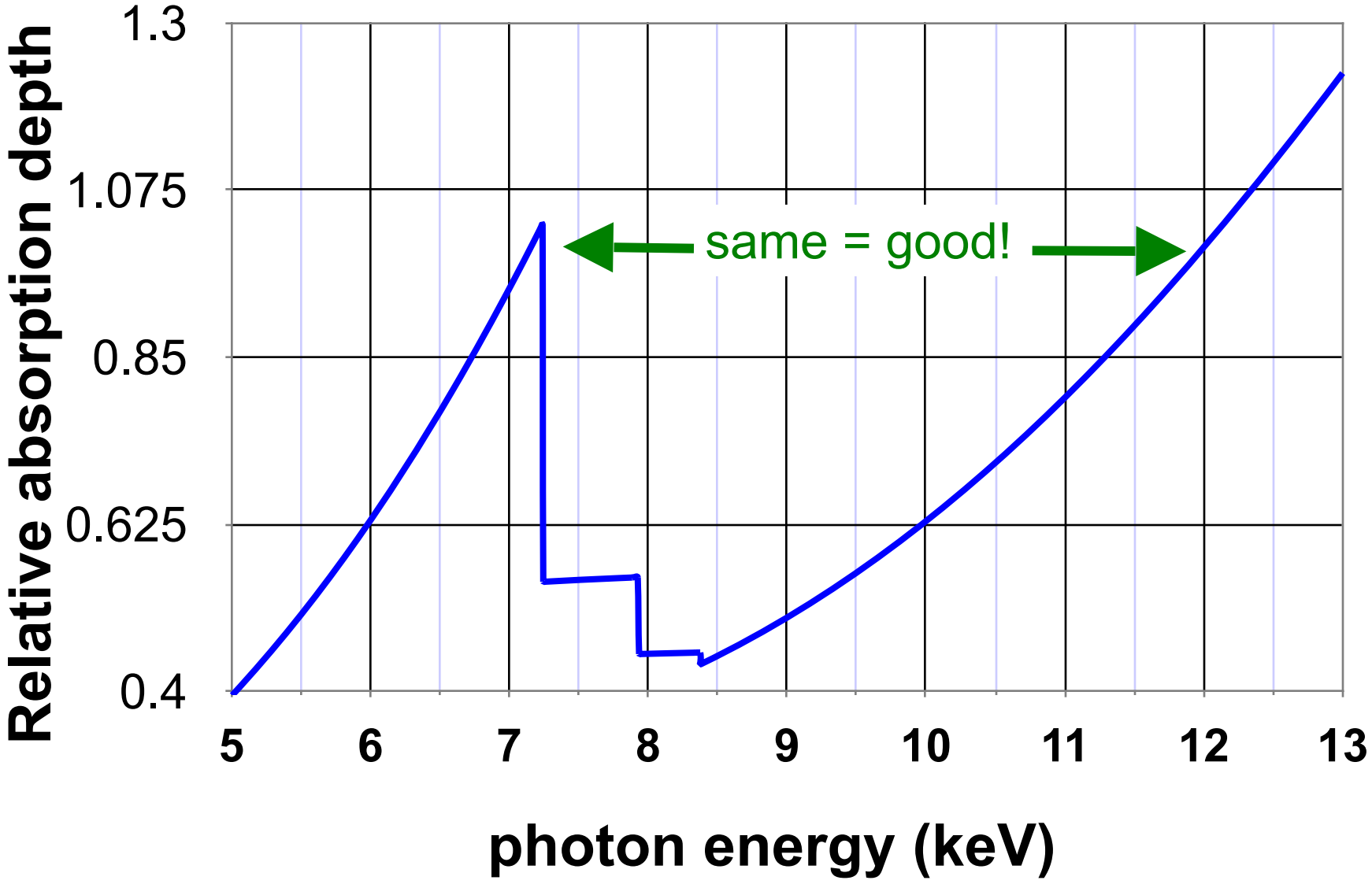

Gadox calibration vs energy

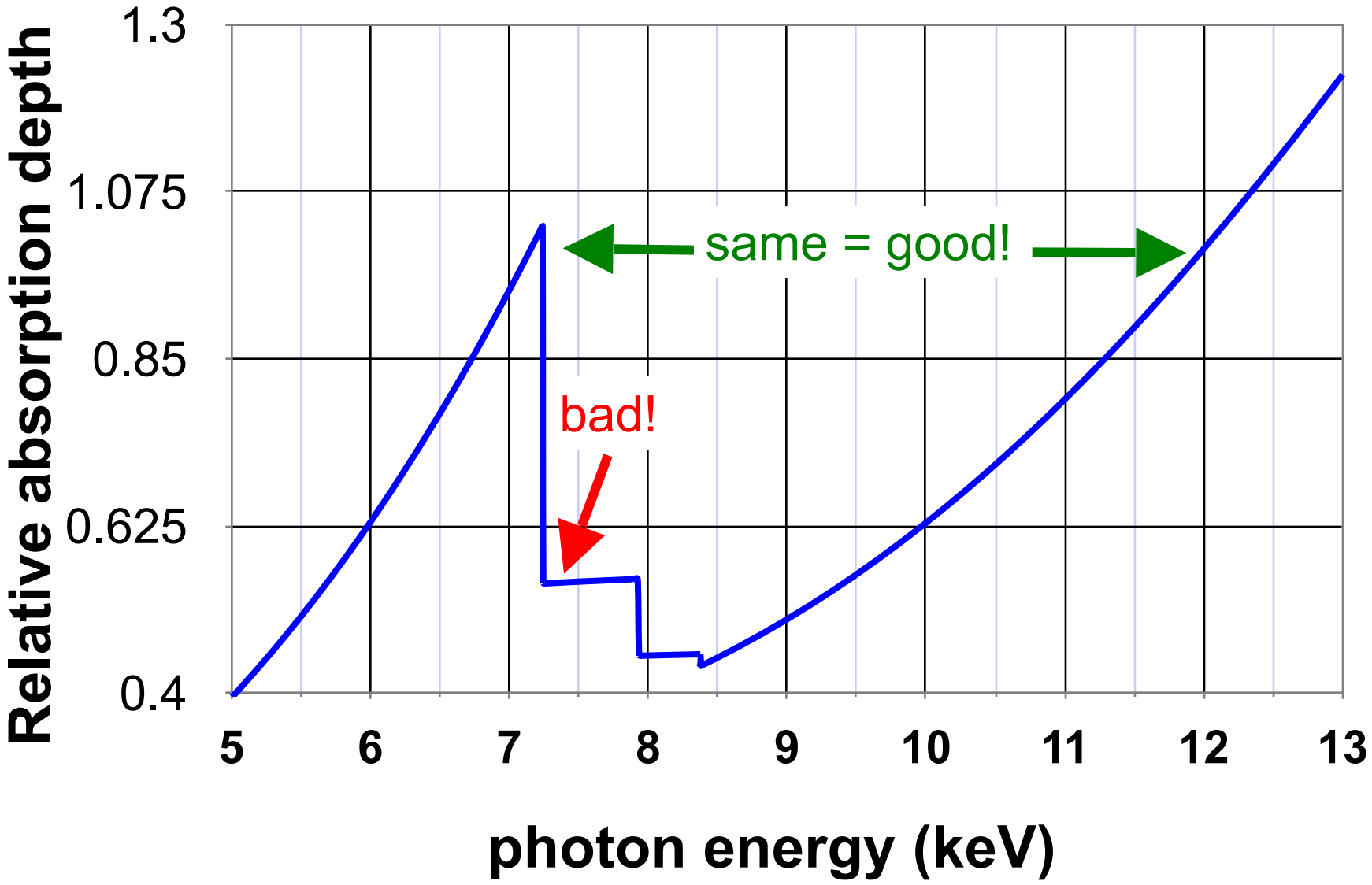

Spatial Heterogeneity in Sharp Spot Sensitivity

Pilatus is not immune!

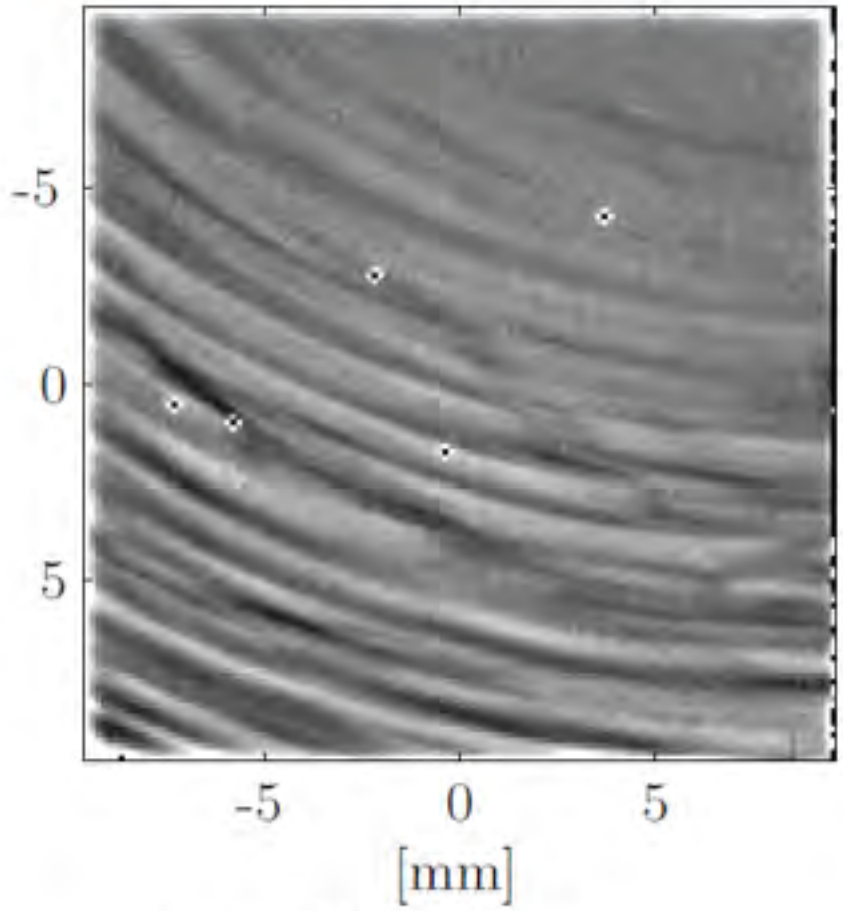

(a) Cu X-Ray Tube

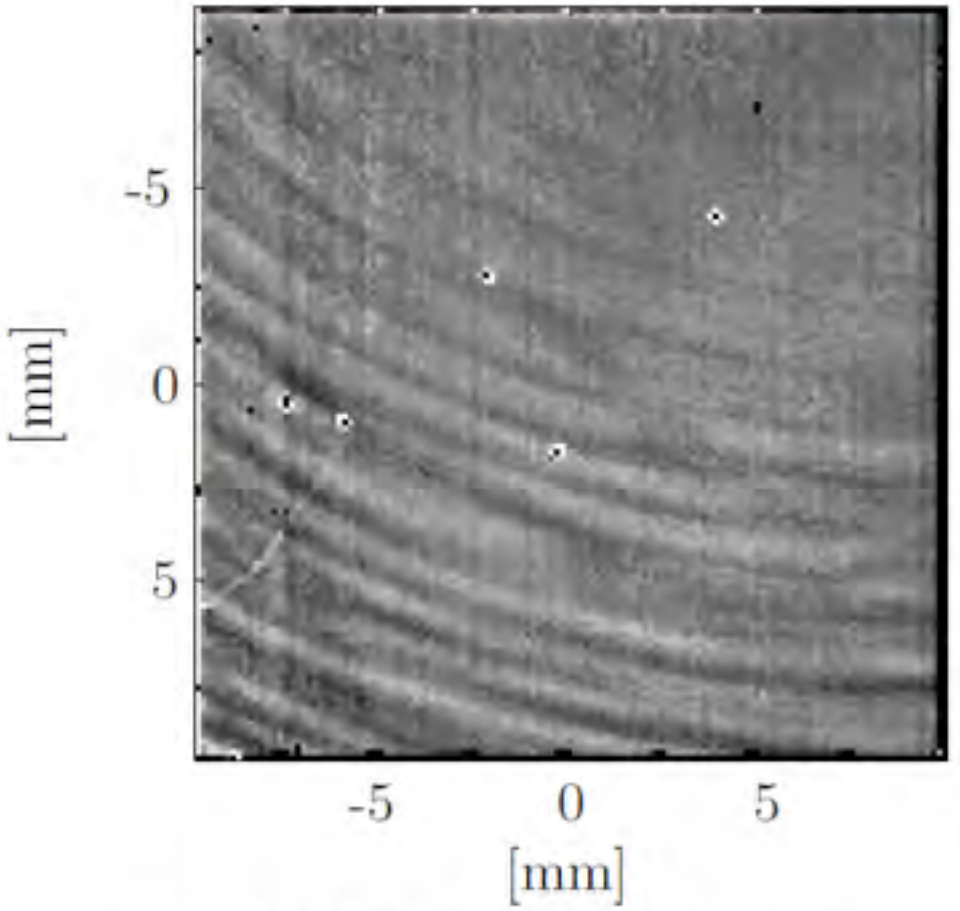

(b) Mo X-Ray Tube (Al attn)

Dan Schuette PhD Thesis (2008) Fig 6.22 page 198, Gruner Lab, Cornell University.

Spatial Heterogeneity in Sharp Spot Sensitivity (SHSSS): Q315r vs Pilatus

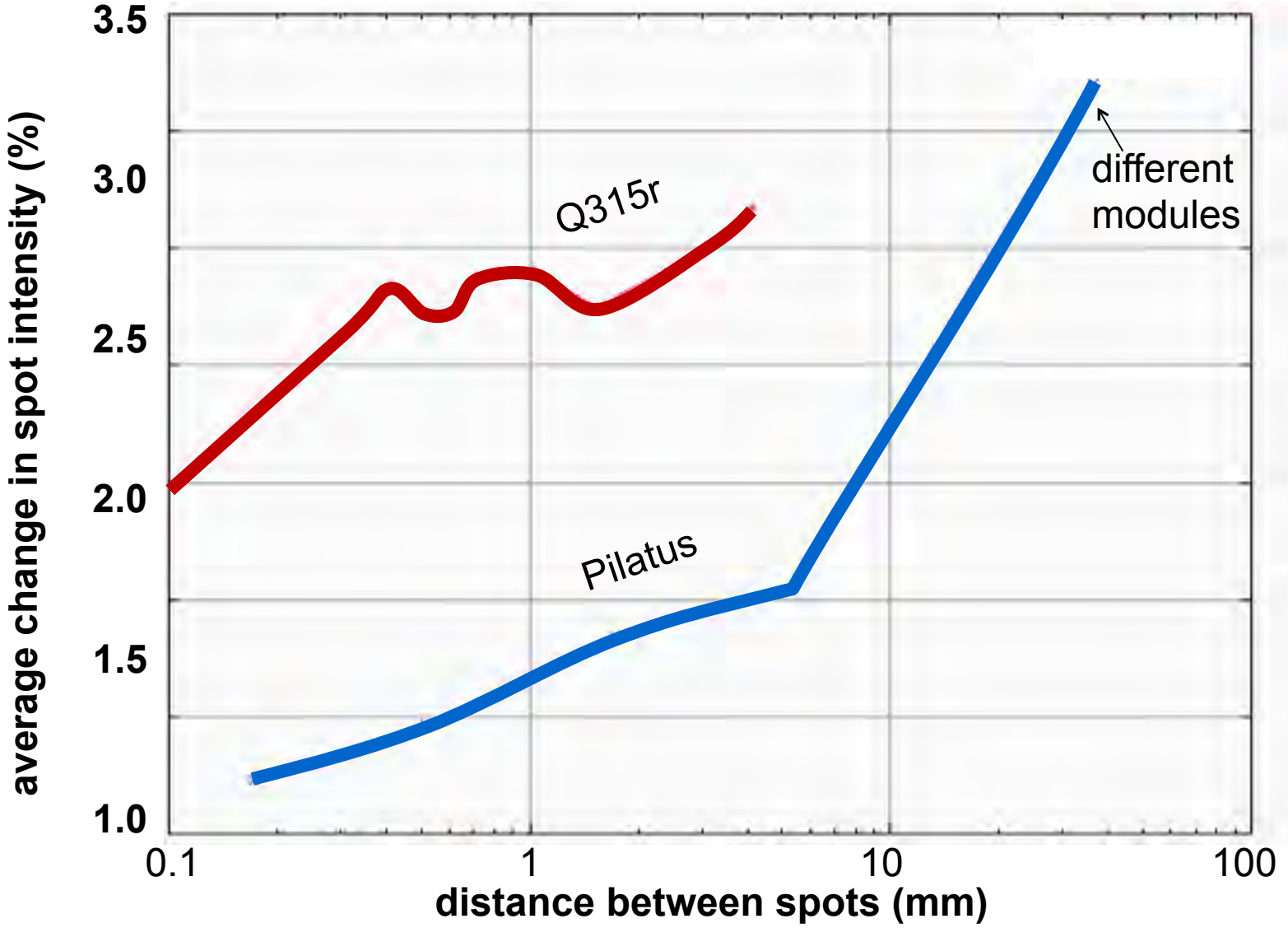

Spatial Heterogeneity in Sharp Spot Sensitivity (SHSSS): Q315r vs Pilatus

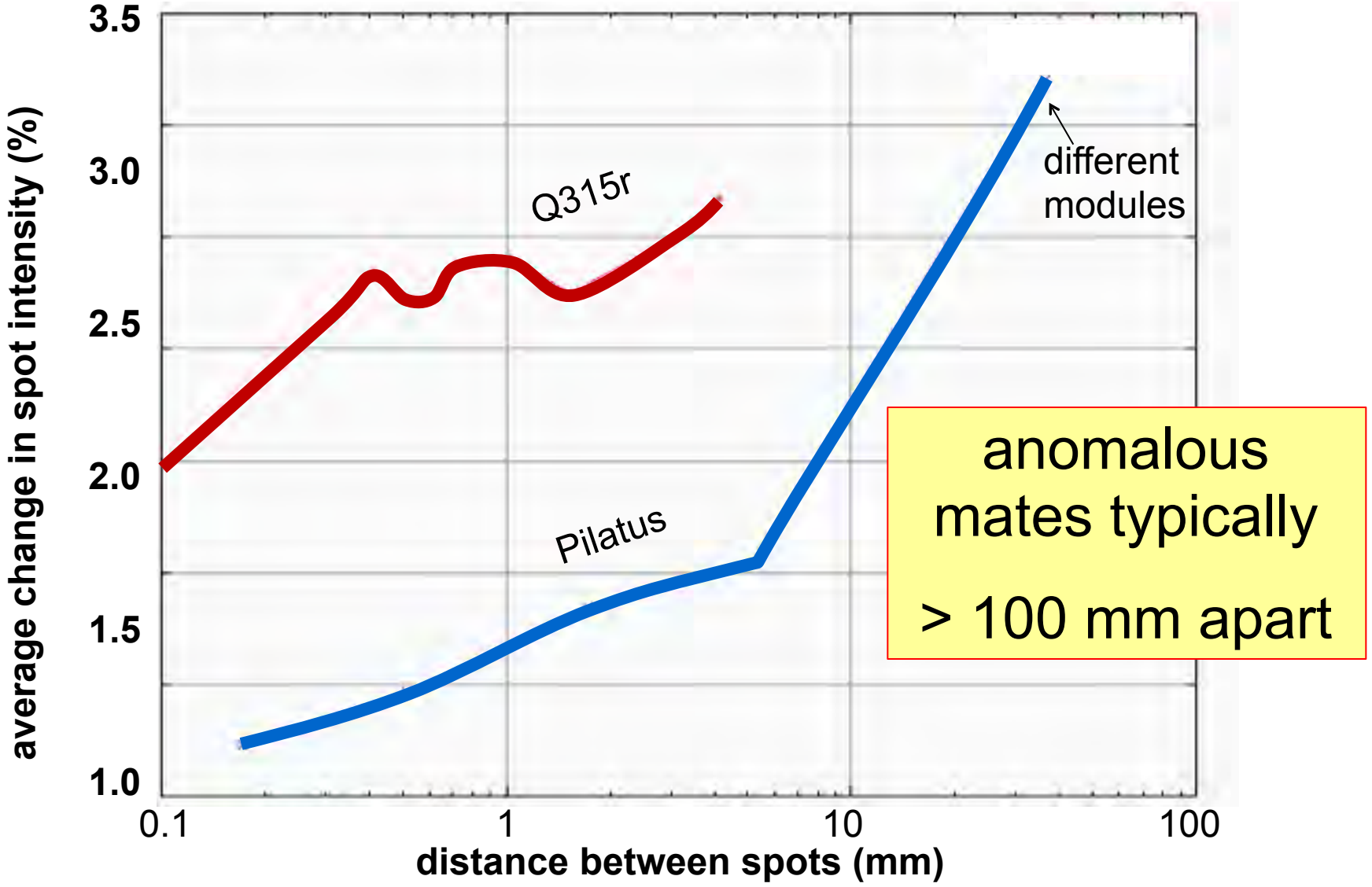

lysozyme: real and reciprocal

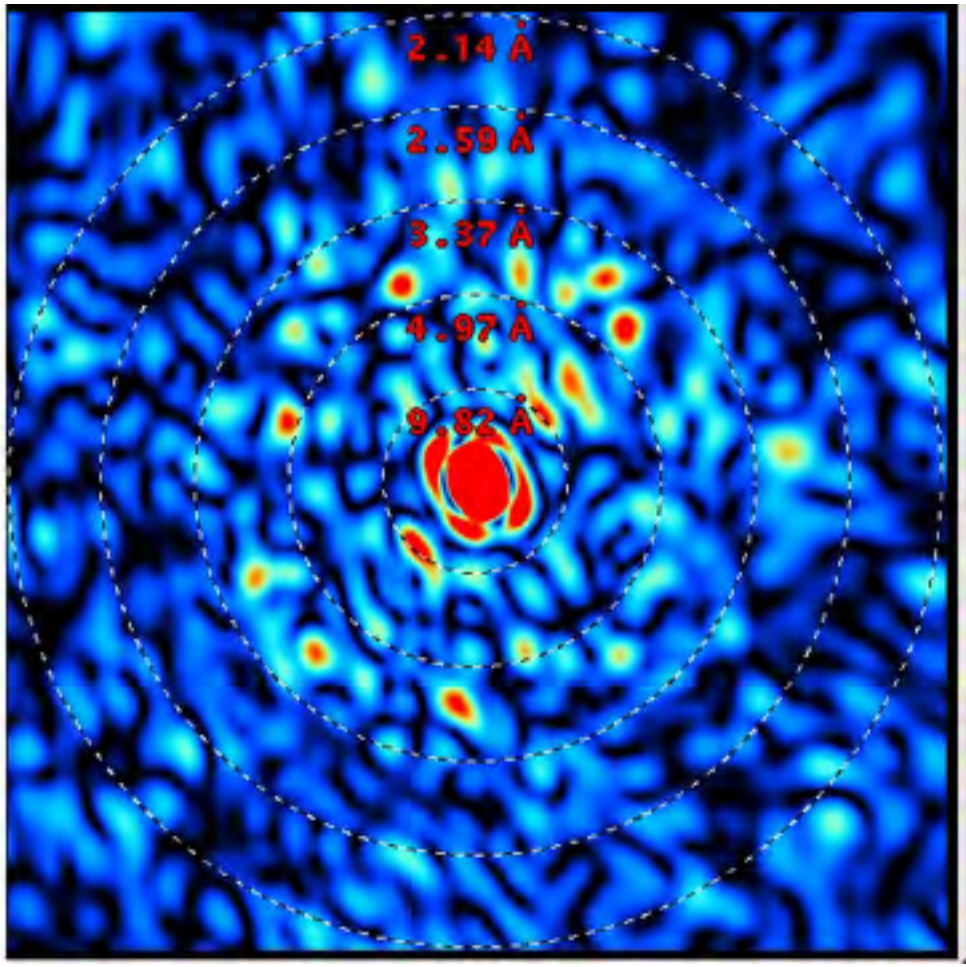

lysozyme: thermal motion

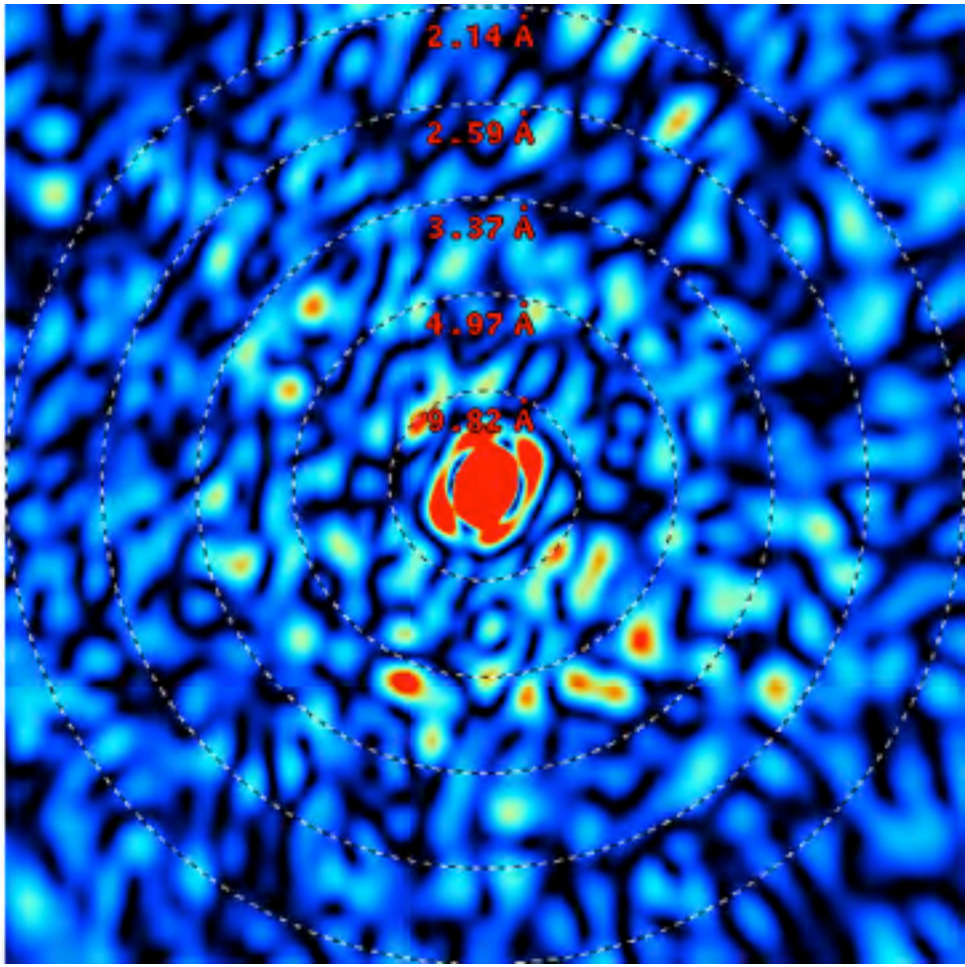

Muybridge’s galloping horse (1878)

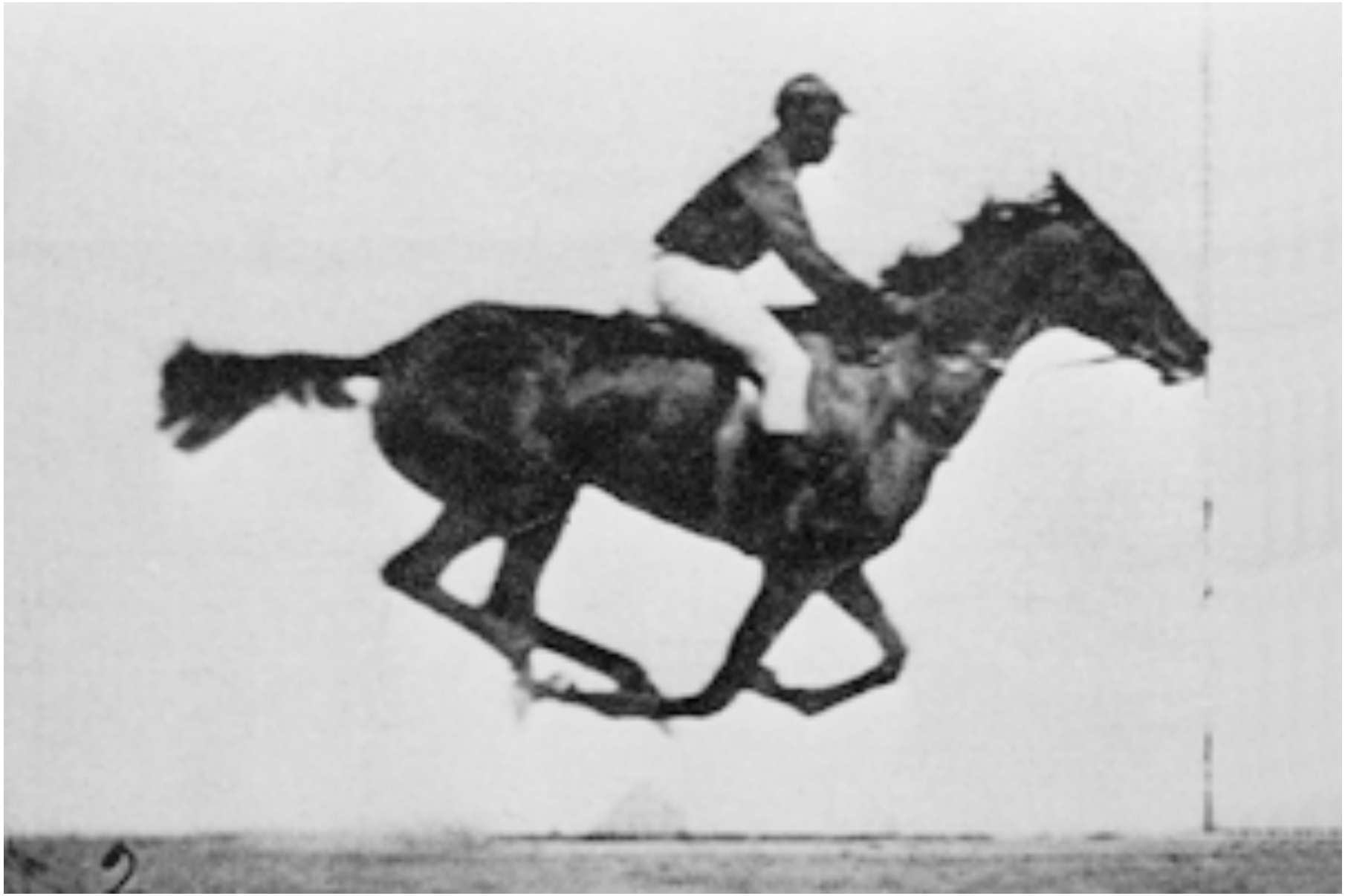

Muybridge's multi-camera

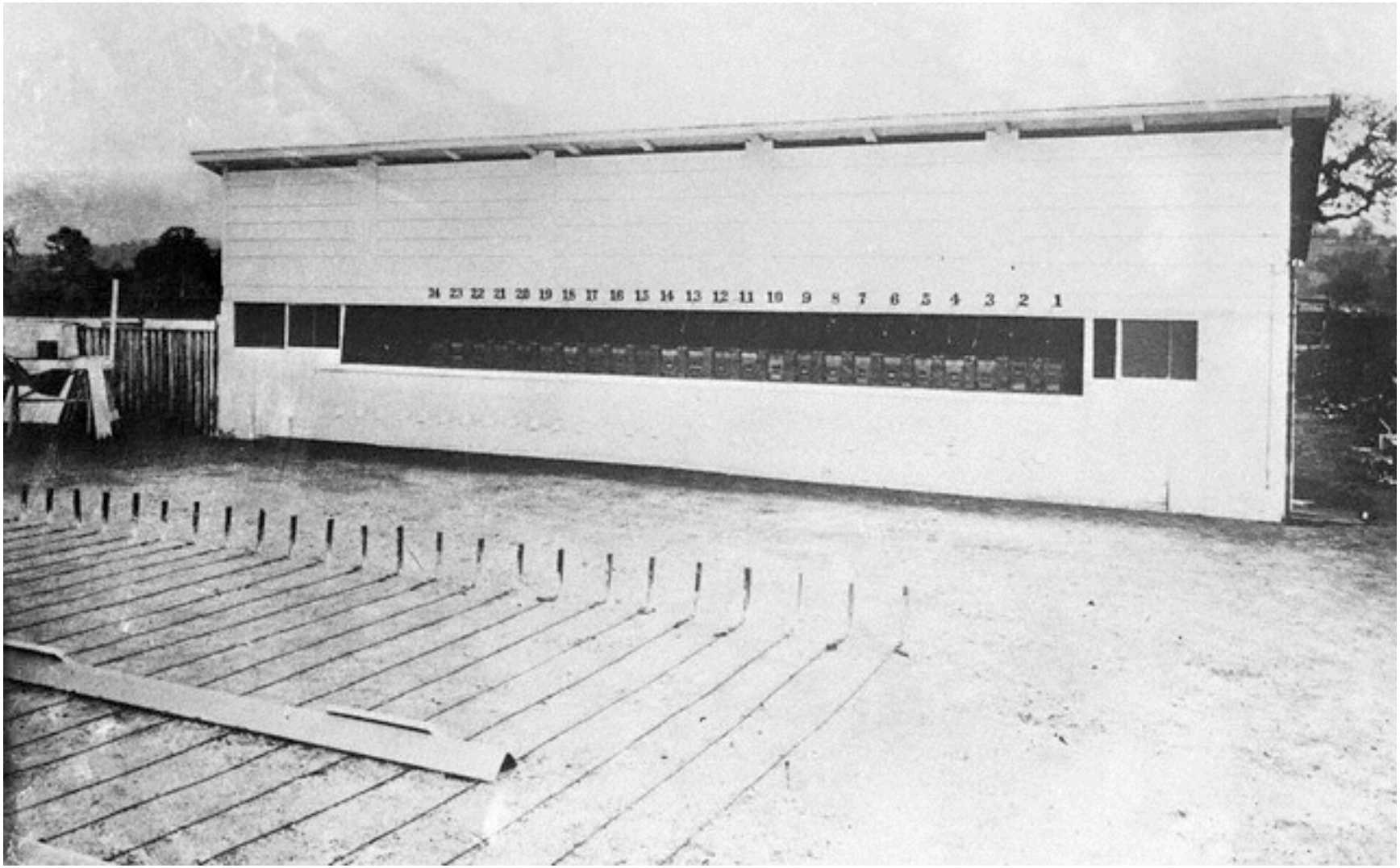

Muybridge's galloping horse (1878)

"Time-resolved" diffraction

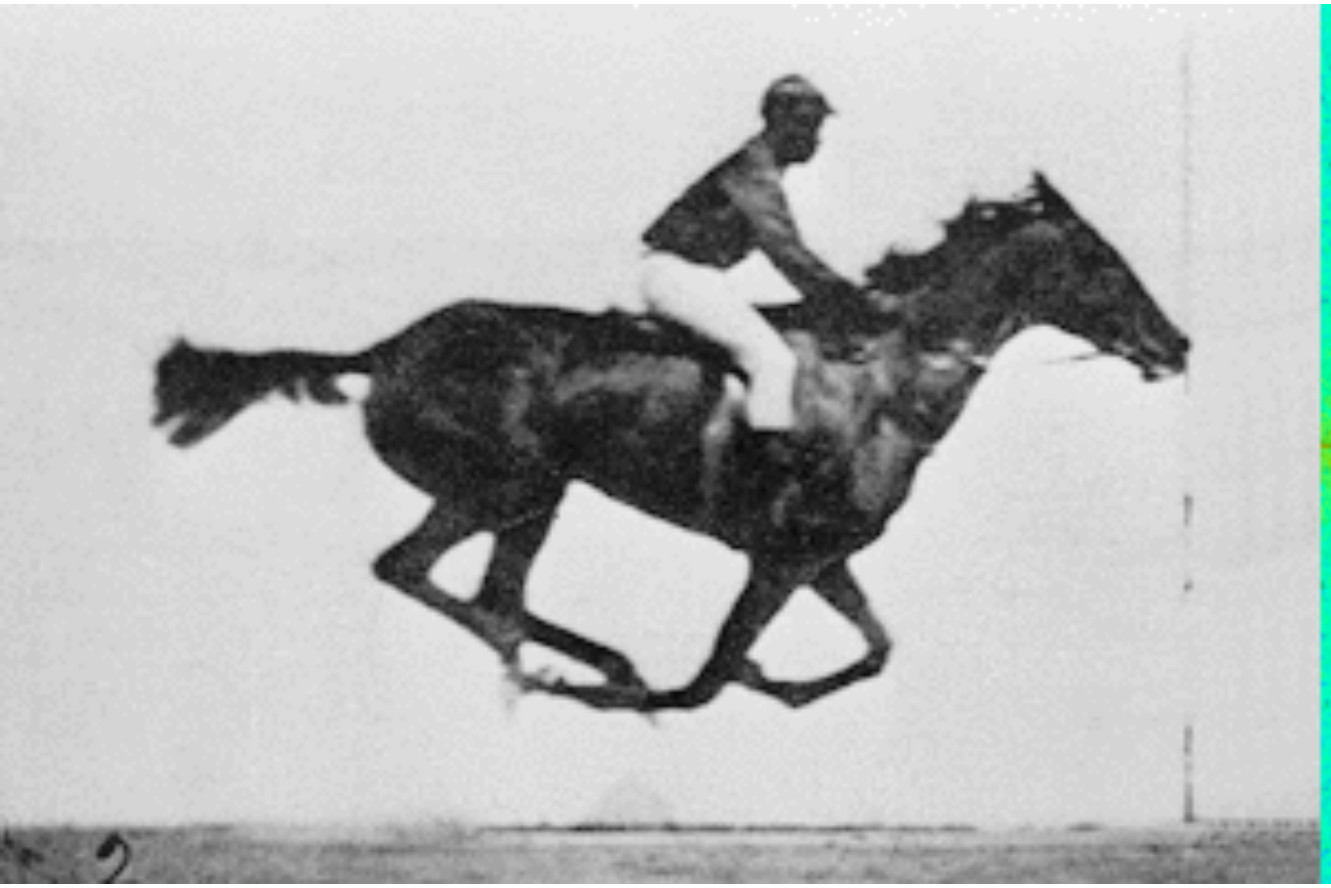

Real space

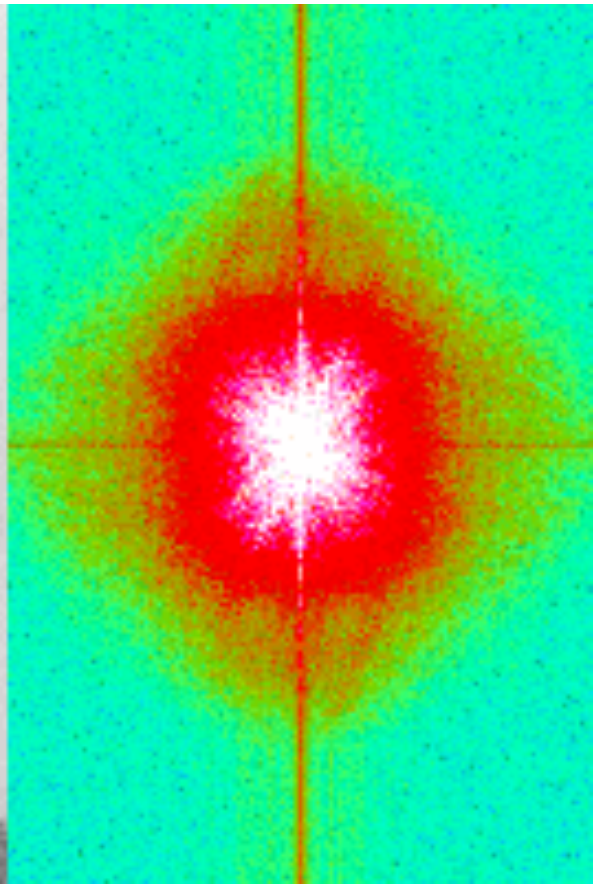

reciprocal

Muybridge's galloping horse (1878)

Average intensity

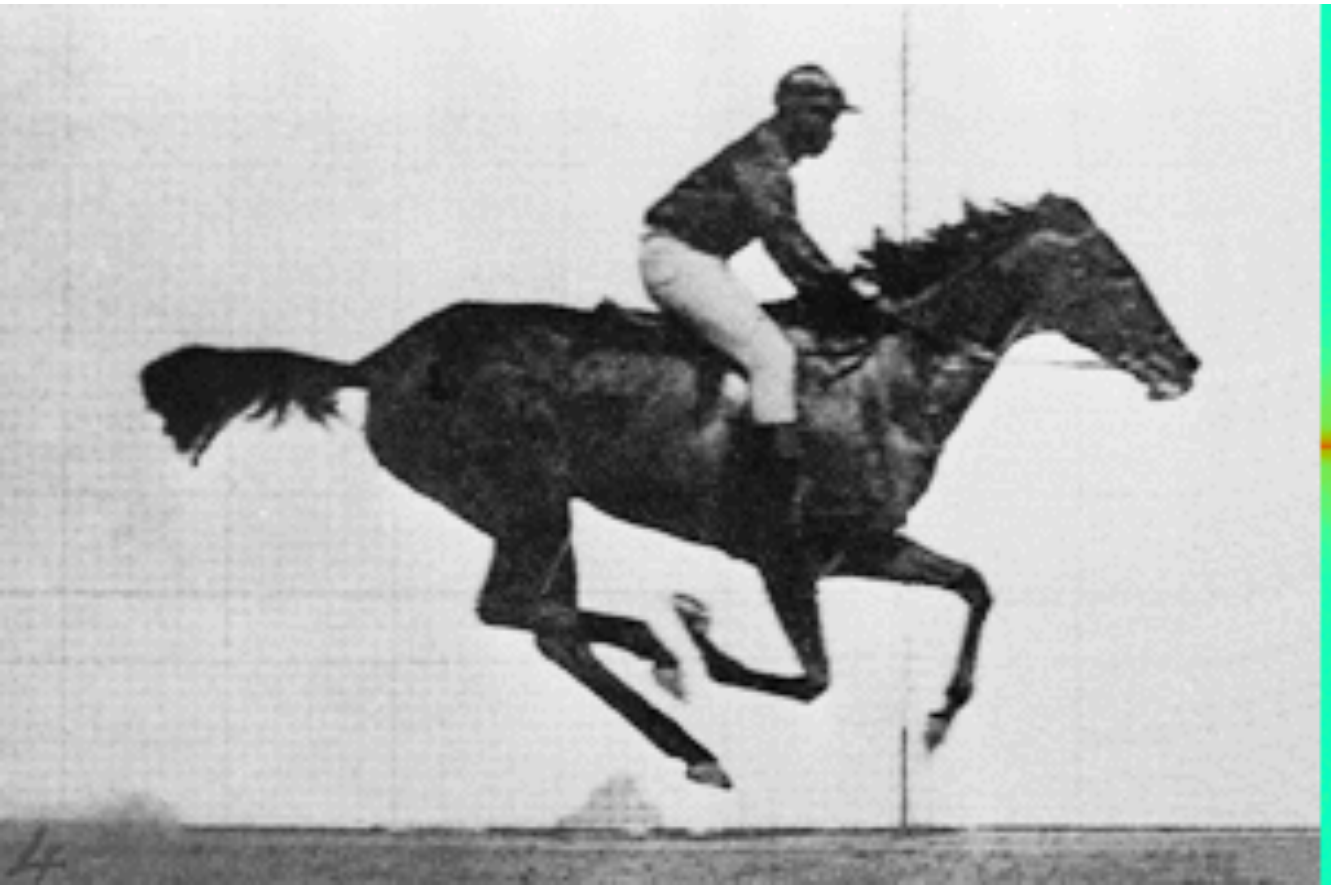

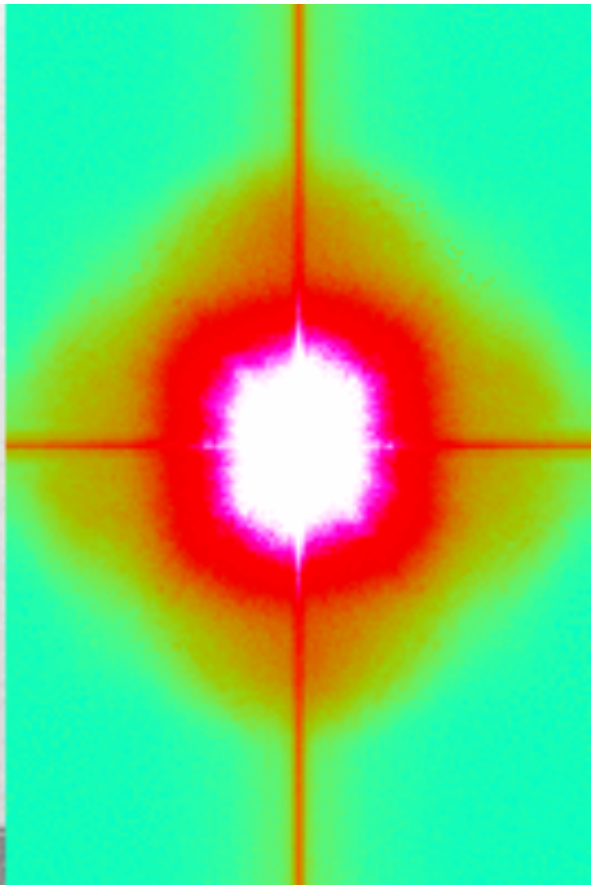

Real space

reciprocal

Muybridge's galloping horse (1878)

Average electron density

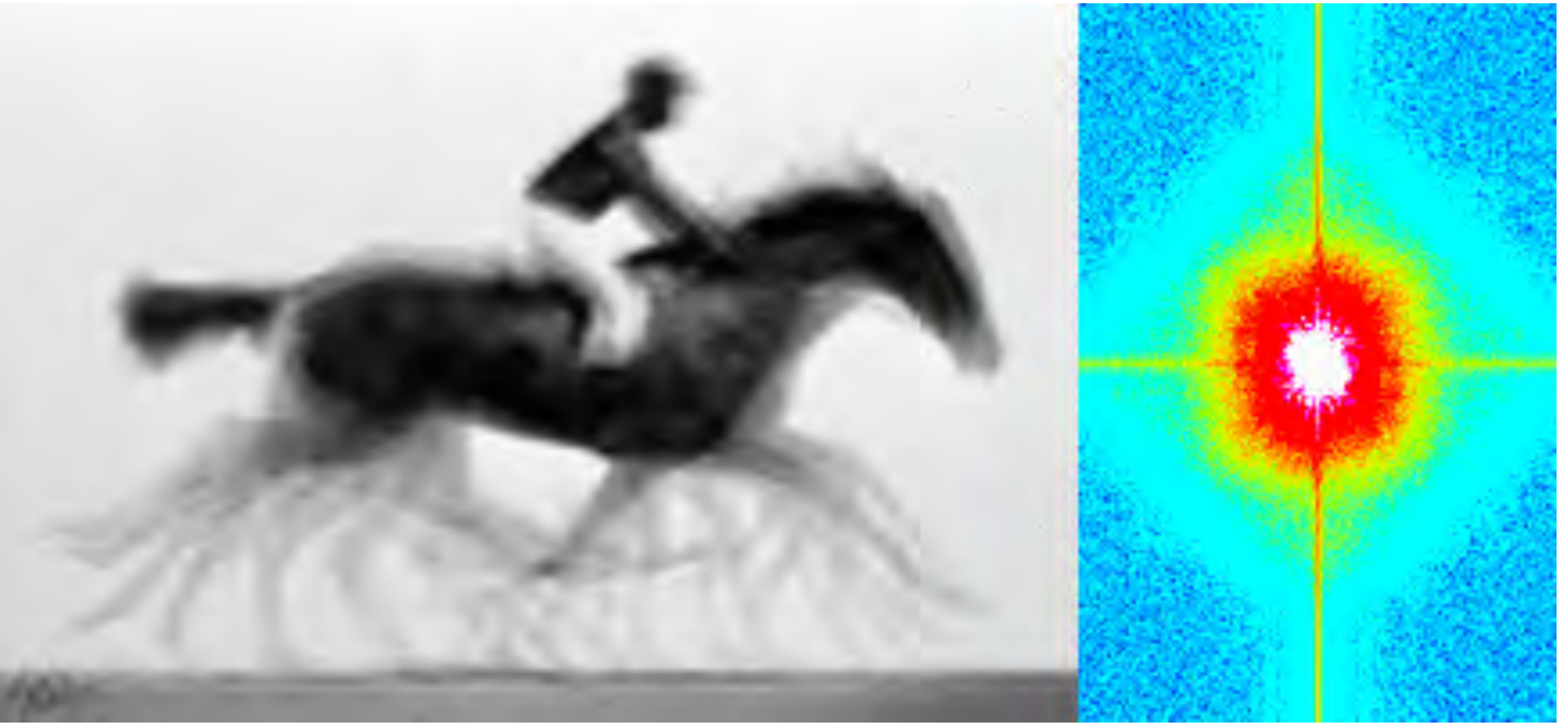

Real space

reciprocal

Muybridge's galloping horse (1878)

Sum(intensity) – Sum(density) = diffuse scatter

Real space

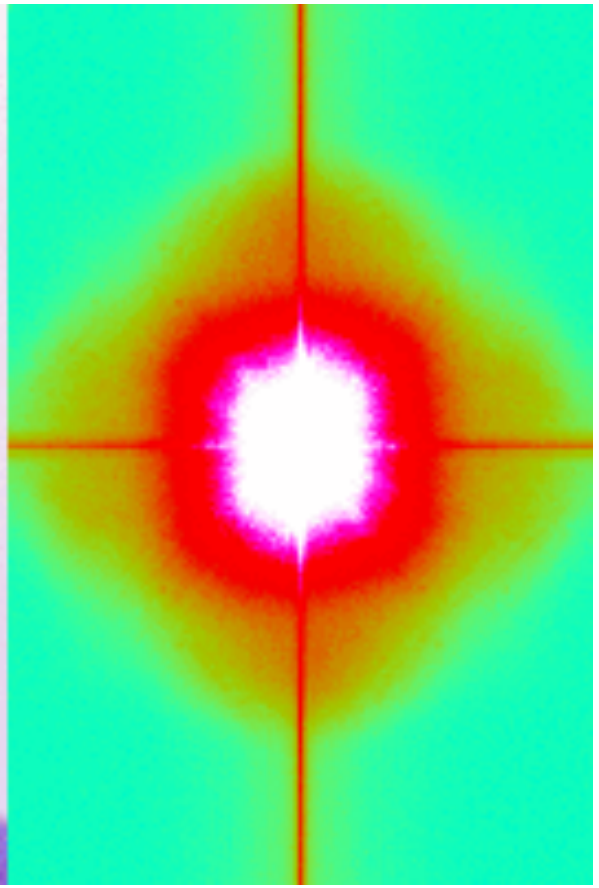

reciprocal

Muybridge's galloping horse (1878)

$F_{incoh} - F_{coherent}$ with density phases

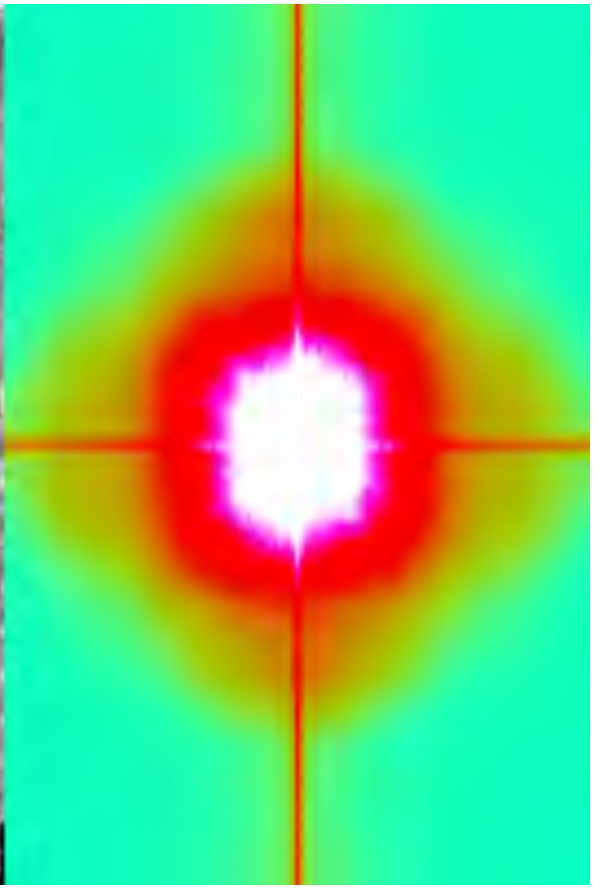

Real space

reciprocal

Muybridge's galloping horse (1878)

RMS variation in density

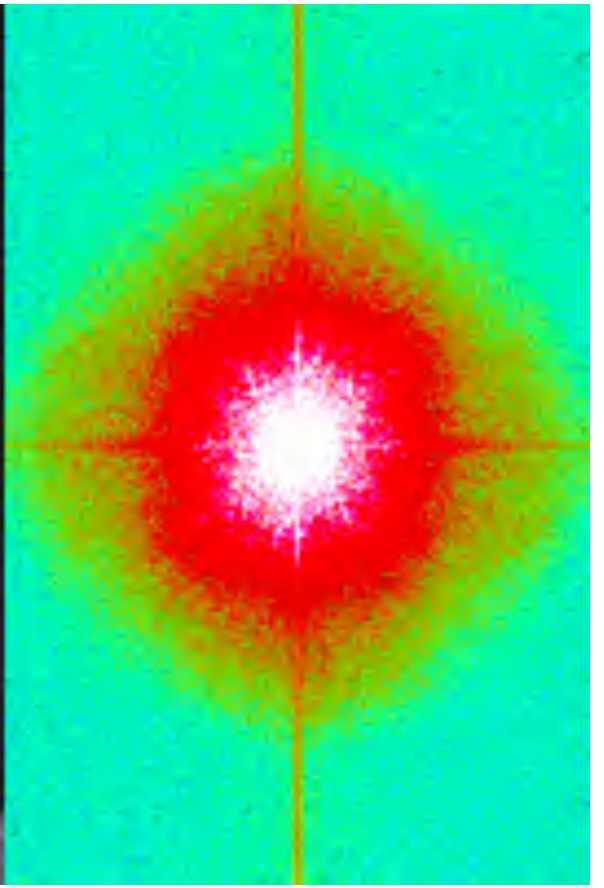

Real space

reciprocal

Supporting a model with data

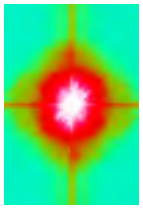

Supporting a model with data

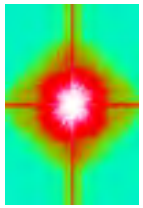

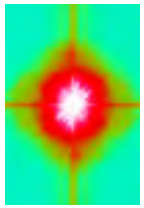

Supporting a model with data

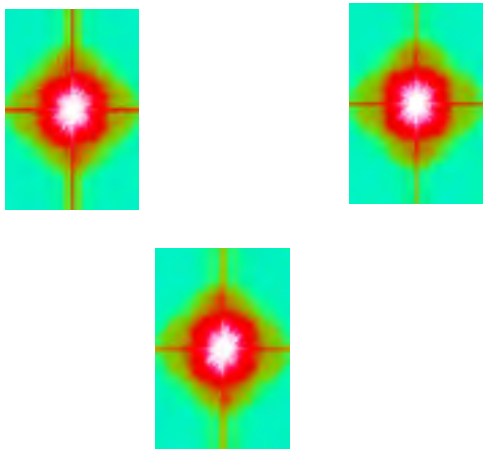

Supporting a model with data

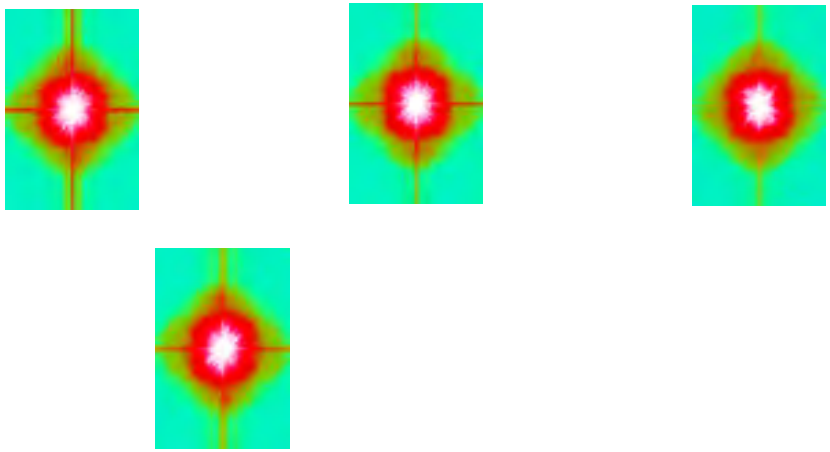

Supporting a model with data

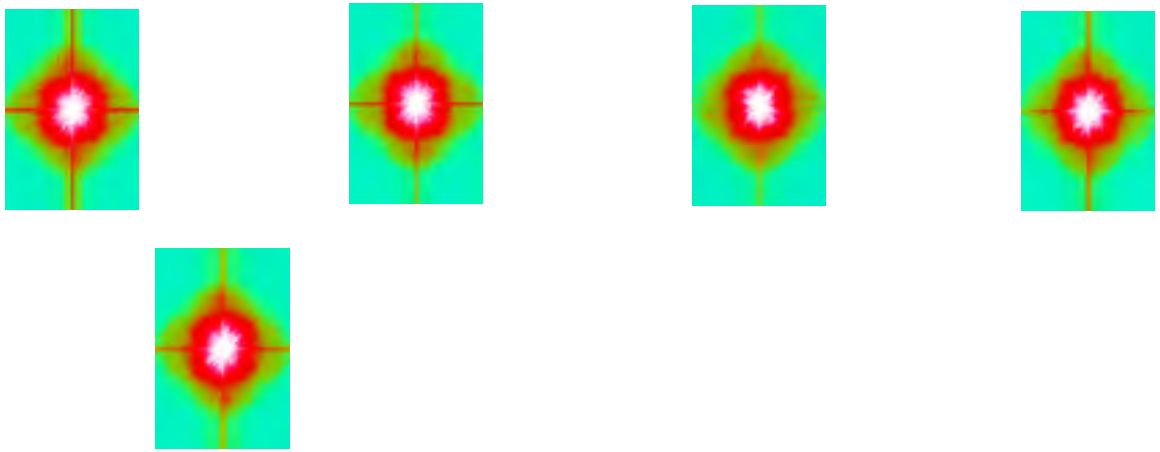

Supporting a model with data

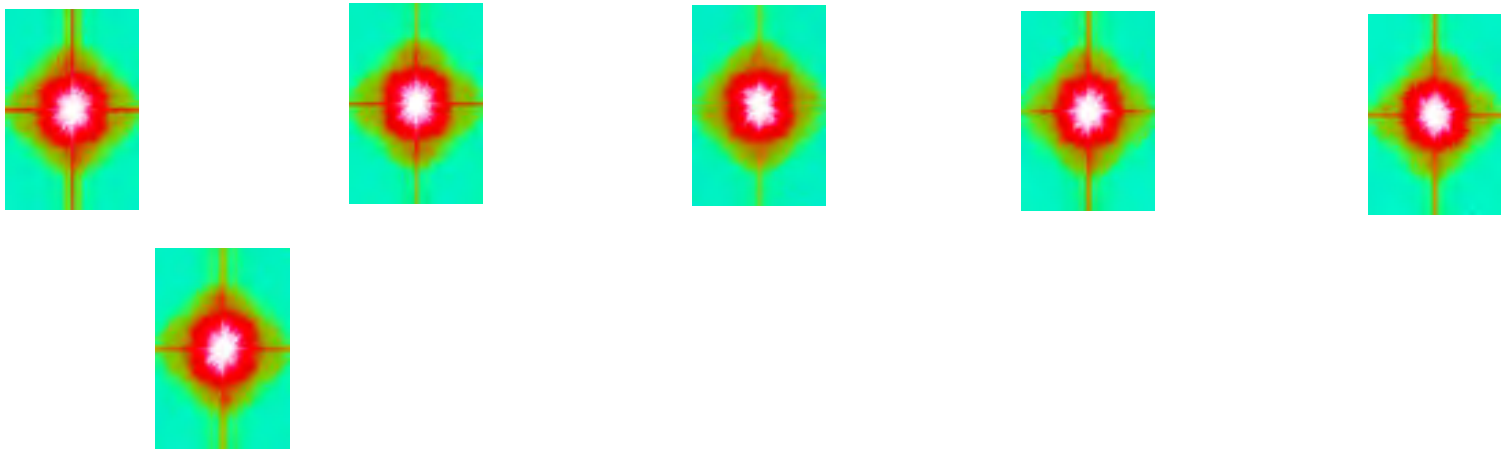

Supporting a model with data

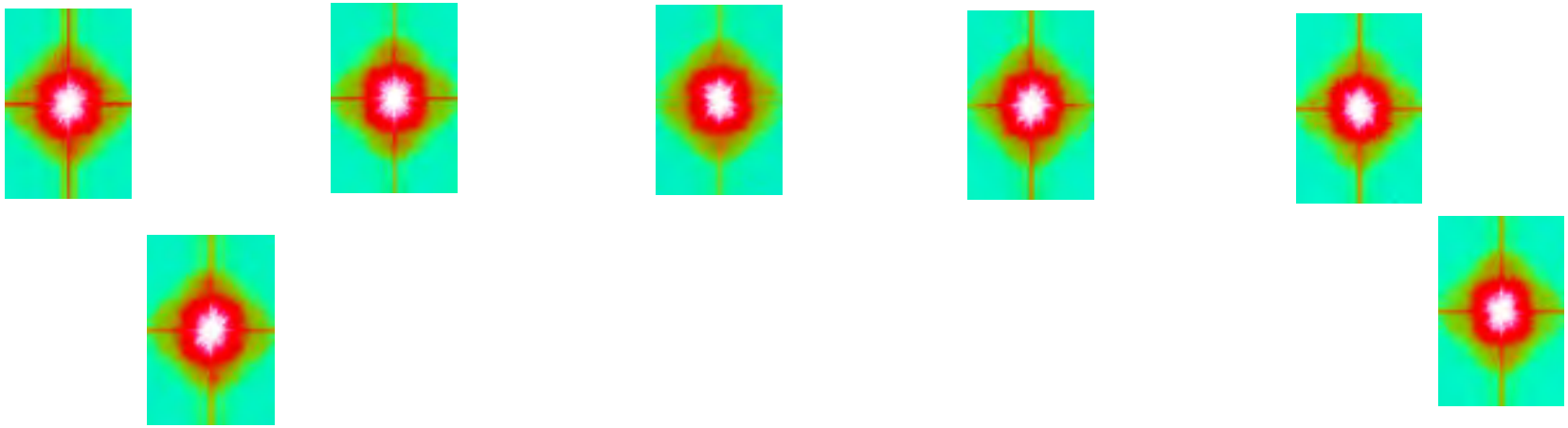

Supporting a model with data

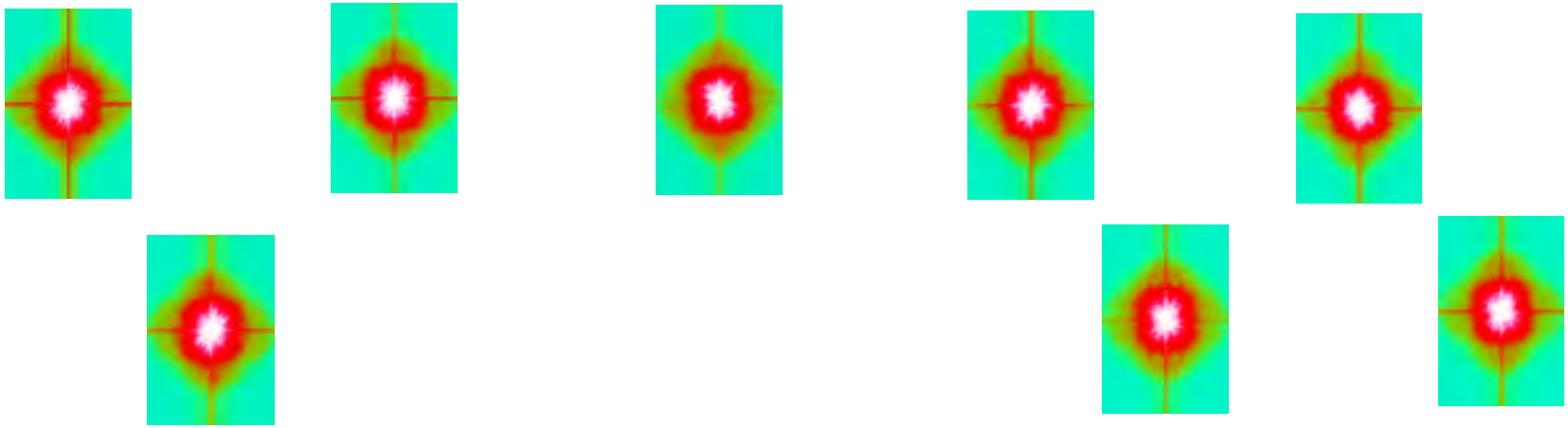

Supporting a model with data

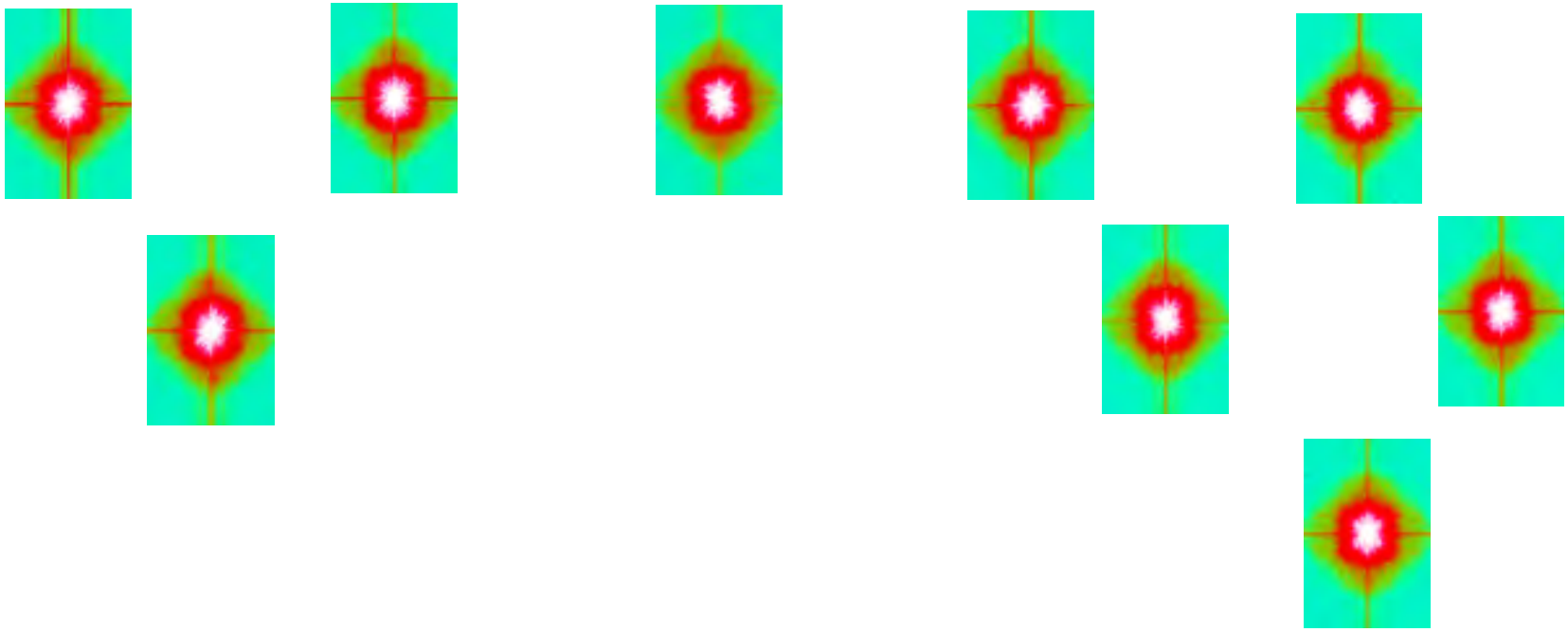

Supporting a model with data

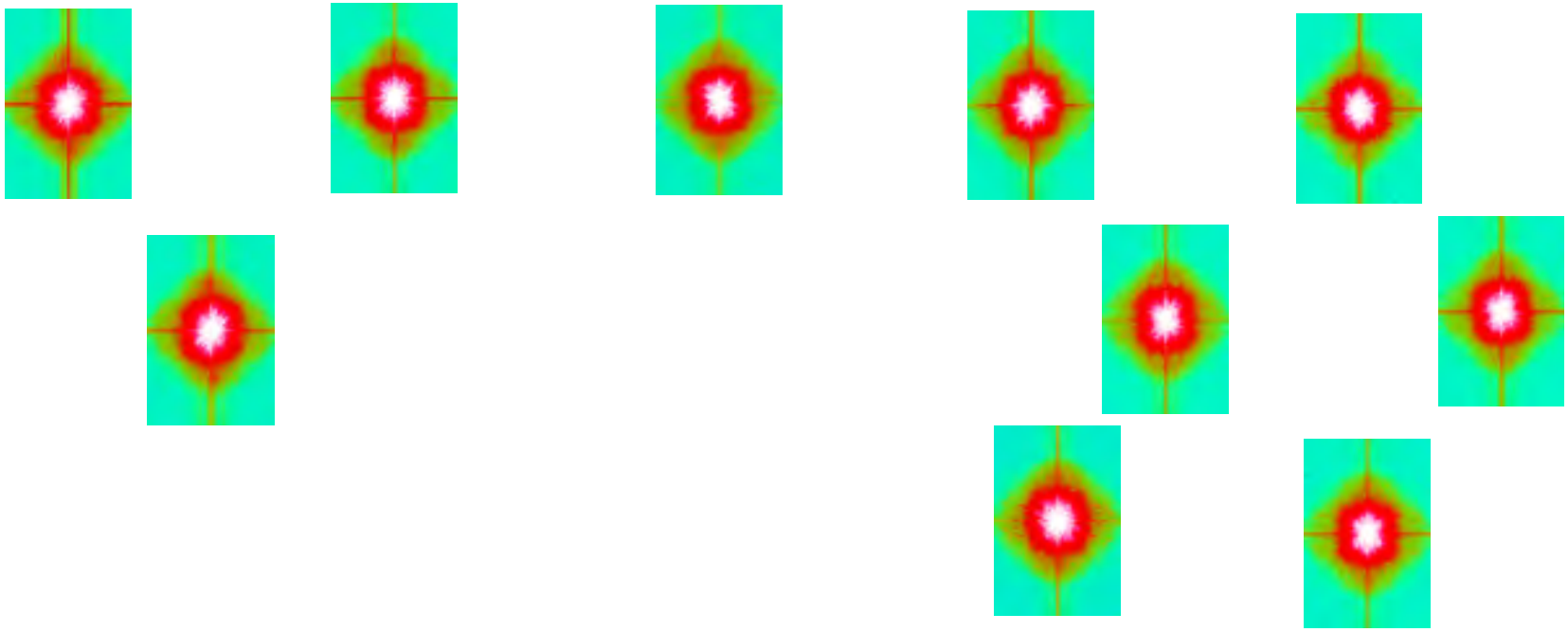

Supporting a model with data

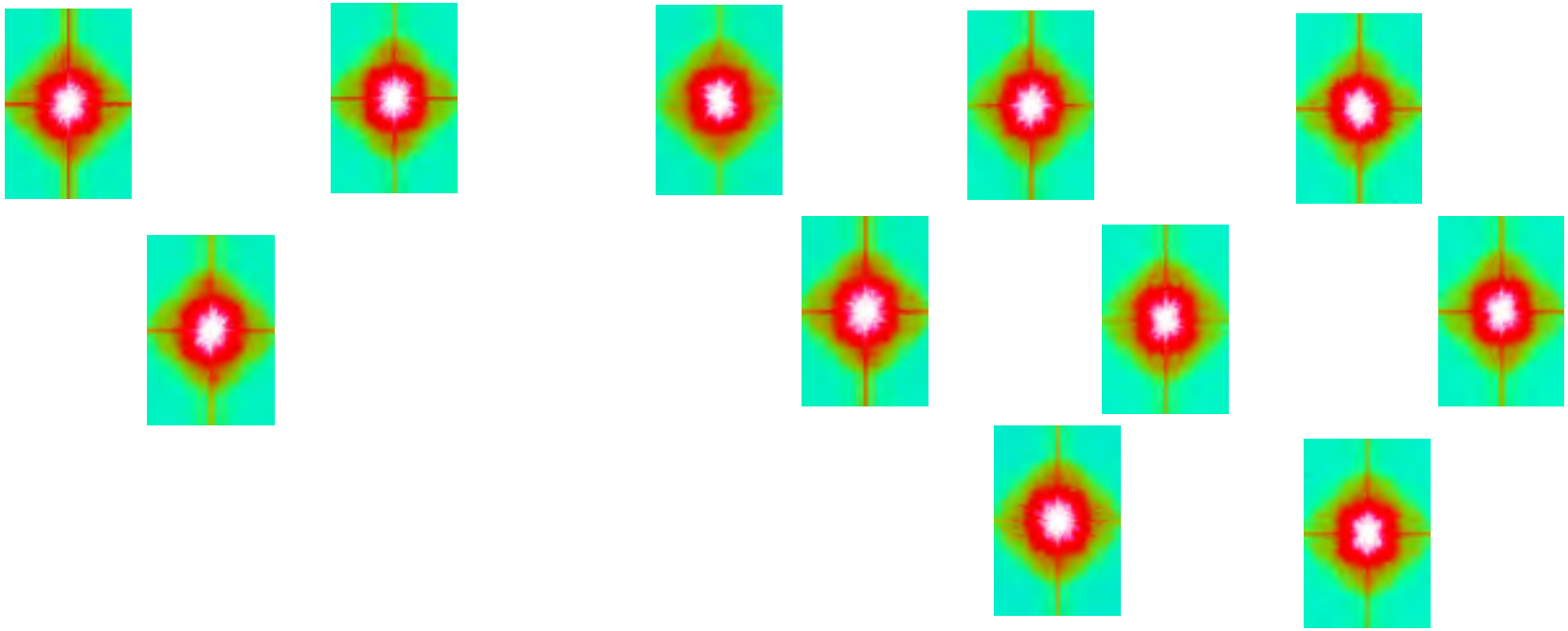

Supporting a model with data

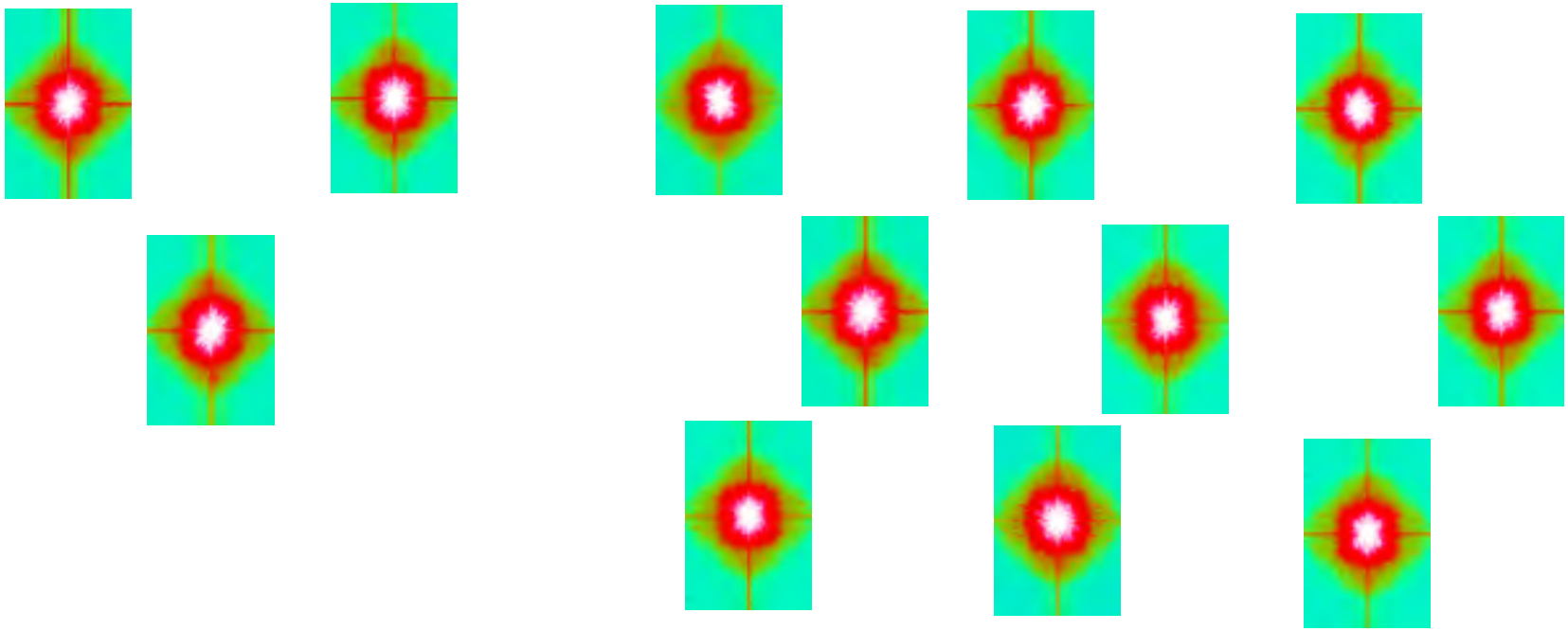

Supporting a model with data

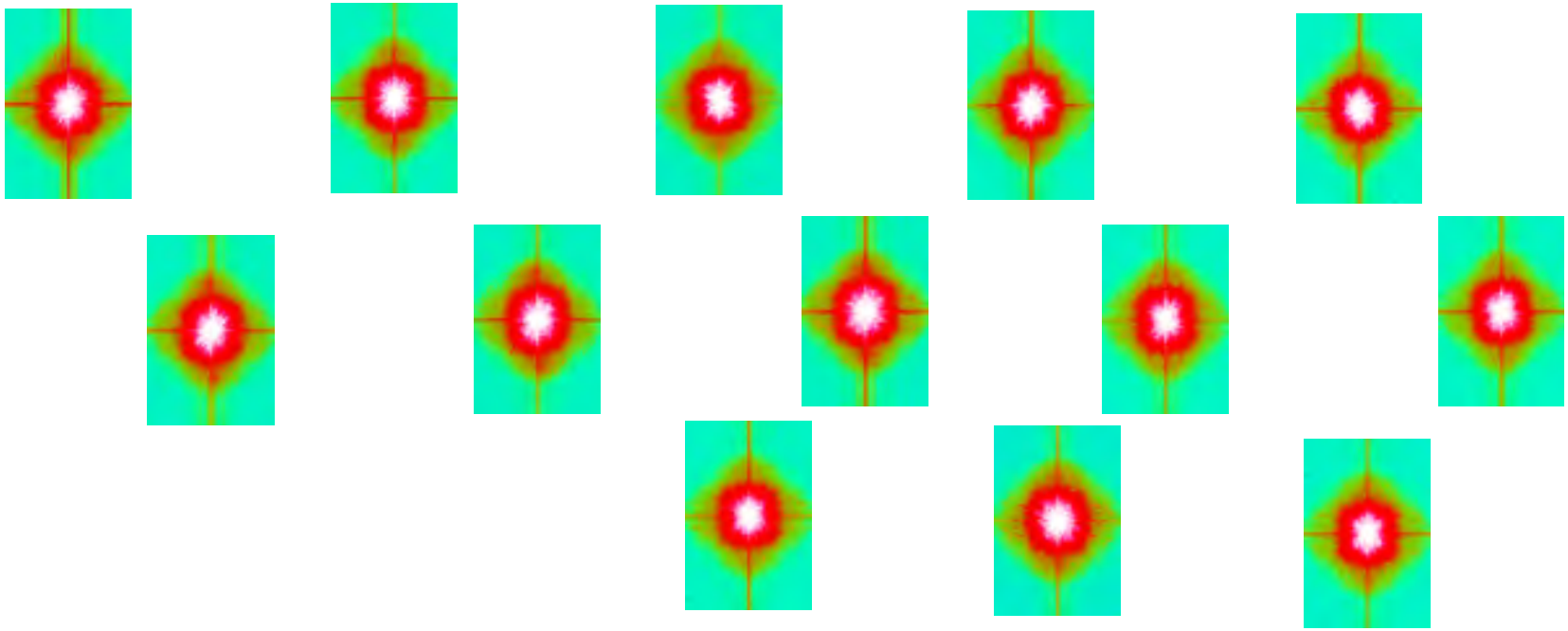

Supporting a model with data

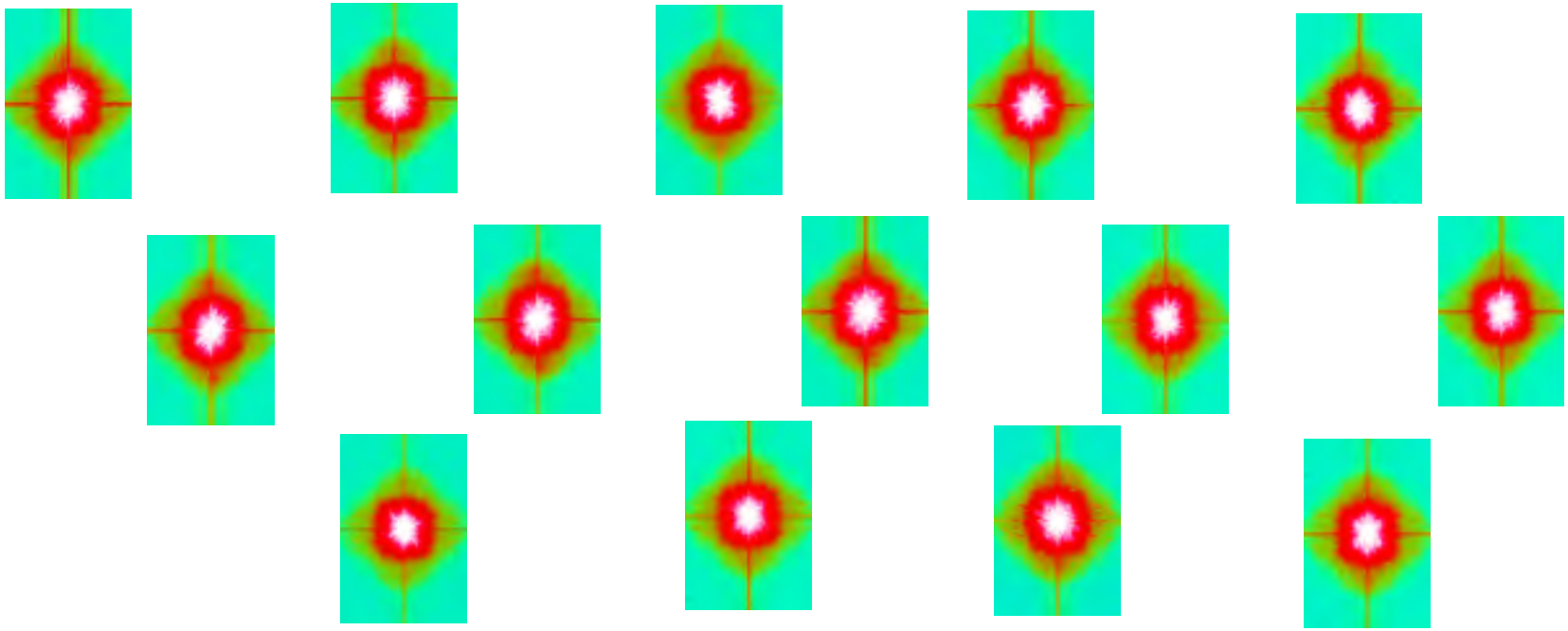

Supporting a model with data

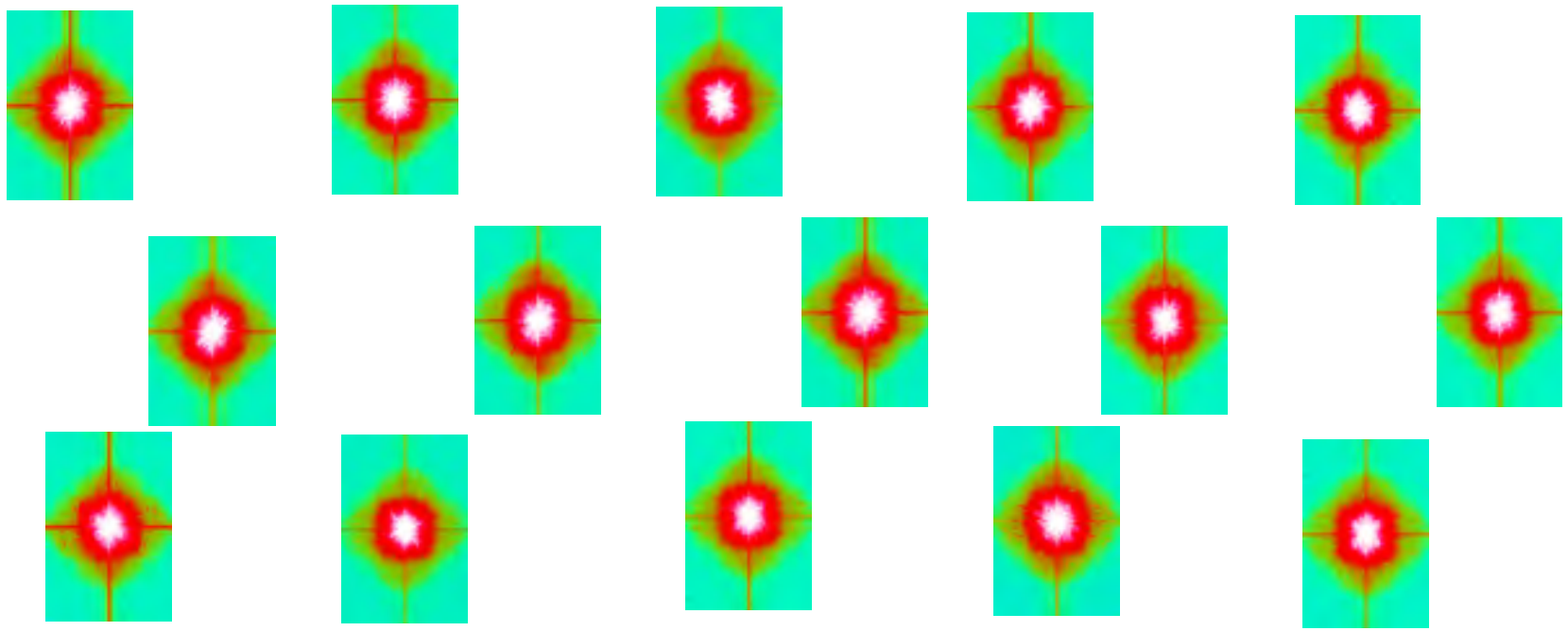

Supporting a model with data

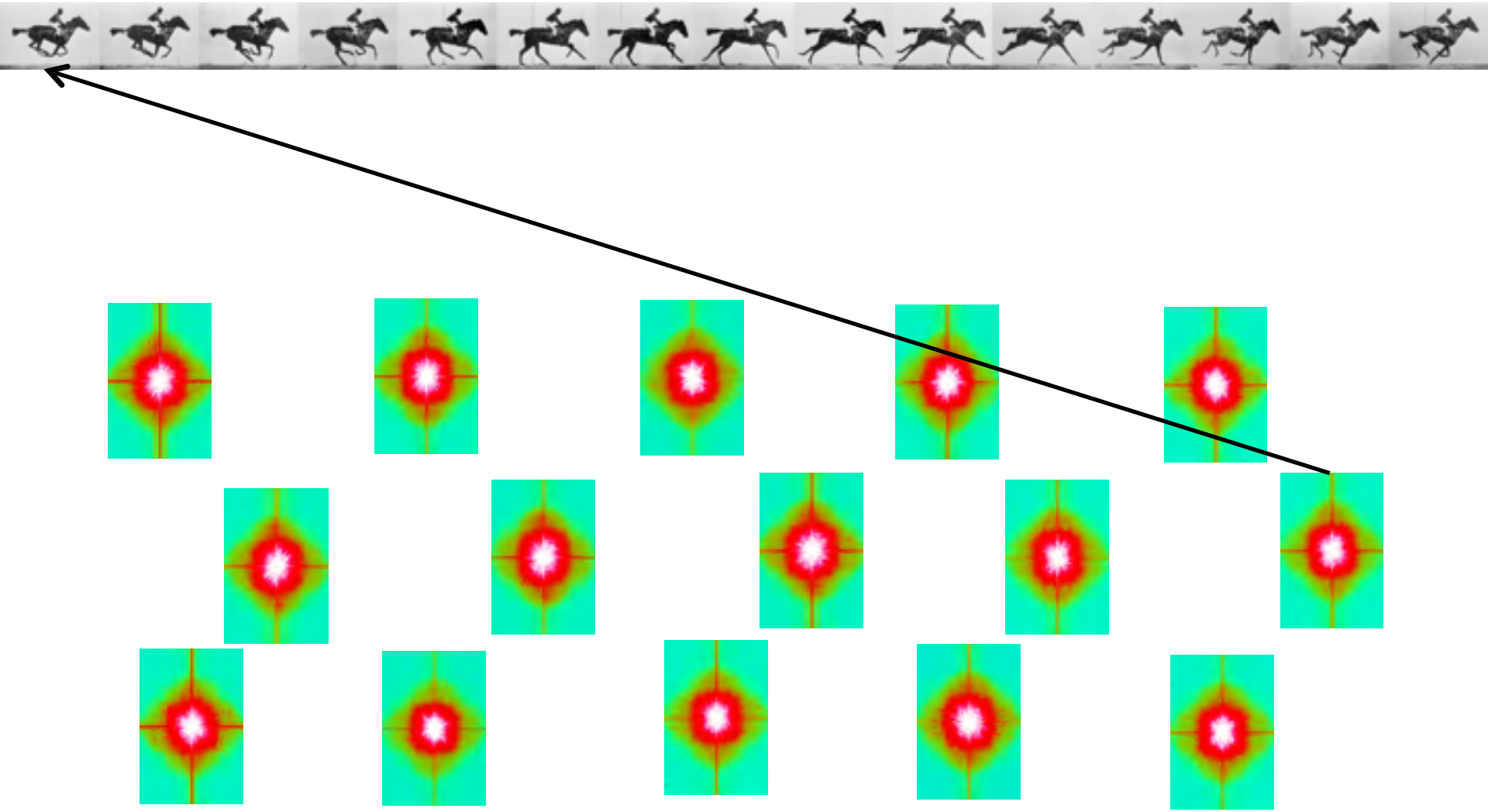

Supporting a model with data

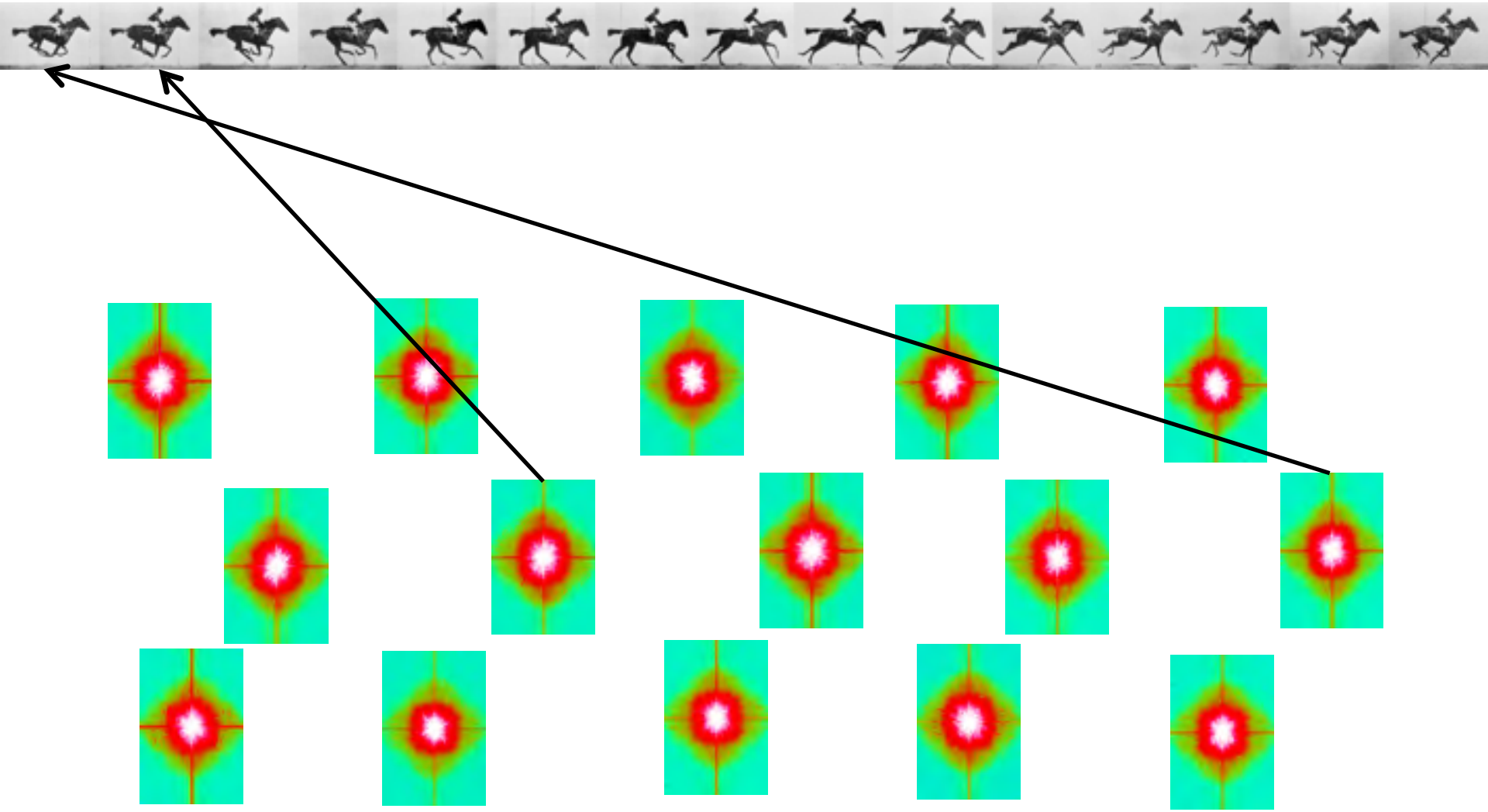

Supporting a model with data

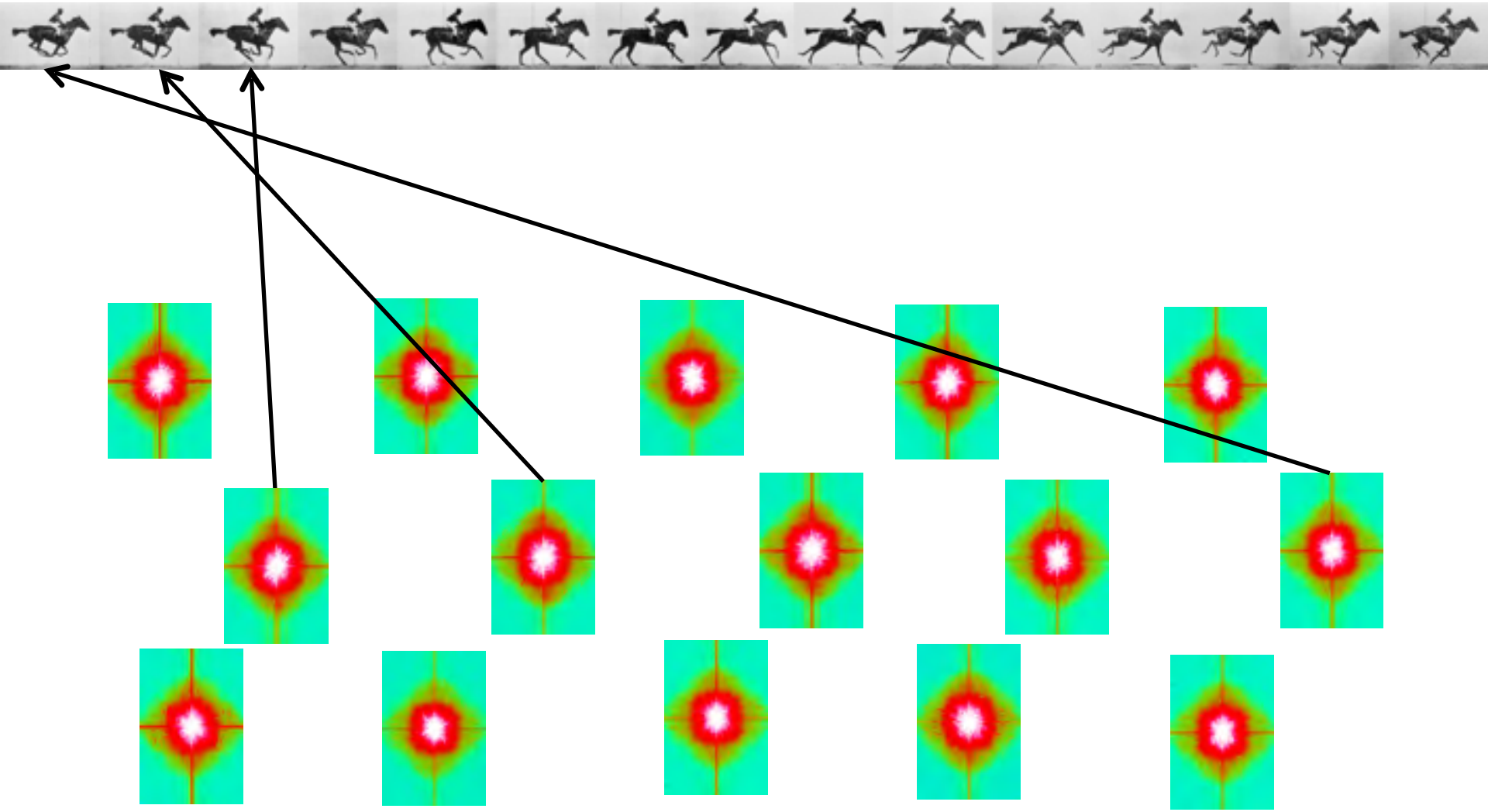

Supporting a model with data

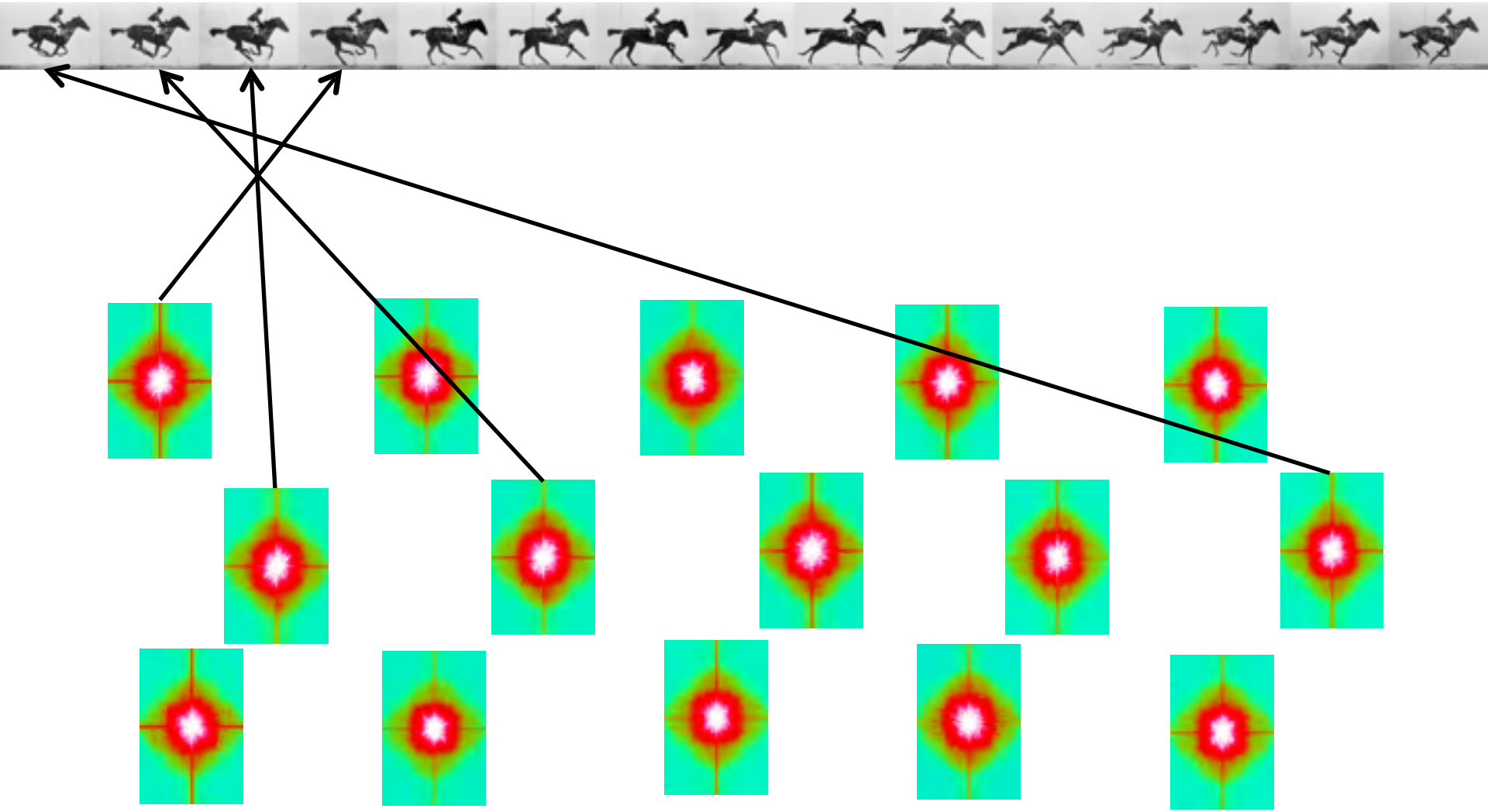

Supporting a model with data

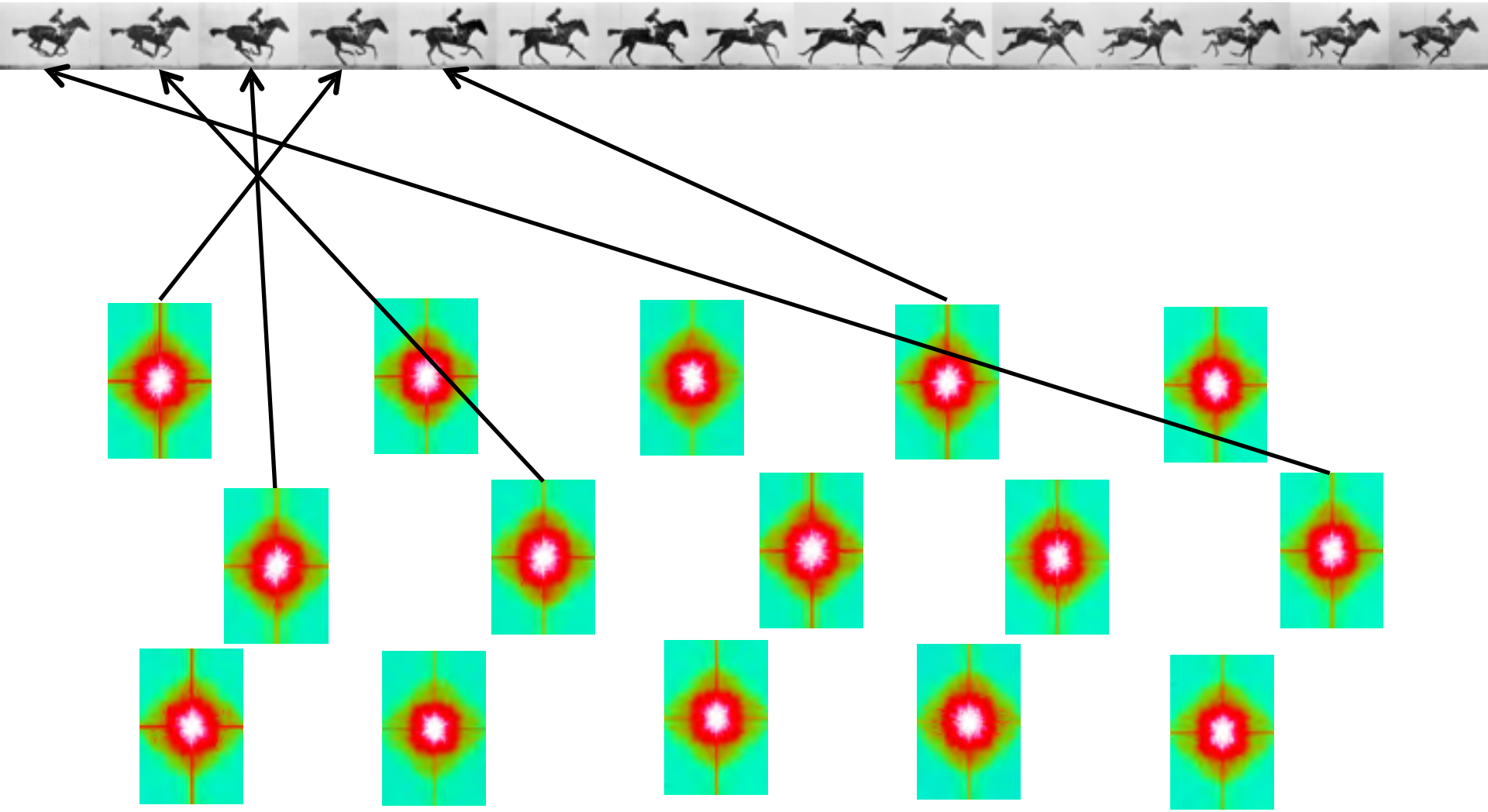

Supporting a model with data

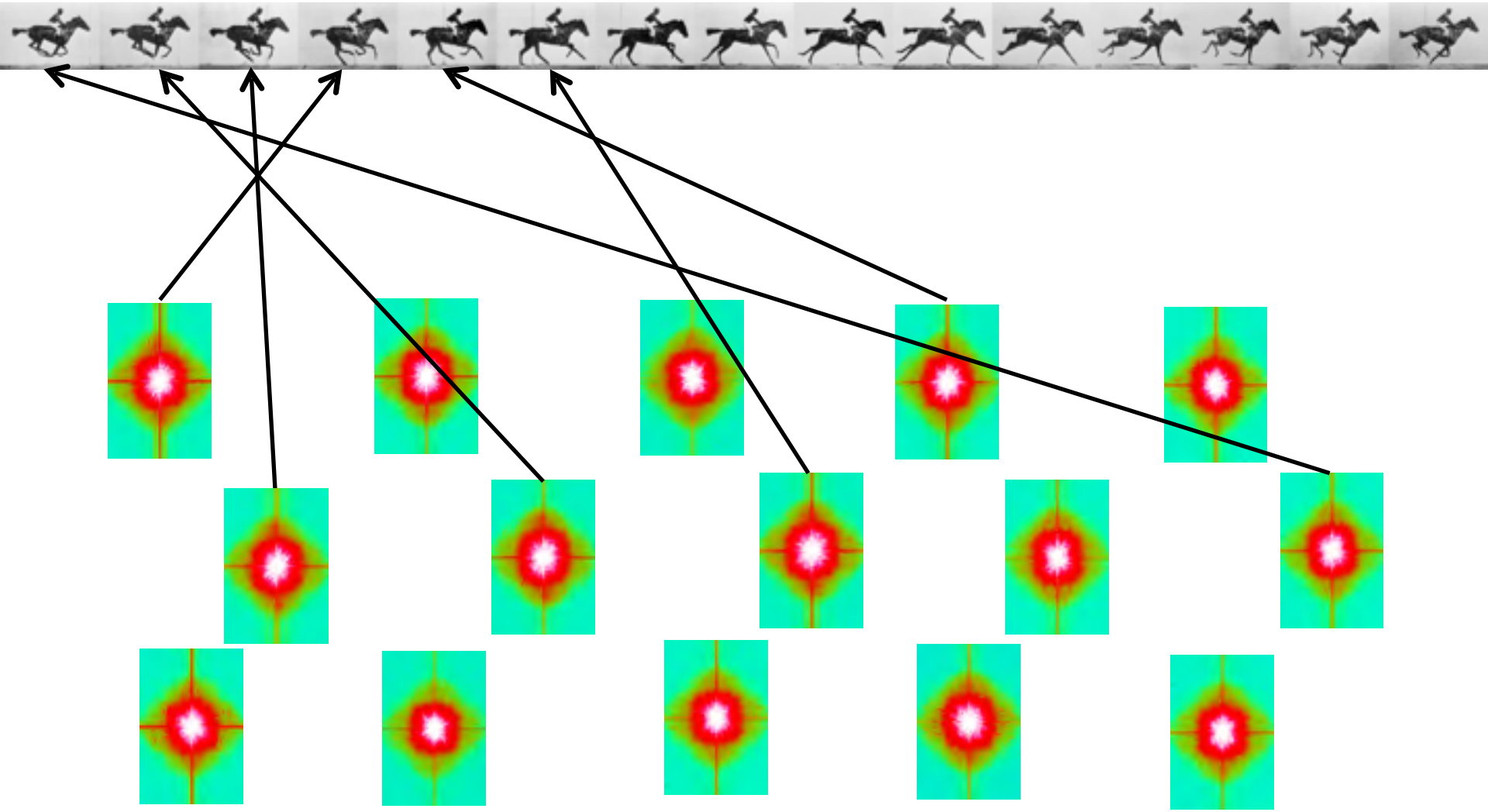

Supporting a model with data

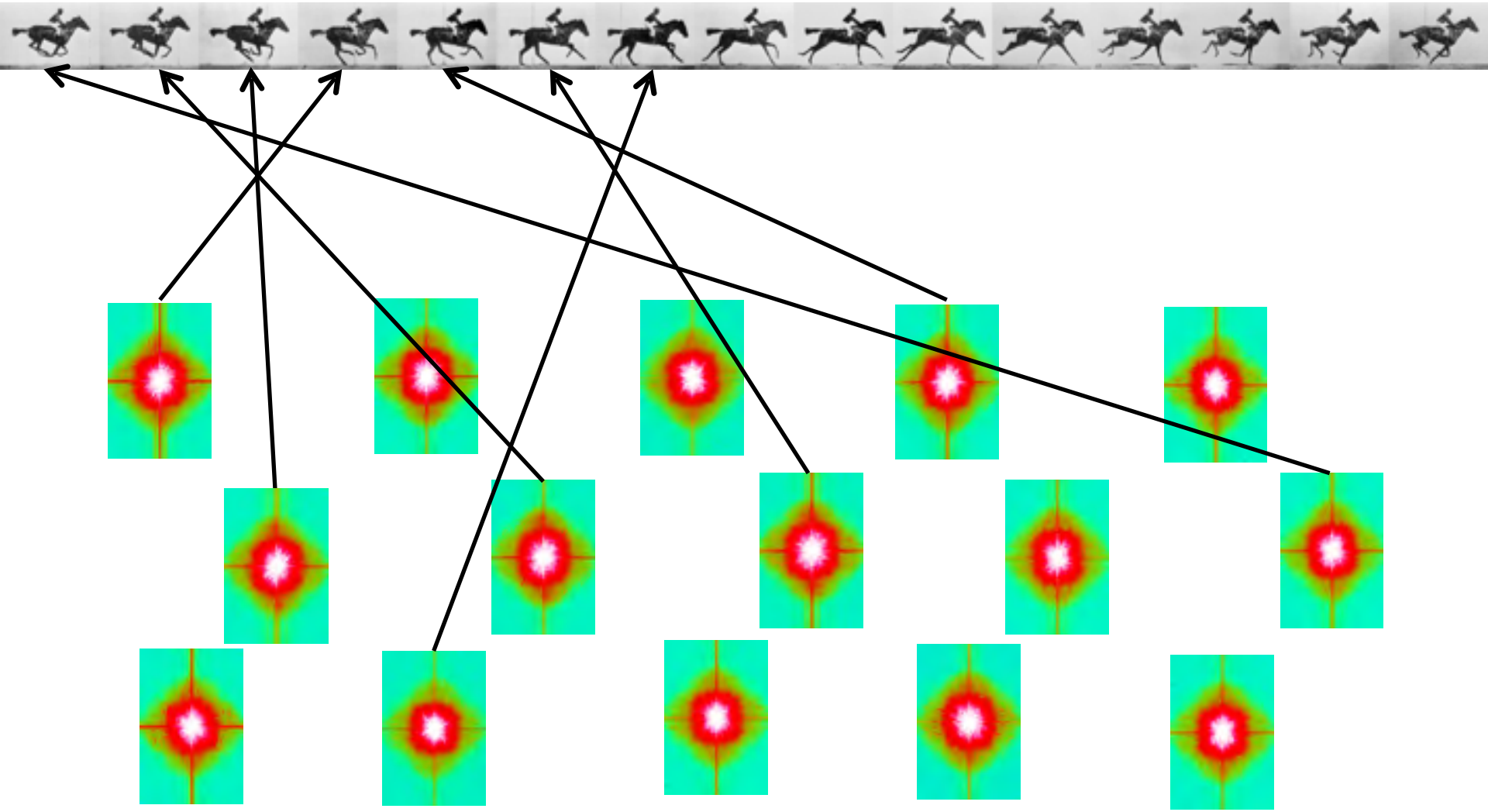

Supporting a model with data

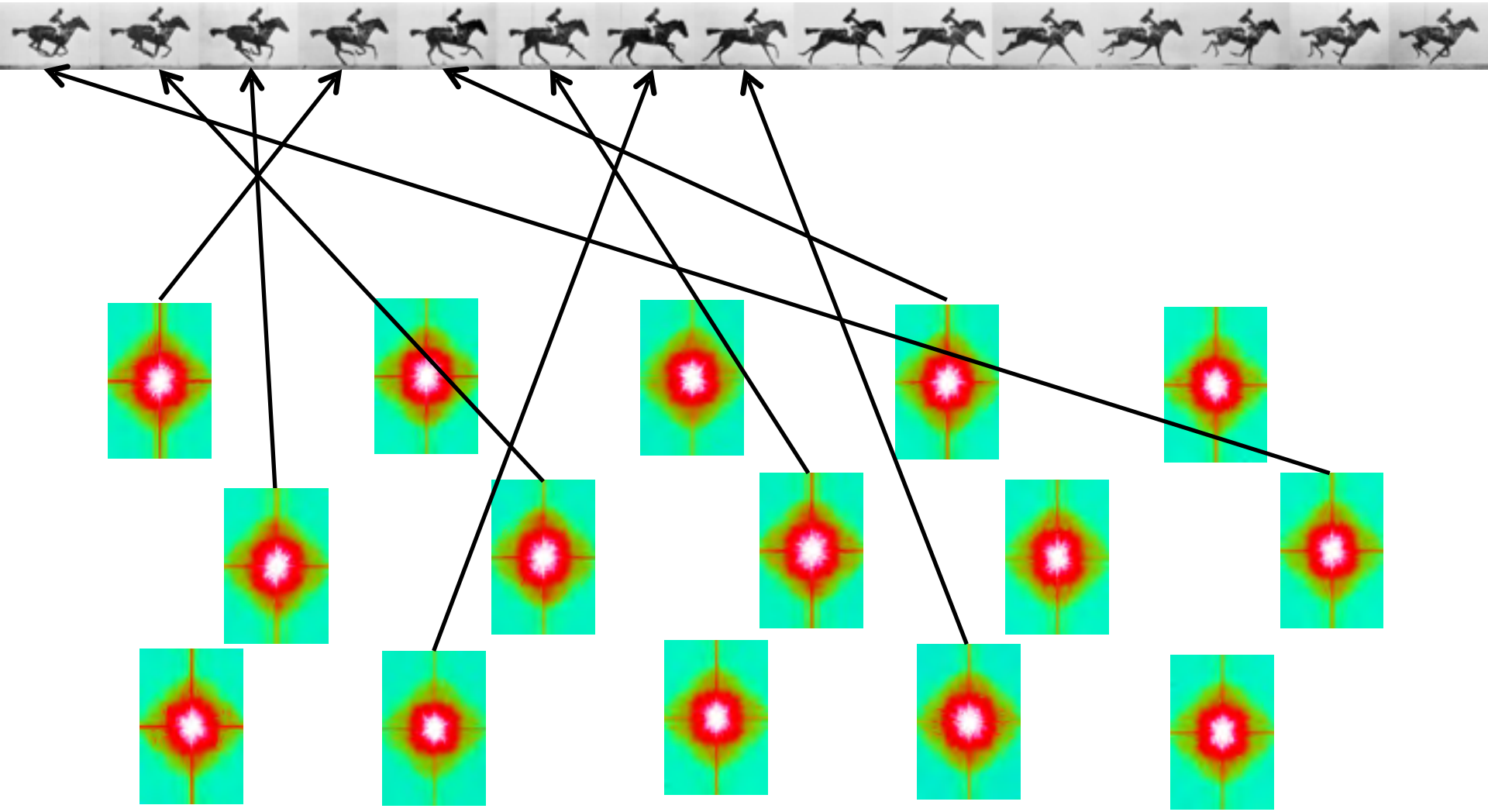

Supporting a model with data

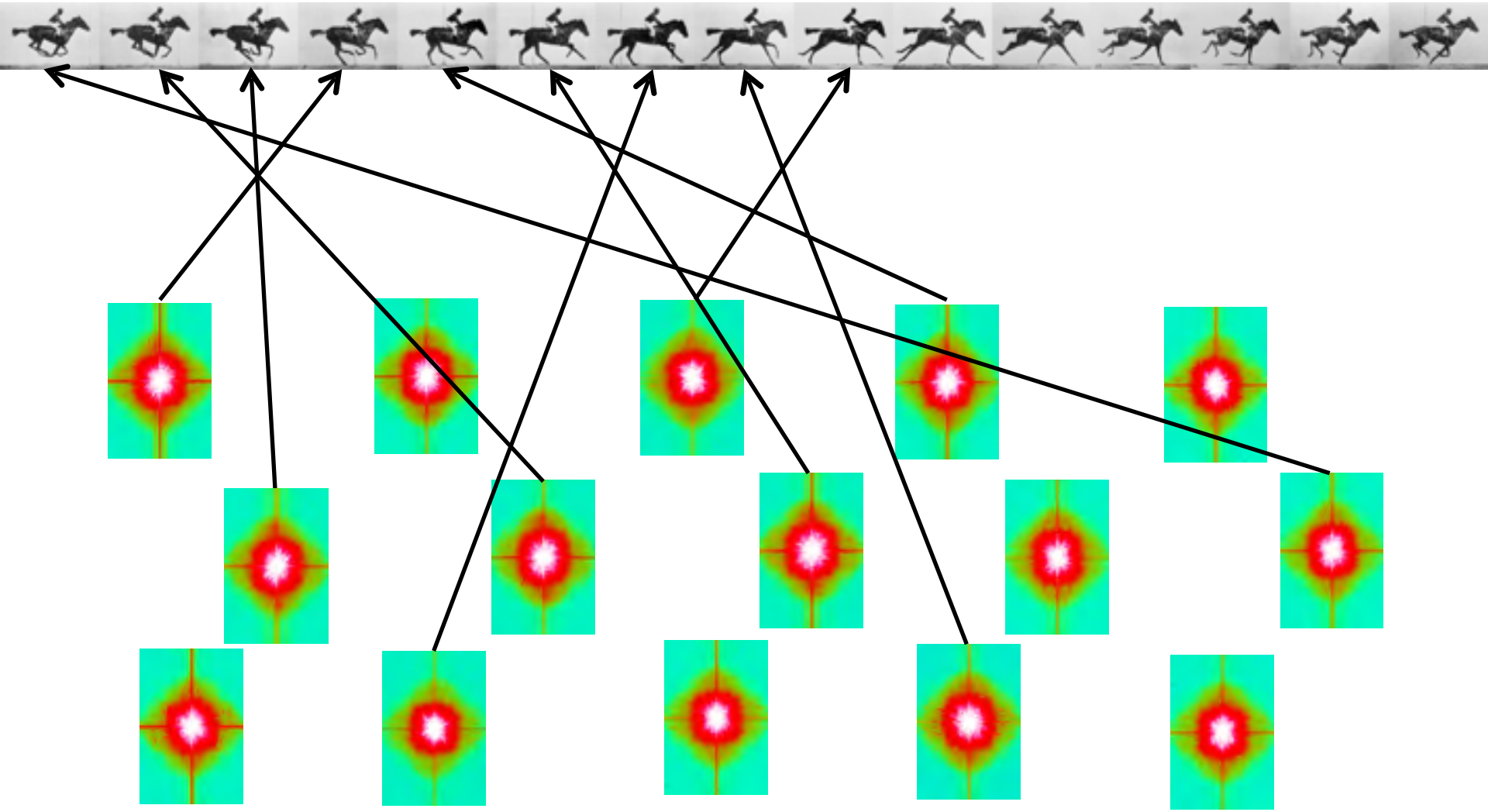

Supporting a model with data

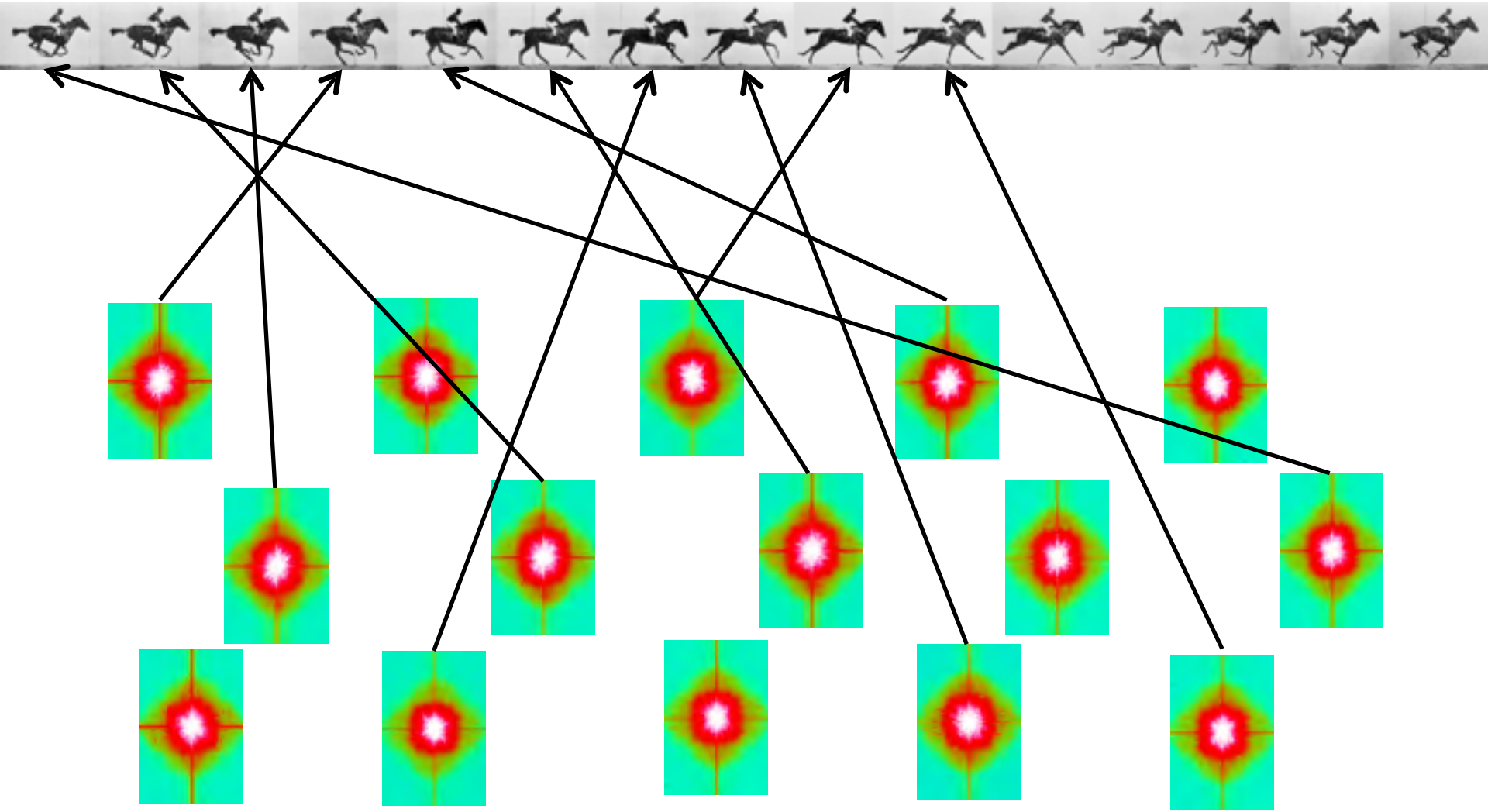

Supporting a model with data

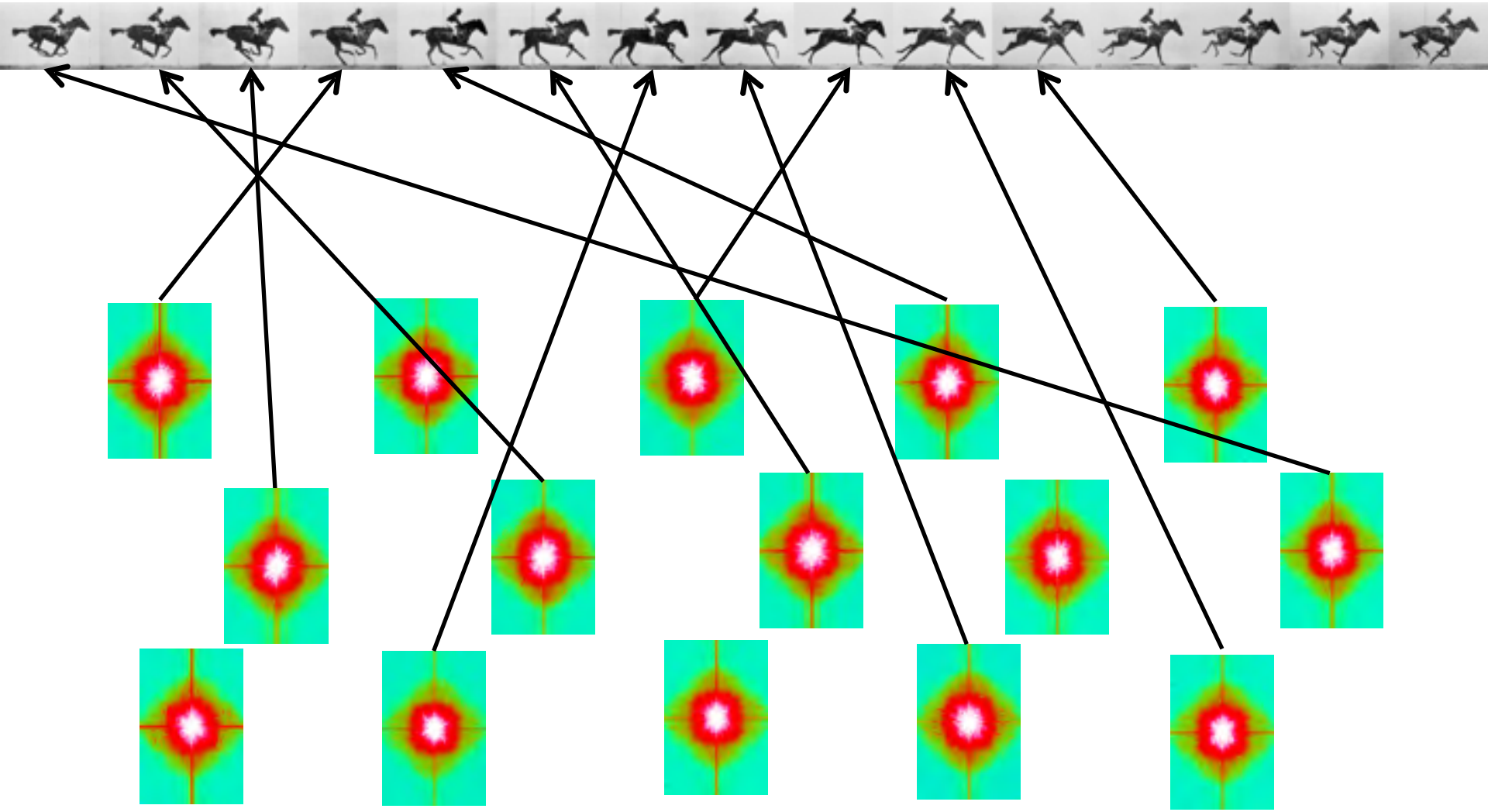

Supporting a model with data

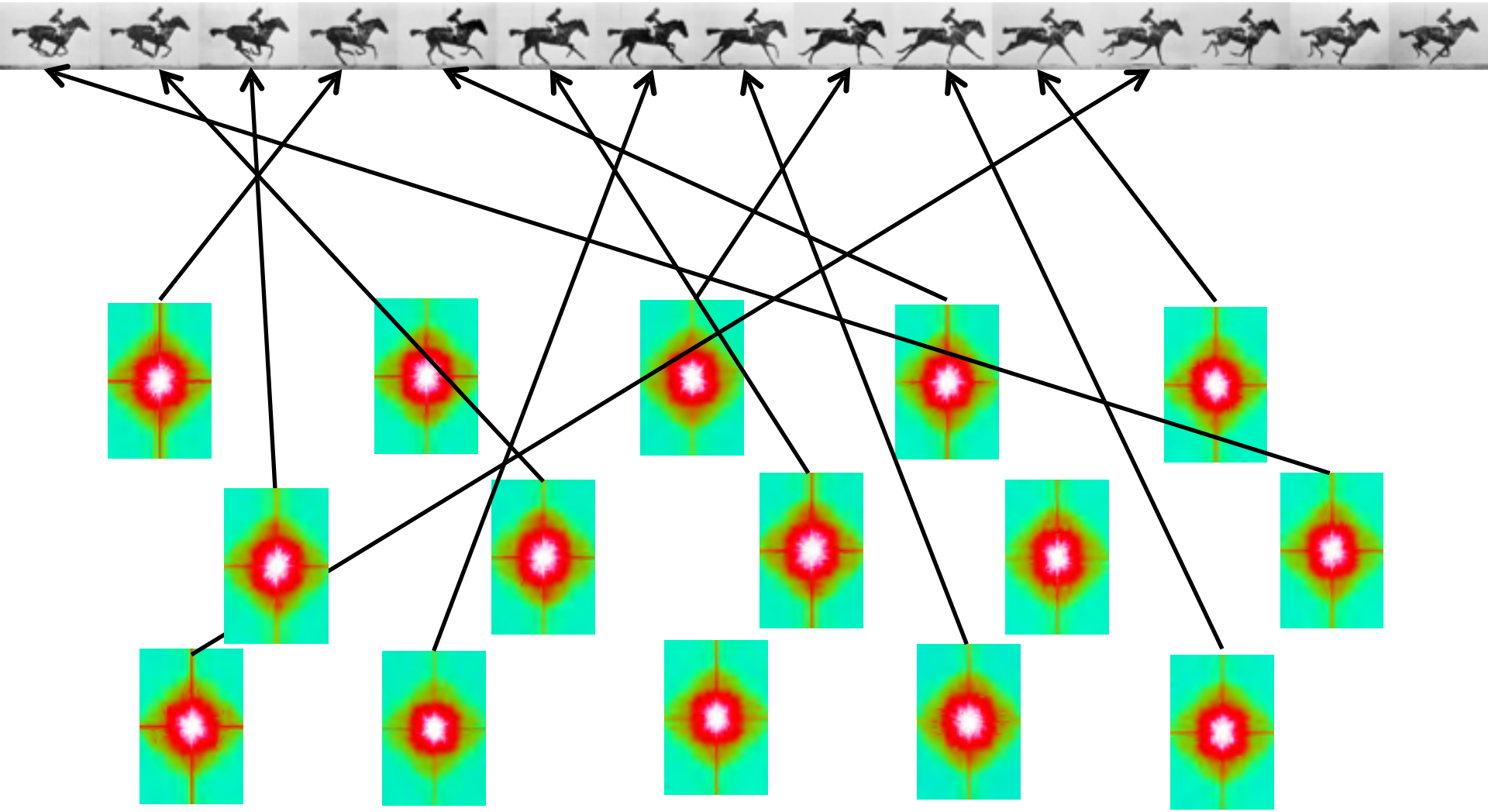

Supporting a model with data

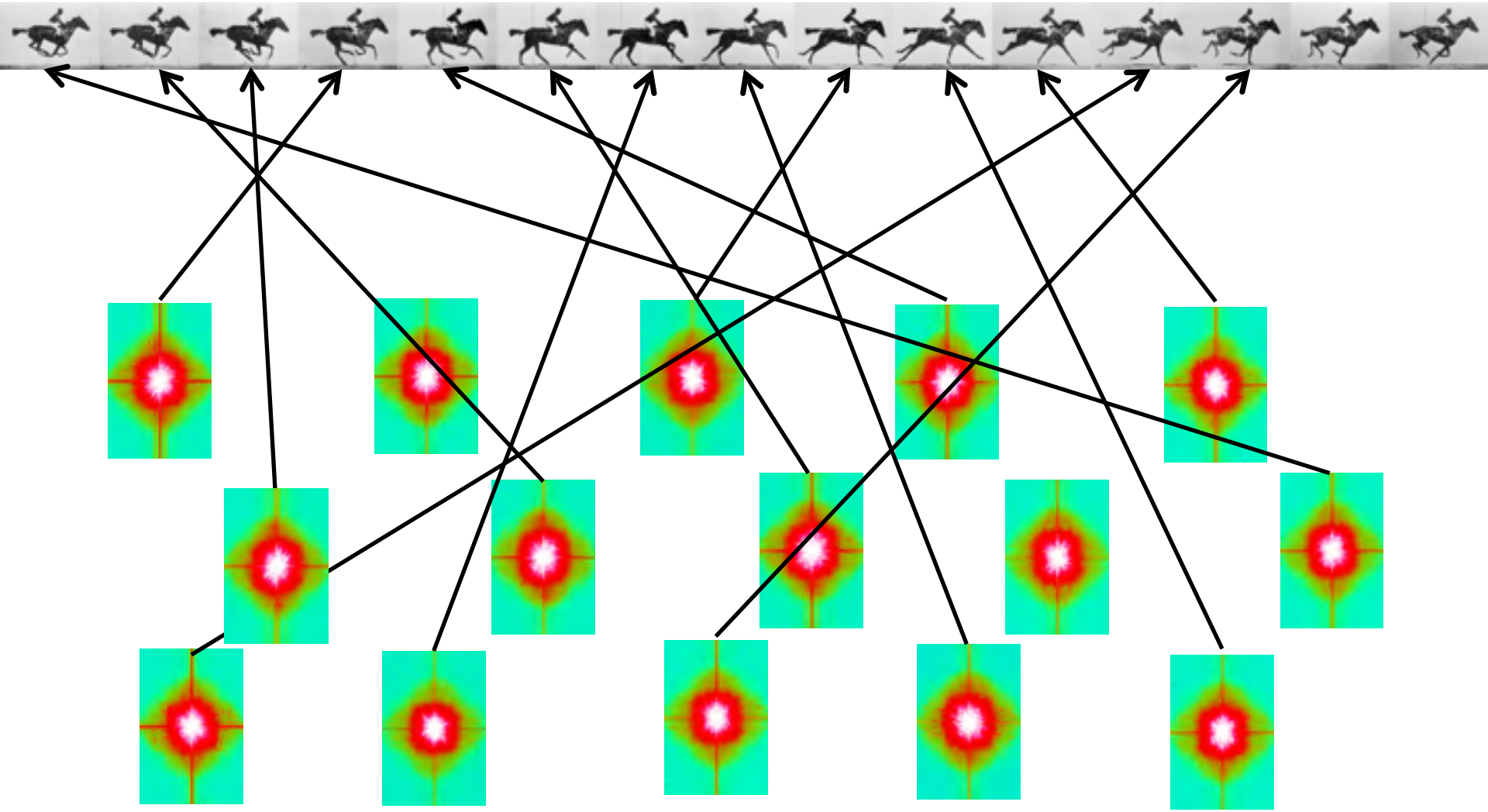

Supporting a model with data

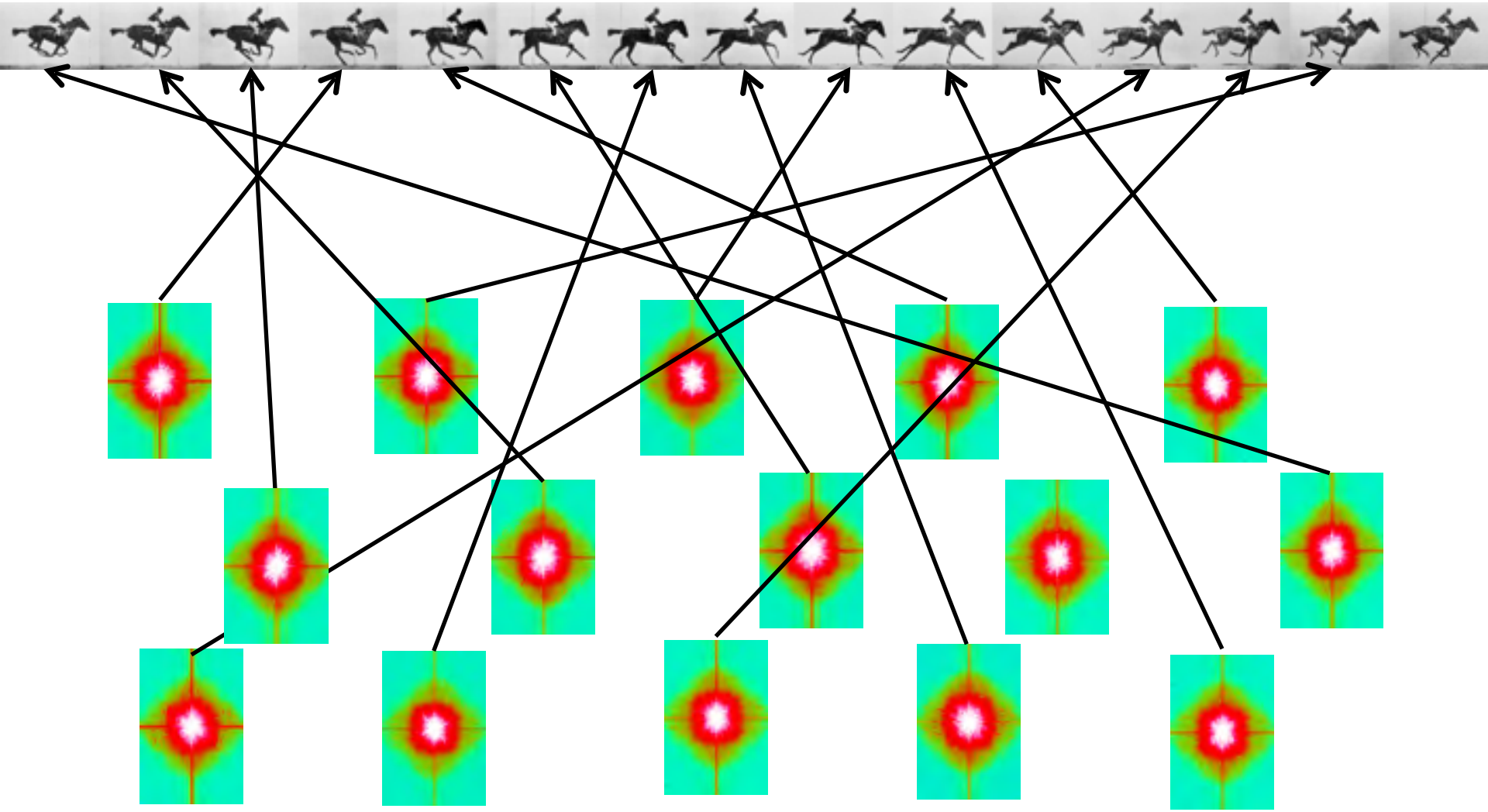

Supporting a model with data

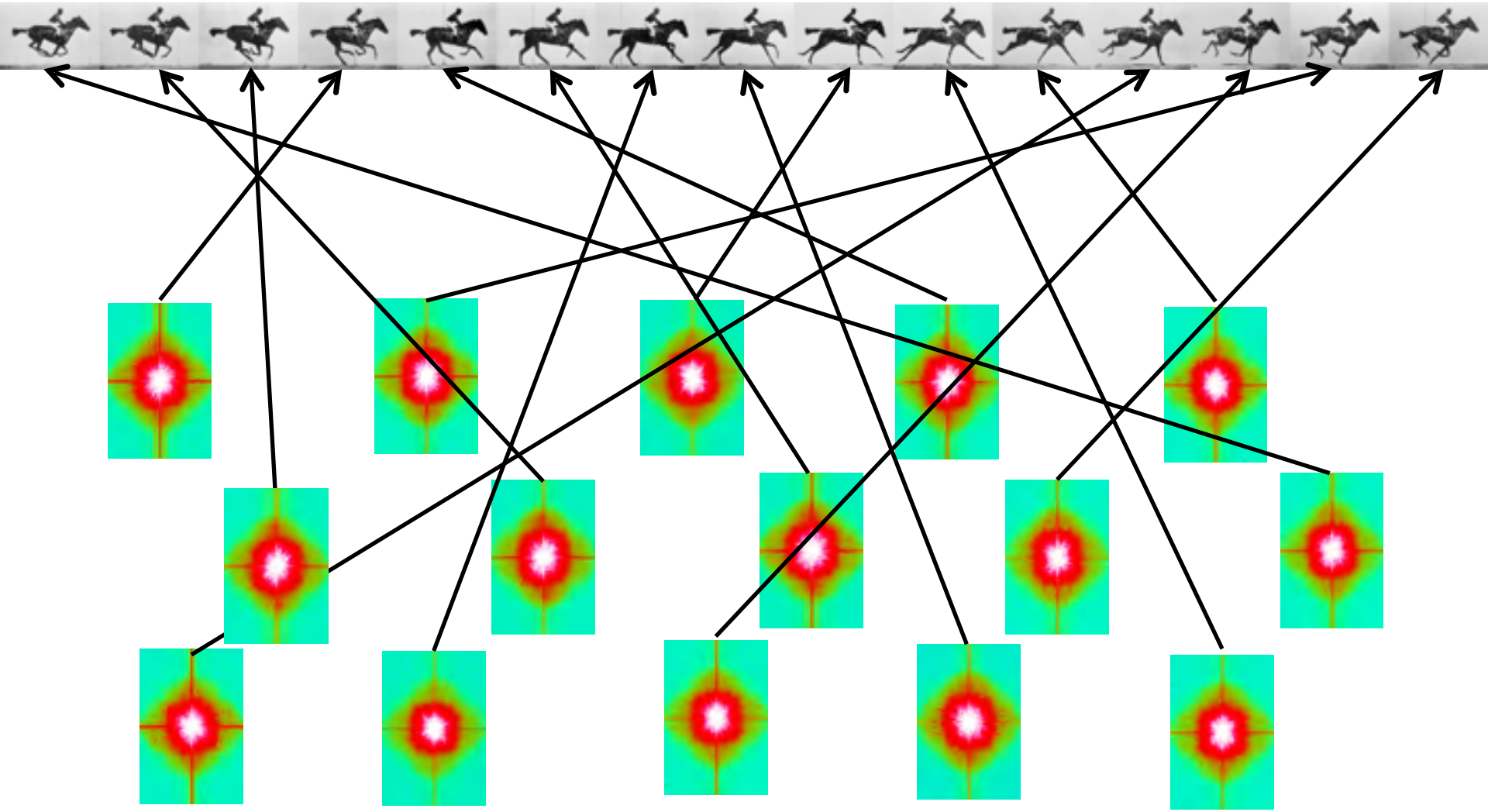

Molecular Dynamics Simulation

using **real**
crystal's lattice

1aho
Scorpion toxin

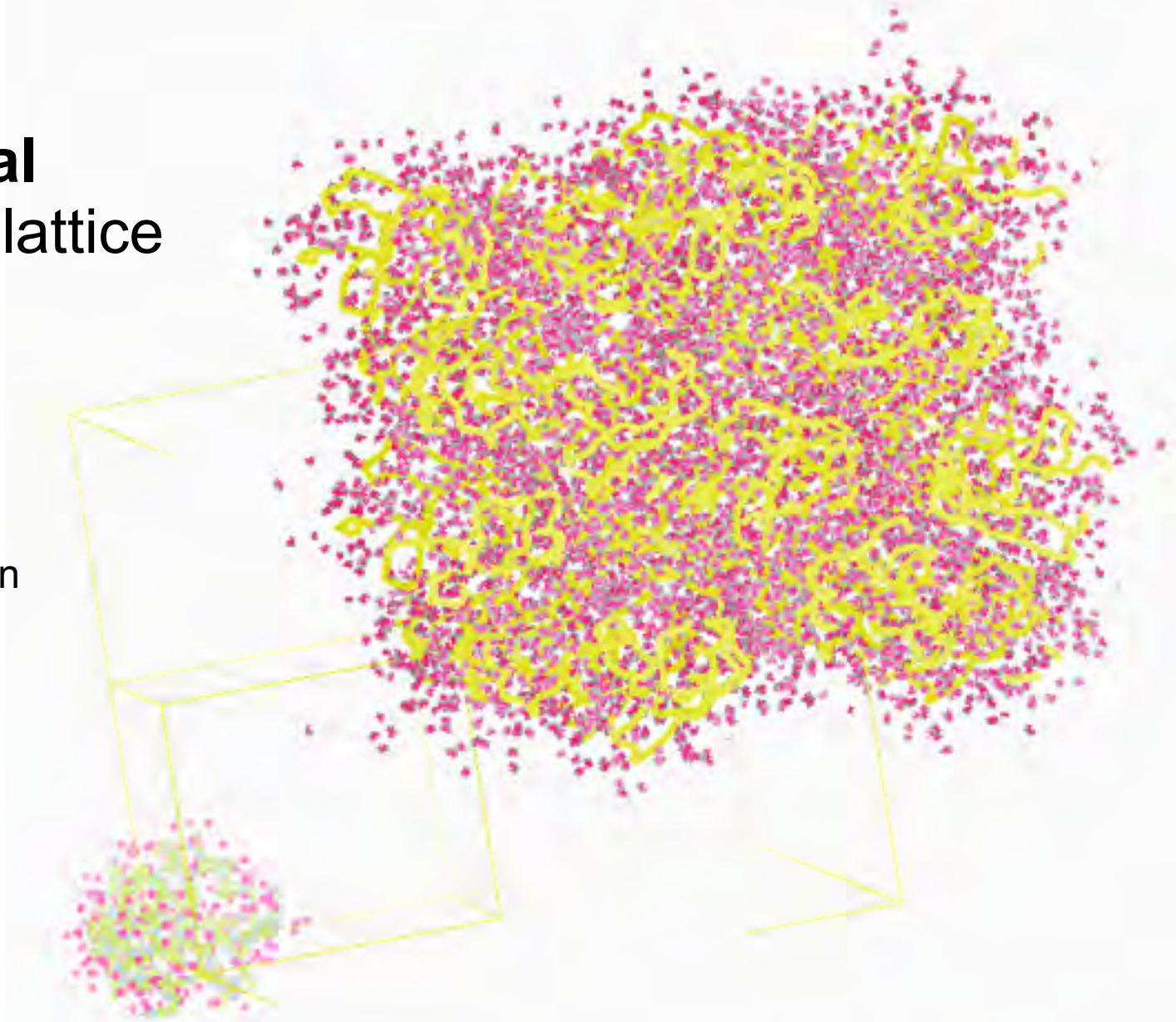

Cerutti *et al.* (2010).*J. Phys. Chem. B* **114**, 12811-12824.

Molecular Dynamics Simulation

using **real**
crystal's lattice

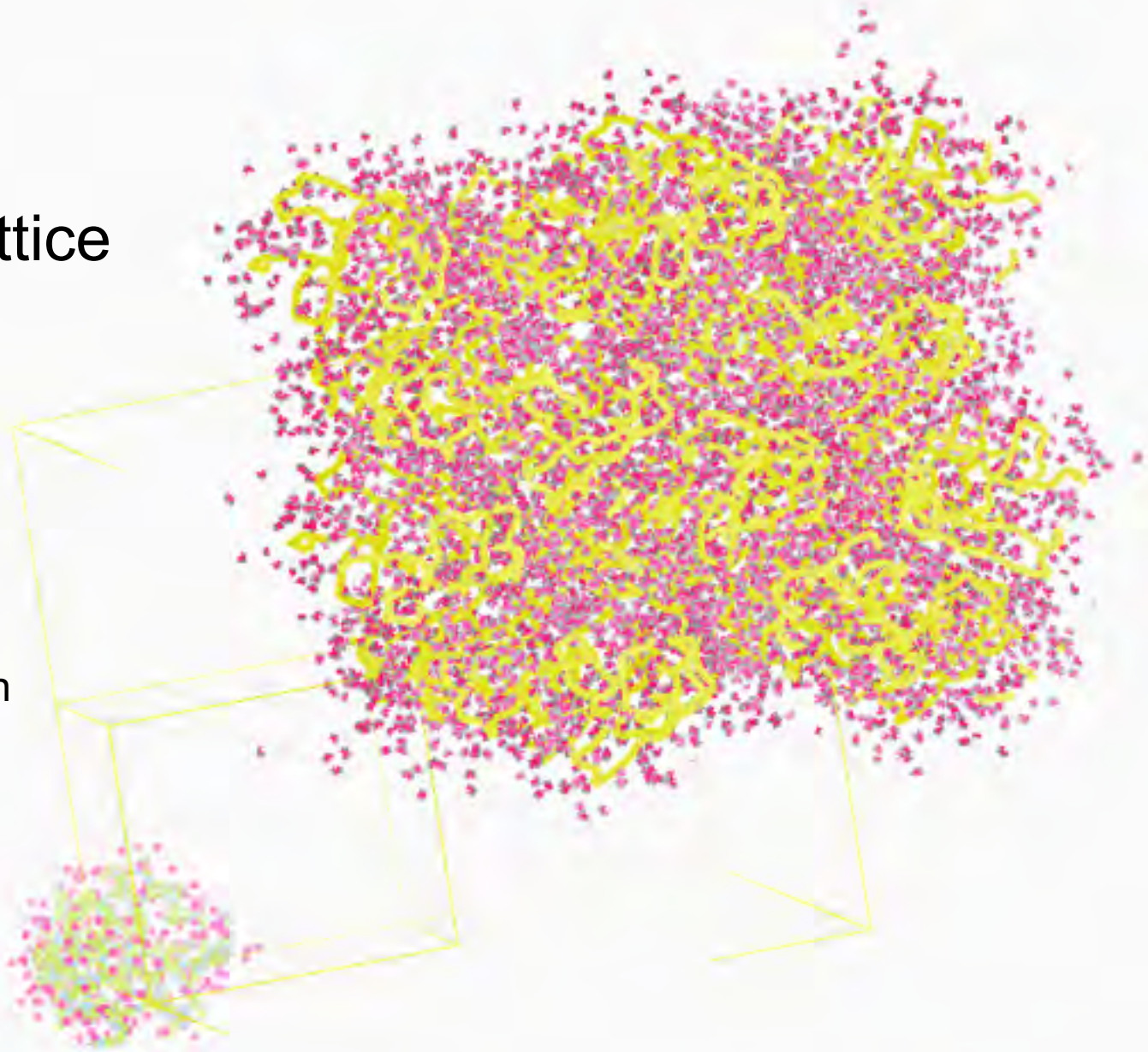

1aho
Scorpion toxin

0.96 Å resolution

Cerutti *et al.* (2010).*J. Phys. Chem. B* **114**, 12811-12824.

Molecular Dynamics Simulation

using **real**
crystal's lattice

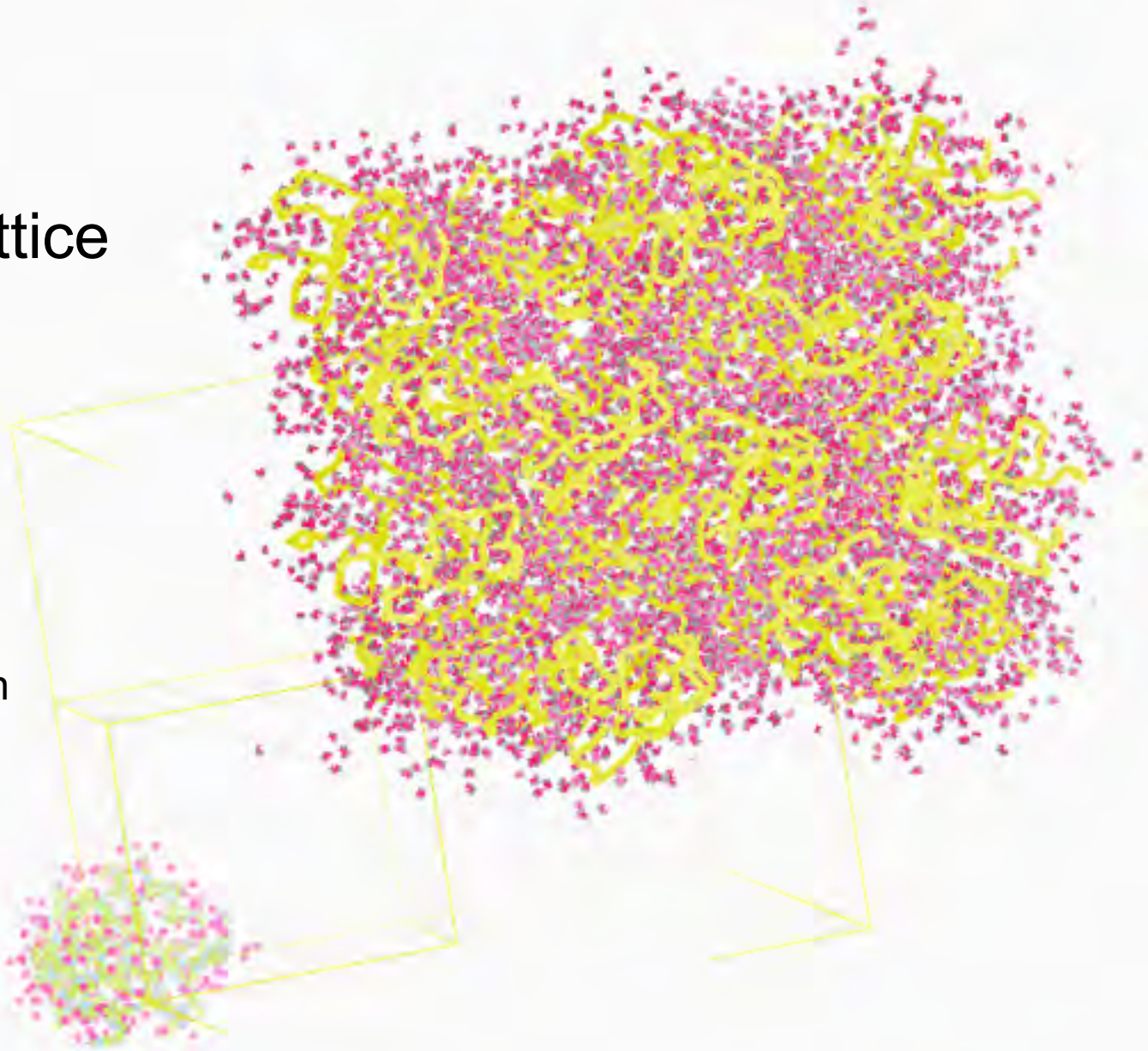

1aho
Scorpion toxin

0.96 Å resolution
64 residues

Cerutti *et al.* (2010).*J. Phys. Chem. B* **114**, 12811-12824.

Molecular Dynamics Simulation

using **real**
crystal's lattice

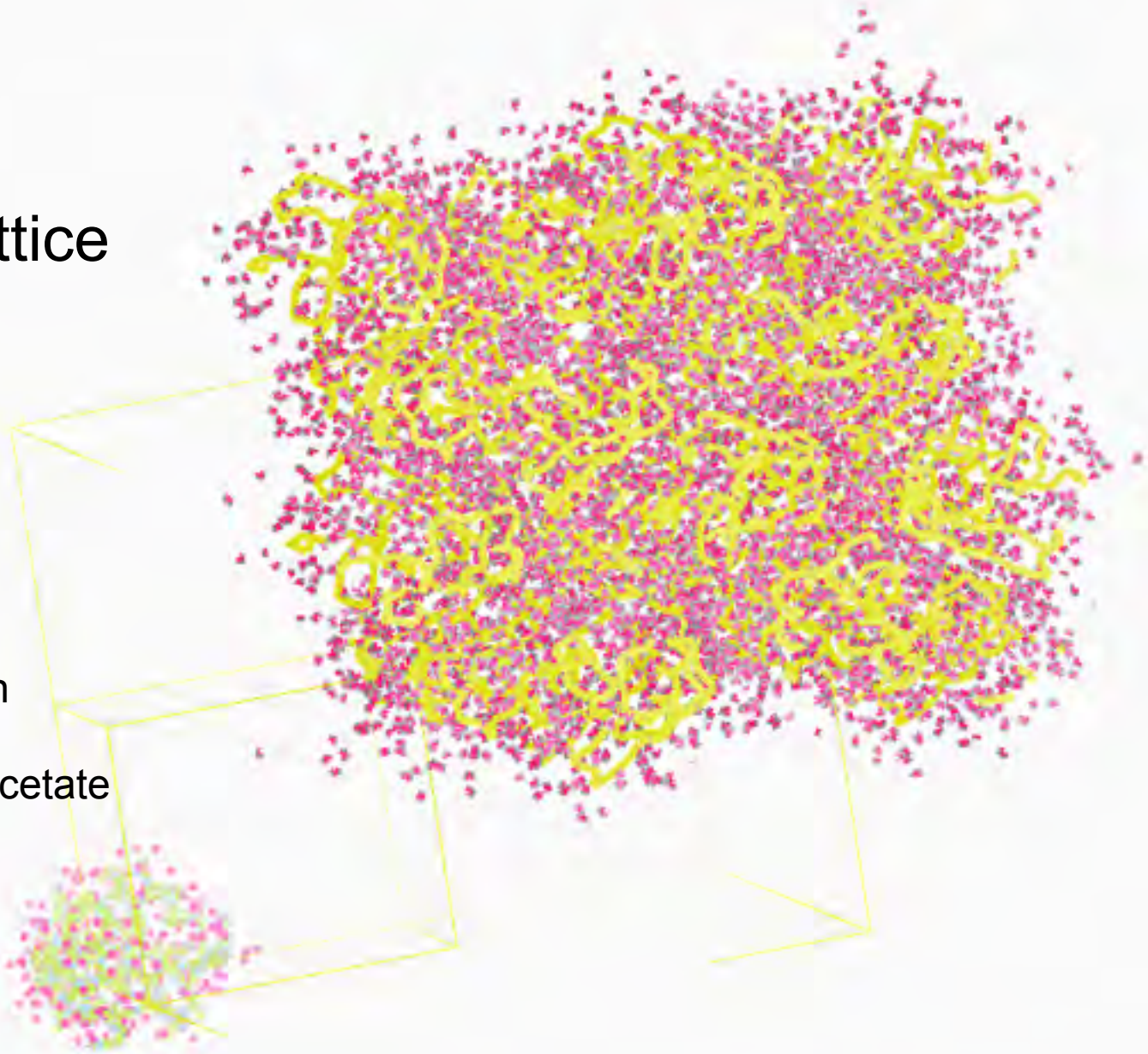

1aho
Scorpion toxin

0.96 Å resolution
64 residues
Solvent: H_20 + acetate

Cerutti *et al.* (2010).*J. Phys. Chem. B* **114**, 12811-12824.

30 conformers from 24,000

Electron density from 24,000 conformers

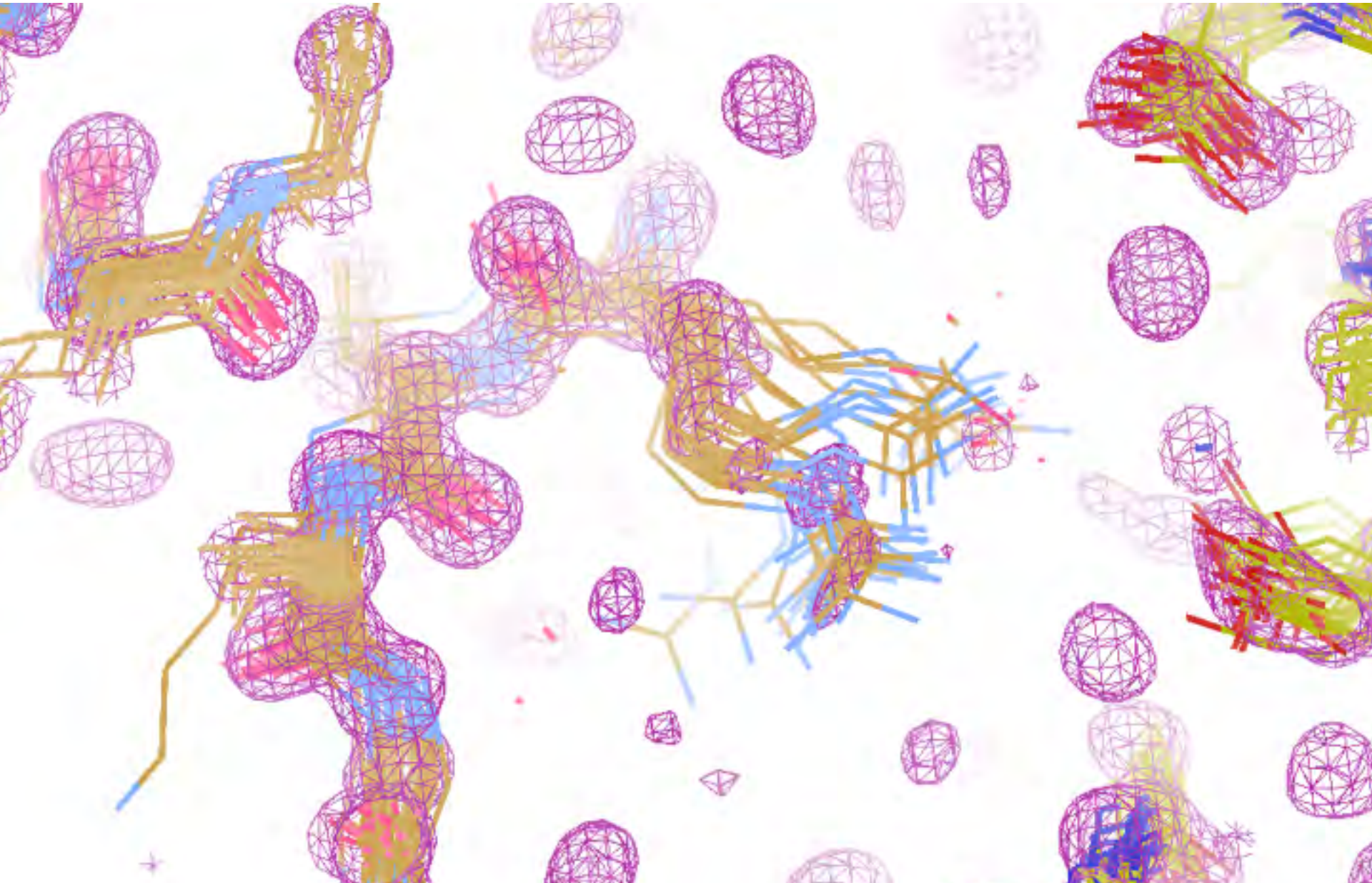

Electron density from 24,000 conformers

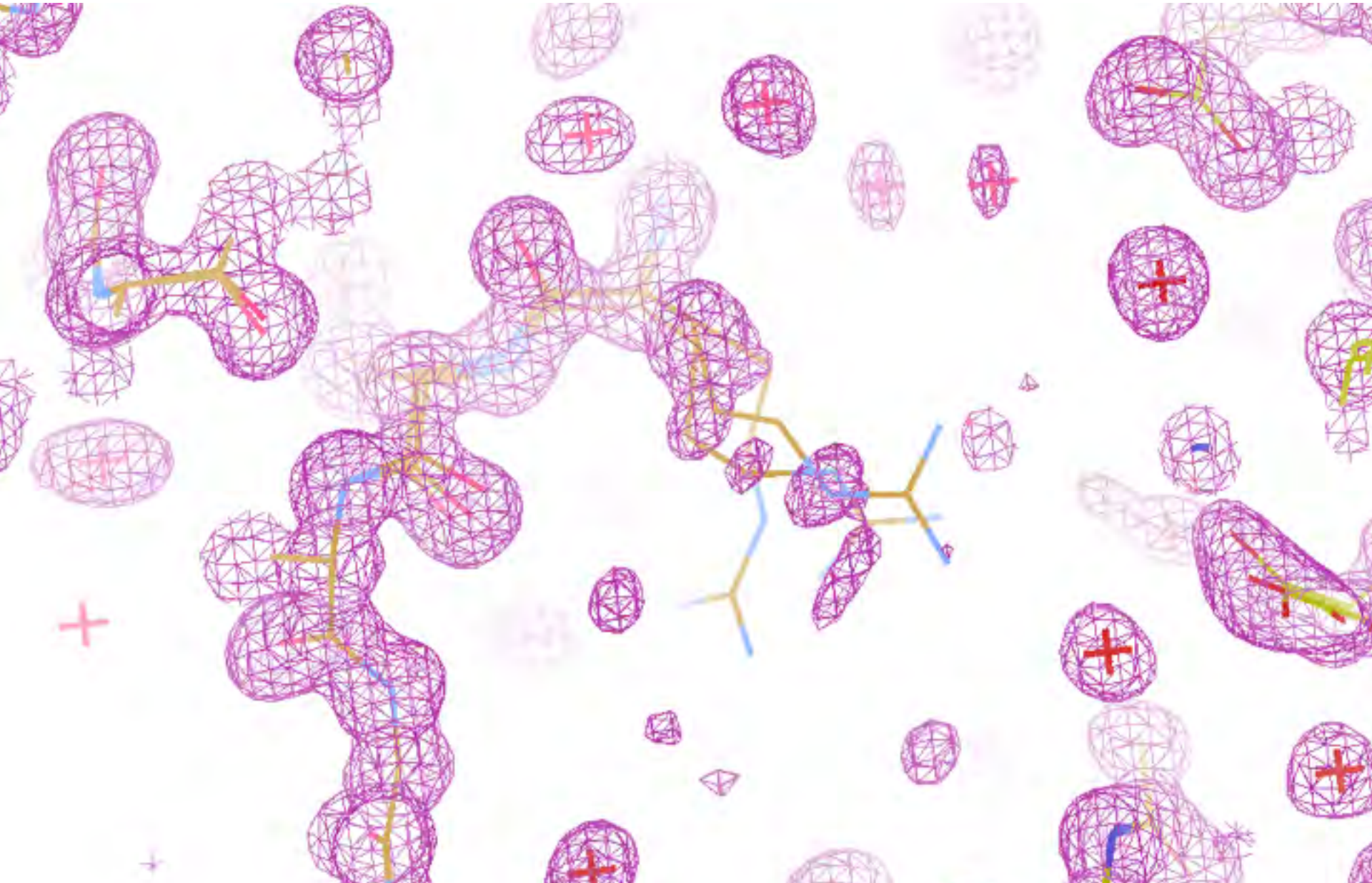

$2F_{sim}$-F_{calc} and F_{sim}-F_{calc} maps

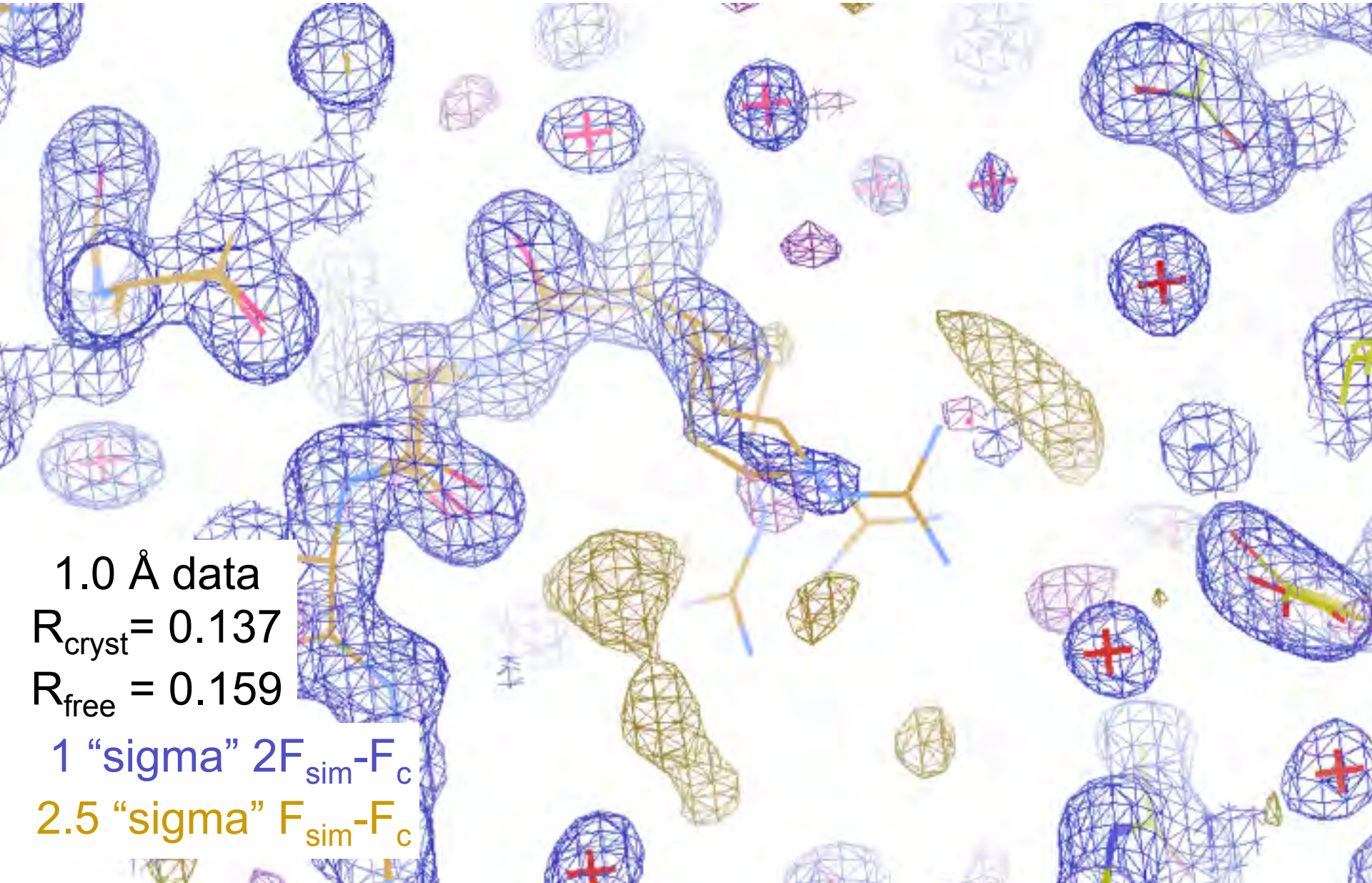

$2F_{sim}$-F_{calc} and (F_{sim} Φ_{sim}) - (F_{calc} Φ_{calc}) maps

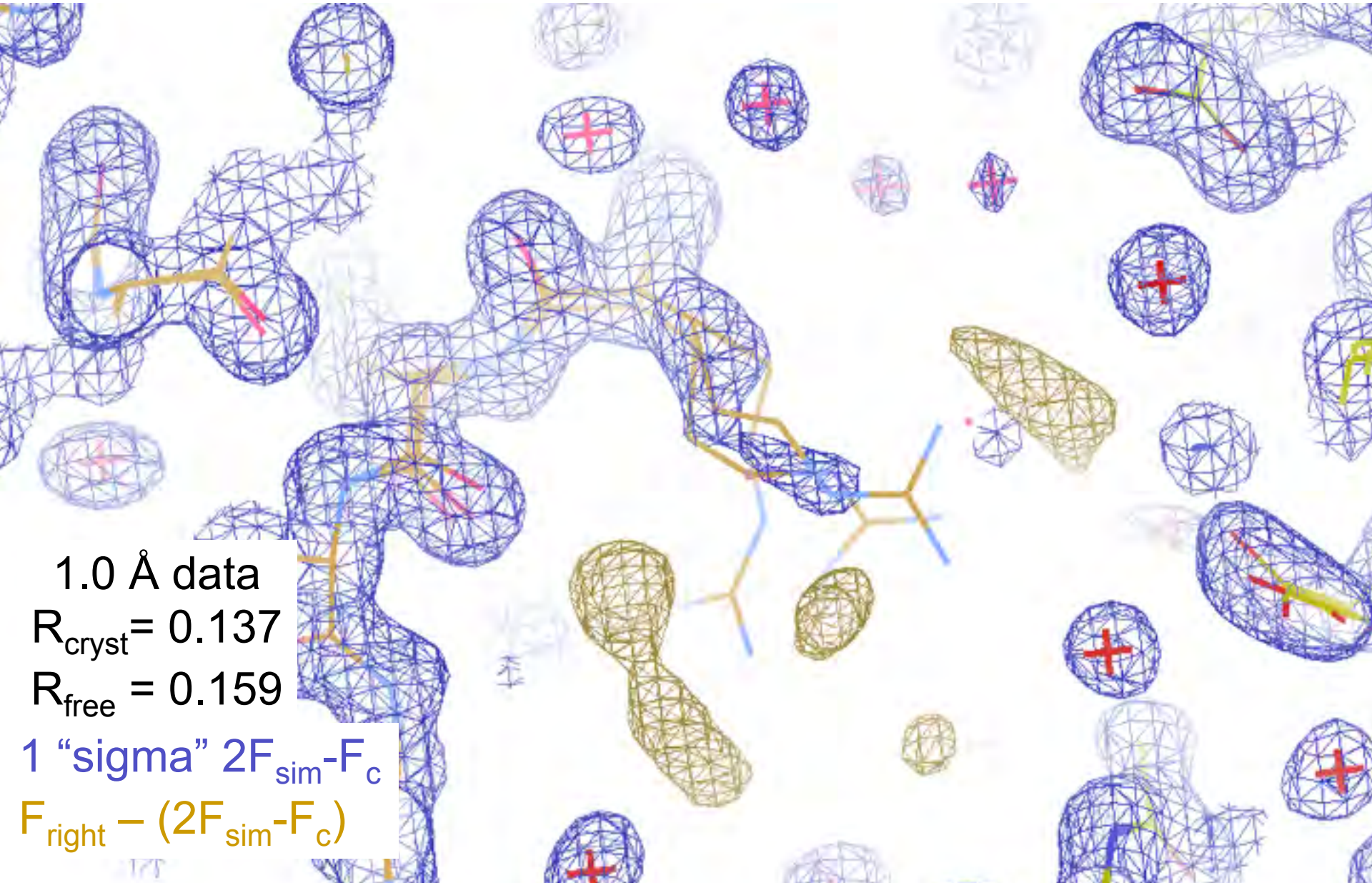

Regular model with real data!

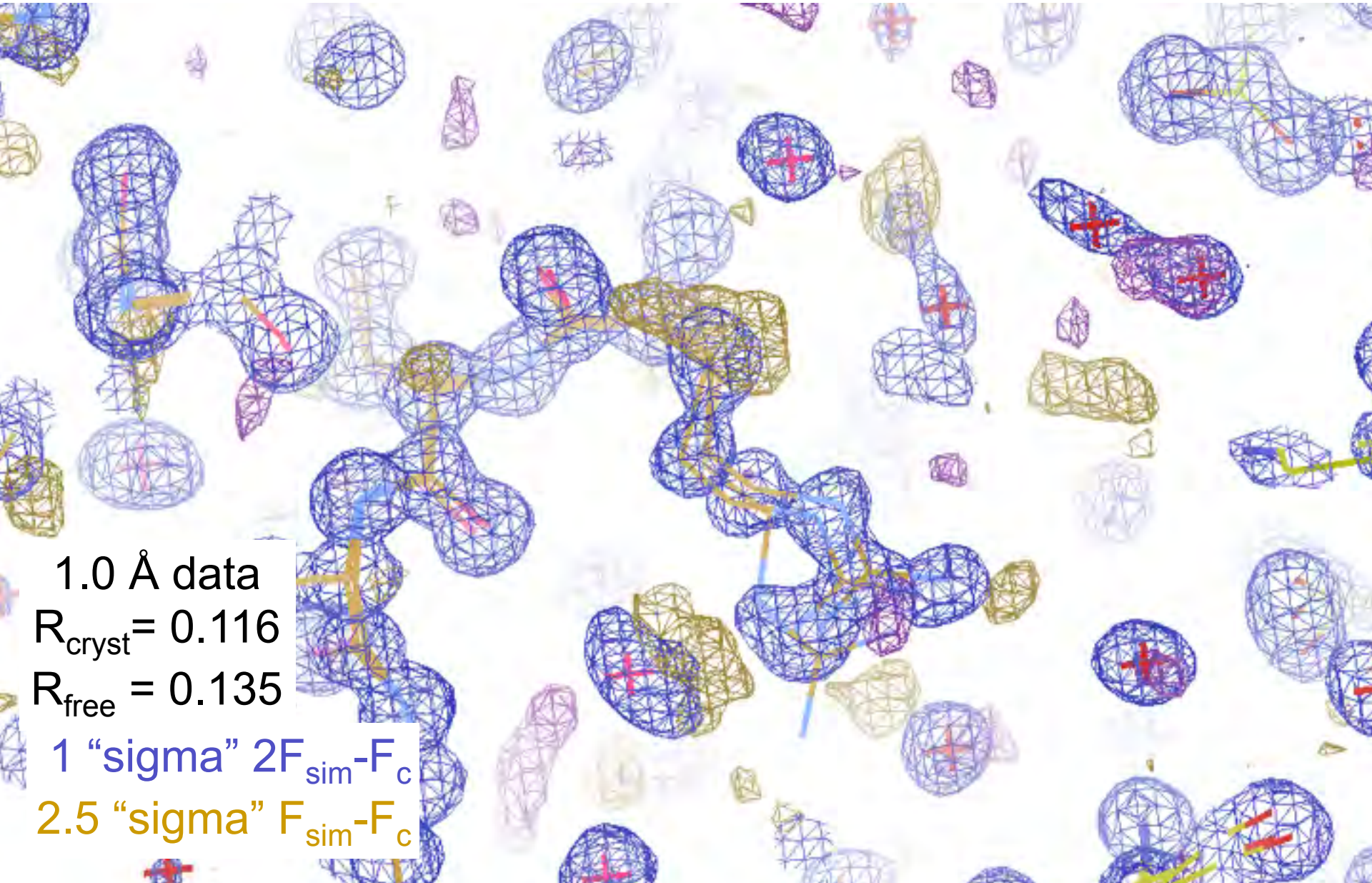

Molecular Dynamics vs Observation

1aho 64-residue scorpion toxin in water to 1.0 Å resolution

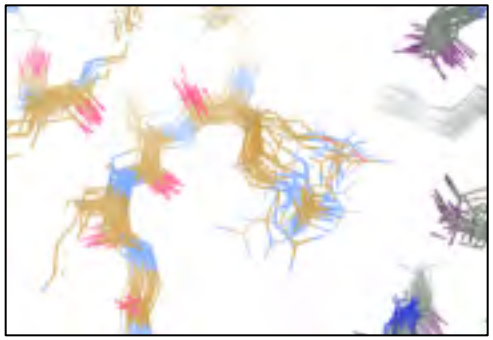

Molecular Dynamics vs Observation

1aho 64-residue scorpion toxin in water to 1.0 Å resolution

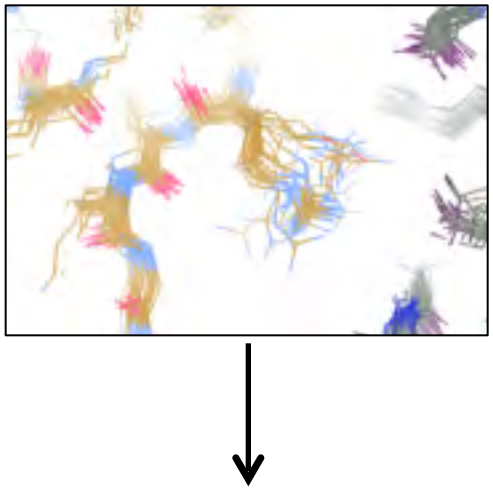

Molecular Dynamics vs Observation

1aho 64-residue scorpion toxin in water to 1.0 Å resolution

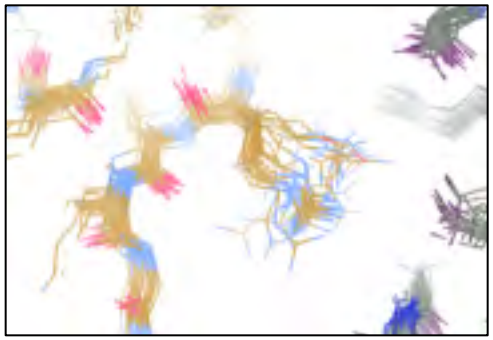

F_{sim}

Molecular Dynamics vs Observation

1aho 64-residue scorpion toxin in water to 1.0 Å resolution

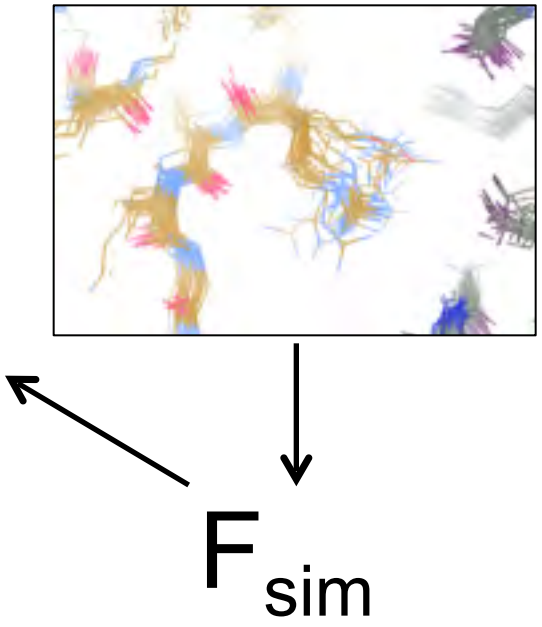

Molecular Dynamics vs Observation

1aho 64-residue scorpion toxin in water to 1.0 Å resolution

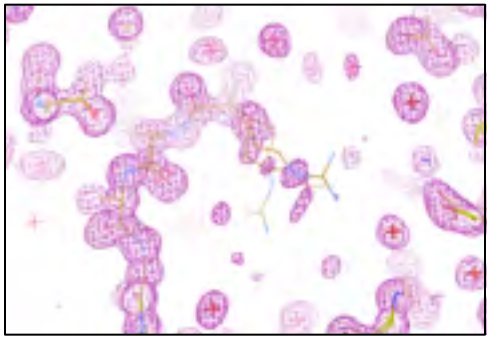

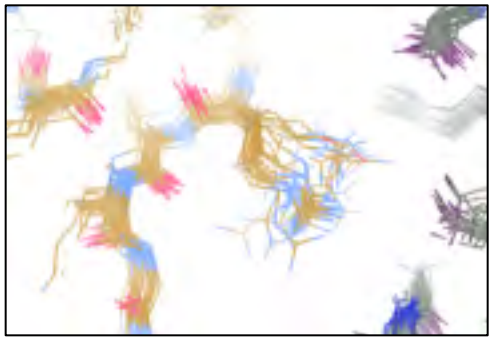

refined_vs_Fsim.pdb

F_{calc} F_{sim}

Molecular Dynamics vs Observation

1aho 64-residue scorpion toxin in water to 1.0 Å resolution

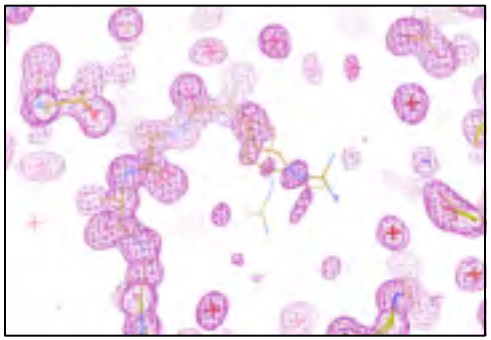

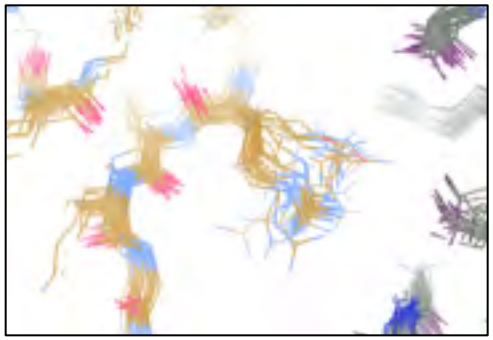

refined_vs_Fsim.pdb

F_{calc} F_{sim}

R_{cryst}= 0.137

Molecular Dynamics vs Observation

1aho 64-residue scorpion toxin in water to 1.0 Å resolution

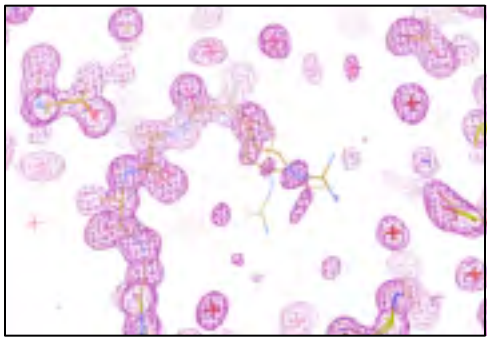

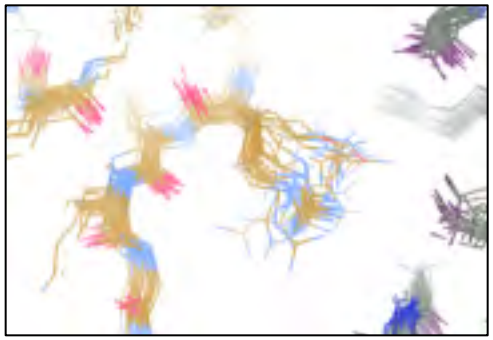

refined_vs_Fsim.pdb

F_{calc} F_{sim}

R_{cryst}= 0.137

Molecular Dynamics vs Observation

1aho 64-residue scorpion toxin in water to 1.0 Å resolution

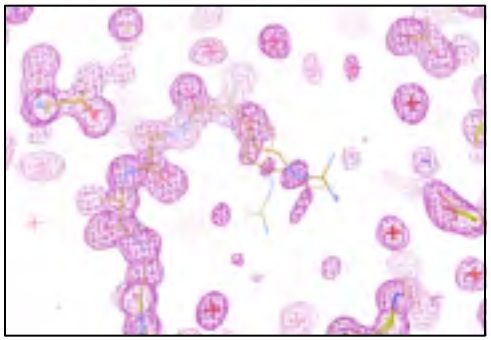

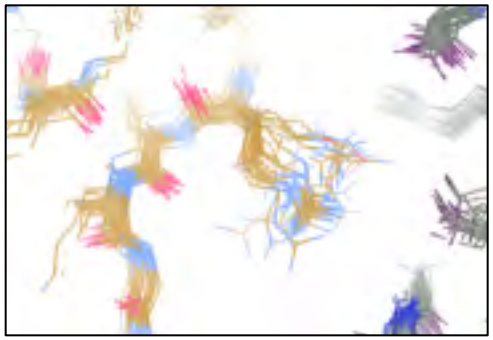

refined_vs_Fsim.pdb

1aho.cif

1aho.pdb

F_{calc}

F_{sim}

R_{cryst}= 0.137

Molecular Dynamics vs Observation

1aho 64-residue scorpion toxin in water to 1.0 Å resolution

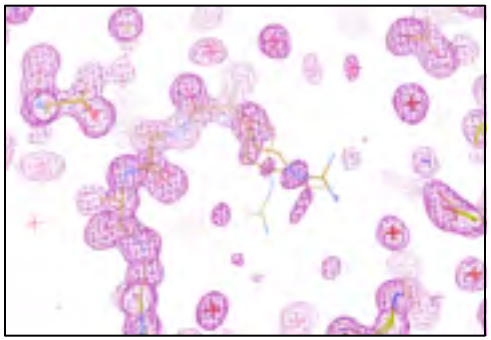

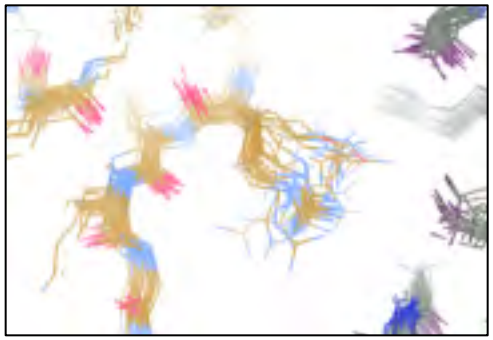

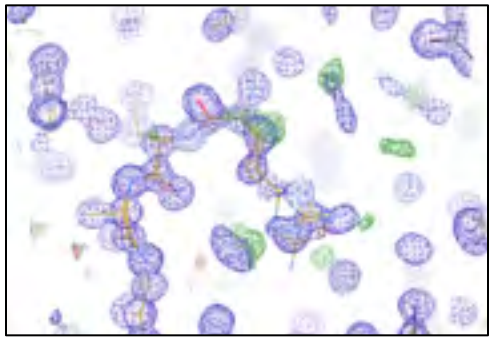

refined_vs_Fsim.pdb

1aho.cif

1aho.pdb

F_{calc}

F_{sim}

R_{cryst}= 0.137

Molecular Dynamics vs Observation

1aho 64-residue scorpion toxin in water to 1.0 Å resolution

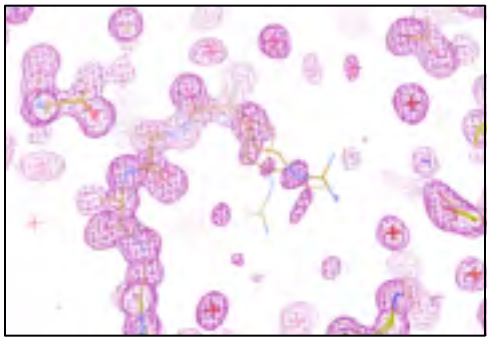

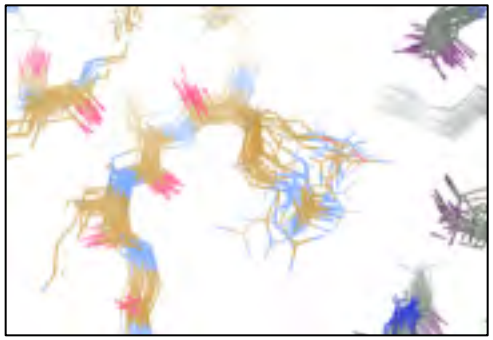

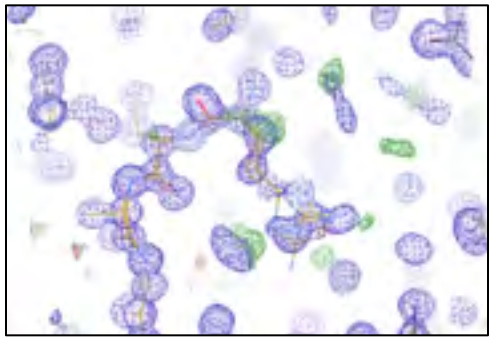

refined_vs_Fsim.pdb

F_{calc}

F_{sim}

1aho.cif

F_{obs}

1aho.pdb

F_{calc}

R_{cryst}= 0.137

Molecular Dynamics vs Observation

1aho 64-residue scorpion toxin in water to 1.0 Å resolution

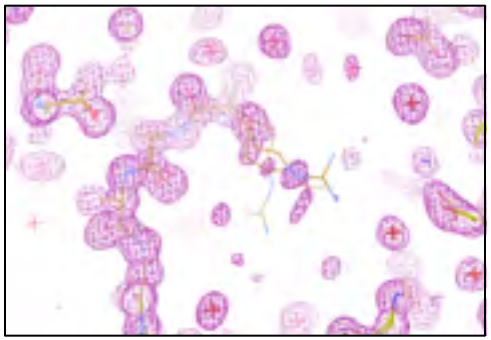

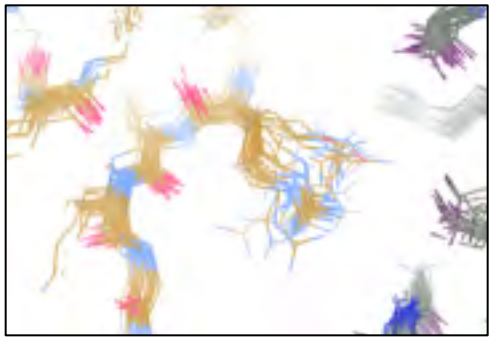

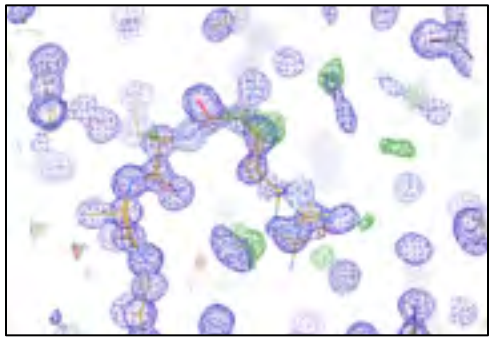

refined_vs_Fsim.pdb

1aho.cif 1aho.pdb

F_{calc} F_{sim} F_{obs} F_{calc}

R_{cryst}= 0.137

R_{cryst}= 0.116

Molecular Dynamics vs Observation

1aho 64-residue scorpion toxin in water to 1.0 Å resolution

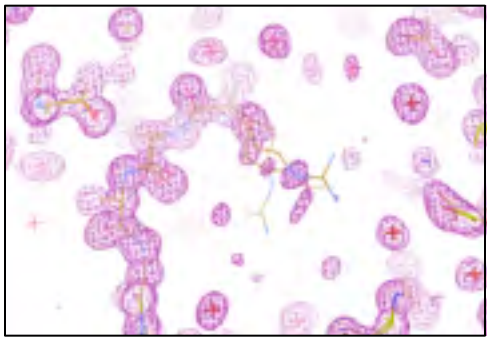

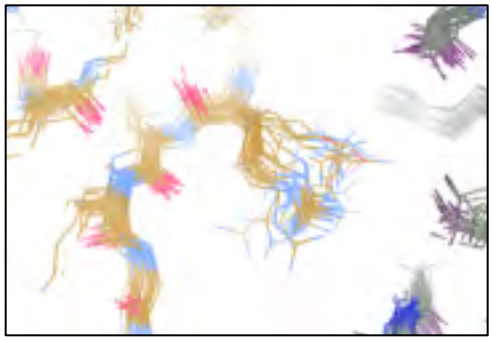

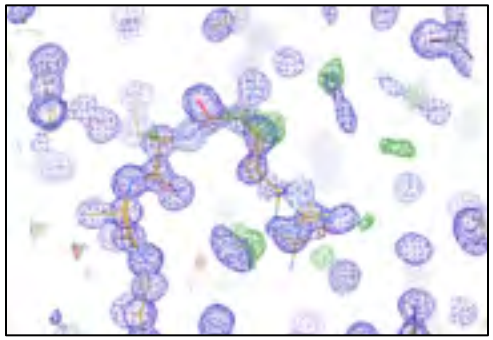

refined_vs_Fsim.pdb

1aho.cif

1aho.pdb

F_{calc} F_{sim} F_{obs} F_{calc}

R_{cryst}= 0.137

R_{cryst}= 0.116

Molecular Dynamics vs Observation

1aho 64-residue scorpion toxin in water to 1.0 Å resolution

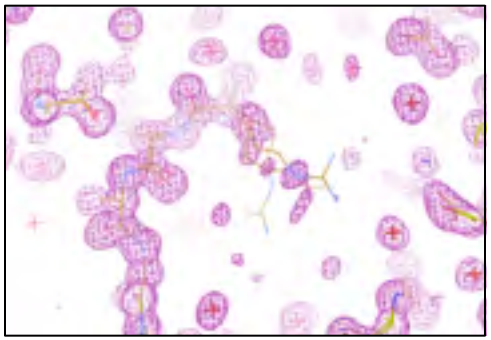

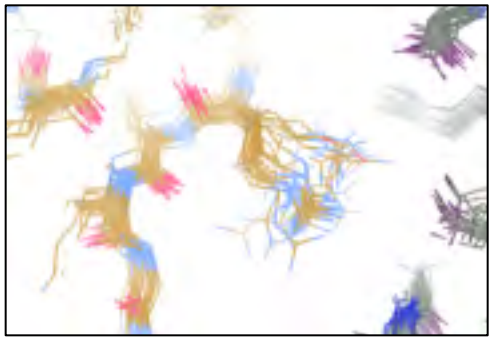

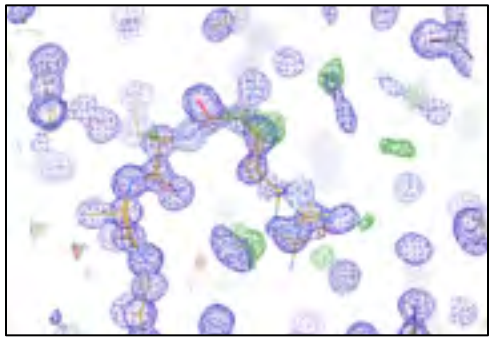

refined_vs_Fsim.pdb

1aho.cif

1aho.pdb

F_{calc} F_{sim} F_{obs} F_{calc}

R_{cryst}= 0.137 R_{free} = R_{cryst}= 0.116

Molecular Dynamics vs Observation

1aho 64-residue scorpion toxin in water to 1.0 Å resolution

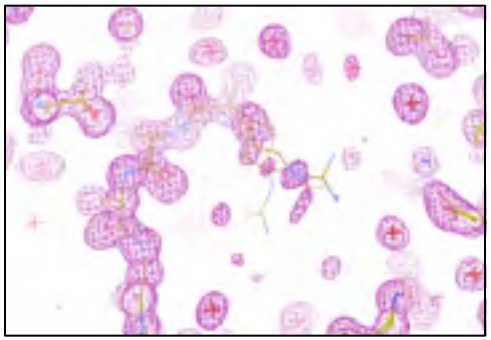

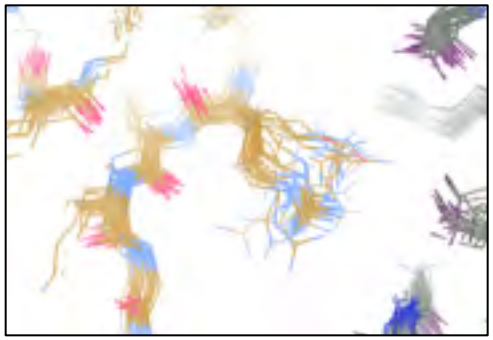

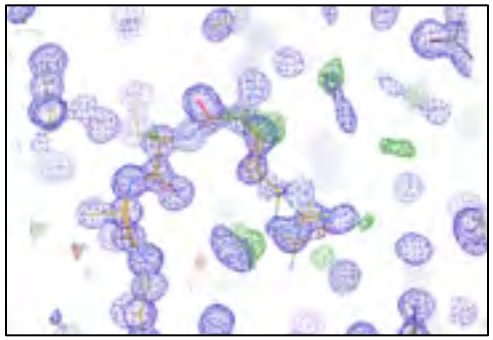

refined_vs_Fsim.pdb

1aho.cif

1aho.pdb

F_{calc} F_{sim} F_{obs} F_{calc}

R_{cryst}= 0.137 R_{free} = 0.69 R_{cryst}= 0.116

Molecular Dynamics vs Observation

1aho 64-residue scorpion toxin in water to 1.0 Å resolution

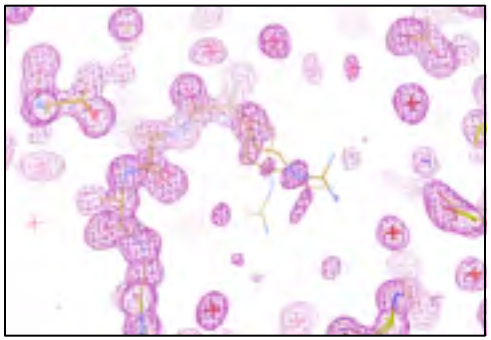

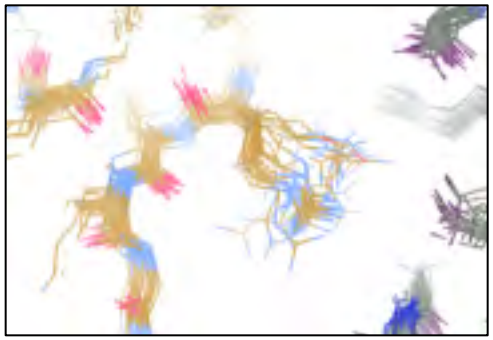

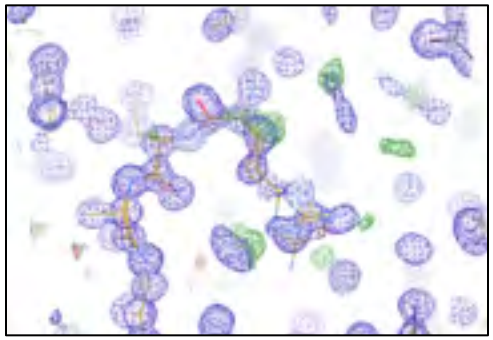

refined_vs_Fsim.pdb

1aho.cif

1aho.pdb

F_{calc} F_{sim} F_{obs} F_{calc}

R_{cryst}= 0.137

R_{free} = 0.69

R_{cryst}= 0.116

R_{free} = 0.48 to 4 Å

Molecular Dynamics vs Observation

1aho 64-residue scorpion toxin in water to 1.0 Å resolution

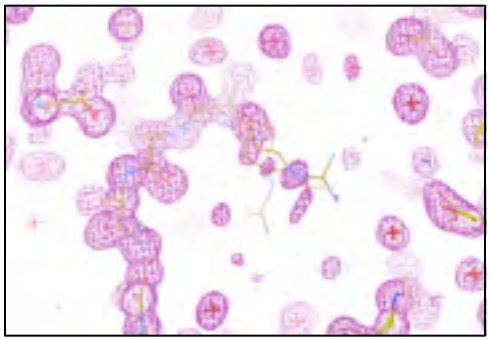

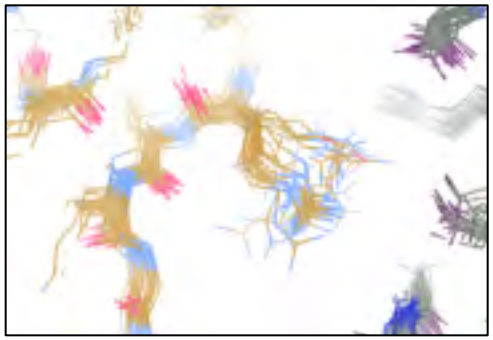

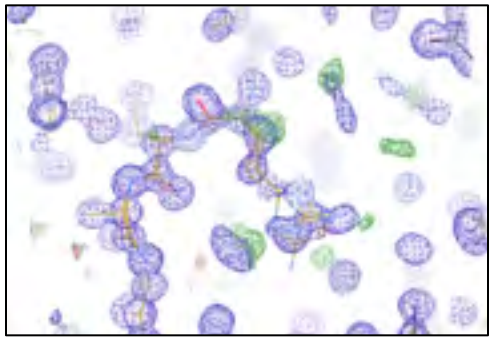

refined_vs_Fsim.pdb

1aho.cif

1aho.pdb

F_{calc} F_{sim} F_{obs} F_{calc}

R_{cryst}= 0.137 R_{free} = 0.69 R_{cryst}= 0.116

R_{free} = 0.48 to 4 Å

rmsd = 1.05 Å

LSQ rmsd = 0.43Å

Molecular Dynamics vs Observation

RMSD
1.05 Å

Molecular Dynamics vs Observation

RMSD
0.45 Å
aligned

Molecular Dynamics vs Observation

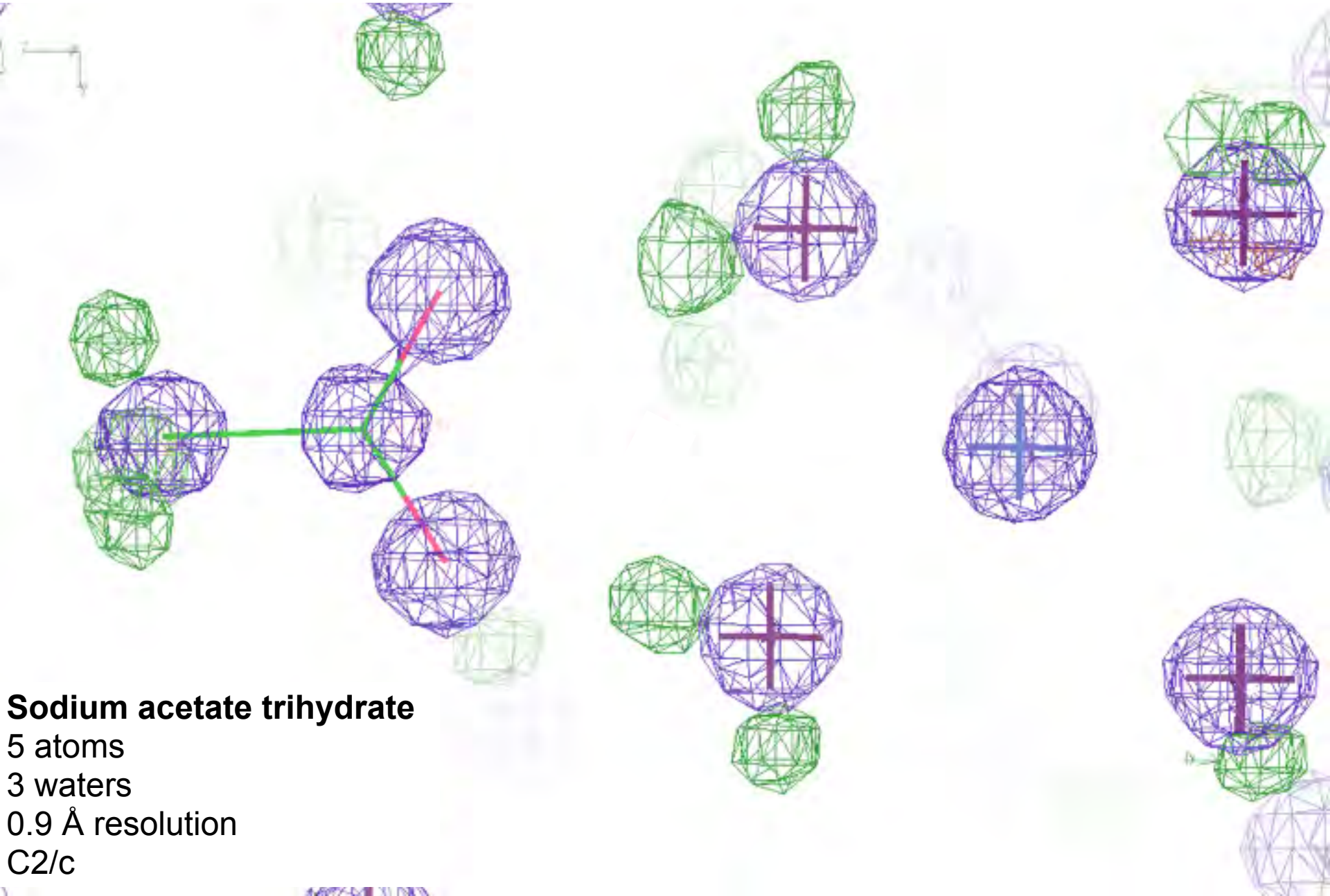

Sodium acetate trihydrate
5 atoms
3 waters
0.9 Å resolution
C2/c

Molecular Dynamics vs Observation

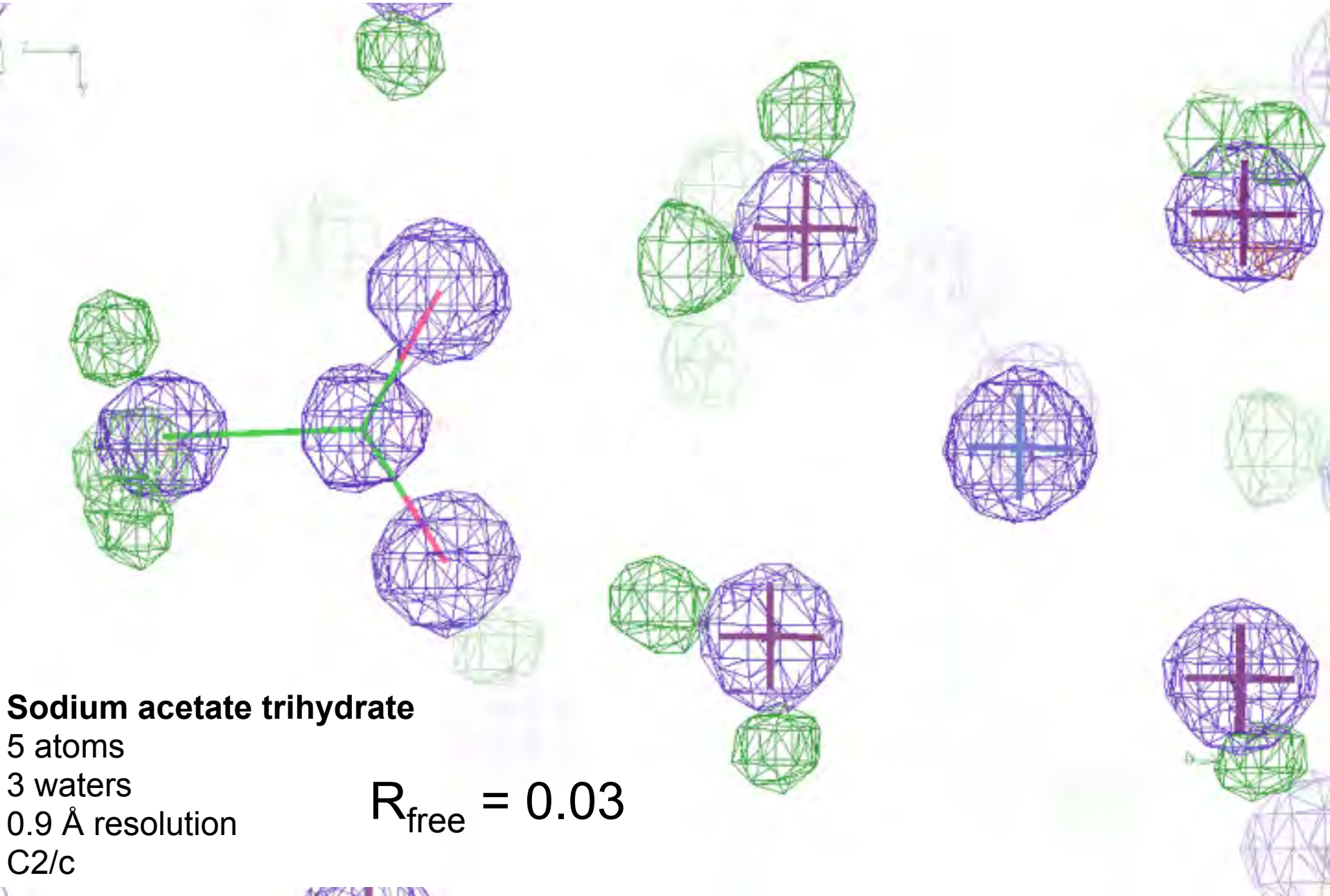

Sodium acetate trihydrate
5 atoms
3 waters
0.9 Å resolution
C2/c

R_{free} = 0.03

Molecular Dynamics vs Observation

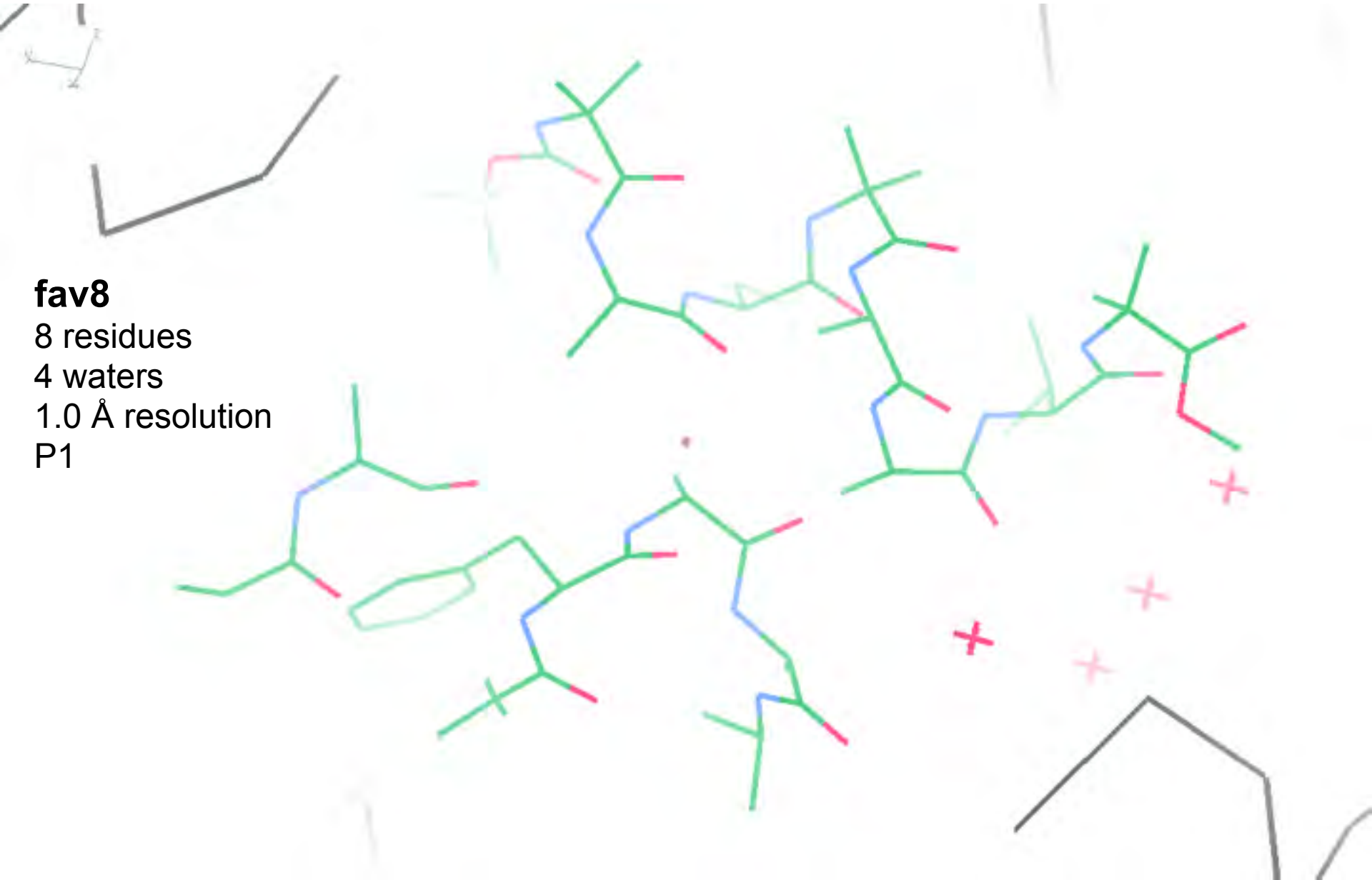

fav8
8 residues
4 waters
1.0 Å resolution
P1

Molecular Dynamics vs Observation

"fav8" 8-residue aromatic peptide with 4 waters to 1.0 Å resolution

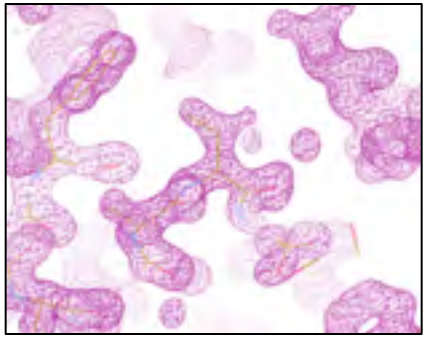

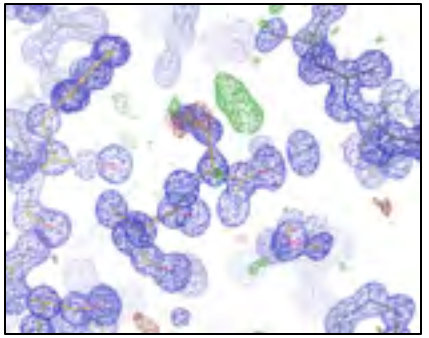

refined_vs_Fsim.pdb

fav8.fcf

fav8.cif

F_{calc} F_{sim} F_{obs} F_{calc}

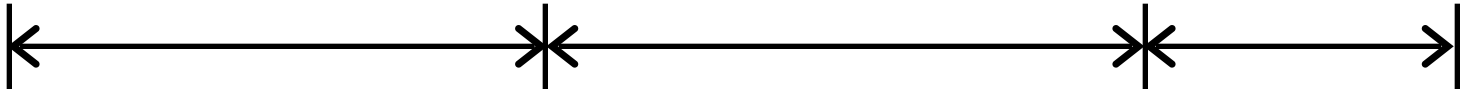

Molecular Dynamics vs Observation

"fav8" 8-residue aromatic peptide with 4 waters to 1.0 Å resolution

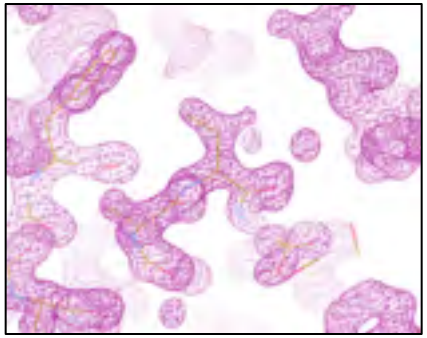

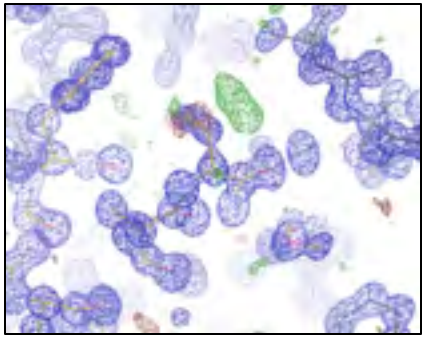

refined_vs_Fsim.pdb

fav8.fcf

fav8.cif

F_{calc} F_{sim} F_{obs} F_{calc}

R_{cryst}= 0.13

Molecular Dynamics vs Observation

"fav8" 8-residue aromatic peptide with 4 waters to 1.0 Å resolution

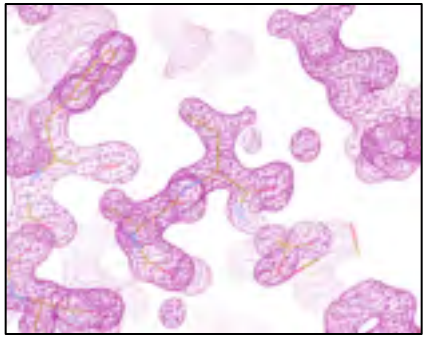

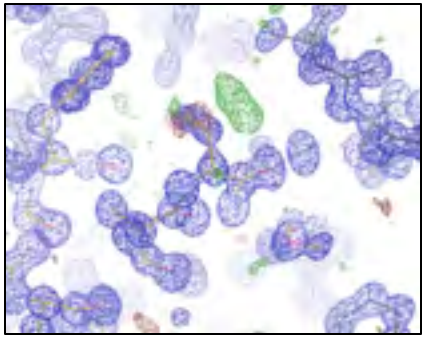

refined_vs_Fsim.pdb

fav8.fcf

fav8.cif

F_{calc} F_{sim} F_{obs} F_{calc}

R_{cryst}= 0.13

R_{cryst}= 0.16

Molecular Dynamics vs Observation

"fav8" 8-residue aromatic peptide with 4 waters to 1.0 Å resolution

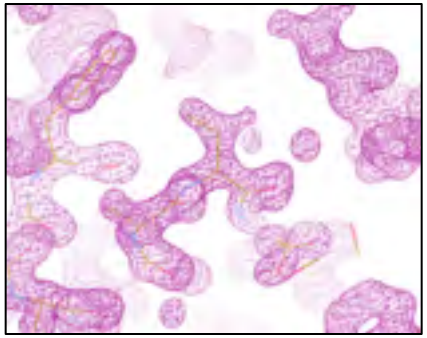

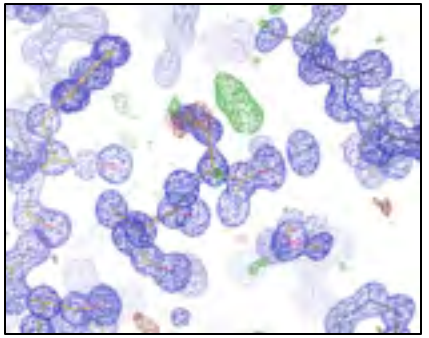

refined_vs_Fsim.pdb

fav8.fcf

fav8.cif

F_{calc} F_{sim} F_{obs} F_{calc}

R_{cryst}= 0.13

R_{cryst}= 0.16

R1 = 0.041
With 4σ cutoff!

Molecular Dynamics vs Observation

"fav8" 8-residue aromatic peptide with 4 waters to 1.0 Å resolution

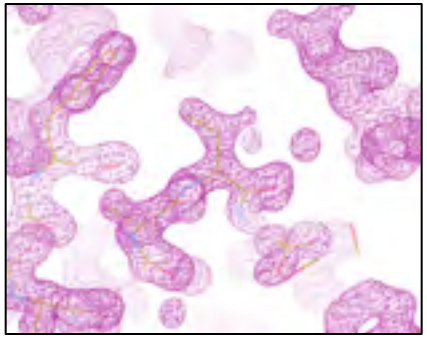

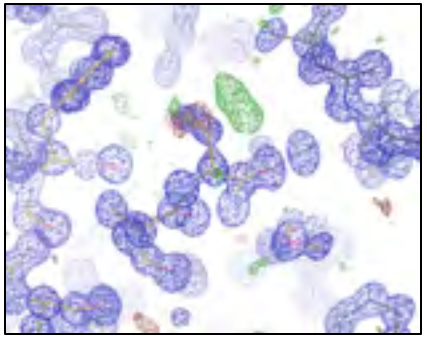

refined_vs_Fsim.pdb

fav8.fcf

fav8.cif

F_{calc} F_{sim} F_{obs} F_{calc}

R_{cryst}= 0.13

R_{free}= 0.23

R_{cryst}= 0.16

R_{free} = 0.20 to 2Å

R1 = 0.041
With 4σ cutoff!

Molecular Dynamics vs Observation

"fav8" 8-residue aromatic peptide with 4 waters to 1.0 Å resolution

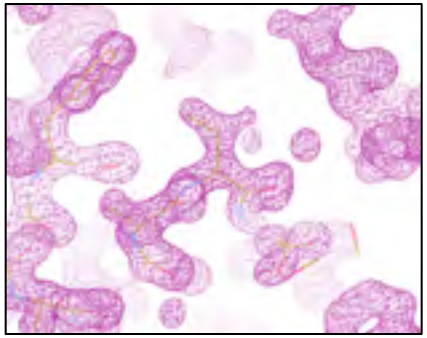

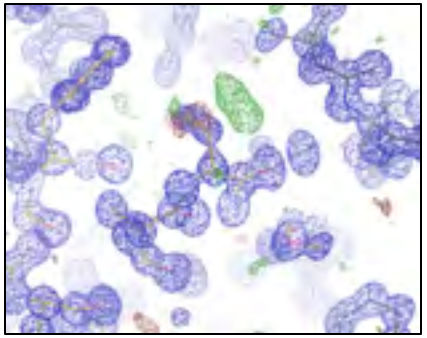

refined_vs_Fsim.pdb

fav8.fcf

fav8.cif

F_{calc} F_{sim} F_{obs} F_{calc}

R_{cryst}= 0.13

R_{free}= 0.23

R_{cryst}= 0.16

R_{free} = 0.20 to 2Å

R1 = 0.041
With 4σ cutoff!

rmsd = 0.20 Å

LSQ rmsd = 0.091Å & 0.15 Å

MD-predicted water structure

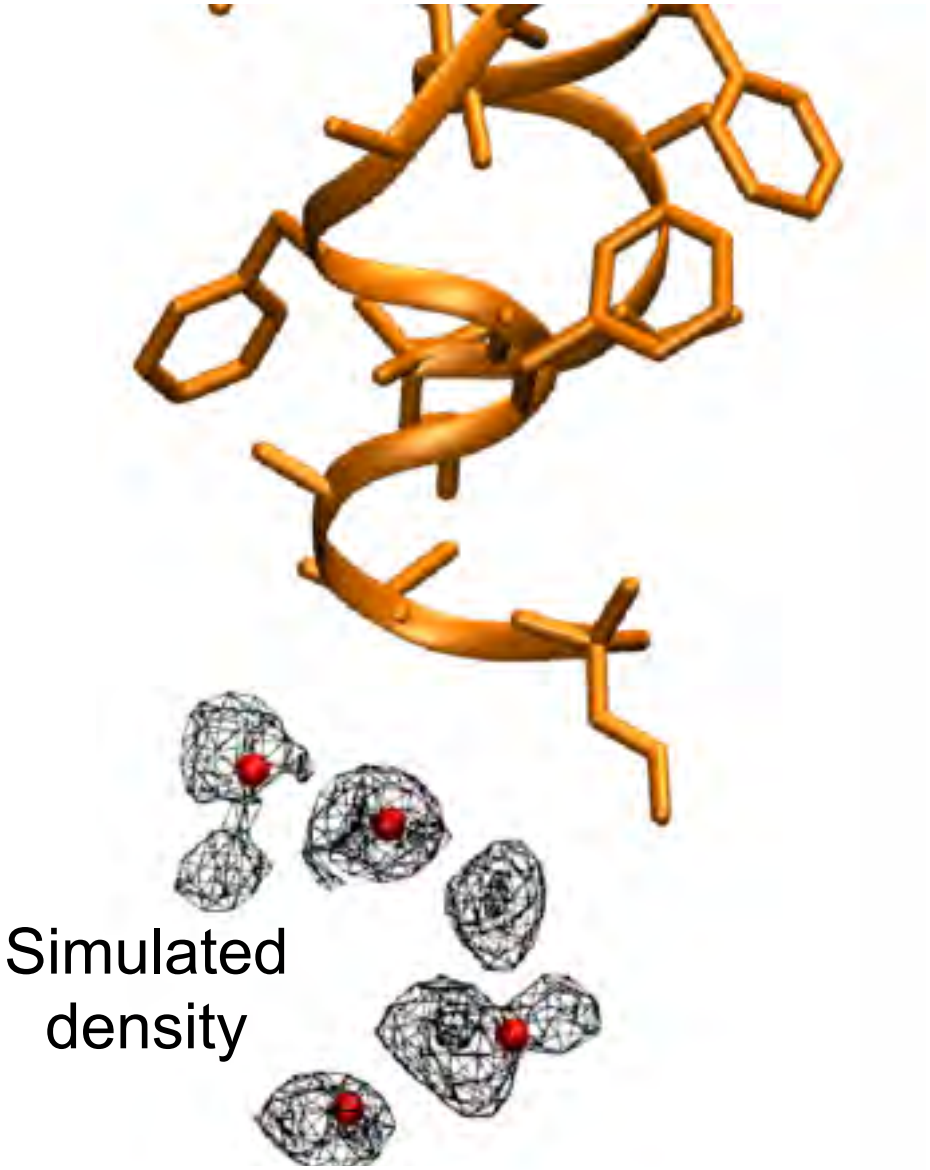

Janowski *et al* (2013) JACS **135**, 7938-7948

MD-predicted water structure

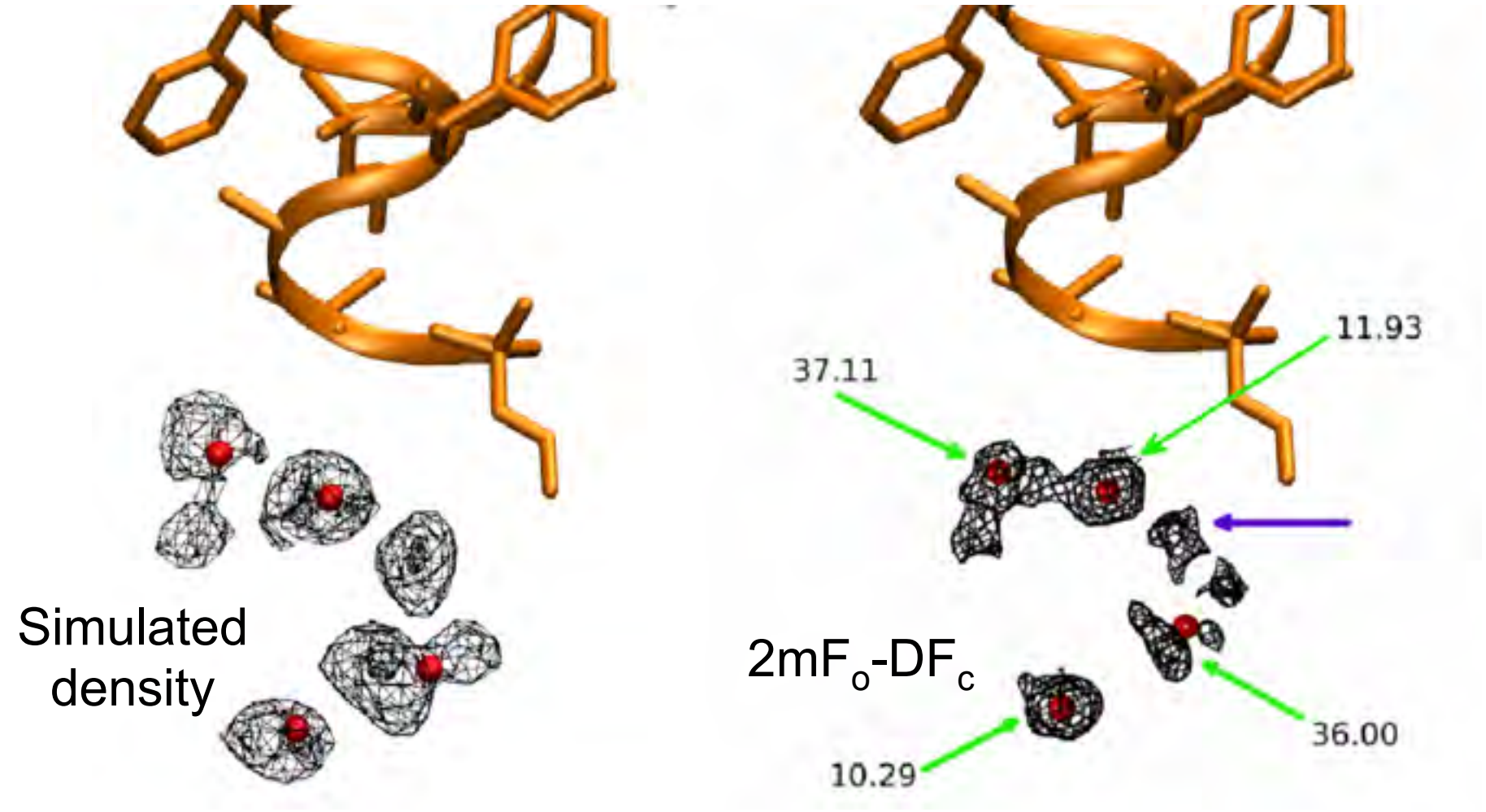

Janowski *et al* (2013) JACS **135**, 7938-7948

MD-predicted Val rotamer

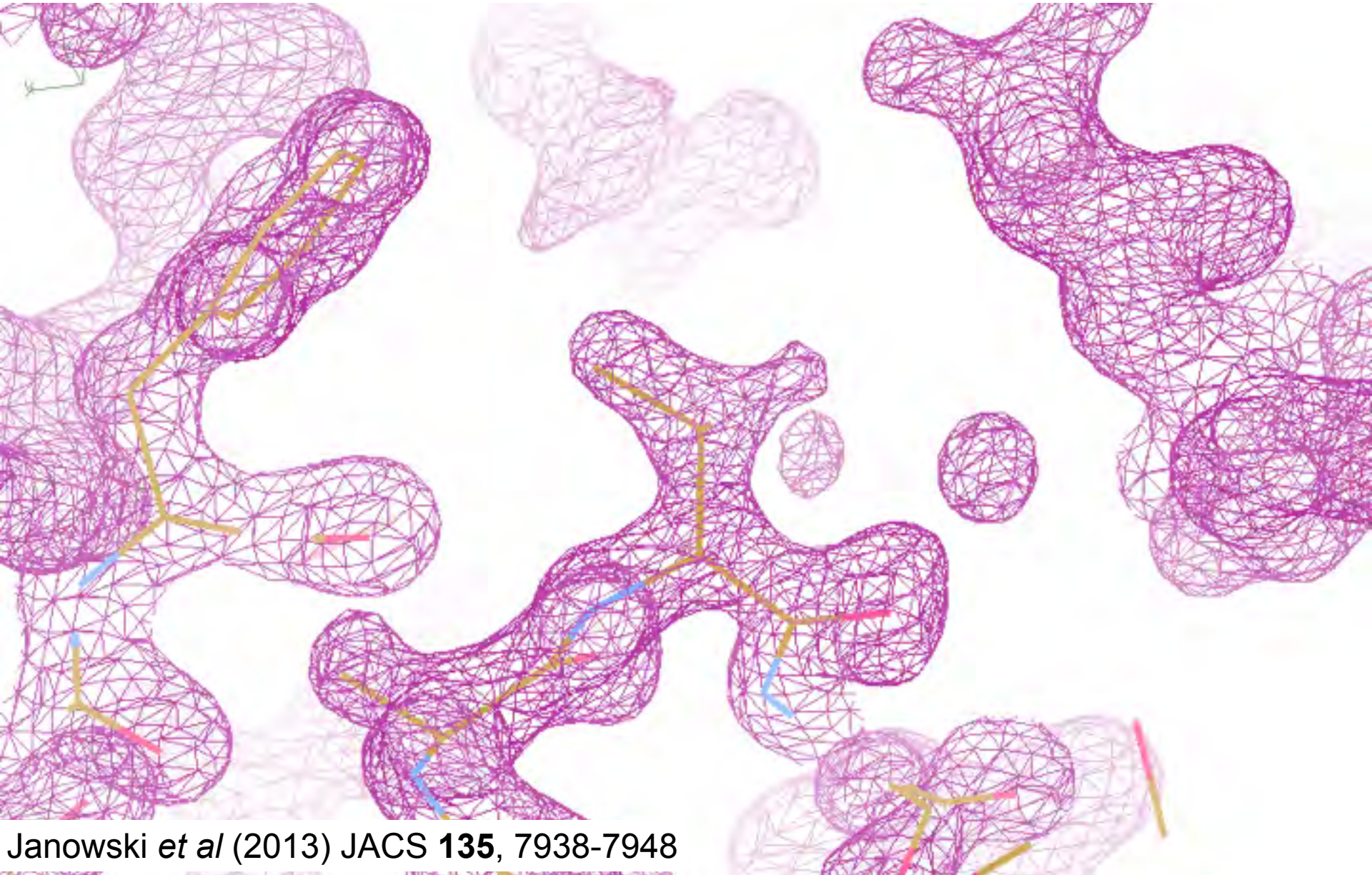

Janowski *et al* (2013) JACS **135**, 7938-7948

MD-predicted Val rotamer

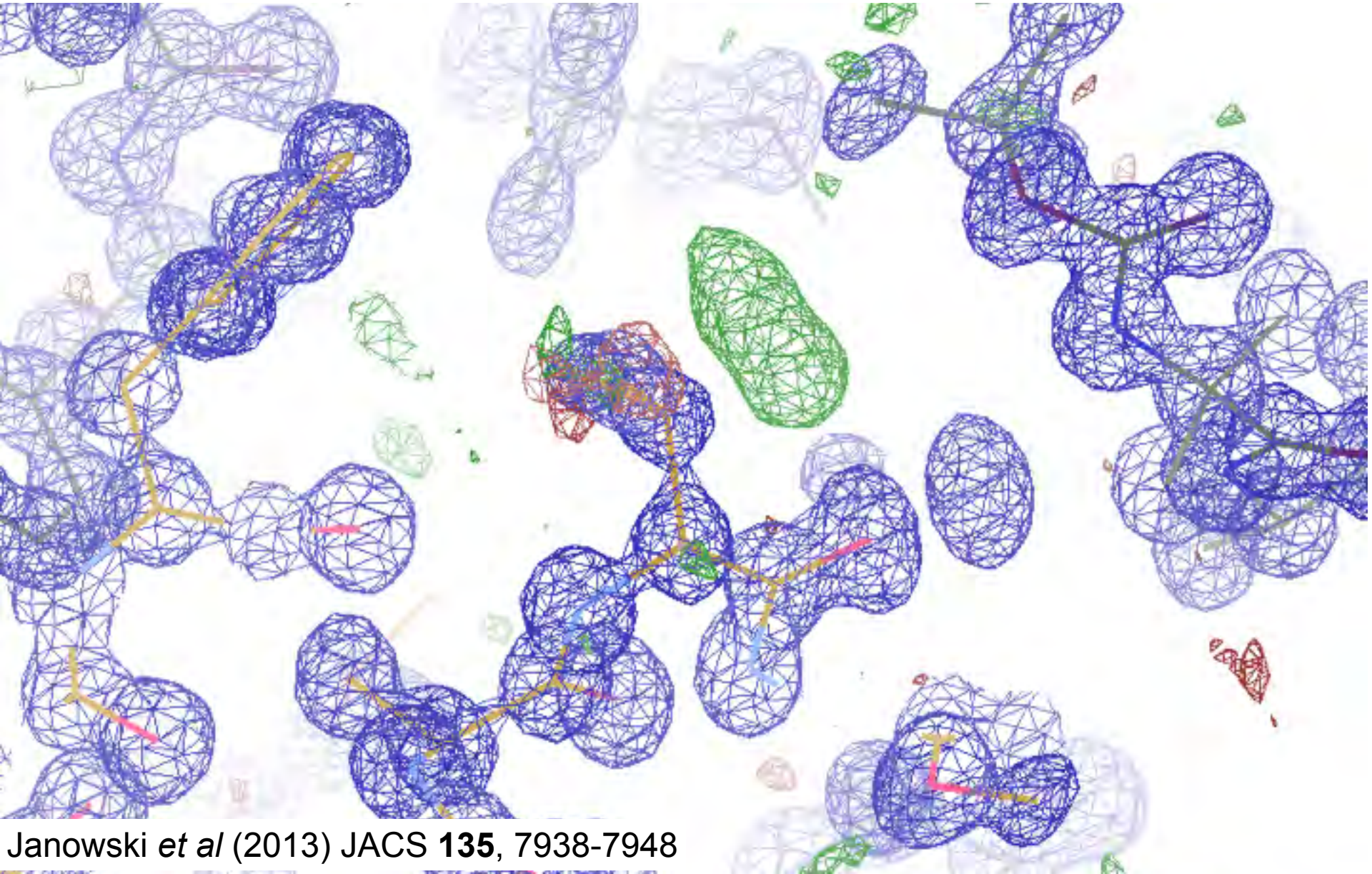

Janowski *et al* (2013) JACS **135**, 7938-7948

MD-predicted Val rotamer

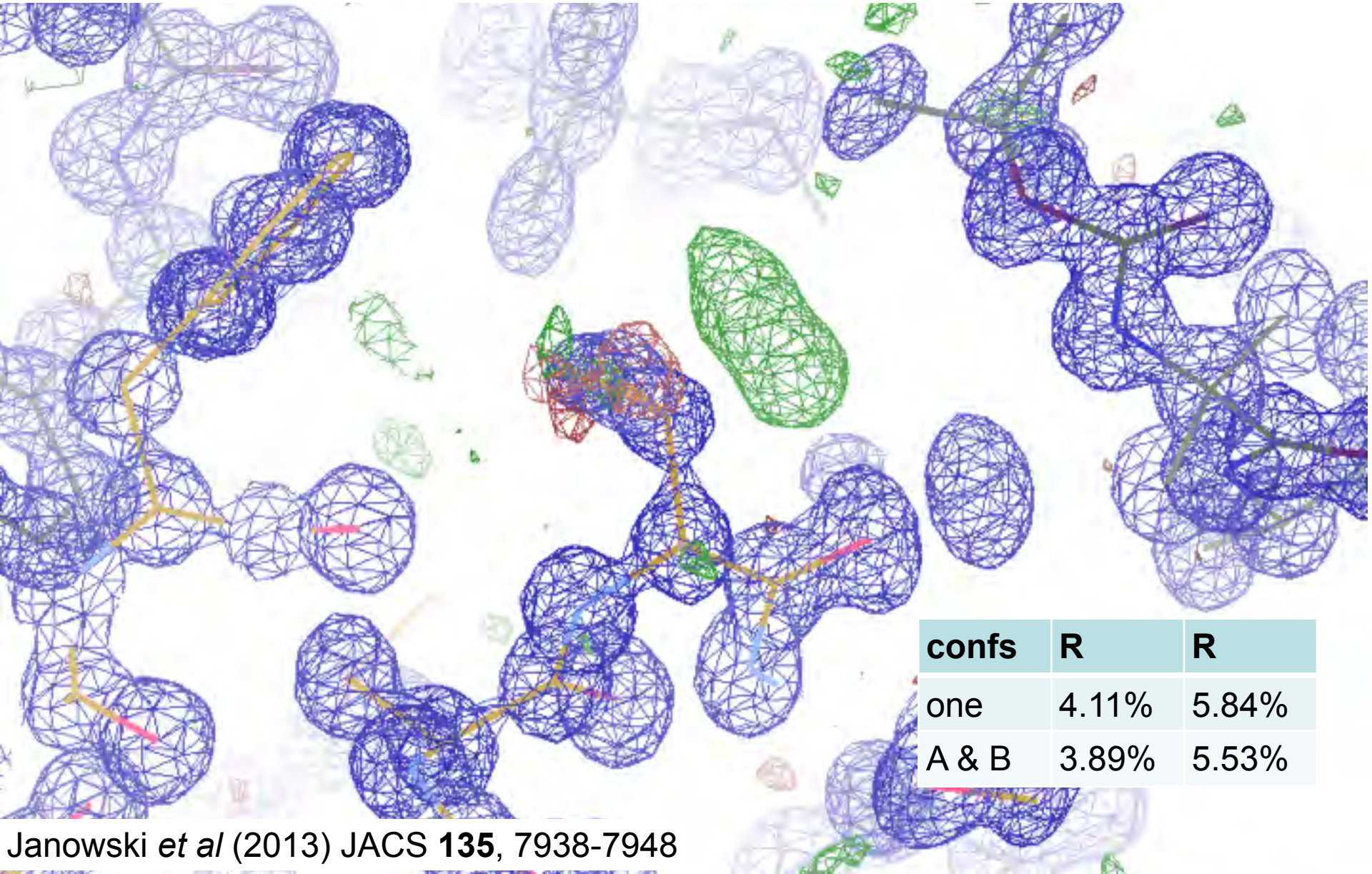

confs	R	R
one	4.11%	5.84%
A & B	3.89%	5.53%

Janowski *et al* (2013) JACS **135**, 7938-7948

MD-predicted Val rotamer

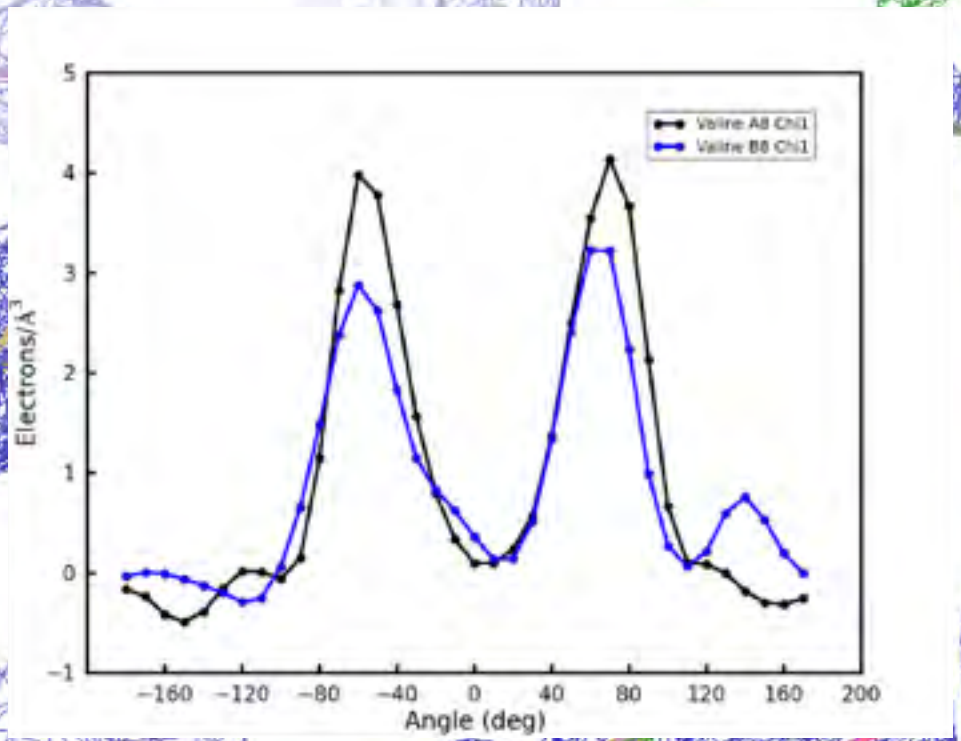

confs	R	R
one	4.11%	5.84%
A & B	3.89%	5.53%

Janowski *et al* (2013) JACS **135**, 7938-7948